

# Advances in the potential treatments of gastrointestinal and liver diseases: Addressing the public health burden

**Edited by**

Mariana Jinga, Adina Turcu-Stiolica  
and Maria Dimitrova

**Published in**

Frontiers in Pharmacology



## FRONTIERS EBOOK COPYRIGHT STATEMENT

The copyright in the text of individual articles in this ebook is the property of their respective authors or their respective institutions or funders. The copyright in graphics and images within each article may be subject to copyright of other parties. In both cases this is subject to a license granted to Frontiers.

The compilation of articles constituting this ebook is the property of Frontiers.

Each article within this ebook, and the ebook itself, are published under the most recent version of the Creative Commons CC-BY licence. The version current at the date of publication of this ebook is CC-BY 4.0. If the CC-BY licence is updated, the licence granted by Frontiers is automatically updated to the new version.

When exercising any right under the CC-BY licence, Frontiers must be attributed as the original publisher of the article or ebook, as applicable.

Authors have the responsibility of ensuring that any graphics or other materials which are the property of others may be included in the CC-BY licence, but this should be checked before relying on the CC-BY licence to reproduce those materials. Any copyright notices relating to those materials must be complied with.

Copyright and source acknowledgement notices may not be removed and must be displayed in any copy, derivative work or partial copy which includes the elements in question.

All copyright, and all rights therein, are protected by national and international copyright laws. The above represents a summary only. For further information please read Frontiers' Conditions for Website Use and Copyright Statement, and the applicable CC-BY licence.

ISSN 1664-8714  
ISBN 978-2-8325-3106-8  
DOI 10.3389/978-2-8325-3106-8

## About Frontiers

Frontiers is more than just an open access publisher of scholarly articles: it is a pioneering approach to the world of academia, radically improving the way scholarly research is managed. The grand vision of Frontiers is a world where all people have an equal opportunity to seek, share and generate knowledge. Frontiers provides immediate and permanent online open access to all its publications, but this alone is not enough to realize our grand goals.

## Frontiers journal series

The Frontiers journal series is a multi-tier and interdisciplinary set of open-access, online journals, promising a paradigm shift from the current review, selection and dissemination processes in academic publishing. All Frontiers journals are driven by researchers for researchers; therefore, they constitute a service to the scholarly community. At the same time, the *Frontiers journal series* operates on a revolutionary invention, the tiered publishing system, initially addressing specific communities of scholars, and gradually climbing up to broader public understanding, thus serving the interests of the lay society, too.

## Dedication to quality

Each Frontiers article is a landmark of the highest quality, thanks to genuinely collaborative interactions between authors and review editors, who include some of the world's best academicians. Research must be certified by peers before entering a stream of knowledge that may eventually reach the public - and shape society; therefore, Frontiers only applies the most rigorous and unbiased reviews. Frontiers revolutionizes research publishing by freely delivering the most outstanding research, evaluated with no bias from both the academic and social point of view. By applying the most advanced information technologies, Frontiers is catapulting scholarly publishing into a new generation.

## What are Frontiers Research Topics?

Frontiers Research Topics are very popular trademarks of the *Frontiers journals series*: they are collections of at least ten articles, all centered on a particular subject. With their unique mix of varied contributions from Original Research to Review Articles, Frontiers Research Topics unify the most influential researchers, the latest key findings and historical advances in a hot research area.

Find out more on how to host your own Frontiers Research Topic or contribute to one as an author by contacting the Frontiers editorial office: [frontiersin.org/about/contact](https://frontiersin.org/about/contact)



# Advances in the potential treatments of gastrointestinal and liver diseases: Addressing the public health burden

## Topic editors

Mariana Jinga — Carol Davila University of Medicine and Pharmacy, Romania

Adina Turcu-Stiolica — University of Medicine and Pharmacy of Craiova, Romania

Maria Dimitrova — Medical University Sofia, Bulgaria

## Topic Coordinator

Amit Khurana — University Hospital RWTH Aachen, Germany

## Citation

Jinga, M., Turcu-Stiolica, A., Dimitrova, M., eds. (2023). *Advances in the potential treatments of gastrointestinal and liver diseases: Addressing the public health burden*. Lausanne: Frontiers Media SA. doi: 10.3389/978-2-8325-3106-8

## Table of contents

- 06 **Editorial: Advances in the potential treatments of gastrointestinal and liver diseases: addressing the public health burden**  
Adina Turcu-Stiolica, Maria Dimitrova and Mariana Jinga
- 09 **Molecular and cellular mechanisms underlying postoperative paralytic ileus by various immune cell types**  
Chao Sui, Liang Tao, Chunhua Bai, Lihua Shao, Ji Miao, Kai Chen, Meng Wang, Qiongyuan Hu and Feng Wang
- 19 **Salvianolic acid B inhibits autophagy and activation of hepatic stellate cells induced by TGF- $\beta$ 1 by downregulating the MAPK pathway**  
Na Jiang, Jing Zhang, Jian Ping and Lieming Xu
- 30 **Hesperidin promotes gastric motility in rats with functional dyspepsia by regulating Drp1-mediated ICC mitophagy**  
Qingling Jia, Li Li, Xiangxiang Wang, Yujiao Wang, Kailin Jiang, Keming Yang, Jun Cong, Gan Cai and Jianghong Ling
- 43 **Alleviating insomnia should decrease the risk of irritable bowel syndrome: Evidence from Mendelian randomization**  
Wenzhao Bao, Li Qi, Yin Bao, Sai Wang and Wei Li
- 53 **Identification of hepatoprotective traditional Chinese medicines based on the structure–activity relationship, molecular network, and machine learning techniques**  
Shuaibing He, Yanfeng Yi, Diandong Hou, Xuyan Fu, Juan Zhang, Xiaochen Ru, Jinlu Xie and Juan Wang
- 72 **Comparison of prognosis between neoadjuvant imatinib and upfront surgery for GIST: A systematic review and meta-analysis**  
Zhen Liu, Zimu Zhang, Juan Sun, Jie Li, Ziyang Zeng, Mingwei Ma, Xin Ye, Fan Feng and Weiming Kang
- 82 **Efficacy and safety of fenofibrate add-on therapy in patients with primary biliary cholangitis refractory to ursodeoxycholic acid: A retrospective study and updated meta-analysis**  
Xuan Guoyun, Ding Dawei, Liu Ning, Hu Yinan, Yang Fangfang, Tian Siyuan, Sun Hao, Yang Jiaqi, Xu Ang, Guo Guanya, Chen Xi, Shang Yulong and Han Ying
- 94 **Effective dose of propofol combined with a low-dose esketamine for gastroscopy in elderly patients: A dose finding study using dixon's up-and-down method**  
Yuling Zheng, Yafei Xu, Bixin Huang, Ying Mai, Yiwen Zhang and Zhongqi Zhang
- 102 **Therapeutic effects and mechanisms of plant-derived natural compounds against intestinal mucositis**  
Cailan Li, Jianhui Xie, Jiahao Wang, Ying Cao, Min Pu, Qihai Gong and Qiang Lu

- 121 **The efficacy of mesalazine on nonspecific terminal ileal ulcers: A randomized controlled trial**  
Junrong Li, Fangmei Ling, Di Guo, Jinfang Zhao, Ling Cheng, Yidong Chen, Mingyang Xu and Liangru Zhu
- 129 **Methanolic *Moringa oleifera* leaf extract protects against epithelial barrier damage and enteric bacterial translocation in intestinal I/R: Possible role of caspase 3**  
O A. Afolabi, T M. Akhigbe, R E. Akhigbe, B A. Alabi, O T. Gbolagun, M E. Taiwo, O O. Fakeye and E O. Yusuf
- 145 **Methotrexate showed efficacy both in Crohn's disease and ulcerative colitis, predictors of surgery were identified in patients initially treated with methotrexate monotherapy**  
Mengyao Wang, Jingwen Zhao, Heran Wang, Changqing Zheng, Bing Chang and Lixuan Sang
- 161 **Based on network pharmacology and molecular docking to explore the protective effect of Epimedii Folium extract on cisplatin-induced intestinal injury in mice**  
Juan Xia, Jun-Nan Hu, Zi Wang, En-Bo Cai, Shen Ren, Ying-Ping Wang, Xiu-Juan Lei and Wei Li
- 179 **Trifluridine/tipiracil as a therapeutic option in real life setting of metastatic colorectal cancer: An efficacy and safety analysis**  
Daniel Sur, Cristina Lungulescu, Ștefan Spînu, Alecsandra Gorzo, Elena-Adriana Dumitrescu, Dan Ionut Gheonea and Cristian-Virgil Lungulescu
- 189 **Host and immunosuppression-related factors influencing fibrosis occurrence post liver transplantation**  
Speranta Iacob, Razvan Iacob, Ioana Manea, Mihaela Uta, Andrei Chiosa, Mona Dumbrava, Gabriel Becheanu, Luminita Stoica, Codruta Popa, Vlad Brasoveanu, Doina Hrehoret, Cristian Gheorghe, Liana Gheorghe, Simona Dima and Irinel Popescu
- 199 **Diagnostic and therapeutic strategies for non-alcoholic fatty liver disease**  
Yajie Fu, Yanzhi Zhou, Linhu Shen, Xuwen Li, Haorui Zhang, Yeqi Cui, Ke Zhang, Weiguo Li, Wei-dong Chen, Shizhen Zhao, Yunfu Li and Wenling Ye
- 219 **Patchouli alcohol improved diarrhea-predominant irritable bowel syndrome by regulating excitatory neurotransmission in the myenteric plexus of rats**  
Wanyu Chen, Lu Liao, Zitong Huang, Yulin Lu, Yukang Lin, Ying Pei, Shulin Yi, Chen Huang, Hongying Cao and Bo Tan
- 235 **Efficacy evaluation of pulmonary hypertension therapy in patients with portal pulmonary hypertension: A systematic review and meta-analysis**  
Ruihua Zhang, Tengfei Li, Yueming Shao, Wei Bai and Xiaoyu Wen

- 248 **Correlation between adenoma detection rate and other quality indicators, and its variability depending on factors such as sedation or indication for colonoscopy**  
Andrei Lucian Groza, Bogdan Silviu Ungureanu, Cristian Tefas, Bogdan Miulescu and Marcel Tanțău
- 258 **Advanced intestinal regulation improves bowel preparation quality in patients with constipation: A systematic review and network meta-analysis**  
Liang Ding, JinNan Duan, Tao Yang, ChaoQiong Jin, Jun Luo and Ahuo Ma



## OPEN ACCESS

EDITED AND REVIEWED BY

Angelo A. Izzo,  
University of Naples Federico II, Italy

\*CORRESPONDENCE

Maria Dimitrova,  
✉ mdimitrova@pharmfac.mu-sofia.bg

RECEIVED 04 July 2023

ACCEPTED 07 July 2023

PUBLISHED 13 July 2023

## CITATION

Turcu-Stiolica A, Dimitrova M and  
Jinga M (2023), Editorial: Advances in the  
potential treatments of gastrointestinal  
and liver diseases: addressing the public  
health burden.*Front. Pharmacol.* 14:1253069.

doi: 10.3389/fphar.2023.1253069

## COPYRIGHT

© 2023 Turcu-Stiolica, Dimitrova and  
Jinga. This is an open-access article  
distributed under the terms of the  
[Creative Commons Attribution License](#)  
(CC BY). The use, distribution or  
reproduction in other forums is  
permitted, provided the original author(s)  
and the copyright owner(s) are credited  
and that the original publication in this  
journal is cited, in accordance with  
accepted academic practice. No use,  
distribution or reproduction is permitted  
which does not comply with these terms.

# Editorial: Advances in the potential treatments of gastrointestinal and liver diseases: addressing the public health burden

Adina Turcu-Stiolica<sup>1</sup>, Maria Dimitrova<sup>2\*</sup> and Mariana Jinga<sup>3</sup><sup>1</sup>Department of Pharmacoeconomics, University of Medicine and Pharmacy of Craiova, Craiova, Romania,<sup>2</sup>Department of Organization and Economy of Pharmacy, Medical University Sofia, Sofia, Bulgaria,<sup>3</sup>Department of Gastroenterology, Carol Davila University of Medicine and Pharmacy, Bucharest, Romania

## KEYWORDS

gastrointestinal, machine learning, plants, efficacy, molecules

## Editorial on the Research Topic

**Advances in the potential treatments of gastrointestinal and liver diseases: addressing the public health burden**

Gastrointestinal and liver diseases continue to pose a significant burden worldwide, both on societies and healthcare systems (Marcellin and Kutala, 2018). With recent advances in studying the pathogenesis of these diseases and the development of therapy and screening strategies for early detection, physicians, pharmacists and policymakers can now address this major public health burden. This includes not only for cancer but also chronic liver diseases and autoimmune diseases (Goebel et al., 2015; World Health Organization, 2022). By doing so, they can improve the therapeutics outcomes, enhance the quality of life of patients, and optimize healthcare costs.

The present Research Topic consists of twenty articles: 3 systematic reviews with meta-analysis, 3 reviews, and 14 original research articles. These articles provide a diverse range of innovative viewpoints on the significance of comprehending the genetic, molecular, and cellular mechanisms associated with gastrointestinal complications and diseases. Such understanding has the potential to guide the advancement of therapies in areas where clinical problems remain unsolved.

Regarding cellular and molecular mechanisms, Sui et al. examined the relationship between various immune cells and postoperative ileus, aiming to provide potential therapeutic solutions for this unresolved clinical issue. Jiang et al. analyzed the potential antifibrotic effects of salvianolic acid B in autophagy in liver fibrosis. Their findings revealed that inducing TGF- $\beta$ 1 resulted in a significant increase in autophagosome formation and autophagic flux in different molecular cascades. Another original research studied by Jia et al. demonstrated the *in vivo* efficacy of hesperidin in promoting gastric motility in rats with functional dyspepsia, suggesting a potential treatment approach for this condition.

Screening and early detection are among the primary priorities of the current European anticancer plan and should be implemented at the national level (Pana et al., 2023). Within our Research Topic, three original research articles emphasized the significance of on national level screening. Groza et al. conducted a study analysing the quality of colonoscopy in Romania as part of colorectal cancer screening. They discovered that the quality of colonoscopy is not consistently monitored and suggested using adenoma detection rate,



polyp detection rate, and adenoma per colonoscopy as monitoring indicators. In their systematic review with meta-analysis, [Ding et al.](#) examined the regimes that could improve bowel cleansing quality for patients undergoing colonoscopy. They emphasized the importance of adequately preparing patients before screening interventions to improve the quality of the results. Additionally, [Fu et al.](#) provided a review describing the current diagnostic methods, therapeutic targets, and therapies for non-alcoholic fatty liver disease.

Irritable bowel syndrome (IBS) is a functional gastrointestinal disorder. [Bao et al.](#) demonstrated that genetic susceptibility to insomnia could increase the risk of IBS. However, they did not observe a causal association between chronotype and IBS, nor did they find that genetic liability to the “morning” chronotype could lower the risk of IBS.

Many of the original research articles contributing to this Research Topic also provided insights on the potential pharmacological effects of plant-derived medicines. [Li et al.](#) conducted a review on the current progress of plant-derived treatments such as terpenoids, flavonoids, quinones, *etc.*, against intestinal mucositis. [He et al.](#) analyzed traditional Chinese medicines as a potential source of hepatoprotective agents. An interesting aspect of their original research was the use of an *in silico* model based on machine learning techniques to discover potential pharmacologically active plants. [Afolabi et al.](#) examined methanolic *Moringa oleifera* leaf extract for its potential protective role against epithelial barrier damage and enteric bacterial translocation in intestinal ischaemia/reperfusion injury. [Chen et al.](#) demonstrated that the patchouli alcohol, extracted from *Pogostemonis Herba*, improves intestinal motility and alleviates IBS-induced diarrheal symptoms. These findings suggest the potential therapeutic efficacy of patchouli alcohol against IBS accompanied with diarrhea.

Network pharmacology and molecular docking are novel methods that contribute to a comprehensive understanding of systems and network biology, as well as the orientation of molecules within binding sites. Currently, these methods are primarily used in the discovery of plant-based, marine-based, and antibiotics drugs ([Aleem et al., 2022](#)). In our Research Topic, [Xia et al.](#) have contributed with a research article that employs these methods to explore the potential *in vivo* protective effect of *Epidemii Folium* on cisplatin-induced intestinal injury in mice. Their findings showed that the extract of *Epidemii Folium* can alleviate cisplatin-induced intestinal damage by modulating oxidative stress, inflammation, and apoptosis.

The utilisation of artificial intelligence and machine-learning in gastroenterology allows the creation of models for predicting prognostics such as mortality ([Ungureanu et al., 2023](#)) or liver protection. [He et al.](#) employed these techniques to predict the hepatoprotective activity of ingredients derived from 12 traditional Chinese medicine, which could aid in the development of new drugs.

Two original research articles examined the efficacy and safety as major criteria for evidence-based therapy decision making. [Li et al.](#) investigated the efficacy of mesalazine in treating nonspecific terminal ileal ulcers and demonstrated no significant difference in clinical or endoscopic efficacy between patients who received mesalazine and those who were followed up without special intervention. [Sur et al.](#)

analyzed the efficacy and safety of trifluridine/tipiracil as a therapeutic option in metastatic colorectal cancer in real life setting for a Romanian cohort of patients. [Liu et al.](#) conducted a meta-analysis showing that neoadjuvant imatinib plus surgery significantly improve overall survival of rectal gastrointestinal stromal tumor compared to upfront surgery. Another meta-analysis, performed by [Zhang et al.](#), focused on changes in hemodynamic and cardiac function in patients with portal pulmonary hypertension (POPH) to understand the effect of pulmonary hypertension agents (including prostacyclin and its analogues, endothelin receptor antagonists, phosphodiesterase 5 inhibitors, soluble guanylate cyclase stimulants, *etc.*) treatment on the entire population of POPH patients.

Primary biliary cholangitis (PBC), a chronic autoimmune intrahepatic cholestatic disease, is still not fully understood. Meta-analyses were performed to better understand its pathogenic mechanisms ([Ionele et al., 2022](#)). [Guoyun et al.](#) updated a meta-analysis to explore the influence of fenofibrate dose and the effectiveness and safety of long-term application on PBC patients, with the aim of improving guideline recommendations.

In the field of gastrointestinal endoscopy, [Zheng et al.](#) determined the optimal dose of propofol combined with esketamine for gastroscopy in elderly patients.

In summary, the articles presented in this Research Topic focus on molecular and cellular mechanisms, the efficacy and safety of established therapies in real-world settings and provide insight into potential therapies derived from plant origins, as well as advanced solutions for screening, diagnosis, and treatment of gastrointestinal and liver diseases.

## Author contributions

AT-S and MD wrote the first draft. MJ commented on it and provided feedback. All authors agreed with submission of the final version.

## Acknowledgments

We are grateful to all the authors and reviewers for their contributions to this Research Topic.

## Conflict of interest

The authors declare that the research was conducted in the absence of any commercial or financial relationships that could be construed as a potential conflict of interest.

## Publisher's note

All claims expressed in this article are solely those of the authors and do not necessarily represent those of their affiliated organizations, or those of the publisher, the editors and the reviewers. Any product that may be evaluated in this article, or claim that may be made by its manufacturer, is not guaranteed or endorsed by the publisher.

## References

- Aleem, M. T., Khan, A., Wen, Z., Yu, Z., Li, K., Shaukat, A., et al. (2022). Molecular docking and in silico simulation of *Trichinella spiralis* membrane-associated progesterone receptor component 2 (Ts-MAPRC2) and its interaction with human PGRMC1. *Biomed. Res. Int.* 2022, 7414198. doi:10.1155/2022/7414198
- Goebel, M., Singal, A. G., Nodora, J., Castañeda, S. F., Martinez, E., Doubeni, C., et al. (2015). How can we boost colorectal and hepatocellular cancer screening among underserved populations? *Curr. Gastroenterol. Rep.* 17 (6), 22. doi:10.1007/s11894-015-0445-1
- Ionele, C. M., Turcu-Stiolica, A., Subtirelu, M. S., Ungureanu, B. S., Cioroianu, G. O., and Rogoveanu, I. (2022). A systematic review and meta-analysis on metabolic bone disease in patients with primary sclerosing cholangitis. *J. Clin. Med.* 11 (13), 3807. doi:10.3390/jcm11133807
- Marcellin, P., and Kutala, B. K. (2018). Liver diseases: A major, neglected global public health problem requiring urgent actions and large-scale screening. *Liver Int.* 38 (Suppl. 1), 2–6. doi:10.1111/liv.13682
- Pana, B. C., Furtunescu, F. L., Turcu-Stiolica, A., Mazilu, L., Ciufu, N., and Ciufu, C. (2023). Digital technology for health shows disparities in cancer prevention between digital health technology users and the general population in Romania. *Front. Oncol.* 13. doi:10.3389/fonc.2023.1171699
- Ungureanu, B. S., Gheonea, D. I., Florescu, D. N., Iordache, S., Cazacu, S. M., Iovanescu, V. F., et al. (2023). Predicting mortality in patients with nonvariceal upper gastrointestinal bleeding using machine-learning. *Front. Med.* 10, 1134835. doi:10.3389/fmed.2023.1134835
- World Health Organization (2022). Elimination of hepatitis by 2030. Available at: [https://www.who.int/health-topics/hepatitis/elimination-of-hepatitis-by-2030#tab=tab\\_1](https://www.who.int/health-topics/hepatitis/elimination-of-hepatitis-by-2030#tab=tab_1) (Accessed June, 2023).



## OPEN ACCESS

## EDITED BY

Adina Turcu-Stolica,  
University of Medicine and Pharmacy of  
Craiova, Romania

## REVIEWED BY

Mari Endo,  
Kitasato University, Japan  
Celine Deraison,  
Institut National de la Santé et de la  
Recherche Médicale (INSERM), France

## \*CORRESPONDENCE

Meng Wang,  
5545840@qq.com  
Qiongyuan Hu,  
qiongyuan\_hu@foxmail.com  
Feng Wang,  
fengwang36@163.com

<sup>†</sup>These authors have contributed equally  
to this work and share first authorship

## SPECIALTY SECTION

This article was submitted to  
Gastrointestinal and Hepatic  
Pharmacology,  
a section of the journal  
Frontiers in Pharmacology

RECEIVED 27 April 2022

ACCEPTED 29 June 2022

PUBLISHED 03 August 2022

## CITATION

Sui C, Tao L, Bai C, Shao L, Miao J,  
Chen K, Wang M, Hu Q and Wang F  
(2022), Molecular and cellular  
mechanisms underlying postoperative  
paralytic ileus by various immune  
cell types.  
*Front. Pharmacol.* 13:929901.  
doi: 10.3389/fphar.2022.929901

## COPYRIGHT

© 2022 Sui, Tao, Bai, Shao, Miao, Chen,  
Wang, Hu and Wang. This is an open-  
access article distributed under the  
terms of the [Creative Commons  
Attribution License \(CC BY\)](#). The use,  
distribution or reproduction in other  
forums is permitted, provided the  
original author(s) and the copyright  
owner(s) are credited and that the  
original publication in this journal is  
cited, in accordance with accepted  
academic practice. No use, distribution  
or reproduction is permitted which does  
not comply with these terms.

# Molecular and cellular mechanisms underlying postoperative paralytic ileus by various immune cell types

Chao Sui<sup>1,2†</sup>, Liang Tao<sup>1†</sup>, Chunhua Bai<sup>1,2†</sup>, Lihua Shao<sup>1</sup>, Ji Miao<sup>1</sup>,  
Kai Chen<sup>1,2</sup>, Meng Wang<sup>1\*</sup>, Qiongyuan Hu<sup>1,2\*</sup> and Feng Wang<sup>1\*</sup>

<sup>1</sup>Department of Gastrointestinal Surgery, Nanjing Drum Tower Hospital, The Affiliated Hospital of  
Nanjing University Medical School, Nanjing, China, <sup>2</sup>Medical School of Nanjing University, Nanjing,  
China

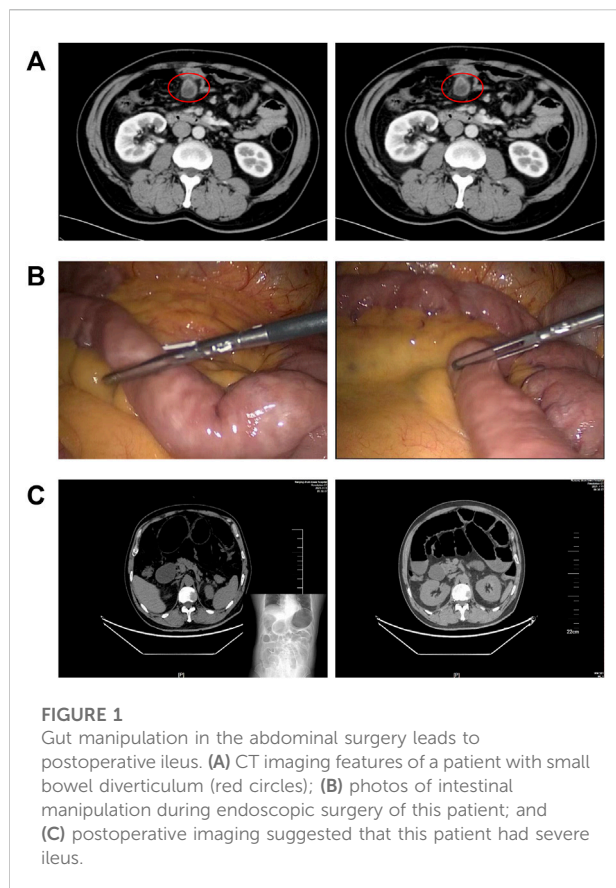
Postoperative ileus (POI) is a well-known complication following gut manipulation or surgical trauma, leading to an impaired gut motility and prolonged postoperative recovery time. Few current therapeutic strategies can prevent POI, and this disorder remains to be a major clinical challenge for patients undergoing surgery. Comprehensive understanding of cellular and molecular mechanisms related to the pathogenesis of POI stimulates the discovery of more promising targets for treatment. POI is closely associated with a series of inflammatory events within the bowel wall, and as key components of inflammatory mechanisms, different types of immune cells, including macrophages, dendritic cells, and T lymphocytes, play significant roles during the development of POI. A variety of immune cells are recruited into the manipulation sites after surgery, contributing to early inflammatory events or impaired gut motility. Our review intends to summarize the specific relationship between different immune cells and POI, mainly focusing on the relevant mechanisms underlying this disorder.

## KEYWORDS

postoperative ileus, inflammatory response, immune cell, macrophage, neutrophil, mast cell

## Introduction

Postoperative ileus (POI), characterized by a transient cessation of gastrointestinal (GI) function, is a common complication following general surgery or gut manipulation (Behm and Stollman, 2003; Hedrick et al., 2018; Thomas, 2019). This clinical dilemma has been a considerable burden on both inpatients and medical resources because of prolonged hospitalization time and increased expenses (Ramirez et al., 2013; Bragg et al., 2015; Wolthuis et al., 2016). Figure 1 presents us the imaging features of a patient with severe POI. Intraoperative intestinal manipulation directly led to the generation of POI, which subsequently resulted in poor prognosis.



Currently, POI is considered to be mainly related to sympathetic neural reflexes, activation of gut opioid receptors and inflammatory reaction, which eventually lead to symptoms such as vomiting, abdominal distension, and delay of defecation in patients (Vather et al., 2013; Vather et al., 2014; Wattoo et al., 2021). Recent evidence suggested that different types of immune cells play a vital role in the genesis of POI (Wattoo et al., 2021), and studies based on it are trying to find a novel potential target for treatment (Mazzotta et al., 2020). However, the relationship between immune cells and POI lacks further investigation and systemic summary. This review intends to provide a general understanding of the mechanisms under POI. It draws together information on effects of various immune cells on paralytic ileus, covering monocytes, macrophages, neutrophils, dendritic cells, mast cells, and T lymphocytes. Other important contributors are also briefly summarized in our review, with emphasis on molecular and cellular mechanisms.

## Mechanisms under postoperative ileus

Several studies have focused on the pathophysiological process of POI in the past few years. Neurogenic as well as inflammatory

mechanisms are considered to be mainly involved in the pathogenesis processes of this disorder (Wehner et al., 2012). It is now widely accepted that a neurogenic component plays a significant role in the early phase of postoperative impairment of gut motility (Lubbers et al., 2010). Activation of sympathetic pathways in response to surgical trauma or gut manipulation is verified to mediate a widespread inhibition of GI function, mostly through suppression of enteric neural reflex pathways (Stakenborg et al., 2017a).

The second phase of ileus is related to an immunological and inflammatory response that consequently leads to a prolonged duration of POI (Venara et al., 2016). Previous evidence in both animal models and humans showed increased leukocyte infiltration after intestinal handling, which begins 3–4 h after surgery and lasts for several days (Kalf et al., 1999; Kalf et al., 2003). This suggests that although early neurogenic mechanism triggers an acute reduction in gut motor activity, the following sustained gut inflammation eventually leads to delayed postoperative dysmotility in the late phase of POI. In addition, another critical factor involved in POI is the use of analgesics, primarily of opioids after surgery. These pain-relieving drugs are able to bind to  $\mu$ -opioid receptors in the GI tract, adding to the potential possibilities of POI.

Current approaches to prevent or treat ileus include non-pharmacological interventions and pharmacological treatments (Wattoo et al., 2021), most of which have poor therapeutic effects and lacks reliable clinical evidence (Delaney et al., 2010; Sammut et al., 2021). Hence, new strategies that target the intimate mechanisms of POI are required to complement current clinical practice and solve existing medical dilemmas (Buscail and Deraison, 2022). Recent studies have focused on the intestinal inflammation during POI, and as key components of inflammatory response, the populations of immune cells including monocytes, macrophages, neutrophils, dendritic cells, mast cells, and T lymphocytes, are proved to be closely linked to the onset of POI. Figure 2 briefly illustrates that different types of immune cells play crucial roles during POI. It is generally accepted that intestinal handling triggers the activation of resident immune cells like macrophages and neutrophils, subsequently leading to the recruitment of more immune cells. On the one hand, activation of immune cells can interact with enteric nervous system (ENS) and transmit stimulation to the spinal cord and in turn increase sympathetic output, which further inhibits myenteric neurons. Meanwhile, they trigger a serious of inflammatory events, subsequently aggravating GI dysfunction. Next, we will mainly summarize and discuss the specific roles of different immune cells in POI and relevant mechanisms implicated in the pathogenesis of this disorder.

## Immune cells in postoperative ileus

### Monocytes and macrophages

Macrophages in the GI tract constitute the major population of macrophages in the body (Mowat and Agace, 2014; Wang

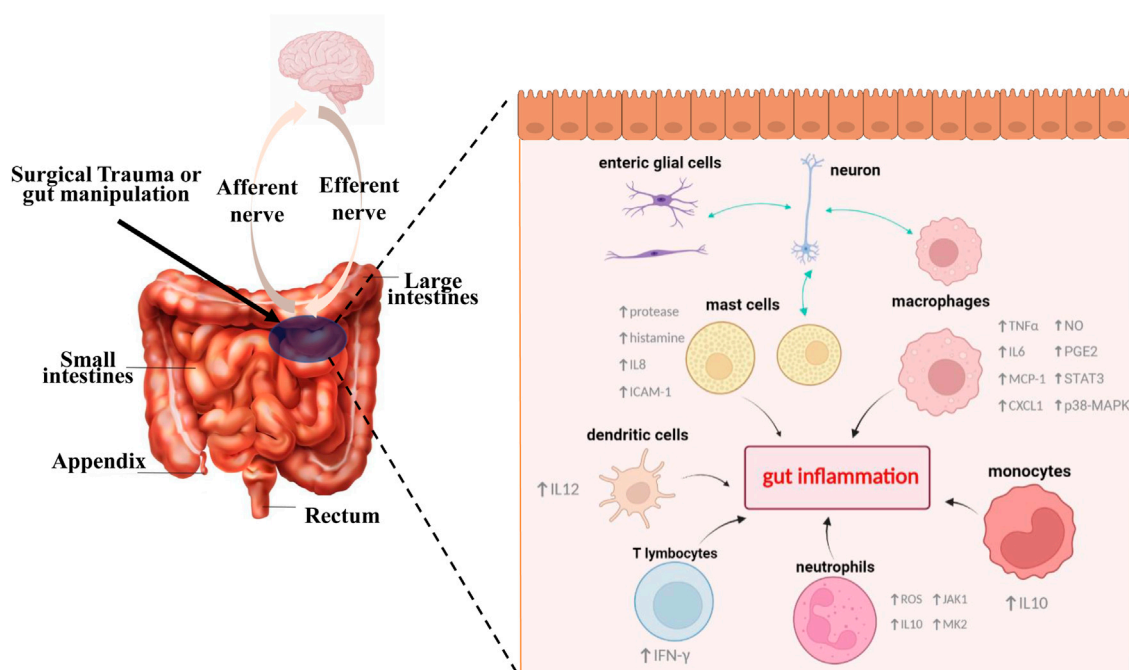


**FIGURE 2**

Different types of immune cells play key roles in the pathophysiologic process of POI. Surgical trauma or gut manipulation triggers the activation of different types of immune cells. In the initial stage, activated cells like mast cells and enteric glial cells can interact with enteric neurons and subsequently transmit stimulation to our brain. Meanwhile, further activation and recruitment of different immune cells such as monocytes, macrophages, neutrophils, dendritic cells, mast cells, and T lymphocytes lead to a series of gut inflammatory cascade events, accompanied by production of varied inflammatory cytokines, activation of transcription factors, and release of other active substances, all of which eventually lead to the generation and aggravation of POI.

et al., 2019). Compared with conventional macrophages, intestinal macrophages have particular features in terms of phenotypic characterization, inflammatory response, and cytokine generation (Yip et al., 2021). It is acknowledged that intestinal macrophages are essential in mediating intestinal immunity and maintaining GI homeostasis (Bain and Mowat, 2014; Bain and Schridde, 2018; Muller et al., 2020). For paralytic ileus, research studies based on reliable animal models suggested that intestinal macrophages, primarily muscularis macrophages, play key roles in the inhibition of gut motility (De Schepper et al., 2018). These resident macrophages in the muscularis layer are activated after gut manipulation or surgical trauma, promoting the development of POI through a series of inflammatory cascade events (Grainger et al., 2017; Mazzotta et al., 2020). TNF $\alpha$  (Matsumoto et al., 2018), IL6 (Wehner et al., 2005), MCP-1 (Türler et al., 2002), CXCL1 (Docsa et al., 2020), and other proinflammatory cytokines or chemokines released from muscularis macrophages contribute to the recruitment of circulating leukocytes and suppress GI function by influencing intestinal muscles and nerves (Wehner et al., 2007; De Schepper et al., 2018). The production of transcription factors such as STAT3 (De Jonge et al., 2005) and p38-MAPK (Wehner et al., 2009) are also upregulated in macrophages during inflammation

and are proved to be associated with POI. Moreover, muscularis macrophages induce the formation of active substances like NO, which inhibit smooth muscle *via* the activation of guanylyl cyclase (Shah et al., 2004; Francis et al., 2010). In addition, activation of macrophages results in the release of prostaglandin E2 by transient receptor potential vanilloid 4 (TRPV4) channels, which further triggers intestinal contraction (Luo et al., 2018). Taken together, muscularis macrophages take part in various inflammatory events that lead to POI, and relevant channels and pathways could be potential targets for treatment.

In contrast to resident muscularis macrophages, the infiltrated macrophages could play protective roles in POI. Farro et al. demonstrated that a population of macrophages, which was exogenously migrated and monocyte-derived, could resolve inflammation and restore intestinal motility in POI, suggesting the functional heterogeneity of different cellular origins (Farro et al., 2017). In addition, Pohl et al. pointed out the different roles of macrophages between small and large intestine. They found that progression of POI in small intestine relied on the iNOS produced by both Ly6C macrophages and Ly6C monocytes, while in colon only the latter secreted iNOS, which indicated a potential role of the intestinal microbiota (Pohl et al., 2017).



Enteric neurons are key players in macrophage-mediated inflammatory response during POI. Vagus nerve stimulation after induction of ileus has been reported to reduce the expression of inflammation-related cytokines (Stakenborg et al., 2017b). This effect depends on  $\alpha 7$  nicotinic receptors ( $\alpha 7$ nAChR) on macrophages, leading to the regression of inflammation and amelioration of POI (Matteoli et al., 2014). In this context, many therapeutic modalities that utilize parallel mechanisms are widely studied (Cipriani et al., 2016; Yang N. N. et al., 2021). Similar to vagus nerve stimulation, the 5-HT<sub>4</sub> receptor (5HT<sub>4</sub>R) agonist accelerates the release of acetylcholine, which subsequently activates  $\alpha 7$ nAChR on muscularis macrophages and eventually reduces the duration of POI after GI surgery (Tsuchida et al., 2011; Stakenborg et al., 2019). Considering that this effect has been confirmed in clinical trials (Gong et al., 2016), 5HT<sub>4</sub>R agonist can act as an effective therapeutic alternative for patients with ileus. It should be noted that not all macrophages express  $\alpha 7$ nAChR, and Stakenborg et al. proved that  $\alpha 7$ nAChR expression was restricted to M2-like pathogenic phenotype. Through culturing macrophages with myenteric ganglia, they discovered that enteric neurons contributed to the induction of  $\alpha 7$ nAChR and the install of M2 phenotype (Stakenborg et al., 2019). Therefore, further studies are required to clarify the relevant phenomena and mechanisms.

Except for a population of resident macrophages, which can sustain their numbers by cell division instead of recruiting monocytes (Mischopoulou et al., 2022), most intestinal macrophages rely on the continuous replenishment of monocytes that extravasate into GI tissue in a CCR2-dependent way (Bain et al., 2013; Bain et al., 2014), and this is also the case during POI. These CCR2-dependent monocyte-derived macrophages help restore GI function after gut manipulation (Farro et al., 2017). CCR2 knock-out mice have fewer monocyte-derived macrophages in muscularis layer due to damaged monocyte migration, which further leads to increased neutrophil-mediated immunopathology. Farro et al. observed that *Ccr2*<sup>-/-</sup> mice show persistent muscular dysfunction and delayed GI transit recovery compared with WT mice upon intestinal handling (Farro et al., 2017), suggesting that targeting circulating monocytes and enhancing macrophage physiological repair functions could be possible strategies for reversing the symptoms of POI.

It should be specifically pointed out that IL10, mainly secreted from monocyte-derived macrophages during POI, plays an important role in the disease. Previous studies have shown that IL10 promotes polarization of macrophages and acts as a macrophage deactivator in the gut inflammation, contributing to faster recovery from ileus (Kontoyiannis et al., 2001; Stoffels et al., 2009; Makita et al., 2015). However, recent evidence suggests that IL10 leads to migration of other immune cells (also see the section on neutrophils below), which induces further inflammation (Stein et al., 2018). Indeed, Stein et al.

pointed out that IL10 secreted by monocyte-derived macrophages aggravated POI, instead of relieving this sort of disorder (Stein et al., 2018).

In conclusion, the current evidence has shown that macrophages activation is crucial in the pathogenesis of POI, and that focusing on underlying molecular and cellular mechanisms may be of great use for clinical treatment. However, further studies are needed so that the observations in animal models can translate into practical therapeutic options.

## Neutrophils

Neutrophils are an indispensable component of innate immune system and act as the first kind of immune cells accumulating in large numbers at sites of inflammation (Sadik et al., 2011; Amulic et al., 2012). Neutrophils are able to release massive amounts of reactive oxygen species (ROS), produce other toxic molecules, and induce neutrophil extracellular traps during their course of reaction (Chen et al., 2021). In addition to their essential functions throughout the body, neutrophils play unique roles in intestinal homeostasis (Fournier and Parkos, 2012) and result in various pathological changes of gut disease such as inflammatory bowel disease (Zhou et al., 2018; Dinallo et al., 2019), colorectal cancer (Yang et al., 2020), and intestinal ischemia-reperfusion injury (Wang et al., 2018). Recent studies have shown that neutrophils are strongly associated with POI. Increased neutrophil infiltration can be observed in intestinal manipulation-induced models of POI, causing the induction of inflammatory mediators (Tsuchida et al., 2011; Maehara et al., 2015). Neutrophils are associated with the recruitment and activation of immune cells in the gut *via* producing cytokines such as CXCL8, IL17, and IL10 (Ferretti et al., 2003; Mantovani et al., 2011). Meanwhile, cytokines and chemokines produced by other immune cells also regulate neutrophil infiltration during intestinal inflammation (Kucharzik et al., 2005).

As highlighted above, IL10 secreted from monocyte-derived macrophages aggravates POI. Recent evidence has proved that IL10 influences neutrophil migration to traumatized sites by regulating the expression of neutrophil chemokines (Stein et al., 2018). Of note, IL-10 deficiency reduces the neutrophil extravasation into the bowel wall, and consequently ameliorates paralytic ileus. This suggests that neutrophils have direct correlation with inflammatory response and other pathological processes in POI. Interestingly, Farro et al. demonstrated that knockout of CCR2 could increase neutrophil-mediated immunopathology and prolong the clinical outcome of POI (Farro et al., 2017). These findings indicate the close relationship between neutrophils and macrophages in POI. They may have complex associations in intestinal inflammation rather than a single synergistic effect.

Janus kinase 1 (JAK1) plays an important role during inflammation and is regarded as a candidate signal pathway involved in regulating inflammatory reactions in intestinal paralysis. Sun et al. found marked activation of JAK1 after gut manipulation, accompanied by increased myeloperoxidase-stained neutrophils (Sun et al., 2019). JAK1 inhibition lowered the infiltration of neutrophils and expression of proinflammatory mediators. In addition, mitogen-activated protein kinase-activated protein kinase 2 (MK2), a downstream molecule of p38, plays an essential role in inflammation (Gorska et al., 2007). In POI, MK2 activation is upregulated, and MK2 inhibitor significantly reduces the number of neutrophils as well as the expression of proinflammatory gene (Liu et al., 2013). Moreover, the selective inhibition of p38 mitogen-activated protein kinase (MAPK) pathway leads to reduction of neutrophil infiltration after gut manipulation (Wehner et al., 2009). Taken together, signal pathways activated during POI are related to neutrophil-mediated inflammation, and from a therapeutic point of view, targeting relevant pathways may have enormous potentialities to prevent POI *via* reducing neutrophil infiltration.

## Dendritic cells

Dendritic cells (DCs) are professional antigen-presenting cells that efficiently sample the environment for foreign antigens and present them to immune system (Chang et al., 2014; Schiavi et al., 2015). In the intestine, dendritic cells are widely distributed within the lamina propria, and they are one of the immune cells central to the initiation of protective proinflammatory as well as tolerogenic immune response, which are pivotal in the maintenance of intestinal homeostasis (Persson et al., 2010; Persson et al., 2013; Worbs et al., 2017). For a long time, studies have focused on the relationship between DCs and intestinal diseases including inflammatory bowel disease and intestinal neoplasms (Bernardo et al., 2018; Yang Z. J. et al., 2021). Considering the inflammatory reaction and immune response in POI, it could be logically inferred that DCs play an irreplaceable role in the pathogenesis and development of this disease.

In fact, the intestinal DCs were observed to be activated in the mouse model of POI, with their numbers increased by 30-fold compared with sham-operated groups, which directly demonstrated the connection between ileus and this kind of immune cells (Engel et al., 2010). DCs secrete a great deal of costimulatory molecules like interleukin-12 (IL12) after surgical trauma, leading to partial activation of T<sub>H</sub>1-memory cells and thus stimulate intestinal macrophages to have more profound impacts on POI (Engel et al., 2010; Koscielny and Kalff, 2011). CCR7, expressed on activated DCs and T cells, is significantly upregulated after gut manipulation, and CCR7<sup>-/-</sup> mice show improved intestinal muscle function in the case of surgical trauma (Koscielny et al., 2011). In addition, Pohl et al. (Pohl

et al., 2017) found that CD103<sup>+</sup>CD11b<sup>+</sup> DCs, a subset of intestinal DCs, triggered the disorder of gut motility, and that lacking such cells consequently reduced the inducible nitric oxide synthase produced by monocytes and macrophages, resulting in the amelioration of POI. As a result, human immune system plays a key role in POI, and as an important component of the immune system, dendritic cells are widely involved in the development of this disorder. Studies on various subpopulations of intestinal DCs provide us more possibilities to clearly understand their roles in POI, allowing them become a novel potential target for POI treatment.

## Mast cells

Previous evidence suggested that mast cells (MCs) are responsible for innate and adaptive immunity, neurogenic inflammation, impaired tissue function, and intestinal barrier dysfunction (Wouters et al., 2016; Traina, 2021), all of which are concerned with POI. The activation of MCs has been proved to be related to POI in both rodent models and clinical setting (De Winter et al., 2012; Berdún et al., 2015). IgE bound to the specific receptor on MCs, which triggered a series of biochemical events. Subsequently, MCs release preformed granule compounds such as cytokines, proteases, and histamine, followed by a proinflammatory response (Galli et al., 2020). MCs have bidirectional communication with nerve endings, making them able to regulate intestinal motility and organ pain (De Winter et al., 2012). In the initial phase, such interactions can be influenced by active substances secreted from MCs, which causes neurogenic inflammation and increased sensitivity. These effects on neurons eventually promote the disturbances of gut motility (Buscail and Deraison, 2022). Previous experiments on mouse models showed that gut manipulation led to mast cell degranulation and this process contributed to the development of leukocyte infiltration, implicating that MCs played a key role in the inflammatory cascade during POI (De Jonge et al., 2004). Moreover, release of mouse mast cell protease-1 (mMCP-1) in the peritoneal fluid was significantly increased after gut manipulation (Peters et al., 2015), further indicating that MCs are key players in POI. Snoek et al. used Kit<sup>W/W<sup>-v</sup></sup> and Kit<sup>W-sh/W-sh</sup> mice that carry different spontaneous mutations in the gene for *ckit* and genetically lack MCs to demonstrate that absence of MCs can reduce the manipulation-induced inflammatory infiltrate and ameliorate GI transit (Snoek et al., 2012). Furthermore, the inflammatory response to intestinal handling in mast cell-deficient mice could be restored through mast cell reconstitution. In addition, evidence has shown that MCs evoke bacterial translocation to mesenteric lymph nodes and are responsible for epithelial barrier dysfunction after intestinal surgery, all of which are proved to be associated with

an increased inflammatory response and delayed GI emptying, suggesting another role of MCs in the pathogenesis of POI (Snoek et al., 2012).

The relationship between MCs and POI has been also verified in clinic as well. A clinical pilot study demonstrated that the handling of intestine triggered mast cell activation and prolonged ileus in patients undergoing gynecological surgery (The et al., 2008). By quantifying mast cell activation and inflammation, the data showed that conventional abdominal hysterectomy resulted in the release of tryptase as well as an increased level of IL6 and IL8, whereas such phenomenon did not occur during minimal invasive surgery. On the other hand, intestinal manipulation-induced mast cell activation upregulated the expression of intercellular adhesion molecule-1 (ICAM-1) that is strongly associated with leucocyte recruitment (The et al., 2008). Hence, faster recovery after minimal invasive surgery may be partly owing to this, and more importantly, targeting MCs as a therapeutic approach for POI has reliable clinical proof of concept (De Giorgio and Barbara, 2008).

Mast cell stabilizers like ketotifen can reduce the release of mast cell mediators and weaken inflammation after abdominal surgery, subsequently leading to an improvement of gastric emptying (The et al., 2009; Rychter et al., 2015). In addition, evidence showed that early enteral nutrition ameliorated POI by stabilizing MCs with a cationic channel protein TRPA1 (Sun et al., 2020). Moreover, Kimura et al. found a new zinc chelator, IPZ-010, and they proved IPZ-010 caused an inhibition of inflammatory response in activated bone marrow-derived MCs, which promotes recovery of GI function after surgery (Kimura et al., 2020). Although some studies based on mouse models questioned the involvement of MCs in POI and opposed mast cell inhibitors as a therapeutic strategy for POI (Gomez-Pinilla et al., 2014), MCs are still regarded as key players in POI development considering the variation of species and current clinical evidence, and the prudent use of mast cell stabilizers could open up new perspectives for POI treatment. In addition, given the numerous differences between mucosal MCs and connective tissue MCs (Reber et al., 2015), investigations on the heterogeneity of mast cell subtypes may be valuable in POI.

## T lymphocytes

Adaptive immune system is crucial to the development of experimental POI, and as an essential cellular counterpart in this immune response, T lymphocyte is closely linked to the pathological process of this disorder. T lymphocytes are widely known to exist in human blood and lymphoid tissue, resident in the gut at the same time (Ma et al., 2019). They have long been observed interacting with gut microbiota to regulate intestinal homeostasis (De Oliveira et al., 2017; Caruso et al., 2020). So far, studies on T

lymphocytes, especially helper T cells, have given us a deeper insight into the molecular and cellular mechanisms involved in POI.

Gut manipulation retarded the transit of orally administered fluorescent dextran in mice, while CD4 knockout mice eliminated such delay and lightened the local inflammatory response, implicating that CD4<sup>+</sup> T helper cells are critical factors involved in POI (Engel et al., 2010). Nevertheless, this effect may be related to the type of T helper effector cells. As a subtype of CD4<sup>+</sup> T cells, T<sub>H</sub>1 cells can be induced mainly by IL-12, and subsequently secrete a variety of cytokines, thereby mediating the cellular immune response and participating in the inflammatory response. Koscielny et al. identified that surgical trauma and local inflammation trigger the release of IL-12, leading to production of large numbers of interferon- $\gamma$  (IFN- $\gamma$ ) by activated T<sub>H</sub>1-memory cells, which consequently enhances the inflammatory process underlying POI and causes GI hypomotility by promoting intestinal macrophages to secrete NO (Koscielny and Kalff, 2011). These findings present us a close connection between T-helper type 1 cell-mediated adaptive immune response and macrophage-mediated innate immune system during POI, assisting us to discover a fire-new way to reduce the duration of POI.

In addition, activated T<sub>H</sub>1 cells at surgical trauma sites can migrate to unmanipulated intestinal segments through the bloodstream, subsequently disseminating ileus over the entire intestinal tract (Engel et al., 2010). Immunosuppressive FTY720 or inhibition of IL-12 can block the T<sub>H</sub>1 cell exit to the portal vein blood and thus prevent POI. These findings provided further evidence that T<sub>H</sub>1 cells are major participants in POI and play irreplaceable roles in its progression.

Despite the well-known role of T<sub>H</sub>1 cells in POI, T<sub>H</sub>2 cells may have an ignorant effect on the disease progression. In fact, recent studies have proved that POI is related to an increase in both T<sub>H</sub>2 cytokines and T<sub>H</sub>2 cells, accompanied by an increased number of mast cells as well as upregulated IgE and histamine plasma levels. This T<sub>H</sub>2 response could be linked to the ROS-mediated activation of NF- $\kappa$ B and p38 MAPK signaling pathways (Lin et al., 2021). In summary, T lymphocyte-mediated immune response has been identified to be a crucial target in the pathological process of POI, but the characteristics of such immune response are not completely understood. Hence, further research is needed to help develop the comprehension of POI to a brand-new phase.

## Other important contributors

An emerging cellular target in the field of neurogastroenterology and GI disorders is the enteric glial

cell that constitutes a crucial part of the enteric nervous system and maintains intestinal homeostasis through interactions with resident immune cells and other cell types (Sharkey, 2015; Yoo and Mazmanian, 2017). Enteric glial cells play a pivotal role in normal gut motility, and disruption of the balance maintained by this cell population consequently leads to motility disorders and GI diseases (Gulbransen and Christofi, 2018; Seguela and Gulbransen, 2021). Notably, studies have revealed that both finger manipulation and high pneumoperitoneum pressure during intestinal surgery cause abnormal mechanical forces on the gut and its mesentery, activating enteric glial cells and converting them to a pathogenic state referred to as a reactive glial phenotype that directly contributes to POI (Mazzotta et al., 2020). Recently, Schneider et al. found that surgical trauma triggers ATP release which further induces a reactive glia phenotype known as “gliosis” (Schneider et al., 2021). The induction of enteric gliosis through ATP depends on the p38-MAPK signaling pathway, and this process subsequently leads to intestinal inflammation and impaired gut motility in POI. Furthermore, P2X2, a relevant ATP receptor, is demonstrated to be linked to ATP-induced enteric gliosis and inflammation. Therefore, blocking enteric glial P2X2 receptors could be a potential therapy in ameliorating POI.

Interstitial cells of Cajal (ICC) are proved to be another contributor to the genesis of POI. Known as intestinal pacemaker cells, ICCs play a significant role in regulating GI motility (Sanders et al., 2014). Kaji et al. demonstrated that the production and propagation of pacemaker potentials *via* ICCs were disrupted through a nitric oxide pathway, further resulting in GI dysmotility after intestinal manipulation (Kaji et al., 2018). This pathological change will be ameliorated as the intestinal inflammation subsides. Hence, it is reasonable to infer that nitric oxide synthase inhibitor may have therapeutic potentials for POI by suppressing the disruption of ICC networks. Moreover, studies have shown that acupuncture protects ICCs in rat models of POI, leading to amelioration of GI function (Deng et al., 2017; Deng et al., 2019). Of note, intestinal mesothelial cells in the abdominal cavity are also involved in the development of POI as the inflammatory response mediated by them is a significant mechanism in many clinical conditions including gut dysmotility (Mihara et al., 2017). Relevant anti-inflammatory pathways regulated by  $\alpha 7$ nAChR expressed on intestinal mesothelial cells may have a therapeutic potential through connectivity with enteric nerves. In addition, other intestinal components like microbiome contribute to POI as well, making POI a complex pathological process.

## Conclusion and future perspectives

POI is an unsolved clinical problem that demands further investigation to find a novel therapy. Recent studies have focused on the immunological and inflammatory response during POI, and comprehensive understanding of relevant cellular mechanisms provides a promising target for POI treatment. As key components of this process, populations of different immune cells are closely related to POI development. Strategies that target macrophages or MCs are already proven to be effective in clinical setting, but they still need further evidence. Our review provides a comprehensive understanding of different types of immune cells in the development of POI, with emphasis on molecular and cellular mechanisms. Although most of their roles have been elucidated in previous studies, the complex interactions between these players are still poorly understood. More promising and effective therapies are likely to evolve from a deep comprehension of relevant mechanisms underlying POI.

## Author contributions

FW, QH, and MW conceptualized and designed the study. CS wrote the original draft. LT, CB, LS, JM, and KC contributed to writing, modifying, and editing the article.

## Funding

This study was supported by the grants from the National Natural Science Foundation of China (82102294).

## Conflict of interest

The authors declare that the research was conducted in the absence of any commercial or financial relationships that could be construed as a potential conflict of interest.

## Publisher's note

All claims expressed in this article are solely those of the authors and do not necessarily represent those of their affiliated organizations, or those of the publisher, the editors, and the reviewers. Any product that may be evaluated in this article, or claim that may be made by its manufacturer, is not guaranteed or endorsed by the publisher.



## References

- Amulic, B., Cazalet, C., Hayes, G. L., Metzler, K. D., and Zychlinsky, A. (2012). Neutrophil function: From mechanisms to disease. *Annu. Rev. Immunol.* 30, 459–489. doi:10.1146/annurev-immunol-020711-074942
- Bain, C. C., Bravo-Blas, A., Scott, C. L., Perdiguero, E. G., Geissmann, F., Henri, S., et al. (2014). Constant replenishment from circulating monocytes maintains the macrophage pool in the intestine of adult mice. *Nat. Immunol.* 15, 929–937. doi:10.1038/ni.2967
- Bain, C. C., and Mowat, A. M. (2014). Macrophages in intestinal homeostasis and inflammation. *Immunol. Rev.* 260, 102–117. doi:10.1111/imr.12192
- Bain, C. C., and Schridde, A. (2018). Origin, differentiation, and function of intestinal macrophages. *Front. Immunol.* 9, 2733. doi:10.3389/fimmu.2018.02733
- Bain, C. C., Scott, C. L., Uronen-Hansson, H., Gudjonsson, S., Jansson, O., Grip, O., et al. (2013). Resident and pro-inflammatory macrophages in the colon represent alternative context-dependent fates of the same Ly6Chi monocyte precursors. *Mucosal Immunol.* 6, 498–510. doi:10.1038/mi.2012.89
- Behm, B., and Stollman, N. (2003). Postoperative ileus: Etiologies and interventions. *Clin. Gastroenterol. Hepatol.* 1, 71–80. doi:10.1053/cgh.2003.50012
- Berdún, S., Bombuy, E., Estrada, O., Mans, E., Rychter, J., Clavé, P., et al. (2015). Peritoneal mast cell degranulation and gastrointestinal recovery in patients undergoing colorectal surgery. *Neurogastroenterol. Motil.* 27, 764–774. doi:10.1111/nmo.12525
- Bernardo, D., Chaparro, M., and Gisbert, J. P. (2018). Human intestinal dendritic cells in inflammatory bowel diseases. *Mol. Nutr. Food Res.* 62, e1700931. doi:10.1002/mnfr.201700931
- Bragg, D., El-Sharkawy, A. M., Psaltis, E., Maxwell-Armstrong, C. A., and Lobo, D. N. (2015). Postoperative ileus: Recent developments in pathophysiology and management. *Clin. Nutr.* 34, 367–376. doi:10.1016/j.clnu.2015.01.016
- Buscail, E., and Deraison, C. (2022). Postoperative ileus: A pharmacological perspective. *Br. J. Pharmacol.* 179, 3283–3305. doi:10.1111/bph.15800
- Caruso, R., Lo, B. C., and Núñez, G. (2020). Host-microbiota interactions in inflammatory bowel disease. *Nat. Rev. Immunol.* 20, 411–426. doi:10.1038/s41577-019-0268-7
- Chang, S. Y., Ko, H. J., and Kweon, M. N. (2014). Mucosal dendritic cells shape mucosal immunity. *Exp. Mol. Med.* 46, e84. doi:10.1038/emmm.2014.16
- Chen, K., Shao, L. H., Wang, F., Shen, X. F., Xia, X. F., Kang, X., et al. (2021). Netting gut disease: Neutrophil extracellular trap in intestinal pathology. *Oxid. Med. Cell. Longev.* 2021, 5541222. doi:10.1155/2021/5541222
- Cipriani, G., Gibbons, S. J., Kashyap, P. C., and Farrugia, G. (2016). Intrinsic gastrointestinal macrophages: Their phenotype and role in gastrointestinal motility. *Cell. Mol. Gastroenterol. Hepatol.* 2, 120–130. doi:10.1016/j.jcmgh.2016.01.003
- De Giorgio, R., and Barbara, G. (2008). Evidence for mast cell involvement in human postoperative ileus: A novel link. *Gut* 57, 5–7. doi:10.1136/gut.2007.131870
- De Jonge, W. J., The, F. O., Van Der Coelen, D., Bennink, R. J., Reitsma, P. H., Van Deventer, S. J., et al. (2004). Mast cell degranulation during abdominal surgery initiates postoperative ileus in mice. *Gastroenterology* 127, 535–545. doi:10.1053/j.gastro.2004.04.017
- De Jonge, W. J., Van Der Zanden, E. P., The, F. O., Bijlsma, M. F., Van Westerloo, D. J., Bennink, R. J., et al. (2005). Stimulation of the vagus nerve attenuates macrophage activation by activating the Jak2-STAT3 signaling pathway. *Nat. Immunol.* 6, 844–851. doi:10.1038/ni1229
- De Oliveira, G. L. V., Leite, A. Z., Higuchi, B. S., Gonzaga, M. I., and Mariano, V. S. (2017). Intestinal dysbiosis and probiotic applications in autoimmune diseases. *Immunology* 152, 1–12. doi:10.1111/imm.12765
- De Schepper, S., Stakenborg, N., Matteoli, G., Verheijden, S., and Boeckstaens, G. E. (2018). Muscularis macrophages: Key players in intestinal homeostasis and disease. *Cell. Immunol.* 330, 142–150. doi:10.1016/j.cellimm.2017.12.009
- De Winter, B. Y., Van Den Wijngaard, R. M., and De Jonge, W. J. (2012). Intestinal mast cells in gut inflammation and motility disturbances. *Biochim. Biophys. Acta* 1822, 66–73. doi:10.1016/j.bbdis.2011.03.016
- Delaney, C. P., Marcello, P. W., Sonoda, T., Wise, P., Bauer, J., Techner, L., et al. (2010). Gastrointestinal recovery after laparoscopic colectomy: Results of a prospective, observational, multicenter study. *Surg. Endosc.* 24, 653–661. doi:10.1007/s00464-009-0652-7
- Deng, J. J., Lai, M. Y., Tan, X., and Yuan, Q. (2019). Acupuncture protects the interstitial cells of Cajal by regulating miR-222 in a rat model of post-operative ileus. *Acupunct. Med.* 37, 125–132. doi:10.1177/0964528419829755
- Deng, J., Yang, S., Yuan, Q., Chen, Y., Li, D., Sun, H., et al. (2017). Acupuncture ameliorates postoperative ileus via IL-6-miR-19a-KIT Axis to protect interstitial cells of cajal. *Am. J. Chin. Med.* 45, 737–755. doi:10.1142/S0192415X17500392
- Dinallo, V., Marafini, I., Di Fusco, D., Laudisi, F., Franzè, E., Di Grazia, A., et al. (2019). Neutrophil extracellular traps sustain inflammatory signals in ulcerative colitis. *J. Crohns Colitis* 13, 772–784. doi:10.1093/ecco-jcc/jjy215
- Docsa, T., Bhattarai, D., Sipos, A., Wade, C. E., Cox, C. S., Jr., Uray, K., et al. (2020). CXCL1 is upregulated during the development of ileus resulting in decreased intestinal contractile activity. *Neurogastroenterol. Motil.* 32, e13757. doi:10.1111/nmo.13757
- Engel, D. R., Koscielny, A., Wehner, S., Maurer, J., Schiwon, M., Franken, L., et al. (2010). T helper type 1 memory cells disseminate postoperative ileus over the entire intestinal tract. *Nat. Med.* 16, 1407–1413. doi:10.1038/nm.2255
- Farro, G., Stakenborg, M., Gomez-Pinilla, P. J., Labeeuw, E., Govers, G., Di Giovangiulio, M., et al. (2017). CCR2-dependent monocyte-derived macrophages resolve inflammation and restore gut motility in postoperative ileus. *Gut* 66, 2098–2109. doi:10.1136/gutjnl-2016-313144
- Ferretti, S., Bonneau, O., Dubois, G. R., Jones, C. E., and Trifileff, A. (2003). IL-17, produced by lymphocytes and neutrophils, is necessary for lipopolysaccharide-induced airway neutrophilia: IL-15 as a possible trigger. *J. Immunol.* 170, 2106–2112. doi:10.4049/jimmunol.170.4.2106
- Fournier, B. M., and Parkos, C. A. (2012). The role of neutrophils during intestinal inflammation. *Mucosal Immunol.* 5, 354–366. doi:10.1038/mi.2012.24
- Francis, S. H., Busch, J. L., Corbin, J. D., and Sibley, D. (2010). cGMP-dependent protein kinases and cGMP phosphodiesterases in nitric oxide and cGMP action. *Pharmacol. Rev.* 62, 525–563. doi:10.1124/pr.110.002907
- Galli, S. J., Gaudenzio, N., and Tsai, M. (2020). Mast cells in inflammation and disease: Recent progress and ongoing concerns. *Annu. Rev. Immunol.* 38, 49–77. doi:10.1146/annurev-immunol-071719-094903
- Gomez-Pinilla, P. J., Farro, G., Di Giovangiulio, M., Stakenborg, N., Némethova, A., De Vries, A., et al. (2014). Mast cells play no role in the pathogenesis of postoperative ileus induced by intestinal manipulation. *PLoS One* 9, e85304. doi:10.1371/journal.pone.0085304
- Gong, J., Xie, Z., Zhang, T., Gu, L., Yao, W., Guo, Z., et al. (2016). Randomised clinical trial: Prucalopride, a colonic pro-motility agent, reduces the duration of post-operative ileus after elective gastrointestinal surgery. *Aliment. Pharmacol. Ther.* 43, 778–789. doi:10.1111/apt.13557
- Gorska, M. M., Liang, Q., Stafford, S. J., Goplen, N., Dharajiyi, N., Guo, L., et al. (2007). MK2 controls the level of negative feedback in the NF-kappaB pathway and is essential for vascular permeability and airway inflammation. *J. Exp. Med.* 204, 1637–1652. doi:10.1084/jem.20062621
- Grainger, J. R., Konkel, J. E., Zangerle-Murray, T., and Shaw, T. N. (2017). Macrophages in gastrointestinal homeostasis and inflammation. *Pflugers Arch.* 469, 527–539. doi:10.1007/s00424-017-1958-2
- Gulbransen, B. D., and Christofi, F. L. (2018). Are we close to targeting enteric glia in gastrointestinal diseases and motility disorders? *Gastroenterology* 155, 245–251. doi:10.1053/j.gastro.2018.06.050
- Hedrick, T. L., Mcevoy, M. D., Mythen, M. M. G., Bergamaschi, R., Gupta, R., Holubar, S. D., et al. (2018). American society for enhanced recovery and perioperative quality initiative joint consensus statement on postoperative gastrointestinal dysfunction within an enhanced recovery pathway for elective colorectal surgery. *Anesth. Analg.* 126, 1896–1907. doi:10.1213/ANE.0000000000002742
- Kaji, N., Nakayama, S., Horiguchi, K., Iino, S., Ozaki, H., Hori, M., et al. (2018). Disruption of the pacemaker activity of interstitial cells of Cajal via nitric oxide contributes to postoperative ileus. *Neurogastroenterol. Motil.* 30, e13334. doi:10.1111/nmo.13334
- Kalff, J. C., Carlos, T. M., Schraut, W. H., Billiar, T. R., Simmons, R. L., Bauer, A. J., et al. (1999). Surgically induced leukocytic infiltrates within the rat intestinal muscularis mediate postoperative ileus. *Gastroenterology* 117, 378–387. doi:10.1053/gast.1999.0029900378
- Kalff, J. C., Türler, A., Schwarz, N. T., Schraut, W. H., Lee, K. K., Twardy, D. J., et al. (2003). Intra-abdominal activation of a local inflammatory response within the human muscularis externa during laparotomy. *Ann. Surg.* 237, 301–315. doi:10.1097/01.SLA.0000055742.79045.7E
- Kimura, H., Yoneya, Y., Mikawa, S., Kaji, N., Ito, H., Tsuchida, Y., et al. (2020). A new zinc chelator, IPZ-010 ameliorates postoperative ileus. *Biomed. Pharmacother.* 123, 109773. doi:10.1016/j.biopha.2019.109773
- Kontoyiannis, D., Kotlyarov, A., Carballo, E., Alexopoulou, L., Blackshear, P. J., Gaestel, M., et al. (2001). Interleukin-10 targets p38 MAPK to modulate ARE-dependent TNF mRNA translation and limit intestinal pathology. *Embo J.* 20, 3760–3770. doi:10.1093/emboj/20.14.3760



- Koscielny, A., Engel, D., Maurer, J., Hirner, A., Kurts, C., and Kalf, J. C. (2011). Impact of CCR7 on the gastrointestinal field effect. *Am. J. Physiol. Gastrointest. Liver Physiol.* 300, G665–G675. doi:10.1152/ajpgi.00224.2010
- Koscielny, A., and Kalf, J. C. (2011). T-helper cell type 1 memory cells and postoperative ileus in the entire gut. *Curr. Opin. Gastroenterol.* 27, 509–514. doi:10.1097/MOG.0b013e32834bb7d7
- Kucharzik, T., Hudson, J. T., 3rd, Lügering, A., Abbas, J. A., Bettini, M., Lake, J. G., et al. (2005). Acute induction of human IL-8 production by intestinal epithelium triggers neutrophil infiltration without mucosal injury. *Gut* 54, 1565–1572. doi:10.1136/gut.2004.061168
- Lin, S., Kühn, F., Schiergens, T. S., Zamyatnin, A. A., Jr., Isayev, O., Gasimov, E., et al. (2021). Experimental postoperative ileus: Is Th2 immune response involved? *Int. J. Med. Sci.* 18, 3014–3025. doi:10.7150/ijms.59354
- Liu, X., Wu, T., and Chi, P. (2013). Inhibition of MK2 shows promise for preventing postoperative ileus in mice. *J. Surg. Res.* 185, 102–112. doi:10.1016/j.jss.2013.05.028
- Lubbers, T., Buurman, W., and Luyer, M. (2010). Controlling postoperative ileus by vagal activation. *World J. Gastroenterol.* 16, 1683–1687. doi:10.3748/wjg.v16.i14.1683
- Luo, J., Qian, A., Oetjen, L. K., Yu, W., Yang, P., Feng, J., et al. (2018). TRPV4 channel signaling in macrophages promotes gastrointestinal motility via direct effects on smooth muscle cells. *Immunity* 49, 107–119. e4. doi:10.1016/j.immuni.2018.04.021
- Ma, H., Tao, W., and Zhu, S. (2019). T lymphocytes in the intestinal mucosa: Defense and tolerance. *Cell. Mol. Immunol.* 16, 216–224. doi:10.1038/s41423-019-0208-2
- Maehara, T., Matsumoto, K., Horiguchi, K., Kondo, M., Iino, S., Horie, S., et al. (2015). Therapeutic action of 5-HT3 receptor antagonists targeting peritoneal macrophages in post-operative ileus. *Br. J. Pharmacol.* 172, 1136–1147. doi:10.1111/bph.13006
- Makita, N., Hizukuri, Y., Yamashiro, K., Murakawa, M., and Hayashi, Y. (2015). IL-10 enhances the phenotype of M2 macrophages induced by IL-4 and confers the ability to increase eosinophil migration. *Int. Immunol.* 27, 131–141. doi:10.1093/intimm/ixu090
- Mantovani, A., Cassatella, M. A., Costantini, C., and Jaillon, S. (2011). Neutrophils in the activation and regulation of innate and adaptive immunity. *Nat. Rev. Immunol.* 11, 519–531. doi:10.1038/nri3024
- Matsumoto, K., Kawanaka, H., Hori, M., Kusamori, K., Utsumi, D., Tsukahara, T., et al. (2018). Role of transient receptor potential melastatin 2 in surgical inflammation and dysmotility in a mouse model of postoperative ileus. *Am. J. Physiol. Gastrointest. Liver Physiol.* 315, G104–G116. doi:10.1152/ajpgi.00305.2017
- Matteoli, G., Gomez-Pinilla, P. J., Nemethova, A., Di Giovangiulio, M., Cailotto, C., Van Bree, S. H., et al. (2014). A distinct vagal anti-inflammatory pathway modulates intestinal muscularis resident macrophages independent of the spleen. *Gut* 63, 938–948. doi:10.1136/gutjnl-2013-304676
- Mazzotta, E., Villalobos-Hernandez, E. C., Fiorda-Diaz, J., Harzman, A., and Christofi, F. L. (2020). Postoperative ileus and postoperative gastrointestinal tract dysfunction: Pathogenic mechanisms and novel treatment strategies beyond colorectal enhanced recovery after surgery protocols. *Front. Pharmacol.* 11, 583422. doi:10.3389/fphar.2020.583422
- Mihara, T., Otsubo, W., Horiguchi, K., Mikawa, S., Kaji, N., Iino, S., et al. (2017). The anti-inflammatory pathway regulated via nicotinic acetylcholine receptors in rat intestinal mesothelial cells. *J. Vet. Med. Sci.* 79, 1795–1802. doi:10.1292/jvms.17-0304
- Mischopoulou, M., D'ambrosio, M., Bigagli, E., Luceri, C., Farrugia, G., Cipriani, G., et al. (2022). Role of macrophages and mast cells as key players in the maintenance of gastrointestinal smooth muscle homeostasis and disease. *Cell. Mol. Gastroenterol. Hepatol.* 13, 1849–1862. doi:10.1016/j.jcmgh.2022.02.017
- Mowat, A. M., and Agace, W. W. (2014). Regional specialization within the intestinal immune system. *Nat. Rev. Immunol.* 14, 667–685. doi:10.1038/nri3738
- Muller, P. A., Matheis, F., and Mucida, D. (2020). Gut macrophages: Key players in intestinal immunity and tissue physiology. *Curr. Opin. Immunol.* 62, 54–61. doi:10.1016/j.coi.2019.11.011
- Persson, E. K., Jaensson, E., and Agace, W. W. (2010). The diverse ontogeny and function of murine small intestinal dendritic cell/macrophage subsets. *Immunobiology* 215, 692–697. doi:10.1016/j.imbio.2010.05.013
- Persson, E. K., Scott, C. L., Mowat, A. M., and Agace, W. W. (2013). Dendritic cell subsets in the intestinal lamina propria: Ontogeny and function. *Eur. J. Immunol.* 43, 3098–3107. doi:10.1002/eji.201343740
- Peters, E. G., De Jonge, W. J., Smeets, B. J., and Luyer, M. D. (2015). The contribution of mast cells to postoperative ileus in experimental and clinical studies. *Neurogastroenterol. Motil.* 27, 743–749. doi:10.1111/nmo.12579
- Pohl, J. M., Gutweiler, S., Thiebes, S., Volke, J. K., Klein-Hitpass, L., Zwanziger, D., et al. (2017). Irf4-dependent CD103(+)CD11b(+) dendritic cells and the intestinal microbiome regulate monocyte and macrophage activation and intestinal peristalsis in postoperative ileus. *Gut* 66, 2110–2120. doi:10.1136/gutjnl-2017-313856
- Ramirez, J. A., McIntosh, A. G., Strehlow, R., Lawrence, V. A., Parekh, D. J., Svatek, R. S., et al. (2013). Definition, incidence, risk factors, and prevention of paralytic ileus following radical cystectomy: A systematic review. *Eur. Urol.* 64, 588–597. doi:10.1016/j.eururo.2012.11.051
- Reber, L. L., Sibillano, R., Mukai, K., and Galli, S. J. (2015). Potential effector and immunoregulatory functions of mast cells in mucosal immunity. *Mucosal Immunol.* 8, 444–463. doi:10.1038/mi.2014.131
- Rychter, J., Ortega, O., Berdun, S., Arenas, C., Lopez, I., Espin, F., et al. (2015). Mast cell degranulation inhibits motor patterns of human ileum and sigmoid colon *in vitro*: Relevance for postoperative ileus. *Neurogastroenterol. Motil.* 27, 1098–1109. doi:10.1111/nmo.12589
- Sadik, C. D., Kim, N. D., and Luster, A. D. (2011). Neutrophils cascading their way to inflammation. *Trends Immunol.* 32, 452–460. doi:10.1016/j.it.2011.06.008
- Sammur, R., Trapani, J., Deguar, J., and Ravasi, V. (2021). The effect of gum chewing on postoperative ileus in open colorectal surgery patients: A review. *J. Perioper. Pract.* 31, 132–139. doi:10.1177/1750458920917015
- Sanders, K. M., Ward, S. M., and Koh, S. D. (2014). Interstitial cells: Regulators of smooth muscle function. *Physiol. Rev.* 94, 859–907. doi:10.1152/physrev.00037.2013
- Schiavi, E., Smolinska, S., and O'mahony, L. (2015). Intestinal dendritic cells. *Curr. Opin. Gastroenterol.* 31, 98–103. doi:10.1097/MOG.0000000000000155
- Schneider, R., Leven, P., Glowka, T., Kuzmanov, I., Lysson, M., Schneiker, B., et al. (2021). A novel P2X2-dependent purinergic mechanism of enteric gliosis in intestinal inflammation. *EMBO Mol. Med.* 13, e12724. doi:10.15252/emmm.202012724
- Seguella, L., and Gulbransen, B. D. (2021). Enteric glial biology, intercellular signalling and roles in gastrointestinal disease. *Nat. Rev. Gastroenterol. Hepatol.* 18, 571–587. doi:10.1038/s41575-021-00423-7
- Shah, V., Lyford, G., Gores, G., and Farrugia, G. (2004). Nitric oxide in gastrointestinal health and disease. *Gastroenterology* 126, 903–913. doi:10.1053/j.gastro.2003.11.046
- Sharkey, K. A. (2015). Emerging roles for enteric glia in gastrointestinal disorders. *J. Clin. Invest.* 125, 918–925. doi:10.1172/JCI76303
- Snoek, S. A., Dhawan, S., Van Bree, S. H., Cailotto, C., Van Diest, S. A., Duarte, J. M., et al. (2012). Mast cells trigger epithelial barrier dysfunction, bacterial translocation and postoperative ileus in a mouse model. *Neurogastroenterol. Motil.* 24, 172–184. e91. doi:10.1111/j.1365-2982.2011.01820.x
- Stakenborg, N., Gomez-Pinilla, P. J., and Boeckxstaens, G. E. (2017a). Postoperative ileus: Pathophysiology, current therapeutic approaches. *Handb. Exp. Pharmacol.* 239, 39–57. doi:10.1007/164\_2016\_108
- Stakenborg, N., Labeeuw, E., Gomez-Pinilla, P. J., De Schepper, S., Aerts, R., Govers, G., et al. (2019). Preoperative administration of the 5-HT4 receptor agonist prucalopride reduces intestinal inflammation and shortens postoperative ileus via cholinergic enteric neurons. *Gut* 68, 1406–1416. doi:10.1136/gutjnl-2018-317263
- Stakenborg, N., Wolthuis, A. M., Gomez-Pinilla, P. J., Farro, G., Di Giovangiulio, M., Bosmans, G., et al. (2017b). Abdominal vagus nerve stimulation as a new therapeutic approach to prevent postoperative ileus. *Neurogastroenterol. Motil.* 29, e13075. doi:10.1111/nmo.13075
- Stein, K., Lysson, M., Schumak, B., Vilz, T., Specht, S., Heesemann, J., et al. (2018). Leukocyte-derived interleukin-10 aggravates postoperative ileus. *Front. Immunol.* 9, 2599. doi:10.3389/fimmu.2018.02599
- Stoffels, B., Schmidt, J., Nakao, A., Nazir, A., Chanthaphavong, R. S., and Bauer, A. J. (2009). Role of interleukin 10 in murine postoperative ileus. *Gut* 58, 648–660. doi:10.1136/gut.2008.153288
- Sun, D. L., Qi, Y. X., Yang, T., Lin, Y. Y., Li, S. M., Li, Y. J., et al. (2020). Early oral nutrition improves postoperative ileus through the TRPA1/CCK1-R-mediated mast cell-nerve axis. *Ann. Transl. Med.* 8, 179. doi:10.21037/atm.2020.01.95
- Sun, Y., Shi, H., Hong, Z., and Chi, P. (2019). Inhibition of JAK1 mitigates postoperative ileus in mice. *Surgery* 166, 1048–1054. doi:10.1016/j.surg.2019.07.016
- The, F. O., Bennink, R. J., Ankum, W. M., Buist, M. R., Busch, O. R., Gouma, D. J., et al. (2008). Intestinal handling-induced mast cell activation and inflammation in human postoperative ileus. *Gut* 57, 33–40. doi:10.1136/gut.2007.120238
- The, F. O., Buist, M. R., Lei, A., Bennink, R. J., Hofland, J., Van Den Wijngaard, R. M., et al. (2009). The role of mast cell stabilization in treatment of postoperative ileus: A pilot study. *Am. J. Gastroenterol.* 104, 2257–2266. doi:10.1038/ajg.2009.268
- Thomas, H. (2019). Prucalopride before surgery alleviates postoperative ileus. *Nat. Rev. Gastroenterol. Hepatol.* 16, 76. doi:10.1038/s41575-019-0106-1

- Traina, G. (2021). The role of mast cells in the gut and brain. *J. Integr. Neurosci.* 20, 185–196. doi:10.31083/jjin.2021.01.313
- Tsuchida, Y., Hatao, F., Fujisawa, M., Murata, T., Kaminishi, M., Seto, Y., et al. (2011). Neuronal stimulation with 5-hydroxytryptamine 4 receptor induces anti-inflammatory actions via  $\alpha$ 7nACh receptors on muscularis macrophages associated with postoperative ileus. *Gut* 60, 638–647. doi:10.1136/gut.2010.227546
- Türler, A., Schwarz, N. T., Türler, E., Kalf, J. C., and Bauer, A. J. (2002). MCP-1 causes leukocyte recruitment and subsequently endotoxemic ileus in rat. *Am. J. Physiol. Gastrointest. Liver Physiol.* 282, G145–G155. doi:10.1152/ajpgi.00263.2001
- Vather, R., O'grady, G., Bissett, I. P., and Dinning, P. G. (2014). Postoperative ileus: Mechanisms and future directions for research. *Clin. Exp. Pharmacol. Physiol.* 41, 358–370. doi:10.1111/1440-1681.12220
- Vather, R., Trivedi, S., and Bissett, I. (2013). Defining postoperative ileus: Results of a systematic review and global survey. *J. Gastrointest. Surg.* 17, 962–972. doi:10.1007/s11605-013-2148-y
- Venara, A., Neunlist, M., Slim, K., Barbieux, J., Colas, P. A., Hamy, A., et al. (2016). Postoperative ileus: Pathophysiology, incidence, and prevention. *J. Visc. Surg.* 153, 439–446. doi:10.1016/j.jvisurg.2016.08.010
- Wang, S., Xie, T., Sun, S., Wang, K., Liu, B., Wu, X., et al. (2018). DNase-1 treatment exerts protective effects in a rat model of intestinal ischemia-reperfusion injury. *Sci. Rep.* 8, 17788. doi:10.1038/s41598-018-36198-2
- Wang, S., Ye, Q., Zeng, X., and Qiao, S. (2019). Functions of macrophages in the maintenance of intestinal homeostasis. *J. Immunol. Res.* 2019, 1512969. doi:10.1155/2019/1512969
- Wattchow, D., Heitmann, P., Smolilo, D., Spencer, N. J., Parker, D., Hibberd, T., et al. (2021). Postoperative ileus—An ongoing conundrum. *Neurogastroenterol. Motil.* 33, e14046. doi:10.1111/nmo.14046
- Wehner, S., Behrendt, F. F., Lyutenski, B. N., Lysson, M., Bauer, A. J., Hirner, A., et al. (2007). Inhibition of macrophage function prevents intestinal inflammation and postoperative ileus in rodents. *Gut* 56, 176–185. doi:10.1136/gut.2005.089615
- Wehner, S., Schwarz, N. T., Hundsdoerfer, R., Hierholzer, C., Tweardy, D. J., Billiar, T. R., et al. (2005). Induction of IL-6 within the rodent intestinal muscularis after intestinal surgical stress. *Surgery* 137, 436–446. doi:10.1016/j.surg.2004.11.003
- Wehner, S., Straesser, S., Vilz, T. O., Pantelis, D., Sielecki, T., De La Cruz, V. F., et al. (2009). Inhibition of p38 mitogen-activated protein kinase pathway as prophylaxis of postoperative ileus in mice. *Gastroenterology* 136, 619–629. doi:10.1053/j.gastro.2008.10.017
- Wehner, S., Vilz, T. O., Stoffels, B., and Kalf, J. C. (2012). Immune mediators of postoperative ileus. *Langenbecks Arch. Surg.* 397, 591–601. doi:10.1007/s00423-012-0915-y
- Wolthuis, A. M., Bislenghi, G., Fieuws, S., De Buck Van Overstraeten, A., Boeckxstaens, G., D'hoore, A., et al. (2016). Incidence of prolonged postoperative ileus after colorectal surgery: A systematic review and meta-analysis. *Colorectal Dis.* 18, O1–O9. doi:10.1111/codi.13210
- Worbs, T., Hammerschmidt, S. I., and Förster, R. (2017). Dendritic cell migration in health and disease. *Nat. Rev. Immunol.* 17, 30–48. doi:10.1038/nri.2016.116
- Wouters, M. M., Vicario, M., and Santos, J. (2016). The role of mast cells in functional GI disorders. *Gut* 65, 155–168. doi:10.1136/gutjnl-2015-309151
- Yang, L., Liu, L., Zhang, R., Hong, J., Wang, Y., Wang, J., et al. (2020). IL-8 mediates a positive loop connecting increased neutrophil extracellular traps (NETs) and colorectal cancer liver metastasis. *J. Cancer* 11, 4384–4396. doi:10.7150/jca.44215
- Yang, N. N., Yang, J. W., Ye, Y., Huang, J., Wang, L., Wang, Y., et al. (2021). Electroacupuncture ameliorates intestinal inflammation by activating  $\alpha$ 7nAChR-mediated JAK2/STAT3 signaling pathway in postoperative ileus. *Theranostics* 11, 4078–4089. doi:10.7150/thno.52574
- Yang, Z. J., Wang, B. Y., Wang, T. T., Wang, F. F., Guo, Y. X., Hua, R. X., et al. (2021). Functions of dendritic cells and its association with intestinal diseases. *Cells* 10, 583. doi:10.3390/cells10030583
- Yip, J. L. K., Balasuriya, G. K., Spencer, S. J., and Hill-Yardin, E. L. (2021). The role of intestinal macrophages in gastrointestinal homeostasis: Heterogeneity and implications in disease. *Cell. Mol. Gastroenterol. Hepatol.* 12, 1701–1718. doi:10.1016/j.jcmgh.2021.08.021
- Yoo, B. B., and Mazmanian, S. K. (2017). The enteric network: Interactions between the immune and nervous systems of the gut. *Immunity* 46, 910–926. doi:10.1016/j.immuni.2017.05.011
- Zhou, G., Yu, L., Fang, L., Yang, W., Yu, T., Miao, Y., et al. (2018). CD177(+) neutrophils as functionally activated neutrophils negatively regulate IBD. *Gut* 67, 1052–1063. doi:10.1136/gutjnl-2016-313535



## OPEN ACCESS

## EDITED BY

Adina Turcu-Stolica,  
University of Medicine and Pharmacy of  
Craiova, Romania

## REVIEWED BY

Ming ming Ni,  
Children's Hospital of Nanjing Medical  
University, China  
Mihaela-Simona Subtirelu,  
University of Medicine and Pharmacy of  
Craiova, Romania

## \*CORRESPONDENCE

Lieming Xu,  
xulieming@shutcm.edu.cn

<sup>†</sup>These authors have contributed equally  
to this work

## SPECIALTY SECTION

This article was submitted to  
Gastrointestinal and Hepatic  
Pharmacology,  
a section of the journal *Front.  
Pharmacol*

RECEIVED 08 May 2022

ACCEPTED 29 June 2022

PUBLISHED 04 August 2022

## CITATION

Jiang N, Zhang J, Ping J and Xu L (2022),  
Salvianolic acid B inhibits autophagy and  
activation of hepatic stellate cells  
induced by TGF- $\beta$ 1 by downregulating  
the MAPK pathway.  
*Front. Pharmacol.* 13:938856.  
doi: 10.3389/fphar.2022.938856

## COPYRIGHT

© 2022 Jiang, Zhang, Ping and Xu. This  
is an open-access article distributed  
under the terms of the [Creative  
Commons Attribution License \(CC BY\)](#).  
The use, distribution or reproduction in  
other forums is permitted, provided the  
original author(s) and the copyright  
owner(s) are credited and that the  
original publication in this journal is  
cited, in accordance with accepted  
academic practice. No use, distribution  
or reproduction is permitted which does  
not comply with these terms.

# Salvianolic acid B inhibits autophagy and activation of hepatic stellate cells induced by TGF- $\beta$ 1 by downregulating the MAPK pathway

Na Jiang<sup>1†</sup>, Jing Zhang<sup>1†</sup>, Jian Ping<sup>1,2</sup> and Lieming Xu<sup>1,2,3,4\*</sup>

<sup>1</sup>Shuguang Hospital Affiliated to Shanghai University of Traditional Chinese Medicine, Shanghai, China, <sup>2</sup>Key Laboratory of Liver and Kidney Diseases, Ministry of Education, Shanghai, China, <sup>3</sup>Institute of Liver Diseases, Shanghai University of TCM, Shanghai, China, <sup>4</sup>Shanghai Key Laboratory of Traditional Chinese Medicine, Shanghai, China

In liver fibrosis, transforming growth factor- $\beta$ 1 (TGF- $\beta$ 1) can stimulate autophagy and activation of hepatic stellate cells (HSCs). Autophagy, playing a crucial role in HSCs activation, is related to liver fibrosis. Increasing evidence have suggested that antifibrosis effects of salvianolic acid B (Sal B) and their mechanisms of action, however, remain unclear. The aim of the article is to understand the role of Sal B in HSCs autophagy in liver fibrosis. Herein, we demonstrated that inducing TGF- $\beta$ 1 led to dramatic increase in autophagosome formation and autophagic flux in JS1 and LX2, which was mediated through the ERK, JNK, and p38 MAPK cascades. TGF- $\beta$ 1 significantly increased the protein of autophagy and liver fibrosis, including LC3BII, ATG5,  $\alpha$ -SMA, and Col.I; Sal B inhibits JS1 autophagy and activation by inhibiting the formation of autophagosomes and autophagic flux. Sal B significantly decreased the LC3BII, ATG5,  $\alpha$ -SMA, and Col.I protein expressions; pretreatment with autophagy inhibitors, chloroquine (CQ) and 3-methyladenine (3-MA) or silencing ATG7 further increase these reductions. However, pretreatment with autophagy agonist, rapamycin (Rapa), or overexpressed ATG5 attenuated this decrease. To further assess the importance of this mechanism, the antibody chip was used to detect the change of phosphorylation protein expression of the MAPK signaling pathway after treating JS1 with Sal B. Eleven differentially expressed proteins were verified. Sal B inhibits activation and autophagy of JS1 induced by TGF- $\beta$ 1 through downregulating the ERK, p38, and JNK signaling pathways, as demonstrated by downregulating p-ERK, p-JNK, and p-p38 MAPK protein expressions. In conclusion, Sal B inhibits autophagy and activation induced by TGF- $\beta$ 1 of HSCs possibly by downregulating the MAPK pathway.

## KEYWORDS

salvianolic acid B, hepatic stellate cells, autophagy, TGF- $\beta$ 1, MAPK signaling pathway

## Introduction

The pathological basis of cirrhosis is hepatic fibrosis. The paradigm of HSCs activation remains the foundation for defining event in hepatic fibrosis (Friedman, 2010). Mechanisms of fibrosis have focused on HSCs, which become fibrogenic myofibroblasts during injury through ‘activation’ (Lee et al., 2015), secreting extracellular matrix protein (ECM) (Friedman, 2008) (Higashi et al., 2017). Hence, inactivation of HSCs can lead to enhancement of fibrolytic activity and could be a potential target of antifibrotic therapy (Jung and Yim, 2017). Yet, the continued discovery of novel pathways and mediators, including endoplasmic reticulum stress, oxidative stress, retinol and cholesterol metabolism, epigenetics, receptor-mediated signals, extracellular vesicle (Shuhei Nakamura, 2018), and autophagy, reveals the complexity of HSCs activation (Tsuchida and Friedman, 2017).

Autophagy is an evolutionally conserved cytoplasmic degradation system, in which varieties of materials are sequestered by a double-membrane structure, autophagosome, and delivered to the lysosomes for the degradation (Gao et al., 2020). Due to the wide varieties of targets, autophagic activity is essential for cellular homeostasis (Gao et al., 2020). Autophagy also plays an important role in energy and nutritional metabolism of the liver (Mizushima et al., 2008). The role of autophagy in liver disease depends on the cell type and the stage of the disease (Allaire et al., 2019). The crucial role of autophagy in protecting hepatocyte from death in response to stress induced liver injury, such as acetaminophen (APAP) overdose (Ni et al., 2012) (Li et al., 2019) (Yan et al., 2018) (Shan et al., 2019), liver injury mediated by death receptors (Amir et al., 2013) (Zhong et al., 2016), Wilson’s disease (Polishchuk et al., 2019), and targeting autophagy as a therapeutic strategy for  $\alpha$ 1-AT deficiency (Mukherjee et al., 2018). Autophagy not only regulates hepatocyte functions but also impacts on non-parenchymal cells such as endothelial cells, macrophages, and hepatic stellate cells (Allaire et al., 2019). A large number of studies demonstrate that the role of autophagy on HSCs activation is complex. Autophagy displays opposite functions depending on the cell type (Allaire et al., 2019). Many studies have shown that selective reduction of autophagy levels of fibrosis-related cells and tissues may be a target for the treatment of liver fibrosis. Activation of HSCs depends on autophagy because the autophagy-mediated degradation of lipid droplets stored in these cells provides energy supply and promotes fibrogenic cell functions (Weiskirchen and Tacke, 2019). Recently, one study showed TGF- $\beta$ 1 treatment increasing both autophagosomes and autolysosomes in LX2 cells, thereby elevating autophagic flux. Ursodeoxycholic acid alleviates experimental liver fibrosis involving inhibition of autophagy flux (Ye et al., 2020). At the same time, many studies have obtained the opposite conclusion. For instance, PDGF induced hepatic stellate cell autophagy inhibiting extracellular vesicle release to attenuate liver fibrosis (Shuhei Nakamura, 2018). Interestingly, we previously showed that TGF- $\beta$ 1 promoted autophagy when it activated HSCs by regulating the

MAPK pathway. Sal B has effects on antifibrotic (Liu et al., 2016) and antihepatic injuries (Lin et al., 2015) (Zhang et al., 2017). Our previous research studies have found that Sal B inhibits the ERK pathway *via* inhibiting phosphorylation of MEK and inhibits the p38 MAPK pathway *via* blocking phosphorylation of MKK3/6 and inhibiting expression of MEF2 in HSCs with or without TGF- $\beta$ 1 stimulation. But the role of Sal B on autophagy is unknown.

In the present study, we demonstrate that TGF- $\beta$ 1 can induce HSCs activation and relate to upregulating autophagy (Zhang et al., 2020a). Sal B can inhibit HSCs activation induced by TGF- $\beta$ 1 through increasing autophagic flux by downregulating the MAPK signaling pathway. Meanwhile, this mechanism participates in liver fibrosis progression.

## Material and methods

### Culture of hepatic stellate cells

JS1, the mouse immortalized stellate cell lines, and LX2, human hepatic stellate cell lines were cultured with Dulbecco’s modified Eagle medium (DMEM, GIBCO, United States) supplemented with 10% FBS, penicillin G (100U/mL, GIBCO, United States) and streptomycin (100  $\mu$ g/mL, GIBCO, United States) with 5% CO<sub>2</sub> at 37°C. TGF- $\beta$ 1 (recombination human TGF- $\beta$ 1, PeproTech, United States) was added to the media for different times, according to the design of different experiments.

Western blotting. Protein quantification was detected by Western blotting. The antibodies used were as follows: the rabbit antibodies were: Col. I (Abcam, #ab34710),  $\alpha$ -SMA (Abcam, #ab32575), Atg5 (CST, #12994), Atg7 (CST, #8558), Beclin1 (CST, #3495), LC3B (sigma, #L7543), JNK (CST, #9258), p-JNK (CST, #4671), ERK (CST, #4695), p-ERK (CST, #4370), p38 (CST, #8690), and p-p38 (CST, #4511). The secondary antibodies were horseradish peroxidase (HRP)-conjugated goat antirabbit (LI-COR, #926–68071) or donkey antimouse (LI-COR, #926–32212). ImageJ software was used for quantification. Data were expressed as relative quantification normalized to GAPDH expression and presented as fold change from unstimulated cells.

Reverse transcription-quantitative (RT-q) PCR: RT-qPCR was performed as previously described to determine the gene expression levels in the culture cells. The following primer pairs were used for the qPCR (Table 1).

### pGMLV-CMV-RFP-GFP-hLC3-Puro lentivirus (purchased from Genomeditech Co., Ltd.) infection of target cells.

The HSCs were seeded in 24-well plates ( $4 \times 10^3$  cell per well) to carry out the pre-infection experiment of the target cells. Before the experiment, different infection holes were set

TABLE T1 Primers used for qPCR analysis

Target	Forward primer	Revers primer
Mouse $\alpha$ -SMA	GGAGAAAATGACCCAGATTA	GAGGCGGATGTTCTCAATCT
Mouse Col.I	CCAGTGGCGGTTATGACTTC	GCTGCGGATGTTCTCAATCT
Mouse LC3B	AGCAATGGCTGTGTAAGACT	CGCTGGTAACATCCCTTTT
Mouse ATG5	CCCCAGCCAACAGATTGA	GCCTCCACTGAACCTGACTG
Mouse ATG7	TACGAGCGAGAAGGATTCAC	CTTGATGGAGCAGGGTAAGA
Mouse BECN1	GAGGGATGGAAGGG	GGGCTGTGGTAAGTA
Mouse GAPDH	AAATGGTGAAGGTCGGTGTG	AGGTCAATGAAGGGGTCGTT

up, according to different MOI, and the amount of lentivirus needed was calculated according to the MOI value and the number of cells. According to the MOI (MOI = 100) value measured by the pre-test, the virus was diluted to the required concentration by using a fresh and complete medium containing 5 g/ml polybrene. After 48 h of infection, each group were incubated with different drugs for corresponding time and then replaced with normal complete medium. Fluorescence changes were observed under a fluorescence inversion microscope and photographed.

Lentiviral autophagy-related gene7(Atg7) short hairpin RNA(shAtg7), which was kindly provided by Professor Mark J. Czaja (Albert Einstein College of Medicine, United States), was cloned into lentiviral vectors. Knockdown and autophagy inhibition was optimal at 5 days after transduction, which was the time point used for the experiments.

### M\_atg5 overexpression stable transgenic Strain (purchased from Genomeditech Co., Ltd.)

The primer sequence design was carried out first, and the primers were synthesized according to the designed sequence, then the target gene fragments were amplified and connected to the over-expression vectors after digestion through different restriction sites at both ends. The connecting products were transferred to the prepared bacterial competent cells, and the monoclonal colonies were sequenced, and the correct clones were compared. That is to say, the target gene was successfully constructed and expressed overexpression vector (PGMLV-6395). 293T tool cells were transfected with the transfected overexpression vectors. Western blot was used to verify the effect of overexpression. 293T cells were transfected with the constructed lentivirus vector and packaging mix. The viral solution was collected, concentrated by ultrafiltration, and then the cell titer was determined. JS1 was infected by lentivirus negative control and packaged ATG5 lentivirus. Overexpression of the target gene was detected by qPCR and Western blot (this stable strain is provided by Genomeditech Co., Ltd.).

## Statistical analysis

Results are representative of at least three independent experiments. All data are expressed as the mean  $\pm$  SD. Statistical analysis was performed using two-tailed Student's *t*-test between two groups or one-factor ANOVA with Student-Newman-Keuls among multiple groups using SPSS21.0 software. *p* value  $\leq 0.05$  was considered statistically significant.

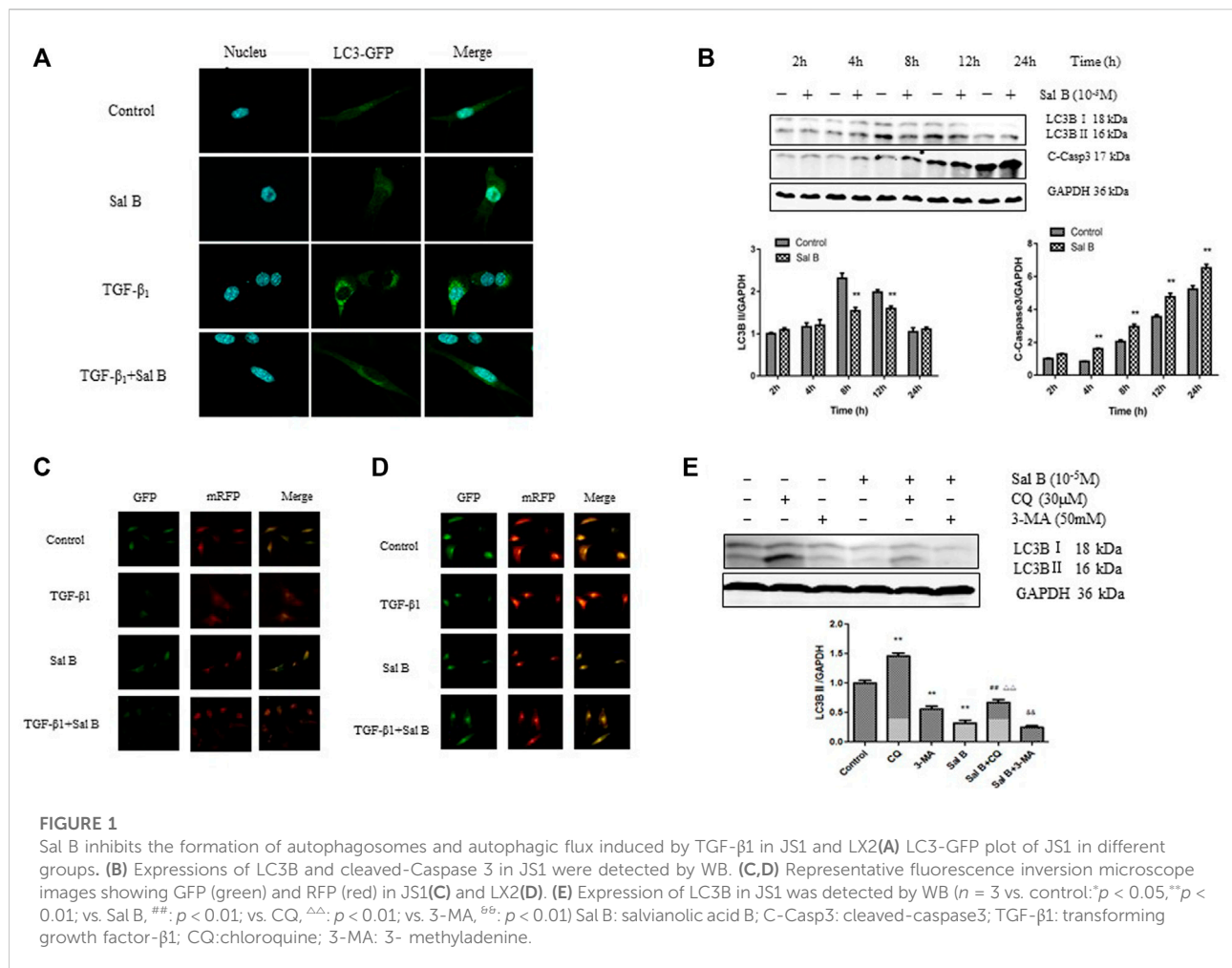
## Results

### Sal B inhibits autophagy of HSCs induced by transforming growth factor- $\beta$ 1

To determine the relationship between Sal B and autophagy activity in liver fibrosis, we detected the expression levels of autophagy-associated protein and autophagic flux in JS1 and (or) LX2. As shown in Figure 1A, JS1 were transfected with an exogenous GFP-LC3B plasmid and then treated with Sal B with or without TGF- $\beta$ 1. The basic autophagy level was lower, LC3-GFP was diffused in the cytoplasm, and only a small amount of green fluorescent dots were observed. GFP-LC3 puncta, which indicates the formation of autophagic vesicles, significantly decreased in the Sal B group compared with the TGF- $\beta$ 1 group in JS1. JS1 were exposed to Sal B at a concentration of  $10^{-5}$ M for 2, 4, 8, 12, and 24 h, and the expressions of the autophagy marker LC3B II and apoptosis marker C-Caspase 3 were assessed. As shown in Figure 1B, Sal B could inhibit the protein expression of LC3B II, especially at 8 and 12 h, but induce the expression of C-Caspase 3 at 4, 8, 12, and 24 h.

To investigate whether Sal B regulates autophagic flux in HSCs activation, pGMLV-CMV-RFP-GFP-hLC3-Puro lentivirus was used. We also confirmed that Sal B inhibited autophagic flux by transfecting JS1 and LX2 with the pGMLV-CMV-RFP-GFP-hLC3-Puro lentivirus. The GFP signal is sensitive to the acidic and/or proteolytic condition of the lysosome lumen, whereas RFP is more stable. Therefore, colocalization of both GFP and RFP fluorescence indicates a compartment that has not fused with a lysosome, such as





autophagosome. In contrast, an RFP signal without GFP corresponds to an autolysosome (Klionsky et al., 2021). Therefore, the cleaved GFP level can be used to monitor autophagic flux. As expected, incubation of JS1 with TGF- $\beta$ 1 resulted in a marked increase in free GFP, whereas pretreatment with Sal B attenuated the TGF- $\beta$ 1-induced increase of cleaved GFP, suggesting that Sal B inhibited the formation of autolysosome and blocked autophagic flux. The exciting thing is that we observed the same results in LX2 (Figures 1C,D).

We then co-treated JS1 with Sal B and autophagic inhibitors CQ and 3-MA, which blocked the upstream and downstream steps of autophagic flux. As shown in Figure 1E, the protein expression of LC3B II was significantly decreased by 3-MA or Sal B and increased by co-treatment of Sal B and CQ; its level decreased significantly compared with CQ, indicating that Sal B can inhibit the formation of autophagosomes and reduced the total amount of autophagosomes; co-treatment with Sal B and 3-MA: the expression of LC3B II further decreased compared with 3-MA, and it can be considered that the combination of Sal B with 3-MA further reduced the formation of autophagosomes

(Figure 1F). These data suggest that Sal B inhibits JS1 autophagy by inhibiting the formation of autophagosomes and autophagic flux.

## Sal B inhibits activation of JS1 through repressing autophagy of JS1 induced by TGF- $\beta$ 1

In order to investigate whether Sal B inhibit autophagy also contributed to HSCs activation, the following experiments were carried out. As shown in Figures 2A,B, Sal B and CQ markedly suppressed the protein expression of Col.I in JS1. Co-treated JS1 with Sal B and CQ further reduced Col.I accumulation. At the same time, we found that TGF- $\beta$ 1 and Rapa, a autophagic agonist, could significantly increase LC3BII, Col.I,  $\alpha$ -SMA, and Atg5 proteins expression, while these proteins were reversed by Sal B, suggesting a possible role of Sal B inhibiting the activation of JS1 by decreasing the formation of autophagosomes.

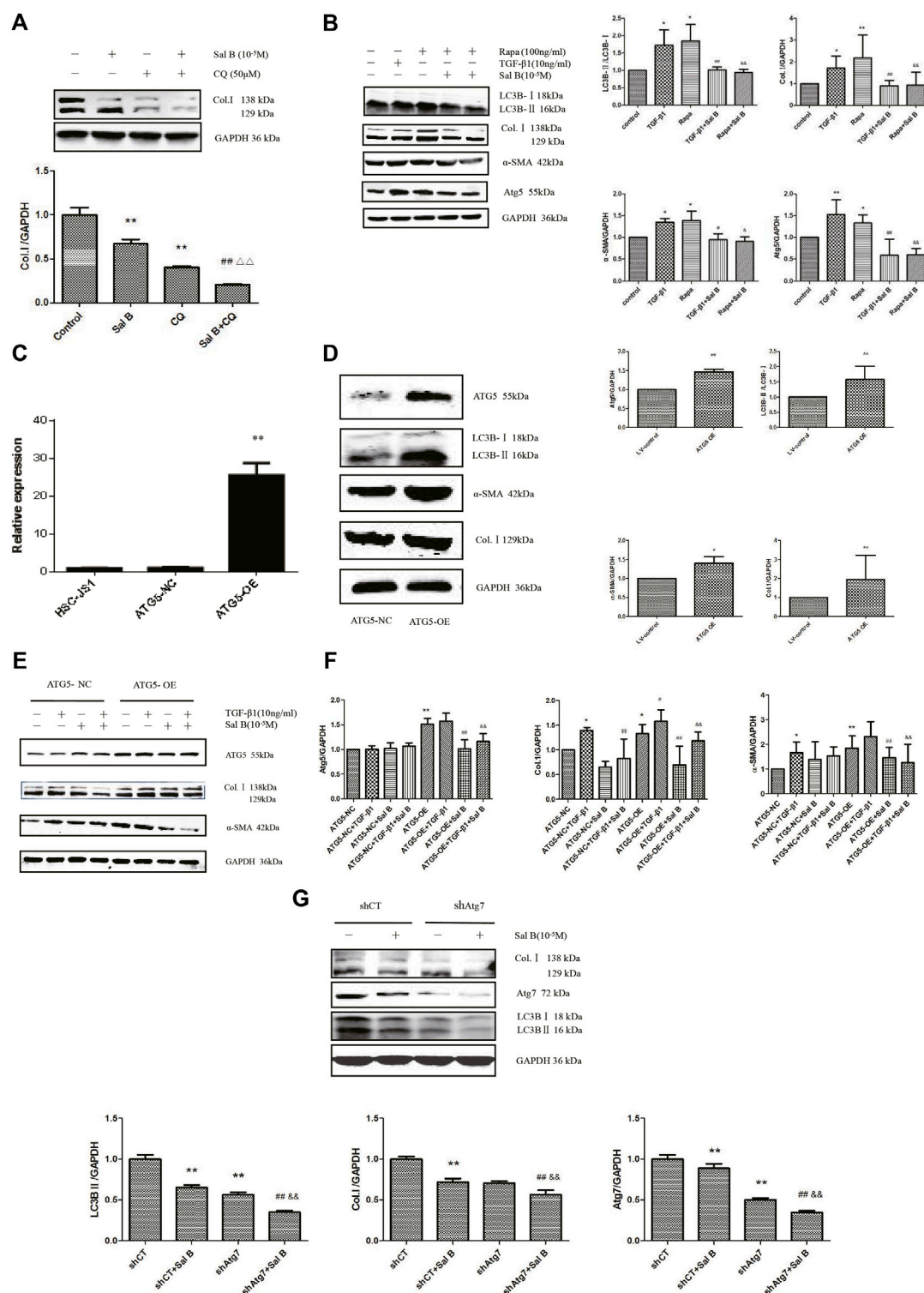


FIGURE 2

Sal B inhibits JS1 activation induced by TGF- $\beta$ 1 through autophagy. (A) Effect of Sal B and CQ, an autophagy inhibitors, on the expression of Col.I in JS1. (B) Effect of Sal B and Rapa, an autophagy agonist, on the expression of Col.I,  $\alpha$ -SMA, Atg5, and LC3B. (C) Expression of ATG5 mRNA was detected by qPCR. (D, F) Effect of ATG5-OE on the expression of Atg5, LC3B,  $\alpha$ -SMA, and Col.I. (E) Effect of Sal B on the expression of ATG5, Col.I, and  $\alpha$ -SMA in overexpression of ATG5 JS1. (G) Effect of Sal B on the expression of Col.I, Atg5, and LC3B in interference of ATG7 JS1.  $N = 3$  ( $N = 3$ , vs. control: \* $p < 0.05$ , \*\* $p < 0.01$ ; vs. Sal B, ###:  $p < 0.01$ ; vs. CQ,  $\Delta\Delta$ :  $p < 0.01$ ; vs. 3-MA,  $\Delta\Delta$ :  $p < 0.01$ ; vs. ATG5-NC, \*:  $p < 0.05$ , \*\*:  $p < 0.01$  (F) vs. ATG5-NC, \*:  $p < 0.05$ , \*\*:  $p < 0.01$ ; vs. ATG5-OE, #:  $p < 0.05$ , \*\*:  $p < 0.01$ ; vs. ATG5-NC + TGF- $\beta$ 1, \*:  $p < 0.05$ , \*\*:  $p < 0.01$ ; vs. ATG5-OE + TGF- $\beta$ 1, #:  $p < 0.05$ , \*\*:  $p < 0.01$ . G vs. shCT, \*\*:  $p < 0.01$ ; vs. shAtg7, ###:  $p < 0.01$ ; vs. shCT + Sal B,  $\Delta\Delta$ :  $p < 0.01$ ). Col.I: collagen type I; Rapa: rapamycin,  $\alpha$ -SMA:  $\alpha$ -smooth muscle actin, LC3B: microtubule-associated protein 1 light chain 3B, ATG5: autophagy-related genes; ATG5-OE: overexpression of ATG5; ATG5-NC: empty vector stable cell lines. shCT: control; shAtg7: small hairpin RNA.

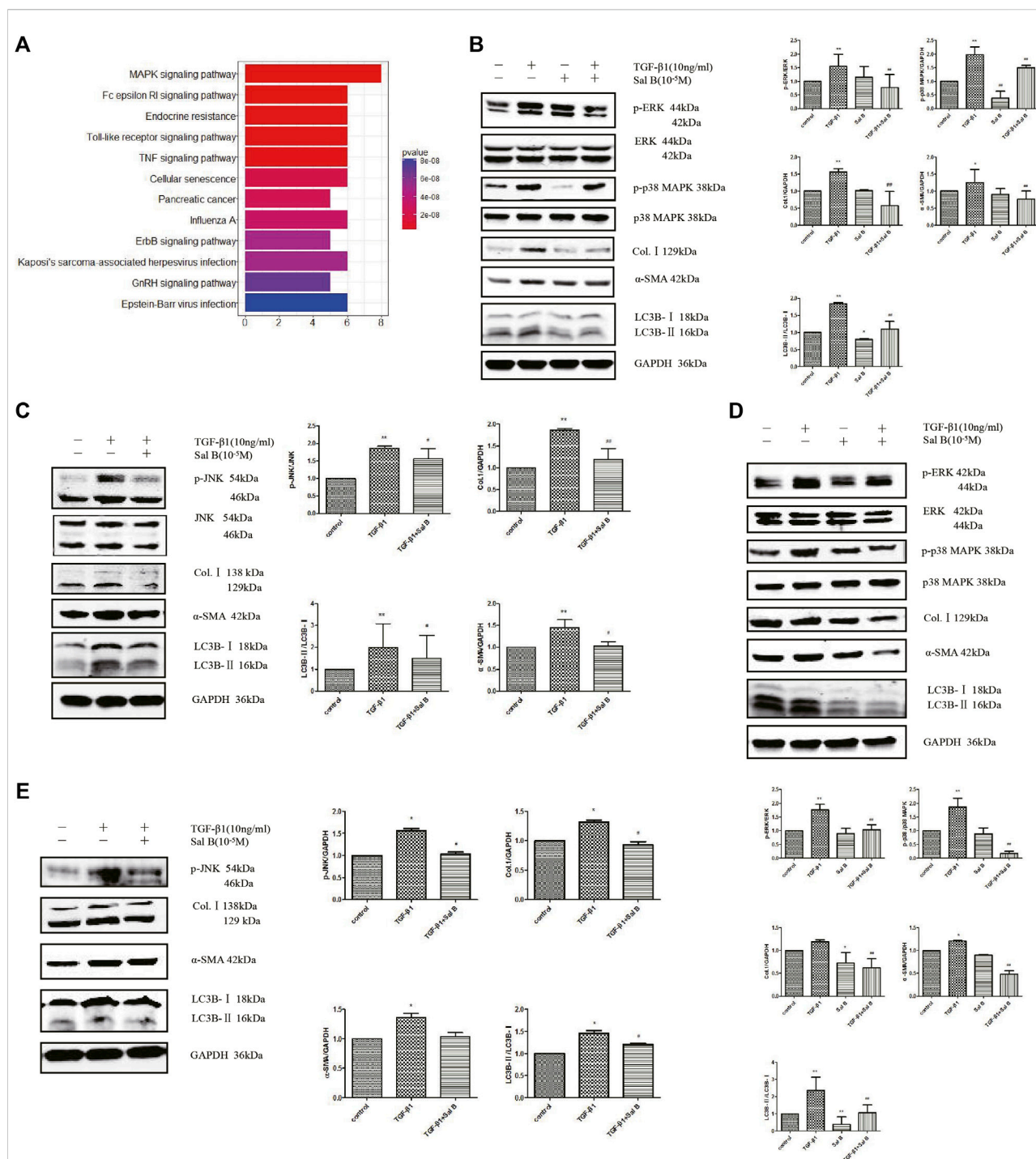
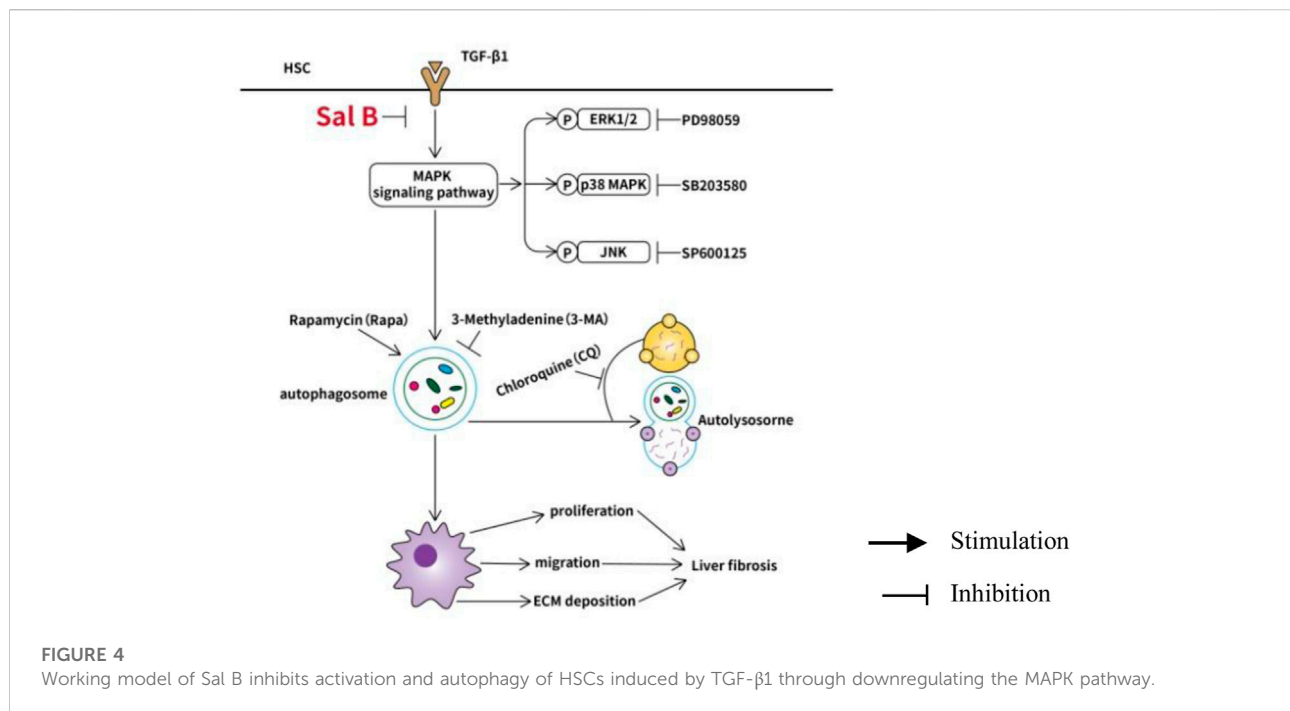


FIGURE 3

Sal B inhibits activation and autophagy of JS1 and LX-2 induced by TGF-β1 through downregulating the MAPK signaling pathway. (A) Protein analysis by MAPK Pathway Phosphorylation Array Kit phosphorylated protein chip (three samples in every group). Expression of p-ERK, p-p38 MAPK, p-JNK, Col.I, α-SMA, and LC3B in JS1 (B,C) or LX-2 (D,E) (vs. control: \* $p < 0.05$ , \*\* $p < 0.01$ ; vs. TGF-β1: \* $p < 0.05$ , \*\* $p < 0.01$ ; vs. TGF-β1+Sal B: \* $p < 0.05$ , \*\* $p < 0.01$ ).

Preclinical studies have shown that activation of autophagy following selective overexpression of certain ATG protein counteracts disease progression (Allaire et al., 2019).

Overexpression of ATG5 extends life in mice and reduces the onset of age-related disease (Jong-Ok Pyo et al., 2013). To further elucidate the role of autophagy on inhibition of HSCs activation



by Sal B, ATG5 was overexpressed. We commissioned Genomeditech Co., Ltd. to complete the overexpression of ATG5 (it is called ATG5-OE afterward) and empty vector stable cell lines (ATG5-NC). The expression of mRNA has shown that ATG5 gene expression in wild-type JS1 was similar to that in ATG5-NC, but ATG5-OE was 25.56 times higher than that in ATG5-NC (Figure 2C). It is mean stable transgenic strain of ATG5 gene overexpression is successful. ATG5-OE dramatically upregulated the protein expressions of ATG5, LC3BII,  $\alpha$ -SMA, and Col. I (Figure 2D); and next is the treatment of stable transgenic strain with TGF- $\beta$ 1 and Sal B. TGF- $\beta$ 1 could further promote the protein expression of Atg5 and  $\alpha$ -SMA compared with ATG5-OE, there was no statistical significance but could significantly promote the protein expression of Col.I. These three proteins markedly decreased by Sal B, indicating an effect of Sal B on autophagy in JS1 activation (Figure 2E). The result of gene expression was similar (Figure 2F).

Then, to further explore the relationship between HSCs activation and autophagy inhibition by Sal B, we established the Atg7 interference model, which was transfected with shAtg7 on the fifth day, and then cells were incubated with 10 ng/ml TGF- $\beta$ 1 or  $10^{-5}$ M Sal B. We also demonstrated that Atg7 interference reversed TGF- $\beta$ 1-mediated upregulation of the expression of the Col. I and LC3B II (Zhang et al., 2020a). At the same time, a Western blotting analysis showed that Sal B could further reduce the expression of Col. I, Atg7, and LC3B II (Figure 2G). These results showed that Sal B could further inhibit the autophagy and activation of JS1 under the autophagy defect induced by shAtg7.

Based on the aforementioned experimental results, we draw a conclusion: Sal B inhibits JS1 activation induced by TGF- $\beta$ 1 through autophagy.

### Sal B inhibits autophagy and activation of HSCs by downregulating the ERK, p38, and JNK pathways.

To explore the mechanism of Sal B inhibiting the autophagy and activation of HSCs, we chose a protein chip from RayBiotech as the research object. The results showed that 11 differentially phosphorylated protein sites expressed were screened out. JNK, p38 MAPK, and its upstream phosphorylated proteins MKK3/6, and upstream phosphorylated proteins of ERK pathways, Mek1, all of them were downregulated (Figure 3A).

Then the aforementioned results are verified. After exposure to TGF- $\beta$ 1 at a dose of 10 ng/ml, the protein expression levels of p-ERK, p-p38 MAPK, p-JNK, Col.I,  $\alpha$ -SMA, and LC3BII increased compared with controls, whereas these markers were markedly inhibited by Sal B. In addition, ERK, p38 MAPK, and JNK protein expressions remained unchanged (Figures 3B,C). Fortunately, we also found the similar results in LX2 (Figures 3D,E).

Collectively, the data indicate that Sal B inhibits activation and autophagy of JS1 in partially mediated ERK, p38, and JNK pathways, and there may be crosstalk between three channels. This possible mechanism of Sal B is shown in Figure 4.



## Discussion

Available evidence suggest Chinese herbal medicine can prevent liver fibrosis. For example, Duhuang Zhechong pill and Gan Shen Fu Fang attenuates liver fibrosis *via* different signaling pathway (Gong et al., 2020) (Du et al., 2020). Among them, Fuzheng Huayu formula has been studied more. Fuzheng Huayu recipe has been used widely for treating liver fibrosis or cirrhosis caused by chronic hepatitis B infection, chronic hepatitis C infection, non-alcoholic steatohepatitis, and so on. A Phase II, randomized, multicenter, double-blind, placebo-controlled study was successfully completed to assess the antifibrotic activity of Fuzheng Huayu tablet in patients with chronic hepatitis C plus hepatic fibrosis in the United States in 2013 (Zhang et al., 2020b). But, the mechanisms are unclear. In this research, we revealed a new mechanism of Sal B, a main drug of Fuzheng Huayu formula, inhibiting HSCs activation. We discovered that reducing autophagic flux also play an important role in Sal B inhibiting HSCs activation induced by TGF- $\beta$ 1 through the downregulated MAPK signaling.

TGF- $\beta$ 1 is a potent fibrogenic cytokine that promotes myofibroblast activation and ECM synthesis (Tschumperlin and Lagares, 2020). HSCs activation is stimulated by several cytokines, in particular TGF- $\beta$ 1, mainly released from Kupffer cells, has been supposed to be the cardinal pro-fibrogenic effector of HSCs (Yongfang Gong and Yang, 2020). Many studies have shown that autophagy operates as a critical quality control mechanism for the maintenance of hepatic homeostasis in both parenchymal [hepatocytes (Fang et al., 2021) (Park et al., 2020)] and non-parenchymal [stellate cells, sinusoidal endothelial cells (Hammoutene et al., 2020), Kupffer cells (Xu et al., 2020)], and compartments (Hazari et al., 2020). We recently showed that TGF- $\beta$ 1 induced autophagy activates hepatic stellate cells *via* the ERK and JNK signaling pathways (Zhang et al., 2020a). Sal B has an obvious effect on antifibrosis. Sal B can inhibit liver fibrosis induced by DMN and CCl<sub>4</sub> in rats *in vivo* (Tao et al., 2021), and it has a therapeutic effect on liver fibrosis, kidney (Gang Yao et al., 2009), and lung fibrosis (Kesireddy et al., 2019) (Stojanović et al., 2020). Sal B can inhibit the proliferation of lung fibroblasts cell and expression of Col. I,  $\alpha$ -SMA, and the production of endogenous TGF- $\beta$ 1 induced by TGF- $\beta$ 1 (Liu et al., 2016). The regulation of Sal B on autophagy varies according to different cell types. For example, Sal B attenuates epithelial-mesenchymal transition in renal fibrosis rats through activating Sirt1-mediated autophagy (He et al., 2020), but in cardiac myocytes, it can inhibit autophagy and protect starving cardiac myocytes (Han et al., 2010). The details presented in our study demonstrate 10<sup>-5</sup>M Sal B could inhibit the activation and proliferation of HSCs induced by TGF- $\beta$ 1. Recent studies suggest that Sal B protects human umbilical vein endothelial cells from oxidative stress at least partially by promoting autophagy *via* activation of the AMPK pathway and downregulation of the mTOR pathway (Gao et al., 2019).

Autophagy may interact with NLRP3 activation to contribute to the development of depression, whereas Sal B can promote autophagy and induce the clearance of NLRP3, thereby resulting in neuro-protective and antidepressant actions (Jiang et al., 2017). These results suggest that Sal B may act as an important role in different cells by regulating autophagy. Our study demonstrated Sal B can decrease the expression of LC3BII, a marker of autophagosome, at different times. Meanwhile, we observed cleaved-Caspase 3, the key enzyme to regulate apoptosis, increased at 8, 12, and 24 h. Autophagy appears before apoptosis, which may be related to the inhibition of autophagy to induce apoptosis.

Sal B inhibited autophagy of JS1 induced by TGF- $\beta$ 1 from the perspective. It is suggested that Sal B can reduce autophagosomes induced by TGF- $\beta$ 1. The effect of Sal B on autophagy flux induced by TGF- $\beta$ 1 is studied. In the next experiment, we used pGMLV-CMV-RFP-GFP-hLC3-Puro lentivirus transfected cells to confirm that Sal B inhibited the formation of autolysosome and blocked autophagic flux in JS1. The interesting thing is that we observed the same results in LX2, and then we used 3-MA and CQ to treat JS1, respectively. The results showed that Sal B and autophagy inhibitor could further decrease the expression of LC3BII. Prior studies have demonstrated that the activation of HSCs can be promoted by induction of autophagy. Lipopolysaccharide induced autophagy resulted in LD loss, RA signaling dysfunction to mediate hepatic stellate cell activation (Chen et al., 2017). Recent studies also have suggested autophagy suppression contributes to inhibition of HSCs activation (Yu et al., 2019) (Ma et al., 2019) (Wang L. et al., 2020). Ursodeoxycholic acid alleviates experimental liver fibrosis involving inhibition of autophagy (Ye et al., 2020). This is consistent with our results. However, there are some opposite results (Hu et al., 2020). For example, hepatic stellate cell autophagy inhibits extracellular vesicle released to attenuate liver fibrosis (Shuhei Nakamura, 2018). This may depend on different cell states and different animal models.

In autophagy research, gene of Atg interference (Wang Z. et al., 2020) and overexpression were used (Zhang et al., 2019). Autophagy is highly dependent on some autophagic proteins, among which ATG5 is a very important protein in autophagic body formation. In our experiment, we established the overexpression of ATG5 (ATG5-OE) and empty vector plasmid (ATG5-NC) transfection stable strain. We detected the protein expressions of Col.I,  $\alpha$ -SMA, Atg5, and LC3BII were significantly increased in ATG5-OE than ATG5-NC. It is suggested that ATG5-OE promotes autophagy and activation in JS1. Then, the study has shown that Sal B can inhibit the activation of HSCs by inhibiting autophagy induced by TGF- $\beta$ 1 and Rapa, as well as ATG5-OE. At the same time, we established the Atg7 interference model. The increase of Col.I, Atg7, and LC3BII induced by TGF- $\beta$ 1 was alleviated by shAtg7. Sal B could further reduce the expressions of Col.I, Atg7, and LC3BII in the shAtg7 model. Its mean Sal B could further inhibit

the autophagy and activation of HSCs under the impaired autophagy induced by shAtg7.

Sal B can inhibit HSCs activation by downregulating autophagy. Next, we will study its mechanism. Our previous research has found (Lv et al., 2010) (Lv and Xu, 2012) (Xu et al., 2012) that Sal B could inhibit HSCs activation induced by TGF- $\beta$ 1 through the MAPK signaling pathway. Qianqian Wang et al. (Wang et al., 2019) reported high glucose caused autophagic cell death by activating the JNK pathway. Previous research had shown autophagy can be regulated by the MAPK signaling pathway (Hanyu et al., 2020) (Chiou et al., 2020). In order to determine the signal pathway of Sal B inhibiting the activation and autophagy of HSCs, we chose a protein chip from RayBiotech. Most focus was on the MAPK signaling pathway. Then, the verification experiments found after exposure to TGF- $\beta$ 1, the level of p-ERK, p-p38 MAPK, p-JNK, Col.I,  $\alpha$ -SMA, and LC3BII protein increased, whereas Sal B significantly reduced the level of these elevated protein. Fortunately, we also found the similar results in LX2.

In summary, the present study demonstrates Sal B inhibits activation and autophagy of HSCs induced by TGF- $\beta$ 1 partly through downregulating the ERK, p38, and JNK pathways, and there may be crosstalk between these channels. These findings provide a rationale for potential clinical applications of Sal B for the prevention or treatment of liver fibrosis.

## Data availability statement

The original contributions presented in the study are included in the article/Supplementary Materials; further inquiries can be directed to the corresponding author.

## References

- Allaire, M., Rautou, P.-E., Codogno, P., and Lotersztajn, S. (2019). Autophagy in liver diseases: Time for translation? *J. Hepatol.* 70, 985–998. doi:10.1016/j.jhep.2019.01.026
- Amir, M., Zhao, E., Fontana, L., Rosenberg, H., Tanaka, K., Gao, G., et al. (2013). Inhibition of hepatocyte autophagy increases tumor necrosis factor-dependent liver injury by promoting caspase-8 activation. *Cell Death Differ.* 20, 878–887. doi:10.1038/cdd.2013.21
- Chen, M., Liu, J., Yang, W., and Ling, W. (2017). Lipopolysaccharide mediates hepatic stellate cell activation by regulating autophagy and retinoic acid signaling. *Autophagy* 13, 1813–1827. doi:10.1080/15548627.2017.1356550
- Chiou, J.-T., Huang, C.-H., Lee, Y.-C., Wang, L.-J., Shi, Y.-J., Chen, Y.-J., et al. (2020). Compound C induces autophagy and apoptosis in parental and hydroquinone-selected malignant leukemia cells through the ROS/p38 MAPK/AMPK/TET2/FOXp3 axis. *Cell Biol. Toxicol.* 36, 315–331. doi:10.1007/s10565-019-09495-3
- Du, Q.-H., Zhang, C.-J., Li, W.-H., Mu, Y., Xu, Y., Lowe, S., et al. (2020). Gan Shen Fu Fang ameliorates liver fibrosis *in vitro* and *in vivo* by inhibiting the inflammatory response and extracellular signal-regulated kinase phosphorylation. *World J. Gastroenterol.* 26, 2810–2820. doi:10.3748/wjg.v26.i21.2810
- Fang, Yuan., Xu, Y., You., Kai, Zhang., Jiaye, Fan, Yang., Li, Yin-Xiong, et al. (2021). Calcitriol alleviates ethanol-induced hepatotoxicity via AMPK-mTOR-mediated autophagy. *Arch. Biochem. Biophys.* 01, 108694. doi:10.1016/j.abb.2020.108694
- Friedman, S. L. (2010). Evolving challenges in hepatic fibrosis. *Nat. Rev. Gastroenterol. Hepatol.* 7, 425–436. doi:10.1038/nrgastro.2010.97
- Friedman, S. L. (2008). Hepatic stellate cells: Protean, multifunctional, and enigmatic cells of the liver. *Physiol. Rev.* 88, 125–172. doi:10.1152/physrev.00013.2007
- Gang Yao, L. X., Wu, Xiaochun, Xu, Lingling, Yang, Junwei, Chen, Huimei, and Chen, H. (2009). Preventive effects of salvianolic acid B on transforming growth factor- $\beta$ 1-induced epithelial-to-mesenchymal transition of human kidney cells. *Biol. Pharm. Bull.* 32, 882–886. doi:10.1248/bpb.32.882
- Gao, J., Wei, B., De Assuncao, T. M., Liu, Z., Hu, X., Ibrahim, S., et al. (2020). Hepatic stellate cell autophagy inhibits extracellular vesicle release to attenuate liver fibrosis. *J. Hepatol.* 73, 1144–1154. doi:10.1016/j.jhep.2020.04.044
- Gao, S., Li, S., Li, Q., Zhang, F., Sun, M., Wan, Z., et al. (2019). Protective effects of salvianolic acid B against hydrogen peroxide-induced apoptosis of human umbilical vein endothelial cells and underlying mechanisms. *Int. J. Mol. Med.* 44, 457–468. doi:10.3892/ijmm.2019.4227
- Gong, Y. F., and Yang, Y. (2020). Activation of nrf2/AREs-mediated antioxidant signalling, and suppression of profibrotic TGF- $\beta$ 1-Smad3 pathway a promising therapeutic strategy for hepatic fibrosis — a review. *Life Sci.* 256, 117909. doi:10.1016/j.lfs.2020.117909

## Author contributions

LX conceived and designed the study, contributed reagents and materials. NJ and JZ performed research and analyzed data. NJ wrote the manuscript. JP analyzed and interpreted the data and revised the manuscript. All authors read and approved the final manuscript.

## Funding

This work was supported by grants from the National Natural Science Foundation of China (No. 81373859). This work was supported by grants from the National Natural Science Foundation of China (No.81573794), and Project of Science and Technology Commission of Shanghai Municipality (No.15401902600).

## Conflict of interest

The authors declare that the research was conducted in the absence of any commercial or financial relationships that could be construed as a potential conflict of interest.

## Publisher's note

All claims expressed in this article are solely those of the authors and do not necessarily represent those of their affiliated organizations, or those of the publisher, the editors, and the reviewers. Any product that may be evaluated in this article, or claim that may be made by its manufacturer, is not guaranteed or endorsed by the publisher.



- Gong, Z. H., Lin, J. Y., Zheng, J., Wei, L. Y., Liu, L., Peng, Y. Z., et al. (2020). Dahuang Zhechong pill attenuates CCl<sub>4</sub>-induced rat liver fibrosis via the PI3K-Akt signaling pathway. *J. Cell. Biochem.* 121, 1431–1440. doi:10.1002/jcb.29378
- Hammoutene, A., Biquard, L., Lasselin, J., Kheloufi, M., Tanguy, M., Vion, A.-C., et al. (2020). A defect in endothelial autophagy occurs in patients with non-alcoholic steatohepatitis and promotes inflammation and fibrosis. *J. Hepatol.* 72, 528–538. doi:10.1016/j.jhep.2019.10.028
- Han, X., Liu, J.-X., and Li, X.-Z. (2010). Salvianolic acid B inhibits autophagy and protects starving cardiac myocytes. *Acta Pharmacol. Sin.* 32, 38–44. doi:10.1038/aps.2010.182
- Hanyu, X., Lanyue, L., Miao, D., Wentao, F., Cangran, C., Hui, S., et al. (2020). Effect of Ganoderma applanatum polysaccharides on MAPK/ERK pathway affecting autophagy in breast cancer MCF-7 cells. *Int. J. Biol. Macromol.* 146, 353–362. doi:10.1016/j.ijbiomac.2020.01.010
- Hazari, Y., Bravo-San Pedro, J. M., Hetz, C., Galluzzi, L., and Kroemer, G. (2020). Autophagy in hepatic adaptation to stress. *J. Hepatol.* 72, 183–196. doi:10.1016/j.jhep.2019.08.026
- He, Y., Lu, R., Wu, J., Pang, Y., Li, J., Chen, J., et al. (2020). Salvianolic acid B attenuates epithelial-mesenchymal transition in renal fibrosis rats through activating Sirt1-mediated autophagy. *Biomed. Pharmacother.* 128, 110241. doi:10.1016/j.biopha.2020.110241
- Higashi, T., Friedman, S. L., and Hoshida, Y. (2017). Hepatic stellate cells as key target in liver fibrosis. *Adv. Drug Deliv. Rev.* 121, 27–42. doi:10.1016/j.addr.2017.05.007
- Hu, Z., Su, H., Zeng, Y., Lin, C., Guo, Z., Zhong, F., et al. (2020). Tetramethylpyrazine ameliorates hepatic fibrosis through autophagy-mediated inflammation. *Biochem. Cell Biol.* 98, 327–337. doi:10.1139/bcb-2019-0059
- Jiang, P., Guo, Y., Dang, R., Yang, M., Liao, D., Li, H., et al. (2017). Salvianolic acid B protects against lipopolysaccharide-induced behavioral deficits and neuroinflammatory response: involvement of autophagy and NLRP3 inflammasome. *J. Neuroinflammation* 14, 239. doi:10.1186/s12974-017-1013-4
- Jong-Ok Pyo, S.-M. Y., Ahn, H., Hye-Hyun, Jihoon, Nah, Hong, Se-Hoon, Tae-in Kam.Kam, T. I., et al. (2013). Overexpression of Atg5 in mice activates autophagy and extends lifespan. *Nat. Commun.* 4, 2300. doi:10.1038/ncomms3300
- Jung, Y. K., and Yim, H. J. (2017). Reversal of liver cirrhosis: current evidence and expectations. *Korean J. Intern. Med.* 32, 213–228. doi:10.3904/kjim.2016.268
- Kesireddy, V. S., Chillappagari, S., Ahuja, S., Knudsen, L., Henneke, I., Graumann, J., et al. (2019). Susceptibility of microtubule-associated protein 1 light chain 3 $\beta$  (MAP1LC3B/LC3B) knockout mice to lung injury and fibrosis. *FASEB J.* 33, 12392–12408. doi:10.1096/fj.201900854R
- Klionsky, D. J., Abdel-Aziz, A. K., Abdelfatah, S., Abdellatif, M., Abdoli, A., Abel, S., et al. (2021). *Guidelines for the use and interpretation of assays for monitoring autophagy*. *Autophagy*. 17, 1–382. 4th edition. doi:10.1080/15548627.2020.1797280
- Lee, Y. A., Wallace, M. C., and Friedman, S. L. (2015). Pathobiology of liver fibrosis: a translational success story. *Gut* 64, 830–841. doi:10.1136/gutjnl-2014-306842
- Li, Y., Ni, H.-M., Jaeschke, H., and Ding, W.-X. (2019). Chlorpromazine protects against acetaminophen-induced liver injury in mice by modulating autophagy and c-Jun N-terminal kinase activation. *Liver Res.* 3, 65–74. doi:10.1016/j.livres.2019.01.004
- Lin, M., Zhai, X., Wang, G., Tian, X., Gao, D., Shi, L., et al. (2015). Salvianolic acid B protects against acetaminophen hepatotoxicity by inducing Nrf2 and phase II detoxification gene expression via activation of the PI3K and PKC signaling pathways. *J. Pharmacol. Sci.* 127, 203–210. doi:10.1016/j.jphs.2014.12.010
- Liu, Q., Chu, H., Ma, Y., Wu, T., Qian, F., Ren, X., et al. (2016). Salvianolic acid B attenuates experimental pulmonary fibrosis through inhibition of the TGF- $\beta$  signaling pathway. *Sci. Rep.* 6, 27610. doi:10.1038/srep27610
- Lv, Z., Song, Y., Xue, D., Zhang, W., Cheng, Y., Xu, L., et al. (2010). Effect of Salvianolic acid B on inhibiting MAPK signaling induced by transforming growth factor- $\beta$ 1 in activated rat hepatic stellate cells. *J. Ethnopharmacol.* 132, 384–392. doi:10.1016/j.jep.2010.05.026
- Lv, Z., and Xu, L. (2012). Salvianolic acid B inhibits ERK and p38 MAPK signaling in TGF- $\beta$ 1-stimulated human hepatic stellate cell line (LX-2) via distinct pathways. *Evidence-Based Complementary Altern. Med.* 2012, 1–11. doi:10.1155/2012/960128
- Ma, J.-Q., Sun, Y.-Z., Ming, Q.-L., Tian, Z.-K., Yang, H.-X., Liu, C.-M., et al. (2019). Ampelopsin attenuates carbon tetrachloride-induced mouse liver fibrosis and hepatic stellate cell activation associated with the SIRT1/TGF- $\beta$ 1/Smad3 and autophagy pathway. *Int. Immunopharmacol.* 77, 105984. doi:10.1016/j.intimp.2019.105984
- Mizushima, N., Levine, B., Cuervo, A. M., and Klionsky, D. J. (2008). Autophagy fights disease through cellular self-digestion. *Nature* 451, 1069–1075. doi:10.1038/nature06639
- Mukherjee, A., Hidvegi, T., Araya, P., Ewing, M., Stolz, D. B., Perlmutter, D. H., et al. (2018). NF- $\kappa$ B mitigates the pathological effects of misfolded  $\alpha$ 1-antitrypsin by activating autophagy and an integrated program of proteostasis mechanisms. *Cell Death Differ.* 26, 455–469. doi:10.1038/s41418-018-0130-7
- Ni, H.-M., Bockus, A., Boggess, N., Jaeschke, H., and Ding, W.-X. (2012). Activation of autophagy protects against acetaminophen-induced hepatotoxicity. *Hepatology* 55, 222–232. doi:10.1002/hep.24690
- Park, H.-S., Song, J.-W., Park, J.-H., Lim, B.-K., Moon, O.-S., Son, H.-Y., et al. (2020). TXNIP/VDUP1 attenuates steatohepatitis via autophagy and fatty acid oxidation. *Autophagy* 17, 2549–2564. doi:10.1080/15548627.2020.1834711
- Polishchuk, E. V., Merolla, A., Lichtmanegger, J., Romano, A., Indrieri, A., Ilyechova, E. Y., et al. (2019). Activation of autophagy, observed in liver tissues from patients with Wilson disease and from ATP7B-deficient animals, protects hepatocytes from copper-induced apoptosis. *Gastroenterology* 156, 1173–1189. e1175. doi:10.1053/j.gastro.2018.11.032
- Shan, S., Shen, Z., Zhang, C., Kou, R., Xie, K., Song, F., et al. (2019). Mitophagy protects against acetaminophen-induced acute liver injury in mice through inhibiting NLRP3 inflammasome activation. *Biochem. Pharmacol.* 169, 113643. doi:10.1016/j.bcp.2019.113643
- Shuhei Nakamura, T. Y., and Yoshimori, T. (2018). Autophagy and longevity. *Autophagy Longev. Mol. Cells* 41, 65–72. doi:10.14348/molcells.2018.2333
- Stojanović, S. D., Fuchs, M., Fiedler, J., Xiao, K., Meinecke, A., Just, A., et al. (2020). Comprehensive bioinformatics identifies key microRNA players in ATG7-deficient lung fibroblasts. *Int. J. Mol. Sci.* 21, 4126. doi:10.3390/ijms21114126
- Tao, S., Duan, R., Xu, T., Hong, J., Gu, W., Lin, A., et al. (2021). Salvianolic acid B inhibits the progression of liver fibrosis in rats via modulation of the Hedgehog signaling pathway. *Exp. Ther. Med.* 23, 116. doi:10.3892/etm.2021.11039
- Tschumperlin, D. J., and Lagares, D. (2020). Mechano-therapeutics: Targeting mechanical signaling in fibrosis and tumor stroma. *Pharmacol. Ther.* 212, 107575. doi:10.1016/j.pharmthera.2020.107575
- Tsuchida, T., and Friedman, S. L. (2017). Mechanisms of hepatic stellate cell activation. *Nat. Rev. Gastroenterol. Hepatol.* 14, 397–411. doi:10.1038/nrgastro.2017.38
- Wang, L., Wang, Y., and Quan, J. (2020a). Exosomal miR-223 derived from natural killer cells inhibits hepatic stellate cell activation by suppressing autophagy. *Mol. Med.* 26, 81. doi:10.1186/s10020-020-00207-w
- Wang, Q.-Q., Zhai, C., Wahafu, A., Zhu, Y.-T., Liu, Y.-H., Sun, L.-Q., et al. (2019). Salvianolic acid B inhibits the development of diabetic peripheral neuropathy by suppressing autophagy and apoptosis. *J. Pharm. Pharmacol.* 71, 417–428. doi:10.1111/jph.13044
- Wang, Z., Sequeira, R. C., Zabalawi, M., Madenspacher, J., Boudyguina, E., Ou, T., et al. (2020b). Myeloid atg5 deletion impairs n-3 PUFA-mediated atheroprotection. *Atherosclerosis* 295, 8–17. doi:10.1016/j.atherosclerosis.2020.01.004
- Weiskirchen, R., and Tacke, F. (2019). Relevance of autophagy in parenchymal and non-parenchymal liver cells for health and disease. *Cells* 8, 16. doi:10.3390/cells8010016
- Xu, H., Zhou, Y., Lu, C., Ping, J., and Xu, L.-M. (2012). Salvianolic acid B lowers portal pressure in cirrhotic rats and attenuates contraction of rat hepatic stellate cells by inhibiting RhoA signaling pathway. *Lab. Invest.* 92, 1738–1748. doi:10.1038/labinvest.2012.113
- Xu, Y., Tang, Y., Lu, J., Zhang, W., Zhu, Y., Zhang, S., et al. (2020). PINK1-mediated mitophagy protects against hepatic ischemia/reperfusion injury by restraining NLRP3 inflammasome activation. *Free Radic. Biol. Med.* 160, 871–886. doi:10.1016/j.freeradbiomed.2020.09.015
- Yan, M., Ye, L., Yin, S., Lu, X., Liu, X., Lu, S., et al. (2018). Glycycomarin protects mice against acetaminophen-induced liver injury predominantly via activating sustained autophagy. *Br. J. Pharmacol.* 175, 3747–3757. doi:10.1111/bph.14444
- Ye, H.-L., Zhang, J.-W., Chen, X.-Z., Wu, P.-B., Chen, L., and Zhang, G. (2020). Ursodeoxycholic acid alleviates experimental liver fibrosis involving inhibition of autophagy. *Autophagy* 24, 117175. doi:10.1016/j.ifs.2019.117175LIFE Sci.

Yu, F., Dong, B., Dong, P., He, Y., Zheng, J., Xu, P., et al. (2019). Hypoxia induces the activation of hepatic stellate cells through the PVT1-miR-152-ATG14 signaling pathway. *Mol. Cell. Biochem.* 465, 115–123. doi:10.1007/s11010-019-03672-y

Zhang, J., Jiang, N., Ping, J., and Xu, L. (2020a). TGF- $\beta$ 1-induced autophagy activates hepatic stellate cells via the ERK and JNK signaling pathways. *Int. J. Mol. Med.* 47, 256–266. doi:10.3892/ijmm.2020.4778

Zhang, M., Liu, H.-L., Huang, K., Peng, Y., Tao, Y.-Y., Zhao, C.-Q., et al. (2020b). Fuzheng Huayu recipe prevented and treated CCl<sub>4</sub>-induced mice liver fibrosis through regulating polarization and chemotaxis of intrahepatic macrophages via CCL2 and CX3CL1. *Evid. Based. Complement. Altern. Med.* 2020, 8591892. doi:10.1155/2020/8591892

Zhang, N., Hu, Y., Ding, C., Zeng, W., Shan, W., Fan, H., et al. (2017). Salvianolic acid B protects against chronic alcoholic liver injury via SIRT1-mediated inhibition of CRP and ChREBP in rats. *Toxicol. Lett.* 267, 1–10. doi:10.1016/j.toxlet.2016.12.010

Zhang, Z., Guo, M., Li, Y., Shen, M., Kong, D., Shao, J., et al. (2019). RNA-binding protein ZFP36/TTP protects against ferroptosis by regulating autophagy signaling pathway in hepatic stellate cells. *Autophagy* 16, 1482–1505. doi:10.1080/15548627.2019.1687985

Zhong, Z., Umemura, A., Sanchez-Lopez, E., Liang, S., Shalpour, S., Wong, J., et al. (2016). NF- $\kappa$ B restricts inflammasome activation via elimination of damaged mitochondria. *Cell* 164, 896–910. doi:10.1016/j.cell.2015.12.057



## OPEN ACCESS

## EDITED BY

Adina Turcu-Stolica,  
University of Medicine and Pharmacy of  
Craiova, Romania

## REVIEWED BY

Majid Sharifi-Rad,  
Zabol University, Iran  
Fuli Zheng,  
Fujian Medical University, China

## \*CORRESPONDENCE

Gan Cai,  
caiganp@126.com  
Jianghong Ling,  
ljh18817424778@163.com

†These authors have contributed equally  
to this work and share first authorship

## SPECIALTY SECTION

This article was submitted to  
Gastrointestinal and Hepatic  
Pharmacology,  
a section of the journal  
Frontiers in Pharmacology

RECEIVED 16 May 2022

ACCEPTED 05 July 2022

PUBLISHED 12 August 2022

## CITATION

Jia Q, Li L, Wang X, Wang Y, Jiang K,  
Yang K, Cong J, Cai G and Ling J (2022),  
Hesperidin promotes gastric motility in  
rats with functional dyspepsia by  
regulating Drp1-mediated  
ICC mitophagy.  
*Front. Pharmacol.* 13:945624.  
doi: 10.3389/fphar.2022.945624

## COPYRIGHT

© 2022 Jia, Li, Wang, Wang, Jiang, Yang,  
Cong, Cai and Ling. This is an open-  
access article distributed under the  
terms of the [Creative Commons  
Attribution License \(CC BY\)](https://creativecommons.org/licenses/by/4.0/). The use,  
distribution or reproduction in other  
forums is permitted, provided the  
original author(s) and the copyright  
owner(s) are credited and that the  
original publication in this journal is  
cited, in accordance with accepted  
academic practice. No use, distribution  
or reproduction is permitted which does  
not comply with these terms.

# Hesperidin promotes gastric motility in rats with functional dyspepsia by regulating Drp1-mediated ICC mitophagy

Qingling Jia<sup>†</sup>, Li Li<sup>†</sup>, Xiangxiang Wang, Yujiao Wang, Kailin Jiang,  
Keming Yang, Jun Cong, Gan Cai\* and Jianghong Ling\*

Department of Gastroenterology, Shuguang Hospital, Shanghai University of Traditional Chinese  
Medicine, Shanghai, China

Hesperidin is one of the main active ingredients of *Citrus aurantium* L. (Rutaceae) and tangerine peel, which have anti-inflammatory and antioxidant effects. In previous study, we found that gastric motility disorder in functional dyspepsia (FD) rats accompanied by excessive autophagy/mitochondrial swelling and even vacuolization in the interstitial cells of cajal (ICC), but the exact mechanism has not yet been investigated. Therefore, we used different doses of hesperidin (50 mg/kg, 100 mg/kg, and 200 mg/kg) to intervene in FD rats, and found that medium doses of hesperidin (100 mg/kg) significantly increased gastric motility in FD rats. Subsequently, FD rats were randomly divided into control group, model group, mdivi-1 group, mdivi-1+hesperidin group and hesperidin group, and mitochondrial division inhibitor (mdivi-1) was injected intraperitoneally to further investigate whether hesperidin could regulate dynamin-related protein 1 (Drp1)-mediated mitophagy in ICC to improve mitochondrial damage. The results showed that compared with the model group, the serum malondialdehyde (MDA) level decreased and the superoxide dismutase (SOD) level increased in the mdivi-1 and hesperidin groups ( $p < 0.001$ ). Transmission electron microscopy (TEM) observed that the mitochondrial nuclear membrane was intact in gastric tissues with a clear internal cristae pattern, and autophagy lysosomes were rare. The co-localization expression of microtubule associated protein 1 light chain 3 (LC3) and voltage dependent anion channel 1 (VDAC1), Drp1 and translocase of the outer mitochondrial membrane 20 (Tom20) was significantly decreased ( $p < 0.001$ ), the protein expression of mitochondrial Drp1, Beclin1 and LC3 were significantly decreased ( $p < 0.001$ ), the protein expression of mitochondrial P62 and ckit in gastric tissue were significantly increased ( $p < 0.05$ ,  $p < 0.001$ ). The above situation was improved more significantly by the synergistic intervention of mdivi-1 and hesperidin. Therefore, hesperidin can improve mitochondrial damage and promote gastric motility in FD rats by regulating Drp1-mediated ICC mitophagy.

## KEYWORDS

hesperidin, functional dyspepsia, mitophagy, mdivi-1, Drp1

## 1 Introduction

Functional dyspepsia (FD) is a common gastrointestinal disorder with a reported global prevalence of 5–11% in the community, which has caused a severe social and economic burden (Talley and Ford, 2015; Jin and Son, 2018; Kim et al., 2018). Currently, gastric motility disorders are considered to be one of the pathophysiological features of FD and are closely associated with dyspepsia symptoms (Asano et al., 2017). Gastric motility is mostly regulated by the autonomic and enteric nervous systems as well as by the interstitial cells of cajal (ICC) (Naganuma et al., 2017). As a pacemaker of gastrointestinal slow-wave activity, ICC plays an important role in intestinal motility by transmitting excitatory and inhibitory signals to affect gastrointestinal motility (Hagger et al., 1997). Ckit is a specific receptor for ICC in the gastrointestinal tract, and ICC is cell that specifically express ckit. Studies have shown that blockade of ICC development in BALB/c mice by the anti-ckit monoclonal antibody ACK2 leads to severe abnormalities in intestinal motility, reduces the number of ICC in the small intestine, and inhibits ICC proliferation and development (Torihashi et al., 1995; Streutker et al., 2007). In our previous study, we found that impaired gastric motility in FD rats was accompanied by excessive autophagy/mitochondrial swelling and even vacuolization of ICC (Tan et al., 2019).

Mitophagy is a form of cellular autophagy that occurs when mitochondria are depolarized and damaged by external stimuli such as oxidative damage, and the damaged mitochondria are wrapped in autophagosomes and fused with lysosomes, thus completing the degradation of the damaged mitochondria (Patergnani and Pinton, 2015; Springer and Macleod, 2016). Mitochondrial division inhibitor (mdivi-1) is a selective inhibitor of dynamin-related protein 1 (Drp1) that inhibits Drp1-mediated mitochondrial division by inhibiting GTPase activity (Duan et al., 2020). Mdivi-1 treatment has been shown to prevent lipopolysaccharide-induced mitophagy and reduce acute lung injury in rats (Luo et al., 2019). Activation of mitophagy via a Drp1-dependent pathway reduced apoptosis and improved renal ischaemia/reperfusion injury-induced renal dysfunction (Li et al., 2018). Furthermore, mdivi-1 prevents the initiation of mitophagy in diabetic cardiomyocytes (Mishra et al., 2014). However, no studies have yet shown how mitophagy plays a role in FD, and further studies are warranted.

Hesperidin, a flavonoid, is one of the main active components of traditional Chinese medicines *Citrus aurantium* L. (Rutaceae) and tangerine peel, and has anti-inflammatory, antioxidant, analgesic, and antihypertensive effects (Iranshahi et al., 2015; Parhiz et al., 2015). Studies have shown that hesperidin can effectively improve gastrointestinal function in rats. For example, hesperidin can improve colonic motility in loeramide-induced constipation rats through the serotonin 4R/cAMP signaling pathway (Wu et al., 2019). Hesperidin may play an anti-ulcer effect by preventing

hemorrhagic injury of gastric mucosa through its antioxidant effect (Bigoniya and Singh, 2014). In addition, hesperidin can reduce oxidative stress and mitochondrial dysfunction by inhibiting DNA Methyltransferase 1-mediated silencing of miR-149, and ameliorate high glucose-induced insulin resistance (Tian et al., 2021). Although hesperidin is known to alleviate FD, its specific mechanism has been rarely studied. Therefore, in this study, we aimed to explore the mechanism of hesperidin through Drp1-mediated ICC mitophagy, improving mitochondrial damage and promoting gastric motility in FD rats.

## 2 Methods and materials

### 2.1 Animals

66 specific pathogen-free (SPF) SD rats, 5–6 weeks old, body weight ( $200 \pm 20$  g), purchased from Zhejiang Weitong Lihua Laboratory Animal Technology Co., Ltd., certificate number SCXK (Zhejiang) 2019-0001, housed in SPF-grade barrier environment at the Experimental Animal Center of Shanghai University of Traditional Chinese Medicine (TCM), with alternating light and dark cycles of 12/12 h, relative temperature ( $22 \pm 2$ )°C and relative humidity ( $55 \pm 2$ )%. This study was approved by the Animal Ethics Committee of Shanghai University of TCM (PZSHUTCM210108004).

### 2.2 Reagents

Hesperidin (Dalian Meilun Biotechnology Co., Ltd., MB6567, Dalian, China), Domperidone Tablets (Xian Janssen Pharmaceutical Ltd., KDJ3YSP, Xian, China), mdivi-1 (Shanghai Selleck, S7162, Shanghai, China), rabbit anti-Drp1 (Abcam, ab184247, Cambridge, UK), rabbit anti-ckit (Cell Signaling Technology, 3074, MA, United States), rabbit anti-Beclin1 (Cell Signaling Technology, 3738S), rabbit anti-P62 (Cell Signaling Technology, 23214S), rabbit anti-LC3 (Cell Signaling Technology, 4108S), rabbit anti-GAPDH (Cell Signaling Technology, 5174S), anti-rabbit IgG, HRP-linked antibody (Cell Signaling Technology, 7074P2), mouse anti-VDAC1 (Santa Cruz Biotechnology, Inc., sc-390996, CA, United States), mouse anti-Tom20 (Santa Cruz Biotechnology, Inc., sc-17764), Bovine Serum Albumin (BSA) (Shanghai Beyotime Biotechnology Co., Ltd., ST023, Shanghai, China), Alexa Fluor 488-labeled Goat Anti-Rabbit IgG (H + L) (Shanghai Beyotime Biotechnology Co., Ltd., A0423), Cy3-labeled Goat Anti-Rat IgG (H + L) (Shanghai Beyotime Biotechnology Co., Ltd., A0507), Antifade Mounting Medium with DAPI (Shanghai Beyotime Biotechnology Co., Ltd., P0131), SDS-PAGE Gel Quick Preparation Kit (Shanghai Beyotime Biotechnology Co., Ltd., P0012AC), Mitochondrial Extraction Kit (Beijing Solarbio Science & Technology Co., Ltd., SM0020,

Beijing, China), EZ-Buffers H 10X TBST Buffer (Shanghai Sangon Biotech Co., Ltd., C520009, Shanghai, China), Reactive Oxygen Species (ROS) Assay Kit (Nanjing Jiancheng Bioengineering Institute, E004-1-1, Nanjing, China), Rat Motilin (MTL) ELISA Kit (Shanghai Biological Technology Co., Ltd. enzyme research, EK-R30889, Shanghai, China), Rat Gastrin (GAS) ELISA Kit (Shanghai Biological Technology Co., Ltd. enzyme research, EK-R30890), Rat Superoxide Dismutase (SOD) ELISA Kit (Shanghai Jianglai Biotechnology Co., Ltd., JL22893, Shanghai, China), Rat Malondialdehyde (MDA) ELISA Kit (Shanghai Jianglai Biotechnology Co., Ltd., JL13297).

## 2.3 Grouping, modelling and drug administration

After 1 w of adaptive feeding, 36 SD rats were randomly divided into control group (C), model group (M), hesperidin low-dose group (Hes + low), hesperidin medium-dose group (Hes + medium), hesperidin high-dose group (Hes + high), and Domperidone (Dompe) group, six rats in each group. All groups, except the control group, were modelled with reference to the modified tail-clamping stimulation method (Wu et al., 2020; Li et al., 2022) for 30 min each time, 2 times/d for 4 w. The dose of gavage was calculated according to the equivalent dose formula of 60 kg adult body weight and rats, and the model group was given saline gavage at 1.5 ml/100 g, the Hes + low group, Hes + medium group, Hes + high group and Dompe group were given 50 mg/kg, 100 mg/kg, 200 mg/kg and 4.5 mg/kg aqueous solution by gavage once in the morning and once in the evening at an interval of 12 h for 4 w. Subsequently, 30 SD rats were randomly divided into control group (C), model group (M), mdivi-1 group (mdivi-1), mdivi-1+hesperidin group (mdivi-1+Hes), hesperidin group (Hes), six rats in each group. Mdivi-1 was injected intraperitoneally once every other week at a dose of 25 mg/kg, and the gavage dose for the Hes group was 100 mg/kg.

## 2.4 Preparation of semi-solid paste

5 g of sodium carboxymethyl cellulose, 8 g of skim milk powder, 4 g of starch, and 4 g of sugar were dissolved in 125 ml of distilled water, and fully mixed to make 150 ml of nutritional semi-solid paste.

## 2.5 Specimen collection and processing

After the last administration, the rats were fasted for 12 h. The next day, the rats in each group were gavaged with the semi-solid paste, and 30 min later, the rats were anesthetized with 2.5% sodium pentobarbital (2.25 ml/kg, ip), dissected along the side of the greater curvature of the stomach, and blood was removed

from the abdominal aorta by flushing with ice-cold saline, then blotted and spread on filter paper. The whole stomach was exposed, the cardia and pylorus were quickly ligated with surgical thread, the connective tissue on the surface of the stomach body was stripped, the mass of the whole stomach was weighed and recorded, the stomach was cut along the greater curvature, the stomach contents were rinsed with saline, the filter paper was blotted dry, the mass of the empty stomach was weighed and recorded, the tissue of the gastric sinus was taken, part of it was fixed in 5% glutaraldehyde and 4% paraformaldehyde respectively, part of it was extracted from the mitochondria according to the instructions of the mitochondrial extraction kit. The rest of the tissue was stored in a refrigerator at  $-80^{\circ}\text{C}$ .

## 2.6 Determination of gastric emptying rate and small intestine propulsion rate by semi-solid paste method

The whole stomach mass, empty stomach mass and semi-solid paste mass were collected and recorded, and the total length of the small intestine and the distance advanced by the semi-solid paste in the small intestine were measured and recorded and calculated according to the following formula: gastric emptying rate =  $[1 - (\text{whole stomach mass} - \text{empty stomach mass}) / \text{semi-solid paste mass}] \times 100\%$ , small intestine propulsion rate (%) =  $\text{distance of semi-solid paste advancing in small intestine} / \text{total length of small intestine} \times 100\%$  (Liang et al., 2018; Zhu et al., 2020).

## 2.7 Histopathological changes in rat gastric antrum tissue observed by H&E staining

After dewaxing, the sections were stained with hematoxylin for 2 min, rinsed with running water for 5 min, stained with eosin for 90 s, rinsed with running water for 10 min, oven at  $60^{\circ}\text{C}$  for 30 min, and sealed with neutral resin to observe the histopathological changes of the gastric antrum tissue in each group.

## 2.8 Observation of mitochondrial structure of interstitial cells of cajal in rat gastric antrum by transmission electron microscope

Gastric antrum tissues were rapidly placed in 2.5% glutaraldehyde fixation for 2 h, rinsed for 10 min  $\times$  2 times, fixed with 1% osmic acid fixative for 2 h, rinsed in double-distilled water for 10 min  $\times$  2 times, dehydrated in steps of



30% → 50% → 70% ethanol for 10 min and then block-stained in 70% ethanol containing 3% dioxin acetate at 4°C, dehydrated in steps of 80% → 95% → 100% → 100% ethanol, and after 10 min × 2 times of epichlorohydrin replacement, Epon812 embedding solution was infiltrated with propylene oxide (1:1, 2 h; 2:1, overnight), and pure Epon812 embedding solution was infiltrated at 37°C for 6 h. Sections were baked at 60°C for 48 h, electronically stained with lead citrate, and observed and photographed by TEM (Hitachi, H-7650, Japan).

## 2.9 Determination of serum motilin, gastrin, superoxide dismutase, malondialdehyde content by enzyme-linked immunosorbent assay

The contents of serum MTL, GAS, SOD and MDA in rats were determined according to the instructions of the ELISA kit. The absorbance A of each sample was read at the wavelength of 450 nm on the microplate reader, and the standard curve was plotted and the concentration value of each sample was calculated according to the curve equation.

## 2.10 Determination of mitochondrial reactive oxygen species activity in rat gastric tissues by spectrophotometer

The fluorescence intensity was measured at excitation wavelength 485 nm and emission wavelength 525 nm using a spectrophotometer, following the steps of the ROS assay kit instructions.

## 2.11 Observation of ckit, light chain 3 and VADC1, dynamin-related protein 1 and translocase of the outer mitochondrial membrane 20 expression in gastric antrum tissue by immunofluorescence

After dewaxing with xylene, the antigen was retrieved with 0.01 mol/L citrate buffer for 15 min, then cooled to room temperature naturally, washed with PBS, blocked with 10% BSA at room temperature for 1 h, primary antibodies (ckit, 1:200; LC3 and VADC1, 1:200; Drp1 and Tom20, 1:200) were added overnight at 4°C. After washing with PBS, fluorescent secondary antibodies Alexa Fluor 488-labeled goat anti-rabbit IgG (H + L) and Cy3-labeled goat anti-rat IgG (H + L) (1:200) were added, respectively. Incubated for 1 h at room temperature and protected from light, washed with PBS, and nuclei stained with DAPI for 5 min. After mounting, the expressions of ckit, LC3 and VADC1, Drp1 and Tom20 were observed with a fluorescence confocal microscope.

## 2.12 Detection the expression of ckit and mitophagy-related proteins dynamin-related protein 1, Beclin1, P62, and light chain 3 in gastric antrum tissue by western blot

Mitochondria were extracted from rat gastric antrum tissue according to the instructions of the mitochondrial extraction kit, protein concentration was determined by BCA, separated by 10% SDS-PAGE electrophoresis for 90 min, transferred by wet transfer method (300 mA, 30–90 min), and closed in 5% skimmed milk for 2 h at room temperature in a shaker, rabbit anti-ckit, Drp1, LC3, Beclin1, P62, and GAPDH (1:1000) was incubated overnight at 4°C in a refrigerator shaker; the next day, the relevant secondary antibody (1:1000) was incubated for 1 h at room temperature, the membrane was washed in TBST buffer for 10 min/time × 3 times, developed in ultra-sensitive ECL luminescent solution, and the gray value of the band was analyzed by Image J.

## 2.13 Statistical analysis

SPSS 24.0 statistical software was used for analysis, and the experimental results were expressed as mean ± standard deviation (means ± SD). One-way ANOVA was used for comparison of means among multiple groups, with  $p < 0.05$  representing a statistically significant difference.

# 3 Results

## 3.1 Effects of different doses of hesperidin on gastric motility in functional dyspepsia rats

### 3.1.1 Effects of different doses of hesperidin on pathological changes of gastric antrum in functional dyspepsia rats

The structure of the gastric antrum was clear, the mucosa was smooth, the glandular structure was regular, and the shape of the epithelial cells and the size of the interstitium of the gastric mucosa were the same in all groups; a small amount of neutrophil infiltration was seen in the model group, the different doses of Hes group, and the Dompe group, and no pathological changes such as erosion and ulceration were seen, see [Figure 1](#) for details.

### 3.1.2 Effects of different doses of hesperidin on gastric emptying rate and small intestinal propulsion rate in functional dyspepsia rats

Compared with the control group, the gastric emptying rate and small intestinal propulsion rate in the model group was significantly decreased ( $p < 0.001$ ). Compared with the model



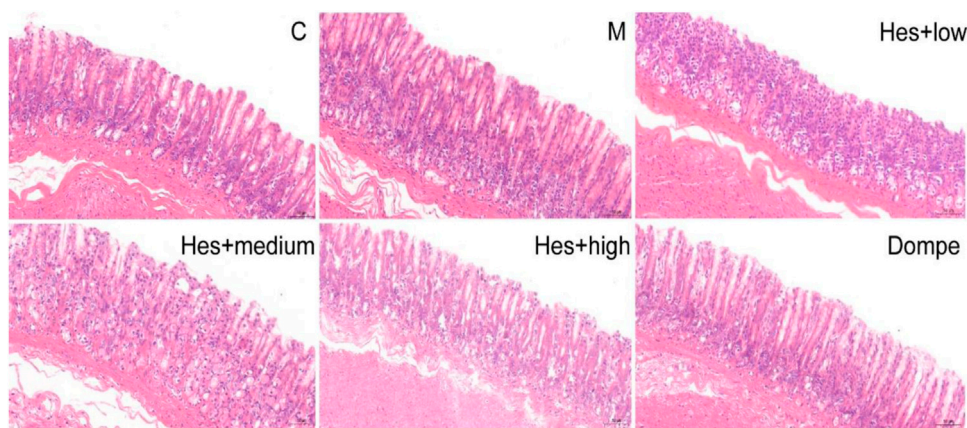


FIGURE 1

H&E staining of rat gastric antrum tissue in each group (H&E,  $\times 200$ ). C, control; M, model; Hes + low, Hesperidin + low; Hes + medium, Hesperidin + medium; Hes + high, Hesperidin + high; Dompe, Domperidone.

TABLE 1 Effects of different doses of hesperidin on gastric emptying rate and small intestinal propulsion rate in functional dyspepsia rats.

Group	n	Gastric emptying rate	Small intestinal propulsion rate
C	6	$0.62 \pm 0.11$	$0.84 \pm 0.05$
M	6	$0.36 \pm 0.09^{***}$	$0.66 \pm 0.08^{***}$
Hes + low	6	$0.39 \pm 0.05$	$0.69 \pm 0.07$
Hes + medium	6	$0.48 \pm 0.08^{\#}$	$0.77 \pm 0.05^{**}$
Hes + high	6	$0.49 \pm 0.06^{**}$	$0.79 \pm 0.05^{***}$
Dompe	6	$0.49 \pm 0.08^{\#}$	$0.78 \pm 0.05^{**}$

C, control; M, model; Hes + low, Hesperidin + low; Hes + medium, Hesperidin + medium; Hes + high, Hesperidin + high; Dompe, Domperidone. Data are presented as means  $\pm$  SD, compared with C,  $^{\#}p < 0.05$ ,  $^{**}p < 0.01$ ,  $^{***}p < 0.001$ , compared with M,  $^{\#}p < 0.05$ ,  $^{**}p < 0.01$ ,  $^{***}p < 0.001$ .

TABLE 2 Effect of different doses of hesperidin on serum motilin (MTL) and gastrin (GAS) contents in functional dyspepsia rats.

Group	n	MLT	GAS
C	6	$556.25 \pm 9.05$	$505.27 \pm 27.27$
M	6	$230.75 \pm 34.84^{***}$	$227.00 \pm 22.59^{***}$
Hes + low	6	$255.02 \pm 44.33$	$262.22 \pm 31.88$
Hes + medium	6	$399.28 \pm 14.52^{***}$	$387.10 \pm 53.15^{***}$
Hes + high	6	$345.97 \pm 11.71^{***}$	$338.98 \pm 7.40^{***}$
Dompe	6	$466.42 \pm 13.62^{***}$	$422.12 \pm 53.25^{***}$

C, control; M, model; Hes + low, Hesperidin + low; Hes + medium, Hesperidin + medium; Hes + high, Hesperidin + high; Dompe, Domperidone. MLT&GAS, pg/ml. Data are presented as means  $\pm$  SD, compared with C,  $^{\#}p < 0.05$ ,  $^{**}p < 0.01$ ,  $^{***}p < 0.001$ , compared with M,  $^{\#}p < 0.05$ ,  $^{**}p < 0.01$ ,  $^{***}p < 0.001$ .

group, the gastric emptying rate and small intestinal propulsion rate in the medium-dose Hes group, high-dose Hes group and Dompe group were significantly increased ( $p < 0.05$ ,  $p < 0.01$ ,  $p < 0.001$ ), as detailed in Table 1.

### 3.1.3 Effects of different doses of hesperidin on serum motilin and gastrin contents in functional dyspepsia rats

Compared with the control group, the serum MTL and GAS contents in model group were significantly decreased ( $p < 0.001$ ); compared with the model group, the serum MTL and GAS contents in medium-dose Hes group, high-dose Hes group and Dompe group were significantly increased ( $p < 0.001$ ), as detailed in Table 2.

### 3.1.4 Effects of different doses of hesperidin on the expression of ckit in the gastric antrum tissue of functional dyspepsia rats

Compared with the control group, the expression of ckit in the model group was significantly decreased ( $p < 0.01$ ); in comparison with the model group, which was increased in the middle-dose Hes group and Dompe group ( $p < 0.05$ ), see Figure 2 for details.

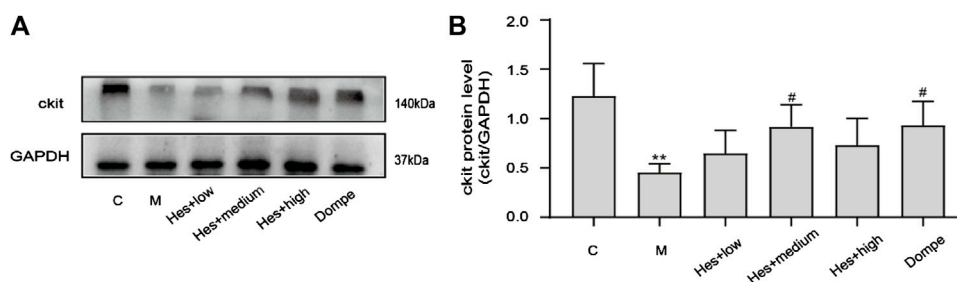


FIGURE 2

Expression of ckit in functional dyspepsia rats detected by Western blot. (A) Western blot. (B) Results of ckit Western blot. C, control; M, model; Hes + low, Hesperidin + low; Hes + medium, Hesperidin + medium; Hes + high, Hesperidin + high; Dompe, Domperidone. Data are presented as means  $\pm$  SD, compared with C, \* $p$  < 0.05, \*\* $p$  < 0.01, compared with M, # $p$  < 0.05.

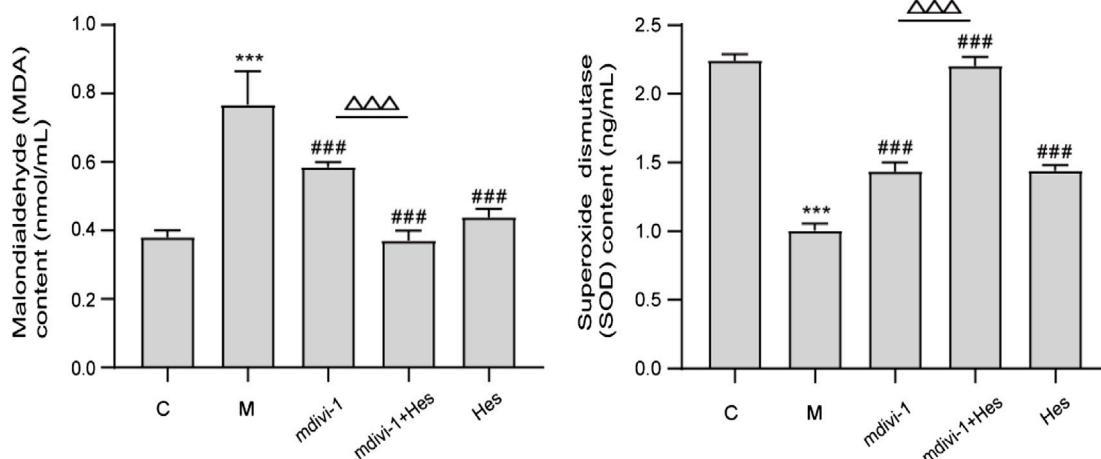


FIGURE 3

Effect of hesperidin on serum malondialdehyde (MDA) and superoxide dismutase (SOD) contents in functional dyspepsia rats. C, control; M, model; mdivi-1+Hes, mdivi-1+Hesperidin; Hes, Hesperidin; MDA, nmol/mL; SOD, ng/mL; Data are presented as means  $\pm$  SD, compared with C, \* $p$  < 0.05, \*\* $p$  < 0.01, \*\*\* $p$  < 0.001, compared with M, # $p$  < 0.05, ### $p$  < 0.01, #### $p$  < 0.001, compared with mdivi-1, ^ $p$  < 0.05, ^^^ $p$  < 0.001, ^^^^ $p$  < 0.0001.

### 3.2 Effect of hesperidin on mitochondrial damage and mitophagy of interstitial cells of cajal in functional dyspepsia rats under mdivi-1 intervention

#### 3.2.1 Effect of hesperidin on serum malondialdehyde and superoxide dismutase content in functional dyspepsia rats

Compared with the control group, the MDA content in the model group was significantly increased ( $p$  < 0.001), whereas SOD content was significantly decreased ( $p$  < 0.001); compared with the model group, the MDA content of mdivi-1 group, mdivi-1+Hes group and Hes group were significantly decreased ( $p$  < 0.001) and SOD content was significantly increased ( $p$  < 0.001); while

compared with the mdivi-1 group, the mdivi-1+Hes group had lower MDA content ( $p$  < 0.001) and higher SOD content ( $p$  < 0.001), as detailed in Figure 3.

#### 3.2.2 Effect of hesperidin on mitochondrial reactive oxygen species activity in functional dyspepsia rats

Compared with the control group, the activity of mitochondrial ROS in the model group was significantly increased ( $p$  < 0.001); compared with the model group, the activity of mitochondrial ROS in the mdivi-1 group, mdivi-1+Hes group and Hes group was significantly decreased ( $p$  < 0.001); and compared with the mdivi-1 group, mdivi-1+Hes group had lower mitochondrial ROS activity ( $p$  < 0.01), see Figure 4 for details.

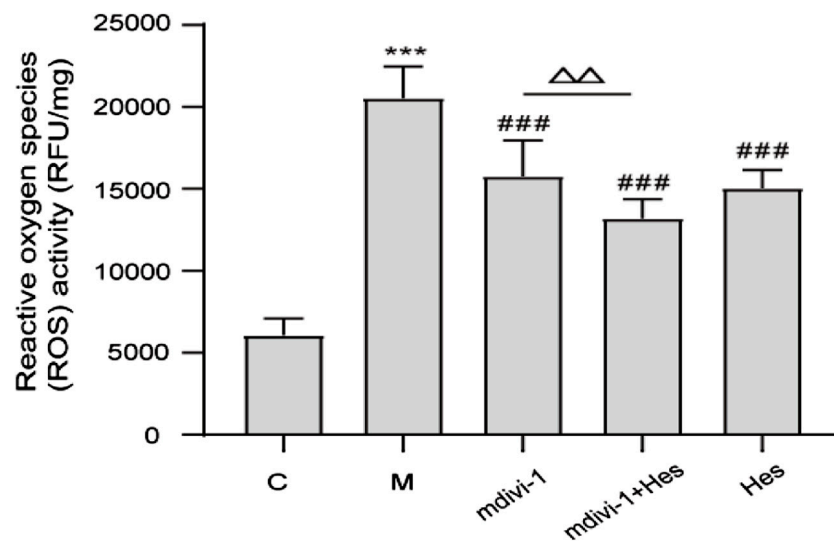


FIGURE 4

Effect of hesperidin on mitochondrial reactive oxygen species (ROS) activity in functional dyspepsia rats. C, control; M, model; mdivi-1+Hes, mdivi-1+Hesperidin; Hes, Hesperidin; ROS, RFU/mg; Data are presented as means  $\pm$  SD, compared with C, \* $p$  < 0.05, \*\* $p$  < 0.01, \*\*\* $p$  < 0.001, compared with M, # $p$  < 0.05, ## $p$  < 0.01, ### $p$  < 0.001, compared with mdivi-1,  $\Delta p$  < 0.05,  $\Delta\Delta p$  < 0.01.

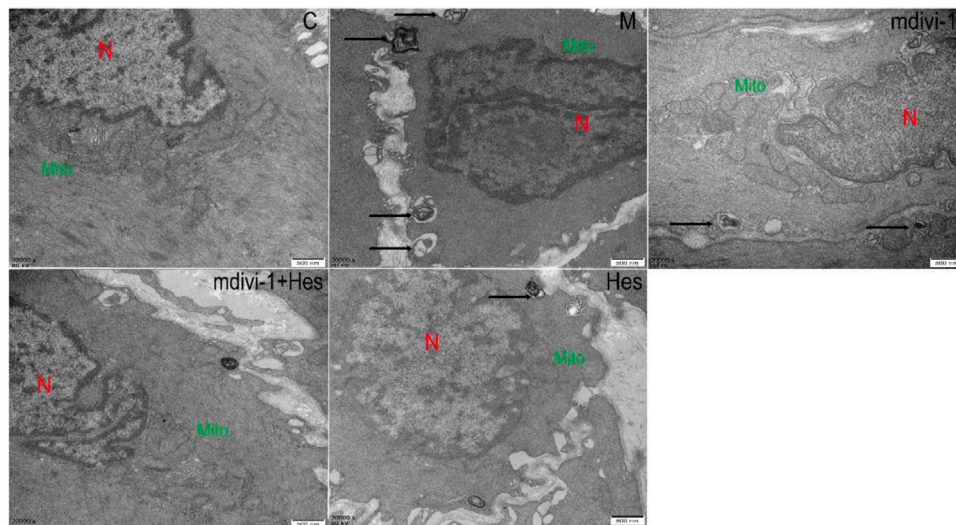


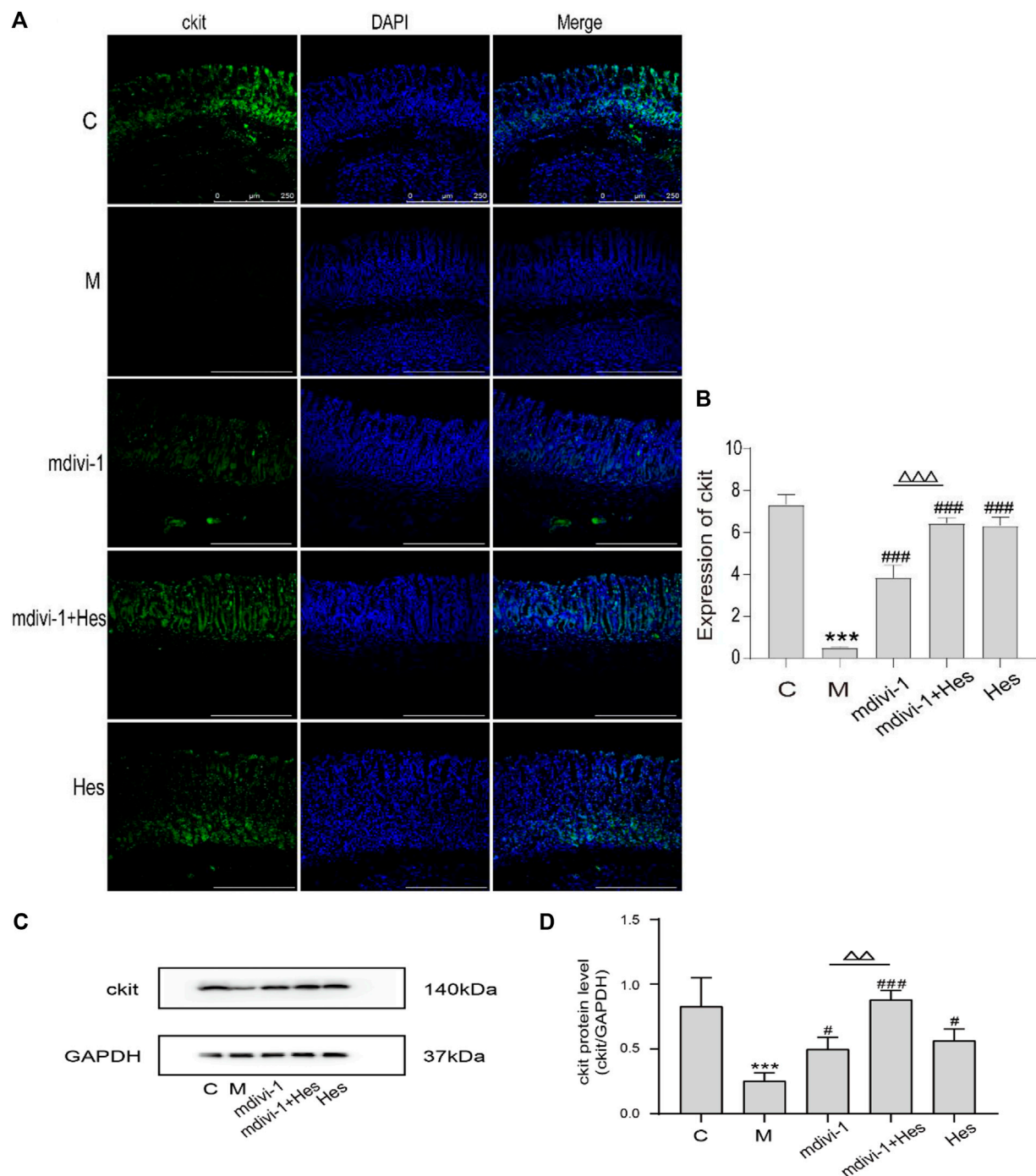
FIGURE 5

Effects of hesperidin on the ultrastructure of the interstitial cells of cajal (ICC) mitochondria in gastric antrum tissue of functional dyspepsia rats (TEM,  $\times 30000$ ). C, control; M, model; mdivi-1+Hes, mdivi-1+Hesperidin; Hes, Hesperidin. Scale bar: 500 nm, N stands for nucleus, Mito for mitochondria, and autolysosomes are marked with arrows.

### 3.2.3 Effect of hesperidin on the ultrastructure of the interstitial cells of cajal mitochondria in gastric antrum tissue of functional dyspepsia rats

In the control group, the rats had a clear morphological structure of ICC with long shuttle shape or oval shape, intact nuclear membrane, high cristae density and large number of

mitochondria in the cytoplasm. In the model group, the mitochondrial morphology was blurred, the number of mitochondria was reduced, the mitochondria were swollen and dilated, vacuolated lesions were present, and a large number of autophagic lysosomes were visible. The mdivi-1 group, mdivi-1+Hes group and Hes group were more

**FIGURE 6**

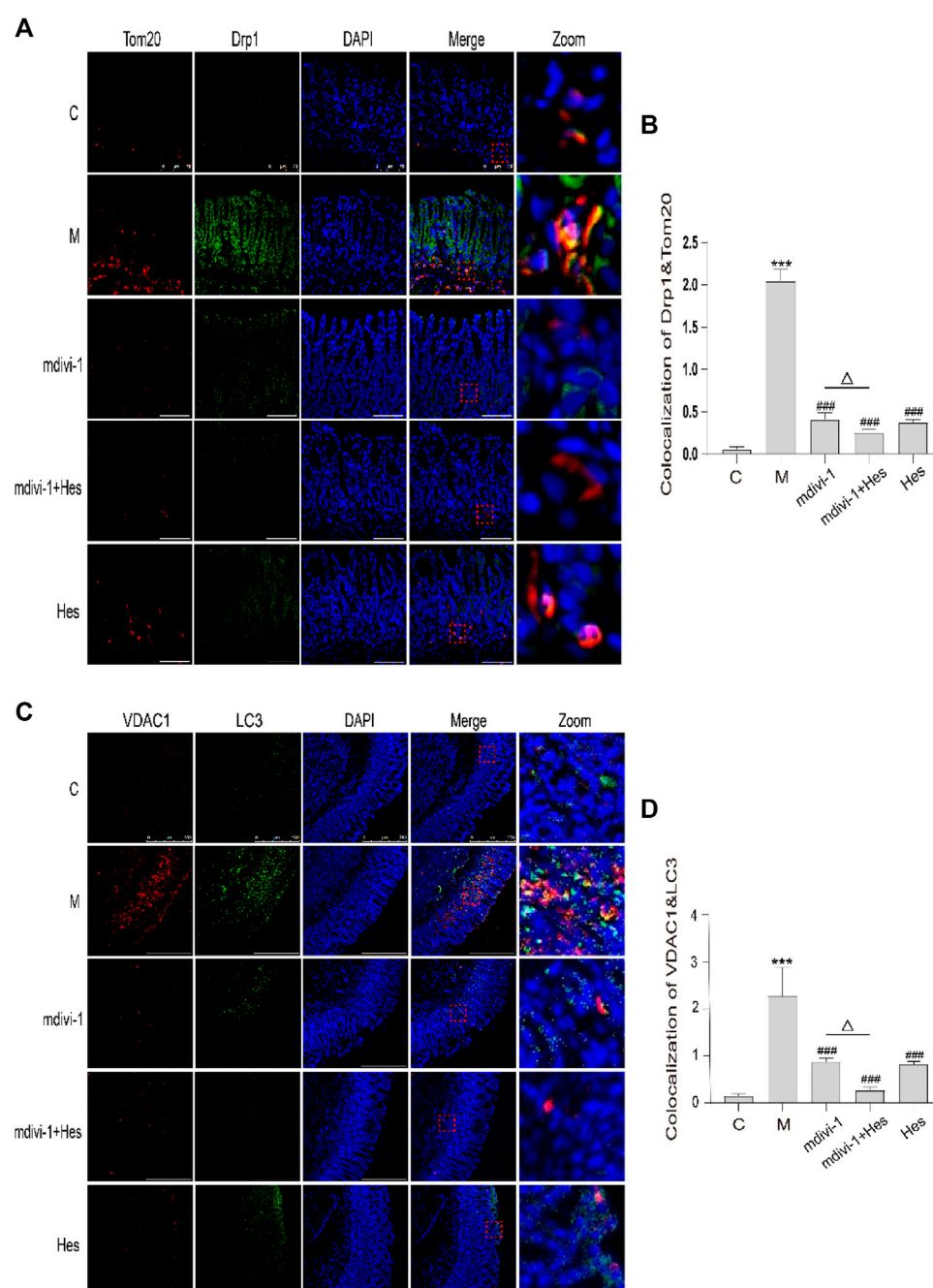
Expression of ckit in functional dyspepsia rats detected by Immunofluorescence and Western blot. **(A)** Immunofluorescence, Scale bar: 250  $\mu$ m.

**(B)** Results of ckit Immunofluorescence. **(C)** Western blot. **(D)** Results of ckit Western blot. C, control; M, model; mdivi-1+Hes, mdivi-1+Hesperidin; Hes, Hesperidin; Data are presented as means  $\pm$  SD, compared with C, \* $p$  < 0.05, \*\* $p$  < 0.01, \*\*\* $p$  < 0.001, compared with M, # $p$  < 0.05, ## $p$  < 0.01, ### $p$  < 0.001, compared with mdivi-1,  $\Delta$  $p$  < 0.05,  $\Delta\Delta$  $p$  < 0.01,  $\Delta\Delta\Delta$  $p$  < 0.001.

structurally intact, with long shuttle-shaped mitochondria, more intact nuclear membranes, higher cristae density and a small number of mitochondria splitting and fusing,

among which, a small number of autophagic lysosomes were visible in the mdivi-1 group and Hes group, as detailed in Figure 5.



**FIGURE 7**

Effects of hesperidin on the fluorescence co-localization expression of dynamin-related protein 1 (Drp1) and translocase of the outer mitochondrial membrane 20 (Tom20), microtubule associated protein 1 light chain 3 (LC3) and voltage dependent anion channel 1 (VDAC1) in gastric antrum of functional dyspepsia rats. **(A)** Immunofluorescence of Drp1 and Tom20, Scale bar: 75  $\mu$ m. **(B)** Colocalization of Drp1 and Tom20 Immunofluorescence. **(C)** Immunofluorescence of LC3 and VDAC1, Scale bar: 250  $\mu$ m **(D)** Colocalization of LC3 and VDAC1 Immunofluorescence. C, control; M, model; mdivi-1+Hes, mdivi-1+Hesperidin; Hes, Hesperidin. Data are presented as means  $\pm$  SD, compared with C, \* $p$  < 0.05, \*\* $p$  < 0.01, \*\*\* $p$  < 0.001, compared with M, # $p$  < 0.05, ## $p$  < 0.01, ### $p$  < 0.001, compared with mdivi-1,  $\Delta p$  < 0.05.



### 3.2.4 The effect of hesperidin on the expression of ckit in gastric antrum of functional dyspepsia rats

The fluorescence results showed that compared with the control group, the expression of ckit in the model group was significantly decreased ( $p < 0.001$ ); compared with the model group, the expression of ckit in the mdivi-1 group, mdivi-1+Hes group and Hes group was significantly increased ( $p < 0.001$ ); and the expression of ckit was higher in the mdivi-1+Hes group compared with the mdivi-1 group ( $p < 0.001$ ); see [Figures 6A,B](#) for details. WB results suggested that compared with the control group, the expression of ckit in the model group was significantly decreased ( $p < 0.001$ ); compared with the model group, the expression of ckit in the mdivi-1 group, mdivi-1+Hes group and Hes group was increased ( $p < 0.05$ ,  $p < 0.001$ ); and the expression of ckit was higher in the mdivi-1+Hes group compared to the mdivi-1 group ( $p < 0.01$ ), as detailed in [Figures 6C,D](#).

### 3.2.5 Effect of hesperidin on fluorescence co-localization of dynamin-related protein 1 and translocase of the outer mitochondrial membrane 20, microtubule associated protein 1 light chain 3 and voltage dependent anion channel 1 in gastric antrum of functional dyspepsia rats

Compared with the control group, the co-localization expression of Drp1 and Tom20 was significantly increased in the model group ( $p < 0.001$ ); compared with the model group, the co-localization expression was significantly decreased in the mdivi-1, mdivi-1+Hes and Hes groups ( $p < 0.001$ ); and the co-localization expression was less in the mdivi-1+Hes group compared with the mdivi-1 group ( $p < 0.05$ ), see [Figures 7A,B](#) for details. Compared with the control group, the co-localization expression of LC3 and VDAC1 was increased in the model group ( $p < 0.001$ ); LC3 and VDAC1 co-localization expression was decreased in the mdivi-1, mdivi-1+Hes and Hes groups compared with the model group ( $p < 0.001$ ); and less co-localization expression was observed in the mdivi-1+Hes group compared to the mdivi-1 group ( $p < 0.05$ ), as detailed in [Figures 7C,D](#).

### 3.2.6 Effects of hesperidin on the protein expression of mitochondrial dynamin-related protein 1, P62, Beclin1, and light chain 3 in functional dyspepsia rats

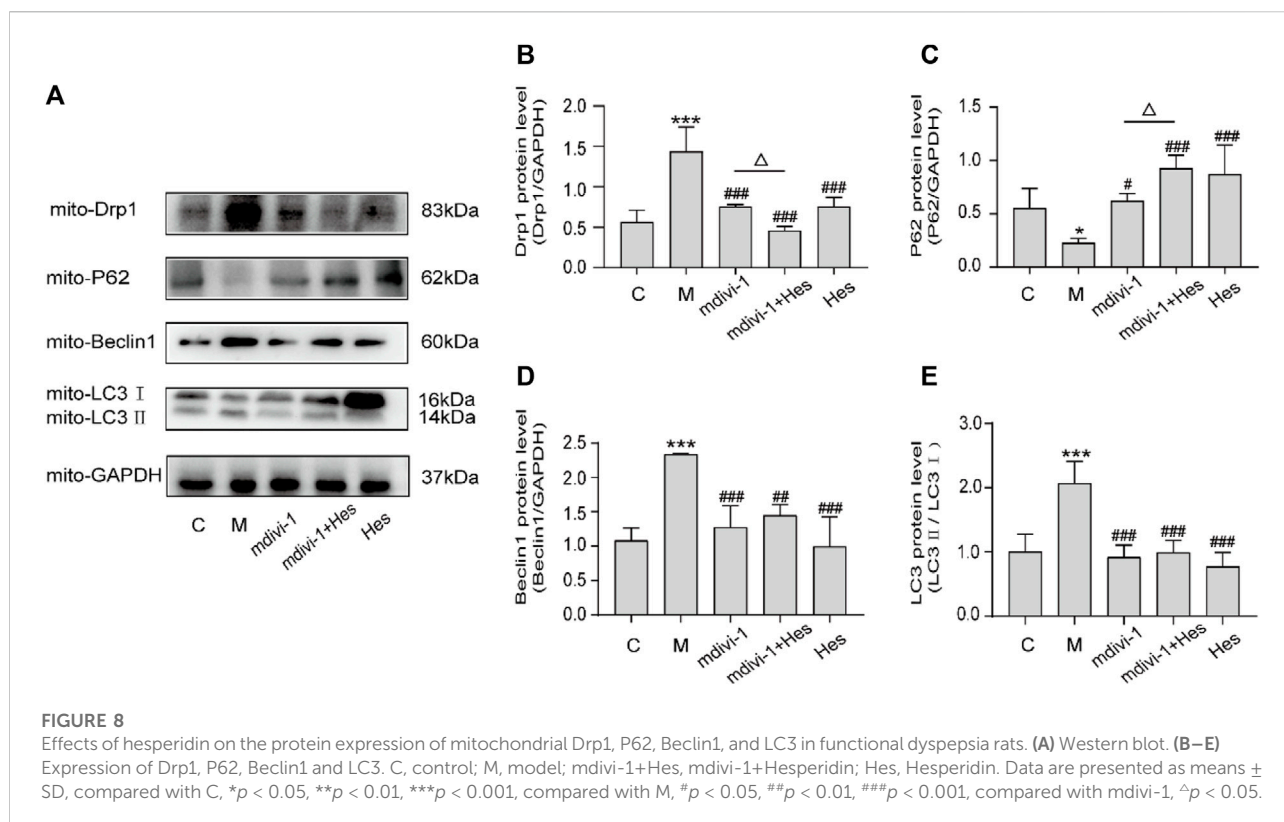
Compared with the control group, the protein expressions of mitochondrial Drp1, Beclin1, and LC3 in the model group were significantly increased ( $p < 0.001$ ), and the protein expression of P62 was decreased ( $p < 0.05$ ); compared with the model group, the protein expressions of Drp1, Beclin1, LC3 in the mdivi-1, mdivi-1+Hes and Hes groups were decreased significantly ( $p < 0.01$ ,  $p < 0.001$ ) and the protein expression of P62 was

significantly higher ( $p < 0.05$ ,  $p < 0.001$ ); and compared with the mdivi-1 group, the mdivi-1+Hes group had lower Drp1 expression ( $p < 0.05$ ) and higher P62 protein expression ( $p < 0.05$ ), as detailed in [Figure 8](#).

## 4 Discussion

The incidence of functional dyspepsia (FD) accounts for approximately 20–40% of gastroenterology outpatient visits and seriously affects the quality of life of patients ([Ohara et al., 2011](#); [Jin and Son, 2018](#)). Related studies have shown that gastrointestinal hormones such as motilin (MTL) and gastrin (GAS) play an important role in the occurrence and development of FD ([Zhao et al., 2015](#); [Deng et al., 2018](#)). MTL can induce enhanced smooth muscle movement of the gastrointestinal tract, promote gastrointestinal peristalsis, and accelerate gastric emptying; GAS acts on almost the entire gastrointestinal tract, promoting contraction of the gastric antrum and gastric body, increasing GAS acts on almost the entire gastrointestinal tract, promotes the contraction of the gastric antrum and gastric body, increases the movement of the gastrointestinal tract, and also promotes the proliferation of the epithelium of the gastrointestinal mucosa. Domperidone improves postprandial epigastric distension, epigastric pain, belching and early satiety in FD patients, and therefore serves as a positive control drug ([Shokry-Shirvani et al., 2012](#)). In this study, H&E staining indicated that no significant organic changes were seen in the gastric antrum tissue of rats in each group, and the gastric emptying rate and small intestine propulsion rate of rats in the model group were significantly lower than those in the control group, which was consistent with the disease characteristics of FD and suggested successful modeling. Compared with the control group, the serum MTL and GAS contents decreased, and ckit protein expression decreased in the model group; after hesperidin intervention, the serum MTL and GAS levels increased, and ckit protein expression increased. Therefore, hesperidin can effectively promote gastric motility in FD rats, and the medium-dose hesperidin was selected for follow-up experiments.

As the main site of reactive oxygen species (ROS) production in cells, mitochondria are responsible for intracellular redox signaling regulation and maintenance of oxidative homeostasis through a range of antioxidants ([Zorov et al., 2014](#)). Oxidative stress can increase ROS and decrease the formation of antioxidant defenses. The reduction in the activity of antioxidant enzymes such as superoxide dismutase (SOD) promotes oxidative attack on cells. Once the redox balance is disrupted, SOD reacts with oxygen molecules and scavenges superoxide anions that are harmful to the organism thus achieving antioxidant stress ([Liu et al., 2020](#); [Dokumacioglu et al., 2021](#)). Malondialdehyde (MDA) is the carbonyl group



produced during lipid peroxidation and is widely used to determine oxidative stress. SOD activity decreases during oxidative stress and produces excess lipid peroxidation product MDA, which can indirectly reflect the degree of mitochondrial peroxidative damage (Tian et al., 2019; Dokumacioglu et al., 2021). The results of this study showed that compared with the control group, the serum MDA content of the model group was increased, the SOD content was decreased, and the mitochondrial ROS level was increased. Transmission electron microscopy (TEM) showed a decrease in the number of mitochondria, swollen and dilated morphology, and even vacuoles in the model group, indicating oxidative stress and mitochondrial damage in the ICC mitochondria of FD rats. Previous studies have further shown that after mdivi-1 intervention, dynamin-related protein 1 (DRP1) is activated by GTPase hydrolysis and oligomerized around the outer mitochondrial outer membrane, which triggers fission and mitochondrial fracture (Rovira-Llopis et al., 2017; Fonseca et al., 2019). The delicate balance between mitochondrial fission and fusion events is disturbed by elevated Drp1 levels, which promotes mitochondrial fission and ultimately impairs mitochondrial function, leading to increased ROS production (Kim et al., 2016; Roy and Sesaki, 2021). If Drp1 protein expression was increased in human umbilical vein endothelial cells under high glucose conditions, increased mitochondrial ROS production and decreased SOD activity induced further mitochondrial fission and apoptosis (Hao et al., 2019). The

results of this study suggested that mdivi-1 intervention reduced mitochondrial ROS and serum MDA levels and increased serum SOD content in gastric antrum tissue compared with the model group, and the morphological structure of ICC mitochondria was clearer and the nuclear membrane was more intact under TEM, suggesting that mdivi-1 intervention could reduce mitochondrial oxidative stress in FD rats. The results of the hesperidin group were similar to those of the mdivi-1 group. However, the mdivi-1+hesperidin group had the lowest ROS and MDA, the highest SOD content, and better morphological structure of ICC mitochondria, suggesting that hesperidin could further reduce mitochondrial oxidative stress and improve mitochondrial damage in FD rats under mdivi-1 intervention.

Mitophagy is a normal physiological activity of cells and is one of the forms of cellular autophagy. Mitophagy refers to the damage that occurs when mitochondria are depolarized in response to external stimuli such as oxidative damage/nutrient deficiency/cellular senescence, and the damaged mitochondria are characteristically encapsulated into autophagosomes and fused with lysosomes, thus completing the degradation of the damaged mitochondria and maintaining intracellular environmental homeostasis. Mitophagy involves three main stages: mitochondrial division, autophagosome assembly and fusion with lysosomes to degrade the damaged mitochondria (Patergnani and Pinton, 2015; Springer and Macleod, 2016; Ma

et al., 2020). TEM suggested that a large number of autophagic lysosomes were visible in ICC cells of the model group compared with the control group; compared with the model group, only a few autophagic lysosomes were visible in the mdivi-1 and hesperidin groups, and no autophagic lysosomes were seen in the mdivi-1+hesperidin group. To further confirm whether the mitochondria were wrapped by autophagosomes, we co-localized the expression of Drp1, a key protein regulating mitophagy, with the mitochondrial marker Tom20; the mitochondrial outer membrane protein VDAC1 and the autophagosomal marker protein LC3 by Immunofluorescence. Compared with the control group, the co-localized expression of Drp1 and Tom20, LC3 and VDAC1 in the model group increased; while the co-localized expression of those in the mdivi-1 group, mdivi-1+hesperidin group and hesperidin group decreased, indicating that mdivi-1 acts as an inhibitor of mitochondrial splitting proteins and reduces mitophagy, and the mitophagy was also significantly improved in the hesperidin group, with the best synergistic effect of hesperidin and mdivi-1, thus revealing that hesperidin could further improve mitophagy in ICC of FD rats under the intervention of mdivi-1.

Drp1 can interact with LC3 and thus induce mitophagy (Wu et al., 2016). LC3 is a marker of mitophagy, and when mitophagy occurs, LC3I is modified by ubiquitination and binds to phosphatidylethanolamine on the surface of autophagic vesicles to form LC3II, which is localized on the surface of autophagosomal membranes, and LC3II and LC3II/LC3I represent to some extent the level of mitochondrial autophagy in the body (Chifenti et al., 2013). P62, a specific substrate for mitophagy, directly binds LC3 and is selectively degraded by autophagy, negatively regulating mitochondrial autophagic activity (Sulkshane et al., 2021). Beclin1 promotes the conversion of LC3I to LC3II and accelerates the fusion of autophagosomes with lysosomes, activating mitophagy, and is a key factor in evaluating mitochondrial autophagic activity (Jakhar et al., 2016). The results revealed that the protein expressions of mitochondrial Drp1, LC3, and Beclin-1 were down-regulated and the expression of P62 protein was increased after mdivi-1 or hesperidin intervention compared with the model group; the expression of ckit in gastric antrum tissues was increased. Mdivi-1, as an inhibitor of mitochondrial splitting proteins, was seen to reduce mitochondrial autophagy and thus exert a pro-gastric motility effect. In the mdivi-1+hesperidin group, the expression of mitochondrial Drp1 protein was lower and the expression of P62 protein was higher; the expression of ckit protein in the gastric antrum tissues was further up-regulated. The above results indicated that mdivi-1 synergistically regulated Drp1-mediated mitochondrial autophagy with hesperidin.

In conclusion, we believe that hesperidin can enhance mitochondrial activity, inhibit ICC mitophagy, and promote

gastric motility in FD rats through the Drp1 signaling pathway, thus effectively preventing and treating FD.

## Data availability statement

The raw data supporting the conclusion of this article will be made available by the authors, without undue reservation.

## Ethics statement

The animal study was reviewed and approved by the Animal Ethics Committee of Shanghai University of Traditional Chinese Medicine.

## Author contributions

JL and GC conceived and designed the study; QJ and LL completed the experiments and collected the data; XW, YW, KJ, KY, and JC prepared the figures and revised the initial manuscript. All authors have read and approved the published version of the manuscript.

## Funding

The work was supported by the National Natural Science Foundation of China (grant No. 82174309 and No. 81973774); the National Administration of TCM: 2019 Project of building evidence based practice capacity for TCM (grant No. ZZ13-042-2, No. 2019XZZX-XH013).

## Conflict of interest

The authors declare that the research was conducted in the absence of any commercial or financial relationships that could be construed as a potential conflict of interest.

## Publisher's note

All claims expressed in this article are solely those of the authors and do not necessarily represent those of their affiliated organizations, or those of the publisher, the editors and the reviewers. Any product that may be evaluated in this article, or claim that may be made by its manufacturer, is not guaranteed or endorsed by the publisher.

## References

- Asano, H., Tomita, T., Nakamura, K., Yamasaki, T., Okugawa, T., Kondo, T., et al. (2017). Prevalence of gastric motility disorders in patients with functional dyspepsia. *J. Neurogastroenterol. Motil.* 23, 392–399. doi:10.5056/jnm16173
- Bigonja, P., and Singh, K. (2014). Ulcer protective potential of standardized hesperidin, a citrus flavonoid isolated from Citrus sinensis. *Rev. Bras. Farmacogn.* 24 (3), 330–340. doi:10.1016/j.bjp.2014.07.011
- Chifenti, B., Locci, M. T., Lazzeri, G., Guagnozzi, M., Dinucci, D., Chiellini, F., et al. (2013). Autophagy-related protein LC3 and Beclin-1 in the first trimester of pregnancy. *Clin. Exp. Reprod. Med.* 40 (1), 33–37. doi:10.5653/term.2013.40.1.33
- Deng, Y., Zhou, X., Xiang, X., Ou, Y., and He, J. (2018). Effect of miRNA-19a on gastrointestinal motility in rats with functional dyspepsia. *Exp. Ther. Med.* 15 (6), 4875–4879. doi:10.3892/etm.2018.6009
- Dokumacioglu, E., Duzcan, I., Iskender, H., and Sahin, A. (2021). RhoA/ROCK-1 signaling pathway and oxidative stress in coronary artery disease patients. *Braz. J. Cardiovasc. Surg.* 1–7, 212–218. doi:10.21470/1678-9741-2020-0525
- Duan, C., Wang, L., Zhang, J., Xiang, X., Wu, Y., Zhang, Z., et al. (2020). Mdivi-1 attenuates oxidative stress and exerts vascular protection in ischemic/hypoxic injury by a mechanism independent of Drp1 GTPase activity. *Redox Biol.* 37, 101706. doi:10.1016/j.redox.2020.101706
- Fonseca, T. B., Sanchez-Guerrero, A., Milosevic, I., and Raimundo, N. (2019). Mitochondrial fission requires DRP1 but not dynamin. *Nature* 570, E34–E42. doi:10.1038/s41586-019-1296-y
- Hagger, R., Finlayson, C., Jeffrey, I., and Kumar, D. (1997). Role of the interstitial cells of Cajal in the control of gut motility. *Br. J. Surg.* 84, 445–450. doi:10.1046/j.1365-2168.1997.02736.x
- Hao, Y., Liu, H., Wei, X., Gong, X., Lu, Z., Huang, Z., et al. (2019). Diallyl trisulfide attenuates hyperglycemia-induced endothelial apoptosis by inhibition of Drp1-mediated mitochondrial fission. *Acta Diabetol.* 56, 1177–1189. doi:10.1007/s00592-019-01366-x
- Iranshahi, M., Rezaee, R., Parhiz, H., Roohbakhsh, A., and Soltani, F. (2015). Protective effects of flavonoids against microbes and toxins: the cases of hesperidin and hesperetin. *Life Sci.* 137, 125–132. doi:10.1016/j.lfs.2015.07.014
- Jakhar, R., Paul, S., Bhardwaj, M., and Kang, S. C. (2016). Astemizole-Histamine induces Beclin-1-independent autophagy by targeting p53-dependent crosstalk between autophagy and apoptosis. *Cancer Lett.* 372 (1), 89–100. doi:10.1016/j.canlet.2015.12.024
- Jin, M., and Son, M. (2018). DA-9701 (motilitone): a multi-targeting botanical drug for the treatment of functional dyspepsia. *Int. J. Mol. Sci.* 19, 4035. doi:10.3390/ijms19124035
- Kim, B., Park, J., Chang, K. T., and Lee, D. S. (2016). Peroxiredoxin 5 prevents amyloid-beta oligomer-induced neuronal cell death by inhibiting ERK-Drp1-mediated mitochondrial fragmentation. *Free Radic. Biol. Med.* 90, 184–194. doi:10.1016/j.freeradbiomed.2015.11.015
- Kim, S. E., Kim, N., Lee, J. Y., Park, K. S., Shin, J. E., Nam, K., et al. (2018). Prevalence and risk factors of functional dyspepsia in health check-up population: a nationwide multicenter prospective study. *J. Neurogastroenterol. Motil.* 24 (4), 603–613. doi:10.5056/jnm18068
- Li, N., Wang, H., Jiang, C., and Zhang, M. (2018). Renal ischemia/reperfusion-induced mitophagy protects against renal dysfunction via Drp1-dependent pathway. *Exp. Cell Res.* 369 (1), 27–33. doi:10.1016/j.yexcr.2018.04.025
- Li, W., Ji, L., Jin, L., Lei, W., Dong, W., Jun, Y., et al. (2022). Auricular vagus nerve stimulation ameliorates Functional Dyspepsia with depressive-like behavior and inhibits the Hypothalamus-Pituitary-Adrenal axis in a rat model. *Dig. Dis. Sci.* 1–13. doi:10.1007/s10620-021-07332-4
- Liang, Q., Yan, Y., Mao, L., Du, X., Liang, J., Liu, J., et al. (2018). Evaluation of a modified rat model for functional dyspepsia. *Saudi J. Gastroenterol.* 24 (4), 228–235. doi:10.4103/sjg.SJG\_505\_17
- Liu, Z., Wang, X., Li, L., Wei, G., and Zhao, M. (2020). Hydrogen sulfide protects against paraquat-induced acute liver injury in rats by regulating oxidative stress, mitochondrial function, and inflammation. *Oxid. Med. Cell. Longev.* 2020, 6325378. doi:10.1155/2020/6325378
- Luo, X., Liu, R., Zhang, Z., Chen, Z., He, J., Liu, Y., et al. (2019). Mitochondrial division inhibitor 1 attenuates mitophagy in a rat model of acute lung injury. *Biomed. Res. Int.* 2019, 2193706. doi:10.1155/2019/2193706
- Ma, M., Lin, X., Liu, H., Zhang, R., and Chen, R. (2020). Suppression of DRP1-mediated mitophagy increases the apoptosis of hepatocellular carcinoma cells in the setting of chemotherapy. *Oncol. Rep.* 43, 1010–1018. doi:10.3892/or.2020.7476
- Mishra, P. K., Nandi, S., and Chavali, V. (2014). Mdivi-1 mitigates cardiac dysfunction by attenuating mitophagy in diabetes (1155.3). *FASEB J.* 28 (51), 1155. doi:10.1096/fasebj.28.1\_supplement.1155.3
- Naganuma, S., Shiina, T., Yasuda, S., Suzuki, Y., and Shimizu, Y. (2017). Histamine-enhanced contractile responses of gastric smooth muscle via interstitial cells of Cajal in the Syrian hamster. *Neurogastroenterol. Motil.* 30 (4), e13255. doi:10.1111/nmo.13255
- Ohara, S., Kawano, T., Kusano, M., and Kouzu, T. (2011). Survey on the prevalence of GERD and FD based on the Montreal definition and the Rome III criteria among patients presenting with epigastric symptoms in Japan. *J. Gastroenterol.* 46 (5), 603–611. doi:10.1007/s00535-011-0382-1
- Parhiz, H., Roohbakhsh, A., Soltani, F., Rezaee, R., and Iranshahi, M. (2015). Antioxidant and anti-inflammatory properties of the citrus flavonoids hesperidin and hesperetin: an updated review of their molecular mechanisms and experimental models. *Phytother. Res.* 29 (3), 323–331. doi:10.1002/ptr.5256
- Patergnani, S., and Pinton, P. (2015). Mitophagy and mitochondrial balance. *Methods Mol. Biol.* 1241, 181–194. doi:10.1007/978-1-4939-1875-1\_15
- Rovira-Llopis, S., Banuls, C., Diaz-Morales, N., Hernandez-Mijares, A., Rocha, M., Victor, V. M., et al. (2017). Mitochondrial dynamics in type 2 diabetes: pathophysiological implications. *Redox Biol.* 11, 637–645. doi:10.1016/j.redox.2017.01.013
- Roy, S., and Sesaki, H. (2021). Reduced levels of Drp1 protect against development of retinal vascular lesions in diabetic retinopathy. *Cells* 10, 1379. doi:10.3390/cells10061379
- Shokry-Shirvani, J., Taheri, H., Shad, E., Bijani, A., and Kashifard, M. (2012). Efficacy of domperidone and pyridostigmine in the treatment of patients with functional dyspepsia: a randomized clinical trial. *Govaresh* 17 (1), 7–12. doi:10.1007/s11655-010-0009-z
- Springer, M. Z., and Macleod, K. F. (2016). In brief: mitophagy: mechanisms and role in human disease. *J. Pathol.* 240 (3), 253–255. doi:10.1002/path.4774
- Streutker, C. J., Huizinga, J. D., Driman, D. K., and Riddell, R. H. (2007). Interstitial cells of Cajal in health and disease. Part I: normal ICC structure and function with associated motility disorders. *Histopathology* 50 (2), 176–189. doi:10.1111/j.1365-2559.2006.02493.x
- Sulkshane, P., Ram, J., Thakur, A., Reis, N., Kleinfeld, O., Glickman, M. H., et al. (2021). Ubiquitination and receptor-mediated mitophagy converge to eliminate oxidation-damaged mitochondria during hypoxia. *Redox Biol.* 45, 102047. doi:10.1016/j.redox.2021.102047
- Talley, N. J., and Ford, A. C. (2015). Functional dyspepsia. *N. Engl. J. Med.* 373 (19), 1853–1863. doi:10.1056/NEJMr1501505
- Tan, R., Zhang, Z., Ju, J., and Ling, J. (2019). Effect of chaihui shugan powder-contained serum on glutamate-induced autophagy of interstitial cells of cajal in the rat gastric antrum. *Evid. Based. Complement. Altern. Med.* 2019, 7318616. doi:10.1155/2019/7318616
- Tian, L., Cao, W., Yue, R., Yuan, Y., Guo, X., Qin, D., et al. (2019). Pretreatment with Tiliandrin improves mitochondrial energy metabolism and oxidative stress in rats with myocardial ischemia/reperfusion injury via AMPK/SIRT1/PGC-1 alpha signaling pathway. *J. Pharmacol. Sci.* 139 (4), 352–360. doi:10.1016/j.jphs.2019.02.008
- Tian, M., Han, Y., Zhao, C., Liu, L., and Zhang, F. (2021). Hesperidin alleviates insulin resistance by improving HG-induced oxidative stress and mitochondrial dysfunction by restoring miR-149. *Diabetol. Metab. Syndr.* 13, 50. doi:10.1186/s13098-021-00664-1
- Torihashi, S., Ward, S. M., Nishikawa, S., Nishi, K., Kobayashi, S., Sanders, K. M., et al. (1995). c-kit-dependent development of interstitial cells and electrical activity in the murine gastrointestinal tract. *Cell Tissue Res.* 280 (1), 97–111. doi:10.1007/BF00304515
- Wu, M., Li, Y., and Gu, Y. (2019). Hesperidin improves colonic motility in Loeramide-induced constipation rat model via 5-Hydroxytryptamine 4R/cAMP signaling pathway. *Digestion* 101 (6), 692–705. doi:10.1159/000501959
- Wu, W., Lin, C., Wu, K., Jiang, L., Wang, X., Li, W., et al. (2016). FUNDC1 regulates mitochondrial dynamics at the ER-mitochondrial contact site under hypoxic conditions. *Embo. J.* 35 (13), 1368–1384. doi:10.15252/embj.201593102
- Wu, Z., Lu, X., Zhang, S., and Zhu, C. (2020). Sini-San regulates the NO-cGMP-PKG pathway in the spinal dorsal horn in a modified rat model of Functional Dyspepsia. *Evid. Based. Complement. Altern. Med.* 3, 3575231. doi:10.1155/2020/3575231
- Zhao, X., Suo, H., Qian, Y., Li, G., Liu, Z., Li, J., et al. (2015). Therapeutic effects of Lactobacillus casei Qian treatment in activated carbon-induced constipated mice. *Mol. Med. Rep.* 12 (2), 3191–3199. doi:10.3892/mmr.2015.3737
- Zhu, J., Tong, H., Ye, X., Zhang, J., Huang, Y., Yang, M., et al. (2020). The effects of low-dose and high-dose decoctions of Fructus aurantii in a rat model of functional dyspepsia. *Med. Sci. Monit.* 26, e919815. doi:10.12659/MSM.919815
- Zorov, D., Juhaszova, M., and Sollott, S. (2014). Mitochondrial reactive oxygen species (ROS) and ROS-induced ROS release. *Physiol. Rev.* 94 (3), 909–950. doi:10.1152/physrev.00026.2013





## OPEN ACCESS

## EDITED BY

Maria Dimitrova,  
Medical University Sofia, Bulgaria

## REVIEWED BY

Peng Wang,  
Anhui Medical University, China  
Sizhi Ai,  
The First Affiliated Hospital of Xinxiang  
Medical University, China

## \*CORRESPONDENCE

Wei Li,  
wli@cmu.edu.cn

## SPECIALTY SECTION

This article was submitted to  
Gastrointestinal and Hepatic  
Pharmacology,  
a section of the journal  
Frontiers in Pharmacology

RECEIVED 21 March 2022

ACCEPTED 06 July 2022

PUBLISHED 16 August 2022

## CITATION

Bao W, Qi L, Bao Y, Wang S and Li W  
(2022), Alleviating insomnia should  
decrease the risk of irritable bowel  
syndrome: Evidence from  
Mendelian randomization.  
*Front. Pharmacol.* 13:900788.  
doi: 10.3389/fphar.2022.900788

## COPYRIGHT

© 2022 Bao, Qi, Bao, Wang and Li. This is  
an open-access article distributed  
under the terms of the [Creative  
Commons Attribution License \(CC BY\)](#).  
The use, distribution or reproduction in  
other forums is permitted, provided the  
original author(s) and the copyright  
owner(s) are credited and that the  
original publication in this journal is  
cited, in accordance with accepted  
academic practice. No use, distribution  
or reproduction is permitted which does  
not comply with these terms.

# Alleviating insomnia should decrease the risk of irritable bowel syndrome: Evidence from Mendelian randomization

Wenzhao Bao<sup>1</sup>, Li Qi<sup>2</sup>, Yin Bao<sup>1</sup>, Sai Wang<sup>2</sup> and Wei Li<sup>2\*</sup>

<sup>1</sup>Department of Anesthesiology, The Affiliated Hospital of Inner Mongolia University for the Nationalities, Tongliao, China, <sup>2</sup>Department of Otorhinolaryngology, The First Hospital of China Medical University, Shenyang, China

**Background:** Associations have been reported between sleep and irritable bowel syndrome (IBS). However, whether there exists a causation between them is still unknown.

**Methods:** We employed the Mendelian randomization (MR) design to explore the causal relationship between sleep and IBS. All genetic associations with sleep-related traits reached genome-wide significance ( $p$ -value  $< 5 \times 10^{-8}$ ). The genetic associations with IBS were obtained from two independent large genome-wide association studies (GWAS), where non-FinnGen GWAS was in the discovery stage and FinnGen GWAS was in the validation stage. Primarily, the inverse-variance weighted method was employed to estimate the causal effects, and a meta-analysis was performed to combine the MR estimates.

**Results:** In the discovery, we observed that genetic liability to the “morning” chronotype could lower the risk of IBS [OR = 0.81 (0.76, 0.86)]. Also, the genetic liability to insomnia can increase the risk of IBS [OR = 2.86 (1.94, 4.23)] and such causation was supported by short sleep duration. In the validation stage, only insomnia displayed statistical significance [OR = 2.22 (1.09, 4.51)]. The meta-analysis suggested two genetically-determined sleep exposures can increase the risk of IBS, including insomnia [OR = 2.70 (1.92, 3.80)] and short sleep duration [OR = 2.46 (1.25, 4.86)]. Furthermore, the multivariable MR analysis suggested insomnia is an independent risk factor for IBS after adjusting for chronotype [OR = 2.32 (1.57, 3.43)] and short sleep duration [OR = 1.45 (1.13, 1.85)]. IBS cannot increase the risk of insomnia in the reverse MR analysis.

**Conclusion:** Genetic susceptibility to insomnia can increase the risk of IBS, and improving sleep quality, especially targeting insomnia, can help to prevent IBS.

**Abbreviations:** IBS, irritable bowel syndrome; MR, Mendelian randomization; GWAS, genome-wide association study; IV, instrument variable; SNP, single nucleotide polymorphism; IVW, inverse variance weighted; FDR, false discovery rate; CRP, C-reactive protein.



# KEYWORDS

sleep disorder, insomnia, irritable bowel syndrome, Mendelian randomization, causal inference

## Introduction

Irritable bowel syndrome (IBS) is a chronic functional disorder of the lower gastrointestinal tract with symptoms including abdominal pain, constipation, or diarrhea. There is a higher prevalence of IBS where up to 20% of the population is affected in their lives (Ford et al., 2020). The patients are mainly young and middle-aged. However, its etiology and pathogenesis are still unclear, which may relate to genetics, intestinal motility, the mental system, psychological stress, infection, and chronic inflammation. In addition to drug therapy, several therapies can alleviate the symptoms of IBS, including dietary adjustment, and psychological and behavioral therapy (Vasant et al., 2021). Therefore, a clear understanding of its risk factors is conducive to identifying the mechanism of IBS considering there is no clear and effective therapeutic schedule for IBS and the disease-associated burden on the health service is heavy (Ford et al., 2020).

Sleep occupies almost 1/3 of our lives. Good quality sleep is essential to maintain physical and mental health (Stern, 2021). Sleep plays an important role in human growth and development, metabolism, and memory function, besides, cardiovascular diseases and metabolic diseases will also be affected by sleep disorders (Ai and Dai, 2018; Ai et al., 2021; Song et al., 2021). A recent study implicated frequent daytime napping should have deleterious effects on cardiometabolic traits and daytime napping shared genetic loci with both cardiometabolic and neurodegenerative traits (Dashti et al., 2021). In addition, insomnia has been identified as an important predictor of depression, anxiety, and neuropathy (Lane et al., 2019). Sleep disorders have been reported to be associated with IBS and may account for a proportion of its pathogenesis (Vege et al., 2004; Wang et al., 2018). For instance, the alterations in day-night rhythms could upregulate circulating cytokines *via* triggering sleep disruption, increasing the risk of IBS (Orr et al., 2020). Furthermore, obstructive sleep apnea, usually accompanied by snoring, was also associated with an increased risk of IBS (Rotem et al., 2003; Orr et al., 2020). However, the causal relationship between different types of sleep disorders and IBS remains poorly understood.

Mendelian randomization (MR) studies used genetic variants to verify causal associations between the predefined exposure and outcome (Emdin et al., 2017). This approach is based on a simple principle: if an exposure trait is a risk factor for a kind of disease, then the locus of genetic variation representing that exposure will also be associated with the disease *via* the exposure. Due to the principle of random allocation during meiosis, gene variant loci are usually inherited stably and independently

of disease status and environment. Based on these assumptions, the MR design is thus similar to randomized controlled trials in clinical practice and is easier to avoid confounding factors and reverse causation to some extent.

In this study, we used the two-sample MR to explore the causal association between eight different sleep disorders and IBS, hoping to clarify the correlation between sleep disorders and IBS and provide novel insights into the prevention and treatment of IBS.

## Methods

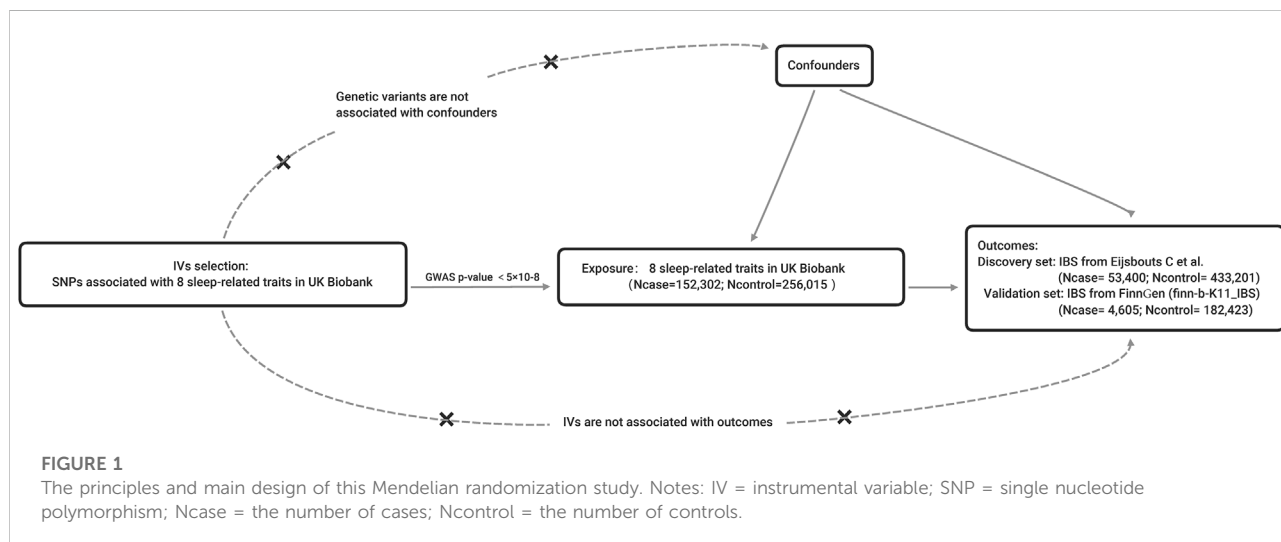
### Data source description

A total of eight sleep-related exposures were included in this study, namely, insomnia, sleep duration (continuous variable), long sleep duration (binary variable), short sleep duration (binary variable), chronotype, “morning” person, daytime nap, and snoring (Table 1). The GWAS of insomnia was analyzed in 453,379 European participants (345,022 cases and 108,357 controls) (Lane et al., 2019). Sleep duration (446,118 Europeans), longer sleep duration (34,184 cases and 305,742 controls), and shorter sleep duration (106,192 cases and 305,742 controls) were extracted from the same GWAS where long sleep duration was defined to be more than 9 h and short sleep duration was less than 6 h (Dashti et al., 2019). The GWAS of chronotype was performed in 449,734 European ancestry individuals and it is a categorical variable, including “Definitely a “morning” person” (coded as 2), “More a “morning” than “evening” person” (coded as 1), “More an “evening” than a “morning” person” (coded as -1), “Definitely an “evening” person” (coded as -2), and “Do not know” or “Prefer not to answer” (coded as 0) (Jones et al., 2019). Similarly, the “morning person” is a binary variable, including 252,287 cases (“Definitely a “morning” person” and “More a “morning” than “evening” person”) and 150,908 controls (“Definitely an “evening” person” and “More an “evening” than a “morning” person”) (Jones et al., 2019). Genetic variants of daytime nap were obtained from a GWAS consisting of 452,633 European individuals, and the phenotype was treated as a continuous variable based on the frequency (Dashti et al., 2021). We extracted genetic variants of snoring from a GWAS consisting of 152,302 cases and 256,015 British ancestry controls (Campos et al., 2020).

Two GWASs of IBS were used, where the discovery set encompassed 53,400 European cases and 433,201 European controls (Eijssbouts et al., 2021) and the validation set was from the FinnGen consortium, including 4,605 cases and 182,423 controls (finn-b-K11\_IBS, <https://www.finnngen.fi/fi>). The IBS cases from UKB should meet at least one of the

TABLE 1 Descriptive information of sleep-related data.

Exposure	Ancestry	Sample size	Covariates	NSNP	R2 (%)	F	PMID
Insomnia	European	345,022 cases and 108,357 controls	age, sex, 10 genetic principal components, and genotyping array	44	0.43	44.09	30,804,566
Sleep duration	European	446,118	age, sex, 10 genetic principal components, genotyping array and genetic relatedness matrix	77	0.72	41.72	30,846,698
Long sleep duration	European	34,184 cases and 305,742 controls	age, sex, 10 genetic principal components, genotyping array and genetic relatedness matrix	12	0.14	40.39	30,846,698
Short sleep duration	European	106,192 cases and 305,742 controls	age, sex, 10 genetic principal components, genotyping array and genetic relatedness matrix	25	0.24	40.46	30,846,698
Chronotype	European	449,734	age, sex, study center and genotyping array	196	2.04	47.73	30,696,823
Morning person	European	252,287 cases and 150,908 controls	age, sex, study center and genotyping array	147	1.64	45.73	30,696,823
Daytime nap	European	452,633	age, sex, 10 genetic principal components, genotyping array and genetic correlation matrix	114	1.25	50.27	33,568,662
Snoring	European	152,302 cases and 256,015	age, sex, genotyping array and the first 20 genetic principal components	43	0.41	39.40	32,060,260



following four conditions (Ford et al., 2020): digestive health questionnaire (DHQ) Rome III: meet Rome III symptom criteria for IBS diagnosis without other diagnostic explanations for these symptoms (Vasant et al., 2021); DHQ “self-report”: answered “yes” to the question “Have you ever been diagnosed with IBS?” (Stern, 2021); Unprompted ‘self-report’: self-reported IBS diagnosis in response to the question “Has a doctor ever told you that you have any serious medical conditions?” (Song et al., 2021); the international code of disease version 10 (ICD-10); with hospital episode statistics indicating being admitted to a hospital due to IBS as the main or secondary ICD-10 diagnosis. The cases from FinnGen all met the ICD-10 standard. The former was adjusted for sex, age, and sex\*age interaction; age<sup>2</sup>, sex\*age<sup>2</sup> interaction; and the first 20 genetic principal components. The

FinnGen GWAS was adjusted for sex, age, the first 10 genetic principal components, genotyping batch, and genetic relatedness matrix. Genomic control has been applied to all these GWASs.

## Mendelian randomization design

The MR should be established based on three principal assumptions (Ford et al., 2020): relevance: the IVs should be closely associated with the exposure (Vasant et al., 2021); independence: the IVs should not be associated with any potential confounders that might influence the exposure or outcome (Stern, 2021); exclusion-restriction: the IVs can only affect the outcome *via* the way of exposure and there were no

other alternative ways (Emdin et al., 2017) (Figure 1). Other additional assumptions should also be satisfied, such as linearity and no interaction between exposure and mediators.

The most important step in MR analysis is selecting appropriate genetic variants as instruments. Genetic variants, usually common single nucleotide polymorphism (SNP) with a minor allele frequency of more than 0.01, were selected as instrumental variables (IVs) if reaching the genome-wide significance (GWAS  $p$ -value  $< 5 \times 10^{-8}$ ), and then they were clumped based on linkage disequilibrium ( $R^2 = 0.01$ ) and distance (10,000 kb). The IBS GWAS with the largest sample size was treated as the discovery set, and the IBS GWAS of FinnGen was the validation set. In the discovery stage, we estimated each exposure's effect on the IBS using a two-sample MR method, and the same method was applied to the validation stage. Only the exposure significant in both discovery and validation stages was assumed to be the causal risk factor.

Furthermore, the results from both the discovery and validation stages were combined using a meta-analysis method. Considering that sleep-related traits were closely correlated, a multivariable MR in the two-sample summary data setting was adopted to explain the independent causal effect as well (Sanderson et al., 2019). Also, a reverse MR was considered to estimate the reverse causation.

## Statistical methods

The F statistic was calculated to assess the IV validity and assess weak instrument bias. Also, the MR Steiger test was performed to guarantee that each IV explained more variance in exposure than that of outcome (Hemani et al., 2017). In MR estimation, the inverse-variance weighted (IVW) method was utilized as the primary analysis, and two complementary methods were adopted as well, including the MR-Egger and weighted median methods (Bowden et al., 2016; Burgess and Thompson, 2017). It should be noted that IVW can obtain an unbiased result only when all IVs are valid, however, MR-Egger and weighted median methods can estimate the causal effect assuming some IVs are invalid. Additionally, the IVW method was also applied in the multivariable MR analysis (Sanderson et al., 2019). In the discovery stage, the false discovery rate (FDR) method was used to control the false-positive results (FDR  $< 0.05$ ).

## Sensitivity analysis

Several methods have been applied to perform sensitivity analyses, including Cochran's Q value for heterogeneity assessment, MR-PRESSO for outliers, and horizontal pleiotropy detection and leave-one-out sensitivity analyses (Verbanck et al., 2018). If there was heterogeneity, the random-effects model for IVW was adopted. The MR-PRESSO method performed the

outlier and distortion tests to detect outliers that might bias the results, and the outliers were eradicated from further analyses. The leave-one-out analysis is another standard method for sensitivity analysis that recalibrates the results after removing SNPs one by one, and the SNP should be a driver for the MR estimates if the results change significantly after removal.

## Power calculation and bias assessment

The power calculation was performed using mRnd (<https://cnsgenomics.shinyapps.io/mRnd/>). The bias caused by sample overlap was assessed by the method proposed by Burgess et al. (<https://sb452.shinyapps.io/overlap/>).

All statistical analyses and data visualization were performed using R programming software 4.1.2 and the used R packages included "TwoSampleMR", "MRPRESSO", "meta", and "forestplot".

## Results

### IV description and validity

The number of IVs for each exposure varied from 12 (long sleep duration) to 196 (chronotype). The F statistic for each SNP was greater than the empirical threshold of 10 (Chen et al., 2022) and the overall F statistic for each exposure was larger than 10 as well, suggesting the results were less likely to be biased by the weak instruments. The MR Steiger test indicated that each IV explained more variance in exposure than that of the outcome, meaning the results might not be biased by the reverse causation.

### Causal associations between sleep and IBS in the discovery stage

In the discovery stage, three exposures were causally associated with IBS after FDR correction (Figure 2). Initially, we observed genetic liability to the "morning" chronotype could lower the risk of IBS [OR = 0.81 (0.76, 0.86),  $p$ -value =  $3.97 \times 10^{-11}$ , FDR =  $3.18 \times 10^{-10}$ ] and it was also supported by it that genetic predisposition to "morning person" tended to reduce the risk of IBS [OR = 0.88 (0.85, 0.92),  $p$ -value =  $6.66 \times 10^{-9}$ , FDR =  $2.66 \times 10^{-8}$ ]. Besides, the genetic liability to insomnia can increase the risk of IBS [OR = 2.86 (1.94, 4.23),  $p$ -value =  $1.26 \times 10^{-7}$ , FDR =  $3.36 \times 10^{-7}$ ] and such causation was evidenced by the fact that the short sleep duration can suggestively increase IBS as well [OR = 2.37 (1.11, 5.07),  $p$ -value = 0.026, FDR = 0.05].

The horizontal pleiotropy test based on the MR-Egger intercept indicated that there was no horizontal pleiotropy (MR-Egger intercept  $p$ -value  $> 0.05$ ), suggesting that there was no need to correct the intercept in the MR analysis.

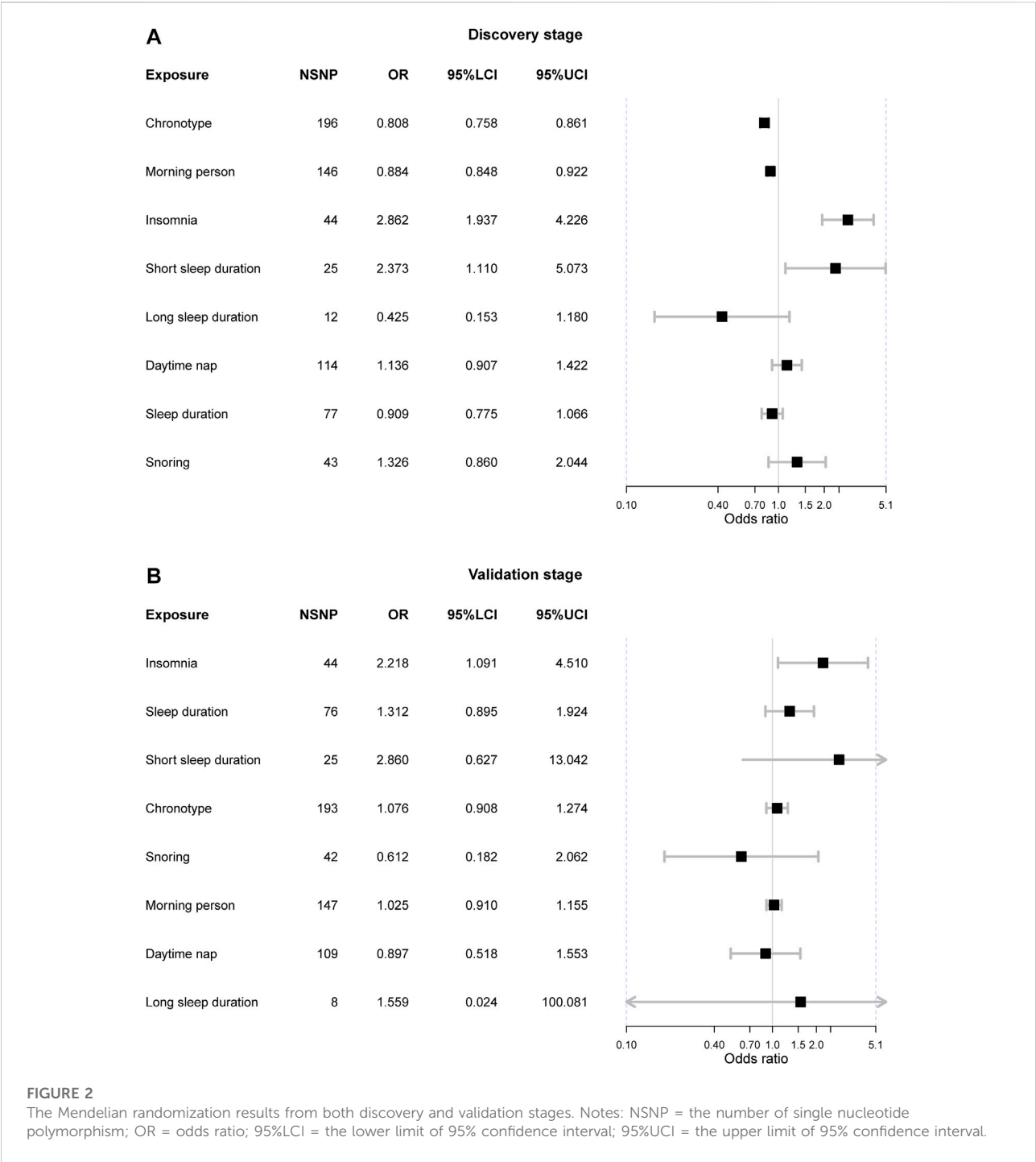


**FIGURE 2**

The Mendelian randomization results from both discovery and validation stages. Notes: NSNP = the number of single nucleotide polymorphism; OR = odds ratio; 95%LCI = the lower limit of 95% confidence interval; 95%UCI = the upper limit of 95% confidence interval.

However, Cochrane’s Q value suggested there existed substantial heterogeneity in all exposure-outcome associations (Q *p*-value < 0.05) except the association between long sleep duration and IBS. The causal relationship between chronotype, “morning” person, insomnia, and IBS remained significant in the weighted median methods (Table 2). Furthermore, the MR-PRESSO method detected outliers in six exposure-outcome associations, and these exposures included chronotype, insomnia, short sleep duration, snoring, sleep duration, and daytime nap. After removal of outliers, the previous observed significant associations were also significant, including chronotype (corrected *p*-value =  $6.49 \times 10^{-11}$ ) and insomnia (corrected *p*-value =  $2.32 \times 10^{-7}$ ) (Table 2). Leave-one-out sensitivity analysis did not detect any other outliers.

TABLE 2 Mendelian randomization results from weighted median and MR-PRESSO methods.

Exposure	Stage	NSNP	Weighted median				MR-PRESSO				P <sub>heterogeneity</sub>	P <sub>pleiotropy</sub>
			OR	95%LCI	95%UCI	p	OR	95%LCI	95%UCI	p		
Chronotype	Discovery	196	0.81	0.74	0.88	0.00	0.81	0.76	0.86	0.00	0.00	0.20
Insomnia	Discovery	44	2.76	1.86	4.09	0.00	2.60	1.81	3.74	0.00	0.00	0.20
Long sleep duration	Discovery	12	0.36	0.09	1.39	0.14	-----	-----	-----	-----	0.86	0.41
Morning person	Discovery	146	0.89	0.84	0.94	0.00	-----	-----	-----	-----	0.02	0.43
Daytime nap	Discovery	114	1.12	0.87	1.43	0.37	1.15	0.94	1.41	0.17	0.00	0.07
Short sleep duration	Discovery	25	1.95	0.92	4.13	0.08	1.96	0.98	3.93	0.06	0.00	0.28
Sleep duration	Discovery	77	0.92	0.77	1.10	0.36	0.91	0.78	1.06	0.22	0.00	0.97
Snoring	Discovery	43	1.51	0.94	2.43	0.09	1.60	1.10	2.32	0.01	0.00	0.48
Chronotype	Validation	193	0.97	0.76	1.26	0.84	-----	-----	-----	-----	0.50	0.45
Insomnia	Validation	44	4.09	1.36	12.30	0.01	-----	-----	-----	-----	0.45	0.25
Long sleep duration	Validation	8	0.37	0.00	45.03	0.69	-----	-----	-----	-----	0.27	0.79
Morning person	Validation	147	1.05	0.89	1.25	0.56	-----	-----	-----	-----	0.26	0.28
Daytime nap	Validation	109	0.97	0.45	2.10	0.95	-----	-----	-----	-----	0.07	0.82
Short sleep duration	Validation	25	3.46	0.41	29.39	0.26	-----	-----	-----	-----	0.92	0.50
Sleep duration	Validation	76	1.11	0.63	1.95	0.71	-----	-----	-----	-----	0.11	0.60
Snoring	Validation	42	0.51	0.11	2.35	0.39	-----	-----	-----	-----	0.03	0.94

NSNP, the number of single nucleotide polymorphism; OR, odds ratio; 95%LCI, the lower limit of 95% confidence interval; 95%UCI, the upper limit of 95% confidence interval; P = the *p*-value of OR; P<sub>heterogeneity</sub> = the *p*-value of heterogeneity test; P<sub>pleiotropy</sub> = the *p*-value of horizontal pleiotropy test.

## Causal associations between sleep and IBS in the validation stage

In the validation stage, only the insomnia indicated statistical significance [OR = 2.22 (1.09, 4.51), *p*-value = 0.028]. Also, such a result was supported by the weighted median method [OR = 4.09 (1.36, 12.30), *p*-value = 0.012]. Neither heterogeneity nor horizontal pleiotropy was detected in the analysis (Cochrane's *Q* *p*-value > 0.05 and MR-Egger intercept *p*-value > 0.05). The MR-PRESSO method did not find outliers that might distort the results, and the leave-one-out sensitivity analysis did not find IV that could drive the results.

We did not observe the causal association between chronotype and IBS [OR = 1.08 (0.91, 1.27), *p*-value = 0.397], nor did the "morning" person [OR = 1.03 (0.91, 1.16), *p*-value = 0.682]. Also, there was no heterogeneity or horizontal pleiotropy.

## Meta-analysis of MR results from the discovery and validation stage

The meta-analysis suggested two genetically-determined sleep exposures can increase the risk of IBS, including insomnia [OR = 2.70 (1.92, 3.80), *p*-value =  $1.27 \times 10^{-8}$ ] and short sleep duration [OR = 2.46 (1.25, 4.86), *p*-value = 0.009] (Figure 3). There was no heterogeneity in these two sleep exposures (*I*<sup>2</sup> = 0% and *Q* *p*-value > 0.05). As for chronotype and "morning" person, the fixed-effects suggested "morning"

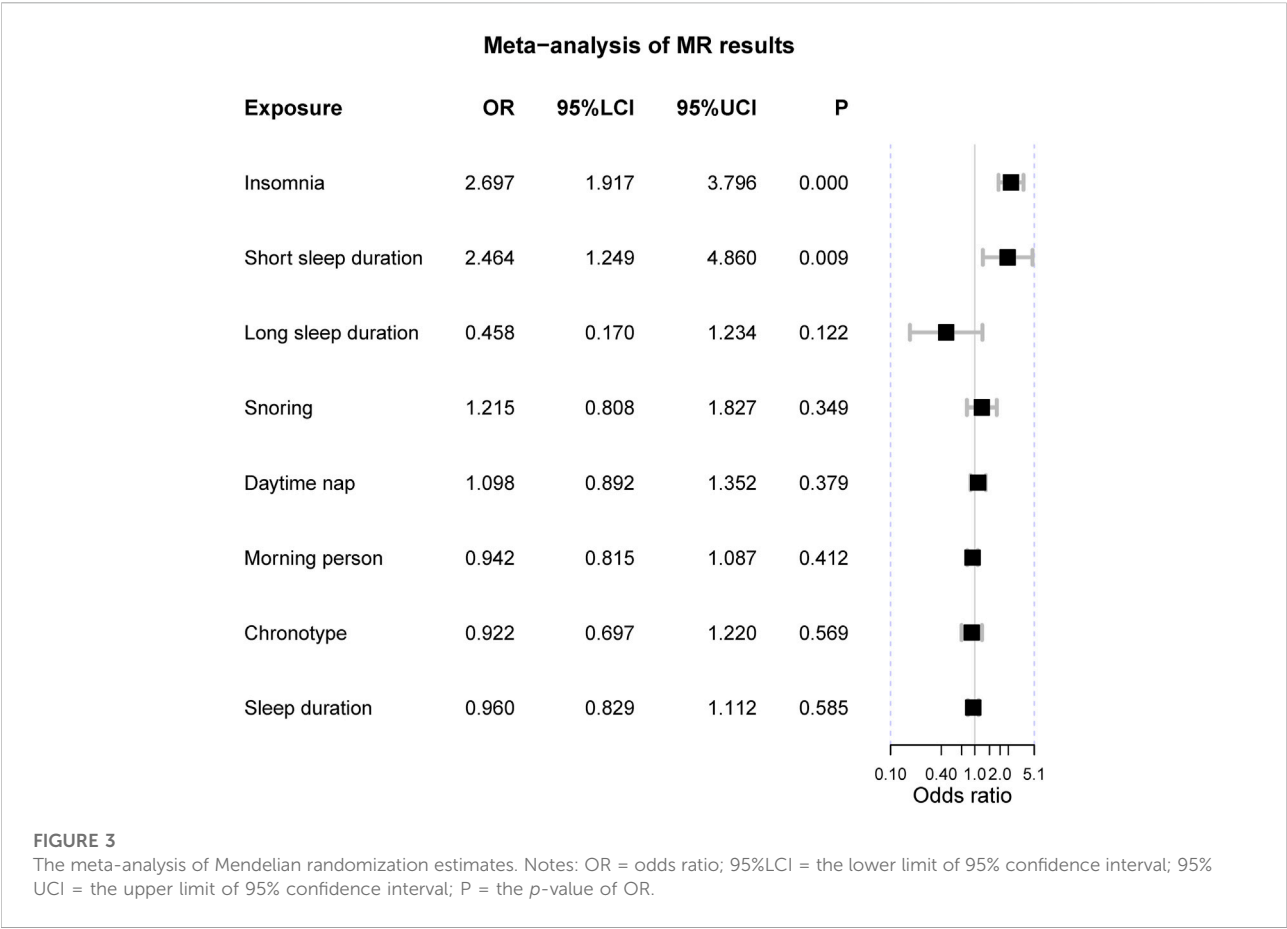
chronotype could decrease the risk of IBS [OR = 0.84 (0.79, 0.89), *p*-value =  $3.88 \times 10^{-9}$ ] and so did the "morning" person [OR = 0.90 (0.86, 0.93), *p*-value =  $9.32 \times 10^{-8}$ ]. However, there was obvious heterogeneity in the meta results of the chronotype and "morning" people and their results were insignificant when using the random-effects model. The other sleep-related exposures should not affect the risk of IBS.

The multivariable MR analysis suggested insomnia is an independent risk factor for IBS after adjusting for chronotype [OR = 2.32 (1.57, 3.43), *p*-value =  $2.67 \times 10^{-5}$ ] in the discovery set while not significant in the validation set. After adjusting for short sleep duration, insomnia can elevate the risk of IBS as well [OR = 1.45 (1.13, 1.85), *p*-value = 0.003] in the discovery set but not in the validation set. The statistical powers were all greater than 80% and the bias caused by sample overlapping in the discovery stage was less than 5%, suggesting sufficient power and validity of this MR study. The reverse MR design ruled out the possibility that IBS could increase the risk of insomnia [OR = 0.87 (0.70, 1.08), *p*-value = 0.231].

## Discussion

Briefly, our MR design was focused on the causal relationship between eight different sleep-related exposures and IBS, and the results indicated that insomnia and short sleep duration can increase the risk of IBS, while there is no sufficient evidence to support that the other sleep-related traits have a causal link with





IBS, including sleep duration (continuous variable), long sleep duration (binary variable), chronotype, “morning” person, daytime nap, and snoring. Since insomnia is also associated with decreased sleep duration, our results suggest that adequate sleep can increase the risk of developing IBS. In addition, the other null associations also support our conclusion that neither chronotype nor snoring affects the incidence of IBS with adequate sleep duration. Also, excessive sleep duration does not alter the risk of IBS either.

Except for the common pathogenic factors such as genetics, epigenetic changes, and infection, many other complex traits are also risk factors for IBS, including an unhealthy lifestyle and psychological stress (Vasant et al., 2021). In modern times, enormous social and psychological stress drives the development of sleep disorders, especially among middle-aged people (Li et al., 2020). The following relevant studies support our findings that insomnia and short sleep duration may affect pathogenesis and promote the development of IBS through the following physiological mechanisms, such as brain-gut-axis, immune disorders, and circadian rhythms.

Although IBS is a functional gastrointestinal disorder, it was considered that dysfunction within the bidirectional gut-brain axis was significantly associated with IBS (2). IBS is also classified

as a disorder of gut-brain interaction since IBS patients often have anxiety and depression, which are also risk factors for IBS in healthy people (Vasant et al., 2021). IBS is thought to often co-occur with mental disorders such as anxiety symptoms and depression, and both of these diseases have a series of biological and psychosocial mechanisms, which are mainly reflected in the gut-brain axis disorders (Staudacher et al., 2021). Meanwhile, sleep behavior is also important to numerous brain functions, including neural cell growth, synaptogenesis, and memory function (Reynolds and O’Hara, 2013; Walker and Stickgold, 2006). Freeman et al. designed a large randomized controlled trial of a psychological intervention for a mental health problem with insomnia, and this study suggested that insomnia is a causal risk factor for the occurrence of mental health problems, and alleviating sleep disorders is particularly important to mental health (Freeman et al., 2017). However, there was a lack of evidence on how insomnia affects the onset of IBS. It should be probable that insomnia might induce intestinal dysfunction via the brain-gut axis since the brain can alter intestinal motility and fluid secretion, intestinal epithelial permeability, and gut microbiota composition (Enck et al., 2016). Besides, insomnia can cause chronic and sustainable stress, which is associated with the onset

and exacerbation of IBS (Chang, 2011). Sleep is fundamental to mental health, furthermore, sleep interventions can prevent mental disease and improve psychological health (Freeman et al., 2017; Espie et al., 2019). Interestingly, the largest GWAS study identified six genetic susceptibility loci that were significantly associated with IBS, four of which were located in genes associated with mood and anxiety (NCAM1, CADM2, PHF2/FAM120A, DOCK9) (Eijsbouts et al., 2021). Such results indicated that IBS shared genetic background with insomnia-associated traits. Further genetic analyses with an enlarged sample size should help to identify shared a genetic loci, which can elucidate how insomnia affects the onset of IBS. And psychotherapy for IBS symptoms, especially cognitive behavioral therapy and hypnosis, is helpful for many IBS patients' symptoms (Chilcot and Moss-Morris, 2013). The accumulating evidence suggests that insomnia can contribute to the increased risk of IBS via mental disorders rising from the gut-brain axis.

To investigate the relationship between sleep restriction and immune function, Circadian et al. recruited nine healthy males to participate in a sleep restriction (4 h of sleep/night for five nights) and sleep recovery protocol (8 h of sleep/night for seven nights), and the results showed that continuous sleep restriction could significantly increase the counts of leukocytes, monocytes, neutrophils, and lymphocytes in peripheral blood, and sleep recovery could partially restore these effects (Lasselin et al., 2015). Furthermore, prolonged periods of wakefulness could increase the soluble tumor necrosis factor- $\alpha$  (TNF- $\alpha$ ) receptor one and interleukin-6 (IL-6) plasma levels in the plasma, which are the messengers connected to the immune and nervous systems (Shearer et al., 2001). In middle-aged and young adults, plasma inflammatory cytokine levels of C-reactive protein (CRP) and IL-6 were significantly elevated in insomnia and short sleep duration populations later after adjustment for confounders, suggesting that clinical interventions targeting sleep disorders might reduce systemic inflammation (Cho et al., 2015). These studies evidenced that sleep insomnia and short sleep duration might play a significant role in contributing to immuno-inflammatory conditions. However, a previous MR study revealed no causal relationship between sleep traits and inflammatory bowel disease (IBD) (Chen et al., 2021). We deemed that IBD is an autoimmune disease that might be largely affected by immune factors, while IBS is a kind of functional intestinal disease that should be affected less. Additionally, the mechanism of autoimmune diseases should be different from that of traditional immune mechanisms, where the immunogen of the former is endogenous while that of the latter is exogenous. Insomnia may affect traditional immune mechanisms, which can affect IBS. Therefore, it is reasonable that insomnia can increase the risk of IBS but not IBD. Meanwhile, high-quality sleep can reduce the incidence rate of infection in both human and animal studies (Ali et al., 2013). In addition, a history of enteric infection is a risk factor for IBS, and patients with a history of enteric infection were more likely to develop IBS than people without a history of acute enteric

infection (Marshall et al., 2010; Cremon et al., 2014). Given this close association between sleep disorders and the immune system, we can explain that insomnia is a risk factor for IBS through the disturbance of immunity. However, attention should be paid to the fact that the alteration of immunity in IBS might not be displayed in laboratory examination.

Circadian rhythm refers to the change of life activities in a cycle of 24 h, a regular cycle established by various physiological functions of organisms to adapt to the diurnal variation of the external environment (Patel et al., 2014). Many recent studies have shown that numerous organ systems are related to circadian oscillations, including the kidney, liver, and gut (Vollmers et al., 2012; Firsov and Bonny, 2018; Godinho-Silva et al., 2019). In the circadian disorganization mice model, the permeability of the intestinal epithelial barrier was significantly increased compared with the control group (Summa et al., 2013). Interestingly, PER2, an important gene in regulating the fundamental molecular basis of biological clocks, has also played an essential role in the regulation of colonic motility (Hoogerwerf et al., 2010; Summa et al., 2013). Above all, alterations in sleep mode are more likely to affect the pathogenesis of digestive diseases such as IBS.

The value of sleep quality is underappreciated in clinical medicine. In this MR study, we found that sleep quality plays an important role for us in preventing IBS. The design of our study was rigorous. MR studies were conducted on IBS GWAS data from two different sample sources successively, and a meta-analysis was conducted on the results of the discovery stage and validation stage to ensure the statistical power and reliability of our results. We suggest that the prevention of insomnia may reduce the risk of brain-gut-axis and immunity disorders, guaranteeing a healthy circadian rhythm to prevent and delay the morbidity and progression of IBS. However, several limitations should be pointed out in this study (Ford et al., 2020): horizontal pleiotropy is a natural flaw of MR design though several statistical methods have been applied to avoid it (Vasant et al., 2021); the target population in this study is mainly of European ancestry and the generalizability of our conclusion might not be applied to other ancestries.

## Conclusion

This Mendelian randomization study found insomnia can increase the risk of irritable bowel syndrome, suggesting that improving sleep quality might be effective in improving irritable bowel syndrome.

## Data availability statement

Publicly available datasets were analyzed in this study. This data can be found here: <https://www.ebi.ac.uk/gwas/>.

## Ethics statement

We used the de-identified summary statistics of each GWAS. Each GWAS study was approved by its Institutional Review Board, and no further ethical approval was needed. The patients/participants provided their written informed consent to participate in this study.

## Author contributions

WL gave the idea and elaborated on the study. WB performed the Mendelian randomization analyses and wrote the draft. LQ gave guidance on statistical methods and software resources and revised the manuscript. YB checked the statistical process and revised the manuscript. SW revised the manuscript. WL was responsible for the accuracy and integrity of this study. All authors gave consent to the publication of this manuscript.

## References

- Ai, S., Zhang, J., Zhao, G., Wang, N., Li, G., So, H. C., et al. (2021). Causal associations of short and long sleep durations with 12 cardiovascular diseases: Linear and nonlinear mendelian randomization analyses in UK biobank. *Eur. Heart J.* 42 (34), 3349–3357. doi:10.1093/eurheartj/ehab170
- Ai, S. Z., and Dai, X. J. (2018). Causal role of rapid-eye-movement sleep on successful memory consolidation of fear extinction. *J. Thorac. Dis.* 10 (3), 1214–1216. doi:10.21037/jtd.2018.01.163
- Ali, T., Choe, J., Awab, A., Wagener, T. L., and Orr, W. C. (2013). Sleep, immunity and inflammation in gastrointestinal disorders. *World J. Gastroenterol.* 19 (48), 9231–9239. doi:10.3748/wjg.v19.i48.9231
- Bowden, J., Davey Smith, G., Haycock, P. C., and Burgess, S. (2016). Consistent estimation in mendelian randomization with some invalid instruments using a weighted median estimator. *Genet. Epidemiol.* 40 (4), 304–314. doi:10.1002/gepi.21965
- Burgess, S., and Thompson, S. G. (2017). Interpreting findings from Mendelian randomization using the MR-Egger method. *Eur. J. Epidemiol.* 32 (5), 377–389. doi:10.1007/s10654-017-0255-x
- Campos, A. I., García-Marín, L. M., Byrne, E. M., Martin, N. G., Cuéllar-Partida, G., Rentería, M. E., et al. (2020). Insights into the aetiology of snoring from observational and genetic investigations in the UK Biobank. *Nat. Commun.* 11 (1), 817. doi:10.1038/s41467-020-14625-1
- Chang, L. (2011). The role of stress on physiologic responses and clinical symptoms in irritable bowel syndrome. *Gastroenterology* 140 (3), 761–765. doi:10.1053/j.gastro.2011.01.032
- Chen, L., Yang, H., Li, H., He, C., Yang, L., Lv, G., et al. (2022). Insights into modifiable risk factors of cholelithiasis: A mendelian randomization study. *Hepatol. Baltim. Md* 75 (4), 785–796. doi:10.1002/hep.32183
- Chen, M., Peng, W. Y., Tang, T. C., and Zheng, H. (2021). Differential sleep traits have No causal effect on inflammatory bowel diseases: A mendelian randomization study. *Front. Pharmacol.* 12, 763649. doi:10.3389/fphar.2021.763649
- Chilcot, J., and Moss-Morris, R. (2013). Changes in illness-related cognitions rather than distress mediate improvements in irritable bowel syndrome (IBS) symptoms and disability following a brief cognitive behavioural therapy intervention. *Behav. Res. Ther.* 51 (10), 690–695. doi:10.1016/j.brat.2013.07.007
- Cho, H. J., Seeman, T. E., Kiefe, C. I., Lauderdale, D. S., and Irwin, M. R. (2015). Sleep disturbance and longitudinal risk of inflammation: Moderating influences of social integration and social isolation in the Coronary Artery Risk Development in Young Adults (CARDIA) study. *Brain Behav. Immun.* 46, 319–326. doi:10.1016/j.bbi.2015.02.023

## Acknowledgments

We would like to thank all investigators for making genetic association estimates openly available.

## Conflict of interest

The authors declare that the research was conducted in the absence of any commercial or financial relationships that could be construed as a potential conflict of interest.

## Publisher's note

All claims expressed in this article are solely those of the authors and do not necessarily represent those of their affiliated organizations, or those of the publisher, the editors, and the reviewers. Any product that may be evaluated in this article, or claim that may be made by its manufacturer, is not guaranteed or endorsed by the publisher.

- Cremon, C., Stanghellini, V., Pallotti, F., Fogacci, E., Bellacosa, L., Morselli-Labate, A. M., et al. (2014). Salmonella gastroenteritis during childhood is a risk factor for irritable bowel syndrome in adulthood. *Gastroenterology* 147 (1), 69–77. doi:10.1053/j.gastro.2014.03.013
- Dashti, H. S., Daghlis, I., Lane, J. M., Huang, Y., Udler, M. S., Wang, H., et al. (2021). Genetic determinants of daytime napping and effects on cardiometabolic health. *Nat. Commun.* 12 (1), 900. doi:10.1038/s41467-020-20585-3
- Dashti, H. S., Jones, S. E., Wood, A. R., Lane, J. M., van Hees, V. T., Wang, H., et al. (2019). Genome-wide association study identifies genetic loci for self-reported habitual sleep duration supported by accelerometer-derived estimates. *Nat. Commun.* 10 (1), 1100. doi:10.1038/s41467-019-08917-4
- Eijsbouts, C., Zheng, T., Kennedy, N. A., Bonfiglio, F., Anderson, C. A., Moutsianas, L., et al. (2021). Genome-wide analysis of 53, 400 people with irritable bowel syndrome highlights shared genetic pathways with mood and anxiety disorders. *Nat. Genet.* 53 (11), 1543–1552. doi:10.1038/s41588-021-00950-8
- Emdin, C. A., Khera, A. V., and Kathiresan, S. (2017). Mendelian randomization. *Mendel. Randomization. Jama.* 318 (19), 1925–1926. doi:10.1001/jama.2017.17219
- Enck, P., Aziz, Q., Barbara, G., Farmer, A. D., Fukudo, S., Mayer, E. A., et al. (2016). Irritable bowel syndrome. *Nat. Rev. Dis. Prim.* 2, 16014. doi:10.1038/nrdp.2016.14
- Espie, C. A., Emsley, R., Kyle, S. D., Gordon, C., Drake, C. L., Siriwardena, A. N., et al. (2019). Effect of digital cognitive behavioral therapy for insomnia on health, psychological well-being, and sleep-related quality of life: A randomized clinical trial. *JAMA psychiatry* 76 (1), 21–30. doi:10.1001/jamapsychiatry.2018.2745
- Firsov, D., and Bonny, O. (2018). Circadian rhythms and the kidney. *Nat. Rev. Nephrol.* 14 (10), 626–635. doi:10.1038/s41581-018-0048-9
- Ford, A. C., Sperber, A. D., Corsetti, M., and Camilleri, M. (2020). Irritable bowel syndrome. *Lancet (London, Engl.* 396 (10263), 1675–1688. doi:10.1016/S0140-6736(20)31548-8
- Freeman, D., Sheaves, B., Goodwin, G. M., Yu, L. M., Nickless, A., Harrison, P. J., et al. (2017). The effects of improving sleep on mental health (OASIS): A randomised controlled trial with mediation analysis. *Lancet. Psychiatry* 4 (10), 749–758. doi:10.1016/S2215-0366(17)30328-0
- Godinho-Silva, C., Domingues, R. G., Rendas, M., Raposo, B., Ribeiro, H., da Silva, J. A., et al. (2019). Light-entrained and brain-tuned circadian circuits regulate ILC3s and gut homeostasis. *Nature* 574 (7777), 254–258. doi:10.1038/s41586-019-1579-3
- Hemani, G., Tilling, K., and Davey Smith, G. (2017). Orienting the causal relationship between imprecisely measured traits using GWAS summary data. *PLoS Genet.* 13 (11), e1007081. doi:10.1371/journal.pgen.1007081

- Hoogerwerf, W. A., Shahinian, V. B., Cornélissen, G., Halberg, F., Bostwick, J., Timm, J., et al. (2010). Rhythmic changes in colonic motility are regulated by period genes. *Am. J. Physiol. Gastrointest. Liver Physiol.* 298 (2), G143–G150. doi:10.1152/ajpgi.00402.2009
- Jones, S. E., Lane, J. M., Wood, A. R., van Hees, V. T., Tyrrell, J., Beaumont, R. N., et al. (2019). Genome-wide association analyses of chronotype in 697, 828 individuals provides insights into circadian rhythms. *Nat. Commun.* 10 (1), 343. doi:10.1038/s41467-018-08259-7
- Lane, J. M., Jones, S. E., Dashti, H. S., Wood, A. R., Aragam, K. G., van Hees, V. T., et al. (2019). Biological and clinical insights from genetics of insomnia symptoms. *Nat. Genet.* 51 (3), 387–393. doi:10.1038/s41588-019-0361-7
- Lasselin, J., Rehman, J. U., Åkerstedt, T., Lekander, M., and Axelsson, J. (2015). Effect of long-term sleep restriction and subsequent recovery sleep on the diurnal rhythms of white blood cell subpopulations. *Brain Behav. Immun.* 47, 93–99. doi:10.1016/j.bbi.2014.10.004
- Li, Y., Li, G., Liu, L., and Wu, H. (2020). Correlations between mobile phone addiction and anxiety, depression, impulsivity, and poor sleep quality among college students: A systematic review and meta-analysis. *J. Behav. Addict.* 9 (3), 551–571. doi:10.1556/2006.2020.00057
- Marshall, J. K., Thabane, M., Garg, A. X., Clark, W. F., Moayyedi, P., and Collins, S. M. (2010). Eight year prognosis of postinfectious irritable bowel syndrome following waterborne bacterial dysentery. *Gut* 59 (5), 605–611. doi:10.1136/gut.2009.202234
- Orr, W. C., Fass, R., Sundaram, S. S., and Scheimann, A. O. (2020). The effect of sleep on gastrointestinal functioning in common digestive diseases. *Lancet. Gastroenterol. Hepatol.* 5 (6), 616–624. doi:10.1016/S2468-1253(19)30412-1
- Patel, V. R., Eckel-Mahan, K., Sassone-Corsi, P., and Baldi, P. (2014). How pervasive are circadian oscillations? *Trends Cell Biol.* 24 (6), 329–331. doi:10.1016/j.tcb.2014.04.005
- Reynolds, C. F., 3rd, and O'Hara, R. (2013). DSM-5 sleep-wake disorders classification: Overview for use in clinical practice. *Am. J. Psychiatry* 170 (10), 1099–1101. doi:10.1176/appi.ajp.2013.13010058
- Rotem, A. Y., Sperber, A. D., Krugliak, P., Freidman, B., Tal, A., Tarasiuk, A., et al. (2003). Polysomnographic and actigraphic evidence of sleep fragmentation in patients with irritable bowel syndrome. *Sleep* 26 (6), 747–752. doi:10.1093/sleep/26.6.747
- Sanderson, E., Davey Smith, G., Windmeijer, F., and Bowden, J. (2019). An examination of multivariable Mendelian randomization in the single-sample and two-sample summary data settings. *Int. J. Epidemiol.* 48 (3), 713–727. doi:10.1093/ije/dyy262
- Shearer, W. T., Reuben, J. M., Mullington, J. M., Price, N. J., Lee, B. N., Smith, E. O., et al. (2001). Soluble TNF-alpha receptor 1 and IL-6 plasma levels in humans subjected to the sleep deprivation model of spaceflight. *J. Allergy Clin. Immunol.* 107 (1), 165–170. doi:10.1067/mai.2001.112270
- Song, Z., Yang, R., Wang, W., Huang, N., Zhuang, Z., Han, Y., et al. (2021). Association of healthy lifestyle including a healthy sleep pattern with incident type 2 diabetes mellitus among individuals with hypertension. *Cardiovasc. Diabetol.* 20 (1), 239. doi:10.1186/s12933-021-01434-z
- Staudacher, H. M., Mikocka-Walus, A., and Ford, A. C. (2021). Common mental disorders in irritable bowel syndrome: Pathophysiology, management, and considerations for future randomised controlled trials. *Lancet. Gastroenterol. Hepatol.* 6 (5), 401–410. doi:10.1016/S2468-1253(20)30363-0
- Stern, P. (2021). The many benefits of healthy sleep. *Sci. (New York, NY)* 374 (6567), 550–551. doi:10.1126/science.abm8113
- Summa, K. C., Voigt, R. M., Forsyth, C. B., Shaikh, M., Cavanaugh, K., Tang, Y., et al. (2013). Disruption of the circadian clock in mice increases intestinal permeability and promotes alcohol-induced hepatic pathology and inflammation. *PLoS One* 8 (6), e67102. doi:10.1371/journal.pone.0067102
- Vasant, D. H., Paine, P. A., Black, C. J., Houghton, L. A., Everitt, H. A., Corsetti, M., et al. (2021). British Society of Gastroenterology guidelines on the management of irritable bowel syndrome. *Gut* 70 (7), 1214–1240. doi:10.1136/gutjnl-2021-324598
- Vege, S. S., Locke, G. R., 3rd, Weaver, A. L., Farmer, S. A., Melton, L. J., 3rd, Talley, N. J., et al. (2004). Functional gastrointestinal disorders among people with sleep disturbances: A population-based study. *Mayo Clin. Proc.* 79 (12), 1501–1506. doi:10.4065/79.12.1501
- Verbanck, M., Chen, C. Y., Neale, B., and Do, R. (2018). Detection of widespread horizontal pleiotropy in causal relationships inferred from Mendelian randomization between complex traits and diseases. *Nat. Genet.* 50 (5), 693–698. doi:10.1038/s41588-018-0099-7
- Vollmers, C., Schmitz, R. J., Nathanson, J., Yeo, G., Ecker, J. R., Panda, S., et al. (2012). Circadian oscillations of protein-coding and regulatory RNAs in a highly dynamic mammalian liver epigenome. *Cell Metab.* 16 (6), 833–845. doi:10.1016/j.cmet.2012.11.004
- Walker, M. P., and Stickgold, R. (2006). Sleep, memory, and plasticity. *Annu. Rev. Psychol.* 57, 139–166. doi:10.1146/annurev.psych.56.091103.070307
- Wang, B., Duan, R., and Duan, L. (2018). Prevalence of sleep disorder in irritable bowel syndrome: A systematic review with meta-analysis. *Saudi J. Gastroenterol.* 24 (3), 141–150. doi:10.4103/sjg.SJG\_603\_17



## OPEN ACCESS

## EDITED BY

Adina Turcu-Stolica,  
University of Medicine and Pharmacy of  
Craiova, Romania

## REVIEWED BY

Salma Jamal,  
Jamia Hamdard University, India  
Samuel Ayodele Egieyeh,  
University of the Western Cape, South  
Africa

## \*CORRESPONDENCE

Jinlu Xie,  
02594@zjhu.edu.cn  
Juan Wang,  
juan\_wangli@163.com

## SPECIALTY SECTION

This article was submitted to  
Gastrointestinal and Hepatic  
Pharmacology,  
a section of the journal  
Frontiers in Pharmacology

RECEIVED 23 June 2022

ACCEPTED 21 July 2022

PUBLISHED 29 August 2022

## CITATION

He S, Yi Y, Hou D, Fu X, Zhang J, Ru X,  
Xie J and Wang J (2022). Identification  
of hepatoprotective traditional Chinese  
medicines based on the  
structure–activity relationship,  
molecular network, and machine  
learning techniques.  
*Front. Pharmacol.* 13:969979.  
doi: 10.3389/fphar.2022.969979

## COPYRIGHT

© 2022 He, Yi, Hou, Fu, Zhang, Ru, Xie  
and Wang. This is an open-access article  
distributed under the terms of the  
[Creative Commons Attribution License  
\(CC BY\)](https://creativecommons.org/licenses/by/4.0/). The use, distribution or  
reproduction in other forums is  
permitted, provided the original  
author(s) and the copyright owner(s) are  
credited and that the original  
publication in this journal is cited, in  
accordance with accepted academic  
practice. No use, distribution or  
reproduction is permitted which does  
not comply with these terms.

# Identification of hepatoprotective traditional Chinese medicines based on the structure–activity relationship, molecular network, and machine learning techniques

Shuaibing He<sup>1</sup>, Yanfeng Yi<sup>2</sup>, Diandong Hou<sup>1</sup>, Xuyan Fu<sup>1</sup>,  
Juan Zhang<sup>3</sup>, Xiaochen Ru<sup>1</sup>, Jinlu Xie<sup>1\*</sup> and Juan Wang<sup>4\*</sup>

<sup>1</sup>Key Laboratory of Vector Biology and Pathogen Control of Zhejiang Province, School of Medicine, Huzhou University, Huzhou Central Hospital, Huzhou, China, <sup>2</sup>Department of Life Sciences and Health, School of Science and Engineering, Huzhou College, Huzhou, China, <sup>3</sup>XinJiang Institute of Chinese Materia Medica and Ethnodrug, Urumqi, China, <sup>4</sup>School of Traditional Chinese Medicine, Zhejiang Pharmaceutical University, Ningbo, China

The efforts focused on discovering potential hepatoprotective drugs are critical for relieving the burdens caused by liver diseases. Traditional Chinese medicine (TCM) is an important resource for discovering hepatoprotective agents. Currently, there are hundreds of hepatoprotective products derived from TCM available in the literature, providing crucial clues to discover novel potential hepatoprotectants from TCMs based on predictive research. In the current study, a large-scale dataset focused on TCM-induced hepatoprotection was established, including 676 hepatoprotective ingredients and 205 hepatoprotective TCMs. Then, a comprehensive analysis based on the structure–activity relationship, molecular network, and machine learning techniques was performed at molecular and holistic TCM levels, respectively. As a result, we developed an *in silico* model for predicting the hepatoprotective activity of ingredients derived from TCMs, in which the accuracy exceeded 85%. In addition, we originally proposed a material basis and a drug property-based approach to identify potential hepatoprotective TCMs. Consequently, a total of 12 TCMs were predicted to hold potential hepatoprotective activity, nine of which have been proven to be beneficial to the liver in previous publications. The high rate of consistency between our predictive results and the literature reports demonstrated that our methods were technically sound and reliable. In summary, systematical predictive research focused on the hepatoprotection of TCM was conducted in this work, which would not only assist screening of potential hepatoprotectants from TCMs but also provide a novel research mode for discovering the potential activities of TCMs.

## KEYWORDS

machine learning, drug discovery, traditional Chinese medicine, predictive model, molecular network, hepatoprotection, structure–activity relationship



# 1 Introduction

As the largest solid organ in the human body, the liver is involved in the regulation of various important physiological processes, including metabolism, drug detoxification, glycogen storage, and bile secretion. In addition, the liver is also considered a major organ that protects against bacterial infection and foreign macromolecule invasion (Bedi et al., 2016). Therefore, dysfunction of the liver will lead to various liver diseases, including hepatitis, hepatic carcinoma, and nonalcoholic fatty liver. It was reported that the liver disease spectrum involved more than 103 liver diseases (Zhao et al., 2008). For hundreds of years, continuous efforts focused on preventing liver dysfunction have been made by scientists and hepatologists while liver diseases are still the major health burdens around the world (Wong et al., 2019). Moreover, recently, the spectrum of liver injury has been constantly changing, increasing the demand for developing novel liver-protecting agents (Huang et al., 2017). In light of these considerations, it is urgent and necessary to expand the spectrum of hepatoprotective drugs. Therefore, efforts focused on discovering potential hepatoprotective drugs are critical for relieving the burdens caused by liver diseases.

As an important branch of complementary and alternative medicine, TCM has made a non-negligible contribution to the development and continuation of human civilization in history. In China, TCM has been used to treat various liver diseases for centuries. In clinical application, lots of TCM products were discovered to have a good hepatoprotective effect. A classic example is silibinin, a flavonolignan derived from *Silybi Fructus*. Both *in vivo* and *in vitro* research practices have shown that silibinin protects liver cells against toxins (Saxena et al., 2022; Song et al., 2022). In clinical trials, silibinin was also used as a supplement to manage some chronic liver diseases (Ferenci et al., 2008). In addition, many other TCM products also exhibited significant liver-protecting effects, including glycyrrhizin, saikosaponin C, curcumin, dioscin, *Lycii Fructus*, *Coptidis Rhizoma*, and *Notoginseng Radix Et Rhizome* (Hong et al., 2015; Lam et al., 2016). All the studies mentioned earlier indicated that TCM is an essential resource for discovering hepatoprotective drugs.

Since it came into the 21st century, vast changes have taken place in the area of medical research. The rapid development of computing science and the continuous accumulation of biomedical data promote the change of the drug research

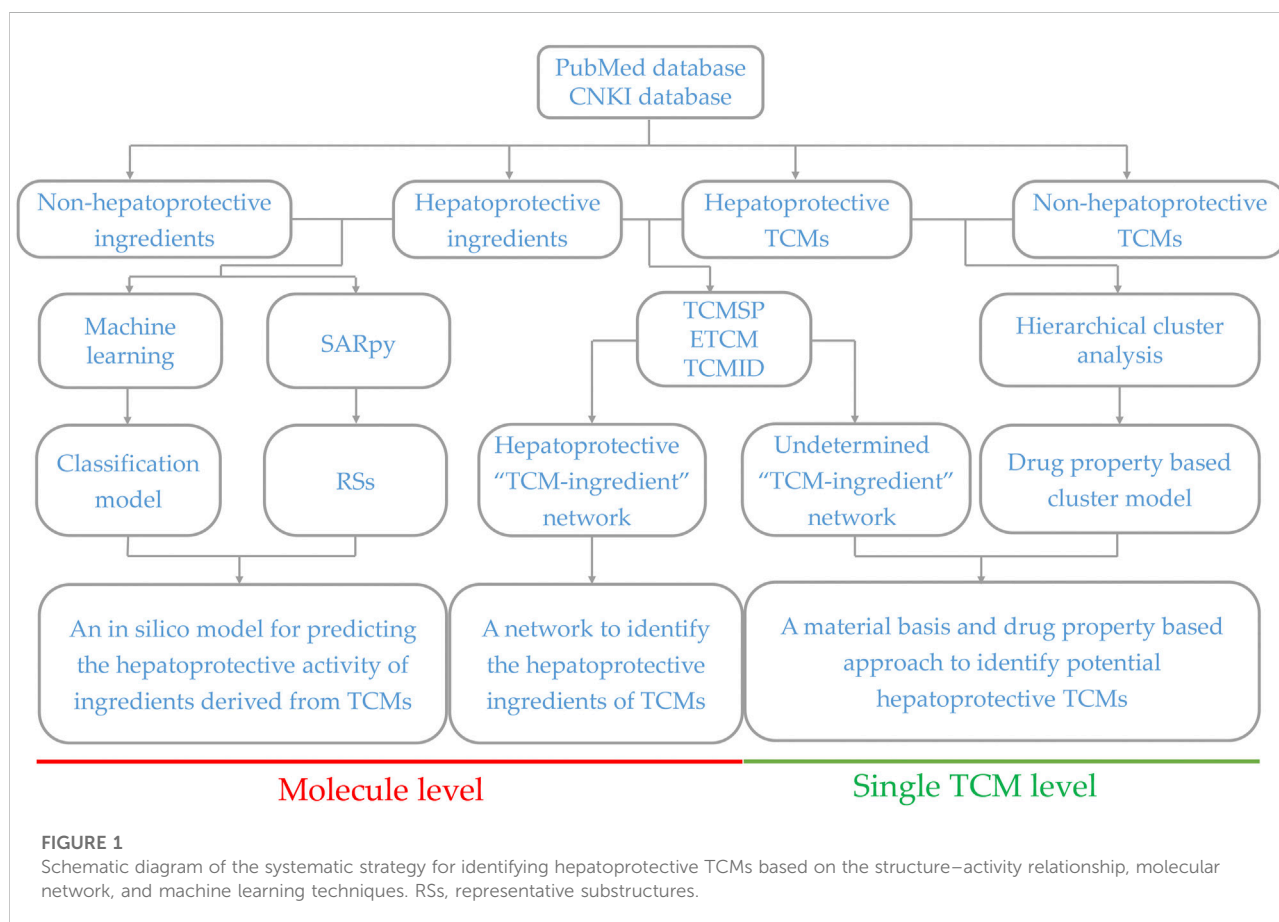


TABLE 1 Predictive power of the models developed based on eight machine learning algorithms.

Algorithm	Parameter	ACC	SE	SP	AUC
Naive Bayes	Default	0.722	0.712	0.754	0.816
J48	C = 0.45	0.825	0.898	0.596	0.712
K-star	B = 41	0.848	0.887	0.725	0.882
IBK	K = 1	0.843	0.877	0.737	0.807
Random forest	Depth = 0	0.872	0.968	0.567	0.884
Bagging	K = 1	0.841	0.879	0.719	0.854
AdaBoost	C = 0.05	0.853	0.922	0.637	0.859
Voting	—	0.865	0.913	0.713	0.890

mode from descriptive research to predictive research. Predictive research has the advantages of saving time, saving labor, and low cost. Furthermore, predictive research dramatically reduces the use of experimental animals in the process of drug research, which is in line with the basic idea of the animal welfare law to minimize the number of animals used in experiments (Moroy et al., 2012). Recently, predictive research has received continuously increasing attention. A series of predictive research studies have been carried out, which significantly promoted the process of drug development and discovery (Medina-Franco and Saldivar-González, 2020; Sessions et al., 2020). In summary, predictive research has become a vital and effective assistant strategy to discover novel drugs.

In history, TCM was primarily used in China and some other Asian countries. Recently, it has been started to be accepted and consumed by many western countries due to its unique effects in treating and preventing some intractable diseases (Martins, 2013; Wu et al., 2015). The widespread use of TCM products around the world encourages researchers to screen novel drugs from TCMs. In particular, with the successful development of artemisinin, expectations are higher to discover novel drugs with high efficacy and little harm from TCMs (Kong and Tan, 2015). Therefore, we believe that comprehensive predictive research focused on TCM-induced hepatoprotection is significant for discovering potential hepatoprotective drugs.

Generally, sufficient data accumulation is necessary for conducting predictive research. Over the past decades, hundreds of TCM products have been reported to be beneficial to the liver, laying a solid foundation for discovering novel potential hepatoprotectants from TCMs *via* predictive research. Therefore, in the current study, systematical predictive research focused on TCM-induced hepatoprotection was conducted based on the hepatoprotective TCMs available in the literature at both molecular and complete singular TCM levels, through which we attempted to provide some valuable clues for discovering novel hepatoprotective agents from TCMs. The detailed experimental design is illustrated in Figure 1.

TABLE 2 Comparison between the KSTAR model and the voting model on the test set.

Algorithm	ACC	SE	SP	AUC
K-star	0.848	0.837	0.884	0.948
Voting	0.871	0.867	0.884	0.953

## 2 Results

### 2.1 Identification of the hepatoprotective activity of ingredients derived from traditional Chinese medicines based on the structure–activity relationship and machine learning

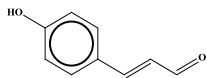
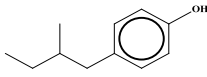
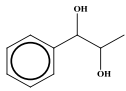
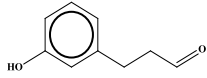
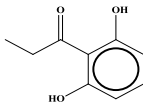
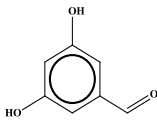
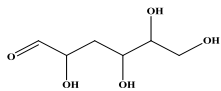
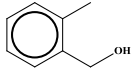
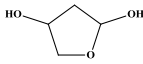
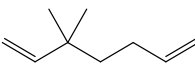
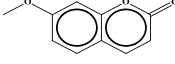
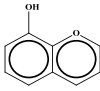
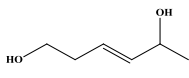
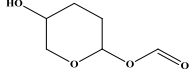
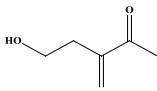
#### 2.1.1 *In silico* model for predicting the hepatoprotective activity of ingredients derived from traditional Chinese medicines

As described in Section 4.1, we established a large-scale dataset for TCM-induced hepatoprotection, including 538 hepatoprotective ingredients and 171 non-hepatoprotective ingredients. Then, seven machine learning algorithms were implemented within 5-fold cross-validation to develop hepatoprotective predictive models. As a result, a total of seven models were attained. As presented in Table 1, ACC (accuracy) of the models varied between 0.722 and 0.872, SE (sensitivity) varied between 0.712 and 0.968, SP (specificity) ranged from 0.567 to 0.754, and the AUC (the area under the receiver-operating characteristic curve) ranged from 0.712 to 0.884.

The most accurate model was generated by the random forest algorithm with an ACC of 0.872. The random forest algorithm also produced the maximum SE (0.968) and AUC (0.884) values. Unfortunately, the SP (0.569) of the random forest model was very poor, which significantly decreased its practical application value. The most satisfactory SP (0.754) was provided by the Naive Bayes algorithm. However, ACC of the Naive Bayes model was only 72.2%, which was significantly lower than that of the other six models. The performance of the IBK model was similar to that of the KSTAR model, whereas the latter's AUC was higher than the former's by 7.5%. Therefore, in terms of comprehensive performance, the model generated by the K-star algorithm seems to be more satisfactory than the others.

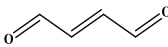
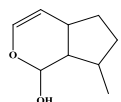
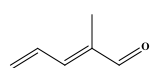
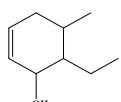
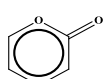
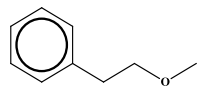
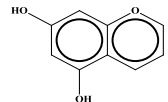
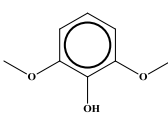
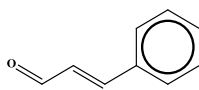
In fact, we also attempted to integrate the advantages of the seven algorithms mentioned earlier *via* voting, aiming to improve the performance of the predictive model. Fortunately, almost all of the indicators of the voting model were higher than those of the KSTAR model slightly both for the training set and for the test set (Table 1 and Table 2). To test the predictive power of the voting model, an external validation set consisting of 135 hepatoprotective ingredients and 43 non-hepatoprotective

TABLE 3 Hepatoprotective RSs and their occurrences.

ID	RS	LR	Hepatoprotection/non-hepatoprotection (percentage)	Distribution of RSs
1		inf	45/0 (100.00%)	General phenylpropanoids (phenylpropionic acids (11); chalcones (4); lignans (3); simple coumarins (2)); phenylethanoid glycosides (9)
2		inf	44/0 (100.00%)	Lignans (34); flavanones/flavanonols (5)
3		inf	39/0 (100.00%)	Flavonoids (25); lignans (dibenzocyclooctadienes (3); tetrahydrofurans (2)); coumarins (6)
4		inf	30/0 (100.00%)	Flavanones/flavanonols (10); lignans (6); phenylpropionic acids (2); alkaloids (4)
5		inf	28/0 (100.00%)	Flavanones/flavanonols (20); dihydrochalcones (4); xanthones (3)
6		inf	25/0 (100.00%)	Tannins (6); flavonoids (6); anthraquinones (6)
7		inf	24/0 (100.00%)	Flavones/flavonols (5); phenylpropionic acids (4); organic acids (4); oleanane-type triterpenoids (5)
8		inf	16/0 (100.00%)	Lignans (5); quinonoids (3)
9		inf	16/0 (100.00%)	Terpenoids (6); steroidal saponins (3); oligosaccharides (3); flavonoids (3)
10		inf	15/0 (100.00%)	Terpenoids (oleanane-type triterpenoids (5); sesquiterpenes (5); others (5))
11		inf	15/0 (100.00%)	Coumarins (simple coumarins (7); pyranocoumarins (5); furanocoumarins (2); others (1))
12		inf	14/0 (100.00%)	Flavones/flavonols (5); xanthones (2); furanocoumarins (3); simple coumarins (2)
13		inf	14/0 (100.00%)	Terpenoids (cucurbitane triterpenoids (4); iridoids (4); others (4))
14		inf	14/0 (100.00%)	Terpenoids (oleanane-type triterpenoids (4); others (2)); simple coumarins (3)
15		inf	12/0 (100.00%)	Terpenoids (kauran diterpenes (3); bicyclic diterpenoids (3); others (1))

(Continued on following page)

TABLE 3 (Continued) Hepatoprotective RSs and their occurrences.

ID	RS	LR	Hepatoprotection/non-hepatoprotection (percentage)	Distribution of RSs
16		inf	12/0 (100.00%)	Quinonoids (naphthoquinones (3); p-Benzoquinones (3))
17		inf	10/0 (100.00%)	Iridoids (10)
18		inf	10/0 (100.00%)	Terpenoids (5); alkaloids (3)
19		inf	10/0 (100.00%)	Terpenoids (oleanane-type triterpenoids (4); others (2))
20		13.08	41/1 (97.62%)	Coumarins (pyranocoumarins (5); furanocoumarins (11); simple coumarins (15); others (3)); cardiac glycosides (4)
21		12.44	39/1 (97.50%)	Phenylethanoid glycosides (10); flavonoids (9); coumarins (pyranocoumarins (4); others (1))
22		12.28	77/2 (97.47%)	Flavonoids (flavones/flavonols (61); others (14))
23		10.53	33/1 (97.06%)	Lignans (dibenzocyclooctadienes (11); aryl naphthalenes (4); biphenylenes (3); others (3)); bibenzyles (4)
24		10.37	65/2 (97.01%)	Phenylpropanoids (phenylpropionic acids (12); others (2)); phenylethanoid glycosides (9); flavonoids (chalcones (7); others (3)); amide alkaloids (5); terpenoids (8)

ingredients was used. Consequently, the model's ACC, SE, SP, and AUC were 0.871, 0.867, 0.884, and 0.953, respectively, indicating that our model was reasonably successful (Table 2). In summary, an *in silico* model for predicting the hepatoprotective activity of ingredients derived from TCMs was constructed for the first time. Both internal and external validation indicated that the model exhibited satisfactory predicting power. All of the predictive models generated in this work are available in [Supplementary File S1](#).

### 2.1.2 Representative substructures for the hepatoprotective activity

To understand the structural preference of the hepatoprotective ingredients, SARpy software was used to extract representative substructures (RSs) for hepatoprotection. As shown in Table 3, a total of 24 RSs were identified. Likelihood ratios (LRs) of the top

19 RSs were infinity, indicating that these substructures were only detected in hepatoprotectants. For the other five RSs, LR ranged from 10.37 to 13.08, demonstrating that the occurrence probabilities of these substructures in hepatoprotectants were 10 times higher than those in non-hepatoprotectants. Considering the high bias of these substructures in hepatoprotectants, we could claim that these RSs mentioned earlier may be highly correlated with liver protection. Therefore, we recommend these RSs be taken into consideration in the design and modification of hepatoprotective drugs.

Moreover, the distribution of the RSs was also explored (Table 3). As a result, we found that a total of 10 RSs [lignans (ID2 and ID23), flavonoids (ID3, ID5, and ID21), terpenoids (ID9, ID13, and ID17), and coumarins (ID11 and ID20)] were largely distributed into specific compound families. In contrast, the other 14 RSs showed lower specificity to the structural category by associating with multiple compound families. It

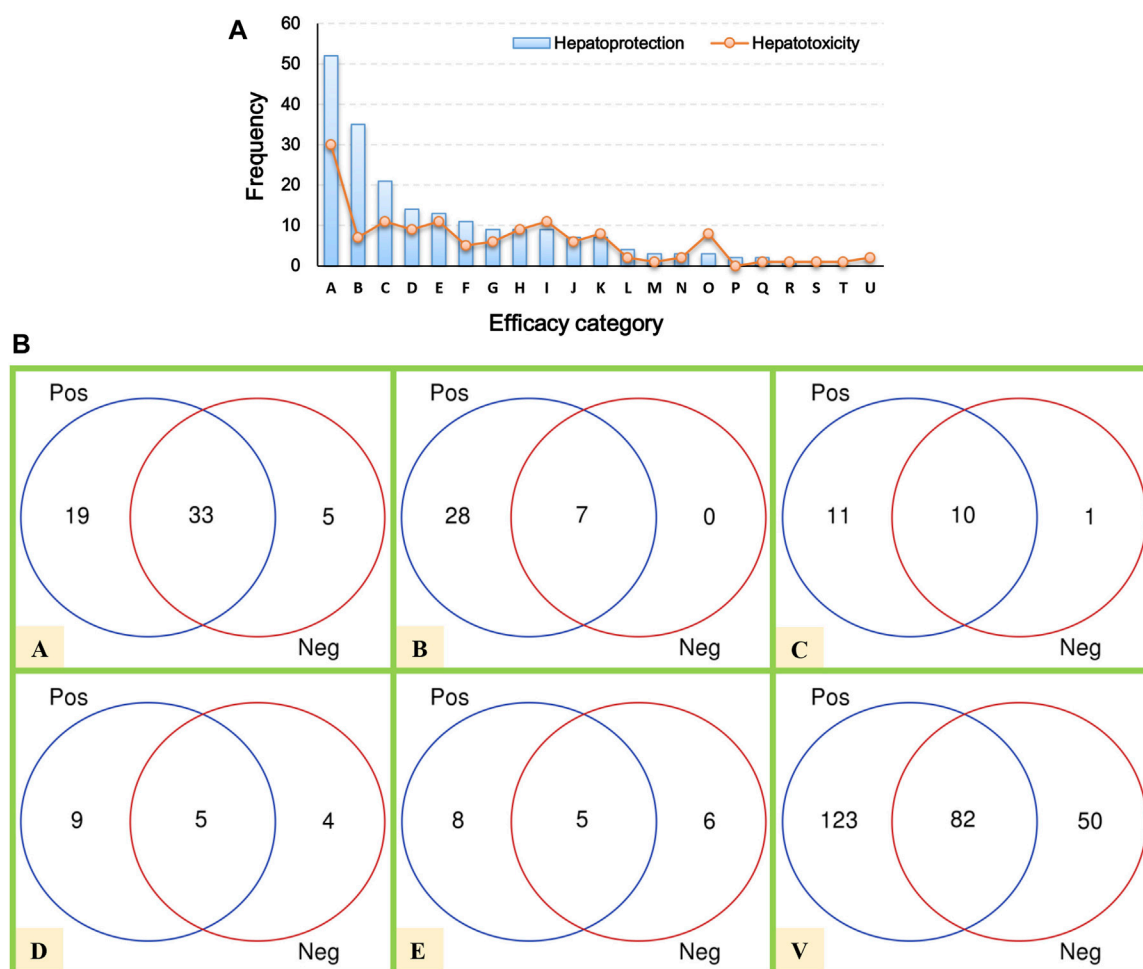


**FIGURE 2**  
Efficacy category analysis. (A) Efficacy category of the hepatoprotective and hepatotoxic TCMs. (B) Overlap between hepatoprotective and hepatotoxic TCMs.

has been a consensus that compounds with similar structures tend to hold consistent activities. Therefore, more attention should be paid to the compound families containing frequent hepatoprotective ingredients when screening hepatoprotective drugs from TCMs.

## 2.2 Comprehensive analysis focused on the hepatoprotective activity of traditional Chinese medicine in the singular traditional Chinese medicine level based on bioinformatics

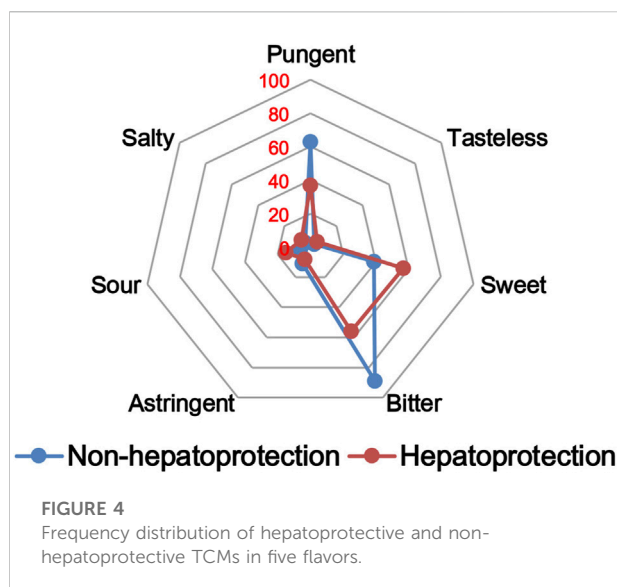
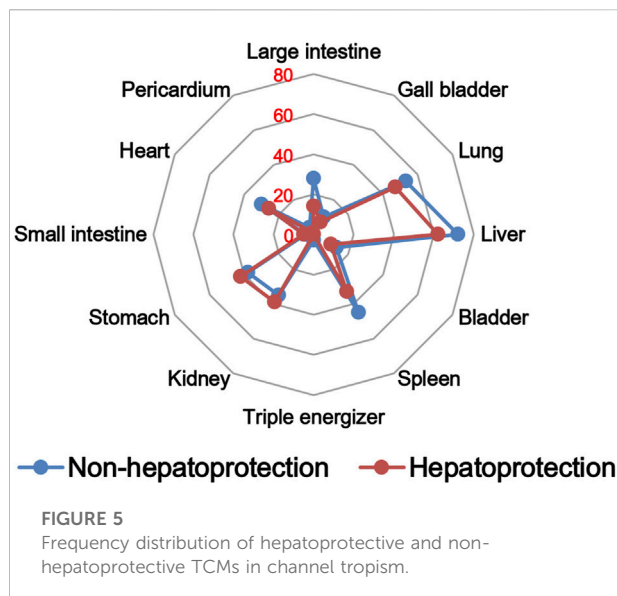
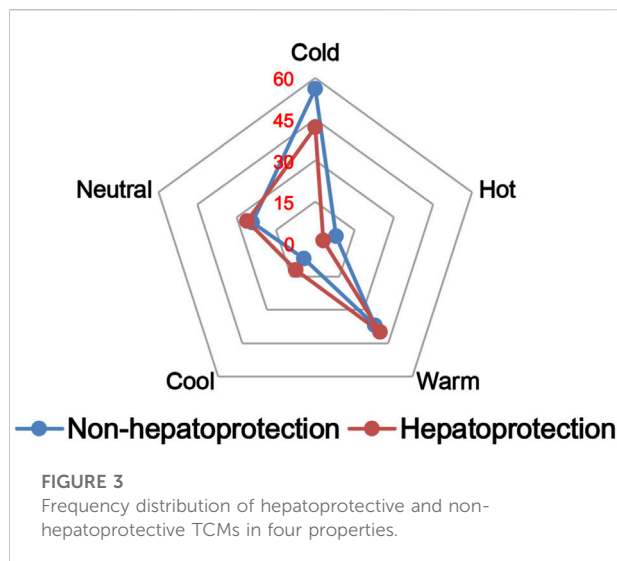
### 2.2.1 Efficacy category analysis

Here, a total of 205 hepatoprotective TCMs were collected (Supplementary File S2). Despite a systematical literature

retrieval being conducted, we must acknowledge that there still existed some hepatoprotective TCMs that escaped from our vision. Therefore, TCMs with the liver-protecting activity included but not limited to those 205 TCMs mentioned earlier. To answer the question of which efficacy categories are rich in hepatoprotective TCMs, a systematical efficacy category analysis was conducted. The results showed that the hepatoprotective TCMs collected in this work were categorized into 18 types. As illustrated in Figure 2A, the antipyretics rank first with a frequency of 52, followed by the tonifying medicinal (35), blood-activating stasis-removing drugs (21), diaphoretics (14), expectorant antitussive antiasthmatics (13), and qi-regulating drugs (11). For the other 12 types of TCMs, the frequencies of hepatoprotective TCMs were less than 10.

In our previous study, a hepatotoxic herb list consisting of 132 members was developed, making it possible to conduct a





comparative analysis between hepatoprotective and hepatotoxic TCMs (He et al., 2019b). As shown in Figure 2A, the TCMs with liver toxicity were divided into 21 types. The antipyretics were the leading cause of herb-induced liver injury with a count of 30. The wind damp-dispelling drugs (11), expectorant antitussive antiasthmatics (11), blood-activating stasis-removing drugs (11), diuretic dampness excreting drugs (9), and diaphoretics (9) rank second, third, fourth, fifth, and sixth, respectively. Further comparative analysis revealed that there existed plenty of overlap between the hepatoprotective and hepatotoxic TCMs (Figure 2B). To be exact, a total of 82 hepatoprotective TCMs were reported to be implicated by liver injury to a different extent, accounting for 40 percent

of the hepatoprotective TCMs collected in this work. The phenomenon mentioned earlier indicates that some hepatoprotective TCMs may exert an adverse effect on liver. Therefore, physicians and hepatologists should keep an eye on hepatoprotectant-induced liver injury in clinical settings.

In summary, the antipyretics, tonifying medicinal, and blood-activating stasis-removing drugs were the three main sources of hepatoprotective TCMs. However, both of the antipyretics and blood-activating stasis-removing drugs were also the most implicated agents of herb-induced liver injury simultaneously. In contrast, as the second major efficacy category of hepatoprotective TCMs, the tonifying medicinal was rarely reported to induce liver toxicity. Therefore, we speculated that tonifying medicinals may be an important and safe source for discovering novel hepatoprotective TCMs.

## 2.2.2 Drug property analysis

The TCM theory considered that the drug property is responsible for specific efficacy and toxicity of TCMs (Ung et al., 2007; Chen et al., 2018). Previous studies have also reported that there exists a certain degree of correlation between drug properties and hepatotoxicity (Liu et al., 2016). To answer the question of whether drug properties are related to the generation of hepatoprotection or not, drug properties of the hepatoprotective TCMs were investigated, including four properties, five flavors, and channel tropism. As there was rarely any literature focusing on the topic of non-hepatoprotection of TCMs, it was difficult to collect non-hepatoprotective TCMs. Therefore, in this study, TCMs with any potential liver toxicity were defined as non-hepatoprotective TCMs. Only those TCMs beneficial to the liver and without liver adverse effects were regarded as

TABLE 4 Results of association rules analysis (support ≥5%, confidence ≥65%, lift >1).

ID	Rule	Support (%)	Confidence (%)	Lift
1	{sweet, kidney} ⇒ {hepatoprotection}	10.59	69.23	1.44
2	{sweet, warm} ⇒ {hepatoprotection}	6.67	73.91	1.53
3	{sour} ⇒ {hepatoprotection}	5.88	71.43	1.48
4	{sweet, liver, kidney} ⇒ {hepatoprotection}	5.49	66.67	1.38
5	{sweet, stomach} ⇒ {hepatoprotection}	6.67	65.38	1.36

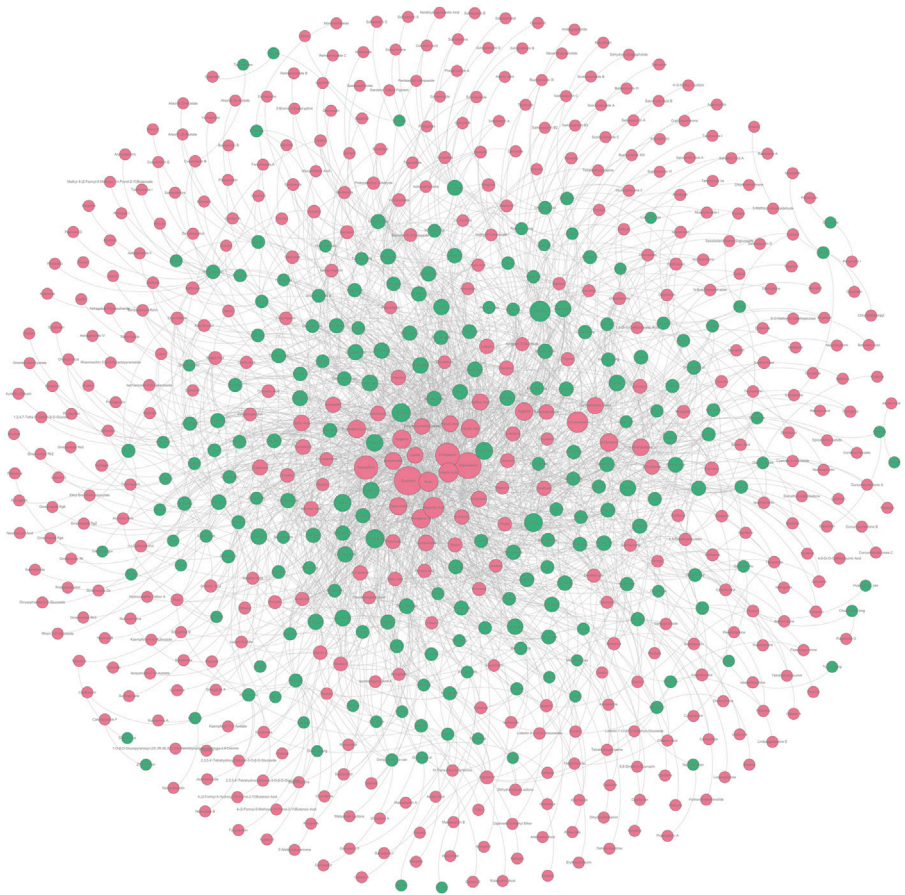
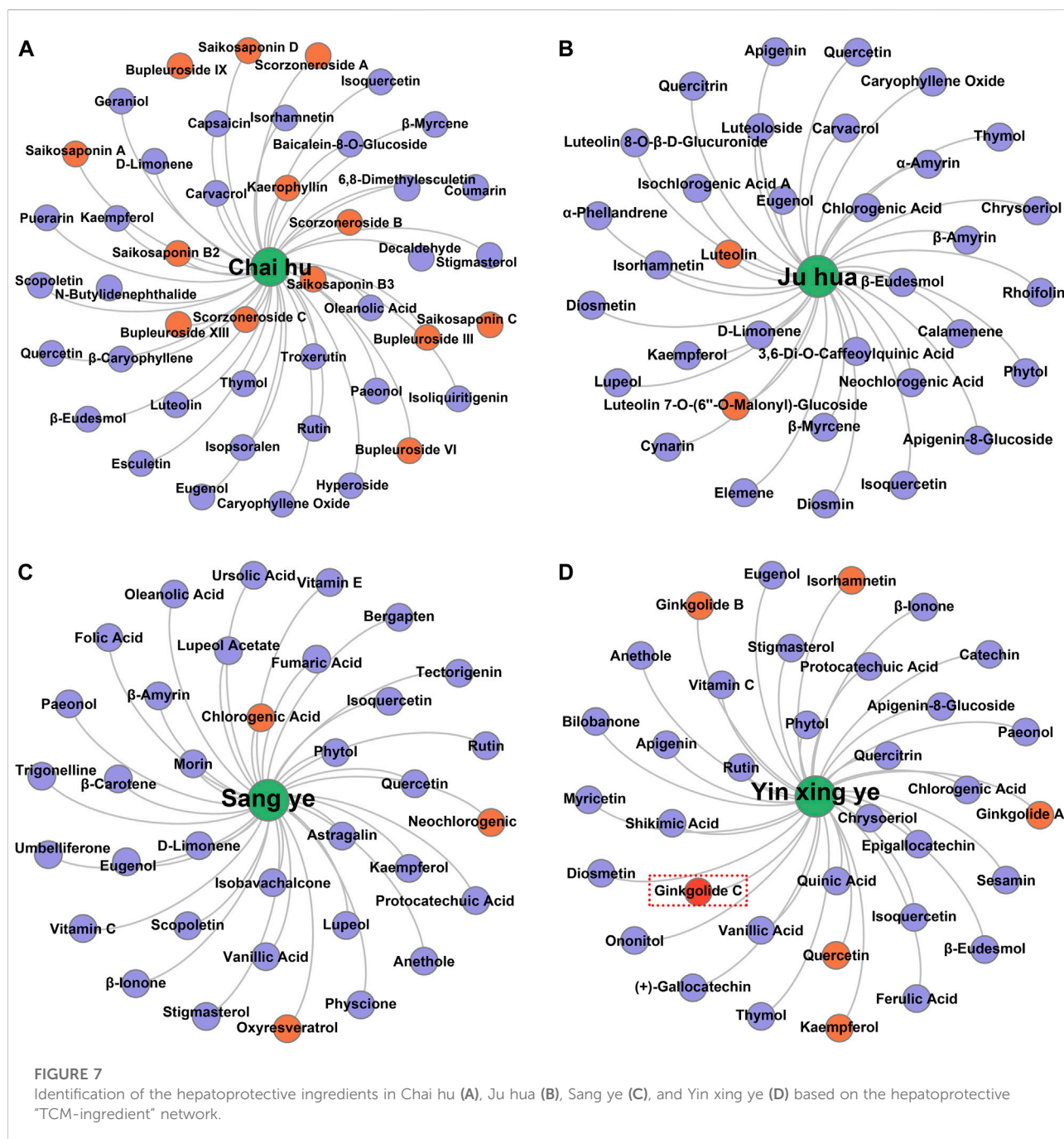


FIGURE 6 “TCM-ingredient” network focused on hepatoprotection. The hepatoprotective TCMs and the hepatoprotective ingredients were displayed by green and red nodes, respectively. If a TCM and an ingredient were connected by a gray line, it indicated that the TCM contained the ingredient.

hepatoprotective TCMs. As a result of this, a total of 123 hepatoprotective TCMs and 132 non-hepatoprotective TCMs were attained and used to conduct drug property analysis (Supplementary File S3). We found that compared to non-hepatoprotective TCMs, hepatoprotective TCMs were inclined to show sour or sweet flavor, whereas less likely to show cold property, bitter flavor, pungent flavor, large

intestine channel, and spleen channel slightly (Figures 3, 4, 5). In fact, pungent flavor was reported to be a risk factor for hepatotoxicity in a previous study (Liu et al., 2016), which was consistent with the phenomenon observed in the present study. To further quantify the difference in drug properties between hepatoprotective and non-hepatoprotective TCMs, the chi-



squared test was conducted. The results indicated that drug properties of the hepatoprotective TCMs were significantly different from those of the non-hepatoprotective TCMs ( $p < 0.05$ ). We must acknowledge that the aforementioned  $p$ -value attained is close to 0.05 ( $p = 0.042$ ). This phenomenon may be due to those hepatoprotective TCMs implicated in herb-induced liver injury being defined as non-hepatoprotective TCMs during the comparative analysis, which decreased the drug property difference between hepatoprotective TCMs and non-

hepatoprotective TCMs to a certain extent. In fact, among those 132 non-hepatoprotective TCMs, a total of 82 TCMs showed biphasic effects on the liver, including hepatoprotection and hepatotoxicity. Nevertheless, there indeed exists significant difference of the drug property between hepatoprotective TCMs and non-hepatoprotective TCMs. Therefore, we can conclude that drug property is related to the generation of hepatoprotection. TCMs with similar drug properties to the hepatoprotective TCMs may exhibit a potential liver-protecting activity.



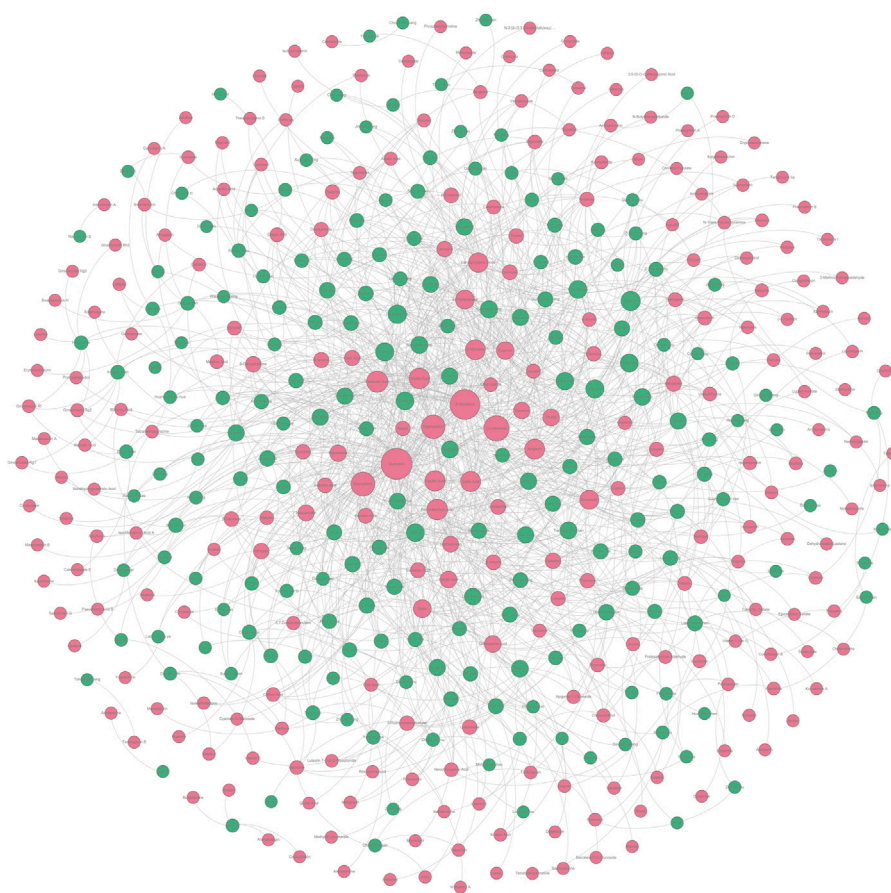


FIGURE 8

Undetermined “TCM-ingredient” network. Green and red nodes represented the TCMs and the hepatoprotective ingredients, respectively. The gray lines connecting the nodes indicated that the TCMs contain the ingredients.

### 2.2.3 Association rules analysis to explore the relationship between the drug property and hepatoprotective activity

In Section 2.2.2, we found that there existed a certain degree of correlation between the drug property and hepatoprotection. To further reveal the detailed association relationship, association rules analysis was conducted. Consequently, a total of five association rules were attained. There was one rule with a single item, three rules with double items, and one rule with triple items (Table 4). The rule with the ID of 3 demonstrated that sour flavor was significantly related to hepatoprotection, which consisted of the TCM theory of “sour into liver” (Wang and Jing, 2019). In addition, sweet flavor showed strong association with hepatoprotection by incorporating with the kidney channel, warm property, or stomach channel, respectively. As the only rule that consisted of triple items, the rule with an ID of 4 involved sweet flavor, liver channel, and kidney channel. The association rules attained previously revealed the relationship between the drug property and hepatoprotection

preliminarily. Theoretically, TCM with these drug properties may have a high potential to generate beneficial effects on the liver.

### 2.2.4 “Traditional Chinese medicine-ingredient” network focused on hepatoprotection

In Section 2.1.1 and Section 2.2.1, we collected a series of potential hepatoprotective ingredients and TCMs. Theoretically, there should exist some associative relationships between these ingredients and TCMs. To discover the detailed relationships, we constructed a “TCM-ingredient” network (Figure 6, Supplementary File S4). The network consisted of 638 nodes and 2262 edges. A total of 205 TCMs and 433 compounds were involved. This network intuitively displayed the association relationships between the hepatoprotective TCMs and ingredients, which may help researchers identify the hepatoprotective ingredients of specific TCMs.

Taking several commonly used TCMs as cases, we identified the hepatoprotective ingredients in Chai Hu (A), Ju Hua (B),

TABLE 5 Top 26 TCMs containing rich liver-protecting ingredients.

ID	TCM	Number of hepatoprotective components	Association rules	Serial number
1	Qian Hu	25	—	U19
2	Ling Xiao Hua	22	1	U16
3	Fu Pen Zi	21	1, 2, 5	U5
4	Gui Zhi	21	4	U10
5	E Bu Shi Cao	20	—	U3
6	Fang Feng	20	4	U4
7	Gao Ben	20	—	U7
8	Jing Jie	20	—	U13
9	Xiang Ru	20	—	U24
10	Qiang Huo	19	—	U20
11	Gao Liang Jiang	18	—	U6
12	Mai Ya	17	3	U17
13	Man Shan Hong	17	—	U18
14	Qing Guo	17	1, 3	U21
15	Tian Shan Xue Lian	17	—	—
16	Che Qian Zi	16	2, 5	U2
17	Hua Ju Hong	16	—	U12
18	Lian Qian Cao	16	—	U15
19	Bai Lian	15	—	U1
20	Gou Gu Ye	15	—	U8
21	Gu Sui Bu	15	—	U9
22	Hu Lu Ba	15	—	U11
23	La Jiao	15	—	U14
24	Wei Ling Cai	15	—	U22
25	Xi He Liu	15	3	U23
26	Zhi Shi	15	1	U25

Serial number corresponds to the TCM ID in Figure 9; ID in column of association rules corresponds to ID in Table 4.

Sang Ye (C), and Yin Xing Ye (D) based on the hepatoprotective “TCM-ingredient” network. As demonstrated in Figure 7, only 13 ingredients were identified to be associated with the hepatoprotective effect of Chai Hu *via* direct literature retrieval (Ashour and Wink, 2011; Lee et al., 2012; Qi et al., 2013; Lin et al., 2015). Interestingly, the hepatoprotective “TCM-ingredient” network discovered 44 hepatoprotective ingredients for Chai Hu. In fact, systematical literature retrieval only led to 2 (Sugawara and Igarashi, 2009), 3 (Lee et al., 2017; Lee et al., 2018), and 6 (Wei et al., 2014; Yang M. H. et al., 2020; Yang Y. et al., 2020; Sarkar et al., 2020) hepatoprotective ingredients for Ju Hua, Sang Ye, and Yin Xing Ye. In contrast, the “TCM-ingredient” network discovered 34, 35, and 34 hepatoprotective ingredients for the corresponding TCMs, respectively. The results mentioned earlier indicated that the hepatoprotective “TCM-ingredient” network was able to identify the hepatoprotective ingredients of TCMs in a more comprehensive and effective way than direct literature retrieval.

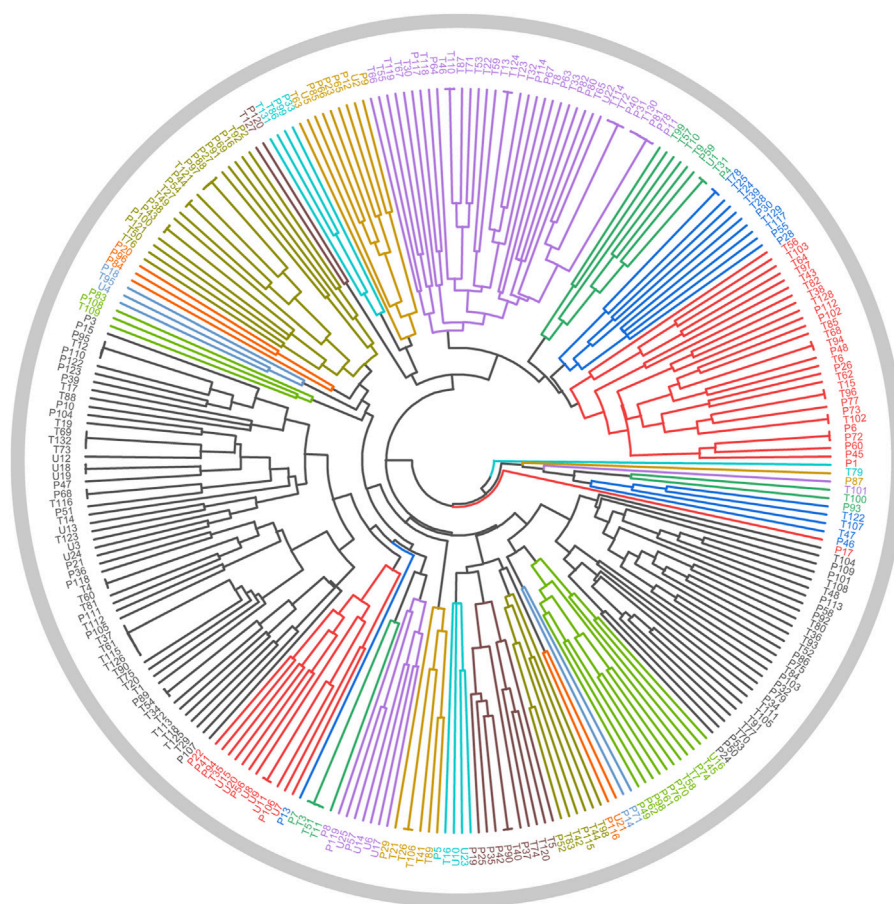
Of note, ginkgolide C, a hepatoprotective ingredient derived from Yin Xing Ye, was not identified successfully by the

hepatoprotective “TCM-ingredient” network. Literature searches found that a total of two studies reported the hepatoprotective activity of ginkgolide C (Huang W. C. et al., 2018; Yang M. H. et al., 2020). However, there was no TCM-related vocabulary that existed in the abstracts or titles of these two studies. Therefore, ginkgolide C escaped our vision when we collected hepatoprotective ingredients and was not included in the hepatoprotective “TCM-ingredient” network. In the future, with the introduction of more hepatoprotective ingredients to the hepatoprotective “TCM-ingredient” network, the network will produce a more satisfactory performance.

### 2.3 Material basis and drug property-based approach to identify potential hepatoprotective traditional Chinese medicines

Theoretically, TCMs may generate a certain degree of liver-protecting effect when they satisfy the following two conditions:



**FIGURE 9**

Cluster analysis based on drug property. The samples with the prefixes of P and T indicated the hepatoprotective TCMs and the non-hepatoprotective TCMs, respectively. U1–U25 represented the 25 samples to be tested.

they contain rich hepatoprotective ingredients and possess similar drug properties to the hepatoprotective TCMs. Therefore, in this section, first, we identified TCMs containing rich hepatoprotective ingredients by constructing an undetermined “TCM-ingredient” network. Then, a comparison between the TCMs containing rich hepatoprotective ingredients and the hepatoprotective TCMs was conducted through cluster analysis. Finally, the TCMs with drug properties similar to those of the hepatoprotective TCMs were considered to be potential hepatoprotective TCMs.

### 2.3.1 Identification of traditional Chinese medicines containing rich liver-protecting ingredients

According to the method mentioned in Section 4.3.4, we constructed an undetermined “TCM-ingredient” network by integrating TCMs and hepatoprotective ingredients. Of note, those 205 hepatoprotective TCMs mentioned in Section 2.2.1 were removed from this network. In other words, for any one of

the TCMs included in this network, whether or not it holds the hepatoprotective activity was unclear. As shown in Figure 8 (Supplementary File S5), the network consisted of 443 nodes and 1376 edges. A total of 197 TCMs and 246 hepatoprotective ingredients were involved. Degree analysis revealed that a total of 26 TCMs contained liver-protecting ingredients greater than 15 (Table 5). Theoretically, the more liver-protecting ingredients a TCM contains, the more likely it is to produce a liver-protecting effect. Therefore, these 26 TCMs were considered as candidate hepatoprotective TCMs.

### 2.3.2 Identification of traditional Chinese medicines with drug properties similar to those of the hepatoprotective TCMs by cluster analysis

In Section 2.2.2, it has been demonstrated that the drug properties of the hepatoprotective TCMs are significantly different from those of the non-hepatoprotective TCMs. Herein, taking the drug properties of the hepatoprotective TCMs (123) and the non-hepatoprotective TCMs (132) as

TABLE 6 Twelve potential hepatoprotective TCMs.

ID	Name	Origin plants	Efficacy category	Hepatoprotective activity
1	Ling Xiao Hua	<i>Campsis grandiflora</i> (Thunb.) K. Schum. and <i>Campsis radicans</i> (L.) Seem	Blood-activating stasis-removing drugs	—
2	Fu Pen Zi	<i>Rubus chingii</i> Hu	Astringent medicinal	Ameliorates CCl <sub>4</sub> -induced liver fibrosis Wu et al. (2022)
3	Gao Ben	<i>Ligusticum sinense</i> Oliv. and <i>Ligusticum jeholense</i> Nakai et Kitag	Diaphoretics	—
4	Gao Liang Jiang	<i>Alpinia officinarum</i> Hance	Warming interior drugs	Anti-hepatoma Zhang et al. (2012); Su et al. (2013); Abass et al. (2018); Fang et al. (2019); anti-hepatitis Luo et al. (2015); nonhepatotoxicity Li et al. (2018)
5	Mai Ya	<i>Hordeum vulgare</i> L.	Digestants	Alleviates alcohol-induced hepatocellular injury Park et al. (2021)
6	Qing Guo	<i>Canarium album</i> Raeusch	Antipyretics	Ameliorates hepatic lipid accumulation Yeh et al. (2018); ameliorates CCl <sub>4</sub> /D-galactosamine-induced liver injury Tamai et al. (1989); Ito et al. (1990)
7	Che Qian Zi	<i>Plantago asiatica</i> L., <i>Plantago depressa</i> Willd	Diuretic dampness excreting drugs	Against lipopolysaccharide-induced liver injury Li et al. (2019)
8	Hu Lu Ba	<i>Trigonella foenum-graecum</i> L.	Tonifying medicinal	Alleviates chemical and drug-induced liver injury (alcohol, thioacetamide, cypermethrin, cadmium, bleomycin, thiamethoxam, adriamycin, AlCl <sub>3</sub> , and gasoline fumes) Kaviarasan et al. (2006); Kaviarasan and Anuradha (2007); Kaviarasan et al. (2007); Kaviarasan et al. (2008); Sushma and Devasena (2010); Lu et al. (2012); Sakr and Abo-El-Yazid (2012); Shivashankara et al. (2012); Belaïd-Nouira et al. (2013); Arafa et al. (2014); Zargar (2014); Qureshi et al. (2016); Kandhare et al. (2017); Abdrabouh (2019); Feki et al. (2019); Fatima Zaidi and Masood (2020); induces hepatoma cell apoptosis Khalil et al. (2015); improves non-alcoholic fatty liver Mohamed et al. (2015); nonhepatotoxicity Serrano (2014)
9	Gou Gu Ye	<i>Ilex cornuta</i> Lindl. ex Paxt	Antipyretics	Prevents high-fat diet-induced fatty liver Liu et al. (2022)
10	Gu Sui Bu	<i>Drynaria fortunei</i> (Kunze) J. Sm	Tonifying medicinal	—
11	Zhi Shi	<i>Citrus aurantium</i> L. and <i>Citrus sinensis</i> Osbeck	Qi-regulating drugs	Alleviates chemical and drug-induced liver injury (acetaminophen, methotrexate, alcohol, and CCl <sub>4</sub> ) Choi et al. (2015); Kim et al. (2016); Lim et al. (2016); Hsouna et al. (2018); He et al. (2019a); Ben Hsouna et al. (2019); Shu et al. (2020); prevents non-alcoholic fatty liver disease Han et al. (2019)
12	La Jiao	<i>Capsicum annuum</i> L.	External medicinal (draw out toxin, resolve putridity)	Attenuates liver fibrosis Sheng et al. (2020); anti-hepatoma carcinoma cell proliferation Chu et al. (2002); induces hepatoma carcinoma cell apoptosis Huang et al. (2009); improves nonalcoholic fatty liver disease Joo et al. (2021); alleviates alcohol-induced liver injury Koneru et al. (2018)

input (Supplementary File S3), hierarchical cluster analysis (Origin 9.0 software) based on Euclidean distance was conducted to develop a cluster model. This model was able to evaluate whether or not the drug properties of specific TCMs were closer to those of the hepatoprotective TCMs. For specific TCM, if it was clustered into the same branch with the hepatoprotective TCMs, its drug property was considered to be closer to the drug properties of the hepatoprotective TCMs. Otherwise, its drug properties were considered to be closer to the drug properties of the non-hepatoprotective TCMs.

In Section 2.3.1, a total of 26 TCMs were found to contain rich liver-protecting ingredients. Of note, Tian Shan Xue Lian lacked channel tropism information and could not be measured by our cluster model. Therefore, only 25 TCMs were put into the cluster model (Figure 9). As a result, a total of 12 TCMs, namely, Ling Xiao Hua, Fu Pen Zi, Gao Ben, Gao Liang Jiang, Mai Ya, Qing Guo, Che Qian Zi, Hu Lu Ba, Gou Gu Ye, Gu Sui Bu, Zhi Shi, and La Jiao, were

discovered to hold similar drug properties to the hepatoprotective TCMs. In summary, these 12 TCMs contained rich liver-protecting ingredients and also held similar drug properties to the hepatoprotective TCMs. Therefore, we speculated that these 12 TCMs may have potential hepatoprotective activity. Detailed descriptions of these 12 TCMs are provided in Table 6.

### 2.3.3 Twelve potential hepatoprotective traditional Chinese medicines

As demonstrated in Table 6, among these 12 potential hepatoprotective TCMs, a total of six TCMs (including Ling Xiao Hua, Gao Ben, Qing Guo, Hu Lu Ba, Gou Gu Ye, and Gu Sui Bu) belonged to the top four efficacy categories of the hepatoprotective TCMs. In other words, about 50% of the novel potential hepatoprotective TCMs were derived from the hepatoprotective TCM-productive efficacy categories, reflecting the reliability of our results to a certain extent.

In Section 2.2.3, we attained five rules which were highly correlated with hepatoprotection. Here, the occurrence frequencies of these five rules in those 25 TCMs were investigated. As a result, the frequency of these rules in these 12 potential hepatoprotective TCMs was 10. However, in the other 13 TCMs, the frequency of these rules was only 3. This phenomenon indicated that these 12 potential hepatoprotective TCMs were more likely to protect the liver than the other 13 TCMs in terms of drug property.

In fact, 9 out of these 12 TCMs were reported to produce beneficial effects to the liver in animal or cell experiments (Table 6). For Ling Xiao Hua and Gao Ben, although they were not reported to treat liver disorders, none of them was implicated by drug-induced liver injury. Direct evidence focused on the liver protection of Gu Sui Bu was unavailable. However, Li Ye Hu Jue (*Drynaria quercifolia* (L.) J. Sm), a form of TCM which has the same effect with Gu Sui Bu, has been demonstrated to exhibit protection against rat liver fibrosis induced by carbon tetrachloride through the Nrf2/ARE and NF $\kappa$ B signaling pathways (Anuja et al., 2018). The results provided by this work were highly consistent with the reports in previous publications and further confirmed the effectiveness of our methods.

### 3 Discussion

In this work, the first contribution is that a comprehensive structure–activity relationship study focused on the hepatoprotective activity of TCMs was conducted. Initially, an *in silico* model for predicting the liver protection of phytoconstituents was developed based on eight machine learning algorithms. Both the five-fold cross-validation and the external validation produced ACC values that exceeded 85%, indicating that the model exhibited satisfactory predicting power. Of note, the imbalance of the dataset may affect the model's performance; a dataset with sufficient non-hepatoprotective phytoconstituents may improve our model's predicting power. Nevertheless, we attempted to develop a model for predicting the hepatoprotection of ingredients derived from TCMs for the first time. This model would contribute to narrowing the scope of candidate drugs in the discovery of novel hepatoprotectants. Second, the structural preference of the hepatoprotective phytoconstituents was investigated. Consequently, a total of 24 RSs for hepatoprotection were identified. Theoretically, phytoconstituents containing these RSs are more likely to produce beneficial effects on the liver. Therefore, these RSs would provide valuable guidance for the design and structural modification of novel hepatoprotectants.

Except the efforts in exploring the hepatoprotection of TCMs in the molecular level, a comprehensive analysis at the level of holistic TCM was also conducted. A total of 205 hepatoprotective TCMs were collected. Efficacy category analysis showed that the

top four efficacy categories were the antipyretics, the tonifying medicinals, the blood-activating stasis-removing drugs, and the diaphoretics, respectively. These four efficacy categories contained many hepatoprotective TCMs. In fact, 6 out of those 12 novel potential hepatoprotective TCMs identified in Section 2.3.2 belonged to the top four efficacy categories, further indicating that these four groups were important sources of the hepatoprotective TCMs. Then, focused on the drug property, a chi-squared test was performed. It showed that the drug properties of the hepatoprotective TCMs were significantly distinguished from those of the non-hepatoprotective TCMs, reflecting that there exists a certain degree of correlation between the drug property and liver-protecting activity. To investigate the detailed relationship, association rules analysis was performed. Subsequently, a total of five association rules were identified. These rules would help explain the liver protection of TCMs from the perspective of the drug property. In fact, more association rules could be attained by decreasing the thresholds of support and confidence. In the current study, the minimum values of the support and confidence were set as 5% and 65%, respectively, which were higher than those in similar studies (Fu et al., 2017).

It has been a consensus that the efficacy of TCM depends on multi-ingredients rather than a single ingredient. Therefore, identifying the hepatoprotective ingredients of specific TCM as complete as possible would help explain its hepatoprotection comprehensively. Generally, researchers compile the efficient ingredients of TCMs through surveying a great deal of literature. However, it is time-consuming and labor-intensive to conduct systematical literature retrieval. Therefore, an efficient and effective method to identify the hepatoprotective ingredients of specific TCM was significant to elucidate its hepatoprotection. In the present study, a “TCM-ingredient” network focused on hepatoprotection was constructed, making it possible to identify the hepatoprotective ingredients of specific TCM efficiently and comprehensively. However, we must acknowledge that there is still some space for improvement in the performance of our hepatoprotective “TCM-ingredient” network. After all, ginkgolide C, one of the hepatoprotective ingredients of Yin Xing Ye, was not successfully discovered. With the introduction of more TCMs and ingredients into the network, it would provide more reliable and complete results in future research.

Another interesting contribution of this work was that a material basis and drug property-based method were originally proposed to discover novel potential hepatoprotective TCMs. This method integrated information on the active ingredients and drug properties of TCMs comprehensively. Based on the method mentioned earlier, a total of 12 potential hepatoprotective TCMs were discovered. Both the efficacy category analysis and the association rules analysis supported the reliability of our results. In addition, 9 out of the 12 potential hepatoprotective TCMs were reported to relieve or treat various types of liver disorders, indicating the effectiveness of our

method further. The hepatoprotective activities of Ling Xiao Hua, Gao Ben, and Gu Sui Bu were not reported. They were expected to be novel hepatoprotective drugs. Therefore, experimental verification focused on the hepatoprotective activities of these three TCMs was urgent and imperative in the next step of our research. One limitation to the method was that the contents of the hepatoprotective ingredients were not taken into consideration. We must acknowledge the importance of the dose-effect relationship. However, it was very difficult to collect the dose effect relationship information of so many hepatoprotective ingredients. When sufficient quantitative data are available, the quantitative methodology study would make great progress. In the future, based on the method proposed in the current study, we believe that more TCMs that were not reported to protect the liver previously will be gradually uncovered to show hepatoprotective effects.

## 4 Materials and methods

### 4.1 Construction of *in silico* models for predicting the hepatoprotective activity of phytoconstituents derived from traditional Chinese medicines

#### 4.1.1 Data sources

In our previous study, focusing on herbal-induced liver injury, we developed a dataset consisting of 664 hepatoprotective phytoconstituents and 216 hepatotoxic phytoconstituents (He et al., 2019b). This dataset laid the foundation for exploring the hepatic effects induced by phytoconstituents based on a data-driven method. Recently, we collected 13 novel hepatoprotective phytoconstituents. They were also added to the dataset of herbal-induced liver protection (Supplementary File S6). Here, the dataset mentioned earlier was utilized to develop a computational molecular model for evaluating the hepatoprotective activity of phytoconstituents. Of note, the phytoconstituents included in the dataset of herbal-induced liver protection were defined as positive samples, whereas the chemical ingredients included in the dataset of herbal-induced liver injury were regarded as negative samples. Both the positive and negative samples were divided into training and test sets in the ratio of 4 to 1 by implementing the Kennard-Stone algorithm. Finally, the training and test sets contained 709 (538 positives and 171 negatives) and 178 (135 positives and 43 negatives) diverse chemicals, respectively (Supplementary File S7).

#### 4.1.2 Molecular descriptor calculation and feature selection

PaDEL-Descriptor (version 2.2.1) (Yap, 2011), a powerful and freely available software application to calculate molecular descriptors and fingerprints, was applied to calculate the two-dimensional (2D) structures of the phytoconstituents. A total of

1444 2D descriptors were taken into consideration, including information on the physicochemical properties and topological geometry properties of the chemicals. With the aim of minimizing the redundancy of the feature variables, the Boruta algorithm (Kursa and Rudnicki, 2010) was implemented to identify feature variables associated with the outcome variable. Thereafter, Pearson's correlation analysis was conducted to eliminate the highly correlated feature variables. The maximum threshold of the Pearson's correlation coefficient was set at 0.90. Finally, a total of 80 non-redundant feature variables were retained and used as input to develop a computational molecular model (Supplementary File S7). Of note, there were six compounds that could not be recognized by PaDEL-Descriptor. Therefore, the total sample size of the training and test sets was 887 rather than 893.

#### 4.1.3 Model construction and evaluation

In the past decades, a series of machine learning algorithms have been proposed by mathematicians and statisticians. However, owing to each algorithm and its own merits, it was difficult to define which one was the best. With the aim of attaining a relatively optimal model, a total of eight algorithms were investigated, including Naive Bayes, J48, K-star, IBK, random forest, Bagging-IBK, AdaBoost-J48, and voting. The rationales of these eight algorithms mentioned earlier have been reviewed in our previous publication (He et al., 2019). In addition, CVPParameterSelection, an effective parameter optimization method, was adopted to confirm the optimum parameters for each algorithm. All of the algorithms mentioned earlier were implemented *via* the Waikato Environment for Knowledge Analysis (WEKA, version 3.8.3) platform within 5-fold cross-validation (Frank et al., 2004).

Three indicators were used to evaluate the predictive ability of the models, including ACC, SE, and SP. These indicators stand for the predictive accuracy of the overall, positive, and negative samples, respectively. In addition, the AUC, an important index for measuring the model's comprehensive performance, was also calculated (Linden, 2006).

### 4.2 Identification of representative substructures for the hepatoprotective activity

SARpy (version 1.0) is a tool to associate structural fragments with specific activity/toxicity (Ferrari et al., 2013). It has been proven to be effective and efficient to extract RSs in many previous studies. Here, it was utilized to identify RSs for hepatoprotection. The minimum thresholds were set at 10 for both the likelihood ratio (LR) and the frequency. The former and the latter indices represent the predictive power and the occurrence number of specific RS, respectively. For a given RS, the greater the LR value, the stronger is its predictive power.



## 4.3 Comprehensive analysis focused on the hepatoprotective activity of traditional Chinese medicines at a singular traditional Chinese medicine level based on bioinformatics

### 4.3.1 Data sources

To collect hepatoprotective TCMs, CNKI (China National Knowledge Infrastructure) and PubMed databases were retrieved according to the procedure listed as follows. First, the publications related to TCMs were identified *via* key phrases of Traditional Chinese Medicine, TCM, herbal, herb, medicinal plant, and botanical. The time span was restricted to between 2012 and 2021. Thereafter, a series of search terms, including hepatotoxicity, liver toxicity, liver injury, liver damage, hepatitis, liver fibrosis, liver failure, liver cancer, hepatoma, liver tumor, liver neoplasms, hepatocellular carcinoma, liver cirrhosis, hepatomegaly, fatty liver, jaundice, cholestasis, liver protection, hepatoprotective, and hepatoprotection, were applied to screen the literature related to TCMs. Only those literature reports associated with herbal-induced hepatoprotection were retained. Finally, hepatoprotective TCMs were collected by reading the literature systematically. Of note, only those TCMs recorded in the Chinese Pharmacopoeia (2020 edition) were taken into consideration in the current study. The efficacy category and the drug property information of each TCM were extracted from TCMSP (Traditional Chinese Medicine Systems Pharmacology Database and Analysis Platform) (Ru et al., 2014) and the Chinese Pharmacopoeia (2020 Edition) (Chinese Pharmacopoeia Commission, 2020), respectively.

### 4.3.2 Statistical analysis

Statistical analysis was performed by SPSS version 17.0 (SPSS Inc., Chicago, United States). The data were presented by frequency. A two-tailed chi-squared test was used for comparing the drug properties (four properties, five flavors, and channel tropism) of the hepatoprotective and non-hepatoprotective TCMs.  $p < 0.05$  was considered statistically significant.

### 4.3.3 Association rules analysis

Association rules analysis was conducted by implementing the Apriori algorithm embedded in the WEKA platform (version 3.8.3) (Frank et al., 2004). The minimum values of support and confidence were set at 5% and 65%, respectively.

### 4.3.4 Construction of the “traditional Chinese medicine-ingredient” network

Over the past decades, many TCM databases have been developed, providing us an opportunity to investigate the relationships between TCMs and chemical components. Here, a total of three typical TCM databases, including TCMSP (Ru et al., 2014), ETCM (Xu et al., 2019), and TCMID (Huang L. et al., 2018), were adopted. By taking the hepatoprotective

ingredients collected in Section 2.1.1 as input, a series of “TCM-ingredient” relationship data were attained. Then, a comparison between the TCMs attained earlier and the hepatoprotective TCMs collected in Section 2.2.1 was conducted. According to whether or not the TCMs were reported to produce beneficial effects on the liver, the “TCM-ingredient” relationships were divided into two categories: hepatoprotective “TCM-ingredient” relationships and undetermined “TCM-ingredient” relationships. Undetermined means that whether the TCMs benefit to the liver or not was unknown. Finally, the former and the latter relationship data were utilized to construct the hepatoprotective “TCM-ingredient” network and an undetermined “TCM-ingredient” network, respectively. To realize the visualization of the network, Gephi (version 0.9.2) software was adopted (Jacomy et al., 2014).

### 4.3.5 Hierarchical cluster analysis

Herein, taking drug properties of the hepatoprotective TCMs (123) and the non-hepatoprotective TCMs (132) as input, hierarchical cluster analysis based on the Euclidean distance was conducted to develop a cluster model. To perform the hierarchical cluster analysis, Origin 9.0 software was used. The drug properties were presented by a binary variable with values of 0 or 1, for example, for TCM Chuan Xiong (Chuanxiong Rhizoma), warm properties, pungent flavor, and entering the liver, gall bladder, and pericardium meridians. Its drug properties were presented as cold 0, hot 0, warm 1, cool 0, neutral 0, pungent 1, bitter 0, sweet 0, sour 0, salty 0, astringent 0, tasteless 0, liver 1, lung 0, stomach 0, spleen 0, kidney 0, heart 0, large intestine 0, gall bladder 1, bladder 0, small intestine 0, pericardium 1, and triple energizer 0.

## 5 Conclusion

In this work, a large-scale dataset of TCM-induced hepatoprotection was constructed through investigating a great deal of literature. Then, the dataset was analyzed based on the structure–activity relationship, molecular network, and machine learning techniques comprehensively. Finally, we developed predictive models for TCM-induced hepatoprotection at the level of molecule and singular TCM, respectively. The model at the molecule level held a strong predictive power with an accuracy greater than 85%. It would provide valuable clues for researchers to screen potential hepatoprotective ingredients from TCMs. The model at the singular TCM level innovatively integrated the material basis and drug property information. It would aid the discovery of novel potential hepatoprotective TCMs. Literature searches showed that the results produced by the singular TCM level model were highly consistent with the reports in previous publications. In summary, we developed effective and reliable predictive models for TCM-induced hepatoprotection at the level of molecule and singular TCM, respectively. Such



comprehensive predictive research would be highly desirable for screening and discovering novel potential hepatoprotectants from TCMs. In addition, the research approaches used in the current study also provided a highlighted mode for discovering the novel functions of TCMs.

## Data availability statement

The original contributions presented in the study are included in the article/Supplementary Material; further inquiries can be directed to the corresponding authors.

## Author contributions

JX and JW conceived the research; SH, YY, and XF collected datasets from the literature; SH carried out all computational analyses and completed the task of manuscript preparation. DH, JZ, and XR contributed to revising and editing the manuscript. All authors have reviewed and approved the manuscript.

## Funding

This work was funded by the National Natural Science Foundation of China (No. 82104540) and the Natural Science Foundation of Zhejiang Province (No. LQ22H280015).

## References

- Abass, S. A., Abdel-Hamid, N. M., Abouzed, T. K., and El-Shishtawy, M. M. (2018). Chemosensitizing Effect of *Alpinia Officinarum* Rhizome Extract in Cisplatin-Treated Rats with Hepatocellular Carcinoma. *Biomed. Pharmacother.* 101, 710–718. doi:10.1016/j.biopha.2018.02.128
- Abdrabouh, A. E. (2019). Liver Disorders Related to Exposure to Gasoline Fumes in Male Rats and Role of Fenugreek Seed Supplementation. *Environ. Sci. Pollut. Res. Int.* 26 (9), 8949–8957. doi:10.1007/s11356-019-04307-x
- Anuja, G. I., Shine, V. J., Latha, P. G., and Suja, S. R. (2018). Protective Effect of Ethyl Acetate Fraction of *Drynaria Quercifolia* against CCl<sub>4</sub> Induced Rat Liver Fibrosis via Nrf2/ARE and NFκB Signalling Pathway. *J. Ethnopharmacol.* 216, 79–88. doi:10.1016/j.jep.2017.11.015
- Arafa, M. H., Mohammad, N. S., and Atteia, H. H. (2014). Fenugreek Seed Powder Mitigates Cadmium-Induced Testicular Damage and Hepatotoxicity in Male Rats. *Exp. Toxicol. Pathol.* 66 (7), 293–300. doi:10.1016/j.etp.2014.04.001
- Ashour, M. L., and Wink, M. (2011). Genus *Bupleurum*: a Review of its Phytochemistry, Pharmacology and Modes of Action. *J. Pharm. Pharmacol.* 63 (3), 305–321. doi:10.1111/j.2042-7158.2010.01170.x
- Bedi, O., Bijjem, K. R. V., Kumar, P., and Gauttam, V. (2016). Herbal Induced Hepatoprotection and Hepatotoxicity: A Critical Review. *Indian J. Physiol. Pharmacol.* 60 (1), 6–21.
- Belaïd-Nouira, Y., Bakhta, H., Haouas, Z., Flehi-Slim, I., Neffati, F., Najjar, M. F., et al. (2013). Fenugreek Seeds, a Hepatoprotector Forage Crop against Chronic AlCl<sub>3</sub> Toxicity. *BMC Vet. Res.* 9, 22. doi:10.1186/1746-6148-9-22
- Ben Hsouna, A., Gargouri, M., Dhifi, W., and Saibi, W. (2019). Antioxidant and Hepato-Preventive Effect of Citrus Aurantium Extract against Carbon Tetrachloride-Induced Hepatotoxicity in Rats and Characterisation of its Bioactive Compounds by HPLC-MS. *Arch. Physiol. Biochem.* 125 (4), 332–343. doi:10.1080/13813455.2018.1461233
- Chen, Z., Cao, Y., He, S., and Qiao, Y. (2018). Development of Models for Classification of Action between Heat-Clearing Herbs and Blood-Activating Stasis-Resolving Herbs Based on Theory of Traditional Chinese Medicine. *Chin. Med.* 13 (1), 12. doi:10.1186/s13020-018-0169-x
- Chinese Pharmacopoeia Commission (2020). *Pharmacopoeia of People's Republic of China*. Beijing: China Medical Science and Technology Press.
- Choi, B. K., Kim, T. W., Lee, D. R., Jung, W. H., Lim, J. H., Jung, J. Y., et al. (2015). A Polymethoxy Flavonoids-Rich Citrus Aurantium Extract Ameliorates Ethanol-Induced Liver Injury through Modulation of AMPK and Nrf2-Related Signals in a Binge Drinking Mouse Model. *Phytother. Res.* 29 (10), 1577–1584. doi:10.1002/ptr.5415
- Chu, Y. F., Sun, J., Wu, X., and Liu, R. H. (2002). Antioxidant and Antiproliferative Activities of Common Vegetables. *J. Agric. Food Chem.* 50 (23), 6910–6916. doi:10.1021/jf020665f
- Fang, D., Xiong, Z., Xu, J., Yin, J., and Luo, R. (2019). Chemopreventive Mechanisms of Galangin against Hepatocellular Carcinoma: A Review. *Biomed. Pharmacother.* 109, 2054–2061. doi:10.1016/j.biopha.2018.09.154
- Fatima Zaidi, S. N., and Masood, J. (2020). The Protective Effect of Fenugreek Seeds Extract Supplementation on Glucose and Lipid Profile in Thioacetamide Induced Liver Damage in Rats. *Pak. J. Pharm. Sci.* 33 (5), 2003–2008.
- Feki, A., Jaballi, I., Cherif, B., Ktari, N., Naifar, M., Makni Ayadi, F., et al. (2019). Therapeutic Potential of Polysaccharide Extracted from Fenugreek Seeds against Thiamethoxam-Induced Hepatotoxicity and Genotoxicity in Wistar Adult Rats. *Toxicol. Mech. Methods* 29 (5), 355–367. doi:10.1080/15376516.2018.1564949
- Ferenci, P., Scherzer, T. M., Kerschner, H., Rutter, K., Beinhart, S., Hofer, H., et al. (2008). Silibinin Is a Potent Antiviral Agent in Patients with Chronic Hepatitis C Not Responding to Pegylated Interferon/ribavirin Therapy. *Gastroenterology* 135 (5), 1561–1567. doi:10.1053/j.gastro.2008.07.072

## Acknowledgments

The authors thank Dr. Shifeng Wang for critically reading and editing the manuscript.

## Conflict of interest

The authors declare that the research was conducted in the absence of any commercial or financial relationships that could be construed as a potential conflict of interest.

## Publisher's note

All claims expressed in this article are solely those of the authors and do not necessarily represent those of their affiliated organizations, or those of the publisher, the editors, and the reviewers. Any product that may be evaluated in this article, or claim that may be made by its manufacturer, is not guaranteed or endorsed by the publisher.

## Supplementary material

The Supplementary Material for this article can be found online at: <https://www.frontiersin.org/articles/10.3389/fphar.2022.969979/full#supplementary-material>

- Ferrari, T., Cattaneo, D., Gini, G., Golbamaki Bakhtyari, N., Manganaro, A., and Benfenati, E. (2013). Automatic Knowledge Extraction from Chemical Structures: the Case of Mutagenicity Prediction. *Sar. QSAR Environ. Res.* 24 (5), 365–383. doi:10.1080/1062936x.2013.773376
- Frank, E., Hall, M., Trigg, L., Holmes, G., and Witten, I. H. (2004). Data Mining in Bioinformatics Using Weka. *Bioinformatics* 20 (15), 2479–2481. doi:10.1093/bioinformatics/bth261
- Fu, X., Song, X., Li, X., Wong, K. K., Li, J., Zhang, F., et al. (2017). Phylogenetic Tree Analysis of the Cold-Hot Nature of Traditional Chinese Marine Medicine for Possible Anticancer Activity. *Evid. Based. Complement. Altern. Med.* 2017, 4365715. doi:10.1155/2017/4365715
- Han, H. Y., Lee, S. K., Choi, B. K., Lee, D. R., Lee, H. J., and Kim, T. W. (2019). Preventive Effect of Citrus Aurantium Peel Extract on High-Fat Diet-Induced Non-alcoholic Fatty Liver in Mice. *Biol. Pharm. Bull.* 42 (2), 255–260. doi:10.1248/bpb.b18-00702
- He, D., Liu, Z., Wang, M., Shu, Y., Zhao, S., Song, Z., et al. (2019a). Synergistic Enhancement and Hepatoprotective Effect of Combination of Total Phenolic Extracts of Citrus Aurantium L. And Methotrexate for Treatment of Rheumatoid Arthritis. *Phytother. Res.* 33 (4), 1122–1133. doi:10.1002/ptr.6306
- He, S., Ye, T., Wang, R., Zhang, C., Zhang, X., Sun, G., et al. (2019). An In Silico Model for Predicting Drug-Induced Hepatotoxicity. *Int. J. Mol. Sci.* 20 (8), 1897. doi:10.3390/ijms20081897
- He, S., Zhang, C., Zhou, P., Zhang, X., Ye, T., Wang, R., et al. (2019b). Herb-Induced Liver Injury: Phylogenetic Relationship, Structure-Toxicity Relationship, and Herb-Ingredient Network Analysis. *Int. J. Mol. Sci.* 20 (15), 3633. doi:10.3390/ijms20153633
- Hong, M., Li, S., Tan, H. Y., Wang, N., Tsao, S. W., and Feng, Y. (2015). Current Status of Herbal Medicines in Chronic Liver Disease Therapy: The Biological Effects, Molecular Targets and Future Prospects. *Int. J. Mol. Sci.* 16 (12), 28705–28745. doi:10.3390/ijms161226126
- Hsouna, A. B., Gargouri, M., Dhifi, W., Saad, R. B., Sayahi, N., Mnif, W., et al. (2018). Potential Anti-inflammatory and Antioxidant Effects of Citrus Aurantium Essential Oil against Carbon Tetrachloride-Mediated Hepatotoxicity: A Biochemical, Molecular and Histopathological Changes in Adult Rats. *Environ. Toxicol.* 34 (4), 388–400. doi:10.1002/tox.22693
- Huang, A., Chang, B., Sun, Y., Lin, H., Li, B., Teng, G., et al. (2017). Disease Spectrum of Alcoholic Liver Disease in Beijing 302 Hospital from 2002 to 2013: A Large Tertiary Referral Hospital Experience from 7422 Patients. *Med. Baltim.* 96 (7), e6163. doi:10.1097/md.00000000000006163
- Huang, L., Xie, D., Yu, Y., Liu, H., Shi, Y., Shi, T., et al. (2018a). TCMID 2.0: a Comprehensive Resource for TCM. *Nucleic Acids Res.* 46 (D1), D1117–d1120. doi:10.1093/nar/gkx1028
- Huang, S. P., Chen, J. C., Wu, C. C., Chen, C. T., Tang, N. Y., Ho, Y. T., et al. (2009). Capsaicin-induced Apoptosis in Human Hepatoma HepG2 Cells. *Anticancer Res.* 29 (1), 165–174.
- Huang, W. C., Chen, Y. L., Liu, H. C., Wu, S. J., and Liou, C. J. (2018b). Ginkgolide C Reduced Oleic Acid-Induced Lipid Accumulation in HepG2 Cells. *Saudi Pharm. J.* 26 (8), 1178–1184. doi:10.1016/j.jsps.2018.07.006
- Ito, M., Shimura, H., Watanabe, N., Tamai, M., Hanada, K., Takahashi, A., et al. (1990). Hepatoprotective Compounds from Canarium Album and Euphorbia Nematocypa. *Chem. Pharm. Bull.* 38 (8), 2201–2203. doi:10.1248/cpb.38.2201
- Jacomy, M., Venturini, T., Heymann, S., and Bastian, M. (2014). ForceAtlas2, a Continuous Graph Layout Algorithm for Handy Network Visualization Designed for the Gephi Software. *PLoS One* 9 (6), e98679. doi:10.1371/journal.pone.0098679
- Joo, H. K., Lee, Y. R., Lee, E. O., Kim, S., Jin, H., Kim, S., et al. (2021). Protective Role of Dietary Capsanthin in a Mouse Model of Nonalcoholic Fatty Liver Disease. *J. Med. Food* 24 (6), 635–644. doi:10.1089/jmf.2020.4866
- Kandhare, A. D., Bodhankar, S. L., Mohan, V., and Thakurdesai, P. A. (2017). Glycosides Based Standardized Fenugreek Seed Extract Ameliorates Bleomycin-Induced Liver Fibrosis in Rats via Modulation of Endogenous Enzymes. *J. Pharm. Bioallied Sci.* 9 (3), 185–194. doi:10.4103/0975-7406.214688
- Kavirasan, S., and Anuradha, C. V. (2007). Fenugreek (Trigonella Foenum Graecum) Seed Polyphenols Protect Liver from Alcohol Toxicity: a Role on Hepatic Detoxification System and Apoptosis. *Pharmazie* 62 (4), 299–304.
- Kavirasan, S., Ramamurthy, N., Gunasekaran, P., Varalakshmi, E., and Anuradha, C. V. (2006). Fenugreek (Trigonella Foenum Graecum) Seed Extract Prevents Ethanol-Induced Toxicity and Apoptosis in Chang Liver Cells. *Alcohol Alcohol* 41 (3), 267–273. doi:10.1093/alcalc/agl020
- Kavirasan, S., Sundarapandian, R., and Anuradha, C. V. (2008). Protective Action of Fenugreek (Trigonella Foenum Graecum) Seed Polyphenols against Alcohol-Induced Protein and Lipid Damage in Rat Liver. *Cell. Biol. Toxicol.* 24 (5), 391–400. doi:10.1007/s10565-007-9050-x
- Kavirasan, S., Viswanathan, P., and Anuradha, C. V. (2007). Fenugreek Seed (Trigonella Foenum Graecum) Polyphenols Inhibit Ethanol-Induced Collagen and Lipid Accumulation in Rat Liver. *Cell. Biol. Toxicol.* 23 (6), 373–383. doi:10.1007/s10565-007-9000-7
- Khalil, M. I., Ibrahim, M. M., El-Gaaly, G. A., and Sultan, A. S. (2015). Trigonella Foenum (Fenugreek) Induced Apoptosis in Hepatocellular Carcinoma Cell Line, HepG2, Mediated by Upregulation of P53 and Proliferating Cell Nuclear Antigen. *Biomed. Res. Int.* 2015, 914645. doi:10.1155/2015/914645
- Kim, T. W., Lee, D. R., Choi, B. K., Kang, H. K., Jung, J. Y., Lim, S. W., et al. (2016). Hepatoprotective Effects of Polymethoxyflavones against Acute and Chronic Carbon Tetrachloride Intoxication. *Food Chem. Toxicol.* 91, 91–99. doi:10.1016/j.fct.2016.03.004
- Koneru, M., Sahu, B. D., Mir, S. M., Ravuri, H. G., Kuncha, M., Mahesh Kumar, J., et al. (2018). Capsaicin, the Pungent Principle of Peppers, Ameliorates Alcohol-Induced Acute Liver Injury in Mice via Modulation of Matrix Metalloproteinases. *Can. J. Physiol. Pharmacol.* 96 (4), 419–427. doi:10.1139/cjpp-2017-0473
- Kong, L. Y., and Tan, R. X. (2015). Artemisinin, a Miracle of Traditional Chinese Medicine. *Nat. Prod. Rep.* 32 (12), 1617–1621. doi:10.1039/c5np00133a
- Kursa, M. B., and Rudnicki, W. R. (2010). Feature Selection with Boruta Package. *J. Stat. Softw.* 36 (11), 1–13.
- Lam, P., Cheung, F., Tan, H. Y., Wang, N., Yuen, M. F., and Feng, Y. (2016). Hepatoprotective Effects of Chinese Medicinal Herbs: A Focus on Anti-inflammatory and Anti-oxidative Activities. *Int. J. Mol. Sci.* 17 (4), 465. doi:10.3390/ijms17040465
- Lee, J. H., Baek, S. Y., Jang, E. J., Ku, S. K., Kim, K. M., Ki, S. H., et al. (2018). Oxyresveratrol Ameliorates Nonalcoholic Fatty Liver Disease by Regulating Hepatic Lipogenesis and Fatty Acid Oxidation through Liver Kinase B1 and AMP-Activated Protein Kinase. *Chem. Biol. Interact.* 289, 68–74. doi:10.1016/j.cbi.2018.04.023
- Lee, T. F., Lin, Y. L., and Huang, Y. T. (2012). Protective Effects of Kaerophyllin against Liver Fibrogenesis in Rats. *Eur. J. Clin. Investig.* 42 (6), 607–616. doi:10.1111/j.1365-2362.2011.02625.x
- Lee, Y. J., Hsu, J. D., Lin, W. L., Kao, S. H., and Wang, C. J. (2017). Upregulation of Caveolin-1 by Mulberry Leaf Extract and its Major Components, Chlorogenic Acid Derivatives, Attenuates Alcoholic Steatohepatitis via Inhibition of Oxidative Stress. *Food Funct.* 8 (1), 397–405. doi:10.1039/c6fo01539e
- Li, F., Huang, D., Nie, S., and Xie, M. (2019). Polysaccharide from the Seeds of Plantago Asiatica L. Protect against Lipopolysaccharide-Induced Liver Injury. *J. Med. Food* 22 (10), 1058–1066. doi:10.1089/jmf.2018.4394
- Li, N., Zhang, Q., Jia, Z., Yang, X., Zhang, H., and Luo, H. (2018). Volatile Oil from *Alpinia Officinarum* Promotes Lung Cancer Regression *In Vitro* and *In Vivo*. *Food Funct.* 9 (9), 4998–5006. doi:10.1039/c8fo01151f
- Lim, S. W., Lee, D. R., Choi, B. K., Kim, H. S., Yang, S. H., Suh, J. W., et al. (2016). Protective Effects of a Polymethoxy Flavonoids-Rich Citrus Aurantium Peel Extract on Liver Fibrosis Induced by Bile Duct Ligation in Mice. *Asian pac. J. Trop. Med.* 9 (12), 1158–1164. doi:10.1016/j.apjtm.2016.10.009
- Lin, L. T., Chung, C. Y., Hsu, W. C., Chang, S. P., Hung, T. C., Shields, J., et al. (2015). Saikosaponin B2 Is a Naturally Occurring Terpenoid that Efficiently Inhibits Hepatitis C Virus Entry. *J. Hepatol.* 62 (3), 541–548. doi:10.1016/j.jhep.2014.10.040
- Linden, A. (2006). Measuring Diagnostic and Predictive Accuracy in Disease Management: an Introduction to Receiver Operating Characteristic (ROC) Analysis. *J. Eval. Clin. Pract.* 12 (2), 132–139. doi:10.1111/j.1365-2753.2005.00598.x
- Liu, H., Li, T., Chen, L., Sha, Z., Pan, M., Ma, Z., et al. (2016). To Set up a Logistic Regression Prediction Model for Hepatotoxicity of Chinese Herbal Medicines Based on Traditional Chinese Medicine Theory. *Evid. Based. Complement. Altern. Med.* 2016, 7273940. doi:10.1155/2016/7273940
- Liu, M., Jia, H., He, Y., Huan, Y., Kong, Z., Xu, N., et al. (2022). Preventive Effects of Ilex Cornuta Aqueous Extract on High-Fat Diet-Induced Fatty Liver of Mice. *Evid. Based. Complement. Altern. Med.* 2022, 7183471. doi:10.1155/2022/7183471
- Lu, K. H., Liu, C. T., Raghu, R., and Sheen, L. Y. (2012). Therapeutic Potential of Chinese Herbal Medicines in Alcoholic Liver Disease. *J. Tradit. Complement. Med.* 2 (2), 115–122. doi:10.1016/s2225-4110(16)30084-0
- Luo, Q., Zhu, L., Ding, J., Zhuang, X., Xu, L., and Chen, F. (2015). Protective Effect of Galangin in Concanavalin A-Induced Hepatitis in Mice. *Drug Des. devel. Ther.* 9, 2983–2992. doi:10.2147/dddt.s80979
- Martins, E. (2013). The Growing Use of Herbal Medicines: Issues Relating to Adverse Reactions and Challenges in Monitoring Safety. *Front. Pharmacol.* 4, 177. doi:10.3389/fphar.2013.00177
- Medina-Franco, J. L., and Saldivar-González, F. I. (2020). Cheminformatics to Characterize Pharmacologically Active Natural Products. *Biomolecules* 10 (11), 1566. doi:10.3390/biom10111566

- Mohamed, W. S., Mostafa, A. M., Mohamed, K. M., and Serwah, A. H. (2015). Effects of Fenugreek, Nigella, and Terminus Seeds in Nonalcoholic Fatty Liver in Obese Diabetic Albino Rats. *Arab. J. Gastroenterol.* 16 (1), 1–9. doi:10.1016/j.ajg.2014.12.003
- Moroy, G., Martiny, V. Y., Vayer, P., Villoutreix, B. O., and Miteva, M. A. (2012). Toward In Silico Structure-Based ADMET Prediction in Drug Discovery. *Drug Discov. Today* 17 (1–2), 44–55. doi:10.1016/j.drudis.2011.10.023
- Park, H., Lee, E., Kim, Y., Jung, H. Y., Kim, K. M., and Kwon, O. (2021). Metabolic Profiling Analysis Reveals the Potential Contribution of Barley Sprouts against Oxidative Stress and Related Liver Cell Damage in Habitual Alcohol Drinkers. *Antioxidants (Basel)* 10 (3), 459. doi:10.3390/antiox10030459
- Qi, F. H., Wang, Z. X., Cai, P. P., Zhao, L., Gao, J. J., Kokudo, N., et al. (2013). Traditional Chinese Medicine and Related Active Compounds: a Review of Their Role on Hepatitis B Virus Infection. *Drug Discov. Ther.* 7 (6), 212–224. doi:10.5582/ddt.2013.v7.6.212
- Qureshi, S., Banday, M. T., Shakeel, I., Adil, S., Mir, M. S., Beigh, Y. A., et al. (2016). Histomorphological Studies of Broiler Chicken Fed Diets Supplemented with Either Raw or Enzyme Treated Dandelion Leaves and Fenugreek Seeds. *Vet. World* 9 (3), 269–275. doi:10.14202/vetworld.2016.269-275
- Ru, J., Li, P., Wang, J., Zhou, W., Li, B., Huang, C., et al. (2014). TCMSP: a Database of Systems Pharmacology for Drug Discovery from Herbal Medicines. *J. Cheminform.* 6, 13. doi:10.1186/1758-2946-6-13
- Sakr, S. A., and Abo-El-Yazid, S. M. (2012). Effect of Fenugreek Seed Extract on Adriamycin-Induced Hepatotoxicity and Oxidative Stress in Albino Rats. *Toxicol. Ind. Health* 28 (10), 876–885. doi:10.1177/0748233711425076
- Sarkar, C., Quispe, C., Jamaddar, S., Hossain, R., Ray, P., Mondal, M., et al. (2020). Therapeutic Promises of Ginkgolide A: A Literature-Based Review. *Biomed. Pharmacother.* 132, 110908. doi:10.1016/j.biopha.2020.110908
- Saxena, N., Dhaked, R. K., and Nagar, D. P. (2022). Silibinin Ameliorates Abrin Induced Hepatotoxicity by Attenuating Oxidative Stress, Inflammation and Inhibiting Fas Pathway. *Environ. Toxicol. Pharmacol.* 93, 103868. doi:10.1016/j.etap.2022.103868
- Serrano, J. (2014). LiverTox: An Online Information Resource and a Site for Case Report Submission on Drug-Induced Liver Injury. *Clin. Liver Dis.* 4 (1), 22–25. doi:10.1002/cld.388
- Sessions, Z., Sánchez-Cruz, N., Prieto-Martínez, F. D., Alves, V. M., Santos, H. P., Jr., Muratov, E., et al. (2020). Recent Progress on Cheminformatics Approaches to Epigenetic Drug Discovery. *Drug Discov. Today* 25 (12), 2268–2276. doi:10.1016/j.drudis.2020.09.021
- Sheng, J., Zhang, B., Chen, Y., and Yu, F. (2020). Capsaicin Attenuates Liver Fibrosis by Targeting Notch Signaling to Inhibit TNF- $\alpha$  Secretion from M1 Macrophages. *Immunopharmacol. Immunotoxicol.* 42 (6), 556–563. doi:10.1080/08923973.2020.1811308
- Shivashankara, A. R., Azmidah, A., Haniadka, R., Rai, M. P., Arora, R., and Baliga, M. S. (2012). Dietary Agents in the Prevention of Alcohol-Induced Hepatotoxicity: Preclinical Observations. *Food Funct.* 3 (2), 101–109. doi:10.1039/c1fo10170f
- Shu, Y., He, D., Li, W., Wang, M., Zhao, S., Liu, L., et al. (2020). Hepatoprotective Effect of Citrus Aurantium L. Against APAP-Induced Liver Injury by Regulating Liver Lipid Metabolism and Apoptosis. *Int. J. Biol. Sci.* 16 (5), 752–765. doi:10.7150/ijbs.40612
- Song, X. Y., Liu, P. C., Liu, W. W., Zhou, J., Hayashi, T., Mizuno, K., et al. (2022). Silibinin Inhibits Ethanol- or Acetaldehyde-Induced Ferroptosis in Liver Cell Lines. *Toxicol. Vitro* 82, 105388. doi:10.1016/j.tiv.2022.105388
- Su, L., Chen, X., Wu, J., Lin, B., Zhang, H., Lan, L., et al. (2013). Galangin Inhibits Proliferation of Hepatocellular Carcinoma Cells by Inducing Endoplasmic Reticulum Stress. *Food Chem. Toxicol.* 62, 810–816. doi:10.1016/j.fct.2013.10.019
- Sugawara, T., and Igarashi, K. (2009). Identification of Major Flavonoids in Petals of Edible Chrysanthemum Flowers and Their Suppressive Effect on Carbon Tetrachloride-Induced Liver Injury in Mice. *Food Sci. Technol. Res.* 15 (5), 499–506. doi:10.3136/fstr.15.499
- Sushma, N., and Devasena, T. (2010). Aqueous Extract of Trigonella Foenum Graecum (Fenugreek) Prevents Cypermethrin-Induced Hepatotoxicity and Nephrotoxicity. *Hum. Exp. Toxicol.* 29 (4), 311–319. doi:10.1177/0960327110361502
- Tamai, M., Watanabe, N., Someya, M., Kondoh, H., Omura, S., Zhang, P. L., et al. (1989). New Hepatoprotective Triterpenes from Canarium Album. *Planta Med.* 55 (1), 44–47. doi:10.1055/s-2006-961822
- Ung, C. Y., Li, H., Kong, C. Y., Wang, J. F., and Chen, Y. Z. (2007). Usefulness of Traditionally Defined Herbal Properties for Distinguishing Prescriptions of Traditional Chinese Medicine from Non-prescription Recipes. *J. Ethnopharmacol.* 109 (1), 21–28. doi:10.1016/j.jep.2006.06.007
- Wang, Y., and Jing, Y. (2019). Explanation the Conception of “Bitter into Heart” Based on Bitter Taste Receptors. *World Latest Med. Inf.* 19 (06), 32–33. doi:10.19613/j.cnki.1671-3141.2019.06.015
- Wei, T., Xiong, F. F., Wang, S. D., Wang, K., Zhang, Y. Y., and Zhang, Q. H. (2014). Flavonoid Ingredients of Ginkgo Biloba Leaf Extract Regulate Lipid Metabolism through Sp1-Mediated Carnitine Palmitoyltransferase 1A Up-Regulation. *J. Biomed. Sci.* 21 (1), 87. doi:10.1186/s12929-014-0087-x
- Wong, M. C. S., Huang, J. L. W., George, J., Huang, J., Leung, C., Eslam, M., et al. (2019). The Changing Epidemiology of Liver Diseases in the Asia-Pacific Region. *Nat. Rev. Gastroenterol. Hepatol.* 16 (1), 57–73. doi:10.1038/s41575-018-0055-0
- Wu, J., Zhang, D., Zhu, B., Wang, S., Xu, Y., Zhang, C., et al. (2022). Rubus Chingii Hu. Unripe Fruits Extract Ameliorates Carbon Tetrachloride-Induced Liver Fibrosis and Improves the Associated Gut Microbiota Imbalance. *Chin. Med.* 17 (1), 56. doi:10.1186/s13020-022-00607-6
- Wu, W.-Y., Yang, W.-Z., Hou, J.-J., and Guo, D.-A. (2015). Current Status and Future Perspective in the Globalization of Traditional Chinese Medicines. *World J. Traditional Chin. Med.* 1 (01), 1–4. doi:10.15806/j.issn.2311-8571.2014.0027
- Xu, H. Y., Zhang, Y. Q., Liu, Z. M., Chen, T., Lv, C. Y., Tang, S. H., et al. (2019). ETCM: an Encyclopaedia of Traditional Chinese Medicine. *Nucleic Acids Res.* 47 (D1), D976–d982. doi:10.1093/nar/gky987
- Yang, M. H., Baek, S. H., Um, J. Y., and Ahn, K. S. (2020a). Anti-neoplastic Effect of Ginkgolide C through Modulating C-Met Phosphorylation in Hepatocellular Carcinoma Cells. *Int. J. Mol. Sci.* 21 (21), 8303. doi:10.3390/ijms21218303
- Yang, Y., Chen, J., Gao, Q., Shan, X., and Lv, Z. (2020b). Study on the Attenuated Effect of Ginkgolide B on Ferroptosis in High Fat Diet Induced Nonalcoholic Fatty Liver Disease. *Toxicology* 445, 152599. doi:10.1016/j.tox.2020.152599
- Yap, C. W. (2011). PaDEL-descriptor: an Open Source Software to Calculate Molecular Descriptors and Fingerprints. *J. Comput. Chem.* 32 (7), 1466–1474. doi:10.1002/jcc.21707
- Yeh, Y. T., Cho, Y. Y., Hsieh, S. C., and Chiang, A. N. (2018). Chinese Olive Extract Ameliorates Hepatic Lipid Accumulation *In Vitro* and *In Vivo* by Regulating Lipid Metabolism. *Sci. Rep.* 8 (1), 1057. doi:10.1038/s41598-018-19553-1
- Zargar, S. (2014). Protective Effect of Trigonella Foenum-Graecum on Thioacetamide Induced Hepatotoxicity in Rats. *Saudi J. Biol. Sci.* 21 (2), 139–145. doi:10.1016/j.sjbs.2013.09.002
- Zhang, H. T., Wu, J., Wen, M., Su, L. J., and Luo, H. (2012). Galangin Induces Apoptosis in Hepatocellular Carcinoma Cells through the Caspase 8/t-Bid Mitochondrial Pathway. *J. Asian Nat. Prod. Res.* 14 (7), 626–633. doi:10.1080/10286020.2012.682152
- Zhao, J., Zhou, G., Sun, Y., Zhou, X., Zhao, Y., Li, W., et al. (2008). Pathological, Epidemiological and Prognostic Studies in 25946 Patients with Liver Disease with Liver Needle Biopsy. *Med. J. Chin. People's Liberation Army* 2008 (10), 1183–1187.



## OPEN ACCESS

## EDITED BY

Adina Turcu-Stolica,  
University of Medicine and Pharmacy of  
Craiova, Romania

## REVIEWED BY

Daniela Calina,  
University of Medicine and Pharmacy of  
Craiova, Romania  
Daniele Pironi,  
Sapienza University of Rome, Italy

## \*CORRESPONDENCE

Fan Feng,  
surgeonfengfan@163.com  
Weiming Kang,  
kangweiming@163.com

## SPECIALTY SECTION

This article was submitted to  
Gastrointestinal and Hepatic  
Pharmacology,  
a section of the journal  
Frontiers in Pharmacology

RECEIVED 11 June 2022

ACCEPTED 19 July 2022

PUBLISHED 29 August 2022

## CITATION

Liu Z, Zhang Z, Sun J, Li J, Zeng Z, Ma M,  
Ye X, Feng F and Kang W (2022),  
Comparison of prognosis between  
neoadjuvant imatinib and upfront  
surgery for GIST: A systematic review  
and meta-analysis.  
*Front. Pharmacol.* 13:966486.  
doi: 10.3389/fphar.2022.966486

## COPYRIGHT

© 2022 Liu, Zhang, Sun, Li, Zeng, Ma, Ye,  
Feng and Kang. This is an open-access  
article distributed under the terms of the  
[Creative Commons Attribution License](https://creativecommons.org/licenses/by/4.0/)  
(CC BY). The use, distribution or  
reproduction in other forums is  
permitted, provided the original  
author(s) and the copyright owner(s) are  
credited and that the original  
publication in this journal is cited, in  
accordance with accepted academic  
practice. No use, distribution or  
reproduction is permitted which does  
not comply with these terms.

# Comparison of prognosis between neoadjuvant imatinib and upfront surgery for GIST: A systematic review and meta-analysis

Zhen Liu<sup>1</sup>, Zimu Zhang<sup>1</sup>, Juan Sun<sup>1</sup>, Jie Li<sup>1</sup>, Ziyang Zeng<sup>1</sup>,  
Mingwei Ma<sup>1</sup>, Xin Ye<sup>1</sup>, Fan Feng<sup>2</sup> and Weiming Kang<sup>1\*</sup>

<sup>1</sup>Department of General Surgery, Peking Union Medical College Hospital, Chinese Academy of Medical Sciences and Peking Union Medical College, Beijing, China, <sup>2</sup>Division of Digestive Surgery, Xijing Hospital of Digestive Diseases, Air Force Medical University, Xi'an, China

**Background:** Significant survival benefit of adjuvant imatinib therapy has been observed in gastrointestinal stromal tumor (GIST). However, the impact of neoadjuvant imatinib on prognosis of GIST remains unclear. This meta-analysis aimed to compare the prognostic impact between upfront surgery and neoadjuvant imatinib plus surgery on GIST.

**Methods:** A comprehensive literature search was performed to identify eligible studies up to 30 Sep 2021, through PubMed, Embase, Web of Science, and Cochrane Library. Studies compared the impact of upfront surgery and neoadjuvant imatinib plus surgery on disease-free (DFS) or overall survival (OS) in patients with GIST were selected.

**Results:** Seven eligible studies with 17,171 patients were included. The reduction rates of tumor size in rectal and mixed site GIST were 33% and 29.8%, respectively. Neoadjuvant imatinib was not significantly associated with DFS compared with no-neoadjuvant therapy in rectal GIST (HR: 0.71, 95% CI: 0.35–1.41). The OS of rectal GIST was significantly improved by neoadjuvant imatinib compared with no-neoadjuvant therapy (HR: 0.36, 95% CI: 0.17–0.75).

**Conclusion:** Neoadjuvant imatinib therapy contributed to tumor shrinkage and R0 resection of rectal GIST. Neoadjuvant imatinib plus surgery significantly improved overall survival of rectal GIST in comparison with upfront surgery.

## KEYWORDS

gastrointestinal stromal tumor, neoadjuvant imatinib, upfront surgery, R0, prognosis, meta-analysis

**Abbreviations:** DFS, disease-free survival; GIST, gastrointestinal stromal tumor; GRADE, the Grading of Recommendations Assessment, Development, and Evaluation system; NCCN, National Comprehensive Cancer Network; NOS, Newcastle-Ottawa Quality Assessment Scale; OS, overall survival; R0, microscopically negative resection margin.



## Introduction

Gastrointestinal stromal tumor is one of the most common mesenchymal tumors arising from the gastrointestinal tract (GI), with an annual incidence of 10 cases per million people globally which accounts for 1–3% of cancers in the entire GI (1, 2). GIST is considered to develop from the gain-of-function mutations of KIT ((Hirota et al., 1998)) and platelet-derived growth factor receptor alpha (PDGFRA) (Heinrich et al., 2003) and can occur anywhere of the GI. The most common site is stomach (60–70%), followed by small intestine (20–30%) and colorectum (5%) (Rubin et al., 2007; Joensuu et al., 2013; Liu et al., 2018).

Surgical resection remains the first choice of curative treatment for primary GIST. Since the first report (Joensuu et al., 2001) of the use of imatinib for metastatic GIST in 2001, various tyrosine kinase inhibitors have been growingly developed and used in clinical treatment of GIST ((Demetri et al., 2002; Demetri et al., 2006; Demetri et al., 2013; Blay et al., 2020; Chen et al., 2020; Heinrich et al., 2020; Chen et al., 2021a)). During this period, significant survival benefit has been observed in those with high-risk GIST who received adjuvant imatinib after surgery (Joensuu et al., 2020). These positive results brought attention to the use of neoadjuvant imatinib for GIST with large size or in special anatomic site. Neoadjuvant therapy has been demonstrated to contribute to the improvement of survival of several malignancies (Das, 2017; Cai et al., 2018; Mittendorf et al., 2020; Chen et al., 2021b). Till now, several retrospective and single-arm studies have reported the feasibility and effectiveness of neoadjuvant therapy on GIST ((Wang et al., 2012; Ling et al., 2021a; Renberg et al., 2022; Wong et al., 2022)). Recent guidelines recommended consideration of neoadjuvant imatinib therapy for patients if the surgical morbidity could be reduced preoperatively (Casali et al., 2018; von Mehren et al., 2020). However, the impact of neoadjuvant imatinib on prognosis of GIST remains unclear due to the absence of strong evidence from randomized controlled trials. Thus, the current meta-analysis aimed to review the relevant literature and provide a comprehensive view of the survival influence of neoadjuvant imatinib on GIST.

## Material and methods

### Search strategy

A systematic search of literature using keywords as “gastrointestinal stromal tumor,” “GIST,” “neoadjuvant,” “preoperative treatment” and “preoperative therapy,” was carried out by two investigators (ZL and ZZ) through PubMed, Embase, Web of Science and Cochrane Library to identify studies that compared the treatment effect between neoadjuvant therapy and upfront surgery for GIST. The search was updated to 30 Sep 2021. Attempts have been made to get additional eligible studies through searching the references

of relevant studies. This study was in compliance with the Preferred Reporting Items for Systematic Reviews and Meta-analyses (PRISMA) guideline (Liberati et al., 2009).

### Selection criteria

Eligible studies were identified by two investigators (ZL and JS) according to the following criteria: (Miettinen et al., 2003) Participants (P): Patients were diagnosed pathologically and immunohistochemically as primary GISTs; (Connolly et al., 2003); Interventions (I) and comparisons (C): Patients received neoadjuvant imatinib followed by surgery and/or adjuvant therapy in research group and upfront surgery and/or adjuvant therapy in control group. The outcomes were compared between research and control groups; (Heinrich et al., 2003); Outcomes (O): Disease-free survival (DFS) and/or overall survival (OS) were/was available or able to be calculated by sufficient data in the studies. When duplicate studies from same center were identified, only the newest or largest study was included. Any discrepancies were resolved by discussion with a third investigator (ZYZ).

### Data extraction

The first author, publication year, country, sample size, tumor site, information of neoadjuvant imatinib, surgery, resection margin, adjuvant therapy, follow-up, DFS and OS were extracted independently by two investigators (SWOY and JL). If the hazard ratio (HR) and 95% confidence interval (CI) were not provided in the studies, we either emailed the corresponding author for original results or calculated these data from the Kaplan-Meier survival curves using the methods reported by Tierney et al. (Tierney et al., 2007). A third observer (MWM) engaged in discussions to resolve any controversial issues.

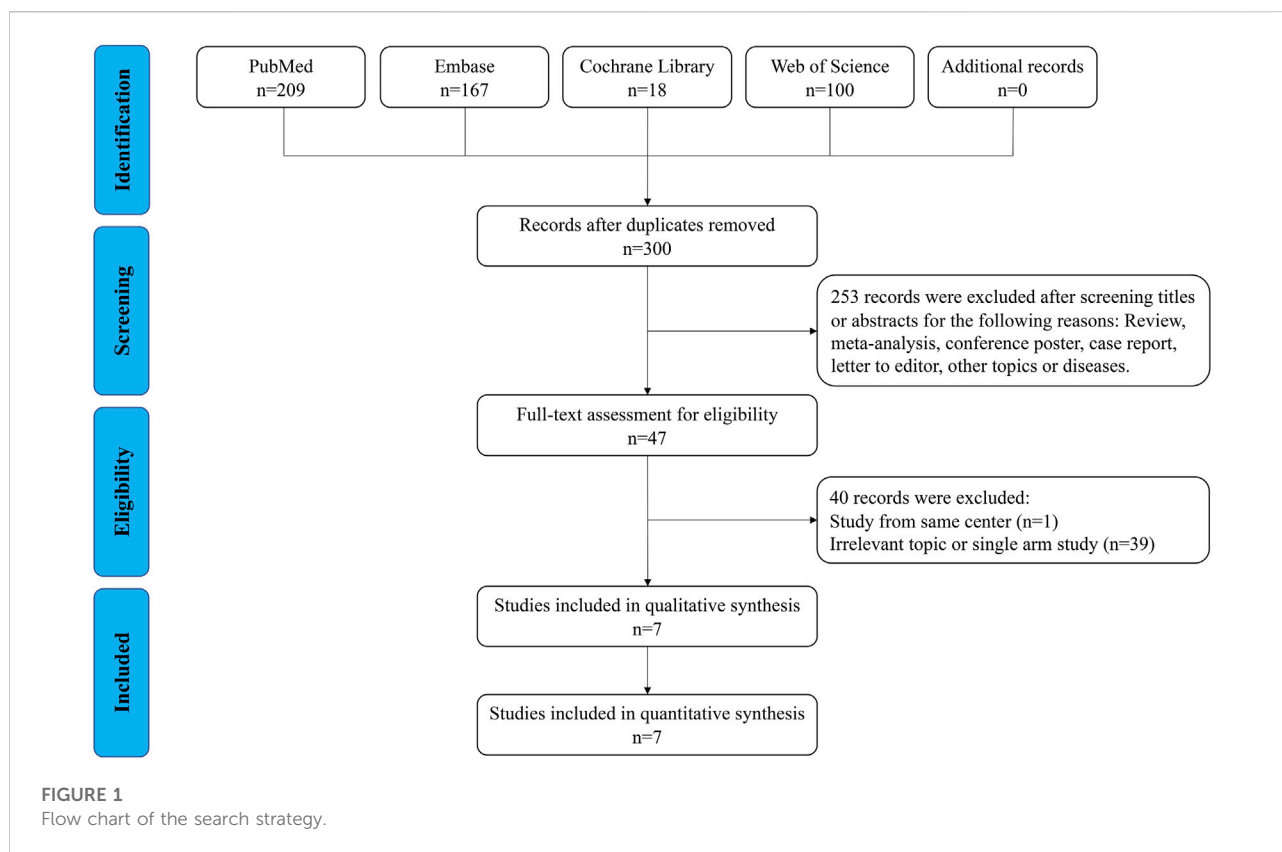
### Quality assessment

Two authors (ZL and ZZ) independently assessed the quality of all included studies using the Newcastle-Ottawa Quality Assessment Scale (NOS) (Stang, 2010) with the highest score of nine, and any discrepancies in the scores were resolved by discussion with a third reviewer (JS).

### Statistical analysis

The pooled survival data were measured using the HR and 95% CI. Some HRs and 95% CIs were extracted from Kaplan-Meier curves using Engauge Digitizer (version 4.1). Statistical





heterogeneity was evaluated using the chi-square test and  $I^2$  statistics. Subgroup analysis was conducted to identify the source of heterogeneity. The random-effects model was used by default because of the nature of these retrospective studies. The estimated results of the fixed-effects model are also provided for reference. Sensitivity analysis was performed to validate the stability of the model by sequentially omitting each study. The publication bias was not performed as fewer than ten studies were included. Statistical analyses were performed using R software 3.6.1 (R Project for Statistical Computing) with the meta package (4.13-0) (Balduzzi et al., 2019). A two-sided  $p < 0.05$  was considered significant. The GRADE profiler software (version 3.6) was used to estimate the level of evidence (Guyatt et al., 2008).

## Results

### Eligible studies in the meta-analysis

As shown in Figure 1, 494 relevant publications were identified through the literature search. After screening and assessment, seven eligible studies (Hawkins et al., 2017; Yan et al., 2018; NS et al., 2020; Yang et al., 2020; Ling et al., 2021b; Marqueen et al., 2021; Yang et al., 2021) with 17,171 patients were included in this meta-analysis (Table 1 and Supplementary

Table S1). There were 1178 patients who received neoadjuvant therapy, and 15,993 patients who received upfront surgery. None of these patients experienced preoperative metastasis. Patients in both groups received adjuvant therapy accordingly. Two studies reported their median reduction rate of tumor size were 29.8% (mixed sites) and 33% (rectum) (Supplementary Table S1), respectively. And in study of Yang 2021 (38), the median tumor size of rectal GIST reduced from 5.8 to 3.8 cm after the use of neoadjuvant imatinib. The NOS scores of the studies ranged from seven to eight, indicating their relatively high quality of methodology. The GRADE evidence profiles of three indicators (resection margin, DFS and OS) were presented in Supplementary Table S2.

### Resection margin

Four studies provided the information of margin resection. Among them, three studies analyzed rectal GIST and one analyzed mixed site GIST (stomach, intestine and enterocoelia). Figure 2A revealed that the R0 resection rate had no significant difference between neoadjuvant imatinib and no-neoadjuvant therapy (HR: 0.54, 95% CI: 0.26–1.10;  $p = 0.99$ ,  $I^2 = 0\%$ ; reference: no-neoadjuvant therapy). In the subgroup analysis of rectal GIST, a trend of higher R0 resection rate ranging from 85.3% to 98.8%

TABLE 1 Summarization of the seven included studies.

Study	Country	Site	Metastasis	Sample size	Neoadjuvant imatinib	Upfront surgery	Follow-up (median, mo)	NOS
Hawkins 2016								7
Rectum-NCDB	USA	Rectum	No	74	21	53	NA	
Yan 2018	China	Mixed <sup>a</sup>	No	191	47	144	NA	8
Ijzerman 2020	Netherlands	Rectum	No	109	78	31	28 (0–115)	8
Yang 2020	China	Rectum	No	64	29	35	41 (1–122)	8
Ling 2021	China	Rectum	No	85	52	33	36.8 (12.7–152.7)	8
Marqueen 2021								8
Total-NCDB	USA	Mixed <sup>b</sup>	No	16,308	865	15,443	44.5 (IQR 22.1–72.5)	
Stomach-NCDB		Stomach	No	10,635	583	10,052		
Yang 2021	China	Rectum		340	86	254	49 (6–215)	8

NCDB, National Cancer Database; NOS, Newcastle–Ottawa Quality Assessment Scale.

<sup>a</sup>Mixed: stomach, intestine and enterocolia.

<sup>b</sup>Mixed: stomach, esophagus, small bowel and colorectum.

was observed in neoadjuvant imatinib group compared with the rate ranging from 74.4% to 92.0% in no-neoadjuvant therapy group (Supplementary Table S1). But the difference was not statistically significant (HR: 0.49, 95% CI: 0.17–1.46;  $p = 0.99$ ,  $I^2 = 0\%$ ; reference: no-neoadjuvant therapy; Figure 2A). Sensitivity analysis was performed by omitting each study sequentially, and the estimated results did not differ significantly, indicating the stability of the model (Figure 2B).

## Disease-free survival

As shown in Figure 3A, DFS data were available in four studies of which the included cases were all rectal GIST. Neoadjuvant imatinib was not significantly associated with DFS compared with no-neoadjuvant therapy (HR: 0.71, 95% CI: 0.35–1.41; reference: no-neoadjuvant therapy), which was consistent with the estimated results of the fixed-effects model (HR: 0.78, 95% CI: 0.46–1.31; reference: no-neoadjuvant therapy), indicating the absence of heterogeneity among studies ( $p = 0.21$ ,  $I^2 = 35\%$ ). Sensitivity analysis was performed by omitting each study sequentially, and the estimated results did not differ significantly, indicating the stability of the model (Figure 3B).

## Overall survival

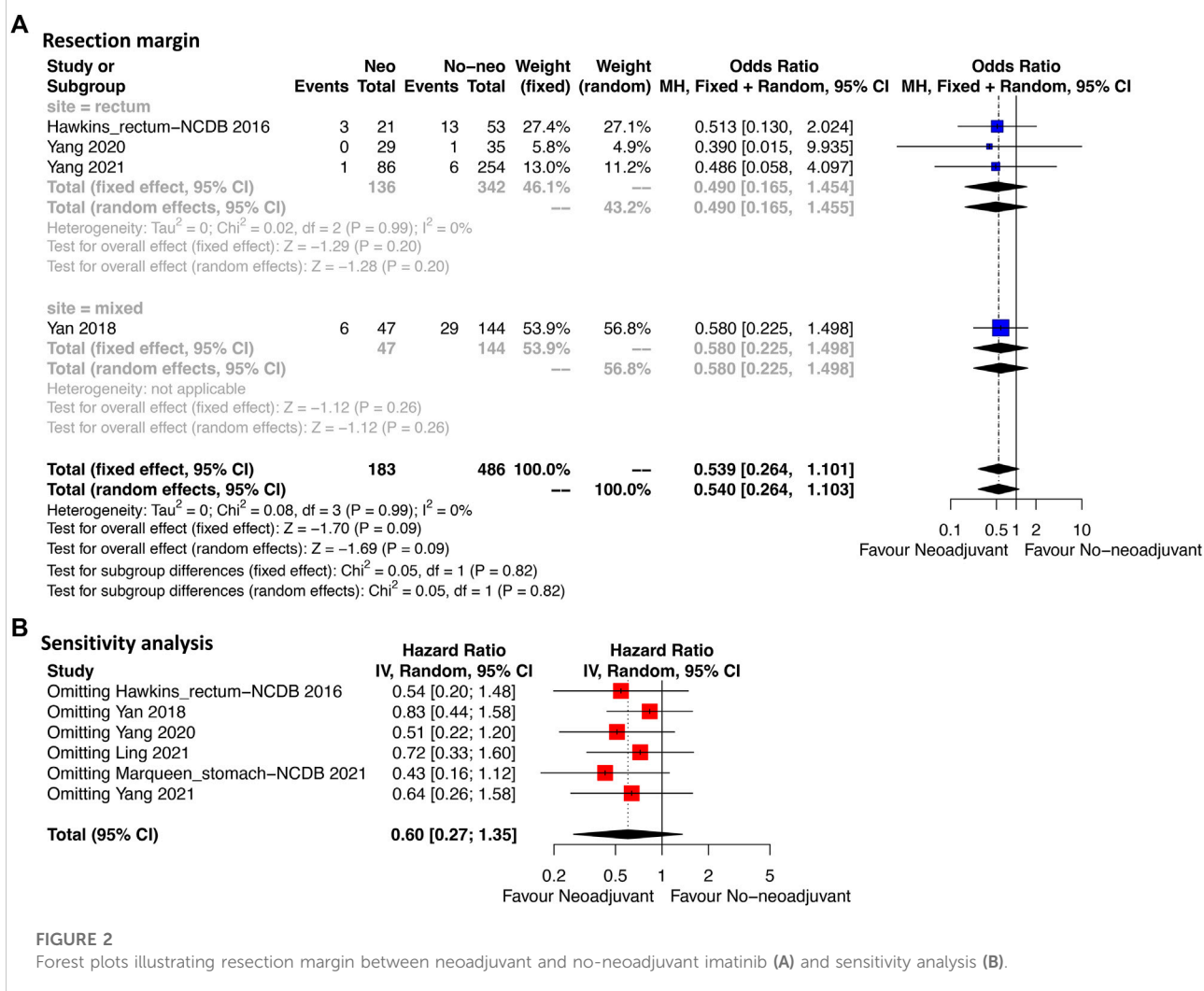
Six studies providing OS data were included (Figure 4A). For the total cases, patients who received neoadjuvant imatinib had similar OS compared with those who received no-neoadjuvant

therapy (HR: 0.52, 95% CI: 0.24–1.14; reference: no-neoadjuvant therapy). However, a moderate heterogeneity was observed ( $p = 0.01$ ,  $I^2 = 65\%$ ). To identify the potential source of heterogeneity, subgroup analysis was performed according to tumor site. A significant decrease of heterogeneity was observed in the subgroup of rectal GIST ( $p = 0.32$ ,  $I^2 = 15\%$ ). In this subgroup, neoadjuvant imatinib was significantly associated with better OS compared with no-neoadjuvant therapy (HR: 0.43, 95% CI: 0.19–1.02), which was consistent with the estimated results of the fixed-effects model (HR: 0.43, 95% CI: 0.21–0.87). Neoadjuvant imatinib significantly improved OS in mixed site GIST (HR: 0.20, 95% CI: 0.05–0.84) but not in gastric GIST (HR: 1.02, 95% CI: 0.94–1.11).

Sensitivity analysis was performed by omitting each study sequentially in rectal GIST subgroup. The result after omitting Yang 2020 was significantly different from that after omitting other three studies which might weaken the credibility of the model (Figure 4B). This might due to the different including criteria in Yang et al.'s study (Yang et al., 2020). Their study mainly compared the transanal and nontransanal surgery for rectal GIST. The prognostic value of neoadjuvant therapy was only analyzed in the multivariate cox model. After omitting the study of Yang 2020 (Figure 4C), the effected result was stable (HR: 0.36, 95% CI: 0.17–0.75) and the heterogeneity additionally decreased ( $p = 0.79$ ,  $I^2 = 0\%$ ) indicating the credibility of the result.

## Discussion

The present study compared the clinical effect of neoadjuvant imatinib and upfront surgery on GIST. The benefits of tumor

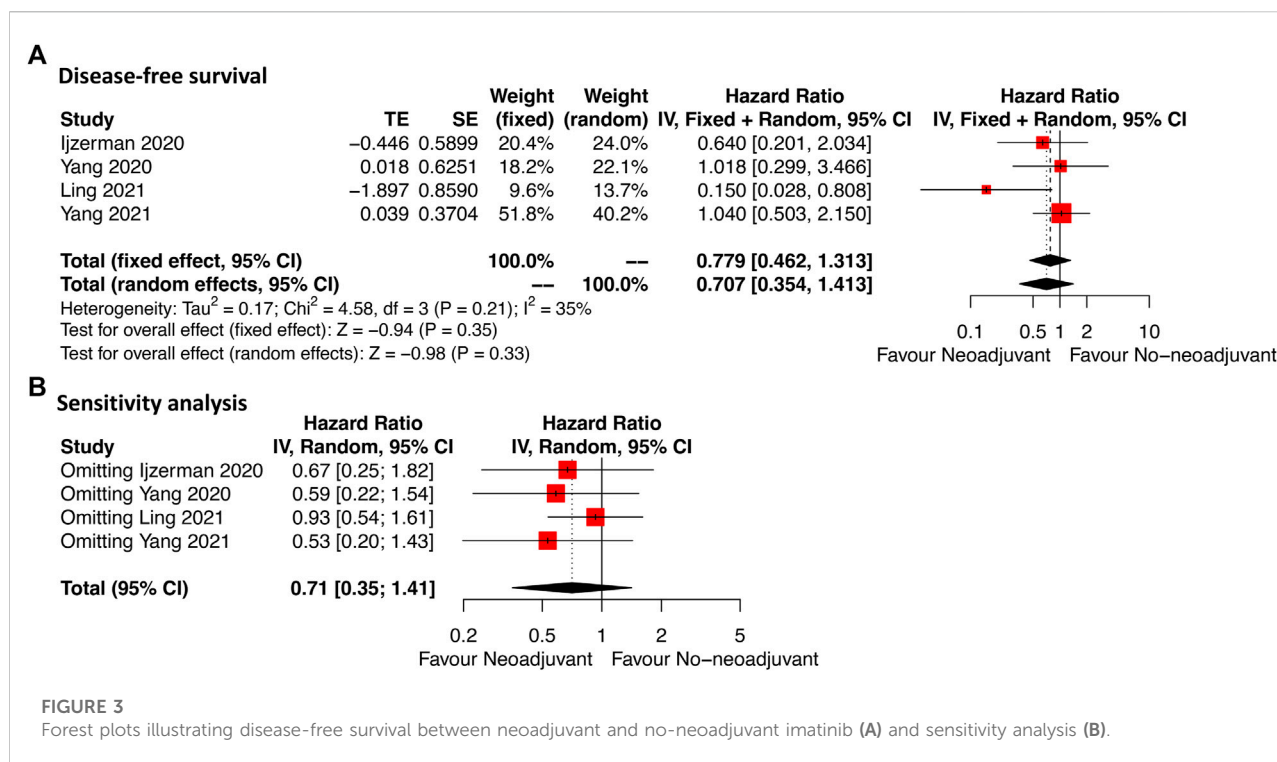


shrinkage as well as improvement of R0 resection rate in rectal GIST were observed after the use of neoadjuvant imatinib therapy. Neoadjuvant imatinib was not significantly associated with DFS compared with no-neoadjuvant therapy in rectal GIST. However, neoadjuvant imatinib significantly improved OS of rectal GIST compared with no-neoadjuvant therapy.

The use of neoadjuvant imatinib has been reported to yield benefits in downstaging to avoid extensive resection in cases of bulky tumors or tumors in particular site, such as rectum (Andtbacka et al., 2007; Fiore et al., 2009; Nishida et al., 2019). A previous observational study (Wilkinson et al., 2015) reported that tumor size and mitotic index significantly reduced after receipt of neoadjuvant imatinib in rectal GIST which allows for less extensive sphincter-preserving surgery. Several studies reported that the sphincter-preserving rate in rectal GIST was 33.3–100% after treatment of neoadjuvant therapy (Kaneko et al., 2019). In the phase II APOLLON trial (Hohenberger et al., 2012), 64% of patients received a less radical surgery after 6 months

treatment of neoadjuvant imatinib. In current meta-analysis, two studies reported their median reduction rate of tumor size were 29.8% (mixed sites) and 33% (rectum) (Supplementary Table S1), respectively. And in study of Yang 2021 (38), the median tumor size of rectal GIST reduced from 5.8 to 3.8 cm after neoadjuvant imatinib. The shrinkage of tumor size is considered to contribute to the achievement of R0 resection.

Complete resection is one of the primary concerns in the treatment of GIST ((Schmieder et al., 2016)). The R0 resection rate was previously reported to be 77.3–100% after treatment of neoadjuvant therapy (Kaneko et al., 2019). In the phase II RTOG 0132 study (Wang et al., 2012) including 31 cases of primary GISTs, a 68% rate of R0 resection (21 cases) was reported within the median neoadjuvant therapy duration of 9.9 weeks. Kurokawa et al. (Kurokawa et al., 2017) reported another phase II study with an achievement of 90% R0 resection rate in large gastric GIST treated with neoadjuvant therapy. This high rate of R0 resection was attributed to the long neoadjuvant



therapy duration of 6 months. Several studies suggested the best duration of neoadjuvant therapy for maximal tumor response is 6–12 months (Bonvalot et al., 2006; Haller et al., 2007; Kurokawa et al., 2017). Which is in line with the 6 months duration or more recommended by NCCN guidelines (von Mehren et al., 2020).

In current meta-analysis, four studies reported the duration of neoadjuvant imatinib which ranged from 6.3 to 10 months (median) indicating a relatively optimal window for tumor response (Supplementary Table S1). The partial response rate in rectal GIST was reported to be 65.9% and 75% by Ling 2021 (36) and Yang 2021 (38), respectively. What is more, the disease control rate achieved 100% in Ling's study (Ling et al., 2021b). Yang et al. (Yang et al., 2021) further reported that the effect of neoadjuvant imatinib is dependent on the genetic type and KIT exon 11 mutation responds better than other types which suggested the importance of genetic sequencing. In the rectal GIST subgroup of current study, a trend of higher R0 resection rate ranging from 85.3% to 98.8% was observed in neoadjuvant imatinib group compared with that ranging from 74.4% to 92.0% in no-neoadjuvant therapy group, though the difference was not significant.

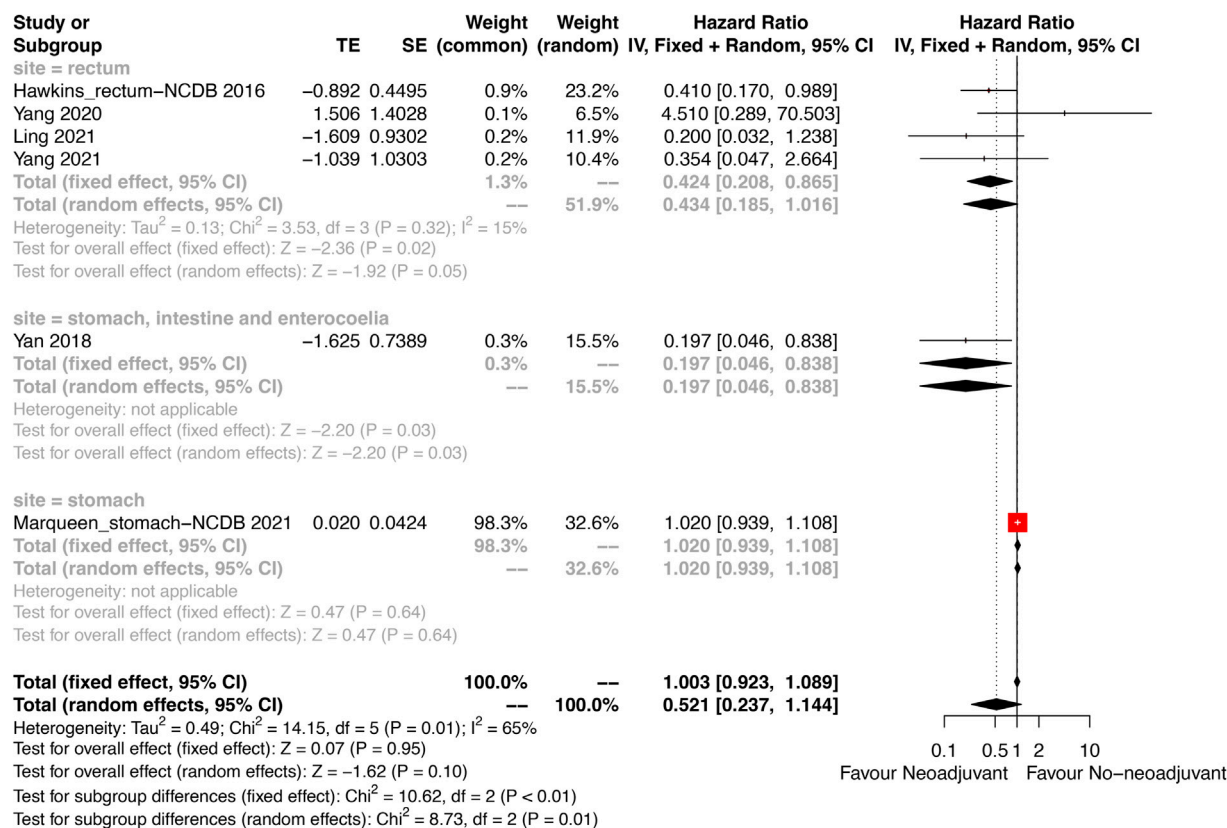
Prognosis is another main indication in the evaluation of efficacy of neoadjuvant therapy which has not been sufficiently reported previously. Hawkins et al. (Hawkins et al., 2017) analyzed 333 cases of rectal GIST enrolled in NCCDB, and the multivariate analysis showed that neoadjuvant therapy was not related with OS. But in the subgroup of tumors that were larger than 5 cm and received radical resection, neoadjuvant therapy

had a significantly higher 5-year OS than no-neoadjuvant therapy (79.2% vs. 51.2%). Ling et al. (Ling et al., 2021b) also demonstrated that neoadjuvant therapy not only reduced tumor size of rectal GIST, but also improved 5-year distant recurrence-free survival and disease-specific survival. But the information of resection margin was not available in their study. In the contrary, a recent multicenter research (Yang et al., 2021) including 340 cases of rectal GISTs from 11 centers in China reported that, the 3-year rates of DFS and OS of those who received neoadjuvant therapy were 95% and 100%, respectively, which were similar in comparison with those of patients who received no-neoadjuvant therapy. Future updated follow-up is warranted for this multicenter study.

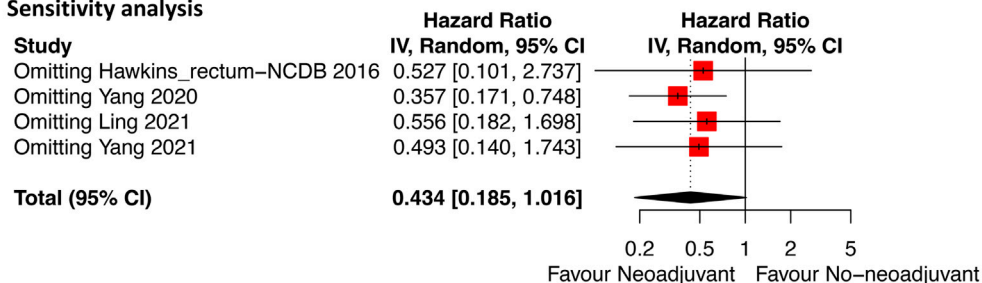
In current meta-analysis, DFS was available in four studies which were all focusing on rectal GIST. The pooled results showed that DFS was not significantly associated with neoadjuvant imatinib in rectal GIST. It is reported that positive margin is possibly associated with the recurrence of GIST but this negative impact disappeared in the era of imatinib due to the use of adjuvant imatinib (Liu et al., 2022). This comparable DFS between neoadjuvant imatinib group and no-neoadjuvant therapy group in current meta-analysis might partly due to the balanced rate of R0 resection between the two groups and the proper use of adjuvant imatinib in both groups. However, the OS was significantly improved after receipt of neoadjuvant imatinib in patients with rectal GIST in present study.

Limitations existed in current study. Firstly, due to the retrospective nature of these eligible studies, some inherent

## A Overall survival



## B Sensitivity analysis



## C Omitting Yan 2018

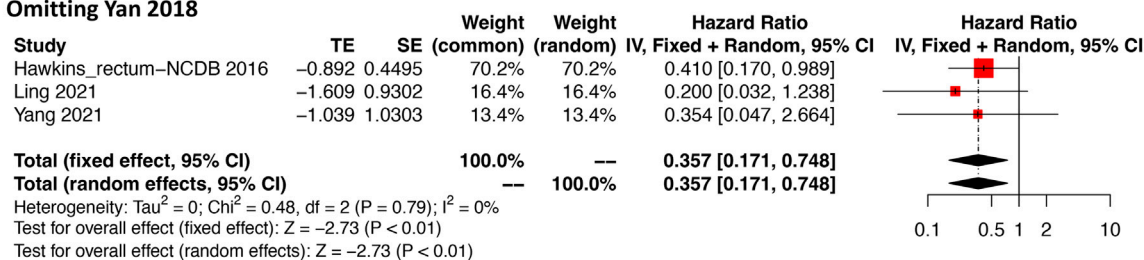


FIGURE 4

Forest plots illustrating overall survival between neoadjuvant and no-neoadjuvant imatinib (A) and sensitivity analyses (B,C).

bias in the study design and process cannot be avoided. Secondly, tumor size and mitotic index as well as their reduction rate after neoadjuvant imatinib were not provided in all eligible studies that

an overview of prognostic factors in GIST other than neoadjuvant imatinib was not available. Thirdly, detailed information of tumor rupture and adjuvant therapy were not



able to be analyzed which were key factors impacting the prognosis of GIST. Fourthly, five out of the seven studies analyzed rectal GIST so further studies focusing on GISTs in other sites are warranted. Fifthly, a multicenter study including 340 cases of rectal GIST from 11 centers in China were included in this meta-analysis which provided relatively firm results for decision-making of neoadjuvant imatinib therapy. However, randomized controlled trials are still lacking and warranted to clarify the role of neoadjuvant imatinib in treatment of GIST.

## Conclusion

Rectal GIST benefits from neoadjuvant imatinib regarding to the achievements of tumor shrinkage and R0 resection. Although neoadjuvant imatinib had no significant advantage on the disease-free survival, patients with rectal GIST who received neoadjuvant imatinib plus surgery had better overall survival than those who received upfront surgery.

## Data availability statement

The original contributions presented in the study are included in the article/[Supplementary Material](#), further inquiries can be directed to the corresponding author.

## Author contributions

Study concepts: WK. Study design: FF. Data acquisition: ZL, ZZ, and JS. Quality control of data and algorithms: ZL and ZZ. Data analysis and interpretation: ZL, SO, and MM. Statistical analysis: ZL and JL. Manuscript preparation: ZL. Manuscript editing: XY. Manuscript review: WK and FF. All authors reviewed the manuscript.

## Funding

This study was supported in part by grants from 1. Wu Jieping Medical Foundation (320.6750.19020 and 320.6750.2020-08-32); 2.

CAMS Innovation Fund for Medical Sciences (2020-I2M-C&T-B-027); 3. Beijing Bethune Charitable Foundation (WCJZL202106); 4. Beijing Xisike Clinical Oncology Research Foundation (Y-HS2019-43).

## Acknowledgments

The authors wish to thank the following collaborators who shared original data in a format that was not available in the original publications: Zifeng Yang, Wentai Guo, Rongkang Huang, Minhui Hu, Huaiming Wang, Hui Wang (*Ann Transl Med* 2020;8(5): 201) and Wenchang Yang, Qian Liu, Guole Lin, Bo Zhang, Hui Cao, Yan Zhao, Lijian Xia, Zhiguo Xiong, Junbo Hu, Yingjiang Ye, Kaixiong Tao, Peng Zhang (*J Surg Oncol*. 2021;124(7): 1128–1135). We also thank all the researchers and study participants for their contributions. Thanks to Siwen Ouyang for the statistical advice.

## Conflict of interest

The authors declare that the research was conducted in the absence of any commercial or financial relationships that could be construed as a potential conflict of interest.

## Publisher's note

All claims expressed in this article are solely those of the authors and do not necessarily represent those of their affiliated organizations, or those of the publisher, the editors and the reviewers. Any product that may be evaluated in this article, or claim that may be made by its manufacturer, is not guaranteed or endorsed by the publisher.

## Supplementary material

The Supplementary Material for this article can be found online at: <https://www.frontiersin.org/articles/10.3389/fphar.2022.966486/full#supplementary-material>

## References

- Andtbacka, R. H., Ng, C. S., Scaife, C. L., Cormier, J. N., Hunt, K. K., Pisters, P. W., et al. (2007). Surgical resection of gastrointestinal stromal tumors after treatment with imatinib. *Ann. Surg. Oncol.* 14, 14–24. doi:10.1245/s10434-006-9034-8
- Balduzzi, S., Rucker, G., and Schwarzer, G. (2019). How to perform a meta-analysis with R: A practical tutorial. *Evid. Based. Ment. Health* 22, 153–160. doi:10.1136/ebmental-2019-300117
- Blay, J. Y., Serrano, C., Heinrich, M. C., Zalcberg, J., Bauer, S., Gelderblom, H., et al. (2020). Ripretinib in patients with advanced gastrointestinal stromal tumours (INVICTUS): A double-blind, randomised, placebo-controlled, phase 3 trial. *Lancet. Oncol.* 21, 923–934. doi:10.1016/S1470-2045(20)30168-6
- Bonvalot, S., Eldweny, H., Pechoux, C. L., Vanel, D., Terrier, P., Cavalcanti, A., et al. (2006). Impact of surgery on advanced gastrointestinal stromal tumors (GIST) in the imatinib era. *Ann. Surg. Oncol.* 13, 1596–1603. doi:10.1245/s10434-006-9047-3
- Cai, Z., Yin, Y., Zhao, Z., Xin, C., Cai, Z., Yin, Y., et al. (2018). Comparative effectiveness of neoadjuvant treatments for resectable gastroesophageal cancer: A Network meta-analysis. *Front. Pharmacol.* 9, 872. doi:10.3389/fphar.2018.00872
- Casali, P. G., Abecassis, N., Aro, H. T., Bauer, S., Biagini, R., Bielack, S., et al. (2018). Gastrointestinal stromal tumours: ESMO-EURACAN clinical practice

guidelines for diagnosis, treatment and follow-up. *Ann. Oncol.* 29, iv68–iv78. doi:10.1093/annonc/mdy095

Chen, D., Jin, Z., Zhang, J., Xu, C., Zhu, K., Ruan, Y., et al. (2021). Efficacy and safety of neoadjuvant targeted therapy vs. Neoadjuvant chemotherapy for stage iiiia EGFR-mutant non-small cell lung cancer: A systematic review and meta-analysis. *Front. Surg.* 8, 715318. doi:10.3389/f surg.2021.715318

Chen, T., Ni, N., Yuan, L., Xu, L., Bahri, N., Sun, B., et al. (2021). Proteasome inhibition suppresses KIT-independent gastrointestinal stromal tumors via targeting hippo/YAP/cyclin D1 signaling. *Front. Pharmacol.* 12, 686874. doi:10.3389/fphar.2021.686874

Chen, Y., Dong, X., Wang, Q., Liu, Z., Dong, X., Shi, S., et al. (2020). Factors influencing the steady-state plasma concentration of imatinib mesylate in patients with gastrointestinal stromal tumors and chronic myeloid leukemia. *Front. Pharmacol.* 11, 569843. doi:10.3389/fphar.2020.569843

Connolly, E. M., Gaffney, E., and Reynolds, J. V. (2003). Gastrointestinal stromal tumours. *Br. J. Surg.* 90, 1178–1186. doi:10.1002/bjs.4352

Das, M. (2017). Neoadjuvant chemotherapy: Survival benefit in gastric cancer. *Lancet. Oncol.* 18, e307. doi:10.1016/S1470-2045(17)30321-2

Demetri, G. D., Reichardt, P., Kang, Y. K., Blay, J. Y., Rutkowski, P., Gelderblom, H., et al. (2013). Efficacy and safety of regorafenib for advanced gastrointestinal stromal tumours after failure of imatinib and sunitinib (GRID): An international, multicentre, randomised, placebo-controlled, phase 3 trial. *Lancet* 381, 295–302. doi:10.1016/S0140-6736(12)61857-1

Demetri, G. D., van Oosterom, A. T., Garrett, C. R., Blackstein, M. E., Shah, M. H., Verweij, J., et al. (2006). Efficacy and safety of sunitinib in patients with advanced gastrointestinal stromal tumour after failure of imatinib: A randomised controlled trial. *Lancet* 368, 1329–1338. doi:10.1016/S0140-6736(06)69446-4

Demetri, G. D., von Mehren, M., Blanke, C. D., Van den Abbeele, A. D., Eisenberg, B., Roberts, P. J., et al. (2002). Efficacy and safety of imatinib mesylate in advanced gastrointestinal stromal tumors. *N. Engl. J. Med.* 347, 472–480. doi:10.1056/NEJMoa020461

Fiore, M., Palassini, E., Fumagalli, E., Pilotti, S., Tamborini, E., Stacchiotti, S., et al. (2009). Preoperative imatinib mesylate for unresectable or locally advanced primary gastrointestinal stromal tumors (GIST). *Eur. J. Surg. Oncol.* 35, 739–745. doi:10.1016/j.ejso.2008.11.005

Guyatt, G. H., Oxman, A. D., Vist, G. E., Kunz, R., Falck-Ytter, Y., Alonso-Coello, P., et al. (2008). Grade: An emerging consensus on rating quality of evidence and strength of recommendations. *BMJ* 336, 924–926. doi:10.1136/bmj.39489.470347

Haller, F., Detken, S., Schulten, H. J., Happel, N., Gunawan, B., Kuhlitz, J., et al. (2007). Surgical management after neoadjuvant imatinib therapy in gastrointestinal stromal tumours (GISTs) with respect to imatinib resistance caused by secondary KIT mutations. *Ann. Surg. Oncol.* 14, 526–532. doi:10.1245/s10434-006-9228-0

Hawkins, A. T., Wells, K. O., Krishnamurthy, D. M., Hunt, S. R., Mutch, M. G., Glasgow, S. C., et al. (2017). Preoperative chemotherapy and survival for large anorectal gastrointestinal stromal tumors: A national analysis of 333 cases. *Ann. Surg. Oncol.* 24, 1195–1201. doi:10.1245/s10434-016-5706-1

Heinrich, M. C., Corless, C. L., Duensing, A., McGreevey, L., Chen, C. J., Joseph, N., et al. (2003). PDGFRα activating mutations in gastrointestinal stromal tumors. *Science* 299, 708–710. doi:10.1126/science.1079666

Heinrich, M. C., Jones, R. L., von Mehren, M., Schoffski, P., Serrano, C., Kang, Y. K., et al. (2020). Avapritinib in advanced PDGFRα D842V-mutant gastrointestinal stromal tumour (NAVIGATOR): A multicentre, open-label, phase 1 trial. *Lancet. Oncol.* 21, 935–946. doi:10.1016/S1470-2045(20)30269-2

Hirota, S., Isozaki, K., Moriyama, Y., Hashimoto, K., Nishida, T., Ishiguro, S., et al. (1998). Gain-of-function mutations of c-kit in human gastrointestinal stromal tumors. *Science* 279, 577–580. doi:10.1126/science.279.5350.577

Hohenberger, P., Langer, C., Wendtner, C. M., Hohenberger, W., Pustowka, A., Wardelmann, E., et al. (2012). Neoadjuvant treatment of locally advanced GIST: Results of APOLLON, a prospective, open label phase II study in KIT- or PDGFRα-positive tumors. *J. Clin. Oncol.* 30, 10031. doi:10.1200/jco.2012.30.15\_suppl.10031

Joensuu, H., Eriksson, M., Sundby Hall, K., Reichardt, A., Hermes, B., Schutte, J., et al. (2020). Survival outcomes associated with 3 Years vs 1 Year of adjuvant imatinib for patients with high-risk gastrointestinal stromal tumors: An analysis of a randomized clinical trial after 10-year follow-up. *JAMA Oncol.* 6, 1241–1246. doi:10.1001/jamaoncol.2020.2091

Joensuu, H., Hohenberger, P., and Corless, C. L. (2013). Gastrointestinal stromal tumour. *Lancet* 382, 973–983. doi:10.1016/S0140-6736(13)60106-3

Joensuu, H., Roberts, P. J., Sarlomo-Rikala, M., Andersson, L. C., Tervahartiala, P., Tuveson, D., et al. (2001). Effect of the tyrosine kinase inhibitor STI571 in a

patient with a metastatic gastrointestinal stromal tumor. *N. Engl. J. Med.* 344, 1052–1056. doi:10.1056/NEJM200104053441404

Kaneko, M., Emoto, S., Muroto, K., Sonoda, H., Hiyoshi, M., Sasaki, K., et al. (2019). Neoadjuvant imatinib therapy in rectal gastrointestinal stromal tumors. *Surg. Today* 49, 460–466. doi:10.1007/s00595-018-1737-5

Kurokawa, Y., Yang, H. K., Cho, H., Ryu, M. H., Masuzawa, T., Park, S. R., et al. (2017). Phase II study of neoadjuvant imatinib in large gastrointestinal stromal tumours of the stomach. *Br. J. Cancer* 117, 25–32. doi:10.1038/bjc.2017.144

Liberati, A., Altman, D. G., Tetzlaff, J., Mulrow, C., Gotzsche, P. C., Ioannidis, J. P., et al. (2009). The PRISMA statement for reporting systematic reviews and meta-analyses of studies that evaluate healthcare interventions: Explanation and elaboration. *BMJ* 339, b2700. doi:10.1136/bmj.b2700

Ling, J. Y., Ding, M. M., Yang, Z. F., Zhao, Y. D., Xie, X. Y., Shi, L. S., et al. (2021). Comparison of outcomes between neoadjuvant imatinib and upfront surgery in patients with localized rectal GIST: An inverse probability of treatment weighting analysis. *J. Surg. Oncol.* 124, 1442–1450. doi:10.1002/jso.26664

Ling, J. Y., Ding, M. M., Yang, Z. F., Zhao, Y. D., Xie, X. Y., Shi, L. S., et al. (2021). Comparison of outcomes between neoadjuvant imatinib and upfront surgery in patients with localized rectal GIST: An inverse probability of treatment weighting analysis. *J. Surg. Oncol.* 124, 1442–1450. doi:10.1002/jso.26664

Liu, Z., Zhang, Y., Yin, H., Geng, X., Li, S., Zhao, J., et al. (2022). Comparison of prognosis between microscopically positive and negative surgical margins for primary gastrointestinal stromal tumors: A systematic review and meta-analysis. *Front. Oncol.* 12, 679115. doi:10.3389/fonc.2022.679115

Liu, Z., Zheng, G., Liu, J., Liu, S., Xu, G., Wang, Q., et al. (2018). Clinicopathological features, surgical strategy and prognosis of duodenal gastrointestinal stromal tumors: A series of 300 patients. *BMC Cancer* 18, 563. doi:10.1186/s12885-018-4485-4

Marqueen, K. E., Moshier, E., Buckstein, M., and Ang, C. (2021). Neoadjuvant therapy for gastrointestinal stromal tumors: A propensity score-weighted analysis. *Int. J. Cancer* 149, 177–185. doi:10.1002/ijc.33536

Miettinen, M., Kopczynski, J., Makhlof, H. R., Sarlomo-Rikala, M., Gyorffy, H., Burke, A., et al. (2003). Gastrointestinal stromal tumors, intramural leiomyomas, and leiomyosarcomas in the duodenum: A clinicopathologic, immunohistochemical, and molecular genetic study of 167 cases. *Am. J. Surg. Pathol.* 27, 625–641. doi:10.1097/0000478-200305000-00006

Mittendorf, E. A., Zhang, H., Barrios, C. H., Saji, S., Jung, K. H., Hegg, R., et al. (2020). Neoadjuvant atezolizumab in combination with sequential nab-paclitaxel and anthracycline-based chemotherapy versus placebo and chemotherapy in patients with early-stage triple-negative breast cancer (IMpassion031): A randomised, double-blind, phase 3 trial. *Lancet* 396, 1090–1100. doi:10.1016/S0140-6736(20)31953-X

Nishida, T., Holmebakk, T., Raut, C. P., and Rutkowski, P. (2019). Defining tumor rupture in gastrointestinal stromal tumor. *Ann. Surg. Oncol.* 26, 1669–1675. doi:10.1245/s10434-019-07297-9

Ns, I. J., Mohammadi, M., Tzanis, D., Gelderblom, H., Fiore, M., Fumagalli, E., et al. (2020). Quality of treatment and surgical approach for rectal gastrointestinal stromal tumour (GIST) in a large European cohort. *Eur. J. Surg. Oncol.* 46, 1124–1130. doi:10.1016/j.ejso.2020.02.033

Renberg, S., Zhang, Y., Karlsson, F., Branstrom, R., Ahlen, J., Jalmell, L., et al. (2022). The role of neoadjuvant imatinib in gastrointestinal stromal tumor patients: 20 years of experience from a tertiary referral center. *Int. J. Cancer* 151, 906–913. doi:10.1002/ijc.34052

Rubin, B. P., Heinrich, M. C., and Corless, C. L. (2007). Gastrointestinal stromal tumour. *Lancet* 369, 1731–1741. doi:10.1016/S0140-6736(07)60780-6

Schmieder, M., Henne-Bruns, D., Mayer, B., Knippschild, U., Rolke, C., Schwab, M., et al. (2016). Comparison of different risk classification systems in 558 patients with gastrointestinal stromal tumors after R0-resection. *Front. Pharmacol.* 7, 504. doi:10.3389/fphar.2016.00504

Stang, A. (2010). Critical evaluation of the Newcastle-Ottawa scale for the assessment of the quality of nonrandomized studies in meta-analyses. *Eur. J. Epidemiol.* 25, 603–605. doi:10.1007/s10654-010-9491-z

Tierney, J. F., Stewart, L. A., Ghersi, D., Burdett, S., and Sydes, M. R. (2007). Practical methods for incorporating summary time-to-event data into meta-analysis. *Trials* 8, 16. doi:10.1186/1745-6215-8-16

von Mehren, M., Kane, J. M., Bui, M. M., Choy, E., Connelly, M., Dry, S., et al. (2020). NCCN guidelines insights: Soft tissue sarcoma, version 1.2021. *J. Natl. Compr. Canc. Netw.* 18, 1604–1612. doi:10.6004/jnccn.2020.0058

Wang, D., Zhang, Q., Blanke, C. D., Demetri, G. D., Heinrich, M. C., Watson, J. C., et al. (2012). Phase II trial of neoadjuvant/adjuvant imatinib mesylate for advanced primary and metastatic/recurrent operable gastrointestinal stromal tumors: Long-term follow-up results of radiation therapy Oncology group 0132. *Ann. Surg. Oncol.* 19, 1074–1080. doi:10.1245/s10434-011-2190-5

Wilkinson, M. J., Fitzgerald, J. E., Strauss, D. C., Hayes, A. J., Thomas, J. M., Messiou, C., et al. (2015). Surgical treatment of gastrointestinal stromal tumour of the rectum in the era of imatinib. *Br. J. Surg.* 102, 965–971. doi:10.1002/bjs.9818

Wong, L. H., Sutton, T. L., Sheppard, B. C., Corless, C. L., Heinrich, M. C., and Mayo, S. C. (2022). Neoadjuvant tyrosine kinase inhibitor therapy for patients with gastrointestinal stromal tumor: A propensity-matched analysis. *Am. J. Surg.* 224, 624–628. doi:10.1016/j.amjsurg.2022.03.045

Yan, L. H., Chen, Z. N., Li, C. J., Chen, J., Qin, Y. Z., Chen, J. S., et al. (2018). Prolonging Gastrointestinal-Stromal-Tumor-free life, an optimal suggestion of

imatinib intervention ahead of operation. *J. Cancer* 9, 3850–3857. doi:10.7150/jca.25263

Yang, W., Liu, Q., Lin, G., Zhang, B., Cao, H., Zhao, Y., et al. (2021). The effect of neoadjuvant imatinib therapy on outcome and survival in rectal gastrointestinal stromal tumors: A multiinstitutional study. *J. Surg. Oncol.* 124, 1128–1135. doi:10.1002/jso.26628

Yang, Z., Guo, W., Huang, R., Hu, M., Wang, H., and Wang, H. (2020). Transanal versus nontransanal surgery for the treatment of primary rectal gastrointestinal stromal tumors: A 10-year experience in a high-volume center. *Ann. Transl. Med.* 8, 201. doi:10.21037/atm.2020.01.55



## OPEN ACCESS

## EDITED BY

Adina Turcu-Stolica,  
University of Medicine and Pharmacy of  
Craiova, Romania

## REVIEWED BY

Claudiu Marinel Ionele,  
Spitalul Clinic Judetean de Urgenta  
Craiova, Romania  
Li Wang,  
Peking Union Medical College Hospital  
(CAMS), China  
Bin Liu,  
Qingdao University, China

## \*CORRESPONDENCE

Han Ying,  
hanying1@fmmu.edu.cn  
Shang Yulong,  
shangyul870222@163.com  
Chen Xi,  
121672361@qq.com

<sup>†</sup>These authors have contributed equally  
to this work

## SPECIALTY SECTION

This article was submitted to Drugs  
Outcomes Research and Policies,  
a section of the journal  
Frontiers in Pharmacology

RECEIVED 19 May 2022

ACCEPTED 20 July 2022

PUBLISHED 30 August 2022

## CITATION

Guoyun X, Dawei D, Ning L, Yinan H,  
Fangfang Y, Siyuan T, Hao S, Jiaqi Y,  
Ang X, Guanya G, Xi C, Yulong S and  
Ying H (2022). Efficacy and safety of  
fenofibrate add-on therapy in patients  
with primary biliary cholangitis  
refractory to ursodeoxycholic acid: A  
retrospective study and updated meta-  
analysis.  
*Front. Pharmacol.* 13:948362.  
doi: 10.3389/fphar.2022.948362

## COPYRIGHT

© 2022 Guoyun, Dawei, Ning, Yinan,  
Fangfang, Siyuan, Hao, Jiaqi, Ang,  
Guanya, Xi, Yulong and Ying. This is an  
open-access article distributed under the  
terms of the [Creative Commons  
Attribution License \(CC BY\)](https://creativecommons.org/licenses/by/4.0/). The use,  
distribution or reproduction in other  
forums is permitted, provided the original  
author(s) and the copyright owner(s) are  
credited and that the original publication  
in this journal is cited, in accordance with  
accepted academic practice. No use,  
distribution or reproduction is permitted  
which does not comply with these terms.

# Efficacy and safety of fenofibrate add-on therapy in patients with primary biliary cholangitis refractory to ursodeoxycholic acid: A retrospective study and updated meta-analysis

Xuan Guoyun<sup>1†</sup>, Ding Dawei<sup>1†</sup>, Liu Ning<sup>2†</sup>, Hu Yinan<sup>1</sup>,  
Yang Fangfang<sup>1</sup>, Tian Siyuan<sup>1</sup>, Sun Hao<sup>1</sup>, Yang Jiaqi<sup>1</sup>, Xu Ang<sup>1</sup>,  
Guo Guanya<sup>1</sup>, Chen Xi<sup>2\*</sup>, Shang Yulong<sup>1\*</sup> and Han Ying<sup>1\*</sup>

<sup>1</sup>National Clinical Research Centre for Digestive Diseases, State Key Laboratory of Cancer Biology, Xijing Hospital of Digestive Diseases, Air Force Medical University (Fourth Military Medical University), Xi'an, China, <sup>2</sup>Medical Service, The Air Force Hospital of Southern Theater of PLA, Guangzhou, China

**Background:** Ursodeoxycholic acid (UDCA) is currently used for the treatment of primary biliary cholangitis (PBC), but some people do not respond well to UDCA. It reported that the combination of fenofibrate and UDCA can improve the clinical indices in these patients. However, more high-quality evidence is needed to improve guideline recommendations.

**Methods:** Through an updated meta-analysis, studies included were valued by the Cochrane Evaluation Manual and Robins-I. Biochemical and clinical indicator changes in UDCA-refractory PBC patients receiving combination therapy were analyzed by Revman 5.42. Then, we explored the influence of fenofibrate dose and the effectiveness and safety of long-term application by retrospective cohort study.

**Results:** Our meta-analysis included nine publications with a total of 389 patients, including 216 treated with UDCA alone and 173 who received combination therapy. The meta-analysis showed that combination therapy was more effective than UDCA monotherapy in decreasing biochemical parameters, such as ALP, GGT, IgM, and TG. However, the occurrence of pruritus and adverse events was slightly higher with combination therapy than with UDCA monotherapy. A total of 156 patients were included in our cohort study: 68 patients underwent UDCA monotherapy, and 88 patients underwent combination therapy. Among UDCA-refractory patients, fenofibrate add-on therapy significantly improved the ALP normalization rate.

**Abbreviations:** ALP, alkaline phosphatase; UDCA, ursodeoxycholic acid; FF, fenofibrate; COM, combination therapy; SD, standard deviation; IV, inverse-variance; CI, confidence interval; df, degrees of freedom; GGT, gamma-glutamyl transferase.

**Conclusion:** The combination of fenofibrate and UDCA can decrease biochemical parameters, of UDCA-refractory PBC patient. Furthermore, the efficacy and safety of long-term combination therapy were also confirmed in our cohort study.

#### KEYWORDS

primary biliary cholangitis, monotherapy, meta-analysis, clinical trial, fenofibrate

## Introduction

Primary biliary cholangitis (PBC), also known as primary biliary cirrhosis, is a chronic autoimmune intrahepatic cholestatic disease (Lleo et al., 2020). Its pathogenesis is not fully understood, but it may be related to abnormal autoimmune responses caused by the interaction of genetic background (Olafsson et al., 2004) and environmental factors (Matsumoto et al., 2022). PBC is mainly observed in middle-aged and elderly women, and the most common presenting symptoms are fatigue and skin pruritus. Serum antimitochondrial antibody (AMA) positivity, especially the positive AMA-M2 subtype, has high sensitivity and specificity for the diagnosis of PBC (Zandanell et al., 2021). At present, ursodeoxycholic acid (UDCA) is still the only drug that has been proven safe and effective in the treatment of PBC by randomized controlled clinical trials (RCT). UDCA can improve biochemical parameters in PBC patients. Several randomized controlled studies and meta-analyses have shown that UDCA can effectively reduce serum total bilirubin (TBIL), alkaline phosphatase (ALP), gamma-glutamyltransferase (GGT), alanine aminotransferase (ALT), aspartate aminotransferase (AST) and cholesterol (CHO) levels (Dat et al., 2021). There are several international criteria for evaluating biochemical response after UDCA treatment (Lammers et al., 2014). Among those criteria, the Paris I and Paris II criteria are frequently used to evaluate biochemical responses to UDCA in patients with advanced PBC (stage III-IV) and early PBC (stage I-II), respectively (Corpechot et al., 2008). Patients with adequate biochemical response to UDCA have a greatly improved survival rate (Harms et al., 2019). However, approximately 40% of patients with PBC have inadequate biochemical response to UDCA monotherapy, so we define them as UDCA-refractory PBC patients. And there is a significant reduction in long-term survival for this group of patients, which is a problem for clinical treatment at present.

There is currently no unified treatment for UDCA-refractory PBC patients (Hirschfield et al., 2021). Scholars from Japan, the United States, Europe and China have successively reported the application of fenofibrate in UDCA-refractory PBC patients (Dohmen et al., 2004; Han et al., 2012; Liberopoulos et al., 2010; Levy et al., 2011; Ohira et al., 2002). A meta-analysis published in 2015 showed that the combination of fenofibrate and UDCA decreased the levels of ALP, GGT, immunoglobulin M (IgM) and triglyceride (TG) compared with UDCA monotherapy, but there was no significant difference in the

improvement of skin pruritus or ALT. In addition, there was no significant difference in the occurrence of adverse events between combination therapy and monotherapy. Whether fenofibrate can improve the long-term outcomes of patients with PBC is unclear (Zhang et al., 2015).

Although fenofibrate has been recommended, the guidelines of various countries and regions do not explicitly recommend the dosage of fenofibrate, and there is no relevant research report on the dosage of fenofibrate (Chinese Society of Hepatology and Chinese Medical Association, 2022; European Association for the Study of the Liver, 2017; Lindor et al., 2018), the meta-analysis is still needed to provide medical evidence. A recent related meta-analysis was the work of Zhang et al., in 2015 (Zhang et al., 2015). Their work was based on the fact that the quality of clinical studies included in their paper needs to be improved. Furthermore, some relevant clinical studies (Cheung et al., 2016; Duan et al., 2018; Hegade et al., 2016) and new evaluation criteria including Robins-I (Sterne et al., 2016) have emerged since 2015. To this end, we try to include higher quality studies, and attempt to carry out subgroup analysis on fenofibrate dose and integrate retrospective cohort study of our center to give more specific opinions for clinical practice.

## Methods

### Identification of studies for inclusion in the meta-analysis

This meta-analysis was registered in INPLASY (registration no. INPLASY202230116). The included studies were identified in English databases, including PubMed, Embase, and The Cochrane Library (updated to December 2021), by a manual search for relevant literature using the search terms “ursodeoxycholic acid”, “UDCA”, “fenofibrate”, “PBC”, “primary biliary cholangitis”, “primary biliary cirrhosis” and “randomized controlled trial”. Further literature was searched to prevent omission.

### Inclusion and exclusion criteria

Studies included in this study met the following five criteria. 1) Randomized controlled trial or clinical controlled trial comparing



combination therapy and UDCA monotherapy. 2) PBC was diagnosed when any two of the following three criteria are met: 1) biochemical evidence of cholestasis (ALP and GGT) is present, and imaging excludes extrahepatic or intrahepatic bold duct obstruction; 2) positive for AMPA/AMA-M2 or other PBC-specific autoantibodies (anti-gp210 antibodies and anti-sp100 antibodies); and 3) histological evidence of nonsuppurative destructive cholangitis and small bile duct disruption. 3) Complete biochemical response to treatment is defined as a decrease in ALP level of more than 40% of the baseline value or ALP level in the normal range after 1 year of UDCA treatment. 4) All patients were not treated with other liver disease medications. 5) For a study produced by the same team, the results with the largest number of cases and most complete data were taken. The studies excluded in this study met the following two criteria. 1) Duplicate documents. 2) Literature with no data to extract.

## Data extraction and assessment of risk of bias

The following data were extracted from each included article: name of the first author, date of publication, sex, age, number of patients, treatment dose and duration, biochemical indices, clinical symptoms, adverse effects, survival rate, etc. Data were independently collected from each study by two researchers (Guoyun Xuan and Ning Liu) to confirm the accuracy of the data. The included studies were evaluated by the researchers according to the Cochrane Evaluation Manual based on the following six aspects: 1. Random assignment method. 2. Concealment of the assignment scheme. 3. Use of blinding. 4. Completeness of the outcome data. 5. Selective reporting of outcomes. 6. Other sources of bias. The risk of bias was also checked independently by the researchers, with answers “Yes” indicating low risk of bias, “No” indicating high risk of bias, and “Unclear” indicating either a lack of information or uncertainty over the potential for bias. Cochrane Reviews often include RCT. Therefore, risk of bias should be assessed for each included study by Robins-I (Lindor et al., 2018). In the current study, the researchers evaluated the included studies based on the following seven dimensions: 1. Bias due to confounding; 2. Bias in selection of participants into the study. 3. Bias in classification of interventions. 4. Bias due to deviations from intended interventions. 5. Bias due to missing data. 6. Bias in measurement of the outcome. 7. Bias in selection of the reported result. The risk of bias in evaluating non-randomized controlled trials was all examined independently by the investigators, and the evaluation results were classified as: “+” indicating low risk of bias, “?” indicating moderate risk of bias, “-” indicating serious risk of bias.

## Clinical study design

A retrospective cohort study was conducted. Patients were divided into “the UDCA group” and “the UDCA + FF group”

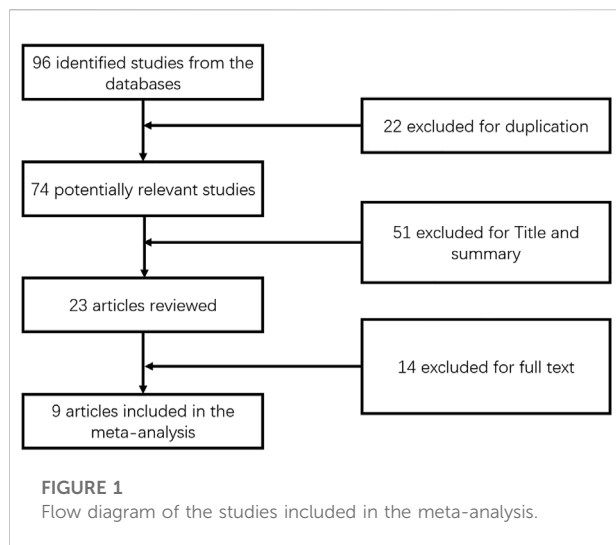
depending on whether they received treatment with UDCA monotherapy or combination therapy of fenofibrate and UDCA. We explored the efficacy and safety of fenofibrate add-on therapy by comparing the clinical characteristics of the two groups. We systematically collected clinical information at presentation and each follow-up. Data included general characteristics, clinical symptoms and serology results. Biochemical response was determined by achieving normal serum ALP levels during follow-up. To evaluate the efficacy of fenofibrate, the primary outcome was the percentage of cases with biochemical responses. Hepatic deterioration was determined by the presence of a decompensatory event (such as hepatic encephalopathy, ascites, or variceal bleeding) and/or progression of the Child-Pugh grade by at least one level (Arroyo et al., 1996). The safety of fenofibrate was assessed primarily in terms of fenofibrate-related symptoms (Levy et al., 2011), hepatotoxicity and nephrotoxicity (detailed characteristics can be seen in [Supplementary Table S1](#)). The Chronic Kidney Disease Epidemiology Collaboration (CKD-EPI) equation was used to calculate eGFR values. The study design was approved by the ethics committee of the Xijing Hospital of the Air Force Military Medical University (KY20151230-5).

## Study population

We analyzed 156 consecutive subjects with PBC who were refractory to prior UDCA monotherapy for 6 months diagnosed and treated in Xijing Hospital of Digestive Diseases (Xi'an, Shaanxi, China) from February 2010 to November 2020. Patients with evidence of concomitant liver disease (autoimmune hepatitis, alcoholic hepatitis, drug-induced liver injury, viral hepatitis, hemochromatosis, and hepatocellular carcinoma) were excluded from our design. A diagnosis of PBC was made if the case met two of the three standards mentioned above. The definition of refractory to UDCA was failure to meet the ALP cutoff value (serum ALP >1.67x ULN) utilized in the Toronto criteria (Corpechot et al., 2011) after 6 months of prior UDCA monotherapy. UDCA and fenofibrate were administered orally at doses of 13–15 mg/kg/d and 200 mg/d, respectively.

## Statistical analysis

In the meta-analysis, the extracted data were processed using the Cochrane systematic evaluation software Revman 5.42 (The Nordic Cochrane Centre, Copenhagen, Denmark; The Cochrane Collaboration, 2012). For dichotomous outcomes, the odds ratio (OR) value and 95% confidence interval (95% CI) were calculated. For continuous variable outcomes, the mean difference (MD) and 95% confidence intervals (CIs) were used. We mainly used the  $\chi^2$  test and the  $I^2$  test to test



heterogeneity ( $p$  value  $<0.10$  or  $I^2$  value  $>50\%$  was considered significant heterogeneity), and then random effect model analysis was performed. Fixed-effects models were used ( $p$  value  $>0.10$  and  $I^2$  value  $<50\%$ ). Subgroup and sensitivity analyses were performed. In our clinical study, SPSS version 26.0 (SPSS Inc., Chicago, IL, United States) was used for all statistical analyses. Continuous variables were described as mean and standard deviation (SD), whereas categorical variables were expressed as median and interquartile range. Categorical data were compared using  $\chi^2$  or Fisher's exact test where appropriate, whereas the Mann-Whitney  $U$  test was used to analyze continuous non-normally distributed variables. Comparisons between biochemical variables at baseline and after treatments were performed using the Wilcoxon signed-rank test for paired date. A two-sided  $p < 0.05$  was considered statistically significant.

## Results

### Description and qualitative assessments of meta-analysis

This meta-analysis included nine publications (Cheung et al., 2016; Dohmen et al., 2004; Duan et al., 2018; Han et al., 2012; Hegade et al., 2016; Liberopoulos et al., 2010; Levy et al., 2011; Ohira et al., 2002; Walker et al., 2009) published from 2002 to 2021, including a total of 389 patients (Figure 1) aged 51–61 years and a follow-up period of 3–24 months. The daily dose of UDCA ranged from 13 to 15 mg/kg day, and the daily dose of fenofibrate was 100–200 mg/day. (Table 1).

Data for the nine studies are shown in Table 2. The nine studies included were also evaluated for quality. Figure 2 shows the evaluation of all included literature relative to each bias risk item. Figure 3 shows the risk of bias summary plot, which is an

assessment of the percentage of risk of bias items arising from all included literature. Those studies include non-randomized studies of interventions (NRSI) as shown in Figure 3. Therefore, risk of bias was assessed for each included study by Robins-I in Figure 4 (Lindor et al., 2018).

### Meta-analysis of biochemical response and adverse events

The results (Table 2) showed that the effect of the combination group in decreasing ALP (MD: 98.08 IU/L, 95% CI: 110.11 to - 86.06,  $p < 0.00001$ ) (Supplementary Figure S1), GGT (MD: 78.57 IU/L, 95% CI: 135.42 to - 21.72,  $p = 0.007$ ) (Supplementary Figure S2), IgM (MD: 80.24 mg/dl, 95% CI: 93.46 to - 67.02,  $p < 0.00001$ ) (Supplementary Figure S5), TG (MD: 0.38 mg/dl, 95% CI: 0.55 to - 0.21,  $p < 0.0001$ ) (Supplementary Figure S6) and other indices were significantly better than those of the UDCA monotherapy group, but there was no statistical significance in the improvement in ALT (MD: 5.40 IU/L, 95% CI: 14.56 to 3.76,  $P: 0.25$ ) (Supplementary Figure S3), AST (MD: 4.89 IU/L, 95% CI: 11.65 to 1.87,  $P: 0.16$ ) (Supplementary Figure S4) or TBIL (MD: 0.44 IU/L, 95% CI: 3.12 to 2.24,  $P: 0.75$ ) (Supplementary Figure S7) level. The incidence of pruritus and adverse events in the combined group were higher than those of the single drug treatment group, but the differences were not obvious [pruritus (MD: 4.08, 95% CI: 1.10 to 15.16,  $P: 0.04$ ) (Supplementary Figure S9); adverse events (MD: 13.44, 95% CI: 1.70 to 105.98,  $P: 0.01$ ) (Supplementary Figure S10)]. The effect of the combined treatment on creatinine (CRE) level was not statistically significant (MD: 9.77 IU/L, 95% CI: 4.05 to 15.49,  $p = 0.0008$ ) (Supplementary Figure S8).

We further grouped the studies according to the dosage of fenofibrate: less than 200 mg/day and 200 mg/day. The subgroup analysis based on identified prognostic indicators was showed in Figure 5 and Figure 6. Although not statistically significant, the results showed that 200 mg per day fenofibrate might achieve stable therapeutic effect in reducing ALP and GGT (Figure 5 and Figure 6).

### Clinical features of patients in the UDCA + FF group and the UDCA group

Figure 7 is the cohort study flowchart. Of the 156 patients with PBC refractory to UDCA, 88 (56%) were treated with combination therapy of fenofibrate and UDCA (UDCA + FF group), and 68 (44%) continued with UDCA monotherapy (the UDCA group). Fenofibrate was administered on average  $18 \pm 12$  months after the start of UDCA. The mean time of exposure to fenofibrate was  $42 \pm 29$  months. No significant differences except for serum GGT, IgG, and TG levels were identified for either group at baseline ( $p < 0.001$ , all) (Table 3). Liver histology data on

TABLE 1 Baseline characteristics of the trials included in the meta-analysis.

References	Publication date	Mean age (years)	UDCA dose (mg/day)	Fenofibrate dose (mg/day)	UDCA		UDCA + FF	
					Course of treatment	Patients(n)	Course of treatment	Patients(n)
Ohira, H. <a href="#">Ohira et al. (2002)</a>	2002	61	600–900	150–200	8 years	7	6 months	7
Dohmen, K. <a href="#">Dohmen et al. (2004)</a>	2004	53	600	100–150	6 months	9	3 months	9
Walker, L. J. <a href="#">Walker et al. (2009)</a>	2009	55	600–900	134–200	23 months	16	23 months	16
Liberopoulos, E. N. <a href="#">Liberopoulos et al. (2010)</a>	2010	57	600	200	8 months	6	2 months	4
Levy, C. <a href="#">Levy et al. (2011)</a>	2011	56	600–900	160	12 months	20	24 months	20
Han, X. F. <a href="#">Han et al. (2012)</a>	2012	51	13–15 mg/kg/day	200	18 months	22	3 months	22
Cheung A C <a href="#">Cheung et al. (2016)</a>	2016	53	600–900	145	12 months	74	11 months	46
Hegade, V. S. <a href="#">Hegade et al. (2016)</a>	2016	56	600–900	200	12 months	23	12 months	23
Duan Weijia <a href="#">Duan et al. (2018)</a>	2018	54	600–900	200	12 months	39	24 months	26

Abbreviations: UDCA, ursodeoxycholic acid; COM, the combination therapy of fenofibrate and UDCA.

TABLE 2 Meta-analysis of clinical events and biochemical parameter changes in the included studies.

Outcome title	Number of studies	Number of participants	Statistical method	Effect size	p-value	I <sup>2</sup> (%)
Alkaline phosphatase level	9	389	Mean difference (IV, Fixed, 95% CI)	-106.29 [-132.56, -80.02]	$p < 0.00001$	48
Gamma-glutamyl transferase	4	86	Mean difference (IV, Fixed, 95% CI)	-78.57 [-135.42, -21.72]	$p = 0.007$	6
Alanine aminotransferase	5	232	Mean difference (IV, Fixed, 95% CI)	-5.40 [-14.56, 3.76]	$p = 0.25$	42
Aspartate aminotransferase	5	232	Mean difference (IV, Fixed, 95% CI)	-4.89 [-11.65, 1.87]	$p = 0.16$	48
Immunoglobulin M	5	114	Mean difference (IV, Fixed, 95% CI)	-80.24 [-93.46, -67.02]	$p < 0.00001$	0
Triglycerides	4	112	Mean difference (IV, Fixed, 95% CI)	-0.38 [-0.55, -0.21]	$p < 0.0001$	40
Total bilirubin	4	112	Mean difference (IV, Fixed, 95% CI)	-0.44 [-3.12, 2.24]	$p = 0.75$	0
Creatinine	4	241	Mean difference (IV, Fixed, 95% CI)	9.77 [4.05, 15.49]	$p = 0.0008$	34
Pruritus	5	228	Odds ratio (M-H, Fixed, 95% CI)	4.08 [1.10, 15.16]	$p = 0.04$	0
Adverse events	6	246	Odds ratio (M-H, Fixed, 96% CI)	13.44 [1.70, 105.98]	$p = 0.01$	0

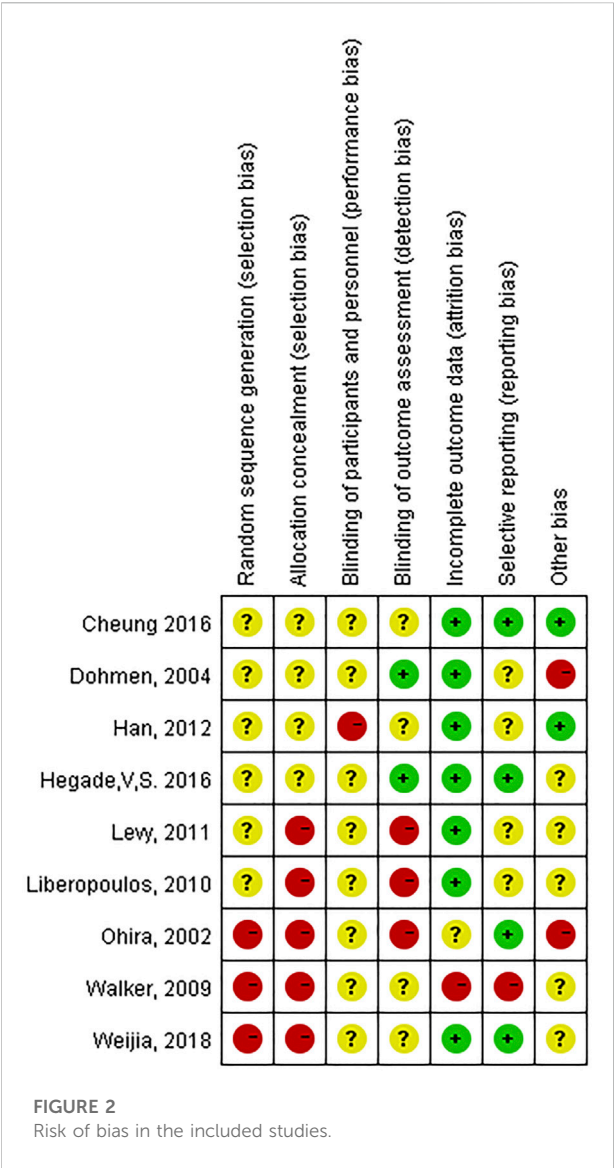
Abbreviations: IV, inverse-variance; CI, confidence interval; M-H, Mantel-Haenszel methods; fixed, fixed effects model.

the stage of fibrosis (results of the last liver biopsy at the time of enrollment) were available in 145 (93%) patients. Depending on the histological findings, a total of 25% of the patients were in advanced stages of disease (Ludwig stage 3 or 4).

## Primary and secondary outcomes

The primary outcome was obtained in 57% of additional fenofibrate-treated cases versus only 10% of UDCA-treated cases ( $p < 0.001$ ) (Figure 8). Univariate analysis of factors related to the biochemical response to fenofibrate showed that six parameters were significantly linked to biochemical response, namely, ALP ( $p = 0.031$ ),

albumin (ALB) ( $p = 0.045$ ), TBIL ( $p < 0.001$ ), CRE ( $p = 0.003$ ), eGFR ( $p = 0.003$ ), and cirrhosis ( $p = 0.020$ ) at baseline (Table 4). As shown in Table 4, multivariate analysis incorporating all variables meeting  $p$  values  $< 0.05$  revealed that the only independent parameter associated with biochemical response to fenofibrate was baseline serum TBIL levels (OR: 0.429; CI: 0.216–0.850;  $p = 0.015$ ). Compared to UDCA-treated cases, fenofibrate-treated cases reported a significantly lower prevalence of hepatic deterioration by study end (35% vs. 18%;  $p = 0.024$ ). Thirty-three patients treated with fenofibrate and twenty patients treated with UDCA underwent at least two liver biopsies at average intervals of 34 (range, 12–84) months and 37 (range, 12–84) months, respectively. Histological progression rates were lower in fenofibrate-treated cases than in



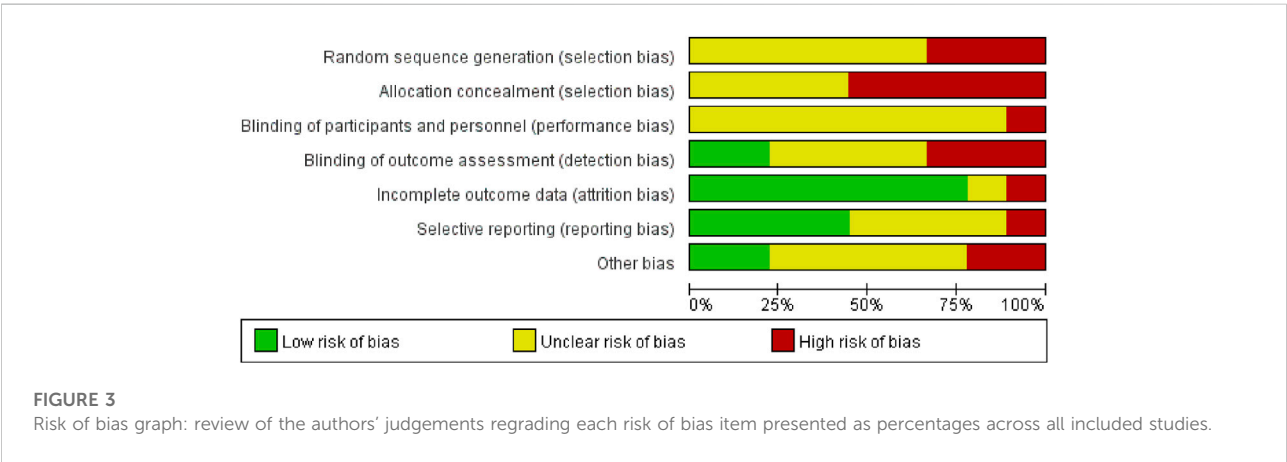
UDCA-treated cases, however this difference was not statistically significant (9% vs. 30%;  $p = 0.112$ ) (Figure 8). W\We also provide images of liver biopsy of one patient before and after combination therapy. (Supplementary Figure S11).

Biochemical measures

Figure 9 shows the dynamic changes in ALP, GGT, ALT, AST, IgM, CHO, TG and TBIL. Biochemical characteristics of patients with UDCA-refractory PBC between “the FF group” and “the UDCA group” after 1 year of treatment were shown in Supplementary Table S2. At 60 months, the level of ALP decreased 73% from baseline in “the UDCA group” and 34% in “the UDCA + FF group” ( $p < 0.001$ , both) (Supplementary Table S3). Similar reductions were found in TG and CHO in “the UDCA + FF group” ( $p < 0.050$ , all) (Supplementary Table S3). The median serum TBIL level in “the UDCA + FF group” was observed to be 32% lower than baseline at 60 months ( $p = 0.047$ ) (Supplementary Table S3). ALT and AST decreased progressively in both groups during follow-up ( $p < 0.05$ , all) (Supplementary Table S3). Compared to “the UDCA group”, significantly lower ALP level was observed in “the UDCA + FF group” during follow-up. No significant differences in TBIL, ALT, AST, TG, CHO were found between the groups (Supplementary Table S3). Elevated ALP levels were observed in five patients after stopping fenofibrate but not UDCA for 0.25–3 months, and four patients reached normal values after resuming fenofibrate therapy.

Safety of additional fenofibrate

Figure 10 shows that BU, CRE, and eGFR remained stable within the normal range in two groups. Adverse events were reported in Supplementary Table S4. Three patients discontinued use of fenofibrate within 1 month: two patients experienced



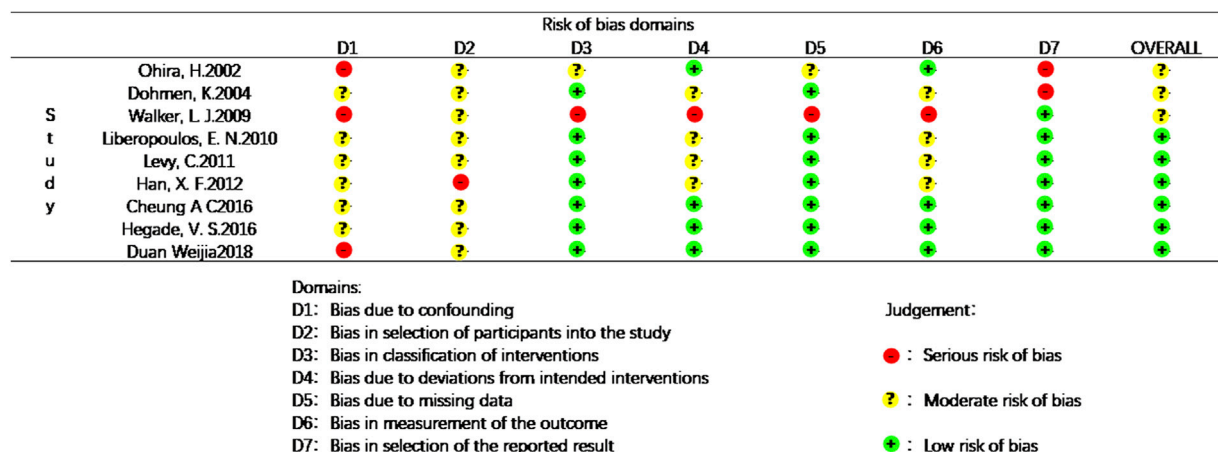


FIGURE 4  
Risk of bias in the included studies based on Robins-I.

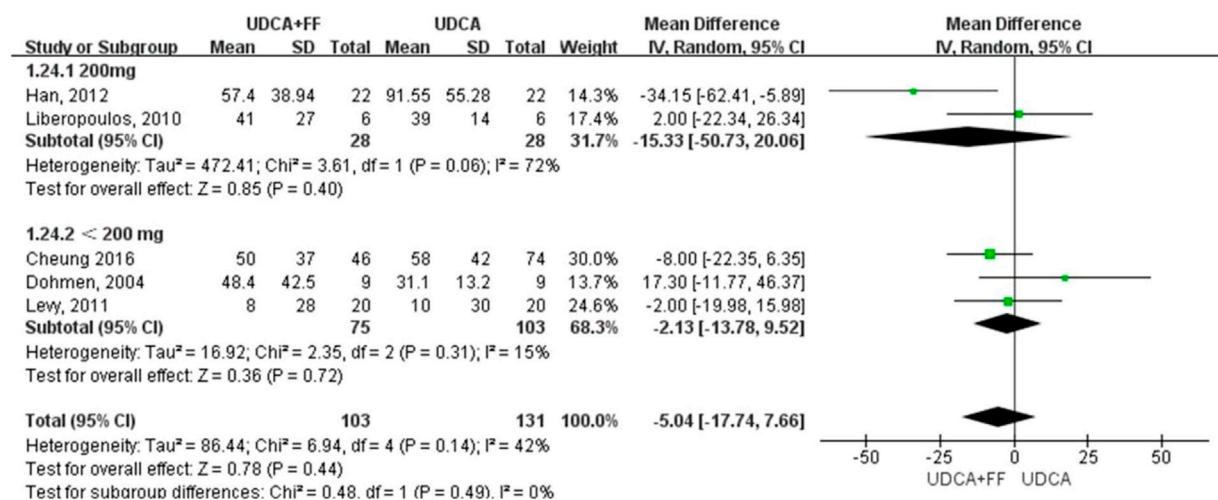


FIGURE 5  
Subgroup analysis of ALP levels in PBC patients treated with monotherapy versus COM.

allergic reactions, and one patient suffered from increased fatigue. Both adverse effects resolved after stopping fenofibrate. Eight patients experienced self-limiting nausea, abdominal pain and bloating in the first 3 months of treatment. Five patients were found to have elevated transaminase levels (ALT or AST, 5–7× ULN) at 12–24 months of treatment with fenofibrate add-on therapy, but ALT levels gradually decreased with continued fenofibrate therapy under monthly monitoring. Four of cirrhotic cases treated with fenofibrate add-on therapy and four of cirrhotic cases treated with UDCA monotherapy experienced severe progression of TBIL levels (>100 mmol/L) (13% vs. 15%;  $p = 1.000$ ). One patient with Child–Pugh B cirrhosis at baseline, who

progressed to Child–Pugh C cirrhosis at 96 months of follow-up, developed renal deterioration with an eGFR of 28 ml/min/1.73 m<sup>2</sup>. No severe adverse events were identified in other patients treated with fenofibrate for more than 12 months.

## Discussion

PBC is a chronic intrahepatic cholestatic disease characterized by a progressive nonsuppurative inflammatory reaction of the intrahepatic bile ducts (Kumagi et al., 2010). UDCA is currently the first-line agent for the treatment of PBC. However, some patients could not benefit from UDCA



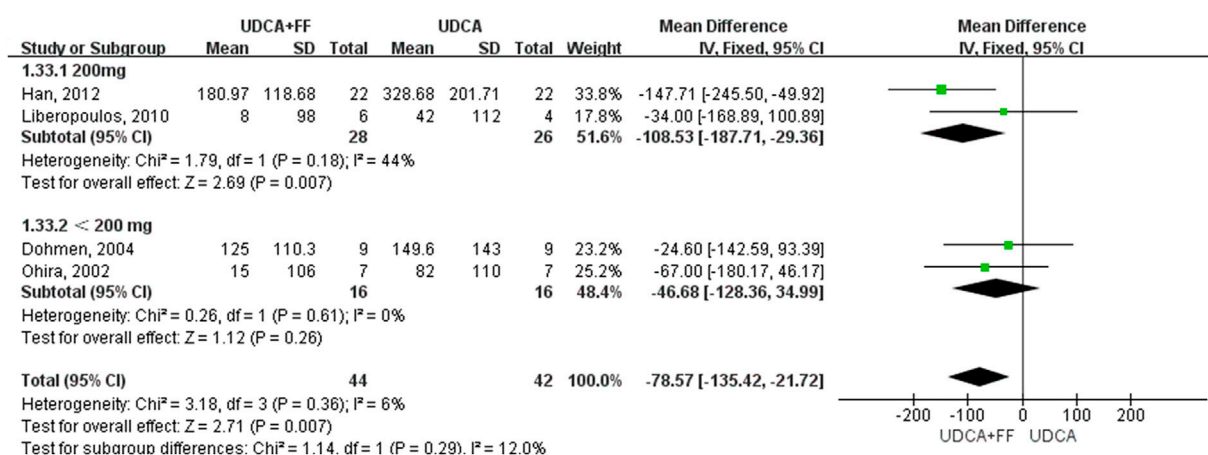


FIGURE 6

Subgroup analysis of GGT levels in PBC patients treated with monotherapy versus COM.

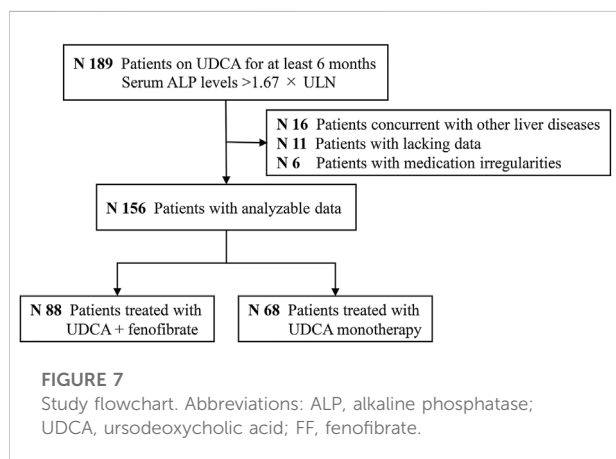


FIGURE 7

Study flowchart. Abbreviations: ALP, alkaline phosphatase; UDCA, ursodeoxycholic acid; FF, fenofibrate.

TABLE 3 Baseline characteristics of patients with UDCA-refractory primary biliary cholangitis treated with “UDCA + FF” or “UDCA monotherapy”.

Characteristic	COM group	UDCA group	p value
	N = 88	N = 68	
Age (mean ± SD)	50 ± 10	52 ± 8	p = 0.424
Female (n, %)	71 (81)	61 (90)	p = 0.121
Follow-up Time (months)	42 ± 26	43 ± 26	p = 0.829
ALP×ULN	2.5 (2.0–3.3)	2.4 (2.0–3.3)	p = 0.677
GGT×ULN	7.9 (4.6–13.0)	5.3 (3.2–8.0)	p < 0.001
ALT×ULN	1.7 (1.2–2.3)	1.5 (1.0–2.3)	p = 0.271
AST×ULN	1.9 (1.4–2.5)	2.0 (1.4–2.7)	p = 0.694
ALB×LLN	1.1 (1.0–1.1)	1.0 (1.0–1.1)	p = 0.203
Tbil×ULN	1.0 (0.8–1.6)	1.0 (0.7–1.5)	p = 0.790
IgG×ULN	0.8 (0.7–0.9)	0.9 (0.8–1.1)	p < 0.001
IgM×ULN	1.2 (0.8–1.8)	1.4 (0.8–1.9)	p = 0.432
TG×LLN	1.0 (0.7–1.5)	0.8 (0.6–1.0)	p < 0.001
BU×ULN	0.6 (0.5–0.7)	0.6 (0.5–0.7)	p = 0.109
Scr×ULN	1.0 (0.9–1.1)	1.0 (0.9–1.1)	p = 0.656
eGFR (ml/min/1.73m2)	97 (91–102)	95 (89–102)	p = 0.216
Fibrosis stage (0–2)/(3–4)	62/21	45/18	p = 0.690

Abbreviations: ALP, alkaline phosphatase; GGT, gamma-glutamyl transferase; ALT, alanine-aminotransferase; AST, aspartate-aminotransferase; ALB, albumin; Tbil, total bilirubin; IgG, immunoglobulin G; IgM, immunoglobulin M; TG, triglyceride; BU, blood urea; Scr, serum creatinine; eGFR, estimated glomerular filtration rate; ULN, upper limit of normal; LLN, lower limit of normal; FF, fenofibrate; UDCA, ursodeoxycholic acid.

treatment. There is a significant reduction in long-term survival for UDCA-refractory PBC patients, which is a problem for clinical treatment. Our meta-analysis included nine publications with a total of 395 patients, showing that combination therapy was more effective than UDCA monotherapy in decreasing biochemical parameters, including ALP, GGT, IgM, and TG. However, the occurrence of pruritus and adverse events was slightly higher with combination therapy than with UDCA monotherapy. Besides, a total of 156 patients were included in our clinical study, finding that fenofibrate add-on therapy significantly improved the ALP normalization rate among UDCA-refractory PBC patients.

Recently, it has been reported that fibrates can be clinically useful in the treatment of hypertriglyceridemia and mixed hyperlipidemia and have anti-inflammatory, antifibrotic, and cholestasis-lowering effects. Fibrates can also ameliorate the biochemical characteristics of patients with PBC (Cancado et al.,

2021); Rosenson et al., 2007, but the change in pruritus symptoms was not obvious. Although many observational studies have been published (Cheung et al., 2016; Corpechot et al., 2018; Duan et al.,

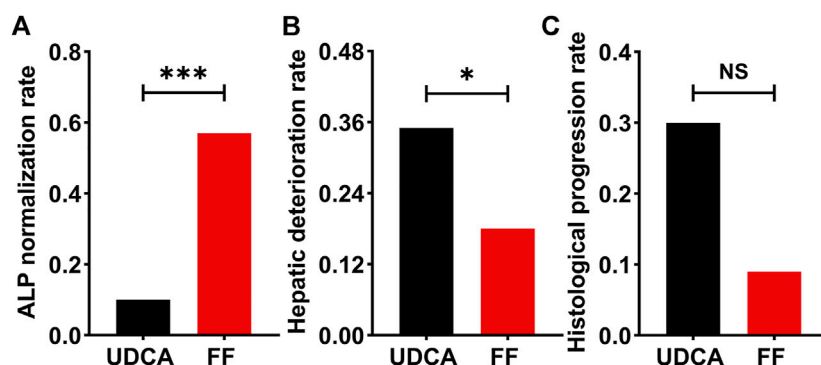


FIGURE 8

The incidence of primary and secondary outcomes in UDCA-refractory PBC patients treated with UDCA + FF (the FF group) or UDCA monotherapy (the UDCA group). (A) ALP normalization rate (B) Hepatic deterioration rate (C) Histological progression rate. Data was analyzed by the chi-squared test. Abbreviations: UDCA, ursodeoxycholic acid; FF, fenofibrate.

TABLE 4 Baseline characteristics of patients with UDCA-refractory primary biliary cholangitis treated with “UDCA + FF” between “ALP normalization group” and “ALP non-normalization group”.

Characteristic	ALP normalization N = 50	ALP non-normalization N = 38	<sup>a</sup> p value	<sup>b</sup> p value	Or (95%CI)
Age (mean)	52 ± 10	48 ± 9	<i>p</i> = 0.073		
Female (n, %)	38 (78)	33 (85)	<i>p</i> = 0.404		
ALP×ULN	2.3 (2.0–3.0)	2.7 (2.2–3.8)	<i>p</i> = 0.031		
GGT×ULN	6.6 (3.7–12.8)	8.4 (6.5–14.6)	<i>p</i> = 0.128		
ALT×ULN	1.5 (1.1–2.1)	1.8 (1.3–2.5)	<i>p</i> = 0.226		
AST×ULN	1.6 (1.3–2.5)	2.2 (1.5–2.8)	<i>p</i> = 0.085		
ALB×LLN	1.1 (1.0–1.1)	1.0 (0.9–1.1)	<i>p</i> = 0.045		
Tbil×ULN	0.9 (0.6–1.3)	1.3 (0.9–2.7)	<i>p</i> < 0.001	<i>p</i> = 0.015	0.429 (0.216–0.850)
IgG×ULN	0.80 (0.69–0.96)	0.75 (0.72–0.86)	<i>p</i> = 0.788		
IgM×ULN	1.15 (0.75–1.78)	1.3 (0.8–1.8)	<i>p</i> = 0.255		
TG×LLN	1.0 (0.7–1.4)	1.1 (0.8–1.8)	<i>p</i> = 0.074		
BU×ULN	0.6 (0.5–0.7)	0.6 (0.5–0.6)	<i>p</i> = 0.225		
Scr×ULN	1.0 (0.9–1.1)	0.9 (0.7–1.0)	<i>p</i> = 0.003		
eGFR (ml/min/1.73m <sup>2</sup> )	94 (89–101)	100 (95–106)	<i>p</i> = 0.003		
Cirrhosis (n, %)	13 (26)	19 (50)	<i>p</i> = 0.020		
Fibrosis stage (0–2)/(3–4)	33/14	29/7	<i>p</i> = 0.424		

Abbreviations: ALP, alkaline phosphatase; GGT, gamma-glutamyl transferase; ALT, alanine-aminotransferase; AST, aspartate-aminotransferase; ALB, albumin; Tbil, total bilirubin; IgG, immunoglobulin G; IgM, immunoglobulin M; TG, triglyceride; BU, blood urea; Scr, serum creatinine; eGFR, estimated glomerular filtration rate; ULN, upper limit of normal; LLN, lower limit of normal; UDCA, ursodeoxycholic acid; FF, fenofibrate; OR, odds ratio; CI, confidence interval.

<sup>a</sup>Univariate analysis.

<sup>b</sup>Multivariate analysis: Logistic regression analysis.

2018; Ghonem et al., 2020), the mechanism by which fibrates reduce the biochemical markers of cholestasis and whether the application of fibrates can improve the survival rate of patients with these diseases remain unclear. In addition, the sample sizes of relevant reports are small, and the follow-up times are different. Thus, the results do not clearly reflect the efficacy and safety of the combination of UDCA and fibrates.

Fenofibrate, a peroxisome proliferator-activated receptor (PPAR)-α-selective agonist, is commonly used for the treatment of hypercholesterolemia and hypertriglyceridemia (Huang et al., 2008). Some studies have shown that fenofibrate can improve biochemical and immunological parameters in UDCA-refractory PBC patients by inhibiting bile acid production (Ghonem et al., 2020) without an

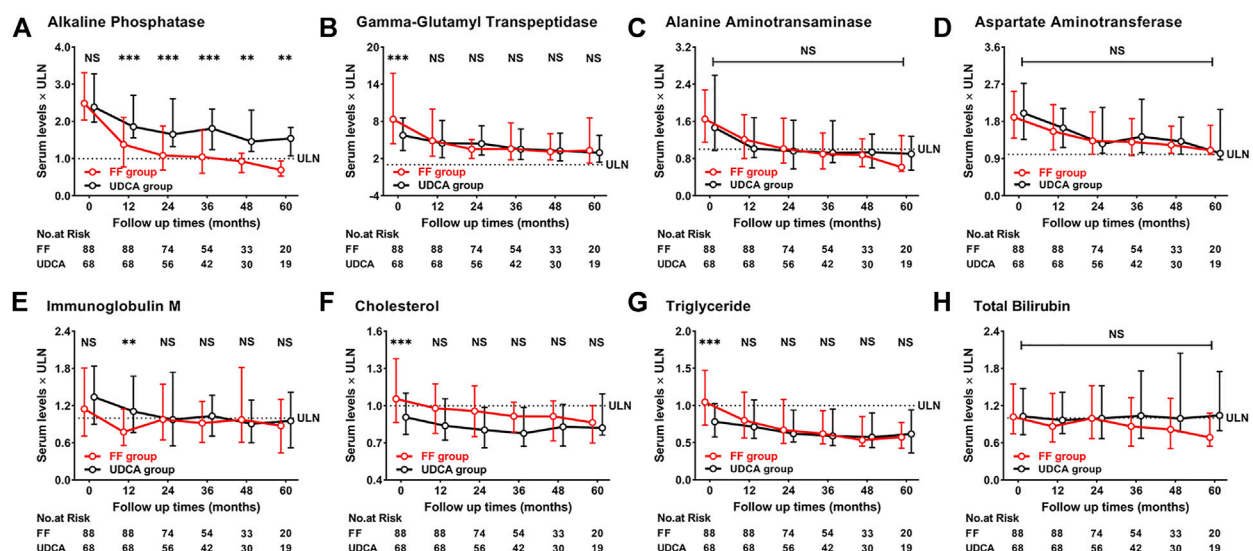


FIGURE 9

Dynamic changes of parameters with follow-up time (A) Alkaline Phosphatase (B) Gamma-Glutamyl Transpeptidase (C) Alanine Aminotransferase (D) Aspartate Aminotransferase (E) Immunoglobulin M (F) Cholesterol (G) Triglyceride (H) Total Bilirubin. Group, patients with UDCA-refractory PBC treated with UDCA + FF (the FF group) or UDCA (the UDCA group). Shown are the median values and interquartile ranges at each follow-up visit. Data was compared with the Mann–Whitney *U* test. Abbreviations: UDCA, ursodeoxycholic acid; FF, fenofibrate; ULN, upper limit of the normal range; LLN, lower limit of the normal range.

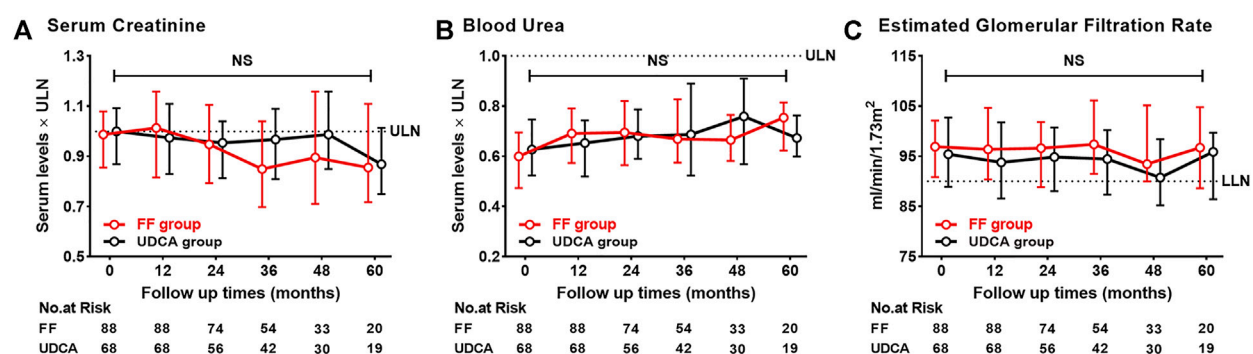


FIGURE 10

Dynamic changes of parameters with follow-up time (A) Serum Creatinine (B) Blood Urea (C) Estimated Glomerular Filtration Rate. Group, patients with UDCA-refractory PBC treated with UDCA + FF (the FF group) or UDCA (the UDCA group). Shown are the median values and interquartile ranges at each follow-up visit. Data was compared with the Mann–Whitney *U* test. Abbreviations: UDCA, ursodeoxycholic acid; FF, fenofibrate; ULN, upper limit of the normal range; LLN, lower limit of the normal range.

increase in adverse events. It was suggested that PPAR-MDR3-PL may be the main anti-cholestatic mechanism of fenofibrate (Ghonem et al., 2014; Kok et al., 2003). Multidrug resistance protein 3 (MDR3) from the bile duct membrane side of hepatocytes is the main determinant of phospholipid secretion (Ros et al., 2003). PPAR agonists can promote the excretion of phosphatidylcholine in bile by upregulating MDR3, reducing the cytotoxicity of bile salt cells, and inhibiting the formation of bile acids. Studies suggest that PPARα may exert anti-inflammatory effects by counter-regulating interference with proinflammatory

transcription factors, such as nuclear factor-κB (NF-κB) (Roglans et al., 2007), signal transduction and activation factors, and other transcription factor pathways to inhibit mRNA and protein expression, thereby reducing p65-mediated gene activation of proinflammatory cytokines (Chen et al., 2014). However, the mechanism of action of UDCA is different. The main function of UDCA is to improve the balance between toxic and nontoxic hydrophobic bile acids and activate the secretion of bile acids, phospholipids, and cholesterol (Poupon, 2012). Therefore, its mechanism of action does not overlap with that of fenofibrate,

and the combination of fenofibrate and UDCA may be more effective than UDCA monotherapy.

There is a lack of multicenter RCTs of fenofibrate combined with UDCA in the treatment of refractory PBC. Therefore, the conclusion of a meta-analysis is still needed to provide medical evidence. At present, fenofibrate is recommended for PBC (Supplementary Table S5). However, there are no guideline giving recommendations on the specific dosage or treatment duration. Clinical practitioners generally refer to the clinical scheme for the treatment of hyperlipidemia, i.e., 200 mg/day.

Thus, we used a meta-analysis to evaluate the efficacy of the combination therapy versus UDCA monotherapy by comparing the changes of parameters in UDCA-refractory PBC patients. Meanwhile, we systematically studied the efficacy and safety of long-term combination therapy in UDCA-refractory PBC patients through our retrospective cohort study. By combining these two aspects of work, our integrated analysis supported the effect of combination therapy on improving the biochemical characteristics of UDCA-refractory PBC and suggested the possible role of dose selection of fenofibrate.

However, there are still deficiencies in this study. Although we first proposed that the dose effect of fenofibrate should be considered, there was no relevant clinical grouping in the clinical trial at our center. Second, although the quality of clinical studies included in the meta-analysis was improved compared with that in 2015, RCT studies still accounted for only a small portion of the included studies. Finally, we mainly evaluated the differences in biochemical indices between combination therapy and monotherapy. Due to the lack of histological evaluation over longer periods, we were unable to confirm whether fenofibrate add-on therapy can delay the histological progression of PBC patient. The safety of combined therapy still needs the support of long-term follow-up data, especially the evaluation of liver histology.

Therefore, we expect that high-quality, well-designed and multicenter RCTs with larger sample sizes will be conducted to comprehensively evaluate the long-term efficacy and safety of UDCA-refractory PBC patients using UDCA in combination with fenofibrate. The results of such studies could help guide the clinical use of fenofibrate in the treatment of UDCA-refractory PBC.

## Conclusion

In summary, combination therapy of fenofibrate and UDCA can improve the main serological indices of UDCA-refractory PBC patients. Moreover, the effectiveness and safety of long-term application of combination therapy were shown in our retrospective cohort study. Finally, a larger sample size and longer follow-up are needed to assess the efficacy and safety of the combination of fenofibrate and UDCA and to observe whether liver histology can be improved with this treatment in longer follow-up.

## Data availability statement

The original contributions presented in the study are included in the article/Supplementary Material, further inquiries can be directed to the corresponding authors.

## Ethics statement

The studies involving human participants were reviewed and approved by The First Affiliated Hospital, the Fourth Military Medical University. The patients/participants provided their written informed consent to participate in this study.

## Author contributions

Conceived and designed the experiments, HY, SY, GG, and CX. Collected the data, XG, TS, and LN. Analyzed the data, XG, HY, DD, and YF. Drafted the manuscript, YJ, SH, XA, and XG. All authors contributed to the article and approved the submitted version.

## Funding

This work was supported by the National Natural Science Foundation of China grants (No. 81820108005, 81770569).

## Conflict of interest

The authors declare that the research was conducted in the absence of any commercial or financial relationships that could be construed as a potential conflict of interest.

## Publisher's note

All claims expressed in this article are solely those of the authors and do not necessarily represent those of their affiliated organizations, or those of the publisher, the editors and the reviewers. Any product that may be evaluated in this article, or claim that may be made by its manufacturer, is not guaranteed or endorsed by the publisher.

## Supplementary material

The Supplementary Material for this article can be found online at: <https://www.frontiersin.org/articles/10.3389/fphar.2022.948362/full#supplementary-material>

## References

- Arroyo, V., Gines, P., Gerbes, A. L., Dudley, F. J., Gentilini, P., Laffi, G., et al. (1996). Definition and diagnostic criteria of refractory ascites and hepatorenal syndrome in cirrhosis. *International Ascites Club. Hepatology* 23 (1), 164–176. doi:10.1002/hep.510230122
- Cancado, G. G. L., Couto, C. A., Guedes, L. V., Braga, M. H., Terrabuo, D. R. B., Cancado, E. L. R., et al. (2021). Fibrates for the treatment of primary biliary cholangitis unresponsive to ursodeoxycholic acid: An exploratory study. *Front. Pharmacol.* 12, 818089. doi:10.3389/fphar.2021.818089
- Chen, K., Li, J., Wang, J., Xia, Y., Dai, W., Wang, F., et al. (2014). Erratum to "15-Deoxy- $\gamma$ 12, 14-prostaglandin J2 reduces liver impairment in a model of ConA-induced acute hepatic inflammation by activation of PPAR $\gamma$  and reduction in NF- $\kappa$ B activity". *PPAR Res.* 2014, 864839. doi:10.1155/2014/864839
- Cheung, A. C., Lapointe-Shaw, L., Kowgier M. Meza-Cardona, J., Hirschfield, G. M., Janssen, H. L. A., et al. (2016). Combined ursodeoxycholic acid (UDCA) and fenofibrate in primary biliary cholangitis patients with incomplete UDCA response may improve outcomes. *Aliment. Pharmacol. Ther.* 43 (2), 283–293. doi:10.1111/apt.13465
- Chinese Society of Hepatology, Chinese Medical Association (2022). Guidelines on the diagnosis and management of primary biliary cholangitis (2021). *Zhonghua Gan Zang Bing Za Zhi* 30 (3), 264–275. doi:10.3760/cma.j.cn112138-20211112-00794-1
- Corpechot, C., Abenavoli, L., Rabahi, N., Chretien, Y., Andreani, T., Johanet, C., et al. (2008). Biochemical response to ursodeoxycholic acid and long-term prognosis in primary biliary cirrhosis. *Hepatology* 48 (3), 871–877. doi:10.1002/hep.22428
- Corpechot, C., Chazouillères, O., and Poupon, R. (2011). Early primary biliary cirrhosis: biochemical response to treatment and prediction of long-term outcome. *J. Hepatol.* 55 (6), 1361–1367. doi:10.1016/j.jhep.2011.02.031
- Corpechot, C., Chazouillères, O., Rousseau, A., Le Gruyer, A., Habersetzer, F., Mathurin, P., et al. (2018). A placebo-controlled trial of bezafibrate in primary biliary cholangitis. *N. Engl. J. Med.* 378 (23), 2171–2181. doi:10.1056/NEJMoa1714519
- Dat, N. Q., Thuy, L. T. T., Hieu, V. N., Hai, H., Hoang, D. V., Thi Thanh Hai, N., et al. (2021). Hexa histidine-tagged recombinant human cytoglobin deactivates hepatic stellate cells and inhibits liver fibrosis by scavenging reactive oxygen species. *Hepatology* 73 (6), 2527–2545. doi:10.1002/hep.31752
- Dohmen, K., Mizuta, T., Nakamuta, M., Shimohashi, N., Ishibashi, H., and Yamamoto, K. (2004). Fenofibrate for patients with asymptomatic primary biliary cirrhosis. *World J. Gastroenterol.* 10 (6), 894–898. doi:10.3748/wjg.v10.i6.894
- Duan, W., Ou, X., Wang, X., Wang, Y., Zhao, X., Wang, Q., et al. (2018). Efficacy and safety of fenofibrate add-on therapy for patients with primary biliary cholangitis and a suboptimal response to UDCA. *Rev. Esp. Enferm. Dig.* 110 (9), 557–563. doi:10.17235/reed.2018.5533/2018
- European Association for the Study of the Liver (2017). EASL Clinical Practice Guidelines: The diagnosis and management of patients with primary biliary cholangitis. *J. Hepatol.* 67 (1), 145–172. doi:10.1016/j.jhep.2017.03.022
- Ghonom, N. S., Ananthanarayanan, M., Soroka, C. J., and Boyer, J. L. (2014). Peroxisome proliferator-activated receptor alpha activates human multidrug resistance transporter 3/ATP-binding cassette protein subfamily B4 transcription and increases rat biliary phosphatidylcholine secretion. *Hepatology* 59 (3), 1030–1042. doi:10.1002/hep.26894
- Ghonom, N. S., Auclair, A. M., Hemme, C. L., Gallucci, G. M., de la Rosa Rodriguez, R., Boyer, J. L., et al. (2020). Fenofibrate improves liver function and reduces the toxicity of the bile acid pool in patients with primary biliary cholangitis and primary sclerosing cholangitis who are partial responders to ursodiol. *Clin. Pharmacol. Ther.* 108 (6), 1213–1223. doi:10.1002/cpt.1930
- Han, X. F., Wang, Q. X., Liu, Y., You, Z. R., Bian, Z. L., Qiu, D. K., et al. (2012). Efficacy of fenofibrate in Chinese patients with primary biliary cirrhosis partially responding to ursodeoxycholic acid therapy. *J. Dig. Dis.* 13 (4), 219–224. doi:10.1111/j.1751-2980.2012.00574.x
- Harms, M. H., van Buuren, H. R., Corpechot, C., Thorburn, D., Janssen, H. L. A., Lindor, K. D., et al. (2019). Ursodeoxycholic acid therapy and liver transplant-free survival in patients with primary biliary cholangitis. *J. Hepatol.* 71 (2), 357–365. doi:10.1016/j.jhep.2019.04.001
- Hegade, V. S., Khanna, A., Walker, L. J., Wong, L. L., Dyson, J. K., and Jones, D. E. J. (2016). Long-term fenofibrate treatment in primary biliary cholangitis improves biochemistry but not the UK-PBC risk score. *Dig. Dis. Sci.* 61 (10), 3037–3044. doi:10.1007/s10620-016-4250-y
- Hirschfield, G. M., Beuers, U., Kupcinskas, L., Ott, P., Bergquist, A., Farkkila, M., et al. (2021). A placebo-controlled randomised trial of budesonide for PBC following an insufficient response to UDCA. *J. Hepatol.* 74 (2), 321–329. doi:10.1016/j.jhep.2020.09.011
- Huang, Z., Zhou, X., Nicholson, A. C., Gotto, A. M., Hajjar, D. P., and Han, J. (2008). Activation of peroxisome proliferator-activated receptor-alpha in mice induces expression of the hepatic low-density lipoprotein receptor. *Br. J. Pharmacol.* 155 (4), 596–605. doi:10.1038/bjp.2008.331
- Kok, T., Bloks, V. W., Wolters, H., Havinga, R., Jansen, P. L. M., Stals, B., et al. (2003). Peroxisome proliferator-activated receptor alpha (PPARalpha)-mediated regulation of multidrug resistance 2 (Mdr2) expression and function in mice. *Biochem. J.* 369 (3), 539–547. doi:10.1042/BJ20020981
- Kumagi, T., Guindi, M., Fischer, S. E., Arenovich, T., Abdalian, R., Coltescu, C., et al. (2010). Baseline ductopenia and treatment response predict long-term histological progression in primary biliary cirrhosis. *Am. J. Gastroenterol.* 105 (10), 2186–2194. doi:10.1038/ajg.2010.216
- Lammers, W. J., van Buuren, H. R., Hirschfield, G. M., Janssen, H. L. A., Invernizzi, P., Mason, A. L., et al. (2014). Levels of alkaline phosphatase and bilirubin are surrogate end points of outcomes of patients with primary biliary cirrhosis: an international follow-up study. *Gastroenterology* 147 (6), 1338–1349. e5; quiz e15. doi:10.1053/j.gastro.2014.08.029
- Levy, C., Peter, J. A., Nelson, D. R., Keach, J., Petz, J., CabReRa, R., et al. (2011). Pilot study: fenofibrate for patients with primary biliary cirrhosis and an incomplete response to ursodeoxycholic acid. *Aliment. Pharmacol. Ther.* 33 (2), 235–242. doi:10.1111/j.1365-2036.2010.04512.x
- Liberopoulos, E. N., Florentin M. Elisaf, M. S., Mikhailidis, D. P., and Tsianos, E. (2010). Fenofibrate in primary biliary cirrhosis: a pilot study. *Open Cardiovasc. Med. J.* 4, 120–126. doi:10.2174/1874192401004010120
- Lindor, K. D., Bowlus, C. L., Boyer, J., Levy, C., and Mayo, M. (2018). Primary biliary cholangitis: 2018 practice guidance from the American association for the study of liver diseases. *Hepatology* 69, 394–419. doi:10.1002/hep.30145
- Lleo, A., Wang, G. Q., Gershwin, M. E., and Hirschfield, G. M. (2020). Primary biliary cholangitis. *Lancet* 396 (10266), 1915–1926. doi:10.1016/S0140-6736(20)31607-X
- Matsumoto, K., Ohfuji, S., Abe, M., Komori, A., Takahashi, A., Fujii, H., et al. (2022). Environmental factors, medical and family history, and comorbidities associated with primary biliary cholangitis in Japan: a multicenter case-control study. *J. Gastroenterol.* 57 (1), 19–29. doi:10.1007/s00535-021-01836-6
- Ohira, H., Sato, Y., Ueno, T., and Sata, M. (2002). Fenofibrate treatment in patients with primary biliary cirrhosis. *Am. J. Gastroenterol.* 97 (8), 2147–2149. doi:10.1111/j.1572-0241.2002.05944.x
- Olafsson, S., Gudjonsson, H., Selmi, C., Amano, K., Invernizzi, P., Podda, M., et al. (2004). Antimitochondrial antibodies and reactivity to N. aromaticivornas proteins in Icelandic patients with primary biliary cirrhosis and their relatives. *Am. J. Gastroenterol.* 99 (11), 2143–2146. doi:10.1111/j.1572-0241.2004.40397.x
- Poupon, R. (2012). Ursodeoxycholic acid and bile-acid mimetics as therapeutic agents for cholestatic liver diseases: an overview of their mechanisms of action. *Clin. Res. Hepatol. Gastroenterol.* 36 Suppl 1, S3–S12. doi:10.1016/S2210-7401(12)70015-3
- Roglans, N., Vila, L., Farre, M., Alegret, M., Sanchez, R. M., Vazquez-Carrera, M., et al. (2007). Impairment of hepatic Stat-3 activation and reduction of PPARalpha activity in fructose-fed rats. *Hepatology* 45 (3), 778–788. doi:10.1002/hep.21499
- Ros, J. E., Libbrecht, L., Geuken, M., Jansen, P. L. M., and Roskams, T. A. D. (2003). High expression of MDRI, MRP1, and MRP3 in the hepatic progenitor cell compartment and hepatocytes in severe human liver disease. *J. Pathol.* 200 (5), 553–560. doi:10.1002/path.1379
- Rosenstock, R. S., Wolff, D. A., Huskin, A. L., Helenowski, I. B., and Rademaker, A. W. (2007). Fenofibrate therapy ameliorates fasting and postprandial lipoproteinemia, oxidative stress, and the inflammatory response in subjects with hypertriglyceridemia and the metabolic syndrome. *Diabetes Care* 30 (8), 1945–1951. doi:10.2337/dc07-0015
- Sterne, J. A., Hernan, M. A., Reeves, B. C., Savovic, J., Berkman, N. D., Viswanathan, M., et al. (2016). ROBINS-I: a tool for assessing risk of bias in non-randomised studies of interventions. *Bmj* 355, i4919. doi:10.1136/bmj.i4919
- Walker, L. J., Newton, J., Jones, D. E. J., and Bassendine, M. F. (2009). Comment on biochemical response to ursodeoxycholic acid and long-term prognosis in primary biliary cirrhosis. *Hepatology* 49 (1), 337–338. doi:10.1002/hep.22670
- Zandanell, S., Strasser, M., Feldman, A., Streibinger, G., Aigner, G., Niederseer, D., et al. (2021). Similar clinical outcome of AMA immunoblot-M2-negative compared to immunoblot-positive subjects over six years of follow-up. *Postgrad. Med.* 133 (3), 291–298. doi:10.1080/00325481.2021.1885945
- Zhang, Y., Li, S., He, L., Wang, F., Chen, K., Li, J., et al. (2015). Combination therapy of fenofibrate and ursodeoxycholic acid in patients with primary biliary cirrhosis who respond incompletely to UDCA monotherapy: a meta-analysis. *Drug Des. Devel. Ther.* 9, 2757–2766. doi:10.2147/DDDT.S79837





## OPEN ACCESS

## EDITED BY

Adina Turcu-Stolica,  
University of Medicine and Pharmacy of  
Craiova, Romania

## REVIEWED BY

Kessarir Thanapirom,  
Royal Free Hospital, United Kingdom  
Mojtaba Akbari,  
Isfahan University of Medical  
Sciences, Iran

## \*CORRESPONDENCE

Zhongqi Zhang,  
jxzzq11@163.com

<sup>†</sup>These authors have contributed equally  
to this work

## SPECIALTY SECTION

This article was submitted to  
Gastrointestinal and Hepatic  
Pharmacology,  
a section of the journal  
Frontiers in Pharmacology

RECEIVED 30 May 2022

ACCEPTED 06 September 2022

PUBLISHED 20 September 2022

## CITATION

Zheng Y, Xu Y, Huang B, Mai Y, Zhang Y  
and Zhang Z (2022), Effective dose of  
propofol combined with a low-dose  
esketamine for gastroscopy in elderly  
patients: A dose finding study using  
dixon's up-and-down method.  
*Front. Pharmacol.* 13:956392.  
doi: 10.3389/fphar.2022.956392

## COPYRIGHT

© 2022 Zheng, Xu, Huang, Mai, Zhang  
and Zhang. This is an open-access  
article distributed under the terms of the  
[Creative Commons Attribution License](https://creativecommons.org/licenses/by/4.0/)  
(CC BY). The use, distribution or  
reproduction in other forums is  
permitted, provided the original  
author(s) and the copyright owner(s) are  
credited and that the original  
publication in this journal is cited, in  
accordance with accepted academic  
practice. No use, distribution or  
reproduction is permitted which does  
not comply with these terms.

# Effective dose of propofol combined with a low-dose esketamine for gastroscopy in elderly patients: A dose finding study using dixon's up-and-down method

Yuling Zheng<sup>1†</sup>, Yafei Xu<sup>2†</sup>, Bixin Huang<sup>1</sup>, Ying Mai<sup>1</sup>,  
Yiwen Zhang<sup>2</sup> and Zhongqi Zhang<sup>1\*</sup>

<sup>1</sup>Department of Anesthesiology, the Affiliated Shunde Hospital of Jinan University, Foshan, China,

<sup>2</sup>Department of Anesthesiology, Shunde Hospital of Southern Medical University, Foshan, China

**Objective:** This study aimed to determine the optimal dose of propofol combined with esketamine to inhibit the response to gastroscopy insertion in elderly patients.

**Methods:** This is a prospective, non-controlled, non-randomized, single-center study. Elderly patients aged 65–80 years were enrolled in the study with the American society of anesthesiologists (ASA) physical status I or II undergoing elective gastroscopy. All patients were administered propofol after an intravenous esketamine at the dosage of 0.3 mg/kg 30 s, the subsequent dose of propofol was determined by the response of the previous patient to gastroscopy insertion (choking, body movement, etc.) using Dixon's up-and-down method. The initial dose of propofol administered to the first elderly patient was 3.0 mg/kg, and the standard ratio of propofol dose in adjacent patients was 0.9. At least six crossover points were obtained before the conclusion of the study. By using Probit analysis the median effective dose (ED<sub>50</sub>), 95% effective dose (ED<sub>95</sub>), and the corresponding 95% confidence interval (CI) for propofol were determined.

**Results:** The study continued until we obtained seven crossover points and 32 elderly patients (17 males and 15 females) were collected. The ED<sub>50</sub> of propofol combined with esketamine inhibiting response to gastroscopy insertion in elderly patients were found to be 1.479 mg/kg (95% CI 1.331–1.592 mg/kg), and ED<sub>95</sub> was found to be 1.738 mg/kg (95% CI 1.614–2.487 mg/kg).

**Conclusion:** According to the present study, propofol combined with 0.3 mg/kg esketamine is safe and effective for elderly patients undergoing gastroscopy. The ED<sub>50</sub> and ED<sub>95</sub> doses of propofol inhibiting response to gastroscopy insertion in elderly patients when combined with 0.3 mg/kg esketamine were 1.479 and 1.738 mg/kg, respectively, without apparent adverse effects.

## KEYWORDS

propofol, esketamine, effective dose, gastroscopy, dose-response relationship

## 1 Introduction

During upper gastrointestinal endoscopy, the endoscope probe stimulates the pharynx when it enters the esophagus. As the pharynx is highly sensitive, patients tend to have nausea, vomiting, choking cough, and even laryngospasm, which can be considerably reduced with an adequate painless procedure. Appropriate sedation enables patients to pass the examination process without difficulty and improves the completion rate and accuracy of endoscopic examination with an enhanced patient and endoscopist satisfaction (Padmanabhan et al., 2017; Nishizawa and Suzuki, 2018). Propofol is a short-acting sedative-hypnotic drug with the characteristics of rapid onset of action, quick recovery, and fewer adverse effects that have been widely used in painless digestive endoscopy (Padmanabhan et al., 2017). Nevertheless, propofol has been reported to possess dose-dependent adverse effects, where overdose increases the risk of respiratory and circulatory depression, while underdose causes airway irritation, pain, limb twitching, and even gastroscopy interruption (Vaessen and Knape, 2016; Delgado et al., 2019), mostly in older patients. In many cases, adjuvants are required because co-administration could not only decrease the required dose of propofol but also reduces the incidence of adverse drug reactions (Nam et al., 2022).

Esketamine is the *s*-enantiomer of ketamine, and its anesthetic effect is approximately threefold that of *R* (-)-ketamine (Zanos et al., 2018). Due to the dose-dependent adverse effects of ketamine, low-dose esketamine can decrease the incidence of anesthesia-related adverse events (Bowdle et al., 1998; Zhan et al., 2022). Due to its sympathomimetic properties and less respiratory and circulatory depression, esketamine could better maintain the hemodynamic stability of elderly patients during induction of anesthesia (Yang et al., 2022b; Li et al., 2022). Therefore, it is an ideal candidate to be used in combination with propofol for gastroscopic examination (Wang et al., 2019). However, there is no clear evidence on the effective dose of propofol in combination with esketamine for elderly patients undergoing gastroscopy. Therefore, we conducted this prospective study intending to assess the ED<sub>50</sub> and ED<sub>95</sub> of propofol combined with 0.3 mg/kg esketamine for a gastroscopy to inhibit the gastroscope insertion (from the pharynx into the esophagus) reaction in elderly patients, thereby providing clinical advice and medication guidance.

## 2 Materials and methods

### 2.1 Study design and patients

This is a prospective, non-controlled, non-randomized, single-center study. The study was registered at the Chinese Clinical Trial Registry ([www.chictr.org.cn](http://www.chictr.org.cn); registration number: ChiCTR2000038242) on 15/09/2020. The registration of clinical trial includes different age groups (pediatric group, young-middle-aged group and elderly group) and the present study

enrolled only elderly patients (age range from 65 to 80). The study was approved by the Medical Ethics Committee of the Shunde Hospital of Southern Medical University (Number: 20200903). All patients undergoing elective gastroscopy from March to May 2021 were enrolled in the study.

### 2.2 Criteria for inclusion and exclusion

Patients were included if they met the following criteria: age between 65 and 80 years, body mass index (BMI) between 18 and 27 kg/m<sup>2</sup>, perform elective gastroscopy, diagnostic gastroscopy, and ASA physical status I or II.

The following exclusion criteria were implemented in this study: refuse to participate; known allergy to either propofol or esketamine; evident difficult airway; chronic pain; mental-related diseases; symptomatic cardiovascular or pulmonary diseases; severe hepatic and kidney function problems; alcohol abuse; those with increased intracranial pressure or intraocular pressure; history of hyperthyroidism; hemostasis, polypectomy or other require any treatments before/during the examination; chronic use of sedative or analgesic drugs.

### 2.3 Anesthesia protocol and endoscopic procedure

Before the painless gastroscopy, all patients were kept fasted for at least 6 h and were then transferred to the examination room and put on oxygen at the rate of 4 L/min through a nasal straw. The Anesthesiologist also measured the mean arterial pressure (MAP), heart rate (HR), and blood oxygen saturation (SpO<sub>2</sub>) of all patients. After opening the patient's peripheral venous access, 500 ml of lactated ringer's solution was infused at a rate of 250 ml/h.

All Anesthesia operations were performed by the same anesthesiologist. Patients were administered intravenous 0.3 mg/kg esketamine (2 ml: 50 mg, Jiangsu Hengrui Medicine China, lot number: 200403BL) and propofol for sedation (20 ml: 0.2 g, Propofol 1% MCT Fresenius Kabi St. Wendel Germany, lot number: 2003085). The dose of propofol administered to elderly patients after 30 s of intravenous esketamine was determined by the response of the previous patient to gastroscope insertion (choking cough, body movement, etc.) using Dixon's up-and-down method. The dose of propofol was increased in the subsequent patient due to an increase in choking cough, body movement, and effect on operations by endoscopists when the gastroscope inserted into the esophagus was deemed "responsive." The dose of propofol was decreased in the subsequent patient if there was no choking cough and no body movement. The initial dose of propofol administered to the first elderly patient was 3.0 mg/kg, and the average ratio of propofol dose in adjacent patients was 0.9. At least six crossover points were obtained before the conclusion of the study.

Following the administration of propofol, an endoscope (OLYMPUS Lucera LCV-260SL) was inserted. All gastroscopic examinations were performed by endoscopists with at least five years of experience. If the patient was “responsive”, a single dose of 20–50 mg of propofol was administered intravenously and repeated to complete the gastroscopy.

Following gastroscopy, the patients were transferred to the post-anesthesia care unit (PACU), where the anesthetist awakened the elderly patient. Similarly, the HR, MAP, and SpO<sub>2</sub> levels were also monitored. The recovery time was recorded. The patient spent at least 30 min in PACU. The criteria for discharge or transfer from PACU to the inpatient unit were typical vital signs, the ability to walk without assistance, and the absence of evident side effects.

The adverse medical events were handled as follows: hypotension (MAP decreased by 30% over the baseline value) was treated with a bolus of 5–10 mg ephedrine; bradycardia (HR < 50 beats/min) was treated with an intravenous injection of 0.25–0.5 mg atropine; respiratory depression (SpO<sub>2</sub><90%) was treated with a mask pressurized or laryngeal mask to maintain ventilation; and in event of nausea and vomiting, a bolus of 2 mg tropisetron was administered.

## 2.4 Outcome assessments

The primary outcome of the current study was the dose of propofol determined for each elderly patient using Dixon’s up-and-down method.

The secondary outcome: HR, MAP, and SpO<sub>2</sub> were measured at the following time points: 5 min after entering the gastroscopy room (T1), immediately after intravenous injection of ketamine (T2), immediately after intravenous injection of propofol (T3), and immediately after the Endoscope was passed into the esophagus (T4), and 1 min after the patient’s recovery (T5). Hypotension, bradycardia, injection pain, post-operative nausea and vomiting (PONV), respiratory depression (SpO<sub>2</sub><90%), emergence agitation, and psychiatric symptoms 24 h following anesthesia were also recorded. Additionally, each dose of propofol used, the duration of the gastroscopy insertion and gastroscopy, and the recovery time were recorded. If the patient frowned or complained of arm pain or ipsilateral limb escape response, this was defined as injection pain. Gastroscopy insertion time was defined as the duration from the pharynx into the esophagus. Recovery time was defined as the duration between propofol cessation and eye-opening on command.

## 2.5 Statistical analysis

The sample size calculation: The total number of participants depends on Dixon’s up-and-down method (Dixon, 1991). This method requires at least six crossover points (non-responsive to responsive) for statistical analysis.

All the statistical analysis were performed using SPSS (version 17.0, SPSS Inc. Chicago, Illinois, United States). Data

were checked for normality using Shapiro-Wilk test, and the appropriate test was next applied as indicated. Data were expressed as mean ± standard deviation (SD), median [range] or *n*. Using repeated measures analysis of variance, the data collected at various time points within the group were analyzed. *p* < 0.05 indicates a statistically significant difference. The ED<sub>50</sub> and ED<sub>95</sub> of propofol and their corresponding CI were analyzed using the Probit test. Microsoft excel software was used to draw a sequential graph and dose-response curve.

## 3 Results

### 3.1 Patients information

A total of 35 elderly patients were enrolled from March to May 2021. Three elderly patients were excluded, and a total of 32 elderly patients successfully completed the study (Figure 1). Table 1 depicts the demographic data of all the elderly enrolled patients. Gastroscopy time was (5.9 ± 1.2) min, recovery time was (11.2 ± 4.3) min, and propofol dose was (119.4 ± 18.3) mg.

### 3.2 Response of gastroscopy insertion

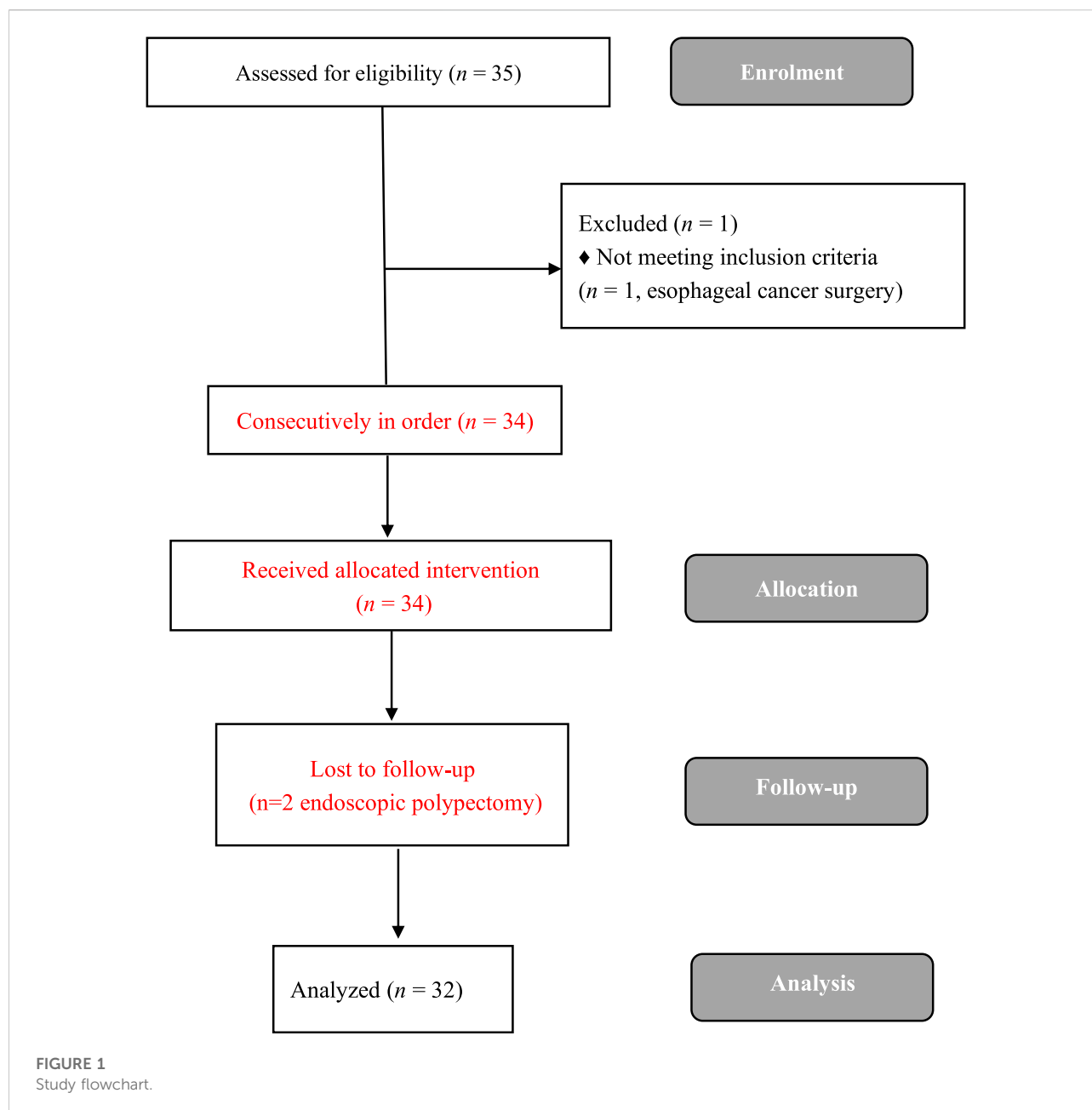
Our study was conducted until data of seven crossover points were collected. Figure 2 shows the sequential response of 32 elderly patients to the up-and-down method of gastroscopy insertion. There were 12 elderly patients who were responsive and given propofol as a remedy.

### 3.3 ED<sub>50</sub> and ED<sub>95</sub> of propofol combined with esketamine

The ED<sub>50</sub> of propofol combined with esketamine inhibiting response to gastroscopy insertion in elderly patients was found to be 1.479 mg/kg (95% CI: 1.331–1.592 mg/kg), while the ED<sub>95</sub> was found to be 1.738 mg/kg (95% CI: 1.614–2.487 mg/kg) (Figure 3).

### 3.4 Hemodynamic changes of patients at different time points

According to repeated measures analysis of variance, MAP and HR fluctuated significantly (*p* < 0.05) over time. MAP significantly increased immediately after intravenous injection of ketamine (T2) time point and dropped significantly immediately after intravenous injection of propofol (T3) time point in comparison to 5 min after entering the gastroscopy room (T1) time point without a significant change in HR and SpO<sub>2</sub> (Table 2).



### 3.5 Anesthesia-related adverse events

The overall incidence of anesthesia-related adverse events was recorded to be 23.3% (Table 3).

## 4 Discussion

The primary objective of this study was to evaluate the effect of low-dose esketamine on the dose of propofol required to achieve the desired degree of sedation without body movement

for gastroscopy in elderly patients and its safety and efficacy. Our research revealed that the ED<sub>50</sub> and ED<sub>95</sub> values for propofol inhibiting the response to gastroscope insertion in patients when combined with 0.3 mg/kg esketamine were found to be 1.479 and 1.738 mg/kg, respectively. The incidence of anesthesia-related complications was recorded to be 23.3% among all patients. All adverse reactions returned rapidly to normal following treatment, and there was no severe cardiovascular incident during gastroscopy. No significant psychiatric symptoms occurred during the telephone follow-up 24 h after the gastroscopy. Thus, the combinational use of propofol and

TABLE 1 Patients' characteristics.

Index

Age (years)	66.5 ± 4.0
Gender (F/M)	14/18
BMI (kg/m <sup>2</sup> )	23.9 ± 2.3
ASA status (I/II)	20/12
Smoking (Y/N)	13/19
Drinking (Y/N)	10/22
Hypertension (Y/N)	26/6
Diabetes (Y/N)	14/18
Gastroscope insertion time (s)	6 [5–22]
Gastrosopy time (min)	5.4 ± 1.2
Recovery time (min)	11.2 ± 4.3
Dose of Propofol (mg)	119.4 ± 18.3

Values are expressed as mean ± SD, median (range) or number of patients.

0.3 mg/kg esketamine is regarded as safe and effective for elderly patients undergoing gastroscopy.

Similar research evaluated the median effective concentration (EC<sub>50</sub>) of propofol and ketamine in elderly gastrointestinal endoscopy patients (Yang et al., 2022b). To determine the EC<sub>50</sub> in their study, propofol was administered using a computer-controlled target-controlled infusion (TCI) pump. We believe that the use of TCI has certain advantages for painless gastrointestinal endoscopy. Still, because gastroscopy requires less time than gastrointestinal endoscopy in the present study, direct injection is simple, convenient, and quick, saving anesthesia time and equipment requirements compared to TCI. Thus, direct injection of propofol is appropriate for gastroscopy. The effective dose of propofol obtained using Dixon's up-and-down method can be utilized to be a better immediate clinically applied medication for gastroscopy.

Like Ketamine, esketamine is an N-methyl-D-aspartate receptor antagonist with analgesic, anesthetic, and sympathomimetic properties and can reduce the incidence of cardiopulmonary depression; however, there is a correlation between effect and dosage, and a small dose of esketamine has greater sedative and analgesic effects than a larger dose (Perez-Ruixo et al., 2021; Yang et al., 2022b; Zheng et al., 2022). Esketamine can be used safely and effectively in elderly patients due to its stable hemodynamics and low incidence of adverse events properties (Yang et al., 2022b). Impaired physical function, the type of surgical procedure, and old age are risk factors for propofol-induced circulatory and respiratory depression (Quine et al., 1995; Eckardt et al., 1999; Bhananker et al., 2006). Therefore, advanced age is also a significant risk factor for adverse events associated with propofol sedation during gastroscopy. Because propofol reduces cardiac output (CO) and systemic vascular resistance (SVR) and causes respiratory depression, it should be administered with caution to elderly patients (Han et al., 2017). After injection of low-dose esketamine, our study revealed that MAP was significantly higher than the baseline blood pressure but had almost no effect on HR and SpO<sub>2</sub>. This transient blood pressure increase could be eliminated by the injection of propofol. Our results were consistent with results reported by Eberl et al., (2020). We believed that it might be due to the sympathomimetic effect of esketamine, which makes it an optimal analgesic and sedative drug for anesthesia in hemodynamically compromised patients. Furthermore, it has been regarded as the drug of choice for elderly patients, in the event of a pre-hospital emergency, burn, and cardiogenic shock patients, as an adjunct to propofol use for sedation (Trimmel et al., 2018; Eberl et al., 2020).

Due to the potential for apnea with propofol, propofol-related respiratory depression occurs frequently reported adverse effects. Ketamine has the unique characteristics of maintaining stable oxygen saturation owing to its ability to exert direct smooth muscle relaxation, bronchodilation effect,

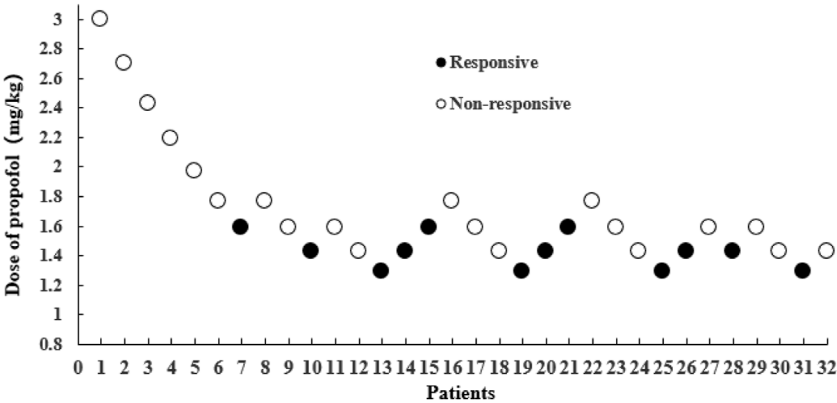
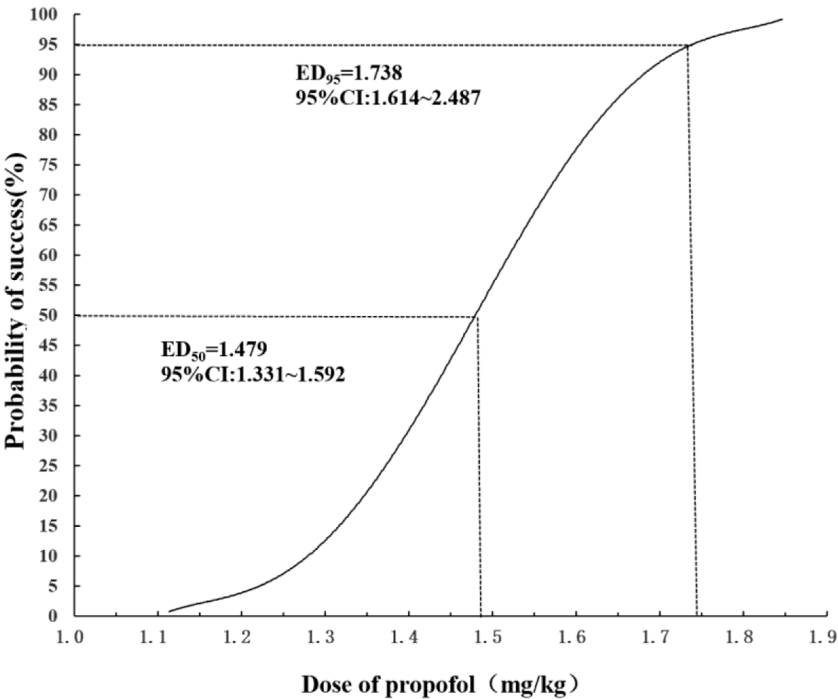


FIGURE 2 The sequential response of 32 elderly patients to gastroscopy insertion with the up-and-down method. The black dot represents "responsive," and the white dot represents "non-responsive".





**FIGURE 3**  
Dose-response curve for propofol plotted using probit analysis.

**TABLE 2** Hemodynamic changes of patients at different time points.

Items	Timepoint					F	p
	T1	T2	T3	T4	T5		
MAP (mmHg)	108.7 ± 14.2	118.3 ± 16.7*	90.3 ± 17.9*	94.9 ± 14.7	99.1 ± 13.6	36.95	<0.001
HR (beats/min)	77.6 ± 13.5	79.6 ± 12.8	74.6 ± 12.4	75.1 ± 10.9	72.3 ± 11.4	6.46	<0.05
SpO <sub>2</sub> (%)	99.8 ± 0.4	99.6 ± 0.3	98.1 ± 1.5	99.7 ± 0.5	99.8 ± 0.4	1.59	0.216

Compared with T1, \**p* < 0.05. Values are expressed as mean ± SD. T1 = 5 min after entering the Gastroscopy room, T2 = immediately after intravenous injection of Ketamine, T3 = immediately after intravenous injection of propofol, T4 = immediately after endoscope passed through the mouth and into the esophagus, and T5 = 1 min after the patient’s recovery (T5).

**TABLE 3** Anesthesia-related adverse events.

**adverse events**

Hypotension	2
Bradycardia	1
PONV	1
SpO <sub>2</sub> < 90 %	2
Injection pain	1
Emergence agitation	0
Psychiatric symptoms after 24 h	0
Total	7 (23.3%)

Values are expressed as the number of patients.

and preserve the laryngeal reflex (Cortinez and Anderson, 2018; Iqbal et al., 2022). However, it should be noted that ketamine-induced sedation can also result in the adverse airway and respiratory events, with an incidence of 1.4%–6.6% (Green et al., 2009). In our study, the incidence and severity of hemodynamic and respiratory adverse events were lower than in other reported studies (Akhondzadeh et al., 2016; Bahrami Gorji et al., 2016). Ketamine is a psychoactive drug that can cause neurological and psychiatric complications, including delirium, hallucinations, and dissociative symptoms. None of patients in our study developed psychiatric symptoms during the follow-up by telephone after 24 h. Propofol may inhibit ketamine-induced expression of c-fos in the posterior cingulate cortex, and that

overexpression of c-fos leads to psychotomimetic side effects of ketamine (Nagata et al., 1998).

With increasing age, the effective dose range of propofol gradually decreases (Yang et al., 2022a). Researchers estimated that the mean induction dose of propofol for elderly patients was 1.7 mg/kg (Schonberger et al., 2021), which was comparable to the outcomes of our study. Opioids such as remifentanyl, sufentanyl, or fentanyl combined with propofol were the most frequently used agents in painless gastroenteroscopy, which can reduce the administered dose of propofol (Zhao et al., 2015; Doganay et al., 2017). Compared to propofol alone or in combination with opioids, propofol combined with ketamine provides sedation and analgesia in addition to the reduction in the risk of cardiovascular and respiratory adverse events (Shah et al., 2011; Nazemroaya et al., 2018). It was observed that propofol used in combination with esketamine reduced the therapeutic dose of propofol in comparison to its lone use for producing similar results during gastrointestinal endoscopy in elderly patients. With the increase in esketamine dose (0–0.5 mg/kg), there was no obvious hypotension, and the recovery time was shortened (Yang et al., 2022b). We, therefore, believed that the low incidence of adverse events in this study was associated with a lower propofol induction dose.

The limitations encountered during the study were: First, considering the safety of the drugs in exploratory trials in elderly patients, we only included patients with ASA I or II and excluded high-risk patients with ASA III and IV. Therefore, the results and conclusions of this study may not apply to other high-risk patients. Second, gastroscopies were performed by 3 different operators (with >5 years of experience), and skills and manipulations of gastroscope insertion may affect the results; therefore, these results may have limited applicability. Thirdly, considering that esketamine may have a greater impact on the effect of general anesthesia and hemodynamics in elderly patients, the anesthesiologists were not blinded to the dose of esketamine used, which may have impacted our findings. Consequently, the current findings require further investigation.

## 5 Conclusion

In conclusion, it was discovered that combining 1.738 mg/kg of propofol with 0.3 mg/kg of esketamine inhibits the response to gastroscope insertion in 95% of elderly patients without noticeable adverse reactions. In the future, we aim to further investigate the optimal dose of propofol for elderly patients in combination with other doses of esketamine for gastroscopy.

## Data availability statement

The original contributions presented in the study are included in the article/supplementary

materials, further inquiries can be directed to the corresponding author.

## Ethics statement

The studies involving human participants were reviewed and approved by Medical Ethics Committee of the Shunde Hospital of Southern Medical University. The patients/participants provided their written informed consent to participate in this study. Written informed consent was obtained from the individual(s) for the publication of any potentially identifiable images or data included in this article.

## Author contributions

In this work, ZZ conceived the study and designed the study. YX, BH and YM contributed to the data collection, performed the data analysis and interpreted the results. YZ wrote the manuscript. YZ (5th author) contributed to the critical revision of article. All authors read and approved the final manuscript.

## Funding

Beijing Medical Award Foundation, Grant/Award Number: YXJL-2021-0307-0584; Guangdong Hospital Pharmacy Research Fund (Medical Special Fund of Xincheng), Grant/Award Number: 2020XC14. Key medical talents training project of Shunde District.

## Acknowledgments

We thank Home for Researchers editorial team ([www.home-for-researchers.com](http://www.home-for-researchers.com)) for language editing service.

## Conflict of interest

The authors declare that the research was conducted in the absence of any commercial or financial relationships that could be construed as a potential conflict of interest.

## Publisher's note

All claims expressed in this article are solely those of the authors and do not necessarily represent those of their affiliated organizations, or those of the publisher, the editors and the reviewers. Any product that may be evaluated in this article, or claim that may be made by its manufacturer, is not guaranteed or endorsed by the publisher.

## References

- Akhondzadeh, R., Ghomeishi, A., Nesioonpour, S., and Nourizade, S. (2016). A comparison between the effects of propofol-fentanyl with propofol-ketamine for sedation in patients undergoing endoscopic retrograde cholangiopancreatography outside the operating room. *Biomed. J.* 39, 145–149. doi:10.1016/j.bj.2015.11.002
- Bahrani Gorji, F., Amri, P., Shokri, J., Alereza, H., and Bijani, A. (2016). Sedative and analgesic effects of propofol-fentanyl versus propofol-ketamine during endoscopic retrograde cholangiopancreatography: A double-blind randomized clinical trial. *Anesth. Pain Med.* 6, e39835. doi:10.5812/aapm.39835
- Bhananker, S. M., Posner, K. L., Cheney, F. W., Caplan, R. A., Lee, L. A., and Domino, K. B. (2006). Injury and liability associated with monitored anesthesia care: A closed claims analysis. *Anesthesiology* 104, 228–234. doi:10.1097/0000542-200602000-00005
- Bowdle, T. A., Radant, A. D., Cowley, D. S., Kharasch, E. D., Strassman, R. J., and Roy-Byrne, P. P. (1998). Psychedelic effects of ketamine in healthy volunteers: Relationship to steady-state plasma concentrations. *Anesthesiology* 88, 82–88. doi:10.1097/0000542-199801000-00015
- Cortez, L. I., and Anderson, B. J. (2018). Advances in pharmacokinetic modeling: Target controlled infusions in the obese. *Curr. Opin. Anaesthesiol.* 31, 415–422. doi:10.1097/ACO.0000000000000619
- Delgado, A. a. A., De Moura, D. T. H., Ribeiro, I. B., Bazarbashi, A. N., Dos Santos, M. E. L., Bernardo, W. M., et al. (2019). Propofol vs traditional sedatives for sedation in endoscopy: A systematic review and meta-analysis. *World J. Gastrointest. Endosc.* 11, 573–588. doi:10.4253/wjge.v11.i12.573
- Dixon, W. J. (1991). Staircase bioassay: The up-and-down method. *Neurosci. Biobehav. Rev.* 15, 47–50. doi:10.1016/s0149-7634(05)80090-9
- Doganay, G., Ekmekci, P., Kazbek, B. K., Yilmaz, H., Erkan, G., and Tuzuner, F. (2017). Effects of alfentanil or fentanyl added to propofol for sedation in colonoscopy on cognitive functions: Randomized controlled trial. *Turk. J. Gastroenterol.* 28, 453–459. doi:10.5152/tjg.2017.16489
- Eberl, S., Koers, L., Van Hoof, J., De Jong, E., Hermanides, J., Hollmann, M. W., et al. (2020). The effectiveness of a low-dose esketamine versus an alfentanil adjunct to propofol sedation during endoscopic retrograde cholangiopancreatography: A randomised controlled multicentre trial. *Eur. J. Anaesthesiol.* 37, 394–401. doi:10.1097/EJA.0000000000001134
- Eckardt, V. F., Kanzler, G., Schmitt, T., Eckardt, A. J., and Bernhard, G. (1999). Complications and adverse effects of colonoscopy with selective sedation. *Gastrointest. Endosc.* 49, 560–565. doi:10.1016/s0016-5107(99)70382-2
- Green, S. M., Roback, M. G., Krauss, B., Brown, L., Mcglone, R. G., Agrawal, D., et al. (2009). Predictors of airway and respiratory adverse events with ketamine sedation in the emergency department: An individual-patient data meta-analysis of 8, 282 children. *Ann. Emerg. Med.* 54, 158–168. doi:10.1016/j.annemergmed.2008.12.011
- Han, S. J., Lee, T. H., Park, S. H., Cho, Y. S., Lee, Y. N., Jung, Y., et al. (2017). Efficacy of midazolam- versus propofol-based sedations by non-anesthesiologists during therapeutic endoscopic retrograde cholangiopancreatography in patients aged over 80 years. *Dig. Endosc.* 29, 369–376. doi:10.1111/den.12841
- Iqbal, A. U., Shuster, M. E., and Baum, C. R. (2022). Ketofol for procedural sedation and analgesia in the pediatric population. *Pediatr. Emerg. Care* 38, 28–33. doi:10.1097/PEC.0000000000002599
- Li, J., Wang, Z., Wang, A., and Wang, Z. (2022). Clinical effects of low-dose esketamine for anaesthesia induction in the elderly: A randomized controlled trial. *J. Clin. Pharm. Ther.* 47, 759–766. doi:10.1111/jcpt.13604
- Nagata, A., Nakao, S., Miyamoto, E., Inada, T., Tooyama, I., Kimura, H., et al. (1998). Propofol inhibits ketamine-induced c-fos expression in the rat posterior cingulate cortex. *Anesth. Analg.* 87, 1416–1420. doi:10.1097/0000539-199812000-00040
- Nam, J. H., Jang, D. K., Lee, J. K., Kang, H. W., Kim, B. W., Jang, B. I., et al. (2022). Committees of quality, M., and conscious sedation of Korean society of gastrointestinal, EPropofol alone versus propofol in combination with midazolam for sedative endoscopy in patients with paradoxical reactions to midazolam. *Clin. Endosc.* 55, 234–239. doi:10.5946/ce.2021.126
- Nazemroaya, B., Majedi, M. A., Shetabi, H., and Salmani, S. (2018). Comparison of propofol and ketamine combination (ketofol) and propofol and fentanyl combination (fenofol) on quality of sedation and analgesia in the lumpectomy: A randomized clinical trial. *Adv. Biomed. Res.* 7, 134. doi:10.4103/abr.abr\_85\_18
- Nishizawa, T., and Suzuki, H. (2018). Propofol for gastrointestinal endoscopy. *United Eur. Gastroenterol. J.* 6, 801–805. doi:10.1177/2050640618767594
- Padmanabhan, A., Frangopoulos, C., and Shaffer, L. E. T. (2017). Patient satisfaction with propofol for outpatient colonoscopy: A prospective, randomized, double-blind study. *Dis. Colon Rectum* 60, 1102–1108. doi:10.1097/DCR.0000000000000909
- Perez-Ruixo, C., Rossenu, S., Zannikos, P., Nandy, P., Singh, J., Drevets, W. C., et al. (2021). Population pharmacokinetics of esketamine nasal spray and its metabolite noresketamine in healthy subjects and patients with treatment-resistant depression. *Clin. Pharmacokinet.* 60, 501–516. doi:10.1007/s40262-020-00953-4
- Quine, M. A., Bell, G. D., McCloy, R. F., Charlton, J. E., Devlin, H. B., and Hopkins, A. (1995). Prospective audit of upper gastrointestinal endoscopy in two regions of england: Safety, staffing, and sedation methods. *Gut* 36, 462–467. doi:10.1136/gut.36.3.462
- Schonberger, R. B., Bardia, A., Dai, F., Michel, G., Yanez, D., Curtis, J. P., et al. (2021). Variation in propofol induction doses administered to surgical patients over age 65. *J. Am. Geriatr. Soc.* 69, 2195–2209. doi:10.1111/jgs.17139
- Shah, A., Mosdossy, G., Mcleod, S., Lehnhardt, K., Peddle, M., and Rieder, M. (2011). A blinded, randomized controlled trial to evaluate ketamine/propofol versus ketamine alone for procedural sedation in children. *Ann. Emerg. Med.* 57, 425–433. doi:10.1016/j.annemergmed.2010.08.032
- Trimmel, H., Helbok, R., Staudinger, T., Jaksch, W., Messerer, B., Schochl, H., et al. (2018). S(+)-ketamine : Current trends in emergency and intensive care medicine. *Wien. Klin. Wochenschr.* 130, 356–366. doi:10.1007/s00508-017-1299-3
- Vaessen, H. H., and Knappe, J. T. (2016). Considerable variability of procedural sedation and analgesia practices for gastrointestinal endoscopic procedures in europe. *Clin. Endosc.* 49, 47–55. doi:10.5946/ce.2016.49.1.47
- Wang, J., Huang, J., Yang, S., Cui, C., Ye, L., Wang, S. Y., et al. (2019). Pharmacokinetics and safety of esketamine in Chinese patients undergoing painless gastroscopy in comparison with ketamine: A randomized, open-label clinical study. *Drug Des. devel. Ther.* 13, 4135–4144. doi:10.2147/DDDT.S224553
- Yang, H., Deng, H. M., Chen, H. Y., Tang, S. H., Deng, F., Lu, Y. G., et al. (2022a). The impact of age on propofol requirement for inducing loss of consciousness in elderly surgical patients. *Front. Pharmacol.* 13, 739552. doi:10.3389/fphar.2022.739552
- Yang, H., Zhao, Q., Chen, H. Y., Liu, W., Ding, T., Yang, B., et al. (2022b). The median effective concentration of propofol with different doses of esketamine during gastrointestinal endoscopy in elderly patients: A randomized controlled trial. *Br. J. Clin. Pharmacol.* 88, 1279–1287. doi:10.1111/bcp.15072
- Zanos, P., Moaddel, R., Morris, P. J., Riggs, L. M., Highland, J. N., Georgiou, P., et al. (2018). Ketamine and ketamine metabolite Pharmacology: Insights into therapeutic mechanisms. *Pharmacol. Rev.* 70, 621–660. doi:10.1124/pr.117.015198
- Zhao, Y. J., Liu, S., Mao, Q. X., Ge, H. J., Wang, Y., Huang, B. Q., et al. (2015). Efficacy and safety of remifentanyl and sufentanil in painless gastroscopic examination: A prospective study. *Surg. Laparosc. Endosc. Percutan. Tech.* 25, e57–60. doi:10.1097/SLE.0000000000000064
- Zheng, X. S., Shen, Y., Yang, Y. Y., He, P., Wang, Y. T., Tao, Y. Y., et al. (2022). ED50 and ED95 of propofol combined with different doses of esketamine for children undergoing upper gastrointestinal endoscopy: A prospective dose-finding study using up-and-down sequential allocation method. *J. Clin. Pharm. Ther.* 47, 1002–1009. doi:10.1111/jcpt.13635
- Zhan, Y., Liang, S., Yang, Z., Luo, Q., Li, S., Li, J., et al. (2022). Efficacy and safety of subanesthetic doses of esketamine combined with propofol in painless gastrointestinal endoscopy: A prospective, double-blind, randomized controlled trial. *BMC Gastroenterol.* 22 (1), 391. doi:10.1186/s12876-022-02467-8



## OPEN ACCESS

## EDITED BY

Adina Turcu-Stolica,  
University of Medicine and Pharmacy of  
Craiova, Romania

## REVIEWED BY

Gordon Stanley Howarth,  
University of Adelaide, Australia  
Michael Thomsen,  
The University of Sydney, Australia

## \*CORRESPONDENCE

Qihai Gong,  
gqh@zmc.edu.cn  
Qiang Lu,  
luqiang@zmu.edu.cn

## SPECIALTY SECTION

This article was submitted to  
Gastrointestinal and Hepatic  
Pharmacology,  
a section of the journal  
Frontiers in Pharmacology

RECEIVED 15 June 2022

ACCEPTED 05 September 2022

PUBLISHED 21 September 2022

## CITATION

Li C, Xie J, Wang J, Cao Y, Pu M, Gong Q  
and Lu Q (2022), Therapeutic effects  
and mechanisms of plant-derived  
natural compounds against  
intestinal mucositis.  
*Front. Pharmacol.* 13:969550.  
doi: 10.3389/fphar.2022.969550

## COPYRIGHT

© 2022 Li, Xie, Wang, Cao, Pu, Gong and  
Lu. This is an open-access article  
distributed under the terms of the  
[Creative Commons Attribution License](#)  
(CC BY). The use, distribution or  
reproduction in other forums is  
permitted, provided the original  
author(s) and the copyright owner(s) are  
credited and that the original  
publication in this journal is cited, in  
accordance with accepted academic  
practice. No use, distribution or  
reproduction is permitted which does  
not comply with these terms.

# Therapeutic effects and mechanisms of plant-derived natural compounds against intestinal mucositis

Cailan Li<sup>1,2,3</sup>, Jianhui Xie<sup>4</sup>, Jiahao Wang<sup>1,2,3</sup>, Ying Cao<sup>5</sup>, Min Pu<sup>5</sup>,  
Qihai Gong<sup>2,3\*</sup> and Qiang Lu<sup>5\*</sup>

<sup>1</sup>Department of Pharmacology, Zunyi Medical University, Zhuhai Campus, Zhuhai, China, <sup>2</sup>Key Laboratory of Basic Pharmacology of Ministry of Education and Joint International Research Laboratory of Ethnomedicine of Ministry of Education, Zunyi Medical University, Zunyi, China, <sup>3</sup>Key Laboratory of Basic Pharmacology of Guizhou Province and School of Pharmacy, Zunyi Medical University, Zunyi, China, <sup>4</sup>The Second Affiliated Hospital of Guangzhou University of Chinese Medicine, Guangzhou, China, <sup>5</sup>Department of Pharmaceutical Sciences, Zunyi Medical University, Zhuhai Campus, Zhuhai, China

Intestinal mucositis is a clinically related adverse reaction of antitumor treatment. Majority of patients receiving high-dose chemical therapy, radiotherapy, and bone-marrow transplant suffer from intestinal mucositis. Clinical manifestations of intestinal mucositis mainly include pain, body-weight reduction, inflammatory symptom, diarrhea, hemoproctia, and infection, which all affect regular nutritional input and enteric function. Intestinal mucositis often influences adherence to antitumor treatment because it frequently restricts the sufferer's capacity to tolerate treatment, thus resulting in schedule delay, interruption, or premature suspension. In certain circumstances, partial and general secondary infections are found, increasing the expenditures on medical care and hospitalization. Current methods of treating intestinal mucositis are provided, which do not always counteract this disorder. Against this background, novel therapeutic measures are extremely required to prevent and treat intestinal mucositis. Plant-derived natural compounds have lately become potential candidates against enteric injury ascribed to the capacity to facilitate mucosal healing and anti-inflammatory effects. These roles are associated with the improvement of intestinal mucosal barrier, suppression of inflammatory response and oxidant stress, and modulation of gut microflora and immune system. The present article aims at systematically discussing the recent progress of plant-derived natural compounds as promising treatments for intestinal mucositis.

## KEYWORDS

intestinal mucositis, natural products, therapeutic action, mechanism, plants

## Introduction

Intestinal mucositis, a clinically significant adverse reaction of antitumor treatment, is characterized by ulcerative lesions along the gastroenteric mucosa (Dahlgren et al., 2021). It appears in nearly 40% of sufferers adopting standard-dose chemotherapy, and over 60% of sufferers receiving high-dose chemotherapy, radiotherapy, and bone-marrow transplantation (Sougiannis et al., 2021). Intestinal mucositis is not only related to a series of remarkable adverse symptoms, including serious diarrhea in 5%–44% of sufferers, obvious body-weight reduction, and decreased nutrient uptake but also associated with the restricted ability of sufferers to tolerate therapy, thus resulting in the delay of succeeding cycles or premature drug withdrawal (Miknevicius et al., 2021).

The clinical signs of intestinal mucositis result from epithelial damage, which is followed by a range of complicated biological events that occur in the diverse cellular and tissular chambers of the mucosa (Batista et al., 2020). Localized and general secondary infections, which increase the expenditures of medical treatment and hospitalization, are found under certain circumstances (Tooley et al., 2009). Therefore, intestinal mucositis poses a significant negative effect on sufferer's clinical outcome, and its complications can even cause death in serious sufferers (van Vliet et al., 2010). There are still no prevention strategies or appropriate therapies for intestinal mucositis. Current treatments primarily focus on relieving the symptoms of intestinal mucositis. To assist the clinical governance of intestinal mucositis, the MASCC/ISOO formulated a guideline including updated information on alternative treatments for this disease (Prisciandaro et al., 2011). These consist of mucosal coating agents, opiates and painkillers, growth factors and

cytokines, antimicrobial agents, cryotherapy, and natural drugs (Kissow, 2015).

Under the circumstances, natural products have attracted much attention and recognition as their prominent bioactivities, including anti-inflammation, antioxidation, immune regulation, and metabolic functions, in the prevention and treatment of intestinal mucositis, cancers, angiopathies, and metabolic and respiratory disorders (Cheah et al., 2014a; da Silva et al., 2021; Wright et al., 2009). A range of preclinical research works have proven that various natural compounds from plants (Figure 1) exerted preventive and therapeutical actions on intestinal mucositis through diversified mechanisms including relieving oxidative injury, decreasing inflammatory reaction, maintaining gut barrier function, and modulating the structure of intestinal microbiome, manifesting that natural compounds possess the potential to stop the progress of intestinal mucositis and delay the clinical course of this disorder (Ribeiro et al., 2016). Thus, in this article, we generalize the pharmacological mechanisms of natural compounds, such as berberine, quercetin, curcumin, baicalein, and luteolin, in preventing and treating intestinal mucositis. These were envisaged to contribute to offering novel ideas for the development of new drugs against intestinal mucositis.

## Methods

For recognizing the studies associated with the effect and mechanism of natural compounds against intestinal mucositis, our team consulted the articles in the following scientific databases from inception until July 2022: Web of Science, PubMed, Google Scholar, and CNKI. The keyword “intestinal

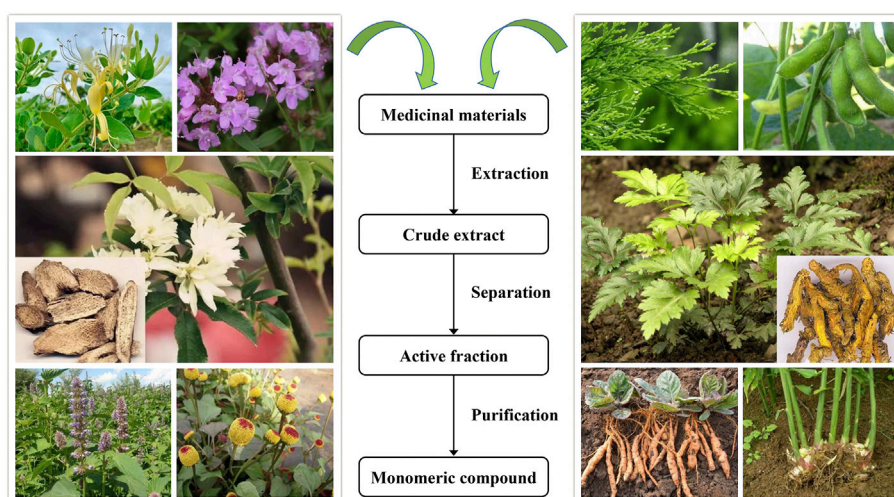


**FIGURE 1**

Various plants of natural compounds for treating intestinal mucositis in the past few decades.



TABLE 1 List of compounds extracted from natural sources.

No.	Compound	Molecular formula	Molecular weight (g/mol)	Main source	Reference
Terpenoids					
1	Costunolide	C <sub>15</sub> H <sub>20</sub> O <sub>2</sub>	232.32	Roots of <i>Aucklandia lappa</i>	Chen et al. (2016)
2	Dehydrocostus	C <sub>15</sub> H <sub>18</sub> O <sub>2</sub>	230.3	Roots of <i>Aucklandia lappa</i>	Chen et al. (2016)
3	Carvacrol	C <sub>10</sub> H <sub>14</sub> O	150.22	Whole-plant of <i>Thymus mongolicus</i> and <i>Origanum vulgare</i>	Alvarenga et al. (2016)
4	Thymol	C <sub>10</sub> H <sub>14</sub> O	150.22	Whole-plant of <i>Thymus vulgaris</i> , <i>Origanum vulgare</i> , and <i>Ocimum gratissimum</i>	Al-Khrashi et al. (2021)
5	Andrographolide	C <sub>20</sub> H <sub>30</sub> O <sub>5</sub>	350.45	Aerial part of <i>Andrographis paniculata</i>	Xiang et al. (2020); Wang et al. (2022)
6	Saikosaponin A	C <sub>42</sub> H <sub>68</sub> O <sub>13</sub>	780.98	Roots of <i>Bupleurum chinense</i> and <i>Bupleurum scorzoniferolium</i>	Ali et al. (2019)
7	Patchouli alcohol	C <sub>15</sub> H <sub>26</sub> O	222.366	Aerial part of <i>Pogostemon cablin</i>	Wu et al. (2020)
8	β-patchoulene	C <sub>15</sub> H <sub>24</sub>	204.351	Aerial part of <i>Pogostemon cablin</i>	Wu et al. (2021)
9	Glycyrrhizic acid	C <sub>42</sub> H <sub>62</sub> O <sub>16</sub>	822.93	Roots and rhizomes of <i>Glycyrrhiza uralensis</i> , <i>Glycyrrhiza inflata</i> , and <i>Glycyrrhiza glabra</i>	Zeeshan et al. (2021)
Flavonoids					
10	Rutin	C <sub>27</sub> H <sub>30</sub> O <sub>16</sub>	610.52	Flowers and fruits of <i>Sophora japonica</i> ; the whole-plant of <i>Ruta graveolens</i>	Fideles et al. (2020)
11	Quercetin	C <sub>15</sub> H <sub>10</sub> O <sub>7</sub>	302.24	Flowers of <i>Sophora japonica</i> ; the leaves of <i>Platycladus orientalis</i> ; and the rhizomes of <i>Alpinia officinarum</i>	Sukhotnik et al. (2018); Lotfi et al. (2021)
12	Luteolin	C <sub>15</sub> H <sub>10</sub> O <sub>6</sub>	286.24	Flowers of <i>Lonicera japonica</i> and <i>Chrysanthemum morifolium</i> and the aerial part of <i>Schizonepeta tenuifolia</i>	Boeing et al. (2020)
13	Baicalein	C <sub>15</sub> H <sub>10</sub> O <sub>5</sub>	270.24	Roots of <i>Scutellaria baicalensis</i>	Wang et al. (2020c)
14	Diadzein	C <sub>15</sub> H <sub>10</sub> O <sub>4</sub>	254.24	Roots of <i>Pueraria lobata</i> ; the seeds of <i>Glycine max</i>	Atiq et al. (2019)
15	Puerarin	C <sub>21</sub> H <sub>20</sub> O <sub>9</sub>	416.38	Roots of <i>Pueraria lobata</i> and <i>Pueraria thomsonii</i>	Wang et al. (2021b)
Quinones					
16	Dihydrotanshinone I	C <sub>18</sub> H <sub>14</sub> O <sub>3</sub>	278.30	Roots and rhizomes of <i>Salvia miltiorrhiza</i>	Wang et al. (2020a)
17	Cryptotanshinone	C <sub>19</sub> H <sub>20</sub> O <sub>3</sub>	296.36	Roots and rhizomes of <i>Salvia miltiorrhiza</i>	Wang et al. (2020b)
Phenylethanoid glycosides					
18	Forsythiaside A	C <sub>29</sub> H <sub>36</sub> O <sub>15</sub>	624.59	Fruits of <i>Forsythia suspensa</i>	Lang et al. (2022)
19	Acteoside	C <sub>29</sub> H <sub>36</sub> O <sub>15</sub>	624.59	Roots of <i>Rehmannia glutinosa</i> and the stems of <i>Cistanche deserticola</i>	Reinke et al. (2015)
Polyphenols					
20	Casuarinin	C <sub>41</sub> H <sub>28</sub> O <sub>26</sub>	936.65	Roots of <i>Melastoma malabathricum</i>	Chen et al. (2022)
21	Curcumin	C <sub>21</sub> H <sub>20</sub> O <sub>6</sub>	368.38	Rhizomes of <i>Curcuma longa</i> , <i>Curcuma aromatica</i> , <i>Curcuma zedoaria</i> , and <i>Acorus calamus</i>	Wang et al. (2021b)
Alkylamide					
22	Spilanthol	C <sub>8</sub> H <sub>8</sub> O <sub>3</sub>	152.15	Flowers of <i>Acmella oleracea</i>	de Freitas-Blanco et al. (2019)
Alkaloid					
23	Berberine	C <sub>20</sub> H <sub>18</sub> ClNO <sub>4</sub>	371.81	Rhizomes of <i>Coptis chinensis</i> , the barks of <i>Phellodendron chinense</i> , and the roots of <i>Berberis soulieana</i>	Chen et al. (2020a); Yue et al. (2021)

mucositis” was adopted for the literature retrieval. All articles with abstracts were taken into account.

After retrieval, the gained articles were strictly filtered. The first screening was conducted in line with the titles and abstracts. The second screening was performed on the basis of the full-text. Finally, all the studies fitting the theme were gathered as the supportive resource of the present review. The exclusion criteria were as follows: crude extracts or oils, not plant-derived natural compounds, and combined therapies.

## Natural compounds against intestinal mucositis

As is well-known, plants are the most significant natural resources for human survival due to their large variety, quantity, and convenient access. The original sources of human food and drugs were mostly derived from plants. To date, the studies on active constituents have primarily

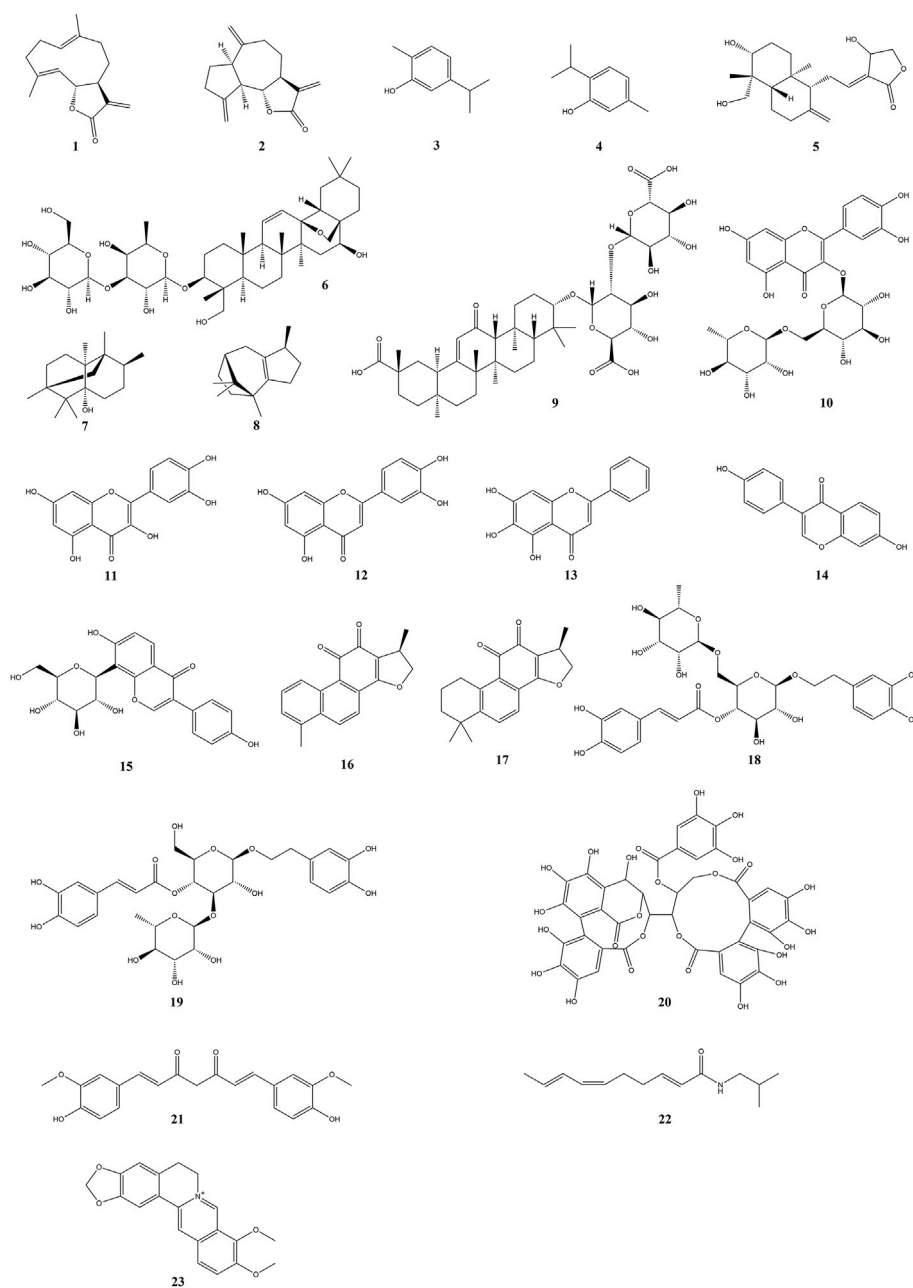


**FIGURE 2**  
Chemical structures of natural compounds in the treatment of intestinal mucositis.

concentrated upon edible and medicinal plants. It is noteworthy that there are plentiful research works on plant-derived natural compounds against intestinal mucositis. In the present research, natural compounds against intestinal mucositis are divided into seven classes, namely, terpenoids, flavonoids, quinones, phenylethanoid glycosides, polyphenols, alkylamides, and alkaloids. The basic, chemical, and pharmacological information of natural compounds used in

the therapy of intestinal mucositis is exhibited in [Table 1](#) and [Figure 2](#) and [Table 2](#), respectively.

## Terpenoids

Costunolide and dehydrocostus belong to natural sesquiterpene lactones, which are the main active constituents

TABLE 2 Summary of the mechanisms of natural compounds against intestinal mucositis.

Name	Model	Effective dosage	Molecular mechanism	Reference
<b>Terpenoids</b>				
Costunolide	5-FU-induced intestinal mucositis in Kunming mice	5 and 20 mg/kg	Upregulation: SOD, IL-10, and occludin  Down-regulation: NF- $\kappa$ B, NO, MDA, TNF- $\alpha$ , COX-2, iNOS, and PCNA	Chen et al. (2016)
Dehydrocostus	5-FU-induced intestinal mucositis in Kunming mice	5 and 20 mg/kg	Upregulation: occludin  Downregulation: NF- $\kappa$ B, NO, TNF- $\alpha$ , COX-2, iNOS, and PCNA	Chen et al. (2016)
Carvacrol	Irinotecan-induced intestinal mucositis in Swiss mice	25, 75, and 150 mg/kg	Upregulation: total leukocytes and NPSH  Downregulation: MPO, TNF- $\alpha$ , IL-1 $\beta$ , KC, NF- $\kappa$ B, COX-2, MDA, and Nox	Alvarenga et al. (2016)
Thymol	5-FU-induced intestinal mucositis in Wistar rats	60, 120 mg/kg	Upregulation: GSH, GPx, SOD, and IL-10  Downregulation: TBARS, NF- $\kappa$ B, TNF- $\alpha$ , COX-2, IL-6, PGE <sub>2</sub> , p38, p38 MAPK, JNK, p-JNK, and TGF- $\beta$	Al-Khrashi et al. (2021)
Andrographolide	5-FU-induced intestinal mucositis in BALB/c mice or NCM460 cells  Irinotecan-induced intestinal mucositis in BALB/c mice or HCT116, HT29, and CT26 cells	12.5, 25, 50, and 100 mg/kg <i>in vivo</i>  0.3, 1, 3, 5, 10, and 20 $\mu$ M <i>in vitro</i>	Upregulation: Bcl-2 and ZO-1  Downregulation: apoptosis, p-p38/p38, p-p53/p53, Bax, C-Casp8/Casp8, C-Casp3/Casp3, TNF- $\alpha$ , IL-1 $\beta$ , IL-6, p-IRF3, p-TBK1, CD-11b, CD-4, CD-8, Cxcl10, Ccl5, IL-18, IFN- $\beta$ , dsDNA, $\gamma$ H2AX, and RAD51	Xiang et al. (2020); Wang et al. (2022)
Saikosaponin A	5-FU-induced intestinal mucositis in BALB/c mice	1, 5, and 10 mg/kg	Upregulation: WBC, RBC, lymphocyte, hemoglobin, GSH, GST, CAT, SOD, Nrf2, HO-1, and <i>Lactobacillus</i> spp.  Downregulation: granulocyte, hematocrit, MDA, IL-1 $\beta$ , IL-6, TNF- $\alpha$ , NO, p-JNK, COX-2, Casp3, and <i>Escherichia coli</i>	Ali et al. (2019)
Patchouli alcohol	5-FU-induced intestinal mucositis in SD mice	10, 20, and 40 mg/kg	Upregulation: IL-10, ZO-1, occludin, claudin-1, mucin-2, <i>Firmicutes</i> , <i>S24</i> , <i>Allobaculum</i> , <i>Erysipelotrichaceae</i> , and <i>Peptostreptococcaceae</i>  Downregulation: TNF- $\alpha$ , IL-1 $\beta$ , IL-6, MPO, TLR2, MyD88, p-I $\kappa$ Ba/I $\kappa$ Ba, NF- $\kappa$ B p65, MLCK, p-MLC/MLC, <i>Proteobacteria</i> , <i>Bacteroidia</i> , <i><math>\epsilon</math>-Proteobacteria</i> , <i><math>\gamma</math>-Proteobacteria</i> , <i>Phascolarctobacterium</i> , <i>Aggregatibacter</i> , <i>Helicobacter</i> , <i>Pasteurellaceae</i> , and <i>Verrucomicrobiaceae</i>	Wu et al. (2020)
$\beta$ -Patchoulene	5-FU-induced intestinal mucositis in IEC-6 cells and SD rats	10, 20, and 40 mg/kg <i>in vivo</i>  20 $\mu$ M <i>in vitro</i>	Upregulation: mucin-2, goblet cells, claudin-1, and occludin  Downregulation: AQP3, PKA, p-MEK1/2/MEK1/2, p-MSK1/MSK1, p-CREB/CREB, VIP, VIPR2, cAMP, PKA, p-MEK1/2/MEK1/2, p-ERK/ERK, p-p38/p38, p-MSK1/MSK1, p-CREB/CREB, P300/CBP, TNF- $\alpha$ , IL-1 $\beta$ , IL-6, IL-10, and p-p65/p65	Wu et al. (2021)
Glycyrrhizic acid	5-FU-induced intestinal mucositis in BALB/c mice	10 mg/kg	Upregulation: goblet cells, GSH, GST, and CAT  Downregulation: TNF- $\alpha$ , IL-1 $\beta$ , and IL-6	Zeeshan et al. (2021)
<b>Flavonoids</b>				
Rutin	5-FU-induced intestinal mucositis in Swiss mice	50, 100, and 200 mg/kg	Upregulation: GSH and goblet cells  Downregulation: MPO, MDA, mast cells, and COX-2	Fideles et al. (2020)
Quercetin	Methotrexate-induced intestinal mucositis in SD rats  5-FU-induced intestinal mucositis in albino mice	5 and 100 mg/kg	Upregulation: BrdU-labeled cells, p-ERK, and CAT  Downregulation: Casp3, MDA, NF- $\kappa$ B, and HIF-1 $\alpha$	Sukhotnik et al. (2018); Lotfi et al. (2021)
Luteolin	Irinotecan-induced intestinal mucositis in Swiss mice	3, 10, and 30 mg/kg	Upregulation: GSH, SOD, CAT, IL-4, IL-10, ZO-1, and occludin	Boeing et al. (2020)

(Continued on following page)

TABLE 2 (Continued) Summary of the mechanisms of natural compounds against intestinal mucositis.

Name	Model	Effective dosage	Molecular mechanism	Reference
Baicalein	5-FU- and irinotecan-induced intestinal mucositis in BALB/c mice	100 mg/kg	Downregulation: ROS, LOOH, MPO, TNF- $\alpha$ , IL-1 $\beta$ , IL-6, PGE <sub>2</sub> , nitrite, and leukocyte Upregulation: <i>Muribaculaceae</i>	Wang et al. (2020c)
Diadzein	5-FU-induced intestinal mucositis in BALB/c mice	1, 5, and 10 mg/kg	Downregulation: IL-6, TNF- $\alpha$ , <i>Bacteroides</i> , <i>Escherichia_Shigella</i> , <i>Parabacteroides</i> , <i>Enterococcus</i> , <i>Clostridium_sensu_stricto_1</i> , and <i>Lactococcus</i> Upregulation: mitotic cells, goblet cells, GSH, GST, CAT, WBC, RBC, lymphocytes, platelets, and <i>Lactobacillus</i> spp. Downregulation: TNF- $\alpha$ , IL-6, IL-1 $\beta$ , p-JNK, MDA, nitrite, granulocytes, and <i>Escherichia coli</i>	Atiq et al. (2019)
Puerarin	5-FU-induced intestinal mucositis in C57BL/6 mice or IEC-6 and Caco-2 cells	50 and 100 mg/kg <i>in vivo</i>  120 $\mu$ M <i>in vitro</i>	Upregulation: SOD and GSH  Downregulation: TNF- $\alpha$ , IL-1 $\beta$ , IL-6, COX-2, iNOS, MDA, MLCK, apoptosis, Bax/Bcl-2, p-STAT3/STAT3, SOCS3, p-JAK1/JAK1, p-JAK2/JAK2, p-JAK3/JAK3, and p-TYK2/TYK2	Wang et al. (2021b)
Quinones				
Dihydrotanshinone I	5-FU- and irinotecan-induced intestinal mucositis in C57BL/6 mice	10 mg/kg	Upregulation: TG, diacylglycerol, <i>Bacteroidetes</i> , <i>Actinobacteria</i> , <i>Akkermansia</i> , <i>Muribaculaceae</i> , <i>Alloprevotella</i> , <i>prevotellaceae_UCG_001</i> , glutamate synthase (NADPH/NADH) small chain, glutamate synthase (ferredoxin), NADH-quinone oxidoreductase subunit F, NADH-quinone oxidoreductase subunit G, and hydroxylamine reductase Downregulation: IL-6, TNF- $\alpha$ , <i>Firmicutes</i> , <i>Proteobacteria</i> , <i>Lactobacillus</i> , <i>Bacteroidetes</i> , glutathione metabolism, ABC transporters, purine metabolism, and bacterial invasion of epithelial	Wang et al. (2020a)
Cryptotanshinone	5-FU- and irinotecan-induced intestinal mucositis in BALB/c mice	20 mg/kg	Upregulation: TG, TG/TC, <i>Muribaculaceae</i> , and <i>Ruminococcaceae_UCG-014</i> Downregulation: IL-6, IL-11, MPO, DAO, TC, and lipase	Wang et al. (2020b)
Phenylethanoid glycosides				
Forsythiaside A	Methotrexate-induced intestinal mucositis in SD rats	40 and 80 mg/kg	Upregulation: goblet cells Downregulation: TNF- $\alpha$ , IL-1 $\beta$ , IL-18, leukocytes, neutrophils, lymphocytes, CD68 positive cells, NLRP3, C-Casp1, and cleaved IL-1 $\beta$	Lang et al. (2022)
Acteoside	Methotrexate-induced intestinal mucositis in C57BL/6 mice	600 $\mu$ g	Downregulation: MPO and MT	Reinke et al. (2015)
Polyphenols				
Casuarinin	5-FU-induced intestinal mucositis in C57BL/6 mice	50 and 100 mg/kg <i>in vivo</i>	Upregulation: PCNA <sup>+</sup> cells, GSH, ZO-1, occludin, <i>Actinobacteria</i> , <i>Lactobacillus murinus</i> , and <i>Lachnospiraceae_NK4A136_group</i>	Chen et al. (2022)
	5-FU-stimulated IEC-6 cells	10, 20, and 30 $\mu$ M <i>in vitro</i>	Downregulation: MDA, MPO, NE, Pr3, CG, IL-1 $\beta$ , TNF- $\alpha$ , <i>Firmicutes/Bacteroidetes</i> , and <i>Candidatus Arthromitus</i>	
Curcumin	5-FU-induced intestinal mucositis in IEC-6 cells	5, 10, and 20 $\mu$ M	Upregulation: E-cadherin Downregulation: apoptosis, TNF- $\alpha$ , IL-1 $\beta$ , IL-6, vimentin, n-cadherin, and p-STAT3	Wang et al. (2021b)
Alkylamide				
Spilanthol	5-FU-induced intestinal mucositis in Swiss mice	10, 20, and 30 mg/kg	Downregulation: MPO	de Freitas-Blanco et al. (2019)
Alkaloid				
Berberine				

(Continued on following page)

TABLE 2 (Continued) Summary of the mechanisms of natural compounds against intestinal mucositis.

Name	Model	Effective dosage	Molecular mechanism	Reference
	5-FU-induced intestinal mucositis in SD rats	50 and 100 mg/kg <i>in vivo</i>	Upregulation: occludin, ZO-1, claudin-1, claudin-7, acetate, propionate, butyrate, glutamine, <i>Firmicutes</i> , <i>Porphyromonadaceae</i> , <i>Lachnospiraceae</i> , <i>Lactobacillus</i> , <i>Clostridiales</i> , <i>Ruminococcus</i> , <i>Prevotella</i> , and <i>Clostridium IV</i>	Chen et al. (2020a); Yue et al. (2021)
	Irinotecan-induced intestinal mucositis in C57BL/6 mice SN38 stimulated NCM460 or Caco-2 cells	50 $\mu$ M <i>in vitro</i>	Downregulation: TNF- $\alpha$ , IL-1 $\beta$ , IL-6, IL-8, COX-2, iNOS, LPS, DAO, GUS, <i>Proteobacteria</i> , and <i>Escherichia Shigella</i>	

of *Aucklandia lappa*. Researches have shown that they have anti-inflammatory, antitumor, and antimicrobial activities (Liu et al., 2021). Chen et al. (2016) have investigated the protective actions and possible mechanisms of costunolide and dehydrocostus in 5-fluorouracil-induced gut mucositis. Male Kunming murines were intraperitoneally administered with 5-fluorouracil (60 mg/kg/day) for five days, and intestinal mucositis was assessed based on the histochemical indexes. Costunolide and dehydrocostus were taken orally once a day for eight days. Continuous 5-fluorouracil therapy resulted in serious intestinal mucositis, which was characterized by morphological injury, decreased ingestion, weight loss, and diarrhea. Experimental results showed that the daily gavage of costunolide or dehydrocostus exerted better protective action than that of the positive drug loperamide and prominently alleviated the seriousness of intestinal mucositis *via* accelerating enteric mucosa recovery, reducing ROS level, and restraining the inflammatory reactions. Therefore, costunolide and dehydrocostus are deemed to be promising therapeutical candidates, which are clinically employed to suppress intestinal mucositis in the course of chemical therapy.

Carvacrol is a phenolic monoterpene originating from various essential plants, such as *Thymus mongolicus* and *Origanum vulgare*. *In vitro* and *in vivo* research works have shown that carvacrol has antioxidative, antibacterial, anti-inflammatory, anticancerous, and hepatoprotective effects (Sharifi-Rad et al., 2018). TRPA1 receptor presents high expression in the enteric mucosa and can recognize cell injury, which manifests the potential relation with gut mucositis. Carvacrol is an activator of TRPA1 receptor and possesses anti-inflammatory activity. Therefore, Alvarenga et al. (2016) have conducted studies to prove the assumed anti-inflammatory and protective effects of carvacrol through TRPA1 activation against gut mucositis treated by CPT-11 in murines. In brief, murines were administered with DMSO, CPT-11, or carvacrol prior to CPT-11. In another group, the mice were treated with HC-030031 (TRPA1 antagonist) for thirty minutes prior to carvacrol exposure. On the seventh day, murine survival and microbemia were evaluated, and the jejunal tissues were

acquired for morphological analysis and determination of oxidative and inflammatory status after mercy killing. Results indicated that carvacrol exerted an anti-inflammatory effect on CPT-11-treated gut mucositis *via* powerful interplays with TRPA1 receptors, causing the reduction of the levels of pro-inflammatory factors (TNF- $\alpha$ , IL-1 $\beta$ , and KC), other inflammatory mediators (MPO, NF- $\kappa$ B, and COX-2), and oxidant stress (GSH, MDA, and NOx). Carvacrol also facilitated the recovery of the structure of villus and recess in the small intestine and improved clinical indexes, including livability, weight changes, leukocyte, and blood bacteria count. Therefore, carvacrol is a prospective candidate drug for treating gut mucositis, and TRPA1 may be a significant therapeutical target for intestinal mucositis.

Thymol, a natural monoterpene phenol, is found in many plants, including *Thymus vulgaris*, *Origanum vulgare*, and *Ocimum gratissimum*. Owing to its various bioactivities, thymol is widely employed in healthcare, animal medicine, food industry, and agriculture. Modern studies have indicated that thymol possesses remarkable beneficial actions, including antimicrobial, antioxidative, anti-inflammatory, anticancer, and immunoregulatory properties (Escobar et al., 2020). Al-Khrashi et al. (2021) have explored the possible protective action and mechanism of thymol on 5-fluorouracil-induced gut mucositis. Murines were injected with 5-fluorouracil (150 mg/kg) and administered with thymol (60 or 120 mg/kg). Pathologic variations, oxidant stress, and inflammatory indicators were evaluated. Results revealed that thymol administration remarkably restrained 5-fluorouracil-induced oxidant stress through decreasing lipid peroxidatic reaction and elevating the intestinal levels of antioxidative systems. Inflammatory indicators, including IL-6, PGE<sub>2</sub>, and COX-2, were also improved. Furthermore, thymol notably suppressed the 5-fluorouracil-induced expression of NF- $\kappa$ B, TNF- $\alpha$ , TGF- $\beta$ 1, p38, p-JNK, and MAPK proteins. Collectively, thymol could alleviate intestinal mucositis *via* the antioxidative and anti-inflammatory roles, which are associated with the inhibition of the TGF- $\beta$ /p38/p-JNK pathway.

Andrographolide is the main active constituent of *Andrographis paniculata* and possesses a diterpenoid lactone



ring. Diversified pharmacological actions of andrographolide have been demonstrated, such as antibacterial, anti-inflammatory, immunoregulatory, antiviral, and anticolitis properties (Kishore et al., 2017). Xiang et al. (2020) probed the protective action and mechanism of andrographolide on 5-fluorouracil-treated gut mucositis. Injection of 5-fluorouracil was conducted for inducing gut mucositis in BALB/c mice. 5-fluorouracil-stimulated NCM460 cells were adopted to probe the potential mechanism of andrographolide *in vitro*. The results indicated that andrographolide markedly relieved 5-fluorouracil-induced weight reduction, diarrhea, and lesions of intestinal crypts and villi. Pro-inflammatory cytokines, including TNF- $\alpha$ , IL-1 $\beta$ , and IL-6, were reduced by andrographolide in colonic and ileal tissues. Moreover, andrographolide significantly inhibited enteric cell apoptosis *in vivo* and *in vitro* through decreasing the expressions of p-p38, p-p53, cleaved caspase-3, cleaved caspase-8, and Bax, and increasing Bcl-2 level. Furthermore, asiatic acid (activator of p38 MAPK) recovered the antiapoptotic effect of andrographolide in NCM460 cells. In addition, Wang et al. (2022) further validated that andrographolide exerted a beneficial role on intestinal mucositis in irinotecan-induced mice and HCT116, CT26, and HT29 cells. Molecular mechanistic studies demonstrated that the andrographolide restrained irinotecan-induced cGAS-STING signaling pathway *via* decreasing the proteic expressions of p-TBK1 and p-IRF3, suppressing the mRNA levels of inflammatory factors (IL-18, TNF- $\alpha$ , and IL-1 $\beta$ ), IFN- $\beta$ , Cxcl10, and Ccl5, and inhibiting the infiltration of immunocytes, including CD11b, CD4, and CD8. The double-stranded DNA release and DNA damage triggered by irinotecan were also mitigated by andrographolide. In conclusion, andrographolide may be beneficial to the sufferers receiving 5-fluorouracil-based chemical therapy.

Saikosaponin-A is a main triterpenoid saponin existed in *Bupleurum falcatum* and *Bupleurum scorzonrifolium*, which manifests anti-inflammatory, antidepressive, antitumor, and immunoregulatory activities (Fu et al., 2015). Ali et al. (2019) demonstrated the protective role of saikosaponin-A on 5-fluorouracil-treated gut mucositis in the murine model. Intestinal mucositis was established in BALB/c murine through injecting 5-fluorouracil for three days, and mucositis was evaluated according to behavior and histochemical analysis. Saikosaponin-A was given one hour prior to 5-fluorouracil treatment for seven days. The results displayed that saikosaponin-A exhibited similar effect to the positive drug mesalazine. Compared with the model group, saikosaponin-A administration notably relieved the severity of intestinal mucositis, including food intake, weight reduction, diarrhea, and death rate in a dosage-dependent manner. The histopathological results also supported the protective action of saikosaponin-A on 5-fluorouracil-induced gut abnormalities, such as villi shrink, crypt stem-cell injury, inflammatory cell infiltration, vacuolation, and edema. Moreover, saikosaponin-A treatment observably suppressed

the pro-inflammatory factors (TNF- $\alpha$ , COX-2, IL-1 $\beta$ , and IL-6) and apoptosis indicators (p-JNK and caspase-3). In addition, saikosaponin-A markedly decreased the level of nitric oxide in enteric tissues, restrained acetic acid-treated Evans blue vasopermeability. In addition, saikosaponin-A administration significantly increased the expressions of antioxidants (Nrf2, HO-1, SOD, GSH, GST, and CAT) and reduced the level of oxidant stress indicator MDA. In brief, the results indicated that saikosaponin-A is a promising drug for treating chemotherapy-induced intestinal mucositis.

Patchouli alcohol, a tricyclic sesquiterpene, is an important active constituent of *Pogostemon cablin*. Up to now, many beneficial effects of patchouli alcohol have been demonstrated, such as anti-inflammatory, antibacterial, anticancer, and anticolitis effects (Lee et al., 2020). Wu et al. (2020) built the murine model of gut mucositis by 5-fluorouracil and administered patchouli alcohol to assess its role on intestinal mucositis. The results indicated that patchouli alcohol manifested similar effect with the positive drug CBL. The general examination (weight, food ingestion, and diarrhea) in animals was adopted to determine the effect of patchouli alcohol on gut mucositis. Inflammatory factors, mucosal barrier proteins, and enteric microbiome were measured to illustrate the potential mechanism of patchouli alcohol against gut mucositis in animals. Experimental results indicated that patchouli alcohol effectually improved weight, food ingestion, and diarrhea in the murine mucositis model, which preliminarily certified the effect of patchouli alcohol. Further tests displayed that patchouli alcohol dramatically reduced the expressions of TNF- $\alpha$ , IL-1 $\beta$ , IL-6, and MPO and elevated the expression of IL-10. Furthermore, the levels of intestinal barrier proteins (e.g., ZO-1, occludin, claudin-1, and mucin-1) and microflora structure were also improved after patchouli alcohol administration in mucositis murines. Therefore, patchouli alcohol may treat intestinal mucositis through decreasing inflammation, sustaining intestinal barrier function, and adjusting gut microbiome.

$\beta$ -patchoulene, a natural sesquiterpene, is one of the active ingredients in *Pogostemon cablin* (Swamy and Sinniah, 2015). Studies have shown that  $\beta$ -patchoulene possesses anti-inflammatory, anticolitis, and hepatoprotective effects. Wu et al. (2021) probed the effect and potential mechanism of  $\beta$ -patchoulene in ameliorating 5-fluorouracil-treated intestinal mucositis in IEC-6 cells and murines. Results indicated that  $\beta$ -patchoulene had similar effect with the positive drug loperamide, prominently restoring cell activity, increasing body weight and food ingestion, and relieving the pathologic diarrhea symptoms in the gut mucositis rats. Aquaporin is significant for maintaining water fluid homeostasis, and its unusual expression is related to pathological diarrhea in intestinal mucositis.  $\beta$ -patchoulene exerted a critical role in restraining AQP3 by the cAMP/PKA/CREB signaling pathway. Moreover, inflammation-caused mucus barrier

damage destroyed water transport and exacerbated diarrhea in intestinal mucositis animals. The function of  $\beta$ -patchoulene on restraining inflammation and restoring the mucus barrier reinforced its adjustment of water transport and therefore relieved diarrhea in gut mucositis murines. In conclusion,  $\beta$ -patchoulene alleviated intestinal mucositis in murines primarily through improving water transport and the mucus barrier, and these activities were related to its role on restraining the cAMP/PKA/CREB signaling pathway.

Glycyrrhizic acid, a triterpene glycoside, is the most significant active constituent of *Glycyrrhiza uralensis*, *Glycyrrhiza inflata*, and *Glycyrrhiza glabra*. Research works have shown that glycyrrhizic acid has anti-inflammatory, antiviral, antioxidative, anticancerous, and immunoregulatory properties (Chen K. et al., 2020). In consideration of the poor pharmacokinetics of glycyrrhizic acid and the prominent therapeutical effect of glycyrrhizic acid-loaded polymeric nanocarriers in intestinal diseases, Zeeshan et al. (2021) investigated their protective role on 5-fluorouracil-induced gut mucositis in murines. Polymeric nanocarrier has been testified to be an effective drug delivery vehicle for the long-range therapy of inflammatory ailments; however, its effect on 5-fluorouracil-induced mucositis has not yet been investigated. Thus, glycyrrhizic acid-loaded polylactic-co-glycolic acid (GA-PLGA) nanoparticle was prepared to assess its preventive and therapeutical effect in 5-fluorouracil-induced mucositis animals. GA-PLGA nanoparticle was produced with an improved double emulsion method, physically and chemically characterized, and tested for *in vitro* drug release. Then, induction of mucositis was conducted by giving 5-fluorouracil to the murines for the first three days, and GA-PLGA nanoparticles were administered to the animals for seven days. GA-PLGA nanoparticle observably decreased the mucositis seriousness concerning body weight, diarrhea scoring, pain, and asitia. Furthermore, 5-fluorouracil caused intestinal histopathologic injury, increased villus-crypt length, decreased goblet-cell quantity, increased pro-inflammatory factors, and restrained antioxidases. Nevertheless, all the deteriorations were restored by GA-PLGA nanoparticle. The results of morphology, behavior, histology, and biochemistry indicated that GA-PLGA nanoparticle was effective, biocompatible, targeted and slow-release nanovehicle drug delivery for enhancing mucoprotective, antiphlogistic, and antioxidative actions in 5-fluorouracil-induced intestinal mucositis.

## Flavonoids

Rutin, also known as vitamin P, is a glycoside of the flavonoid quercetin, derived from many edible and officinal plants, such as *Saussurea involucreata*, *Hippophae rhamnoides*, *Ruta graveolens*, and *Sophora japonica*. Extensive research works have shown that rutin possesses antimicrobial, anti-

inflammatory, anticancerous, and antidiabetic effects (Ganeshpurkar and Saluja, 2017). Fideles et al. (2020) investigated the function of rutin on 5-fluorouracil-induced experimental gut mucositis. The Swiss murines were randomly separated into seven groups: saline, 5-fluorouracil, rutin-50, rutin-100, rutin-200, celecoxib, and celecoxib + rutin-200 groups. The animals were weighed every day. After therapy, the mice were executed and fragments of the small intestine were gathered to assess the histopathologic changes, the levels of MDA, MPO and GSH, mastocyte and goblet cell amount, and COX-2 vitality. Moreover, the immunohistochemical analysis was also conducted in the study. Rutin administration suppressed 5-fluorouracil-induced histopathologic variations and decreased the oxidant stress through decreasing MDA level and elevating GSH level. Moreover, rutin alleviated the inflammatory reaction *via* reducing MPO vitality, enteric mastocytosis, and COX-2 activity. The result indicated that the COX-2 pathway might be one of the potential protective targets of rutin in treating 5-fluorouracil-induced intestinal mucositis.

Quercetin, a natural flavonoid, isolated from many medicinal and edible plants, such as *Sophora japonica*, *Platycladus orientalis*, and *Alpinia officinarum*. Modern studies have shown that quercetin has antioxidative, anti-inflammatory, antibacterial, and antineoplastic activities (Li et al., 2016). Sukhotnik et al. (2018) assessed the protective effect of quercetin on methotrexate-treated gut injury in SD rats. Results indicated that quercetin notably decreased the enteric damage scores, increased the enteral and mucosal weight of the jejunum and ileum, the protein level in ileum, the length of villi in the ileum, and the depth of crypts in the jejunum and ileum. Moreover, quercetin treatment markedly improved cell proliferation in both the jejunum and ileum through upregulating p-ERK protein expression and downregulating caspase-3. These results indicated that quercetin could restrain gut injury and promote gut restoration after methotrexate-induced gut mucositis. In addition, Lotfi et al. (2021) further found that quercetin and its nanoemulsion formulations exhibited protective effects on 5-fluorouracil-treated gut mucositis in mice. The oxidant-antioxidant balance was regulated by quercetin *via* increasing CAT level and decreasing MDA concentration, and HIF-1 $\alpha$  and NF- $\kappa$ B expression.

Luteolin is a usual flavone derived from many kinds of plants, including fruits, vegetables, and Chinese herbal medicines. A great deal of research has shown that luteolin possesses antioxidative, anticancerous, antiallergic, and anti-inflammatory activities (Aziz et al., 2018). Boeing et al. (2020) investigated the role and mechanism of luteolin against irinotecan-treated gut mucositis in murines. Clinical symptoms, histologic, oxidized, and inflammatory indicators were examined, along with the potential effect of luteolin on the antineoplastic role of irinotecan. The results indicated that luteolin improved irinotecan-induced gut injury through

decreasing weight loss and diarrhea scores and suppressing the shortening of the dodecadactylon and colon. Histologic examination proved that luteolin restrained villi shortening, vacuolation, and cell apoptosis and maintained the mucoprotein level in the dodecadactylon and colon. Furthermore, luteolin administration alleviated irinotecan-induced oxidant stress through decreasing the expressions of ROS and LOOH and increasing endogenous antioxidants and suppressed inflammatory symptoms through reducing MPO vitality, TNF- $\alpha$ , IL-1 $\beta$ , IL-6 productions, and elevating IL-4 and IL-10 productions. Disruption of the tight junctions ZO-1 and occludin could also be reversed by luteolin administration. It is noteworthy that luteolin had no effect on the anticancer role of irinotecan. In brief, luteolin may be a promising candidate to inhibit intestinal mucositis caused by irinotecan.

Baicalein, a natural flavone, is predominantly found in the roots of *Scutellaria baicalensis*. It has been proven that baicalein possesses antioxidative, antiviral, antibacterial, anti-inflammatory, antiallergenic, and antitumor effects (Dinda et al., 2017). Wang et al. (2020c) estimated the therapeutic effect of baicalein against chemotherapy-induced gut mucositis in murines. Simultaneously, the role of enteric microflora modulation in the therapeutic action of baicalein was explored. Male BALB/c murines were randomly separated into three groups, namely, the normal control, model, and experimental groups. Apart from normal control group, murines were treated with 5-fluorouracil and irinotecan to establish the intestinal mucositis model. Baicalein notably decreased the DAI of intestinal mucositis animals and the levels of IL-6 and TNF- $\alpha$  in serum. There were remarkable discrepancies in the constitution of the intestinal microflora among groups based on the analyses of  $\alpha$ -diversity,  $\beta$ -diversity and the species discrepancies. In comparison with the normal group, the *Ruminococcaceae\_UCG\_014* and *Lachnospiraceae* in murines of the model group were markedly reduced, while *Bacteroides*, *Escherichia\_Shigella*, *Enterococcus*, *Parabacteroides*, *Clostridium\_sensu\_stricto\_1*, and *Lactococcus* were observably elevated. After baicalein treatment, the levels of *Bacteroides*, *Escherichia\_Shigella*, *Parabacteroides*, *Enterococcus*, *Clostridium\_sensu\_stricto\_1*, and *Lactococcus* were notably reduced and *Muribaculaceae* was elevated. The levels of IL-6 and TNF- $\alpha$  in the serum of the three groups were positively related to the levels of *Clostridium\_sensu\_stricto\_1*, *Lactococcus*, *Bacteroides*, and *Enterococcus* based on the association analysis. The present research indicated the promising efficacy of baicalein on intestinal mucositis murines. Modulation of intestinal microflora possibly exerted a crucial role in the therapeutic effect of baicalein.

Diadzein is a natural isoflavone mainly extracted from *Pueraria lobata* and soybeans. Extensive pharmacologic actions of diadzein were proven, including anticancer, anti-inflammatory, and antidiabetic activities (Feng et al., 2015). Atiq et al. (2019) investigated the effect of diadzein on gut mucositis treated with 5-fluorouracil and paid close attention to oxidant stress and inflammatory indicators in murines. Animals were given 5-fluorouracil to induce mucositis once

daily for three days, and diadzein was given once daily for seven days. The results showed that diadzein exerted a comparable effect with the positive drug mesalazine. Administration of diadzein decreased the seriousness of mucosa damage in a dosage-dependent manner. Diadzein prominently suppressed weight reduction, alleviated diarrhea, and improved histopathologic deformity related to inflammatory symptoms. Furthermore, diadzein observably improved the enteric wall histopathology through decreasing infiltration and arrested restraint of antioxidant via 5-fluorouracil treatment. Nitrite levels in enteric tissues were decreased by diadzein, which accorded with the regulation of inflammatory mediators. In addition, diadzein also improved the microbial profile through decreasing the count of pathogens and increasing the level of probiotic bacteria. Collectively, this research indicated that diadzein possessed prominent protective effect against mucositis in 5-fluorouracil-treated mucositis model, and the therapeutic effect of diadzein may be associated with the restraint of oxidant stress and inflammatory response.

Puerarin, a natural isoflavone, is the major constituent derived from the roots of *Pueraria lobata*. Research works have shown that puerarin has antitumor, antiviral, antioxidative, and anti-inflammatory effects (Zhang, 2019). Wang L. et al. (2021) built a murine model of gut mucositis through intraperitoneally injecting 5-fluorouracil and then administering puerarin for seven days. Regular indices including weight, food intake, and diarrhea were measured to assess the effect of puerarin on gut mucositis in murines. The function of gut barrier was also assessed through determining the serum recovery of fluorescein isothiocyanate-4kD dextran. The expressions of inflammatory factors, oxidative reactions, and apoptosis marker proteins were examined to illuminate the potential mechanism of puerarin against gut mucositis. Results suggested that the model murines appeared representative symptoms and histopathologic variations of 5-fluorouracil-induced gut mucositis. Drastic inflammatory symptoms, oxidation reactions, cell apoptosis, and JAK were significantly stimulated. Puerarin reduced the expressions of inflammation-related proteins, oxidation reactions and apoptosis in 5-fluorouracil-induced mucositis through blocking JAK activation. In conclusion, puerarin reduced inflammatory symptoms, oxidation reactions and apoptosis, and protected enteric barrier function to alleviate 5-fluorouracil-treated gut mucositis via suppressing JAK activation. This work suggested that puerarin might be a promising natural JAK depressor for the treatment of 5-fluorouracil-induced intestinal mucositis.

## Quinones

Dihydrotanshinone I is an important active constituent in *Salvia miltiorrhiza*, which has been reported to exert antitumor,

anti-inflammatory, and cardioprotective roles (Chen et al., 2019). Wang et al. (2020a) probed the action of dihydrotanshinone I against intestinal mucositis induced by 5-fluorouracil and irinotecan in murines. They determined the level of enteric mucosa injury and inflammatory reaction in gut mucositis animals with or without dihydrotanshinone I treatment. Body weight and DAI of murines were daily examined. H&E staining was adopted to assess the pathologic injury. The levels of IL-6, TNF- $\alpha$ , TG, and diacylglycerol in serums were measured using commercial kits. The variations of fecal microbiome were also probed via 16S rRNA high throughput sequencing. Spearman association analyses were employed to assess the relevance between fecal microbiome and inflammatory cytokines. Tax4Fun was used to explore the possible role of gut microflora. The result indicated that dihydrotanshinone I markedly decreased the DAI score, enteric mucosa injury, and inflammatory reaction in gut mucositis murines by reducing the serum IL-6 and TNF- $\alpha$  levels. Moreover, there was close relationship between fecal microbiome and inflammatory cytokines. Dihydrotanshinone I effectively restored the maladjusted faecal microbiome and increased the level of *Akkermansia*. Dihydrotanshinone I also improved bacteria species, which facilitated butyric acid metabolism or were negatively related to inflammatory cytokines. In addition, species improved by dihydrotanshinone I in faecal microbiome were possibly associated with the glutamine level and ammonia oxidization. In brief, this research indicated that dihydrotanshinone I effectually alleviated gut mucositis caused by 5-fluorouracil and irinotecan in murines. Adjustment of the composition and function of fecal microbiome possibly exerted an important effect in the therapeutical action of dihydrotanshinone I in intestinal mucositis animals.

Cryptotanshinone is a natural quinone compound predominantly existed in *Salvia miltiorrhiza*. Studies have indicated that cryptotanshinone has anti-inflammatory, anticancerous, antibacterial, neuroprotective, and cardioprotective effects (Li et al., 2021). Wang et al. (2020b) explored the therapeutical action of cryptotanshinone on chemotherapy-induced gut mucositis in murines. Chemotherapy-caused gut mucositis was induced through intraperitoneally injecting 5-fluorouracil and irinotecan for four days. A pseudo-sterile murine model was established through intragastrically administering mixed antibiotics (metronidazole, vancomycin, and penicillin). Weight, DAI, and feces of murines were daily examined and the levels of inflammatory cytokines, TC, TG, and lipase vitality in serums or colon mucosa of intestinal mucositis animals were measured. They also probed the constitution and relative abundance of fecal microflora. The relation of the relative abundance of fecal microflora and environmental aspects was further analyzed. Cryptotanshinone observably reduced DAI, and the expressions of IL-6, IL-11, MPO, and DAO in the serums of intestinal mucositis murines. Cryptotanshinone effectually

elevated the level of TG while decreased TC and lipase vitality in the serums. It was indicated that the incidence of chemotherapy-induced mucositis in the pseudoaseptic model group was prominently decreased. In the meantime, there was no remarkable discrepancy in the levels of inflammatory cytokines and TG/TC ratio between the pseudoaseptic model and normal control groups. There was a prominent discrepancy in the diversity and constitution of fecal microbiome among groups. Furthermore, cryptotanshinone recovered the constitution of fecal microbiome close to normal and observably elevated the levels of *Muribaculaceae* and *Ruminococcaceae\_UCG-014*. Specially, *Ruminiclostridium* and *Muribaculaceae* showed a remarkable positive relation to TG but a negative relation to DAO, MPO, IL-6, lipase, and TC. In brief, cryptotanshinone effectually relieved gut mucositis in murines induced by 5-fluorouracil and irinotecan through modulating the fecal microbiome, inflammatory cytokines, and serum lipids.

## Phenylethanoid glycosides

Forsythiaside A is the major active constituent derived from *Forsythia suspensa* and has excellent biological activities. Pharmacological research works have proven that forsythiaside A has remarkable activities in treating multiple diseases, including inflammation, virus and bacterial infection, oxidative stress, and hepatic damage (Gong et al., 2021). Lang et al. (2022) explored the effect and mechanism of forsythiaside A on chemotherapy-induced gut mucositis in murines. In brief, for three days, male SD murines were treated with 7 mg/kg methotrexate to induce intestinal mucositis and simultaneously administered with 40 or 80 mg/kg forsythiaside A for seven days. The result indicated that the final body weight and daily food uptake were elevated, and the DAI score was decreased by forsythiaside A administration. The methotrexate-treated rats exhibited pathologic changes including inflammatory infiltration, mucosa layer destruction, gland expansion, enteric villus structure disorder, and goblet cell reduction, whereas administration with 80 mg/kg forsythiaside A showed obvious beneficial roles. ELISA assay further indicated that the serum levels of TNF- $\alpha$ , IL-1 $\beta$ , and IL-18 in methotrexate-induced animals were decreased after forsythiaside A administration. Furthermore, forsythiaside A reduced the amounts of leukocytes, neutrophils, and lymphocytes in peripheral blood. Western blotting and immunofluorescence results showed that the expressions of NLRP3, cleaved caspase 1 and cleaved IL-1 $\beta$  and CD68 positive rate were reduced in methotrexate-induced murines after forsythiaside A treatment. In conclusion, forsythiaside A effectively restrained methotrexate-induced intestinal mucositis through alleviating the activation of NLRP3 inflammasome.

Acteoside is an important active component, which mainly exists in medicinal plants like *Rehmannia glutinosa* and



*Cistanche deserticola*. At present, acteoside has been found to exert anti-inflammatory, antioxidative, and anticancer effects (Zhou et al., 2020). Reinke et al. (2015) explored the effect of acteoside in the treatment of intestinal mucositis. C57BL/6 murine was administered daily with 600 µg acteoside for five days before inducing intestinal mucositis and throughout the experiment. Induction of intestinal mucositis was conducted by methotrexate, and mice were executed on the fifth and eleventh days after methotrexate. The dodecadactylon, jejunum, and ileum were collected to examine MPO vitality, MT expression, and histological features. Acteoside decreased histological severity scores by 75, 78, and 88% in the dodecadactylon, jejunum and ileum in comparison with the methotrexate controls on the fifth day, respectively. Acteoside also decreased crypt depth by 49, 51, and 33% and elevated villus height by 19, 38, and 10% in the dodecadactylon, jejunum, and ileum in comparison with the methotrexate controls on the fifth day, respectively. Moreover, acteoside reduced the MT level by 50% in comparison with the methotrexate control murine on the fifth day. Moreover, acteoside reduced the MPO level by 60 and 30% in the dodecadactylon and jejunum in comparison with the methotrexate controls on the fifth day, respectively. The results indicated that acteoside relieved methotrexate-induced intestinal mucositis probably through suppressing inflammation.

## Polyphenols

*Melastoma malabathricum* is a common herb and mainly adopted to treat multiple gastrointestinal diseases in China (Al-Sayed et al., 2020). Chen et al. (2022) isolated an active compound casuarinin from the root of *Melastoma malabathricum* and explored the therapeutic effect and mechanism of casuarinin in 5-fluorouracil-treated gut mucositis murines. Results indicated that casuarinin notably improved 5-fluorouracil-induced body weight loss and ingestive reduction, and also prominently reversed villus atrophy, restored the proliferative activity of the enteric crypts, and restrained inflammatory symptoms and enteric barrier dysfunction in the murine model of 5-fluorouracil-treated gut mucositis. Moreover, casuarinin also reversed 5-fluorouracil-induced intestinal microflora dysbiosis, especially the level of *Actinobacteria*, *Candidatus Arthromitus*, *Lactobacillus murinus*, and the Firmicutes-to-Bacteroidetes ratio. In conclusion, casuarinin could improve 5-fluorouracil-treated gut mucositis by favorably regulating inflammation, gut barrier dysfunction, and intestinal microflora imbalance. Therefore, casuarinin might be a prospective candidate for the treatment of intestinal mucositis.

Curcumin, a natural diketone, mainly exists in *Curcuma longa*, *Curcuma aromatica*, *Curcuma zedoaria*, and *Acorus calamus*. For a long time, curcumin has been widely used in

the food industry as a common natural pigment, and also exhibits antioxidative, antibacterial, antiviral, antitumor, and anti-inflammatory activities (Hewlings and Kalman, 2017). Considering the anticancer effect of curcumin and its protective effect in intestinal diseases, Wang et al. (2021) explored the role of curcumin in inflammation and enteric epithelial cell injury in gut mucositis animals. 5-fluorouracil was adopted to induce intestinal mucositis in gut epithelia cells, and diverse levels of curcumin were given. Experimental data indicated that curcumin effectively alleviated 5-fluorouracil-induced injury to IEC-6 cells, restrained the expressions of inflammatory factors, increased cell vitality, and exerted antiapoptotic role on IEC-6 cells. RNA sequencing analyses and experimental verification demonstrated that curcumin exerted protective effect on 5-fluorouracil-induced gut mucositis in enteric epithelia cells through inhibiting the IL-6/STAT3 signaling pathway. In conclusion, the results manifested that curcumin may be a potential therapeutical candidate in preventing and treating chemotherapy-induced intestinal mucositis.

## Alkylamide

Spilanthol, a major alkylamide from *Acmella oleracea*, possesses narcose, analgesic, and anti-inflammatory actions (Silveira et al., 2018). de Freitas-Blanco et al. (2019) assessed the effect of spilanthol on gut mucositis in Swiss murine elicited by 5-fluorouracil. Continuous dose of 5-fluorouracil led to gut mucositis and consequently decreased food ingestion and weight reduction. Experimental data suggested that spilanthol (30 mg/kg) prominently reduced the seriousness of gut mucositis, restrained histopathologic deterioration, and increased the villi length in mice administered with spilanthol compared with the 5-fluorouracil treatment group. Though a few pro-inflammatory factors were not quantifiable in any group, reduction of MPO vitality was obvious in mice administered with spilanthol. In brief, the results indicated that spilanthol efficiently decreased the inflammatory symptoms in gut mucositis mice treated with 5-fluorouracil, and this natural compound may be a potential therapeutical candidate for gut mucositis.

## Alkaloid

Berberine is a natural isoquinoline alkaloid existed in a lot of medicinal plants including *Coptis chinensis*, *Phellodendron chinense*, and *Berberis soulieana*. Modern pharmacological studies have shown that berberine possesses hypoglycemic, hypolipidemic, antibacterial, and anti-inflammatory activities (Kumar et al., 2015). Chen H. T. et al. (2020) explored the function and mechanism of berberine on gut mucositis rats



treated by 5-fluorouracil. Results indicated that berberine treatment exhibited decreased weight loss, reduced diarrhea score, and increased colon length in 5-fluorouracil-induced gut mucositis rats. Meanwhile, berberine dramatically increased the occludin level in ileum and lowered the D-lactic acid content in serum. In addition, berberine prominently restrained inflammatory response through inhibiting the production of intestinal inflammatory cytokines TNF- $\alpha$ , IL-6, and IL-1 $\beta$ . Moreover, berberine reversed the changes of fecal metabolites and regulated metabolic pathways via increasing the levels of acetate, butyrate, propionate, and glutamine. Importantly, berberine effectively modulated the gut microbiota structure. The relative abundance of *Firmicutes*, *Porphyromonadaceae*, *Lachnospiraceae*, *Lactobacillus*, *Clostridiales*, *Ruminococcus*, *Prevotella*, and *Clostridium IV* was upregulated, while *Proteobacteria* and *Escherichia\_Shigella* were decreased by berberine treatment. Significantly, fecal transplantation from berberine-treated rats could relieve intestinal mucosal injury. Yue et al. (2021) also found that berberine conspicuously ameliorated gut mucositis in irinotecan-treated mucositis murines and SN38-stimulated NCM460 or Caco-2 cells. The underlying mechanism might be closely associated with the suppression of pro-inflammatory mediators (including COX-2, iNOS, TNF- $\alpha$ , IL-8, and IL-1 $\beta$ ), bacterial GUS activity and the improvement of mucosal barrier integrity by elevating the protein expression of ZO-1, occludin, and claudin-1 and decreasing the levels of LPS, DAO, and FITC-dextran fluorescence. In summary, these results offered novel clues into the potential usage of berberine in preventing and treating intestinal mucositis.

## Discussion

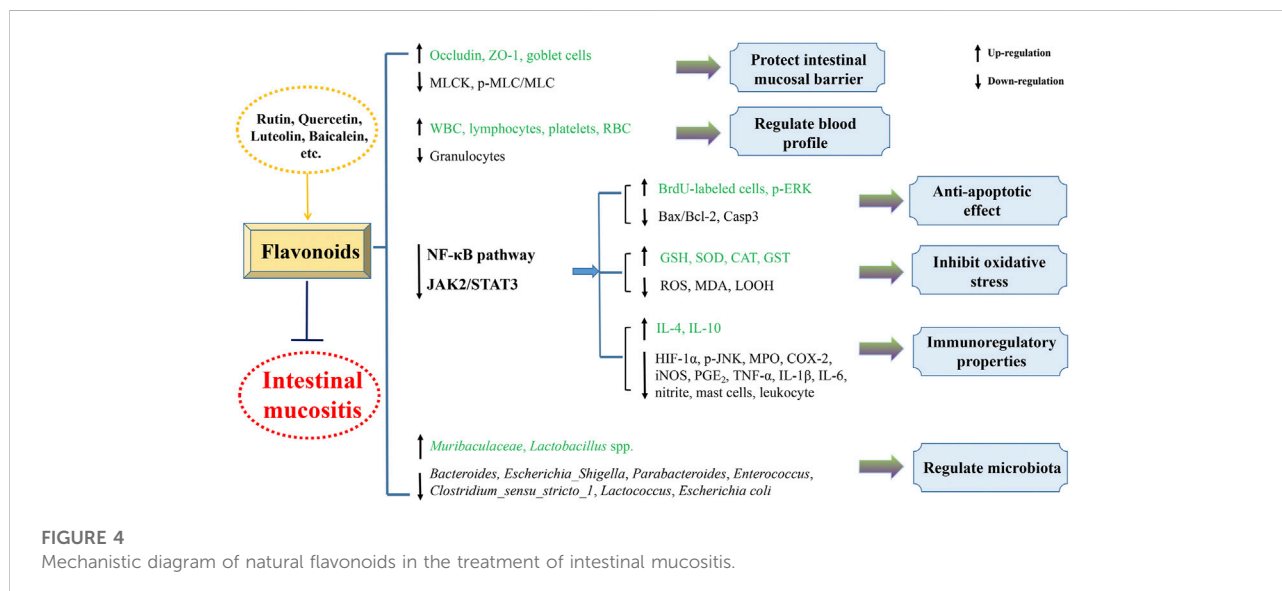
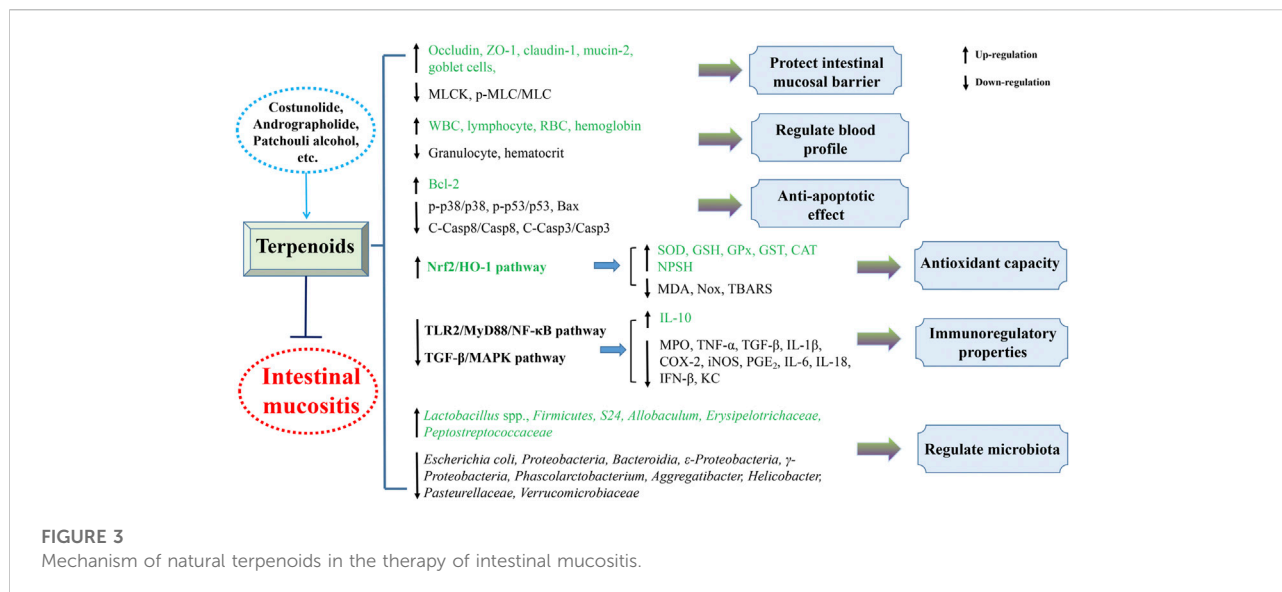
Chemotherapy for malignant tumors can cause changes in the structure and function of the gastrointestinal tract. 5-fluorouracil, an important chemotherapeutic drug, is widely used to treat advanced colorectal carcinoma and malignant tumors in head and neck (Cheah et al., 2014b; Huang et al., 2022). Consecutive oral administration of 5-fluorouracil leads to serious toxic reactions, especially gut mucositis, which is mainly ascribed to the destruction of intestinal structure and integrity. Moreover, epithelial cell apoptosis, oxidative stress, inflammatory response, and intestinal microflora disorder are closely associated with the deterioration of intestinal mucositis.

Intestinal barrier is composed of epithelia barrier and mucosal layer. The intact mucosal layer is a barrier to stop water runoff and eliminate inspiratory foreign matters, including microorganisms, inflammatory cells, and pollutants (Bajka et al., 2015; Zhao and Maynard, 2022). When intestinal mucositis appeared, slime layer is exhausted with reduced level of mucins (mucin-1 and mucin-2) and goblet cell dysregulation

(Kawashima et al., 2015; Thorpe et al., 2020). Malfunction of the mucus layer, in turn, exacerbated inflammatory symptoms and impaired the water-holding capability of the gastrointestinal tract, caused aquaporins over expression, and ultimately resulted in serious diarrhea in intestinal mucositis murines (Ikarashi et al., 2016). In the current review, patchouli alcohol,  $\beta$ -patchoulene, glycyrrhizic acid, rutin, and forsythiaside A could effectively improve the content of goblet cells or mucins. Of note,  $\beta$ -patchoulene enhanced the mucus layer function and decreased aquaporin 3 level, thus recovering the murine's water-holding capability. The association analysis also showed that aquaporin 3 and diarrhea symptoms were strongly associated with mucus layer function.

Intestinal epithelia establish the maximal and most significant barrier between inner and outer surroundings. Research works have indicated that enteric epithelium barrier is destroyed in gastrointestinal disorders, such as ulcerative colitis and gut mucositis (Xiong et al., 2019; Jin et al., 2022). TJs are the apical adhesive junction complexes in epithelial cells of mammals. Deficiency of TJs results in an enhancement in enteric penetrability and promotes the development of enteric inflammation (Panwar et al., 2021). TJ membrane-spanning proteins, such as ZO-1, ZO-2, occludin, and claudins, exert a synergic action in controlling the entry and exit of ionic solute and maintaining enteric penetrability. ZO is a kind of cytoplasmic scaffolding protein, which anchors TJ membrane protein to the cytoskeleton through interaction (Skamrahl et al., 2021). Claudins are the critical constituents of intercellular TJs and take charge of paracytic solute flux (Tanaka et al., 2015). As a necessary membrane-spanning protein, occludin is significant for TJ integrity. In addition, MLCK exerts a key effect in TNF- $\alpha$ -induced enteric penetrability. MLCK restraint stops MLC phosphorylation and maintains enteric TJ barrier, leading to the inhibition of enteric inflammation (Wang J. et al., 2021). Current research works have found a destruction of the enteric intercellular structure, with an increase in enteric penetrability, reduced TJs levels, and abnormal high expressions of MLC, MLCK and p-MLC proteins in mucositis murines. However, patchouli alcohol,  $\beta$ -patchoulene, luteolin, casuarinin, and berberine exhibited beneficial action on enteric penetrability by elevating the levels of TJs (ZO-1, claudin-1, or occludin), thus resulting in further maintaining enteric epithelia barrier. Moreover, the increased level of MLCK and p-MLC were significantly inhibited by puerarin and patchouli alcohol treatments.

Inflammatory infiltration is a typical feature of mucositis. MPO vitality and pro-inflammatory factors have been found to increase under inflammatory conditions (Li et al., 2020). Excessive production of ROS and uncontrolled inflammatory symptoms could disturb enteric homeostasis, change the normal microflora and stimulate a sequence of acute reactions to injure cells and tissues, resulting in mucosa damage and mucositis



(Boeing et al., 2020). The content of antioxidases decreases or cannot remove superfluous ROS, resulting in elevated oxidative stress and cell injury (Yoneda et al., 2021). Moreover, convincing evidence have demonstrated that elevated expressions of inflammatory factors were strongly related to the destruction of enteric mucosa barrier (Tappenden, 2008). Research works have indicated that 5-fluorouracil treatment could elevate the expressions of pro-inflammatory cytokines (COX-2, iNOS, IL-6, IL-1 $\beta$ , and TNF- $\alpha$ ), reduce antioxidant enzymes (SOD, GST, and CAT), and induce mucosa injury (Aghabozorgi et al., 2020). However, costunolide, thymol, saikosaponin A, rutin, luteolin, and casuarinin have been proven to possess anti-inflammatory

action and relieve oxidative stress by reducing the generation of pro-inflammatory factors and elevating the expressions of antioxidants.

TLRs possess critical effects in adjusting the enteric epithelia barrier and congenital immunization. TLR2 induce NF- $\kappa$ B activation to regulate the gene levels of inflammatory mediators by Toll/IL-1 receptor domain with adapter protein MyD88 (Takeuchi and Akira, 2002; Zhang et al., 2021). Proper expression of TLR2 insures antiapoptotic action, resulting in the adjustment of TJs in enteric epithelia cells (Lin et al., 2013). NF- $\kappa$ B is a significant coordinator of congenital and adaptive immunoreactions, taking part in the regulation of

inflammatory symptoms and cell cycle. NF- $\kappa$ B activation induces the abnormal expression of its downstream genes, including iNOS, COX-2, chemokines, adhesion molecules, and pro-inflammatory factors (Luqman and Pezzuto, 2010). In addition, STAT3 is a cellular signal transcription factor, which plays a key role in hyperplasia, differentiation, transference, and survival. Enduring STAT3 activation is deemed to accelerate chronic inflammation, which elevates susceptibility of healthy cells to carcinogenesis (Lei et al., 2021). When the enteric mucosa is activated, increased IL-6 can stimulate the phosphorylation of STAT3 and feedback to NF- $\kappa$ B (Ke et al., 2015). In the present review, patchouli alcohol, thymol, puerarin, and forsythiaside A remarkably restrained intestinal mucositis in animal or cell models, which was intimately associated with the suppression of TLR2/MyD88/NF- $\kappa$ B, IL-6/STAT3, TGF- $\beta$ /MAPK, and NLRP3 signaling pathways.

Intestinal microbiota homeostasis is a significant element for gastrointestinal health. Numerous research works have shown that gut microflora disorder exhibits a crucial effect in gastrointestinal diseases, including colitis, bacterial dysentery, and chemotherapy-induced mucositis (Varankovich et al., 2015). Microbial diversity analysis has shown that compared with the normal group, the intestinal microbial structure of mucositis animals changed significantly. Moreover, microflora takes part in the change of inflammatory cell factors (Li et al., 2017). *Bacteroides*, *Bifidobacterial*, *Lactobacilli*, *Escherichia*, *Helicobacter*, and *Parabacteroides* are strongly associated with the progression and seriousness of mucositis. *Bifidobacterial* and *Lactobacilli* are indicated to be capable of restraining NF- $\kappa$ B activation, increasing TJs protein level, and reducing enteric penetrability (Khokhlova et al., 2012; Wu et al., 2016). *Bacteroides*, *Escherichia*, *Helicobacter*, and *Parabacteroides* are often deemed to be the pathogenic bacteria or conditioned pathogens (Zhang et al., 2018). For instance, rises in *Parabacteroides* and *Bacteroides* amounts contribute to colitis in murines, *Helicobacter pylori* infection contributes to peptic ulcer disorder and stomach tumors, and *Escherichia* is profitable for gut inflammation *in vivo*. *Bifidobacterium infantis* alleviates Th1 cell reaction through adjusting cell factors and differentiation-related factors in chemotherapy-induced gut mucositis murines (Mi et al., 2017). In terms of *Lactobacillus*, it contributes to reducing the colonic pH and the development of pathogens (Yeung et al., 2020). In this review article, 5-fluorouracil induced structure disorder of intestinal microflora characterized by elevated *Bacteroides*, *Escherichia coli*, *Proteobacteria*, *Bacteroidia*, *Proteobacteria*, *Helicobacter*, *Pasteurellaceae*, *Verrucomicrobiaceae*, and reduced relative abundances of *Bacterioidetes*, *Lactobacillus* spp., *Actinobacteria*, and *Lactobacillus murinus*, which were reversed by saikosaponin A, patchouli alcohol, baicalein, daidzein, dihydrotanshinone, casuarinin, and berberine treatment.

## Conclusion

The present review generalizes the significant and beneficial roles of plant-derived natural compounds in attenuating intestinal mucositis in pioneering endeavor. Their protective mechanisms against intestinal mucositis might involve improving intestinal barrier function, decreasing enterocyte apoptosis, regulating gut microbiota, and inhibiting inflammatory reaction and oxidant stress predominantly through blocking TLR2/MyD88/NF- $\kappa$ B, TGF- $\beta$ /MAPK, JAK2/STAT3, Nrf2/HO-1, and NLRP3 inflammasome pathways (Figures 3, 4). Taken together, these findings provide experimental and scientific evidence for utilizing plant-derived natural compounds as drug candidates to treat intestinal mucositis. However, further in-depth preclinical and clinical trials are warranted to clarify the molecular mechanism to facilitate the potential clinical transformation of natural compounds like costunolide, andrographolide, patchouli alcohol, and berberine in the treatment of intestinal mucositis.

## Author contributions

QL conducted the design of the study. CL, QL, and JX performed the literature searching. CL, QL, JW, YC, and MP designed the figures and tables. CL wrote the manuscript. QG and QL revised the manuscript. All authors have approved the final version.

## Funding

This study was financially supported by the National Natural Science Foundation of China (Nos. 82003771 and 82160785), Science and Technology Foundation of Guizhou Province (Nos. QKHJC-ZK[2021] YB514 and QKHJC-ZK[2021] YB525).

## Conflict of interest

The authors declare that the research was conducted in the absence of any commercial or financial relationships that could be construed as a potential conflict of interest.

## Publisher's note

All claims expressed in this article are solely those of the authors and do not necessarily represent those of their affiliated organizations, or those of the publisher, the editors, and the reviewers. Any product that may be evaluated in this article, or claim that may be made by its manufacturer, is not guaranteed or endorsed by the publisher.

## References

- Aghabozorgi, A. S., Sarabi, M. M., Jafarzadeh-Esfehani, R., Koochakkhani, S., Hassanzadeh, M., Kavousipour, S., et al. (2020). Molecular determinants of response to 5-fluorouracil-based chemotherapy in colorectal cancer: The undisputable role of micro-ribonucleic acids. *World J. Gastrointest. Oncol.* 12 (9), 942–956. doi:10.4251/wjgo.v12.i9.942
- Al-Khrashi, L. A., Badr, A. M., Al-Amin, M. A., and Mahran, Y. F. (2021). Thymol ameliorates 5-fluorouracil-induced intestinal mucositis: Evidence of down-regulatory effect on TGF- $\beta$ /MAPK pathways through NF- $\kappa$ B. *J. Biochem. Mol. Toxicol.* 36 (1), e22932. doi:10.1002/jbt.22932
- Al-Sayed, E., Michel, H. E., Khatib, M. A., El-Shazly, M., and Singab, A. N. (2020). Protective role of casuarinin from *Melaleuca leucadendra* against ethanol-induced gastric ulcer in rats. *Planta Med.* 86 (1), 32–44. doi:10.1055/a-1031-7328
- Ali, J., Khan, A. U., Shah, F. A., Ali, H., Ul Islam, S., Kim, Y. S., et al. (2019). Mucoprotective effects of Saikosaponin-A in 5-fluorouracil-induced intestinal mucositis in mice model. *Life Sci.* 239, 116888. doi:10.1016/j.lfs.2019.116888
- Alvarenga, E. M., Souza, L. K. M., Araujo, T. S. L., Nogueira, K. M., Sousa, F. B. M., Araujo, A. R., et al. (2016). Carvacrol reduces irinotecan-induced intestinal mucositis through inhibition of inflammation and oxidative damage via TRPA1 receptor activation. *Chem. Biol. Interact.* 260, 129–140. doi:10.1016/j.cbi.2016.11.009
- Atiq, A., Shal, B., Naveed, M., Khan, A., Ali, J., Zeeshan, S., et al. (2019). Diadzein ameliorates 5-fluorouracil-induced intestinal mucositis by suppressing oxidative stress and inflammatory mediators in rodents. *Eur. J. Pharmacol.* 843, 292–306. doi:10.1016/j.ejphar.2018.12.014
- Aziz, N., Kim, M. Y., and Cho, J. Y. (2018). Anti-inflammatory effects of luteolin: A review of *in vitro*, *in vivo*, and *in silico* studies. *J. Ethnopharmacol.* 225, 342–358. doi:10.1016/j.jep.2018.05.019
- Bajka, B. H., Rigby, N. M., Cross, K. L., Macierzanka, A., and Mackie, A. R. (2015). The influence of small intestinal mucus structure on particle transport *ex vivo*. *Colloids Surf. B Biointerfaces* 135, 73–80. doi:10.1016/j.colsurfb.2015.07.038
- Batista, V. L., da Silva, T. F., de Jesus, L. C. L., Coelho-Rocha, N. D., Barroso, F. A. L., Tavares, L. M., et al. (2020). Probiotics, Prebiotics, synbiotics, and paraprobiotics as a therapeutic alternative for intestinal mucositis. *Front. Microbiol.* 11, 544490. doi:10.3389/fmicb.2020.544490
- Boeing, T., de Souza, P., Specia, S., Somensi, L. B., Mariano, L. N. B., Cury, B. J., et al. (2020). Luteolin prevents irinotecan-induced intestinal mucositis in mice through antioxidant and anti-inflammatory properties. *Br. J. Pharmacol.* 177 (10), 2393–2408. doi:10.1111/bph.14987
- Cheah, K. Y., Howarth, G. S., and Bastian, S. E. P. (2014a). Grape seed extract dose-responsively decreases disease severity in a rat model of mucositis; Concomitantly enhancing chemotherapeutic effectiveness in colon cancer cells. *PLoS One* 9 (1), e85184. doi:10.1371/journal.pone.0085184
- Cheah, K. Y., Howarth, G. S., Bindon, K. A., Kennedy, J. A., and Bastian, S. E. P. (2014b). Low molecular weight procyanidins from grape seeds enhance the impact of 5-fluorouracil chemotherapy on caco-2 human colon cancer cells. *PLoS One* 9 (6), e98921. doi:10.1371/journal.pone.0098921
- Chen, H. T., Zhang, F., Li, R. R., Liu, Y., Wang, X. Y., Zhang, X. J., et al. (2020a). Berberine regulates fecal metabolites to ameliorate 5-fluorouracil induced intestinal mucositis through modulating gut microbiota. *Biomed. Pharmacother.* 124, 109829. doi:10.1016/j.biopha.2020.109829
- Chen, K. J., Huang, Y. L., Kuo, L. M., Chen, Y. T., Hung, C. F., and Hsieh, P. W. (2022). Protective role of casuarinin from *Melastoma malabathricum* against a mouse model of 5-fluorouracil-induced intestinal mucositis: Impact on inflammation and gut microbiota dysbiosis. *Phytomedicine*. 101, 154092. doi:10.1016/j.phymed.2022.154092
- Chen, K., Yang, R., Shen, F. Q., and Zhu, H. L. (2020b). Advances in pharmacological activities and mechanisms of glycyrrhizic acid. *Curr. Med. Chem.* 27 (36), 6219–6243. doi:10.2174/092986732566619101115407
- Chen, X. P., Yu, J., Zhong, B. L., Lu, J. H., Lu, J. J., Li, S. J., et al. (2019). Pharmacological activities of dihydrotanshinone I, a natural product from *Salvia miltiorrhiza* Bunge. *Pharmacol. Res.* 145, 104254. doi:10.1016/j.phrs.2019.104254
- Chen, Y. L., Zheng, H., Zhang, J. Z., Wang, L., Jin, Z. X., and Gao, W. Y. (2016). Reparative activity of costunolide and dehydrocostus in a mouse model of 5-fluorouracil induced intestinal mucositis. *RSC Adv.* 6 (7), 5249–5258. doi:10.1039/c5ra22371g
- da Silva, K. S., da Silveira, B. C., Bueno, L. R., da Silva, L. C. M., Fonseca, L. D., Fernandes, E. S., et al. (2021). Beneficial effects of polysaccharides on the epithelial barrier function in intestinal mucositis. *Front. Physiol.* 12, 714846. doi:10.3389/fphys.2021.714846
- Dahlgren, D., Sjoblom, M., Hellstrom, P. M., and Lennernas, H. (2021). Chemotherapeutics-induced intestinal mucositis: Pathophysiology and potential treatment strategies. *Front. Pharmacol.* 12, 681417. doi:10.3389/fphar.2021.681417
- de Freitas-Blanco, V. S., Monteiro, K. M., de Oliveira, P. R., de Oliveira, E. C. S., Braga, L. E. D., de Carvalho, J. E., et al. (2019). Spilanthal, the principal alkylamide from *Acmella oleracea*, attenuates 5-fluorouracil-induced intestinal mucositis in mice. *Planta Med.* 85 (3), 203–209. doi:10.1055/a-0715-2002
- Dinda, B., Dinda, S., DasSharma, S., Banik, R., Chakraborty, A., and Dinda, M. (2017). Therapeutic potentials of baicalin and its aglycone, baicalein against inflammatory disorders. *Eur. J. Med. Chem.* 131, 68–80. doi:10.1016/j.ejmech.2017.03.004
- Escobar, A., Perez, M., Romanelli, G., and Blustein, G. (2020). Thymol bioactivity: A review focusing on practical applications. *Arab. J. Chem.* 13 (12), 9243–9269. doi:10.1016/j.arabjc.2020.11.009
- Feng, G., Sun, B., and Li, T. Z. (2015). Daidzein attenuates lipopolysaccharide-induced acute lung injury via toll-like receptor 4/NF- $\kappa$ B pathway. *Int. Immunopharmacol.* 26 (2), 392–400. doi:10.1016/j.intimp.2015.04.002
- Fideles, L. D., de Miranda, J. A. L., Martins, C. D., Barbosa, M. L. L., Pimenta, H. B., Pimentel, P. V. D., et al. (2020). Role of rutin in 5-fluorouracil-induced intestinal mucositis: Prevention of histological damage and reduction of inflammation and oxidative stress. *Molecules* 25 (12), 2786. doi:10.3390/molecules25122786
- Fu, Y. H., Hu, X. Y., Cao, Y. G., Zhang, Z. C., and Zhang, N. S. (2015). Saikosaponin A inhibits lipopolysaccharide-oxidative stress and inflammation in human umbilical vein endothelial cells via preventing TLR4 translocation into lipid rafts. *Free Radic. Biol. Med.* 89, 777–785. doi:10.1016/j.freeradbiomed.2015.10.407
- Ganeshpurkar, A., and Saluja, A. K. (2017). The pharmacological potential of rutin. *Saudi Pharm. J.* 25 (2), 149–164. doi:10.1016/j.jsps.2016.04.025
- Gong, L., Wang, C., Zhou, H., Ma, C., Li, Y., Peng, C., et al. (2021). A review of pharmacological and pharmacokinetic properties of forsythiaside A. *Pharmacol. Res.* 169, 105690. doi:10.1016/j.phrs.2021.105690
- Hewlings, S. J., and Kalman, D. S. (2017). Curcumin: A review of its effects on human health. *Foods* 6 (10), 92. doi:10.3390/foods6100092
- Huang, X. X., Ke, K., Jin, W. W., Zhu, Q. R., Zhu, Q. C., Mei, R. Y., et al. (2022). Identification of genes related to 5-fluorouracil based chemotherapy for colorectal cancer. *Front. Immunol.* 13, 887048. doi:10.3389/fimmu.2022.887048
- Ikarashi, N., Kon, R., and Sugiyama, K. (2016). Aquaporins in the colon as a new therapeutic target in diarrhea and constipation. *Int. J. Mol. Sci.* 17 (7), 1172. doi:10.3390/ijms17071172
- Jin, S. Z., Guan, T. X., Wang, S., Hu, M. X., Liu, X. Y., Huang, S. Q., et al. (2022). Dioscin alleviates cisplatin-induced mucositis in rats by modulating gut microbiota, enhancing intestinal barrier function and attenuating TLR4/NF- $\kappa$ B signaling cascade. *Int. J. Mol. Sci.* 23 (8), 4431. doi:10.3390/ijms23084431
- Kawashima, R., Kawakami, F., Maekawa, T., Yamamoto, H., Koizumi, W., and Ichikawa, T. (2015). Elemental diet moderates 5-fluorouracil-induced gastrointestinal mucositis through mucus barrier alteration. *Cancer Chemother. Pharmacol.* 76 (2), 269–277. doi:10.1007/s00280-015-2790-z
- Ke, X., Hu, G. H., Fang, W. Y., Chen, J. T., Zhang, X., Yang, C. B., et al. (2015). Qing Hua Chang Yin inhibits the LPS-induced activation of the IL-6/STAT3 signaling pathway in human intestinal Caco-2 cells. *Int. J. Mol. Med.* 35 (4), 1133–1137. doi:10.3892/ijmm.2015.2083
- Khokhlova, E. V., Smeianov, V. V., Efimov, B. A., Kafarskaia, L. I., Pavlova, S. I., and Shkoporov, A. N. (2012). Anti-inflammatory properties of intestinal bifidobacterium strains isolated from healthy infants. *Microbiol. Immunol.* 56 (1), 27–39. doi:10.1111/j.1348-0421.2011.00398.x
- Kishore, V., Yarla, N. S., Bishayee, A., Putta, S., Malla, R., Neelapu, N. R. R., et al. (2017). Multi-targeting andrographolide and its natural analogs as potential therapeutic agents. *Curr. Top. Med. Chem.* 17 (8), 845–857. doi:10.2174/1568026616666160927150452
- Kissow, H. (2015). Glucagon-like peptides 1 and 2: Intestinal hormones implicated in the pathophysiology of mucositis. *Curr. Opin. Support. Palliat. Care* 9 (2), 196–202. doi:10.1097/SPC.0000000000000132
- Kumar, A., EkavaliChopra, K., Mukherjee, M., Pottabathini, R., and Dhull, D. K. (2015). Current knowledge and pharmacological profile of berberine: An update. *Eur. J. Pharmacol.* 761, 288–297. doi:10.1016/j.ejphar.2015.05.068
- Lang, W. Y., Cheng, M., Zheng, X., Zhao, Y. P., Qu, Y. L., Jia, Z., et al. (2022). Forsythiaside A alleviates methotrexate-induced intestinal mucositis in rats by modulating the NLRP3 signaling pathways. *Int. Immunopharmacol.* 103, 108466. doi:10.1016/j.intimp.2021.108466



- Lee, H. S., Lee, J., Smolensky, D., and Lee, S. H. (2020). Potential benefits of patchouli alcohol in prevention of human diseases: A mechanistic review. *Int. Immunopharmacol.* 89 (A), 107056. doi:10.1016/j.intimp.2020.107056
- Lei, W. R., Liu, D. X., Sun, M., Lu, C. X., Yang, W. W., Wang, C. Y., et al. (2021). Targeting STAT3: A crucial modulator of sepsis. *J. Cell. Physiol.* 236 (11), 7814–7831. doi:10.1002/jcp.30394
- Li, C. L., Ai, G. X., Wang, Y. F., Lu, Q., Luo, C. D., Tan, L. H., et al. (2020). Oxyberberine, a novel gut microbiota-mediated metabolite of berberine, possesses superior anti-colitis effect: Impact on intestinal epithelial barrier, gut microbiota profile and TLR4-MyD88-NF-kappa B pathway. *Pharmacol. Res.* 152, 104603. doi:10.1016/j.phrs.2019.104603
- Li, H. L., Lu, L., Wang, X. S., Qin, L. Y., Wang, P., Qiu, S. P., et al. (2017). Alteration of gut microbiota and inflammatory cytokine/chemokine profiles in 5-fluorouracil induced intestinal mucositis. *Front. Cell. Infect. Microbiol.* 7, 455. doi:10.3389/fcimb.2017.00455
- Li, H. Y., Gao, C. D., Liu, C., Liu, L. J., Zhuang, J., Yang, J., et al. (2021). A review of the biological activity and pharmacology of cryptotanshinone, an important active constituent in Danshen. *Biomed. Pharmacother.* 137, 111332. doi:10.1016/j.biopha.2021.111332
- Li, Y., Yao, J. Y., Han, C. Y., Yang, J. X., Chaudhry, M. T., Wang, S. N., et al. (2016). Quercetin, inflammation and immunity. *Nutrients* 8 (3), 167. doi:10.3390/nu8030167
- Lin, N., Xu, L. F., and Sun, M. (2013). The protective effect of trefoil factor 3 on the intestinal tight junction barrier is mediated by toll-like receptor 2 via a pi3k/akt dependent mechanism. *Biochem. Biophys. Res. Commun.* 440 (1), 143–149. doi:10.1016/j.bbrc.2013.09.049
- Liu, X. N., Li, H. M., Wang, S. P., Zhang, J. Z., and Liu, D. L. (2021). Sesquiterpene lactones of *Aucklandia lappa*: Pharmacology, pharmacokinetics, toxicity, and structure-activity relationship. *Chin. Herb. Med.* 13 (2), 167–176. doi:10.1016/j.chmed.2020.11.005
- Lotfi, M., Kazemi, S., Shirafkan, F., Hosseinzadeh, R., Ebrahimpour, A., Barary, M., et al. (2021). The protective effects of quercetin nano-emulsion on intestinal mucositis induced by 5-fluorouracil in mice. *Biochem. Biophys. Res. Commun.* 585, 75–81. doi:10.1016/j.bbrc.2021.11.005
- Luqman, S., and Pezzuto, J. M. (2010). NFkappaB: A promising target for natural products in cancer chemoprevention. *Phytother. Res.* 24 (7), 949–963. doi:10.1002/ptr.3171
- Mi, H., Dong, Y., Zhang, B., Wang, H. N., Peter, C. C. K., Gao, P., et al. (2017). Bifidobacterium infantis ameliorates chemotherapy-induced intestinal mucositis via regulating T cell immunity in colorectal cancer rats. *Cell. Physiol. Biochem.* 42 (6), 2330–2341. doi:10.1159/000480005
- Miknevicius, P., Zulpaitė, R., Leber, B., Strupas, K., Stiegler, P., and Schemmer, P. (2021). The impact of probiotics on intestinal mucositis during chemotherapy for colorectal cancer: A comprehensive review of animal studies. *Int. J. Mol. Sci.* 22 (17), 9347. doi:10.3390/ijms22179347
- Panwar, S., Sharma, S., and Tripathi, P. (2021). Role of barrier integrity and dysfunctions in maintaining the healthy gut and their health outcomes. *Front. Physiol.* 12, 715611. doi:10.3389/fphys.2021.715611
- Prisciandaro, L. D., Geier, M. S., Butler, R. N., Cummins, A. G., and Howarth, G. S. (2011). Evidence supporting the use of probiotics for the prevention and treatment of chemotherapy-induced intestinal mucositis. *Crit. Rev. Food Sci. Nutr.* 51 (3), 239–247. doi:10.1080/10408390903551747
- Reinke, D., Kritas, S., Polychronopoulos, P., Skaltsounis, A. L., Aliagannis, N., and Tran, C. D. (2015). Herbal substance, acteoside, alleviates intestinal mucositis in mice. *Gastroenterol. Res. Pract.* 2015, 327872. doi:10.1155/2015/327872
- Ribeiro, R. A., Wanderley, C. W. S., Wong, D. V. T., Mota, J. M. S. C., Leite, C. A. V. G., Souza, M. H. L. P., et al. (2016). Irinotecan- and 5-fluorouracil-induced intestinal mucositis: Insights into pathogenesis and therapeutic perspectives. *Cancer Chemother. Pharmacol.* 78 (5), 881–893. doi:10.1007/s00280-016-3139-y
- Sharifi-Rad, M., Varoni, E. M., Iriti, M., Martorell, M., Setzer, W. N., Contreras, M. D., et al. (2018). Carvacrol and human health: A comprehensive review. *Phytother. Res.* 32 (9), 1675–1687. doi:10.1002/ptr.6103
- Silveira, N., Sandjo, L. P., and Biavatti, M. W. (2018). Spilanthal-containing products: A patent review (1996–2016). *Trends Food Sci. Technol.* 74, 107–111. doi:10.1016/j.tifs.2018.02.012
- Skamrahl, M., Pang, H. T., Ferle, M., Gottwald, J., Rubeling, A., Maraschini, R., et al. (2021). Tight junction ZO proteins maintain tissue fluidity, ensuring efficient collective cell migration. *Adv. Sci.* 8 (19), 2100478. doi:10.1002/adv.202100478
- Sougiannis, A. T., VanderVeen, B. N., Davis, J. M., Fan, D. P., and Murphy, E. A. (2021). Understanding chemotherapy-induced intestinal mucositis and strategies to improve gut resilience. *Am. J. Physiol. Gastrointest. Liver Physiol.* 320 (5), G712–G719. doi:10.1152/ajpgi.00380.2020
- Sukhotnik, I., Moati, D., Shaoul, R., Loberman, B., Pollak, Y., and Schwartz, B. (2018). Quercetin prevents small intestinal damage and enhances intestinal recovery during methotrexate-induced intestinal mucositis of rats. *Food Nutr. Res.* 62, 1327. doi:10.29219/fnr.v62.1327
- Swamy, M. K., and Sinniah, U. R. (2015). A comprehensive review on the phytochemical constituents and pharmacological activities of *Pogostemon cablin* Benth.: An aromatic medicinal plant of industrial importance. *Molecules* 20 (5), 8521–8547. doi:10.3390/molecules20058521
- Takeuchi, O., and Akira, S. (2002). MyD88 as a bottle neck in Toll/IL-1 signaling. *Curr. Top. Microbiol. Immunol.* 270, 155–167. doi:10.1007/978-3-642-59430-4\_10
- Tanaka, H., Takechi, M., Kiyonari, H., Shioi, G., Tamura, A., and Tsukita, S. (2015). Intestinal deletion of Claudin-7 enhances paracellular organic solute flux and initiates colonic inflammation in mice. *Gut* 64 (10), 1529–1538. doi:10.1136/gutjnl-2014-308419
- Tappenden, K. A. (2008). Inflammation and intestinal function: Where does it start and what does it mean? *JPEN. J. Parenter. Enter. Nutr.* 32 (6), 648–650. doi:10.1177/0148607108325177
- Thorpe, D., Butler, R., Sultani, M., Vanhoecke, B., and Stringer, A. (2020). Irinotecan-induced mucositis is associated with goblet cell dysregulation and neural cell damage in a tumour bearing DA rat model. *Pathol. Oncol. Res.* 26 (2), 955–965. doi:10.1007/s12253-019-00644-x
- Tooley, K. L., Howarth, G. S., and Butler, R. N. (2009). Mucositis and non-invasive markers of small intestinal function. *Cancer Biol. Ther.* 8 (9), 753–758. doi:10.4161/cbt.8.9.8232
- van Vliet, M. J., Harmsen, H. J. M., de Bont, E. S. J. M., and Tissing, W. J. E. (2010). The role of intestinal microbiota in the development and severity of chemotherapy-induced mucositis. *PLoS Pathog.* 6 (5), e1000879. doi:10.1371/journal.ppat.1000879
- Varankovich, N. V., Nickerson, M. T., and Korber, D. R. (2015). Probiotic-based strategies for therapeutic and prophylactic use against multiple gastrointestinal diseases. *Front. Microbiol.* 6, 685. doi:10.3389/fmicb.2015.00685
- Wang, J., Zhao, H., Lv, K., Zhao, W., Zhang, N., Yang, F., et al. (2021a). Pterostilbene ameliorates DSS-induced intestinal epithelial barrier loss in mice via suppression of the NF-kappa B-mediated MLCK-MLC signaling pathway. *J. Agric. Food Chem.* 69 (13), 3871–3878. doi:10.1021/acs.jafc.1c00274
- Wang, L., Song, B. H., Hu, Y., Chen, J., Zhang, S. S., Chen, D. P., et al. (2021b). Puerarin ameliorates 5-fluorouracil-induced intestinal mucositis in mice by inhibiting JAKs. *J. Pharmacol. Exp. Ther.* 379 (2), 147–155. doi:10.1124/jpet.121.000677
- Wang, L., Wang, R., Wei, G. Y., Wang, S. M., and Du, G. H. (2020a). Dihydrotanshinone attenuates chemotherapy-induced intestinal mucositis and alters fecal microbiota in mice. *Biomed. Pharmacother.* 128, 110262. doi:10.1016/j.biopha.2020.110262
- Wang, L., Wang, R., Wei, G. Y., Wang, S. M., and Du, G. H. (2020b2020). Study on the therapeutic effects and mechanism of cryptotanshinone on mice with chemotherapy-induced mucositis. *Acta Pharm. Sin.* 55 (8), 1801–1811.
- Wang, R., Wang, L., Wei, G. Y., Liu, N. N., Zhang, L., Wang, S. M., et al. (2020c2020). The effect and mechanism of baicalein on regulating gut microbiota and improving chemotherapy-induced intestinal mucositis in mice. *Acta Pharm. Sin.* 55 (5), 868–876.
- Wang, X. Y., Zhang, B., Lu, Y., Xu, L., Wang, Y. J., Cai, B. Y., et al. (2021). RNA-seq and *in vitro* experiments reveal the protective effect of curcumin against 5-fluorouracil-induced intestinal mucositis via IL-6/STAT3 signaling pathway. *J. Immunol. Res.* 2021, 8286189. doi:10.1155/2021/8286189
- Wang, Y. Y., Wei, B., Wang, D. P., Wu, J. J., Gao, J. H., Zhong, H. Q., et al. (2022). DNA damage repair promotion in colonic epithelial cells by andrographolide downregulated cGAS-STING pathway activation and contributed to the relief of CPT-11-induced intestinal mucositis. *Acta Pharm. Sin. B* 12 (1), 262–273. doi:10.1016/j.japsb.2021.03.043
- Wright, T. H., Yazbeck, R., Lymn, K. A., Whitford, E. J., Cheah, K. Y., Butler, R. N., et al. (2009). The herbal extract, Iberogast, improves jejunal integrity in rats with 5-Fluorouracil (5-FU)-induced mucositis. *Cancer Biol. Ther.* 8 (10), 923–929. doi:10.4161/cbt.8.10.8146
- Wu, J. Z., Gan, Y. X., Li, M. X., Chen, L. P., Liang, J. L., Zhuo, J. Y., et al. (2020). Patchouli alcohol attenuates 5-fluorouracil-induced intestinal mucositis via TLR2/MyD88/NF-kB pathway and regulation of microbiota. *Biomed. Pharmacother.* 124, 109883. doi:10.1016/j.biopha.2020.109883
- Wu, J. Z., Gan, Y. X., Luo, H. J., Xu, N., Chen, L. P., Li, M. Y., et al. (2021).  $\beta$ -Patchoulene ameliorates water transport and the mucus barrier in 5-fluorouracil-induced intestinal mucositis rats via the cAMP/PKA/CREB signaling pathway. *Front. Pharmacol.* 12, 689491. doi:10.3389/fphar.2021.689491
- Wu, Y. P., Zhu, C., Chen, Z., Chen, Z. J., Zhang, W. N., Ma, X. Y., et al. (2016). Protective effects of *Lactobacillus plantarum* on epithelial barrier disruption caused



by enterotoxigenic *Escherichia coli* in intestinal porcine epithelial cells. *Vet. Immunol. Immunopathol.* 172, 55–63. doi:10.1016/j.vetimm.2016.03.005

Xiang, D. C., Yang, J. Y., Xu, Y. J., Zhang, S., Li, M., Zhu, C., et al. (2020). Protective effect of andrographolide on 5-Fu induced intestinal mucositis by regulating p38 MAPK signaling pathway. *Life Sci.* 252, 117612. doi:10.1016/j.lfs.2020.117612

Xiong, Y. J., Deng, Z. B., Liu, J. N., Qiu, J. J., Guo, L., Feng, P. P., et al. (2019). Enhancement of epithelial cell autophagy induced by sinensetin alleviates epithelial barrier dysfunction in colitis. *Pharmacol. Res.* 148, 104461. doi:10.1016/j.phrs.2019.104461

Yeung, C. Y., Chiau, J. S. C., Cheng, M. L., Chan, W. T., Chang, S. W., Chang, Y. H., et al. (2020). Modulations of probiotics on gut microbiota in a 5-fluorouracil-induced mouse model of mucositis. *J. Gastroenterol. Hepatol.* 35 (5), 806–814. doi:10.1111/jgh.14890

Yoneda, J., Nishikawa, S., and Kurihara, S. (2021). Oral administration of cystine and theanine attenuates 5-fluorouracil-induced intestinal mucositis and diarrhea by suppressing both glutathione level decrease and ROS production in the small intestine of mucositis mouse model. *BMC Cancer* 21 (1), 1343. doi:10.1186/s12885-021-09057-z

Yue, B., Gao, R. Y., Lv, C., Yu, Z. L., Wang, H., Geng, X. L., et al. (2021). Berberine improves irinotecan-induced intestinal mucositis without impairing the anti-colorectal cancer efficacy of irinotecan by inhibiting

bacterial beta-glucuronidase. *Front. Pharmacol.* 12, 774560. doi:10.3389/fphar.2021.774560

Zeeshan, M., Atiq, A., Ul Ain, Q., Ali, J., Khan, S., and Ali, H. (2021). Evaluating the mucoprotective effects of glycyrrhizic acid-loaded polymeric nanoparticles in a murine model of 5-fluorouracil-induced intestinal mucositis via suppression of inflammatory mediators and oxidative stress. *Inflammopharmacology* 29 (5), 1539–1553. doi:10.1007/s10787-021-00866-z

Zhang, L. (2019). Pharmacokinetics and drug delivery systems for puerarin, a bioactive flavone from traditional Chinese medicine. *Drug Deliv.* 26 (1), 860–869. doi:10.1080/10717544.2019.1660732

Zhang, X. J., Yuan, Z. W., Qu, C., Yu, X. T., Huang, T., Chen, P. V., et al. (2018). Palmatine ameliorated murine colitis by suppressing tryptophan metabolism and regulating gut microbiota. *Pharmacol. Res.* 137, 34–46. doi:10.1016/j.phrs.2018.09.010

Zhang, X., Wan, Y., Feng, J., Li, M., and Jiang, Z. (2021). Involvement of TLR2/4-MyD88-NF-kappa B signaling pathway in the pathogenesis of intracranial aneurysm. *Mol. Med. Rep.* 23 (4), 230. doi:10.3892/mmr.2021.11869

Zhao, Q., and Maynard, C. L. (2022). Mucus, commensals, and the immune system. *Gut Microbes* 14 (1), 2041342. doi:10.1080/19490976.2022.2041342

Zhou, Y. Q., Zhu, J. L., Shao, L. Y., and Guo, M. M. (2020). Current advances in acteoside biosynthesis pathway elucidation and biosynthesis. *Fitoterapia* 142, 104495. doi:10.1016/j.fitote.2020.104495

## Glossary

<b>AQP3</b> aquaporin 3	<b>MPO</b> myeloperoxidase
<b>CAT</b> catalase	<b>MT</b> metallothionein
<b>CBL</b> live combined bifidobacterium	<b>NF-<math>\kappa</math>B</b> nuclear factor kappa-B
<b>C-Casp</b> cleaved caspase	<b>NE</b> neutrophil elastase
<b>CG</b> cathepsin G	<b>NO<sub>x</sub></b> nitrogen oxide
<b>COX-2</b> cyclooxygenase-2	<b>NPSH</b> non-protein sulfhydryl
<b>CPT-11</b> irinotecan hydrochloride	<b>Nrf2</b> nuclear factor erythroid 2-related factor 2
<b>CREB</b> element-binding protein	<b>PCNA</b> proliferating cell nuclear antigen
<b>DAI</b> disease activity index	<b>p-ERK</b> phosphorylated extracellular signal-related kinase
<b>DAO</b> diamine oxidase	<b>p-IRF3</b> phosphorylated interferon regulatory factor 3
<b>DMSO</b> dimethylsulfoxide	<b>PGE2</b> prostaglandin E2
<b>5-FU</b> 5-fluorouracil	<b>p-JNK</b> phosphorylated c-Jun N terminal kinase
<b>GPx</b> glutathione peroxidase	<b>PKA</b> protein kinase A
<b>GSH</b> glutathione	<b>Pr3</b> proteinase 3
<b>GST</b> glutathione S-transferase	<b>p-STAT3</b> phosphorylated signal transducer and activator of transcription
<b>GUS</b> $\beta$ -glucuronidase	<b>p-TBK1</b> phosphorylated TANK-binding kinase 1
<b>HIF-1<math>\alpha</math></b> hypoxia-inducing factor 1 $\alpha$	<b>p-TYK</b> phosphorylated TYK
<b>HO-1</b> hemoxygenase-1	<b>ROS</b> reactive oxygen species
<b>IFN</b> interferon	<b>SD</b> Sprague–Dawley
<b>iNOS</b> inducible nitric oxide synthase	<b>SOCS3</b> suppressor of cytokine signaling 3
<b>IL</b> interleukin	<b>SOD</b> superoxide dismutase
<b>JAK</b> janus kinase	<b>STAT3</b> signal transducers and activators of transcription 3
<b>KC</b> keratinocyte chemoattractant	<b>TBARS</b> thiobarbituric acid reactive substances
<b>LOOH</b> lipid hydroperoxides	<b>TC</b> total cholesterol
<b>LPS</b> lipopolysaccharide	<b>TG</b> triglyceride
<b>MAPK</b> mitogen-activated protein kinase	<b>TJ</b> tight junction
<b>MASCC/ISO</b> mucositis study group of the multinational association of supportive care in cancer/international society of oral oncology	<b>TNF</b> tumor necrosis factor
<b>MDA</b> malondialdehyde	<b>TRPA1</b> transient receptor potential cation channel, subfamily A, member 1
<b>MLC</b> myosin light chain	<b>TYK</b> tyrosine kinase
<b>MLCK</b> myosin light chain kinase	<b>Tyr</b> tyrosinase
	<b>ZO-1</b> zonula occludens



## OPEN ACCESS

## EDITED BY

Mariana Jinga,  
Carol Davila University of Medicine and  
Pharmacy, Romania

## REVIEWED BY

Luiz Jardelino De Lacerda Neto,  
Federal University of Campina Grande,  
Brazil  
Seifollah Bahramikia,  
Lorestan University, Iran

## \*CORRESPONDENCE

Liangru Zhu,  
zhuliangru@hust.edu.cn

<sup>†</sup>These authors have contributed equally  
to this work

## SPECIALTY SECTION

This article was submitted to  
Gastrointestinal and Hepatic  
Pharmacology,  
a section of the journal  
Frontiers in Pharmacology

RECEIVED 08 July 2022

ACCEPTED 07 September 2022

PUBLISHED 23 September 2022

## CITATION

Li J, Ling F, Guo D, Zhao J, Cheng L,  
Chen Y, Xu M and Zhu L (2022), The  
efficacy of mesalazine on nonspecific  
terminal ileal ulcers: A randomized  
controlled trial.  
*Front. Pharmacol.* 13:989654.  
doi: 10.3389/fphar.2022.989654

## COPYRIGHT

© 2022 Li, Ling, Guo, Zhao, Cheng,  
Chen, Xu and Zhu. This is an open-  
access article distributed under the  
terms of the [Creative Commons  
Attribution License \(CC BY\)](https://creativecommons.org/licenses/by/4.0/). The use,  
distribution or reproduction in other  
forums is permitted, provided the  
original author(s) and the copyright  
owner(s) are credited and that the  
original publication in this journal is  
cited, in accordance with accepted  
academic practice. No use, distribution  
or reproduction is permitted which does  
not comply with these terms.

# The efficacy of mesalazine on nonspecific terminal ileal ulcers: A randomized controlled trial

Junrong Li<sup>1†</sup>, Fangmei Ling<sup>1†</sup>, Di Guo<sup>2</sup>, Jinfang Zhao<sup>3</sup>,  
Ling Cheng<sup>4</sup>, Yidong Chen<sup>1</sup>, Mingyang Xu<sup>1</sup> and Liangru Zhu<sup>1\*</sup>

<sup>1</sup>Division of Gastroenterology, Union Hospital, Tongji Medical College, Huazhong University of Science and Technology, Wuhan, China, <sup>2</sup>Department of Geriatrics, Wuhan Central Hospital, Wuhan, China, <sup>3</sup>Center for Life Sciences, Tsinghua University, Beijing, China, <sup>4</sup>Department of Gastroenterology, The First Peoples Hospital of Nanyang City, Henan, China

**Background:** Nonspecific terminal ileal ulcers are one of the common ulcerative diseases in terminal ileum. However, the studies about treatment efficacy are scarce. We aimed to investigate the efficacy of mesalazine in the treatment of this disease.

**Methods:** Eighty-two patients with nonspecific terminal ileal ulcers who sought outpatient medical treatment in the Division of Gastroenterology, Wuhan Union Hospital, from April 2016 to January 2019 were enrolled and randomly divided into two groups. The experimental group took mesalazine orally, 4.0 g/d, once a day for 3 months. The control group was followed up without special intervention. The primary endpoint was the endoscopic remission rate at the 6<sup>th</sup> and 12<sup>th</sup> month. Secondary endpoints included the clinical remission rate at the 1<sup>st</sup>, 6<sup>th</sup> and 12<sup>th</sup> month and adverse events (ChiCTR1900027503).

**Results:** About the endoscopic efficacy, the remission rate of the experimental group and control group was 73.2 versus 61.0% at the 6<sup>th</sup> month (RR = 1.20, 95% CI 0.88~1.63,  $p = 0.24$ ) and 87.8 versus 78.0% at the 12<sup>th</sup> month (RR = 1.13, 95% CI 0.92~1.37,  $p = 0.24$ ). About the clinical efficacy, the remission rate was 70.3 versus 43.8% at the 1<sup>st</sup> month (RR = 1.61, 95%CI 1.03~2.51,  $p = 0.03$ ), 83.8 versus 68.8% at the 6<sup>th</sup> month (RR = 1.22, 95%CI 0.93~1.60,  $p = 0.14$ ) and 91.9 versus 81.3% at the 12<sup>th</sup> month (RR = 1.13, 95%CI 0.93~1.37,  $p = 0.34$ ). During follow-up, no patients were diagnosed with Crohn's disease or intestinal tuberculosis, and no patients developed significant complications.

**Conclusion:** For patients with nonspecific terminal ileal ulcers, there is no disease progression over a short term. In addition, there is no significant difference in clinical or endoscopic efficacy between patients who received mesalazine and patients who are followed up without special intervention.

## KEYWORDS

randomized controlled trial, nonspecific ulcers, terminal ileum, mesalazine, efficacy

## 1 Introduction

In recent years, due to the deepening awareness in intestinal diseases, the wide application of endoscopy, capsule endoscopy and other endoscopic techniques, and the improvement in endoscopic surgical and diagnostic skills, the detection rate and diagnosis rate of terminal ileal ulcers have been significantly improved (Jeong et al., 2008; Greaves and Pochapin, 2006; Courville et al., 2009). The terminal ileum is a common site for small intestinal lesions. Crohn's disease (CD), intestinal tuberculosis (ITB), nonsteroid anti-inflammatory drug (NSAID)-related enteropathy and nonspecific terminal ileal ulcers are common ulcerative diseases occurring at the end of ileum (Goulart et al., 2016). Nonspecific terminal ileal ulcers are a chronic ulcerative disease located in the terminal ileum. The understanding of this disease is still incomplete, such as the pathogenesis, clinical characteristics, diagnosis and treatment, and they need to be further studied. A study showed that there were no specific gastrointestinal symptoms or signs in patients with nonspecific terminal ileal ulcers, which were thus easily ignored by clinicians. Some patients even had no obvious clinical manifestations, and ulcers were found during routine endoscopic examinations (Kim et al., 2021). Currently, there is no standard treatment for patients with nonspecific terminal ileal ulcers (Karnam et al., 2001).

Mesalazine, also known chemically as 5-aminosalicylic acid (5-ASA), is commonly used in the treatment of ulcerative colitis (UC). Mesalazine exerts an anti-inflammatory effect on the intestinal wall after taken orally. Because of the anti-ulcer and antioxidant efficacy, mesalazine is not only used in the treatment of UC, but also in other diseases (Beiranvand, 2021). A research showed that mesalazine significantly attenuated NSAID-induced mucosal injury in patients with small bowel enteropathy (Rácz et al., 2013). In addition, a recent study showed that 5-ASA also exerted ameliorative and protective effects on ethanolic gastric ulcers in experimental rats by strengthening the antioxidant defense system of gastric mucosal cells (Beiranvand and Bahramikia, 2020). Relevant studies revealed that mesalazine yielded mild adverse reactions and was a relatively safe drug (Klotz, 2012). Therefore, mesalazine might be an effective and safe drug for nonspecific terminal ileal ulcers. At present, the relevant studies are scarce. Mesalazine was used in the treatment of patients with nonspecific small intestinal ulcers in a study and showed that the patient symptoms improved to varying degrees. However, the disappearance of ulcers in patients was not associated with the use of mesalazine (Wang et al., 2011). Based on the above background, this study focused on the clinical and endoscopic efficacy of mesalazine in treating patients with nonspecific terminal ileal ulcers and analyzed the clinical, endoscopic and histopathological characteristics of the disease. The primary endpoint was the endoscopic

remission rate at the 6<sup>th</sup> and 12<sup>th</sup> month. The secondary endpoints were clinical remission rate at the 1<sup>st</sup>, 6<sup>th</sup> and 12<sup>th</sup> month and adverse events.

## 2 Materials and methods

### 2.1 Study design

This was an observer-blinded, prospective randomized-controlled trial. The study was approved by the Ethics Committee of Tongji Medical College, Huazhong University of Science and Technology, Ethics No. 2018-S (493), and was registered on the Chinese Clinical Trial Registry website with the registration number of ChiCTR1900027503. The sample size was calculated according to the remission rate from the previous studies and experience before our study. The remission rate in the experimental group and control group was anticipated to be 90 and 65%, respectively. The estimated sample size was 32 patients per group with a risk of 0.05 and a power of 0.80, using PASS 15.0 software. Considering 20% dropout, at least 40 subjects in each group were needed in this study.

### 2.2 Study subjects

A total of 86 patients with nonspecific terminal ileal ulcers sought outpatient medical treatment in the Division of Gastroenterology, Union Hospital, Tongji Medical College, Huazhong University of Science and Technology from April 2016 to January 2019, among whom 4 patients under 18 years old were excluded. The remaining 82 patients were randomly assigned into either the experimental group or the control group by computer-generated randomization. In the experimental group, 41 patients were given mesalazine tablets orally at 4.0 g/d, and once a day for 3 months (drug manufacturer: FERRING INTERNATIONAL CENTER SA, Import Drug Registration No. H20181183). Forty-one cases in the control group were observed and followed up without special intervention, and a light diet was highlighted in both groups.

### 2.3 Inclusion and exclusion criteria

Inclusion criteria: ① Patients signed their informed consent voluntarily; ② >18 years old, no limitation on sex; ③ Endoscopy revealed ulcers in the terminal ileum or terminal ileitis, with no limitations on size or number of ulcers; ④ No ulcers were found in other parts of the intestinal tract by computed tomography enterography (CTE), magnetic resonance enterography (MRE) or capsule endoscopy within 1 month. ⑤ Pulmonary computed tomography (CT) imaging, purified protein derivative (PPD),

T-cell spot test (T-SPOT) and tuberculosis antibody results were normal; ⑥ The patients tested negative for cytomegalovirus DNA and Epstein-Barr virus DNA; ⑦ Histopathology showed nonspecific ulcers, and the surrounding mucosa showed nonspecific inflammatory changes, with no granulomas or crypts change.

Exclusion criteria: ① Patients with ulcerative disease in terminal ileum such as CD, ITB, ischemic enteropathy, infectious (bacterial, viral, fungal) enteritis, and eosinophilic enteritis; ② Patients with characteristics of CD such as fistulas, perianal lesions, skip lesions under endoscopy or imaging, longitudinal/cobblestone appearance ulcers, transmural inflammation or non-caseating granuloma. ③ Patients with caseating granuloma or positive stain/culture for acid fast-bacillus. ④ Patients who received NSAIDs, potassium chloride tablets, diuretics or herbal remedy in the last 6 months; ⑤ Patients with previous abdominal surgery; ⑥ Patients with digestive system tumors; ⑦ Patients who were pregnant or lactating; ⑧ Patients who were allergic to salicylic acid drugs.

## 2.4 Follow-up and outcomes

The primary endpoint was the endoscopic remission rate at the 6<sup>th</sup> and 12<sup>th</sup> month. Secondary endpoints included the clinical remission rate at the 1<sup>st</sup>, 6<sup>th</sup> and 12<sup>th</sup> month and adverse events. All patients were followed up for 12 months. If symptoms disappeared completely and no related complications occurred, then the clinical efficacy was determined to be cured. If symptoms improved without affecting the patients' daily life or work, then the clinical efficacy was determined to be improved. If there was no improvement or symptoms were aggravated, then the clinical efficacy was determined to be ineffective. Endoscopy images were read by two experienced endoscopists who did not know about the grouping of patients. If there were no erosions, ulcers, congestion or edema in the terminal ileum mucosa, then it was determined to be cured. If the lesions were fewer or smaller, they were considered to be improved. If the endoscopic appearance was not improved or even worse, the treatment was deemed ineffective. Remission rate equaled cured rate plus improved rate.

## 2.5 Statistical analysis

Statistical analysis was performed using SPSS 23.0. For numerical data, those conforming to a normal distribution were expressed as the mean  $\pm$  standard deviation. Those conforming to a skewed distribution were represented by the median. A t test was used for data conforming to a normal distribution, and a nonparametric test was used for comparisons between groups for data conforming to a skewed distribution.

Categorical variables were presented as the number and percentage of patients and were analyzed by the chi-square test or Fisher's exact test. Results were expressed as risk ratios (RR) with 95% confidence intervals (CI).  $P < 0.05$  was considered statistically significant.

## 3 Results

Eighty-two patients were finally enrolled, including 52 males (63.4%) and 30 females (36.6%), with an average age of  $42.84 \pm 12.73$  years (range, 18~70) and a median course of 24 months (range, 1~312). The baseline characteristics were compared in Table 1.

The clinical manifestations included abdominal pain in 47 cases (57.3%), diarrhea in 15 cases (18.3%), abdominal distension in 15 cases (18.3%), shapeless stools in 13 cases (15.9%), constipation in 7 cases (8.5%), bloody stools in 6 cases (7.3%), tenesmus in 3 cases (3.7%) and mucous stools in 3 cases (3.7%). Thirteen patients (15.9%) had no obvious clinical manifestations. Clinical manifestations were shown in Figure 1.

Endoscopic manifestations included ulcers or erosions, with hyperemia and edema in the terminal ileum mucosa (one representative case was shown in Figure 2). In addition, the size of ulcers were  $\leq 5$  mm in 80 patients (97.6%), multiple in 71 cases (86.6%) and superficial in 79 cases (96.3%). The endoscopic features including ulcer size, number and depth were shown in Figures 3A–C, respectively.

In this study, the histopathological manifestations revealed chronic inflammatory changes in the terminal ileum mucosal tissues, which may be accompanied by lymphoproliferative tissues. and there were no granulomatous lesions or crypts change (one representative case was shown in Figure 4).

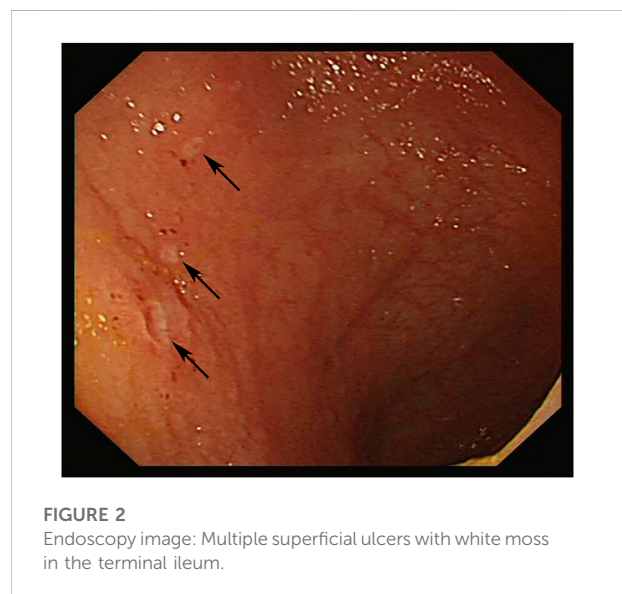
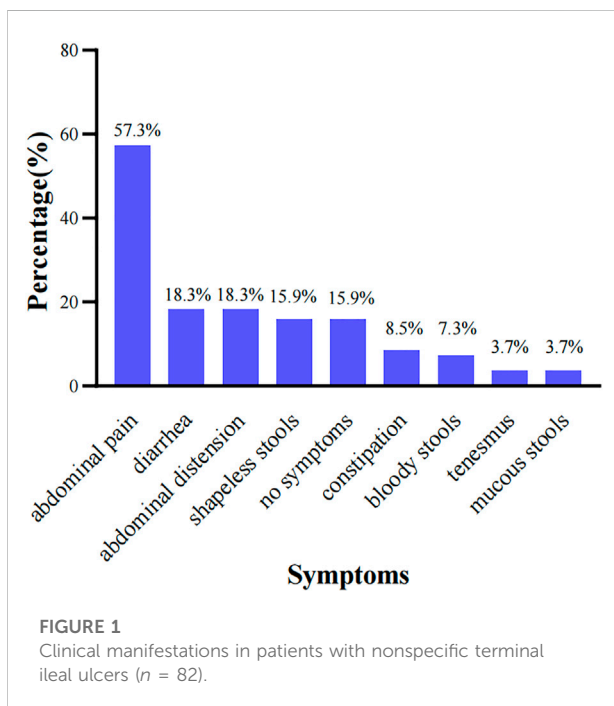
### 3.1 Primary outcome

At the 6<sup>th</sup> month, 8 cases were cured, 22 cases were improved, 11 cases were ineffective, and the endoscopic remission rate was 73.2% in the experimental group. In the control group, 7 cases were cured, 18 cases were improved, 16 cases were ineffective, and the endoscopic remission rate was 61.0%. There was no statistically significant difference in endoscopic efficacy (RR = 1.20, 95%CI 0.88~1.63,  $p = 0.24$ ). At the 12<sup>th</sup> month, 9 cases were cured, 27 were improved, 5 were ineffective, and the endoscopic remission rate was 87.8% in the experimental group. In the control group, 10 cases were cured, 22 were improved, 9 were ineffective, and the endoscopic remission rate was 78.0%. There was no statistically significant difference in endoscopic efficacy (RR = 1.13, 95% CI 0.92~1.37,  $p = 0.24$ ). The comparison of endoscopic efficacy between two groups was shown in Table 2.



TABLE 1 Baseline features of the patients, compared between 2 groups.

Patients		Experimental group	Control group	<i>p</i>
Male-female ratio		1.93:1	1.56:1	0.65
Average age (years)		43.71 ± 13.44	41.98 ± 12.08	0.54
Median course (months)		12	24	0.06
Smoking	current	10	7	0.71
	past	5	6	
	never	26	28	
Drinking	current	12	11	0.47
	past	2	0	
	never	27	30	
Clinical manifestations	abdominal pain	26	21	0.65
	diarrhea	6	9	
	abdominal distension	9	6	
	shapeless stools	6	7	
	constipation	2	5	
	bloody stools	4	2	
	tenesmus	1	2	
	mucous stools	1	2	
	no symptoms	4	9	

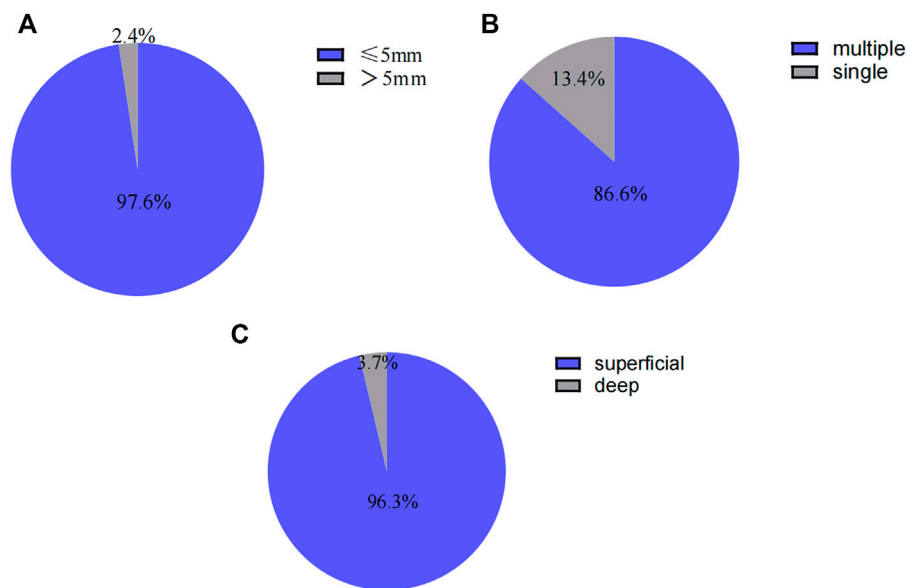


## 3.2 Secondary outcomes

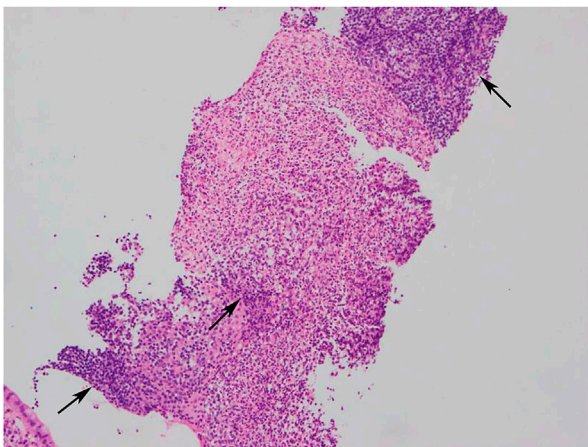
### 3.2.1 Clinical remission rate

There were no obvious clinical manifestations in 13 patients (4 in the experimental group and 9 in the control group), so they

were not included in the clinical efficacy evaluation. In the experimental group, 7 cases were cured, 19 cases were improved, 11 cases were ineffective, and the clinical remission rate was 70.3% at the 1<sup>st</sup> month. In the control group, 5 cases were cured, 9 cases were improved, 18 cases were ineffective, and the clinical remission rate was 43.8% at the 1<sup>st</sup> month. The difference in clinical efficacy between the two groups was statistically significant (RR = 1.61, 95%CI 1.03~2.51, *p* = 0.03). At the 6<sup>th</sup> month in the experimental group, 9 patients were cured, 22 were

**FIGURE 3**

(A) Endoscopic features in patients with nonspecific terminal ileal ulcers (ulcer size). (B) Endoscopic features in patients with nonspecific terminal ileal ulcers (ulcer number). (C) Endoscopic features in patients with nonspecific terminal ileal ulcers (ulcer depth).

**FIGURE 4**

Histopathology image (HEX100): Chronic inflammatory changes in mucosal tissues, lymphocytic infiltration and numerous inflammatory cells exudation and necrosis.

improved, and 6 had ineffective treatment, and the clinical remission rate was 83.8%. In the control group, 6 cases were cured, 16 cases were improved, 10 cases were ineffective, and the clinical remission rate was 68.8%. There was no statistically significant difference in clinical efficacy (RR = 1.22, 95%CI 0.93~1.60,  $p = 0.14$ ). At the 12<sup>th</sup> month, 11 patients in the experimental group were cured, 23 were improved, 3 had

ineffective treatment, and the clinical remission rate was 91.9%. In the control group, 8 cases were cured, 18 cases were improved, 6 cases were ineffective, and the clinical remission rate was 81.3%. There was no statistically significant difference in clinical efficacy between the two groups (RR = 1.13, 95%CI 0.93~1.37,  $p = 0.34$ ) as shown in Table 3.

### 3.2.2 Adverse events

In the experimental group, only 2 patients showed slight abdominal distension and nausea, respectively, which was not serious enough to stop the medication.

## 4 Discussion

Nowadays, terminal ileal ulcers are increasingly common under endoscopy. A study included 1497 patients who underwent ileocolonoscopy, and found that 74 patients (5.0%) had terminal ileal ulcers (Mehta et al., 2017). Terminal ileal ulcers may be caused by a wide variety of diseases, including CD, NSAID, ITB, eosinophilic enteritis and so on (Dilauro and Crum-Cianflone, 2010). In addition, there are a significant part of patients with nonspecific terminal ileal ulcers. For example, in the previously mentioned study, about 40% of 74 patients were diagnosed with this disease (Mehta et al., 2017). Nonspecific terminal ileal ulcers are a nonspecific ulcer of the small intestine that occurs in the terminal ileum and does not involve the rest part of the small intestine or the upper

TABLE 2 Endoscopic efficacy comparison of the patients between 2 groups ( $n = 82$ ).

Follow-up	Groups	Remission rate (%)		Ineffective rate (%)	$p$	RR (95%CI)
		Cured rate (%)	Improved rate (%)			
6 <sup>th</sup> month	Experimental group	8 (19.5)	22 (53.7)	11 (26.8)	0.24	1.20 (0.88~1.63)
	Control group	7 (17.1)	18 (43.9)	16 (39.0)		
12 <sup>th</sup> month	Experimental group	9 (22.0)	27 (65.9)	5 (12.2)	0.24	1.13 (0.92~1.37)
	Control group	10 (24.4)	22 (53.7)	9 (22.0)		

TABLE 3 Clinical efficacy comparison of the patients between 2 groups ( $n = 69$ ).

Follow-up	Groups	Remission rate (%)		Ineffective rate (%)	$p$	RR (95%CI)
		Cured rate (%)	Improved rate (%)			
1 <sup>st</sup> month	Experimental group	7 (18.9)	19 (51.4)	11 (29.7)	0.03	1.61 (1.03~2.51)
	Control group	5 (15.6)	9 (28.1)	18 (56.3)		
6 <sup>th</sup> month	Experimental group	9 (24.3)	22 (59.5)	6 (16.2)	0.14	1.22 (0.93~1.60)
	Control group	6 (18.8)	16 (50.0)	10 (31.3)		
12 <sup>th</sup> month	Experimental group	11 (29.7)	23 (62.2)	3 (8.1)	0.34	1.13 (0.93~1.37)
	Control group	8 (25.0)	18 (56.3)	6 (18.8)		

digestive tract, which pathogenesis is still unclear. Due to the long disease course, some patients were misdiagnosed as functional bowel disease before being diagnosed with nonspecific terminal ileal ulcers (Wang et al., 2011).

A study showed that the common clinical manifestations of patients with nonspecific terminal ileal ulcers included abdominal pain, diarrhea, abdominal distension, constipation and bloody stools. Besides, fever and weight loss were less common than patients with CD and ITB (Kedia et al., 2016). In this study, most patients presented with abdominal pain, diarrhea, abdominal distension, shapeless stools, constipation or bloody stools, and no patients presented with fever or significant weight loss, which was consistent with the previous study (Zhong et al., 2020). The endoscopic manifestations included multiple, superficial and small ulcers without intestinal stricture or malformation. Histopathological manifestations revealed nonspecific inflammation, without granulomas, eosinophil infiltration or viral inclusions. In addition, the endoscopic manifestations were not always parallel to the clinical manifestations, and there were no new clinical manifestations or complications such as intestinal perforation or intestinal obstruction during a follow-up period of 7 years (Wang et al., 2011). Therefore, it was suggested in some studies that routine biopsy was not required for patients with

terminal ileal ulcers who did not consider the diagnosis of IBD (Velidedeoğlu et al., 2015). In this study, 82 patients presented with nonspecific endoscopic and histopathological manifestations, with a benign disease course, which was basically consistent with other related studies.

No effective medications are validated for the treatment of nonspecific terminal ileal ulcers, and symptomatic treatment is the main choice in clinical. A study indicated that the symptoms and endoscopic manifestations in some patients could be improved to varying degrees when they were observed and followed up without medications (Kim et al., 2021). Mesalazine has been used in the treatment of UC since the 1940s, and is currently a commonly used medication for mild to moderate UC (Chibba and Moss, 2020). It was reported that the mechanisms of action may include blocking the production of proinflammatory factors, downregulating the production of anti-angiogenic factors and promoting the healing of intestinal epithelial wounds (MacDermott, 2000; Desreumaux and Ghosh, 2006; Lyakhovich and Gasche, 2010). The adverse reactions of mesalazine are minor and generally well tolerated in patients of different age groups, without dose-related side effects (Sehgal et al., 2018; Cuffari et al., 2016). Therefore, mesalazine may be an effective medication for the treatment of nonspecific terminal ileal ulcers. However, the related studies

are scarce, and especially randomized controlled trials about mesalazine in the treatment of nonspecific terminal ileal ulcers are currently lacking. There was a study in which 2 patients with nonspecific small intestinal ulcers were treated orally with symptomatic treatment including mesalazine, and their symptoms improved to varying degrees, but the ulcers persisted or recurred (Wang et al., 2011). In our study, among 41 patients treated with mesalazine, 30 cases (73.2%) and 36 cases (87.8%) achieved endoscopic remission at the 6<sup>th</sup> and 12<sup>th</sup> month, respectively, which was not significantly different from 25 cases (61.0%) and 32 cases (78.0%) in the control group. Similarly, there was no significant difference in clinical remission rate at the 6<sup>th</sup> and 12<sup>th</sup> month between two groups. Therefore, regular follow-up without medications might be a better choice for patients with nonspecific terminal ileal ulcers in clinical practice.

There were several advantages in our study. Firstly, this is the first research to focus on the clinical and endoscopic efficacy of mesalazine in treating patients with nonspecific terminal ileal ulcers. And our study was a prospective randomized controlled trial, with accurate data and small bias. In addition, repeated clinical and endoscopic follow-up within 12 months demonstrated the prognosis of patients in different periods, as well as the efficacy of mesalazine compared with the control. However, our study also has the following limitations: insufficient patient enrollment and follow-up period; the endoscopic remission rate at the 1<sup>st</sup> month could not be analyzed because most patients were reluctant to undergo the preparation process for colonoscopy. Besides, patients in the control group received no drugs, and it is obvious for them to know the grouping, so psychological factors cannot be ruled out for the results. Multi-center, large-scale and long-term prospective randomized controlled trials are needed for further study.

## 5 Conclusion

Common clinical manifestations in patients with nonspecific terminal ileal ulcers include abdominal pain, diarrhea, abdominal distension, constipation and bloody stools, and about 16% of patients have no obvious clinical manifestations. Endoscopic manifestations include ulcers or erosions, with hyperemia and edema in the terminal ileum mucosa. Histopathology shows chronic inflammatory changes in the terminal ileum mucosal tissues. No new symptoms or intestinal complications occurs during the 12-month follow-up. In addition, there is no significant difference in clinical or endoscopic efficacy between patients who receive mesalazine and patients who are followed up without special intervention, which needs to be further explored in future clinical studies.

## Data availability statement

The original contributions presented in the study are included in the article/supplementary material, further inquiries can be directed to the corresponding author.

## Ethics statement

The studies involving human participants were reviewed and approved by the Ethics Committee of Tongji Medical College, Huazhong University of Science and Technology. The patients/participants provided their written informed consent to participate in this study. Written informed consent was obtained from the individual(s) for the publication of any potentially identifiable images or data included in this article.

## Author contributions

JL and FL contributed to patient follow-up and completed the article; DG, JZ, LC, YC, and MX contributed to information collection and data analysis; LZ designed the study and provided critical review of the manuscript. All authors read and approved the final manuscript.

## Funding

The study was supported by the National Key R&D Program of China (2018YFC0114600) and National Natural Science Foundation of China (No. 82170547 and No.81873558).

## Conflict of interest

The authors declare that the research was conducted in the absence of any commercial or financial relationships that could be construed as a potential conflict of interest.

## Publisher's note

All claims expressed in this article are solely those of the authors and do not necessarily represent those of their affiliated organizations, or those of the publisher, the editors and the reviewers. Any product that may be evaluated in this article, or claim that may be made by its manufacturer, is not guaranteed or endorsed by the publisher.

## References

- Beiranvand, M. (2021). A review of the biological and pharmacological activities of mesalazine or 5-aminosalicylic acid (5-ASA): An anti-ulcer and anti-oxidant drug. *Inflammopharmacology* 29 (5), 1279–1290. doi:10.1007/s10787-021-00856-1
- Beiranvand, M., and Bahramikia, S. (2020). Ameliorating and protective effects mesalazine on ethanol-induced gastric ulcers in experimental rats. *Eur. J. Pharmacol.* 888, 173573. doi:10.1016/j.ejphar.2020.173573
- Chibbar, R., and Moss, A. C. (2020). Mesalamine in the initial therapy of ulcerative colitis. *Gastroenterol. Clin. North Am.* 49 (4), 689–704. doi:10.1016/j.gtc.2020.07.002
- Courville, E. L., Siegel, C. A., Vay, T., Wilcox, A. R., Suriawinata, A. A., and Srivastava, A. (2009). Isolated asymptomatic ileitis does not progress to overt Crohn disease on long-term follow-up despite features of chronicity in ileal biopsies. *Am. J. Surg. Pathol.* 33 (9), 1341–1347. doi:10.1097/PAS.0b013e3181ad25b6
- Cuffari, C., Pierce, D., Korczowski, B., Fyderek, K., Van Heusen, H., and Hossack, S. (2016). Randomized clinical trial: Pharmacokinetics and safety of multimatrix mesalazine for treatment of pediatric ulcerative colitis. *Drug Des. devel. Ther.* 10, 593–607. doi:10.2147/DDDT.S95316
- Desreumaux, P., and Ghosh, S. (2006). Review article: Mode of action and delivery of 5-aminosalicylic acid - new evidence. *Aliment. Pharmacol. Ther.* 24, 2–9. doi:10.1111/j.1365-2036.2006.03069.x
- Dilauro, S., and Cianflone, N. F. C. (2010). Ileitis: When it is not Crohn's disease. *Curr. Gastroenterol. Rep.* 12 (4), 249–258. doi:10.1007/s11894-010-0112-5
- Goulart, R. A., Barbalho, S. M., Gasparini, R. G., and de Carvalho, A. C. (2016). Facing terminal ileitis: Going beyond Crohn's disease. *Gastroenterol. Res.* 9 (1), 1–9. doi:10.14740/gr698w
- Greaves, M. L., and Pochapin, M. (2006). Asymptomatic ileitis: Past, present, and future. *J. Clin. Gastroenterol.* 40 (4), 281–285. doi:10.1097/01.mcg.0000210104.59370.66
- Jeong, S. H., Lee, K. J., Kim, Y. B., Kwon, H. C., Sin, S. J., and Chung, J. Y. (2008). Diagnostic value of terminal ileum intubation during colonoscopy. *J. Gastroenterol. Hepatol.* 23 (1), 51–55. doi:10.1111/j.1440-1746.2007.05151.x
- Karnam, U. S., Rosen, C. M., and Raskin, J. B. (2001). Small bowel ulcers. *Curr. Treat. Options Gastroenterol.* 4 (1), 15–21. doi:10.1007/s11938-001-0043-1
- Kedia, S., Kurrey, L., Pratap Mouli, V., Dhingra, R., Srivastava, S., and Pradhan, R. (2016). Frequency, natural course and clinical significance of symptomatic terminal ileitis. *J. Dig. Dis.* 17 (1), 36–43. doi:10.1111/1751-2980.12307
- Kim, J. H., Lee, J. Y., Park, Y. E., Lee, J. H., Park, J., and Kim, T. O. (2021). Clinical course of terminal ileal ulcers observed incidentally during colonoscopy. *Dig. Dis. Sci.* 66 (12), 4423–4428. doi:10.1007/s10620-020-06781-7
- Klotz, U. (2012). The pharmacological profile and clinical use of mesalazine (5-aminosalicylic acid). *Arzneimittelforschung.* 62 (2), 53–58. doi:10.1055/s-0031-1299685
- Lyakhovich, A., and Gasche, C. (2010). Systematic review: Molecular chemoprevention of colorectal malignancy by mesalazine. *Aliment. Pharmacol. Ther.* 31 (2), 202–209. doi:10.1111/j.1365-2036.2009.04195.x
- MacDermott, R. P. (2000). Progress in understanding the mechanisms of action of 5-aminosalicylic acid. *Am. J. Gastroenterol.* 95 (12), 3343–3345. doi:10.1111/j.1572-0241.2000.03342.x
- Mehta, V., Gupta, A., Mahajan, R., Narang, V., Midha, V., and Sood, N. (2017). Symptomatic isolated terminal ileal ulcers: Etiology and clinical significance. *Endosc. Int. Open* 5 (7), E539–E546. doi:10.1055/s-0043-100688
- Rácz, I., Szalai, M., Kovács, V., Regőczy, H., Kiss, G., and Horváth, Z. (2013). Mucosal healing effect of mesalazine granules in naproxen-induced small bowel enteropathy. *World J. Gastroenterol.* 19 (6), 889–896. doi:10.3748/wjg.v19.i6.889
- Sehgal, P., Colombel, J. F., Aboubakr, A., and Narula, N. (2018). Systematic review: Safety of mesalazine in ulcerative colitis. *Aliment. Pharmacol. Ther.* 47 (12), 1597–1609. doi:10.1111/apt.14688
- Velidedeoglu, M., Enes Ankan, A., Zengin, A. K., ArikAn, A. E., and Zengin, A. K. (2015). Diagnostic value of terminal ileum biopsies in patients with abnormal terminal ileum mucosal appearance. *Ulus. Cerrahi Derg.* 31 (3), 152–156. doi:10.5152/UCD.2015.2756
- Wang, W., Wang, Z., Yang, Y., Linghu, E., and Lu, Z. (2011). Long-term follow-up of nonspecific small bowel ulcers with a benign course and no requirement for surgery: Is this a distinct group? *BMC Gastroenterol.* 11, 51. doi:10.1186/1471-230X-11-51
- Zhong, Q., Zhang, A., Huang, J., Yan, W., Lin, J., and Huang, Q. (2020). Analysis and follow up of endoscopy results in 1099 patients with terminal ileum lesions. *Can. J. Gastroenterol. Hepatol.* 2020, 8838613. doi:10.1155/2020/8838613





## OPEN ACCESS

## EDITED BY

Maria Dimitrova,  
Medical University Sofia, Bulgaria

## REVIEWED BY

Silvio Terra Stefanello,  
Institut für Physiologie II, Germany  
Milton Prabu,  
Annamalai University, India  
Giovanna Baron,  
University of Milan, Italy  
Laiba Arshad,  
Forman Christian College, Pakistan  
Enilton A Camargo,  
Federal University of Sergipe, Brazil

## \*CORRESPONDENCE

R E. Akhigbe,  
akhigberoland@gmail.com

## SPECIALTY SECTION

This article was submitted to  
Gastrointestinal and Hepatic  
Pharmacology,  
a section of the journal  
Frontiers in Pharmacology

RECEIVED 07 July 2022

ACCEPTED 05 September 2022

PUBLISHED 23 September 2022

## CITATION

Afolabi OA, Akhigbe TM, Akhigbe RE,  
Alabi BA, Gbolagun OT, Taiwo ME,  
Fakeye OO and Yusuf EO (2022),  
Methanolic *Moringa oleifera* leaf extract  
protects against epithelial barrier  
damage and enteric bacterial  
translocation in intestinal I/R: Possible  
role of caspase 3.  
*Front. Pharmacol.* 13:989023.  
doi: 10.3389/fphar.2022.989023

## COPYRIGHT

© 2022 Afolabi, Akhigbe, Akhigbe, Alabi,  
Gbolagun, Taiwo, Fakeye and Yusuf.  
This is an open-access article  
distributed under the terms of the  
Creative Commons Attribution License  
(CC BY). The use, distribution or  
reproduction in other forums is  
permitted, provided the original  
author(s) and the copyright owner(s) are  
credited and that the original  
publication in this journal is cited, in  
accordance with accepted academic  
practice. No use, distribution or  
reproduction is permitted which does  
not comply with these terms.

# Methanolic *Moringa oleifera* leaf extract protects against epithelial barrier damage and enteric bacterial translocation in intestinal I/R: Possible role of caspase 3

O A. Afolabi<sup>1</sup>, T M. Akhigbe<sup>2,3</sup>, R E. Akhigbe<sup>1,3\*</sup>, B A. Alabi<sup>4</sup>,  
O T. Gbolagun<sup>1</sup>, M E. Taiwo<sup>1</sup>, O O. Fakeye<sup>1</sup> and E O. Yusuf<sup>1</sup>

<sup>1</sup>Department of Physiology, Ladoké Akintola University of Technology, Ogbomoso, Oyo, Nigeria,

<sup>2</sup>Department of Agronomy, Osun State University, Osogbo, Osun, Nigeria, <sup>3</sup>Reproductive Biology and Toxicology Research Laboratory, Oasis of Grace Hospital, Osogbo, Osun, Nigeria, <sup>4</sup>Department of Pharmacology, Bowen University, Ogbomoso, Nigeria

**Background:** Activation of caspase 3 has been implicated in the pathogenesis of I/R injury in various organs, but there is a paucity of data on its role in IIRI. Also, no reports were found on the beneficial role of methanolic *Moringa oleifera* leaf extract (MMOLE) in IIRI. This study investigated the involvement of caspase 3 in IIRI, and the impact of MMOLE in IIRI.

**Methods:** Male Wistar rats were randomized into five groups; the sham-operated group that was sham-operated and received 0.5 ml of distilled water for 7 days prior to sham surgery, and the IIRI, februxostat (FEB) +IIRI, low dose MMOLE (LDMO)+IIRI, and high dose MMOLE (HDMO)+IIRI groups that underwent I/R and also received 0.5 ml of distilled water, 10 mg/kg of februxostat, 200 mg/kg of MMOLE, and 400 mg/kg of MMOLE respectively for 7 days prior to I/R. Markers of hepatic function, oxidative stress, and inflammation as well as enteric bacterial translocation and histoarchitecture integrity of intestinal and hepatic tissues were evaluated. The bioactive components of MMOLE were also determined by GC-MS.

**Results:** As revealed by GC-MS, the active bioactive components of MMOLE were thiosemicarbazone, hydrazine, 1,3-dioxolane, octanoic acid, 1,3-

**Abbreviations:** AST, aspartate transaminase; ALT, alanine transferase; Caspase 3, cysteine-aspartic protease 3; EMB, eosin-methylene blue; GC-MS, Gas chromatography-mass spectrophotometric; GGT, gamma-glutamyl transferase; GPx, glutathione peroxidase; GSH, reduced glutathione; Hb, haematocrit count; IL-6, interleukin-6; IR, ischaemia/reperfusion; IIRI, intestinal ischaemia/reperfusion injury; LDH, lactate dehydrogenase; MCCA, Mac Conkey agar; MCHC, mean corpuscular haemoglobin concentration; MCV, mean corpuscular volume; MDA, malondialdehyde; MODS, multiple organ dysfunction syndrome; MPO, myeloperoxidase; NA, nutrient agar; NF- $\kappa$ B, nuclear factor kappa-light-chain-enhancer of activated B cells; PCV, packed cell volume; RBC, red blood cell count; ROS, reactive oxygen species; WBC, white blood cell count; SIRS, systemic inflammatory response syndrome (SIRS); SOD, superoxide dismutase; TNF- $\alpha$ , tumour necrotic factor- $\alpha$ .

benzenediamine, 9-octadecenoic acid, oleic acid, nonadecanoic acid, 3-undecanone, phosphonic acid, and cyclopentanecarboxylic acid. MMOLE alleviated IIRI-induced rise in intestinal and hepatic injury markers, malondialdehyde, TNF- $\alpha$ , IL-6, and myeloperoxidase activities. MMOLE improved IIRI-induced suppression of reduced glutathione, thiol and non-thiol proteins, and superoxide dismutase, catalase and glutathione peroxidase activities. These were associated with suppression of IIRI-induced caspase 3 activity and bacterial translocation. Histopathological evaluation revealed that MMOLE attenuated IIRI-induced alterations in intestinal and hepatic histoarchitecture integrity. MMOLE also militated against increased absolute and relative intestinal and hepatic weight, intestinal and hepatic injuries, epithelial mucosal barrier dysfunction, and enteric bacterial translocation associated with IIRI by downregulating oxidative stress-mediated activation of caspase 3.

**Conclusion:** IIRI is associated with a rise in caspase 3 activity. Also, MMOLE confers protection against IIRI, possibly due to its constituent bioactive molecules, especially hydrazine, 9-octadecenoic acid, 1,3-dioxolane, oleic acid, and nonadecanoic acid.

#### KEYWORDS

Apoptosis, bacterial translocation, hepatic function, inflammation, ischaemia/reperfusion, *Moringa oleifera*, oxidative stress, torsion/detorsion

## 1 Introduction

Intestinal ischaemia/reperfusion injury (IIRI) is a life-threatening condition with high morbidity and mortality. It is associated with several pathologies such as small bowel transplantation, septic shock, cardiopulmonary resuscitation, and mesenteric artery embolization (Wen et al., 2020). IIRI involves a series of pathological events stimulated by abrupt disruption of blood flow and subsequent establishment of blood flow, leading to increased generation of reactive oxygen species (ROS), inflammation, and apoptosis (Liu et al., 2020). This cascade of events alters the integrity of the intestinal mucosal barrier, thus facilitating bacterial translocation (BT) and the release of endotoxins into the liver and eventually into the systemic circulation to affect remote organs such as the lungs and the kidneys (Park et al., 1990; Kubes, 1993). This may eventually culminate in systemic inflammatory response syndrome (SIRS), multiple organ dysfunction (MODS), and multiple organ failure (MOF) (Feng et al., 2017).

Although the mechanisms associated with IIRI and BT is yet to be fully understood, it has been demonstrated that oxidative stress (an imbalance between ROS generation and scavenging) (Akhigbe and Ajayi, 2021) and pro-inflammatory cytokines play a key role (Mallick et al., 2004). Hence, the use of antioxidants with anti-inflammatory activities, such as *M. oleifera*, may be useful in the management of IIRI and its attendant complications.

*M. oleifera*, a member of the family Moringaceae popularly called drumstick, is a small to medium sized tree that is about 10–15 m high and is widely cultivated in Asia, West Indies, South America, and Nigeria (Sreelatha and Padma, 2009). In Nigeria, it is known by different names; 'Okwe oyibo' in Igbo, 'Gawara' or 'Habiwal' in Hausa and 'Adagba maloye' or 'Ewe Igbale' in Yoruba. Studies have shown that various parts of the plant (especially the leaves, seeds and roots) have medicinal value. *Moringa oleifera* has been demonstrated to possess analgesic, antipyretic, anti-diabetic, and hypotensive properties (Saka et al., 2020). It has also been reported to exert antioxidant (Charoensin, 2014; Saka et al., 2020), anti-inflammatory (Cheenpracha et al., 2010), and antimicrobial/antibacterial (Rahman et al., 2009) activities. Although various parts of the plants exert these activities, the leaves have been reported to be commonly used due to its wide range of beneficial biological activities (Xu et al., 2019). The biological activities of *Moringa oleifera* have been attributed to its phytochemical constituents, viz. carotenoids, vitamins, minerals, amino acids, saponins, terpenoid, sterols, glycosides, alkaloids, flavonoids, tannins, anthraquinones, and phenolics (Siddhuraju and Becker, 2003; Anwar et al., 2007; Saka et al., 2020). Although, reports on the effect of *Moringa oleifera* on caspase 3-mediated apoptosis are scarce, it is likely that *Moringa oleifera*-mediated maintenance of redox balance and modulation of cytokines suppresses caspase 3 activity. Thus, we speculated that *Moringa oleifera* prevents IIRI-induced hepato-intestinal injury and BT by inhibiting oxidative stress, inflammation, and apoptosis.

Therefore, this study evaluated the effect of methanolic *Moringa oleifera* leaf extract (MMOLE) in IIRI and IIRI-induced BT, and also confirmed whether or not suppression of oxidative stress, inflammation, and caspase 3-mediated apoptosis mediate the effect of MMOLE in IIRI.

## 2 Materials and methods

### 2.1 Plant collection

Fresh leaves of *M. oleifera* were harvested at California area, Ogbomoso, Oyo State, Nigeria (8.1333°N, 4.2356°E). Plants were collected monthly throughout year 2020 and mixed together to avoid the influence of seasonal variation. The plant was identified and authenticated by Dr. Mrs. Ogundola of the Botany Unit, Department of Pure and Applied Biology, Ladoke Akintola University of Technology, Ogbomoso. The name of the botanical was confirmed on <http://www.theplantlist.org> (accessed on 20 July 2021). A voucher specimen, LHO 616, was obtained and kept in the Herbarium at the Department of Botany, Ladoke Akintola University of Technology, Ogbomoso, Nigeria.

### 2.2 Preparation of plant extract

Methanolic *M. oleifera* leaf extract (MMOLE) was made as earlier reported (Sofowora, 1993; Ogundola et al., 2021). Fresh leaves of *Moringa oleifera* were air-dried for 2 weeks and pulverized using electric blender. About 500 g of the obtained sample was soaked in 70% methanol for 72 h (3 days). After 3 days, the samples were filtered with muslin paper to separate the residue from the filtrate. The filtrate was then poured inside the round bottom flask of the Soxhlet apparatus and heated for 1 hour at 60°C, then poured inside a beaker and placed in a water bath for concentration at 100°C for 24 h. The obtained yield was 11.72%.

### 2.3 Gas chromatography-mass spectrophotometric analysis

The constituent bioactive molecules of methanolic *M. oleifera* leaf extract were identified by gas chromatography-mass spectrophotometric (GC-MS) analysis following established methods (Mamza et al., 2012). The database of National Institute of Standard and Technology (NIST) was employed in interpreting the mass spectrum of GC-MS to ascertain the name, molecular weight and structure of the obtained bioactive molecules.

## 2.4 Experimental animals

The present study was conducted in the animal house of the Department of Physiology, Ladoke Akintola University of Technology, Ogbomoso, Nigeria. Ethical approval was obtained from the Ethics Review Committee of the Faculty of Basic Medical Sciences of the institution. Fifty adult male Wistar rats of similar weight ( $190 \pm 5$  g) were used for this study. Animals were allowed to feed on standard rat chow and drink water ad libitum. Animals were humanely cared for in accordance with the guidelines for the care and use of laboratory animals as published by the US National Institutes of Health (NIH Publication No. 85-23, revised 1996).

## 2.5 Experimental design

Animals were allowed to acclimatize for 2 weeks, and then randomized into five groups ( $n = 10$ ). The sham group was sham-operated and received 0.5 ml of distilled water for 7 days prior to the sham operation, while the IIRI, febuxostat (FEB) +IIRI, low dose methanolic *Moringa oleifera* leaf extract (LDMO)+IIRI, and high dose methanolic *Moringa oleifera* leaf extract (HDMO)+IIRI groups underwent I/R procedure. In addition to the I/R procedure, IIRI, FEB + IIRI, LDMO + IIRI, and HDMO + IIRI received 0.5 ml of distilled water, 10 mg/kg of febuxostat, 200 mg/kg of methanolic *M. oleifera* leaf extract, and 400 mg/kg of methanolic *M. oleifera* leaf extract respectively for 7 days prior to I/R procedure. Febuxostat was used as a standard control drug with anti-inflammatory and antioxidant properties that protect against I/R injury (Tsuda et al., 2012; Saban-Ruiz et al., 2013). The drugs were administered *via* gavage. The doses of febuxostat (Khames et al., 2017) and *M. oleifera* (Kirisattayakul et al., 2013) were as previously reported.

IIRI was induced as previously reported (Yildiz et al., 2009) with some modifications. Animals were weighed and anesthetized with 10 mg/kg of Xylazine and 50 mg/kg of Ketamine. The abdomen was cleaned with 10% povidone iodine, a ventral midline incision was made on the abdomen and the intestine was mobilised. About Five 5 cm of the ileum was measured proximally from the ilio-cecal junction and a further 5 cm measured proximal to the first 5 cm. The most proximal 5 cm of ileum was folded on itself and twisted 720°clockwise. The twisted ileum was then anchored to the anterior abdominal wall by placing a 3-0 chromic suture round it and through the avascular part of the mesentery. The abdomen was then closed lightly with 3-0 chromic suture after which the animal was left for 45 minutes. At the expiration of the 45 min of ischemia, the abdomen was reopened. Loss of pulsation was observed to confirm that ischemia has occurred. Reperfusion was induced by reopening the abdomen, untwisting the ileum and closing the abdomen again. The animals were then left for 24 h.

## 2.6 Sacrifice and tissue collection

After 24 h of reperfusion, animals were euthanized, blood was obtained via retro-orbital vein, and the reperused intestine and liver were immediately harvested, and weighed after separating adhering structures. The relative intestinal weight was determined as the weight of the intestine divided by the body weight multiplied by 100, while the relative hepatic weight was determined as the weight of the liver divided by the body weight multiplied by 100.

Portions of the intestinal and hepatic tissues were homogenized in appropriate volume of cold phosphate buffer saline using a glass homogenizer. The homogenates were centrifuged at 10,000 g for 15 min in cold centrifuge at 4°C to obtain the supernatant fractions.

Also, portions of the intestinal and hepatic tissues were obtained and fixed in 10% formalin-phosphate-buffered saline at 4°C overnight for histopathological examination.

## 2.7 Biochemical analyses

### 2.7.1 Haematological indices

A drop of blood was used to prepare a peripheral blood smear. The peripheral blood smear was stained with modified Wright Geimsa using an automated slide stainer (Hematek, Miles, Elkhart, IN). The peripheral blood smear was used to determine red blood cell count (RBC), platelet count, and white blood cell count (WBC) and differentials. The remaining blood sample was subjected to complete/full blood count analysis with an automated hematology instrument (Abbott Cell-Dyn 3500 Hematology Analyzer, Abbott Labs, Abbott Park, IL) for haematocrit (Hb), packed cell volume (PCV), mean corpuscular volume (MCV), mean corpuscular haemoglobin concentration (MCHC), platelet count and differential white blood cell counts for lymphocytes, and granulocytes.

### 2.7.2 Tissue injury markers

The activities of aspartate transaminase (AST), alanine transferase (ALT), and gamma-glutamyl transferase (GGT) in the intestinal and hepatic tissue were assayed by spectrophotometry as previously reported (Saka et al., 2011).

### 2.7.3 Markers of oxidative stress and antioxidant levels

The intestinal and hepatic concentrations of malondialdehyde (MDA) and reduced glutathione (GSH) (Akhigbe et al., 2021), and the activities of superoxide dismutase (SOD), catalase, and glutathione peroxidase (GPx) (Hamed et al., 2021; Hamed et al., 2022) in the intestinal and hepatic tissues were assayed by spectrophotometry as previously

reported. Thiol and non-thiol proteins were assayed by colorimetry as earlier reported (Jocelyn, 1987; Hu, 1994).

### 2.7.4 Markers of inflammation

Myeloperoxidase (MPO) activities in the intestinal and hepatic tissues were determined by colorimetric methods as earlier documented (Hamed et al., 2021). The intestinal and hepatic levels of tumour necrotic factor- $\alpha$  (TNF- $\alpha$ ) and interleukin-6 (IL-6) were determined using ELISA kits (Elabscience Biotechnology Inc., United States) according to the manufacturers' guidelines.

### 2.7.5 Marker of apoptosis

The activities of caspase 3 in the intestinal and hepatic tissues were assayed using ELISA kits (Elabscience Biotechnology Inc., United States) according to the manufacturers' guidelines.

## 2.8 Microbiological analysis

Bacterial translocation was determined as previously reported (Ozkan et al., 2009) under strict sterile conditions. Briefly, some portions of the intestinal and hepatic tissues were cut into pieces with a sterile blade and added to 1 ml of Mueller-Hinton Broth. The samples were homogenized and about 100  $\mu$ l of each sample was inoculated into nutrient agar (NA), eosin-methylene blue (EMB), and Mac Conkey agar (MCCA) for colony counts. The cultures were incubated for 48 h and observed for the presence of growth under either aerobic or anaerobic conditions.

## 2.9 Histopathological analysis

Formalin-phosphate-buffered saline-fixed intestinal and hepatic tissues were dehydrated and embedded in paraffin wax. About 5  $\mu$ m thick sections were cut and stained with hematoxylin-eosin and examined under light microscope by two pathologists who were blinded to the study protocol. Photomicrographs were taken at  $\times 100$  and  $\times 400$  magnifications.

Intestinal (Chiu et al., 1970) and hepatic (Eckhoff et al., 2002) histomorphological damage was scored using the Chiu and Eckhoff's score respectively. The mean values for each variable obtained by both pathologists were used as the values of the variables.

The digital photomicrographs obtained were imported into ImageJ Software (NIH, Bethesda, MD, United States) with specific plugins for quantification. The villus height and crypt depth were determined by two experts. The mean values for each variable obtained by both experts were used as the values of the variables.

TABLE 1 Effect of intestinal ischaemia/reperfusion (I/R) and methanolic *Moringa oleifera* leaf extract on full blood count.

	Sham	IIRI	FEB + IIRI	LDMO + IIRI	HDMO + IIRI
RBC ( $\times 10^{12}/L$ )	6.66 $\pm$ 0.29	7.44 $\pm$ 0.64 <sup>a</sup>	7.52 $\pm$ 0.64 <sup>a</sup>	8.34 $\pm$ 0.20 <sup>a,b,c</sup>	7.47 $\pm$ 0.12 <sup>a,d</sup>
Hb (g/dl)	13.02 $\pm$ 0.68	14.78 $\pm$ 0.41 <sup>a</sup>	14.22 $\pm$ 0.48 <sup>a</sup>	16.08 $\pm$ 0.52 <sup>a,b,c</sup>	14.84 $\pm$ 0.29 <sup>a,d</sup>
PCV (%)	36.4 $\pm$ 1.67	39.90 $\pm$ 0.68 <sup>a</sup>	38.74 $\pm$ 1.36 <sup>a</sup>	41.24 $\pm$ 0.60 <sup>a,c</sup>	42.48 $\pm$ 0.77 <sup>a,b,c</sup>
MCV (fL)	54.69 $\pm$ 1.16	53.73 $\pm$ 0.65	54.30 $\pm$ 1.52	57.50 $\pm$ 0.86 <sup>a,b,c</sup>	54.24 $\pm$ 0.89 <sup>d</sup>
MCHC (g/L)	345.20 $\pm$ 12.74	354.80 $\pm$ 3.39	362.80 $\pm$ 7.43 <sup>a</sup>	359.60 $\pm$ 6.60 <sup>a</sup>	366.20 $\pm$ 3.74 <sup>a</sup>
WBC ( $10^9/L$ )	9.87 $\pm$ 0.30	13.03 $\pm$ 1.14 <sup>a</sup>	5.12 $\pm$ 0.56 <sup>a,b</sup>	8.28 $\pm$ 0.74 <sup>a,b,c</sup>	8.24 $\pm$ 0.79 <sup>a,b,c</sup>
Lymphocytes (%)	74.74 $\pm$ 1.45	61.90 $\pm$ 1.74 <sup>a</sup>	60.30 $\pm$ 2.18 <sup>a</sup>	63.90 $\pm$ 0.69 <sup>a,c</sup>	63.08 $\pm$ 2.56 <sup>a</sup>
Granulocytes (%)	16.83 $\pm$ 0.65	27.83 $\pm$ 1.91 <sup>a</sup>	13.00 $\pm$ 1.14 <sup>a,b</sup>	22.35 $\pm$ 0.71 <sup>a,b,c</sup>	26.13 $\pm$ 2.09 <sup>a,c,d</sup>
Platelets ( $10^9/L$ )	361.00 $\pm$ 42.45	335.30 $\pm$ 15.95	483.60 $\pm$ 33.50 <sup>a,b</sup>	469.50 $\pm$ 50.33 <sup>a,b</sup>	579.80 $\pm$ 8.26 <sup>a,b,c,d</sup>

<sup>a</sup> $p < 0.05$  versus sham, <sup>b</sup> $p < 0.05$  versus IIRI, <sup>c</sup> $p < 0.05$  versus FEB+IIRI, <sup>d</sup> $p < 0.05$  versus LDMO+IIRI

Data were analyzed by one-way ANOVA followed by Tukey's post hoc test. Values are expressed as mean  $\pm$  SD of 10 rats per group.

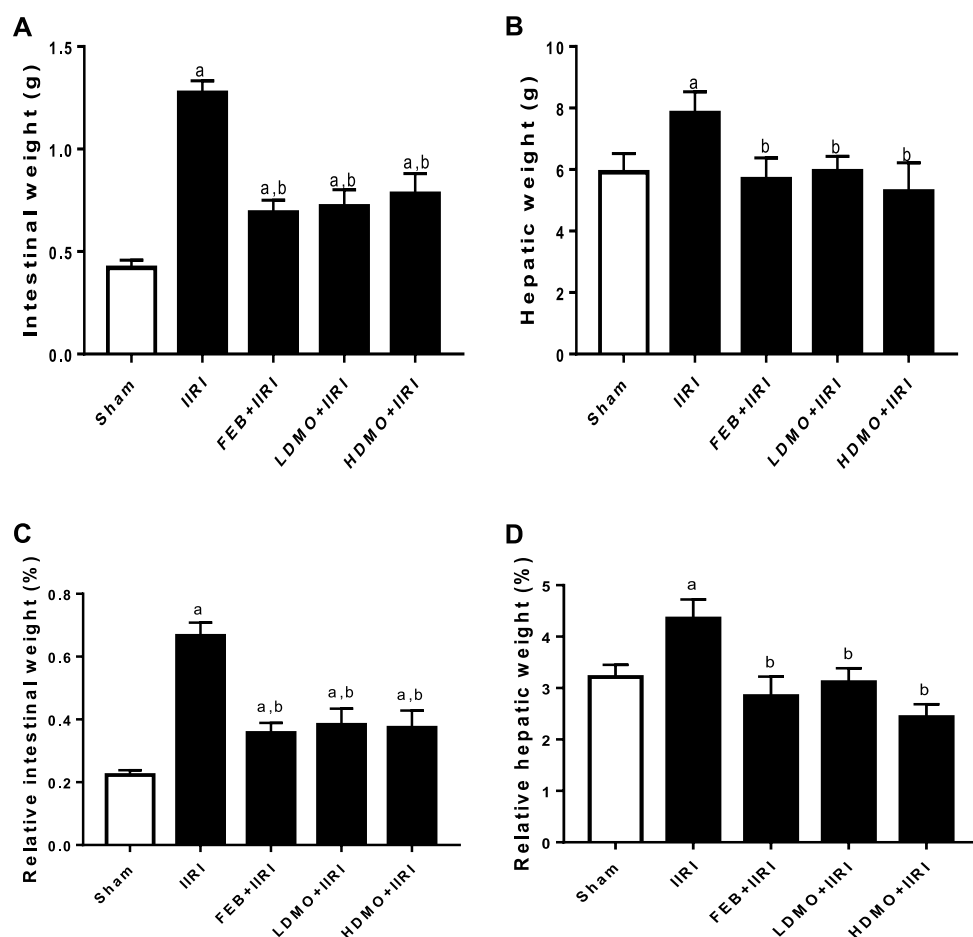


FIGURE 1

Effect of intestinal ischaemia/reperfusion (I/R) and methanolic *Moringa oleifera* leaf extract on intestinal weight (A), hepatic weight (B), relative intestinal weight (C), and relative hepatic weight (D). IIRI: Intestinal ischaemia/reperfusion injury, FEB: febuxostat, LDMO: low dose *Moringa oleifera*, HDMO: high dose *Moringa oleifera*, <sup>a</sup> $p < 0.05$  versus sham, <sup>b</sup> $p < 0.05$  versus IIRI. Data were analyzed by one-way ANOVA followed by Tukey's post hoc test. Values are expressed as mean  $\pm$  SD of 10 rats per group.



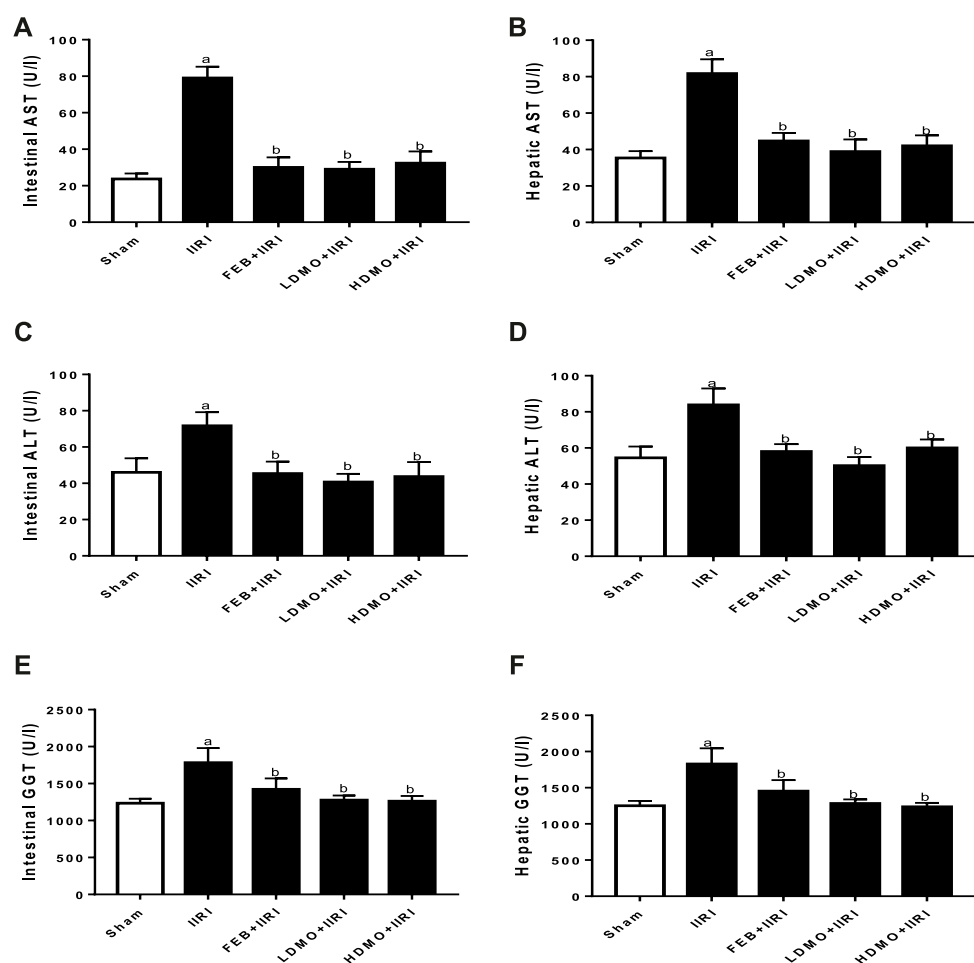


FIGURE 2

Effect of intestinal ischaemia/reperfusion (I/R) and methanolic *Moringa oleifera* leaf extract on intestinal (A) and hepatic aspartate transaminase, AST (B), intestinal (C) and hepatic alanine transaminase, ALT (D), and intestinal (E) and hepatic gamma-glutamyltransferase, GGT (F). IIRI: Intestinal ischaemia/reperfusion injury, FEB: febuxostat, LDMO: low dose *Moringa oleifera*, HDMO: high dose *Moringa oleifera*, <sup>a</sup>  $p < 0.05$  versus sham, <sup>b</sup>  $p < 0.05$  versus IIRI. Data were analyzed by one-way ANOVA followed by Tukey's post hoc test. Values are expressed as mean  $\pm$  SD of 10 rats per group.

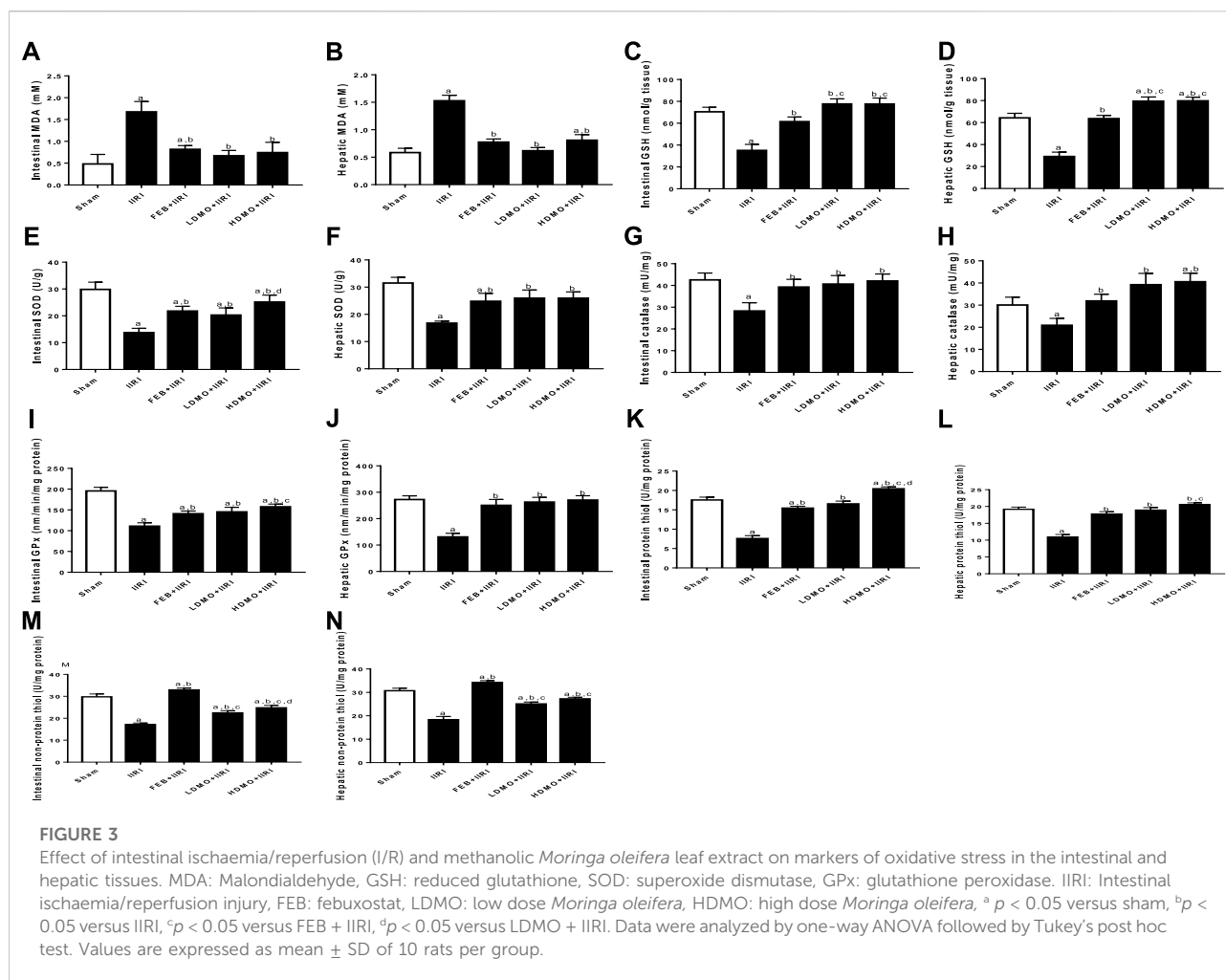
## 2.10 Statistical analysis

GraphPad Prism (Versions 7.00) was used for data analysis. D'Agostino Pearson Omnibus and Shapiro-Wilk normality tests were conducted to ascertain that the data set were normally distributed. Comparisons of mean values were made by Analysis of variance (ANOVA) followed by Tukey's posthoc test for pair-wise comparison. Data are presented as means  $\pm$  standard deviations. A  $p$  value  $< 0.05$  was considered significant.

## 3 Results

### 3.1 Bioactive compounds of methanolic *M. oleifera* leaf extract

Supplementary Table S1 and Supplementary Figure S1 show the bioactive compounds of methanolic *M. oleifera* leaf extract as revealed by GC-MS. It was observed that cyclopentanecarboxylic acid had the highest retention time (18.676 min), followed by phosphonic acid (17.072 min) and



3-undecanone (16.023 min), while thiosemicarbazone had the least (2.631 min) followed by hydrazine (3.987 min) and 1,3-dioxolane (5.379 min). Hydrazine was found to be the highest compound (14.50%), followed by 9-octadecenoic acid (8.74%), 1,3-dioxolane (2.92%), and oleic acid (2.14%). The chemical properties of these organic constituents are shown in Table 1 and the chemical structures are provided in Supplementary Figure S2.

### 3.2 Organ weight

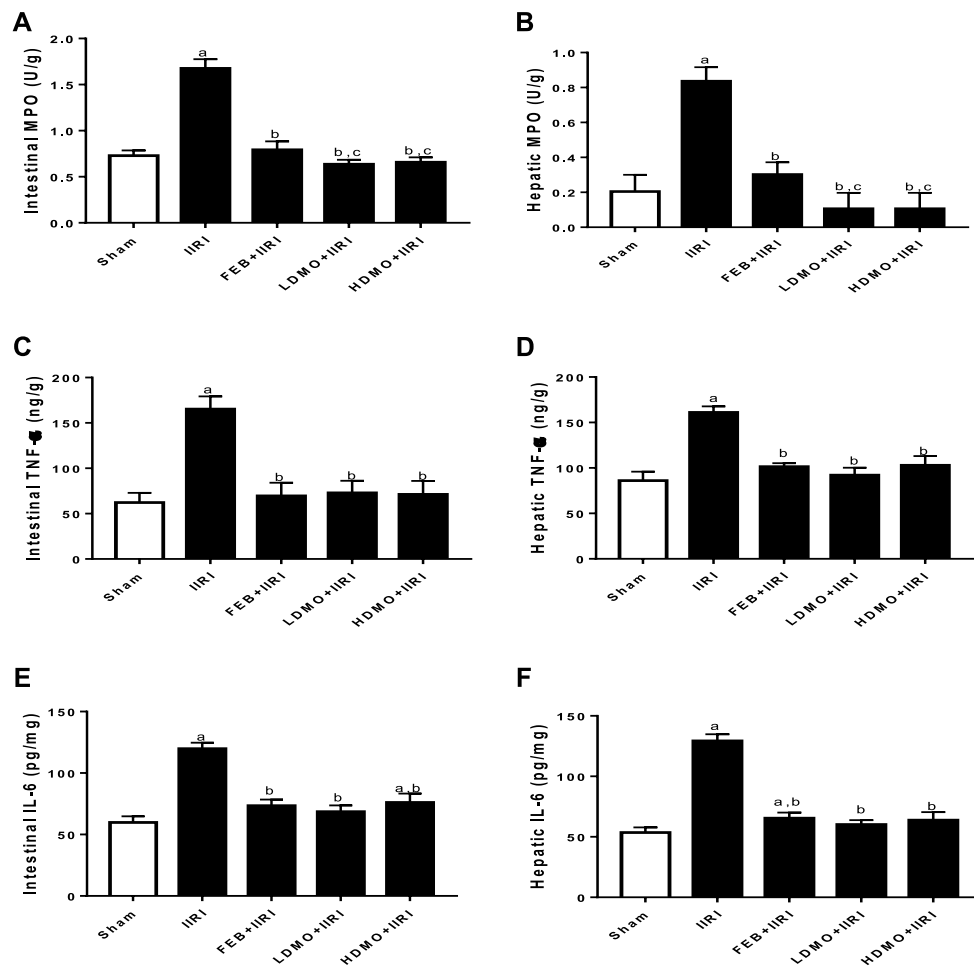
As shown in Figure 1, I/R led to a significant increase in the absolute and relative intestinal and hepatic weight compared with the animals in the sham group. I/R-induced increase in the absolute and relative intestinal and hepatic weight were significantly attenuated by FEB, LDMO, and HDMO. The effects of MMOLE on absolute and relative intestinal and hepatic weight were not dose-dependent.

### 3.3 Intestinal and hepatic injury markers

To investigate the effect of IIRI and MMOLE on tissue injury markers, AST, ALP, and GGT activities were estimated (Figure 2). It was noted that intestinal I/R significantly elevated intestinal and hepatic AST, ALP, and GGT activities compared with the sham group. I/R-induced rise in injury markers was significantly attenuated by FEB, LDMO, and HDMO. The effects of MMOLE on these injury markers were not dose-dependent.

### 3.4 Markers of oxidative stress and inflammation

IIRI significantly increased intestinal and hepatic MDA. The observed I/R-led rise in MDA was significantly abrogated by FEB, LDMO, and HDMO. In addition, I/R caused a considerable reduction in intestinal and hepatic GSH, thiol

**FIGURE 4**

Effect of intestinal ischaemia/reperfusion (I/R) and methanolic *Moringa oleifera* leaf extract on markers of inflammation in the intestinal and hepatic tissues. MPO: Myeloperoxidase, TNF- $\alpha$ : tumour necrotic factor- $\alpha$ , IL-6: interleukin-6. IIRI: Intestinal ischaemia/reperfusion injury, FEB: febuxostat, LDMO: low dose *Moringa oleifera*, HDMO: high dose *Moringa oleifera*, <sup>a</sup> $p < 0.05$  versus sham, <sup>b</sup> $p < 0.05$  versus IIRI, <sup>c</sup> $p < 0.05$  versus FEB + IIRI. Data were analyzed by one-way ANOVA followed by Tukey's post hoc test. Values are expressed as mean  $\pm$  SD of 10 rats per group.

and non-thiol protein concentrations as well as SOD, catalase, and GPx activities. I/R-driven decline in these antioxidants was significantly blocked by FEB, LDMO, and HDMO. Although the effects of MMOLE on enzymatic and non-enzymatic antioxidants were observed to be dose-independent, MMOLE exerted a dose-dependent effect on intestinal levels of thiol and non-thiol protein, and SOD activity (Figure 3).

In addition, intestinal I/R caused a marked increase in intestinal and hepatic MPO activities and TNF- $\alpha$  and IL-6 concentrations compared with the sham-operated group. I/R-driven rise in these inflammatory markers were significantly ameliorated by FEB, LDMO, and HDMO treatments. The effects of MMOLE on MPO, TNF- $\alpha$ , and IL-6 were dose-independent (Figure 4).

### 3.5 Apoptotic markers

Intestinal I/R significantly upregulated intestinal and hepatic caspase 3 activities compared with the sham group. I/R-driven rise in caspase 3 activities was significantly abrogated by FEB, LDMO, and HDMO treatments. The effect of MMOLE treatment on caspase 3 activity was not dose-dependent (Figure 5).

### 3.6 Intestinal and hepatic histoarchitecture

Histopathological examinations revealed that the sham-operated rats had normal villi from mucosal layer with mild

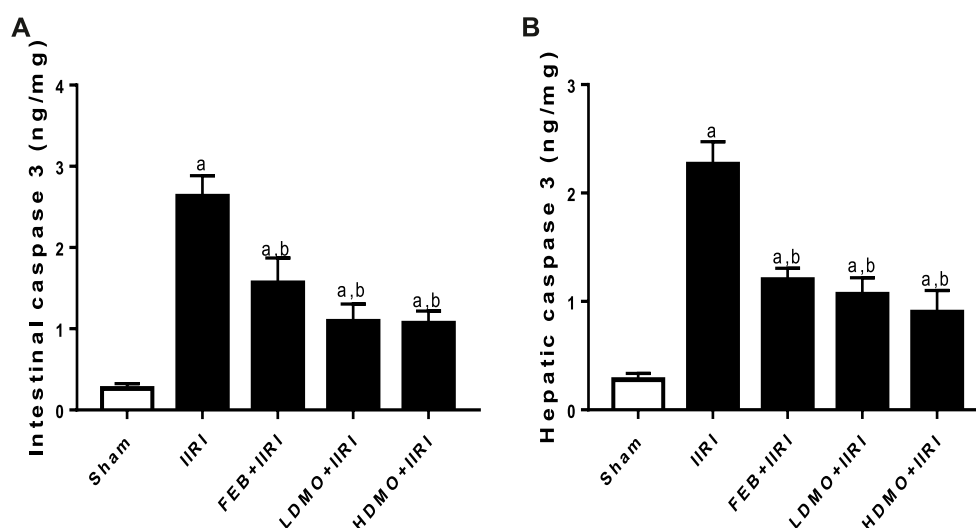


FIGURE 5

Effect of intestinal ischaemia/reperfusion (I/R) and methanolic *Moringa oleifera* leaf extract on caspase 3 activities in the intestinal and hepatic tissues. IIRI: Intestinal ischaemia/reperfusion injury, FEB: febuxostat, LDMO: low dose *Moringa oleifera*, HDMO: high dose *Moringa oleifera*, <sup>a</sup>  $p < 0.05$  versus sham, <sup>b</sup>  $p < 0.05$  versus IIRI, <sup>c</sup>  $p < 0.05$  versus FEB + IIRI. Data were analyzed by one-way ANOVA followed by Tukey's post hoc test. Values are expressed as mean  $\pm$  SD of 10 rats per group.

lymphocyte infiltration in the lumen, moderate inter-glandular infiltration of inflammatory cells in the propria showed, and moderate infiltration of inflammatory cells in the submucosal layer. However, IIRI led to moderately inflamed villi from mucosal layer with moderate infiltration by inflammatory cells, severe infiltration of the lumen by lymphocytes and polymorphs, severe inter-glandular infiltration of inflammatory cells in the propria, and moderate to severe infiltration of the submucosal layer by inflammatory cells. The febuxostat FEB + IIRI showed well preserved villi from mucosal layer, mild inflammatory cells infiltration of the lumen and lamina propria, and a well-preserved submucosal layer and circular muscle. MMOLE treatments, in low and high doses, preserved the villi, although there was moderate lymphocytic infiltration and mild inter-glandular infiltration of inflammatory cells of the lumen and propria respectively. Animals treated with LDMO had normal submucosal layer, while those treated with HDMO had mildly infiltrated submucosal layer (Figure 6).

In addition, the sham-operated rats showed preserved hepatic histoarchitecture with normal central venules, portal triads, hepatocytes, and sinusoids. IIRI led to moderately congested central venules and mildly dilated sinusoids with normal hepatocytes. FEB + IIRI rats showed mildly congested central venules, mildly dilated sinusoids, with normal hepatocytes. MMOLE treatments showed normal central venules without congestion and normal hepatocytes with mildly dilated sinusoids (Figure 7).

Figure 8 shows the histomorphological changes in the intestinal and hepatic tissues using the Chiu and Eckhoff's

scores respectively. When compared with the sham-operated, IIRI led to increased intestinal injury (evidenced by increased Chiu's score) and hepatic injury (evidenced by increased Eckhoff's score). Administration of FEB, LDMO, and HDMO significantly blunted IIRI-induced intestinal and hepatic injury. The impact of *M. oleifera* on IIRI-driven intestinal and hepatic injury was not dose-dependent. Furthermore, significantly shorter villus length and reduced crypt depth were seen in IIRI rats compared to the sham-operated. IIRI-led reductions in villus length and crypt depth were blunted by FEB and MMOLE administrations. MMOLE improved the villus length and crypt depth in a dose-dependent manner.

### 3.7 Bacterial translocation

IIRI significantly increased the bacteria count in intestinal and hepatic tissues compared with the sham-operated group in all the culture media used. FEB and MMOLE treatments significantly reduced IIRI-led rise in bacteria count. Interestingly, although the bactericidal activity of MMOLE was not dose-dependent, it significantly reduced bacteria count at the low and high doses when compared FEB treatment (Figure 9).

#### 3.7.1 9 Haematological indices

When compared with the control, IIRI significantly reduced lymphocyte and platelet counts, increased RBC, Hb, PCV, WBC, and granulocytes, but did not alter MCV and MCHC. FEB

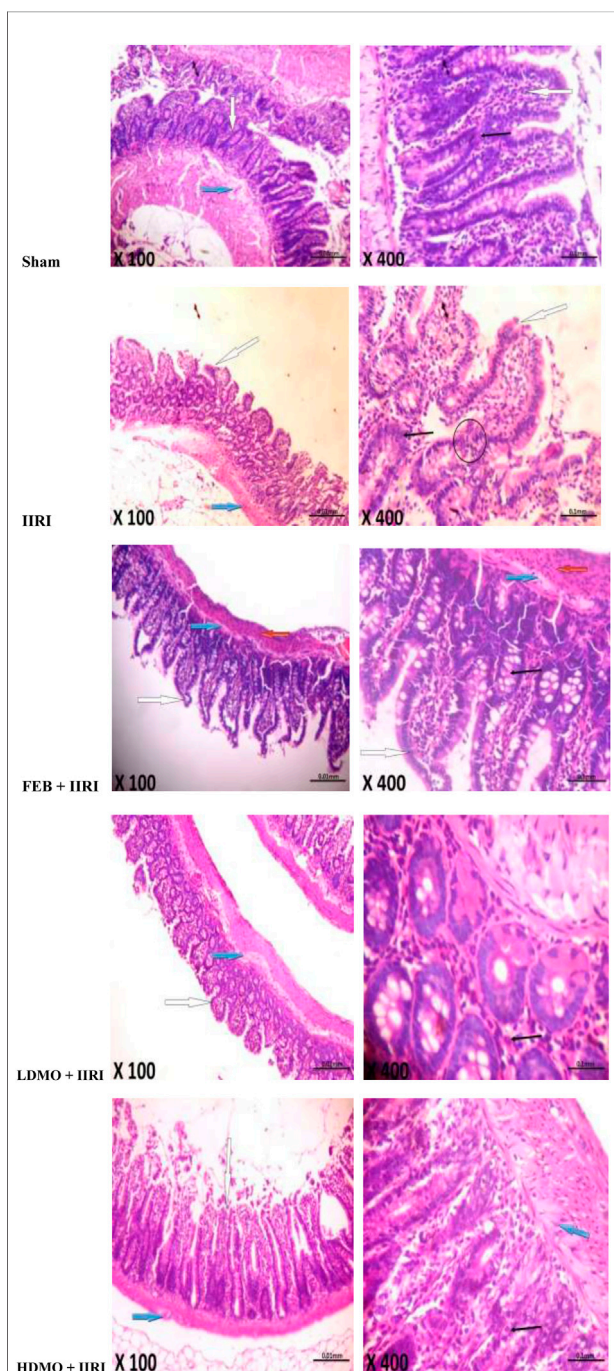


FIGURE 6

Effect of intestinal ischaemia/reperfusion (I/R) and methanolic *Moringa oleifera* leaf extract on intestinal histoarchitecture. The sham-operated rats showed normal villi from mucosal layer (white arrow). The lumen showed mild lymphocytes infiltration and the propria showed moderate inter-glandular infiltration of inflammatory cells (slender arrow). The submucosal layer was moderately infiltrated by inflammatory cells (blue arrow). The intestinal ischaemia/reperfusion injury (IIRI) group showed moderately inflamed villi from mucosal layer which is moderately infiltrated by inflammatory cells (white arrow) and neutrophils (circle). The lumen showed severe infiltration of lymphocytes and polymorphs, and the propria showed severe

(Continued)

## FIGURE 6 (Continued)

inter-glandular infiltration of inflammatory cells (slender arrow). The submucosal layer appeared moderately to severely infiltrated by inflammatory cells (blue arrow). The februxostat (FEB) + IIRI showed well preserved villi from mucosal layer (white arrow). The lumen showed mild inflammatory cells infiltration, and the lamina propria showed mild infiltration of inflammatory cells (slender arrow). The submucosal layer appeared normal (blue arrow) and the circular muscle appeared normal (red arrow). The low dose *Moringa oleifera* (LDMO) + IIRI animals showed normal villi from mucosal layer (white arrow). The lumen showed moderate lymphocytes infiltration and the propria showed mild inter-glandular infiltration of inflammatory cells (slender arrow). The submucosal layer appeared normal (blue arrow). The high dose *Moringa oleifera* (HDMO) + IIRI animals showed normal villi from mucosal layer (white arrow). The lumen showed moderate lymphocytes infiltration and the propria showed moderate inter-glandular infiltration of inflammatory cells (slender arrow). The submucosal layer appeared mildly infiltrated (blue arrow).

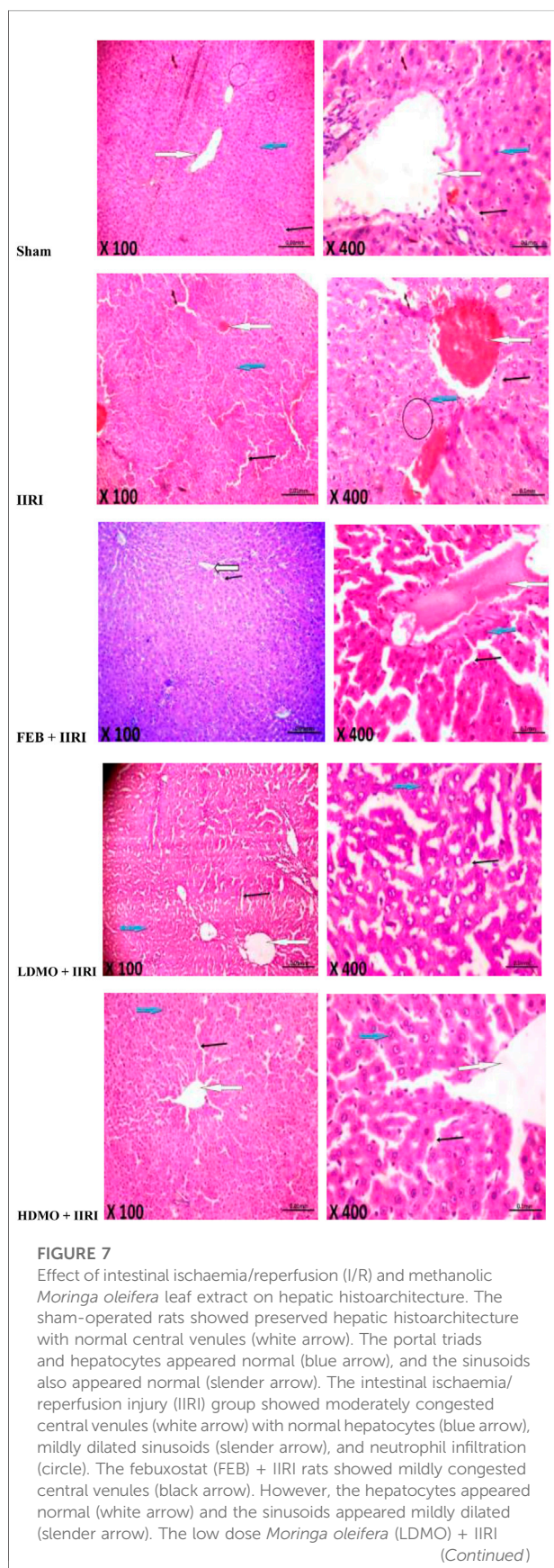
treatment prevented IIRI-induced rise in WBC and platelet counts and granulocyte. Interestingly, LDMO, but not HDMO, increased RBC count, Hb, and MCHC when compared with the control and IIRI groups; while HDMO and LDMO reduced IIRI-induced rise in WBC count and increased IIRI-induced reduction in platelet count. The effects of MMOLE on RBC, Hb, granulocytes, and platelets were dose-dependent (Table 1).

## 4 Discussion

Caspase 3-mediated apoptosis has been incriminated in the pathogenesis of I/R injury in various organs (Afolabi et al., 2021; Ba et al., 2021; Zhu et al., 2021; Afolabi et al., 2022; Huang et al., 2022; Zhu et al., 2022). However, the role of caspase 3 in the intestinal tract, a bacteria-filled organ, has not been well explored. Also, the possible medicinal benefit of *M. oleifera*, a herbal nutraceutical used in folklore medicine for its anti-inflammatory properties, in IIRI has not been reported. This study revealed that MMOLE-mediated caspase 3 suppression may play a role in its protection against IIRI-induced epithelial barrier dysfunction, bacterial translocation, and hepatic injury. We demonstrated that MMOLE attenuated intestinal mucosal injury, and intestinal and extraintestinal bacterial counts normally seen in IIRI. Downregulation of caspase 3 by MMOLE likely inhibits enteric bacterial intrusion via multiple pathways, including enhancement of epithelial barrier integrity via maintenance of cellular antioxidants and direct antimicrobial activity.

Our findings of increased number of bacterial colonies in the liver are in line with previous studies which revealed increased epithelial permeability and bacterial translocation in IIRI (Hsiao et al., 2009; Huang et al., 2010). The increased permeability could have resulted from the disruption of the intestinal barrier arising



**FIGURE 7 (Continued)**

animals showed normal central venules without congestion (white arrow). The hepatocytes appeared normal (blue arrow) and the sinusoids appeared mildly dilated (slender arrow). The high dose *Moringa oleifera* (HDMO) + IIRI animals showed normal central venules (white arrow). The hepatocytes appeared normal (blue arrow) and the sinusoids appeared mildly dilated (slender arrow).

from oxidative damage to the membranes and subsequent apoptotic denudation of the intestinal epithelium (Hu et al., 2019). The current study showed that MMOLE pretreatment significantly reduced intestinal and hepatic bacterial counts, which was coupled with reduced intestinal mucosal injury and hepatic damage, as well as improved villus length and crypt depth. The attenuation of IIRI-induced bacterial translocation and reduction of WBC and granulocytes (indicators of bacterial infection) by MMOLE may be ascribed to its antimicrobial and/or antioxidant activities. This finding corroborates previous reports on the antimicrobial effects (Rahman et al., 2009) and antioxidant (Charoensin, 2014; Saka et al., 2020) properties of MMOLE. Rahman and his colleagues (2009) reported that the leaf juice and extracts of *M. oleifera* exerted antibacterial activities against tested gram positive and gram negative bacteria, suggestive of the presence of broad spectrum bioactive compounds in the herbal nutraceutical. Abalaka et al. (2012) also demonstrated the activity of *M. oleifera* leaf extract against gram positive and gram negative bacteria, confirming that *M. oleifera* exhibits broad spectrum antibacterial activities. Thus, it is reasonable to infer that MMOLE-mediated reduction in bacterial translocation in IIRI is due to, at least in part, its antibacterial potentials.

The preservation of cellular antioxidants that was associated with preserved intestinal and hepatic cytoarchitecture in MMOLE-treated rats suggests that the botanical conferred cellular protection in IIRI. Cellular antioxidants are integral parts of tissues that protect the cell against ROS-mediated oxidative injury (Hamed et al., 2022). SOD converts superoxide radicals into dioxygen and hydrogen peroxide, which is further broken down into water and molecular oxygen by catalase (Akhigbe et al., 2020). GSH scavenges ROS, while GPx metabolizes hydrogen peroxide and also oxidizes GSH (Aquilano et al., 2014). Sreelatha and Padma (2009) demonstrated that *M. oleifera* leaf extract exhibited strong scavenging effect on 2,2-diphenyl-2-picryl hydrazyl (DPPH) free radical, superoxide radical and nitric oxide radical, thus protects against oxidative damage to biomolecules. Charoensin (2014) also reported the radical scavenging activities of *M. oleifera* leaf extracts. Hence, MMOLE-driven suppression of MDA and upregulation of enzymatic and non-enzymatic antioxidants in IIRI explains, at least partly, the observed preserved intestinal and hepatic cytoarchitecture and maintenance of villus length and crypt depth in MMOLE-treated rats.

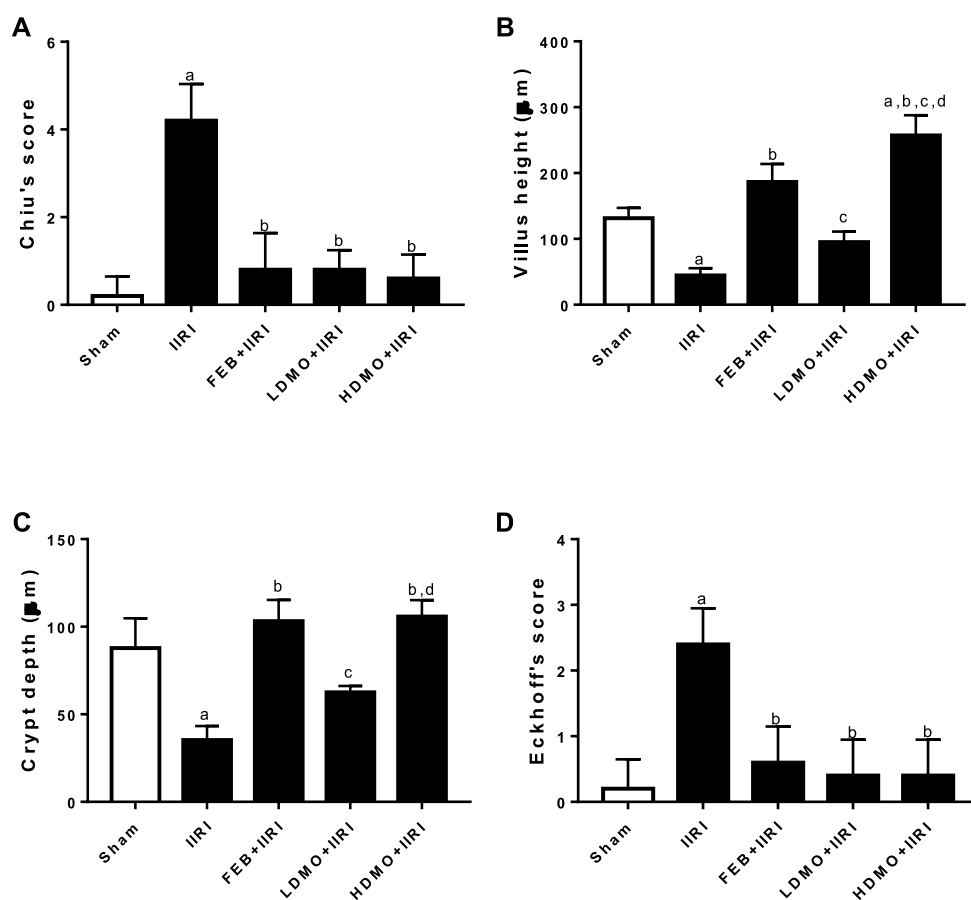


FIGURE 8

Effect of intestinal ischaemia/reperfusion (I/R) and methanolic *Moringa oleifera* leaf extract on intestinal injury using Chiu's score (A), villi height (B), crypt depth (C), and hepatic injury using Eckhoff's score (D). IIRI: Intestinal ischaemia/reperfusion injury, FEB: febuxostat, LDMO: low dose *Moringa oleifera*, HDMO: high dose *Moringa oleifera*, <sup>a</sup> $p < 0.05$  versus sham, <sup>b</sup> $p < 0.05$  versus IIRI, <sup>c</sup> $p < 0.05$  versus FEB + IIRI, <sup>d</sup> $p < 0.05$  versus LDMO + IIRI. Data were analyzed by one-way ANOVA followed by Tukey's post hoc test. Values are expressed as mean  $\pm$  SD of 10 rats per group.

Oxidative stress has been established as a cause and/or consequence of inflammation. Oxidative stress triggers the translocation of nuclear factor kappa-light-chain-enhancer of activated B cells (NF- $\kappa$ B) to the nucleus and induces the transcription of several deleterious pro-inflammatory genes (Won et al., 2006; Hamed et al., 2022). In addition, oxidative stress upregulates pro-inflammatory cytokines such as TNF- $\alpha$  and IL-6 that in turn activate NF- $\kappa$ B (Akhigbe and Ajayi, 2020; Hamed et al., 2022), prime neutrophil infiltration (Sheppard et al., 2005), and promote ROS-induced oxidative stress (Akhigbe and Ajayi, 2020). It is therefore plausible to surmise that MMOLE blunted IIRI-induced neutrophil accumulation (evidenced by reduced MPO activity) by suppressing ROS-driven upregulation of TNF- $\alpha$  and IL-6, indicating the anti-inflammatory and antioxidant activities of MMOLE. This agrees with the report of Omodanisi et al. (2017) that demonstrated the anti-inflammatory and antioxidant activities of MMOLE in diabetes-induced nephrotoxic rats. It is also in

consonance with the report of Xu et al. (2019) that demonstrated the anti-inflammatory and antioxidant activities of the crude extracts of *M. oleifera* leaves.

In an organ full of commensal bacteria such as the intestine, epithelial barrier disruption by oxido-inflammatory damage is key in extraintestinal bacterial translocation (Kubes, 1993; Liu et al., 2020). It is likely that caspase 3-mediated apoptosis also play a role in altering the epithelial mucosa integrity and promoting microbial dissemination. Based on this hypothesis, we evaluated whether IIRI may upregulate caspase 3 activity. It is worth noting that IIRI-led epithelial denudation and villus deformation was not only associated with oxidative stress and upregulation of inflammatory cytokines, it was also coupled with enhanced caspase 3 activity. It is likely that caspase 3, an executioner of apoptosis (Akhigbe and Ajayi, 2020), was activated by IIRI-induced oxido-inflammatory response, resulting in the cleavage of downstream death

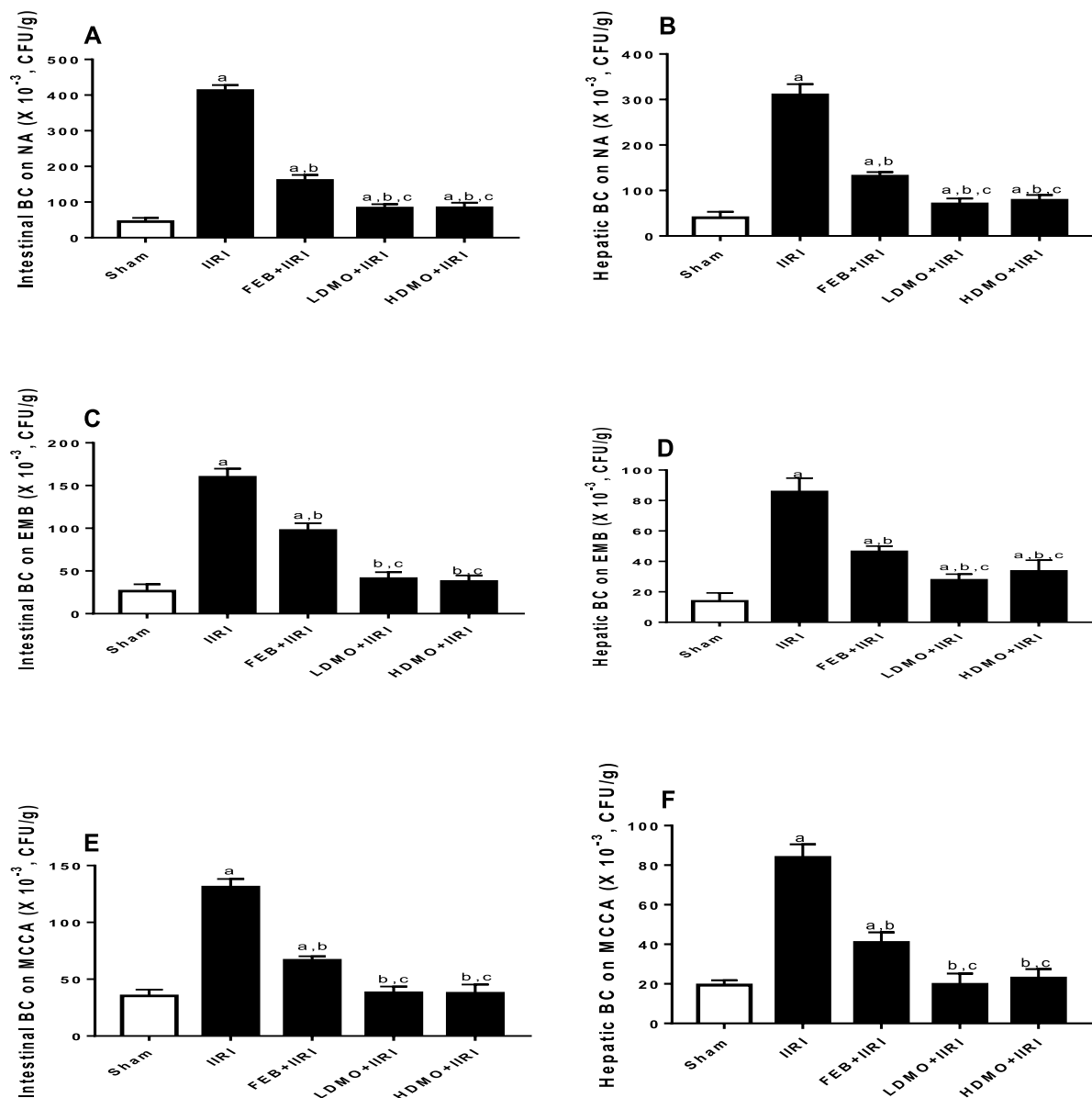


FIGURE 9

Effect of intestinal ischaemia/reperfusion (I/R) and methanolic *Moringa oleifera* leaf extract on intestinal and hepatic bacterial count (BC) using nutrient agar (NA), eosin-methylene blue (EMB), and Mac Conkey agar (MCCA) culture media for colony count. IIRI: Intestinal ischaemia/reperfusion injury, FEB: febuxostat, LDMO: low dose *Moringa oleifera*, HDMO: high dose *Moringa oleifera*, <sup>a</sup>  $p < 0.05$  versus sham, <sup>b</sup>  $p < 0.05$  versus IIRI, <sup>c</sup>  $p < 0.05$  versus FEB + IIRI. Data were analyzed by one-way ANOVA followed by Tukey's post hoc test. Values are expressed as mean  $\pm$  SD of 10 rats per group.

substrates and amplification of upstream death cascade that culminate in apoptosis (Akhigbe and Ajayi, 2020). To this end, it is safe to conclude that activation of caspase 3 is essential in the pathogenesis of epithelial barrier damage, enteric bacterial translocation, and hepatic injury in IIRI. Interestingly, MMOLE promoted epithelial restitution and militated against epithelial barrier damage, enteric bacterial

translocation, and hepatic injury in IIRI. Thus, the protective activity of MMOLE in IIRI is via downregulation of oxidative stress-dependent caspase 3 activation.

The observed biological activities of MMOLE may be ascribed to its constituents bioactive molecules, especially hydrazine, 9-octadecenoic acid, 1,3-dioxolane, oleic acid, and nonadecanoic acid. Hydrazine has been reported to exert

antioxidant antimicrobial activities (Shen et al., 2010). Also, 9-octadecenoic acid has been demonstrated to exert antimicrobial activities against gram positive and gram negative bacteria (Stenz et al., 2008; Garba and Garba, 2017). In addition, 1,3-dioxolane and its derivatives have been reported to possess radical scavenging and antimicrobial activities (Nobre et al., 2014). This molecule and its derivatives have also been demonstrated to act as effective modulators to combat multidrug resistance (Schmidt et al., 2007), thus improving their antimicrobial activities. Oleic acid has been shown to exert anti-inflammatory (Earlia et al., 2019) and antibacterial activities (McGaw et al., 2002; Zheng et al., 2005). The antibacterial property of thiosemicarbazone (Khan et al., 2014) may also contribute to the biological activities of MMOLE.

## 5 Conclusion

In conclusion, methanolic *M. oleifera* leaf extract protects against epithelial mucosal barrier disruption, bacterial translocation, and hepatic injury caused by IIRI via downregulation of oxidative stress-mediated caspase 3 activation and the antimicrobial activities of its constituents bioactive molecules. This study has some limitations. First, GC-MS, instead of high performance liquid chromatography (HPLC), was used to characterize the constituent bioactive molecules of methanolic *M. oleifera* leaf extract due to availability. This possibly provided a limited view of the active compounds in the extract. Also, the pathways evaluated are limited. Future studies evaluating the roles of other apoptotic pathways in IIRI, the bioactive components of methanolic *M. oleifera* leaf extract using HPLC, and the protective potentials of methanolic *M. oleifera* leaf extract against identified pathways are recommended.

## Data availability statement

The original contributions presented in the study are included in the article/Supplementary Material, further inquiries can be directed to the corresponding author.

## References

- Abalaka, M. E., Daniyan, S. Y., Oyeleke, S. B., and Adeyemo, S. O. (2012). The antibacterial evaluation of *Moringa oleifera* leaf extracts on selected bacterial pathogens. *J. Microbiol. Res. Rosemead, Calif.* 2 (2), 1–4. doi:10.5923/j.microbiology.20120202.01
- Afolabi, O., Alabi, B., Omobowale, T., Oluranti, O., and Iwalewa, O. (2021). Cysteamine mitigates torsion/detorsion-induced reperfusion injury via inhibition

## Ethics statement

The animal study was reviewed and approved by Ethics Review Committee of the Faculty of Basic Medical Sciences of the institution.

## Author contributions

OA, TA, RA, and BA conceived and designed the study. OA, RA, and BA supervised and managed the project. OG, MT, OF, and EY performed the experiments. TA and RA analyzed the data and made all the figures. TA and RA wrote the first draft of the manuscript. OA, TA, RA, BA, OG, MT, OF, and EY revised the manuscript for intellectual content. All authors read and approved the final manuscript.

## Funding

The study was funded by the authors' financial contributions.

## Conflict of interest

The authors declare that the research was conducted in the absence of any commercial or financial relationships that could be construed as a potential conflict of interest.

## Publisher's note

All claims expressed in this article are solely those of the authors and do not necessarily represent those of their affiliated organizations, or those of the publisher, the editors and the reviewers. Any product that may be evaluated in this article, or claim that may be made by its manufacturer, is not guaranteed or endorsed by the publisher.

## Supplementary material

The Supplementary Material for this article can be found online at: <https://www.frontiersin.org/articles/10.3389/fphar.2022.989023/full#supplementary-material>

of apoptosis, oxidative stress and inflammatory responses in experimental rat model. *Andrologia* 54 (1), e14243. doi:10.1111/and.14243

Afolabi, O. A., Anyogu, D. C., Hamed, M. A., Odetayo, A. F., Adeyemi, D. H., and Akhigbe, R. E. (2022). Glutamine prevents upregulation of NF- $\kappa$ B signaling and caspase 3 activation in ischaemia/reperfusion-induced testicular damage: An animal model. *Biomed. Pharmacother.* 150, 113056. doi:10.1016/j.biopha.2022.113056



- Akhigbe, R., and Ajayi, A. (2020). Testicular toxicity following chronic codeine administration is via oxidative DNA damage and up-regulation of NO/TNF- $\alpha$  and caspase 3 activities. *PLoS ONE* 15 (3), e0224052. doi:10.1371/journal.pone.0224052
- Akhigbe, R., and Ajayi, A. (2021). The impact of reactive oxygen species in the development of cardiometabolic disorders: A review. *Lipids Health Dis.* 20, 23. doi:10.1186/s12944-021-01435-7
- Akhigbe, R. E., Hamed, M. A., Odetayo, A. F., Akhigbe, T. M., Ajayi, A. F., and Ajibogun, F. A. H. (2021). Omega-3 fatty acid rescues ischaemia/perfusion-induced testicular and sperm damage via modulation of lactate transport and xanthine oxidase/uric acid signaling. *Biomed. Pharmacother.* 142, 111975. doi:10.1016/j.biopha.2021.111975
- Akhigbe, R. E., Ajayi, L. O., Adelakun, A. A., Olorunnisola, O. S., and Ajayi, A. F. (2020). Codeine-induced hepatic injury is via oxido-inflammatory damage and caspase-3-mediated apoptosis. *Mol. Biol. Rep.* 47, 9521–9530. doi:10.1007/s11033-020-05983-6
- Anwar, F., Latif, S., Ashraf, M., and Gilani, A. H. (2007). Moringa oleifera: A food plant with multiple medicinal uses. *Phytother. Res.* 21, 17–25. doi:10.1002/ptr.2023
- Aquilano, K., Baldelli, S., and Ciriolo, M. R. (2014). Glutathione: New roles in redox signaling for an old antioxidant. *Front. Pharmacol.* 5, 196. doi:10.3389/fphar.2014.00196
- Ba, J., Wang, X., Du, S., Wang, P., Wang, Y., Quan, L., et al. (2021). Study on the protective effects of danshen-honghua herb pair (DHHP) on myocardial ischaemia/reperfusion injury (MIRI) and potential mechanisms based on apoptosis and mitochondria. *Pharm. Biol.* 59 (1), 335–346. doi:10.1080/13880209.2021.1893346
- Charoensin, S. (2014). Antioxidant and anticancer activities of *Moringa oleifera* leaves. *J. Med. Plants Res.* 8 (7), 318–325. doi:10.5897/jmpr2013.5353
- Cheenpracha, S., Park, E., Yoshida, W. Y., Barit, C., Wall, M., Pezzuto, J. M., et al. (2010). Potential anti-inflammatory phenolic glycosides from the medicinal plant *Moringa oleifera* fruits. *Bioorg. Med. Chem.* 18, 6598–6602. doi:10.1016/j.bmc.2010.03.057
- Chiu, C., McArdle, A. H., Brown, R., Scott, H. J., and Gurd, F. N. (1970). Intestinal mucosal lesion in low-flow states. A morphological, hemodynamic, and metabolic reappraisal. *Arch. Surg.* 101, 478–483.
- Eckhoff, D. E., Bilbao, G., Frenette, L., Thompson, J. A., and Contreras, J. L. (2002). 17-Beta-estradiol protects the liver against warm ischemia/reperfusion injury and is associated with increased serum nitric oxide and decreased tumor necrosis factor- $\alpha$ . *Surgery* 132 (2), 302–309.
- Earlia, N., MuslemSuhendra, R., Amin, M., Prakoeswa, C. R. S., Khairan, et al. (2019). GC/MS analysis of fatty acids on *Pliek U* oil and its pharmacological study by molecular docking to Filaggrin as a drug candidate in atopic dermatitis treatment. *ScientificWorldJournal*. 2019, 8605743. doi:10.1155/2019/8605743
- Feng, D., Yao, J., Wang, G., Li, Z., Zu, G., Li, Y., et al. (2017). Inhibition of p66Shc-mediated mitochondrial apoptosis via targeting prolyl-isomerase Pin1 attenuates intestinal ischemia/reperfusion injury in rats. *Clin. Sci. (Lond.)* 131 (8), 759–773. doi:10.1042/CS20160799
- Garba, S., and Garba, I. (2017). Anti-diarrhoeal properties of Cis-9-octadecanoic acid isolated from *Landolphia owariensis* plant. *Org. Med. Chem. Int. J.* 3 (4), 103. doi:10.19080/OMCIJ.2017.03.555619
- Hamed, M. A., Akhigbe, T. M., Akhigbe, R. E., Aremu, A. O., Oyedokun, P. A., Gbadamosi, J. A., et al. (2022). Glutamine restores testicular glutathione-dependent antioxidant defense and upregulates NO/cGMP signaling in sleep deprivation-induced reproductive dysfunction in rats. *Biomed. Pharmacother.* 148, 112765. doi:10.1016/j.biopha.2022.112765
- Hamed, M. A., Aremu, G. O., and Akhigbe, R. E. (2021). Concomitant administration of HAART aggravates anti-Koch-induced oxidative hepatorenal damage via dysregulation of glutathione and elevation of uric acid production. *Biomed. Pharmacother.* 137, 111309. doi:10.1016/j.biopha.2021.111309
- Hsiao, J. K., Huang, C. Y., Lu, Y. Z., Yang, C. Y., and Yu, L. C. H. (2009). Magnetic resonance imaging detects intestinal barrier dysfunction in a rat model of acute mesenteric ischemia/reperfusion injury. *Invest. Radiol.* 44, 329–335. doi:10.1097/RLI.0b013e3181a16762
- Hu, M. (1994). Measurement of protein thiol groups and glutathione in plasma. *Methods Enzymol.* 233, 380–385. doi:10.1016/s0076-6879(94)33044-1
- Hu, Q., Ren, H., Li, G., Wang, D., Zhou, Q., Wu, J., et al. (2019). STING-mediated intestinal barrier dysfunction contributes to lethal sepsis. *EBioMedicine* 41, 497–508. doi:10.1016/j.ebiom.2019.02.055
- Huang, C. Y., Hsiao, J. K., Lu, Y. Z., Lee, T. C., and Yu, L. C. H. (2010). Anti-apoptotic PI3K/Akt signaling by sodium/glucose transporter 1 reduces epithelial barrier damage and bacterial translocation in intestinal ischemia. *Lab. Invest.* 91, 294–309. doi:10.1038/labinvest.2010.177
- Huang, R., Zhao, Z., Jiang, X., Li, W., Zhang, L., Wang, B., et al. (2022). Liposomal chrysin attenuates hepatic ischaemia-reperfusion injury: Possible mechanism via inhibiting NLRP3 inflammasome. *J. Pharm. Pharmacol.* 74 (2), 216–226. doi:10.1093/jpp/rgab153
- Jocelyn, P. C. (1987). Spectrophotometric assay of thiols. *Methods Enzymol.* 143, 44–67. doi:10.1016/0076-6879(87)43013-9
- Khames, A., Khalaf, M. M., Gad, A. M., and Abd El-Raouf, O. M. (2017). Ameliorative effects of sildenafil and/or febuxostat on doxorubicin-induced nephrotoxicity in rats. *Eur. J. Pharmacol.* 805, 118–124. doi:10.1016/j.ejphar.2017.02.046
- Khan, S. A., Asiri, A. M., Al-Amry, K., and Malik, M. A. (2014). Synthesis, characterization, electrochemical studies, and *in vitro* antibacterial activity of novel Thiosemicarbazone and its Cu(II), Ni(II), and Co(II) complexes. *ScientificWorldJournal*. 2014, 592375. doi:10.1155/2014/592375
- Kirisattayakul, W., Wattanathorn, J., Tong-Un, T., Muchimapura, S., Wannanon, P., and Jittiwat, J. (2013). Cerebroprotective effect of Moringa oleifera against focal ischemic stroke induced by middle cerebral artery occlusion. *Oxid. Med. Cell. Longev.* 2013, 951415. doi:10.1155/2013/951415
- Kubes, P. (1993). Polymorphonuclear leukocyte-endothelium interactions: A role for pro-inflammatory and anti-inflammatory molecules. *Can. J. Physiol. Pharmacol.* 71, 88–97. doi:10.1139/y93-013
- Liu, C., Ding, R., Huang, W., Miao, L., Li, J., and Li, Y. (2020). Sevoflurane protects against intestinal ischemia-reperfusion injury by activating peroxisome proliferator-activated receptor gamma/nuclear factor-kb pathway in rats. *Pharmacology* 105 (3–4), 231–242. doi:10.1159/000503727
- Mallick, I. H., Yang, W., Winslet, M. C., and Seifalian, A. M. (2004). Ischemia-reperfusion injury of the intestine and protective strategies against injury. *Dig. Dis. Sci.* 49, 1359–1377. doi:10.1023/b:ddas.0000042232.98927.91
- Mamza, U. T., Sodipo, O. A., and Khan, I. Z. (2012). Gas chromatography-mass spectrometry (gc-ms) analysis of bioactive components of *Phyllanthus amarus* leaves. *Int. Res. J. Plant Sci.* 3 (10), 208–215.
- McGaw, L. J., Jager, A. K., and Van Staden, J. (2002). Antibacterial effects of fatty acids and related compounds from plants. *South Afr. J. Bot.* 68, 417–423. doi:10.1016/s0254-6299(15)30367-7
- Nobre, P. C., Borges, E. L., Silva, C. M., Casaril, A. M., Martinez, D. M., Lenardao, E. J., et al. (2014). Organochalcogen compounds from glycerol: Synthesis of new antioxidants. *Bioorg. Med. Chem.* 22, 6242–6249. doi:10.1016/j.bmc.2014.08.018
- Ogundola, A. F., Akhigbe, R. E., Saka, W. A., Adeniyi, A. O., Adeshina, O. S., Babalola, D. O., et al. (2021). Contraceptive potential of *Andrographis paniculata* is via androgen suppression and not induction of oxidative stress in male Wistar rats. *Tissue Cell* 73, 101632. doi:10.1016/j.tice.2021.101632
- Omodanisi, E. I., Aboua, Y. G., and Oguntibeju, O. O. (2017). Assessment of the anti-hyperglycaemic, anti-inflammatory and antioxidant activities of the methanol extract of *Moringa oleifera* in diabetes-induced nephrotoxic male Wistar rats. *Molecules* 22, 439. doi:10.3390/molecules22040439
- Ozkan, O. V., Yuzbasioglu, M. F., Ciralik, H., Kurutas, E. B., Yonden, Z., Aydin, M., et al. (2009). Resveratrol, a natural antioxidant, attenuates intestinal ischemia/reperfusion injury in rats. *Tohoku J. Exp. Med.* 218, 251–258. doi:10.1620/tjem.218.251
- Park, P. O., Haglund, U., Bulkley, G. B., and Falt, K. (1990). The sequence of development of intestinal tissue injury after strangulation ischemia and reperfusion. *Surgery* 107, 574–580.
- Rahman, M. M., Sheik, M. M., Sharmin, S. A., Islam, M. S., Rahman, M. A., Rahman, M. M., et al. (2009). Antibacterial activity of leaf juice and extracts of *Moringa oleifera* Lam. against some human pathogenic bacteria. *CMU. J. Nat. Sci.* 8 (2), 219–227.
- Saban-Ruiz, J., Alonso-Pacho, A., Fabregate-Fuente, M., and Gonzalez-Quevedo, C. D. (2013). Xanthine oxidase inhibitor febuxostat as a novel agent postulated to act against vascular inflammation. *Antinflamm. Antiallergy. Agents Med. Chem.* 12, 94–99. doi:10.2174/1871523011312010011
- Saka, W. A., Akhigbe, R. E., Ishola, O. S., Ashamu, E. A., Olayemi, O. T., and Adeleke, G. E. (2011). Hepatotherapeutic effect of Aloe vera in alcohol-induced hepatic damage. *Pak. J. Biol. Sci.* 14, 742–746. doi:10.3923/pjbs.2011.742.746
- Saka, W. A., Ayoade, T. E., Akhigbe, T. M., and Akhigbe, R. E. (2020). *Moringa oleifera* seed oil partially abrogates 2, 3-dichlorovinyl dimethyl phosphite (Dichlorvos)-induced cardiac injury in rats: Evidence for the role of oxidative stress. *J. Basic Clin. Physiol. Pharmacol.* 32, 237–246. doi:10.1515/jbcpp-2019-0313
- Schmidt, M., Ungvari, J., Glode, J., Dobner, B., and Langner, A. (2007). New 1, 3-dioxolane and 1, 3-dioxane derivatives as effective modulators to overcome multidrug resistance. *Bioorg. Med. Chem.* 15, 2283–2297. doi:10.1016/j.bmc.2007.01.024
- Shen, W., Qiu, Q., Wang, Y., Miao, M., Li, B., Zhang, T., et al. (2010). Hydrazine as a nucleophile and antioxidant for fast aminolysis of RAFT polymers in Air. *Macromol. Rapid Commun.* 31, 1444–1448. doi:10.1002/marc.201000154



- Sheppard, F. R., Kelher, M. R., Moore, E. E., McLaughlin, N. J. D., Banerjee, A., and Silliman, C. C. (2005). Structural organization of the neutrophil NADPH oxidase: Phosphorylation and translocation during priming and activation. *J. Leukoc. Biol.* 78, 1025–1042. doi:10.1189/jlb.0804442
- Siddhuraju, P., and Becker, K. (2003). Antioxidant properties of various solvent extracts of total phenolic constituents from three different agroclimatic origins of drumstick tree (*Moringa oleifera* Lam.) leaves. *J. Agric. Food Chem.* 51 (8), 2144–2155. doi:10.1021/jf020444+
- Sofowora, A. (1993). *Medicinal plant and traditional medicine in africa*. New York, NY, USA: Chichester John Wiley and Sons, 256.
- Sreelatha, S., and Padma, P. R. (2009). Antioxidant activity and total phenolic content of *Moringa oleifera* leaves in two stages of maturity. *Plant Foods Hum. Nutr.* 64, 303–311. doi:10.1007/s11130-009-0141-0
- Stenz, L., Francois, P., Fischer, A., Huyghe, A., Tangomo, M., Hernandez, D., et al. (2008). Impact of oleic acid (cis-9-octadecenoic acid) on bacterial viability and biofilm production in *Staphylococcus aureus*. *FEMS Microbiol. Lett.* 287, 149–155. doi:10.1111/j.1574-6968.2008.01316.x
- Tsuda, H., Kawada, N., Kaimori, J., Kitamura, H., Moriyama, T., Rakugi, H., et al. (2012). Febuxostat suppressed renal ischemia-reperfusion injury via reduced oxidative stress. *Biochem. Biophys. Res. Commun.* 427, 266–272. doi:10.1016/j.bbrc.2012.09.032
- Wen, X. L. S., Ling, Y., Chen, S., Deng, Q., Yang, L., Li, Y., et al. (2020). HMGB1-associated necroptosis and Kupffer cells M1 polarization underlies remote liver injury induced by intestinal ischemia/reperfusion in rats. *FASEB J.* 34, 4384–4402. doi:10.1096/fj.201900817R
- Won, J. H., Im, H. T., Kim, Y. H., Yun, K. J., Park, H. J., Choi, J. W., et al. (2006). Antiinflammatory effect of buddlejasaponin IV through the inhibition of iNOS and COX-2 expression in RAW 264.7 macrophages via the NF-kappaB inactivation. *Br. J. Pharmacol.* 148, 216–225. doi:10.1038/sj.bjp.0706718
- Xu, Y.-B., Chen, G.-L., and Guo, M.-Q. (2019). Antioxidant and anti-inflammatory activities of the crude extract of *Moringa oleifera* from Kenya and their correlations with flavonoids. *Antioxidants* 8, 296. doi:10.3390/antiox8080296
- Yildiz, F., Terzi, A., Coban, S., Celik, H., Aksoy, N., Bitiren, M., et al. (2009). Protective effects of resveratrol on small intestines against intestinal ischemia-reperfusion injury in rats. *J. Gastroenterol. Hepatol.* 24, 1781–1785. doi:10.1111/j.1440-1746.2009.05945.x
- Zheng, C. J., Yoo, J.-S., Lee, T.-G., Cho, H.-Y., Kim, Y.-H., and Kim, W.-G. (2005). Fatty acid synthesis is a target for antibacterial activity of unsaturated fatty acids. *FEBS Lett.* 579, 5157–5162. doi:10.1016/j.febslet.2005.08.028
- Zhu, J., Qiu, J.-G., Xu, W.-T., Ma, H.-X., and Jiang, K. (2021). Alamandine protects against renal ischaemia-reperfusion injury in rats via inhibiting oxidative stress. *J. Pharm. Pharmacol.* 73 (11), 1491–1502. doi:10.1093/jpp/rgab091
- Zhu, T., Fang, B.-Y., Meng, X.-B., Zhang, S.-X., Wang, H., Gao, G., et al. (2022). Folium *Ginkgo* extract and tetramethylpyrazine sodium chloride injection (Xingxiong injection) protects against focal cerebral ischaemia/reperfusion injury via activating Akt/Nrf2 pathway and inhibiting NLRP3 inflammasome activation. *Pharm. Biol.* 60 (1), 195–205. doi:10.1080/13880209.2021.2014895



## OPEN ACCESS

## EDITED BY

Adina Turcu-Stolica,  
University of Medicine and Pharmacy of  
Craiova, Romania

## REVIEWED BY

Sabina Wiecek,  
Medical University of Silesia, Poland  
Luis Andrés Lopez-Fernández,  
Instituto de Investigación Sanitaria  
Gregorio Marañon, Spain

## \*CORRESPONDENCE

Bing Chang,  
cb000216@163.com  
Lixuan Sang,  
sanglixuan2008@163.com

<sup>†</sup>These authors have contributed equally  
to this work

## SPECIALTY SECTION

This article was submitted to  
Gastrointestinal and Hepatic  
Pharmacology,  
a section of the journal  
Frontiers in Pharmacology

RECEIVED 17 July 2022

ACCEPTED 12 September 2022

PUBLISHED 26 September 2022

## CITATION

Wang M, Zhao J, Wang H, Zheng C,  
Chang B and Sang L (2022),  
Methotrexate showed efficacy both in  
Crohn's disease and ulcerative colitis,  
predictors of surgery were identified in  
patients initially treated with  
methotrexate monotherapy.  
*Front. Pharmacol.* 13:996065.  
doi: 10.3389/fphar.2022.996065

## COPYRIGHT

© 2022 Wang, Zhao, Wang, Zheng,  
Chang and Sang. This is an open-access  
article distributed under the terms of the  
[Creative Commons Attribution License](#)  
(CC BY). The use, distribution or  
reproduction in other forums is  
permitted, provided the original  
author(s) and the copyright owner(s) are  
credited and that the original  
publication in this journal is cited, in  
accordance with accepted academic  
practice. No use, distribution or  
reproduction is permitted which does  
not comply with these terms.

# Methotrexate showed efficacy both in Crohn's disease and ulcerative colitis, predictors of surgery were identified in patients initially treated with methotrexate monotherapy

Mengyao Wang<sup>1</sup>, Jingwen Zhao<sup>1</sup>, Heran Wang<sup>1</sup>,  
Changqing Zheng<sup>1</sup>, Bing Chang<sup>2\*†</sup> and Lixuan Sang<sup>1\*†</sup>

<sup>1</sup>Department of Gastroenterology, Shengjing Hospital of China Medical University, Shenyang, China,

<sup>2</sup>Department of Gastroenterology, The First Affiliated Hospital of China Medical University, Shenyang, China

**Objective:** This study aimed to evaluate methotrexate efficacy in patients with Crohn's disease (CD) and ulcerative colitis (UC), and identify predictors of surgery for patients who were initially treated with methotrexate monotherapy.

**Design:** We performed a retrospective analysis of 34,860 patients with inflammatory bowel disease (IBD) in the IBD Bioresource (United Kingdom) prior to 9 November 2021. Logistic regression was used to identify factors associated with methotrexate efficacy. The data were randomly stratified into training and testing sets (7:3). Nomograms were developed based on Cox regression analysis outcomes. The predictive accuracy and discriminative ability were determined using the concordance index (C-index) and calibration curves.

**Results:** Overall, 1,042 patients (CD: 791, UC: 251) were included. Independent factors associated with effective methotrexate monotherapy were younger age at diagnosis, latest therapy period, exclusive upper gastrointestinal tract disease (for CD), and longer duration between diagnosis and methotrexate initiation (for UC). For CD, predictors in the nomogram were gender, treatment era, tolerance, lesion site, perianal involvement, disease behaviour, and biologics requirements (C-index: 0.711 and 0.732 for training and validation cohorts, respectively). For UC, the factors were age at diagnosis and sex (C-index: 0.784 and 0.690 for training and validation cohorts, respectively). Calibration curves

**Abbreviation:** IBD, inflammatory bowel disease; CD, Crohn's disease; UC, ulcerative colitis; IBDU, IBD-unclassified; RCT, randomised control trial; ECCO, The European Crohn's and Colitis Organisation; OR, odds ratio; CI, confidence interval; GI, gastrointestinal tract.

demonstrated good agreement between predictions and actual observations.

#### KEYWORDS

inflammatory bowel disease, methotrexate monotherapy, prognostic analysis, Crohn's disease, ulcerative colitis

## Introduction

Inflammatory bowel diseases (IBD), including ulcerative colitis (UC), Crohn's disease (CD), and IBD-unclassified (IBDU), are disorders of chronic intestinal inflammation characterised by repeated aggravation and remission. Its increasing incidence has caused a huge economic burden on patients and country's healthcare systems (Kaplan, 2015; Rosen et al., 2015; Ng et al., 2017; Coward et al., 2019). Conventional immunomodulators, including methotrexate and thiopurines, have been the mainstay of IBD treatment for decades, especially to maintain remission in steroid-dependent or steroid-refractory patients (Sales-Campos et al., 2015; Torres et al., 2020a; Ran et al., 2021; Raine et al., 2022).

Methotrexate, which was initially developed in 1948 for the treatment of leukemia (Gabbani et al., 2016), has been clinically used for other diseases, including IBD, psoriasis, and rheumatoid arthritis (Tung and Maibach, 1990; Rajitha et al., 2017). Due to hepatotoxicity and gastrointestinal symptoms, patients treated with methotrexate should routinely undergo a full blood count and liver and pancreatic function tests during the treatment period (Cervoni et al., 2020; Vasudevan et al., 2020; Ran et al., 2021). In recent years, with the emergence of biological agents and concerns regarding their adverse effects, the application of methotrexate in IBD has been questioned.

The European Crohn's and Colitis Organisation (ECCO) Guidelines on Therapeutics for patients with CD recommend parenteral administration of methotrexate for the maintenance of remission in steroid-dependent patients (Torres et al., 2020b). A multicentre randomised control trial (RCT) (Feagan et al., 1995) study of 141 patients with chronically active CD found that after 16 weeks, 37 patients (39.4%) in the methotrexate group were in clinical remission compared with 9 patients (19.1%) in clinical remission in the placebo group ( $p = 0.025$ ), moreover the methotrexate group had received less prednisone than the placebo group ( $p = 0.025$ ). However, there is not enough evidence supporting methotrexate for the maintenance of remission in UC patients. A French study (Carbonnel et al., 2016) assessed the efficacy of methotrexate in inducing UC steroid-free remission, after 16 weeks, methotrexate group was not superior to placebo with regards to induction of steroid-free remission ( $p = 0.15$ ). Moreover, more patients in the placebo group experienced continued UC disease activity that required withdrawal from the aforementioned study. Further studies are needed to determine the effectiveness of methotrexate in UC maintenance therapy.

IBD has become a global problem characterised by a lifelong relapsing-remitting course, which diminishes the quality of life of patients and increases the consumption of healthcare resources. Thus, long-term efficacy is an important aspect of IBD treatment. A prior meta-analysis of 44 cohort studies suggested that for diagnosed patients, the 1-, 5- and 10- year surgery risk for patients with UC (colectomy with or without an ileal pouch-anal anastomosis) was 2.8%, 7.0%, and 9.6%, respectively, and for patients with CD (intestinal resection) was 12.3%, 18.0%, and 26.2%, respectively (Tsai et al., 2021). Because of the overall burden of IBD and its multifactorial aetiology, efforts should be made to improve the medical management of these inflammatory conditions. Identifying factors associated with surgery can help optimise the treatment plan.

## Methods

Here, we analyses the effectiveness of methotrexate in IBD treatment using the United Kingdom IBD BioResource ([www.ibdbioresource.nihr.ac.uk](http://www.ibdbioresource.nihr.ac.uk)), which launched in 2016 as part of the United Kingdom National Institute for Health Research BioResource (Parkes, 2019). The database contained a large number of patients whose information were ascertained at enrolment and updated annually, including demographic, clinical characteristics, and treatment informations. All patients signed consent forms allowing their information to be used by investigators. To obtain these data, a data application was submitted to IBD BioResource.

## Patient population

A total of 34,860 patients in over 100 hospitals in the United Kingdom signed up before the data lock on 9 November 2021.

The following patients were excluded: 1) those whose basic information on IBD or treatment response was missing; 2) those who underwent surgery in the same year of methotrexate initiation; 3) those who started or were on biological therapy in the year of methotrexate initiation; and 4) those for whom we could not determine whether biological therapy or surgery overlapped the period of methotrexate monotherapy. Patients with UC who underwent colectomy prior to methotrexate initiation were also excluded. Surgery is common in CD progression; therefore, those who underwent surgery before

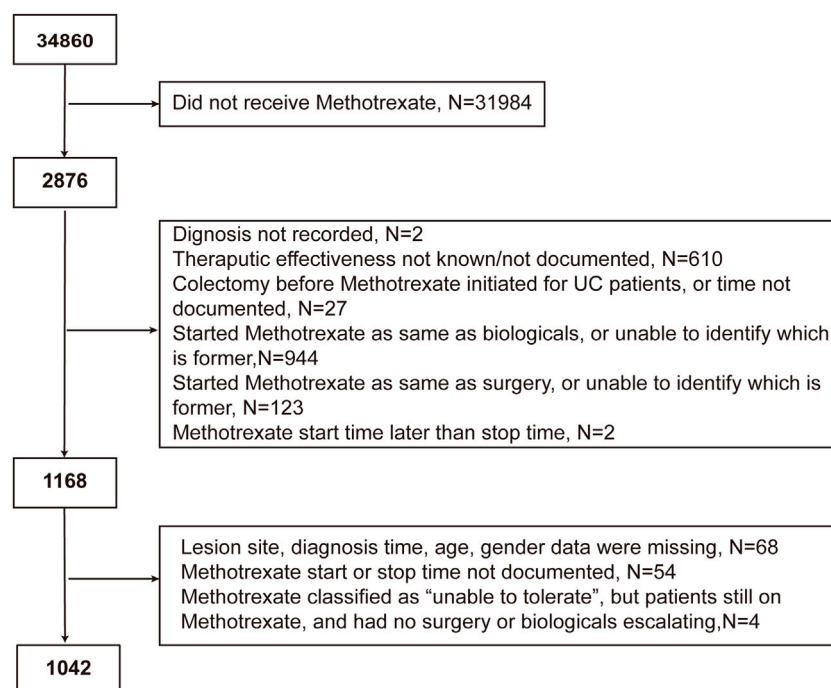


FIGURE 1

Flowchart of the study cohort depicting the inclusion and exclusion of patients from the analysis.

methotrexate initiation were not excluded. IBDU was classified as UC in our study, since we were able to find UC-related information of IBDU patients in the database.

## Treatment effectiveness

Effectiveness was evaluated by asking the question, “Did methotrexate work?” Effectiveness was defined as answering “yes” and avoiding escalation to alternative (biologics and/or surgical) treatment during the methotrexate treatment. We also discussed the treatment duration between the initiation of methotrexate and escalation to biologics or surgery (whichever occurred first), which also reflected the effectiveness of methotrexate.

## Definitions in study

The diagnosis of IBD was made based on radiographic, endoscopic, histologic criteria, or physician judgment. For CD, disease location were classified as “ileal” (L1), “colonic” (L2), “ileo-colonic” (L3), “exclusive upper gastrointestinal tract (GI) Crohn’s” (L4); disease behaviour were classified as “stenosing”, “internal penetrating” and “inflammatory and others”; internal penetrating disease was defined if patients had evidence of entero-enteric or entero-vesicular fistulae, intra-abdominal

abscesses or intestinal perforation; perianal involvement including tags, fissures, ulcers, perianal abscess, simple fistula (single fistula, little clinical problem), complex fistula (more than one or branching or recto-vaginal or major problem); surgery including colectomy, ileal or jejunal resection and the treatment of complications such as drainage of perianal abscess, perianal fistula repairment. For UC, disease location were divided into “proctitis” (E1), “left sided” (E2), “extensive” (E3); surgery referred colectomy. Smoking history included current and past smoking. In Cox regression, biologics requirement referred to that patients requiring biologics after methotrexate initiation and before surgery; glucocorticoid requirement referred to that patients receiving intravenous glucocorticoids before or after methotrexate initiation, but before surgery.

## Statistical analysis

Continuous variables are presented as mean  $\pm$  SD or median  $\pm$  interquartile range (IQR), while categorical variables are presented as percentages or proportions. Continuous variables were analysed using Student’s t-tests or paired t-tests, as appropriate, while categorical variables were analysed using the chi-square or Fisher’s exact test. The Cochran-Mantel-Haenszel (CMH) test was applied to compare effectiveness of methotrexate between UC and CD,

TABLE 1 Demographic and clinical characteristics and adverse reactions in 1042 patients who were treated with methotrexate monotherapy.

	CD (N = 791)			UC (N = 251)		
Age at diagnosis, median (IQR)	30.0 (20.0, 46.0)			38.0 (27.0, 49.0)		
Gender						
Male	330 (41.7%)			130 (51.8%)		
Female	461 (58.3%)			121 (48.2%)		
Smoke history						
No	481 (60.8%)			155 (61.8%)		
Yes	310 (39.2%)			96 (38.2%)		
CD Lesion						
Ileal (L1)	260 (32.9%)					
Colonic (L2)	232 (29.3%)					
Ileo-colonic (L3)	289 (36.5%)					
Exclusive upper GI Crohn's (L4)	10 (1.3%)					
Perianal involvement	220 (27.8%)					
Behaviour						
Stenosing	224 (28.3%)					
Internal penetrating	70 (8.8%)					
Inflammatory and others	497 (62.8%)					
UC Lesion						
Proctitis (E1)				22 (8.8%)		
Left sided (E2)				123 (49.0%)		
Extensive (E3)				106 (42.2%)		
Adverse reactions ( $\chi^2$ test of tolerating and intolerating groups)	Tolerate (N = 632)	Unable to tolerate (N = 159)	<i>p</i> value	Tolerate (N = 229)	Unable to tolerate (N = 22)	<i>p</i> value
Abdominal pain and diarrhea	14 (2.2%)	10 (6.3%)	<b>0.016</b>	3 (1.3%)	1 (4.5%)	0.310
Blood cell decrease	6 (0.9%)	3 (1.9%)	0.390	1 (0.4%)	0 (0.0%)	1.000
Deranged LFTs	26 (4.1%)	16 (10.1%)	<b>0.005</b>	8 (3.5%)	1 (4.5%)	0.570
Flu-like symptoms	14 (2.2%)	10 (6.3%)	<b>0.016</b>	3 (1.3%)	1 (4.5%)	0.310
Nausea	64 (10.1%)	48 (30.2%)	<b>&lt;0.001</b>	14 (6.1%)	7 (31.8%)	<b>&lt;0.001</b>
Others	63 (10.0%)	50 (31.4%)	<b>&lt;0.001</b>	35 (15.3%)	2 (9.1%)	0.750

Significant *p* values shown in bold; CD, Crohn's disease; UC, ulcerative colitis; CI, confidence interval; GI, gastrointestinal tract; IQR, interquartile ranges.

using stratified treatment initiation periods every 5 years. Multivariable logistic regression was performed to compare methotrexate effectiveness between patients with UC and CD, adjusting for age at diagnosis, gender, smoking history, treatment era, and time interval from diagnosis to methotrexate initiation. Next, univariate and multivariable logistic regression analyses were used to identify independent risk factors of methotrexate monotherapy effectiveness within UC and CD using the same covariates as above, but also including disease location (variables with  $p < 0.2$  were included in multivariable regression). The CD and UC cohorts were randomly divided into training and validation cohorts at a ratio of 7:3. Univariate Cox regression was then used to screen for variables that were significantly correlated with surgery occurrence in the training group with the same covariates as above, but also included biologics, glucocorticoid treatment, and previous surgery. Predictors with  $p < 0.2$  were fed into multivariable Cox regression

model. Backward stepwise selection based on Akaike's information criterion (AIC) was used to further eliminate redundant variables. The performance of the nomogram was evaluated using the concordance index (C-index) and a calibration curve in both the training and validation cohorts. A larger C-index indicates more accurate prognostic stratification. A *p*-value threshold of  $<0.05$  was considered statistically significant in the adjusted models. All statistical analyses were performed using the R software (version 4.1.0).

## Results

### Patient population

Of the 34,860 participants in the IBD BioResource at the data lock, 2876 (8.25%) had been treated with methotrexate (76.7%



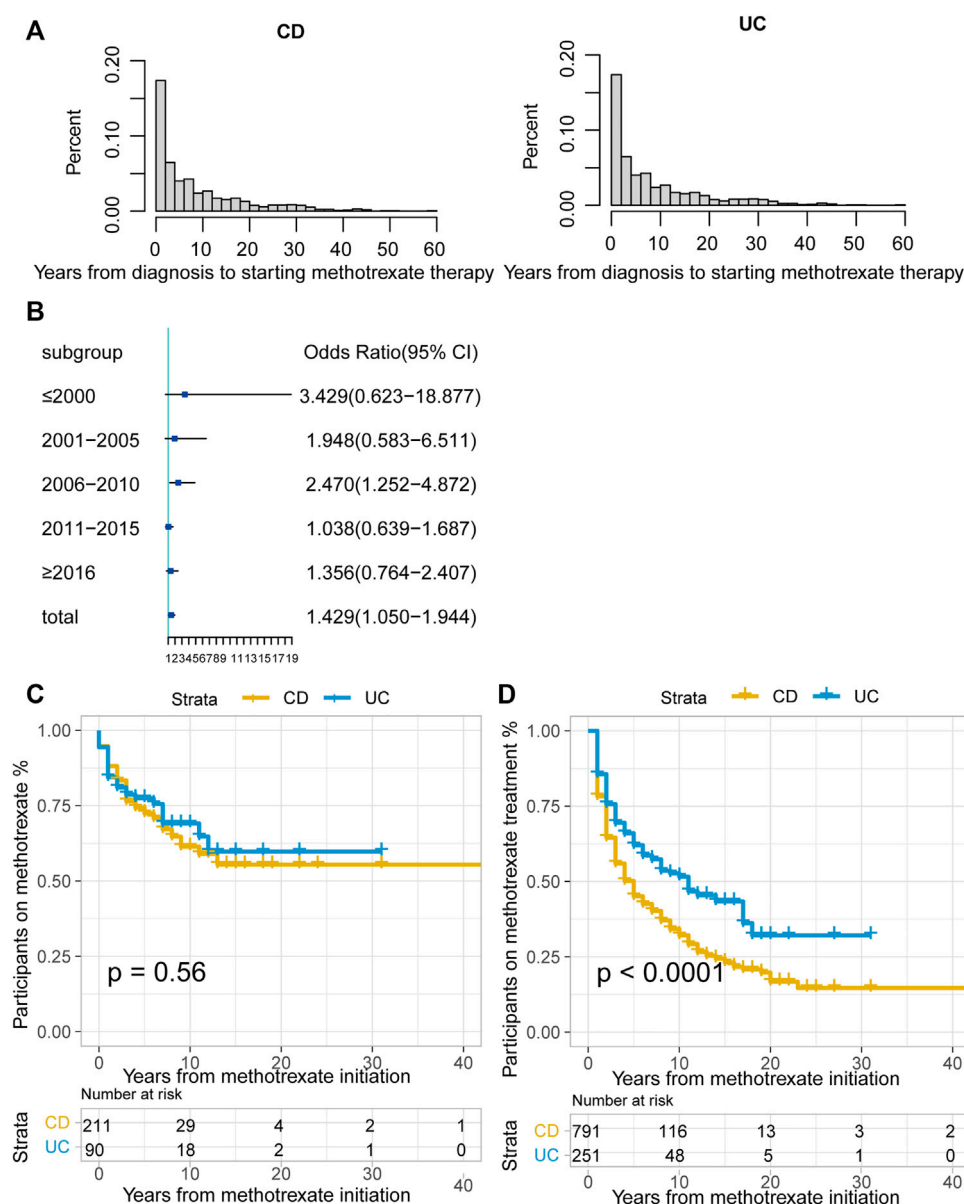


FIGURE 2

(A) Time interval (years) between CD or UC diagnosis and methotrexate monotherapy; (B) Odds ratio (OR) of methotrexate monotherapy being effective in UC vs. CD stratified by therapy period. The horizontal coordinates are OR values, blue boxes indicate OR values for every era, and black solid lines indicate 95% confidence intervals (CI) for OR values; (C) The Kaplan-Meier curve shows the duration of methotrexate treatment in patients in whom methotrexate monotherapy was considered effective; (D) The Kaplan-Meier curve shows the duration of effective methotrexate monotherapy without requirement for treatment escalation ( $p < 0.0001$  for log-rank test). (CD, Crohn's disease; UC, ulcerative colitis).

with CD, 21.7% with UC, and 1.6% with IBDU), either as monotherapy or combined with biologics. As shown in Figure 1, 1042 participants met the criteria for assessment of the effectiveness of methotrexate monotherapy [791 CD and 251 UC (including 15 IBDU cases)]. The baseline patient characteristics are presented in Table 1. The median age at CD and UC diagnosis was 30 and 38 years, respectively. Nausea was the most common adverse reaction in both

patients with CD and UC. Patients who could not tolerate methotrexate were prone to have a nauseous reaction (CD: 30.2% vs. 10.1%,  $p < 0.001$ ; UC: 31.8% vs. 6.1%,  $p < 0.001$ ).

Among the 1042 patients, 181 (17.4%) were unable to tolerate and had to stop methotrexate. The median duration of methotrexate treatment was 2 years (IQR: <1–6 years) for patients with CD and 3 years (IQR: 1–7 years) for patients with UC. The median time from diagnosis to methotrexate

TABLE 2 Multivariable analysis of factors affecting methotrexate monotherapy effectiveness.

Factor	Hazard ratio	95% CI	p Value
Diagnosis			
UC	1.359	0.988–1.863	
CD	reference		0.058
Therapy period	1.262	1.089–1.467	<b>0.002</b>
Time from diagnosis to methotrexate initiation	1.033	1.017–1.049	<b>&lt;0.001</b>
Gender			<b>0.023</b>
Female	1.395	1.049–1.861	
Male	Reference		
Age at diagnosis	1.038	1.027–1.050	<b>&lt;0.001</b>
Smoking history			0.131
Yes	0.795	0.589–1.069	
No	Reference		

Significant *p* values shown in bold; CD, Crohn's disease; UC, ulcerative colitis; CI, confidence interval.

initiation was 5 years in both patients with CD and UC (Figure 2A). A total of 486 (61.44%) patients with CD and 106 (42.2%) with UC received biologics after methotrexate monotherapy.

## Effectiveness of methotrexate monotherapy

Overall, 28.9% (301/1042) cases were regarded as effective, without escalation to biologics or surgery during treatment. Methotrexate monotherapy was effective in 35.5% of patients with UC (94/251) and a lower proportion of patients with CD (26.7%; 211/791,  $p = 0.001$ ). In methotrexate-tolerant group, it was effective in 39.3% of patients with UC and 32.8% of patients with CD ( $p = 0.074$ ).

According to the CMH test stratified by the treatment initiation era (every 5 years), methotrexate appeared to be more effective in UC than in CD (odds ratio [OR]: 1.429, 95% confidence interval [CI]: 1.050–1.944,  $p = 0.023$ ). The test of homogeneity of ORs indicated that there was no heterogeneity in the OR values of each therapy area ( $p = 0.237$ ). We used the forest map to display the OR values of each era, and the results were meaningful only for the 2006–2010 period (Figure 2B). There were no statistically significant differences between the treatment effectiveness of CD and UC in most eras.

Among patients with CD, the effective ratio of methotrexate monotherapy increased, whereas patients with UC showed a decreasing trend, except in the period after 2016 (Supplementary Figure S1). We then incorporated the treatment era along with other possible confounding factors into the multivariable logistic regression analysis (Table 2). The results demonstrated that there were no statistically significant differences in methotrexate

effectiveness between CD and UC (OR: 1.359, 95% CI: 0.988–1.863,  $p = 0.058$ ).

## Clinical characteristics and methotrexate monotherapy effectiveness

For patients with CD, multivariable analysis showed that after controlling for confounding factors, methotrexate monotherapy appeared to be more effective in older patients (OR: 1.028 per year; 95% CI: 1.017–1.040;  $p < 0.001$ ). In addition, the more recent the treatment, the better the treatment outcomes with methotrexate (OR: 1.363, 95% CI: 1.152–1.623,  $p = 0.001$ ). Patients with exclusive upper gastrointestinal tract disease were considered to receive more effective treatment than those with ileo-colon involvement (OR: 3.797, 95% CI: 0.973–14.855,  $p = 0.049$ ). Univariate logistic regression showed statistical significance for gender, disease behaviour, and perianal involvement; however, no statistical significance was obtained with multivariable logistic regression. No correlation was found between smoking history and the time from diagnosis to methotrexate initiation (Table 3).

For patients with UC, univariate logistic regression showed statistical significance for age, gender, smoking history, treatment eras, and time from diagnosis to methotrexate initiation; after controlling for confounding factors, the multivariable analysis only demonstrated statistical significance for the time interval from diagnosis to methotrexate initiation (Table 3).

## Duration of effective treatment

For patients in whom methotrexate monotherapy was deemed effective (301), 68.8% (207) were still treated with methotrexate at the time of data lock. The Kaplan-Meier curve illustrated that over

TABLE 3 Univariate and multivariable logistic regression analyses were performed to identify factors affecting the effectiveness of methotrexate monotherapy in patients with CD and UC.

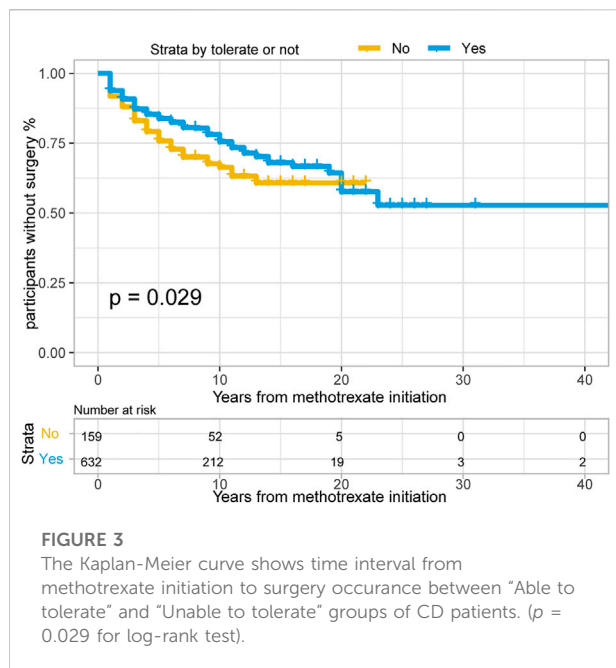
Factor	CD				UC			
	Univariable		Multivariable		Univariable		Multivariable	
	OR and 95%CI	<i>p</i> Value	OR and 95% CI	<i>p</i> Value	OR and 95%CI	<i>p</i> Value	OR and 95% CI	<i>p</i> Value
Age at diagnosis	1.036 (1.025–1.047)	<b>&lt;0.001</b>	1.028 (1.017–1.040)	<b>&lt;0.001</b>	1.013 (0.995–1.033)	<b>0.168</b>	1.009 (0.989–1.029)	0.391
Gender		<b>0.050</b>		0.143		<b>0.140</b>		
Female	1.384 (1.002–1.922)		1.293 (0.919–1.829)		1.477 (0.881–2.488)			
Male	Reference		Reference		Reference			
Smoking history		0.909				<b>0.076</b>		0.164
Yes	0.981 (0.709–1.353)				1.613 (0.951–2.737)		1.492 (0.848–2.625)	
No	Reference				Reference		Reference	
Therapy period	1.550 (1.318–1.833)	<b>&lt;0.001</b>	1.363 (1.152–1.623)	<b>0.001</b>	1.224 (0.934–1.626)	<b>0.152</b>	1.213 (0.923–1.614)	0.173
CD location								
Ileal	1.454 (0.988–2.146)	<b>0.058</b>	0.991 (0.652–1.505)	0.965				
Colonic	1.487 (1.000–2.216)	<b>0.050</b>	1.232 (0.806–1.883)	0.334				
Exclusive upper GI Crohn's	3.587 (0.970–13.275)	<b>0.049</b>	3.797 (0.973–14.855)	<b>0.049</b>				
Ileo-colonic	Reference		Reference					
UC location								
Proctitis (E1)					1.142 (0.436–2.892)	0.781		
Left sided (E2)					0.825 (0.479–1.421)	0.487		
Extensive (E3)					Reference			
Behaviour								
Stenosing	0.665 (0.457–0.955)	<b>0.030</b>	0.863 (0.579–1.274)	0.462				
Internal penetrating	0.431 (0.210–0.813)	<b>0.014</b>	0.709 (0.333–1.402)	0.345				
Inflammatory and other	Reference		Reference					
Perianal involvement		<b>0.002</b>		0.245				
Yes	0.540 (0.364–0.787)		0.781 (0.511–1.178)					
No	Reference		Reference					
Time from diagnosis to methotrexate initiation	1.005 (0.990–1.020)	0.482		1.041 (1.011–1.071)	<b>0.006</b>	1.056 (1.021–1.092)	<b>0.002</b>	

Significant *p* values shown in bold; CD, Crohn's disease; UC, ulcerative colitis; OR, odds ratio; CI, confidence interval; GI, gastrointestinal tract.

50% of this group was still on methotrexate at data lock in both the CD and UC groups. (Figure 2C,  $p = 0.56$ , log-rank test).

Of the patients treated with methotrexate monotherapy, 532 (51.1%) required treatment escalation after a median time of 5 years in the CD group, 11 years in the UC group, and earlier escalation in the CD group. (Figure 2D;  $p < 0.0001$  for the log-rank test).

Of the patients treated with methotrexate monotherapy, at 1 and 3 years, 78.3% and 55.9% of patients with CD and 85.7% and 69.5% of patients with UC, respectively, remained on methotrexate and did not require treatment escalation to biologics or surgery (Supplementary Table S1).



## Development and validation of prognostic nomograms for predicting surgery in CD patients treated initially with methotrexate monotherapy

In total, 382/791 patients with CD (48.3%) treated with methotrexate monotherapy underwent surgery, 202/791 (25.5%) patients underwent at least two surgeries, and 198/791 (25.0%) underwent surgery after methotrexate initiation. The rates of 1-, 3- and 5- years no-surgery were 93.4%, 86.4% and 82.1%, respectively. A total of 159 patients with CD could not tolerate treatment, and their treatment time interval to surgery was modestly shorter than that of the 632 methotrexate-tolerant patients (Figure 3;  $p = 0.029$  for the log-rank test).

Surgery occurrence and time interval in the treatment process are important indicators of treatment effectiveness. A total of 791 patients with CD were randomly divided into training and validation cohorts at a ratio of 7:3. There was no statistically significant difference between the two groups (Supplementary Table S2). Finally, the variables included in the nomogram were sex, disease location, disease behaviour, perianal involvement, tolerance, treatment period, and biological requirements based on outcomes of Cox regression (Table 4; Figure 4). The C-index was 0.711 [0.664–0.758] in the training cohort and 0.732 [0.661–0.803] in the validation cohort. As shown in Figure 5, the calibration curves showed good agreement between predictions of 1-, 3-, and 5- year of surgery occurrence and the actual observations in both the training and validation cohorts.

## Establishment and validation of prognostic nomograms for predicting surgery in UC patients treated initially with methotrexate monotherapy

Of the 251 patients with UC, 15 (6.0%) underwent colectomy. The indications for colectomy included acute severe colitis in 6 patients (40%), chronic continuous colitis in 6 patients (40%), dysplasia in 1 patient (6.7%), and undocumented reasons in 2 patients. The 1-, 3- and 5- years no-surgery rates were 97.6%, 96.0%, and 95.1%, respectively. Overall, 4/22 (18.2%) patients who were unable to tolerate methotrexate required colectomy, compared with 11/229 (4.8%) patients who could tolerate methotrexate. Time to colectomy was shorter in individuals unable to tolerate methotrexate than in those able to tolerate methotrexate (Figure 6,  $p = 0.013$  for log-rank test).

251 UC patients with were randomly divided into training and validation cohorts at a ratio of 7:3. There was no statistically significant difference between the two groups (Supplementary Table S3). All factors were analysed using univariate regression analysis to identify potential risk variables. Potential risk factors ( $p < 0.2$  in univariate regression analysis) were selected for stepwise regression analysis with backward selection procession by AIC. Finally, the variables included in the nomogram were sex and age at UC diagnosis (Table 4; Figure 7). The C-index was 0.784 [0.600–0.968] and 0.690 [0.502–0.878] in the training and validation cohorts, respectively. As shown in Figure 8, the calibration curves showed good agreement between the predictions of surgery occurrence and the actual observations in both the training and validation cohorts.

## Discussion

Through this retrospective study that enrolled 791 patients with CD and 251 with UC, we report the first large-scale study assessing the clinical characteristics and patient-level outcomes of patients with CD and UC treated with methotrexate, using the IBD BioResource. Currently, non-biological treatments remain valuable approaches for patients with IBD; however, their long-term outcome data remain sparse. In our study, 8.25% of patients had been treated with methotrexate, either as a monotherapy or combination therapy, and methotrexate provided an effective long-term treatment for 35.5% of patients with UC and 26.7% with CD without escalation therapy. A multicentre retrospective study in the Netherlands suggested that 86%, 63%, 47%, and 20% of patients with CD who were treated with methotrexate monotherapy obtained clinical benefits at 6, 12, 24, and 60 months, respectively (Seinen et al., 2013). Our study also evaluated the tolerability and safety of methotrexate; of the 1042 patients, 181 (17.4%) patients were unable to tolerate and had to stop methotrexate, consistent with previous studies (Herfarth et al., 2016). Nausea was the most common adverse

TABLE 4 Univariate and multivariable Cox regression for determining factors affecting surgery in patients with CD and UC treated with methotrexate monotherapy.

Factor	CD				UC			
	Univariable		Multivariable (backward stepwise)		Univariable		Multivariable (backward stepwise)	
	OR and 95% CI	<i>p</i> Value	OR and 95% CI	<i>p</i> Value	OR and 95% CI	<i>p</i> Value	OR and 95% CI	<i>p</i> Value
Age at diagnosis	0.981 (0.969–0.992)	<b>&lt;0.001</b>			0.940 (0.885–0.998)	<b>0.042</b>	0.936 (0.880–0.996)	<b>0.038</b>
Gender		<b>0.019</b>		<b>0.040</b>		<b>0.083</b>		0.070
Female	0.681 (0.494–0.938)		0.710 (0.512–0.985)		0.156 (0.019–1.274)		0.143 (0.018–1.172)	
Male	Reference		Reference		Reference		Reference	
Smoking history		0.638				0.472		
Yes	0.924 (0.666–1.283)				0.555 (0.112–2.759)			
No	Reference				Reference			
Therapy period	0.769 (0.663–0.892)	<b>&lt;0.001</b>	0.810 (0.695–0.943)	<b>0.007</b>	0.928 (0.449–1.920)	0.841		
Disease location								
Ileal	0.740 (0.509–1.075)	0.114	0.935 (0.624–1.401)	0.745				
Colonic	0.418 (0.271–0.645)	<b>&lt;0.001</b>	0.537 (0.342–0.841)	<b>0.007</b>	<0.001 (0- Infinity)	0.999		
Exclusive upper GI Crohn's	1.001 (0.315–3.181)	0.998	1.510 (0.462–4.936)	0.495	0.518 (0.124–2.172)	0.368		
Ileo-colonic	Reference		Reference		Reference			
Behaviour								
Stenosing	2.137 (1.495–3.053)	<b>&lt;0.001</b>	1.843 (1.272–2.671)	<b>0.001</b>				
Internal penetrating	3.815 (2.453–5.933)	<b>&lt;0.001</b>	2.775 (1.734–4.441)	<b>&lt;0.001</b>				
Inflammatory and other	Reference		Reference					
Perianal involvement		<b>&lt;0.001</b>		<b>0.009</b>				
Yes	1.923 (1.391–2.659)		1.609 (1.125–2.299)					
No	Reference		Reference					
Time from diagnosis to methotrexate initiation	0.991 (0.974–1.008)	0.286		1.000 (0.918–1.088)	0.991			
Tolerate		<b>0.074</b>		<b>0.004</b>		<b>0.079</b>		
Yes	0.716 (0.497–1.032)		0.560 (0.379–0.828)		0.238 (0.048–1.179)			
No	Reference		Reference		Reference			
Previous surgery		<b>0.043</b>						
Yes	1.403 (1.011–1.947)							
No	Reference							
Biologics requirement		<b>0.151</b>		<b>0.004</b>		0.664		
Yes	0.790 (0.572–1.090)		0.605 (0.430–0.852)		1.36 (0.340–5.438)			
No	Reference		Reference		Reference			
Glucocorticoid requirement		0.459				0.998		

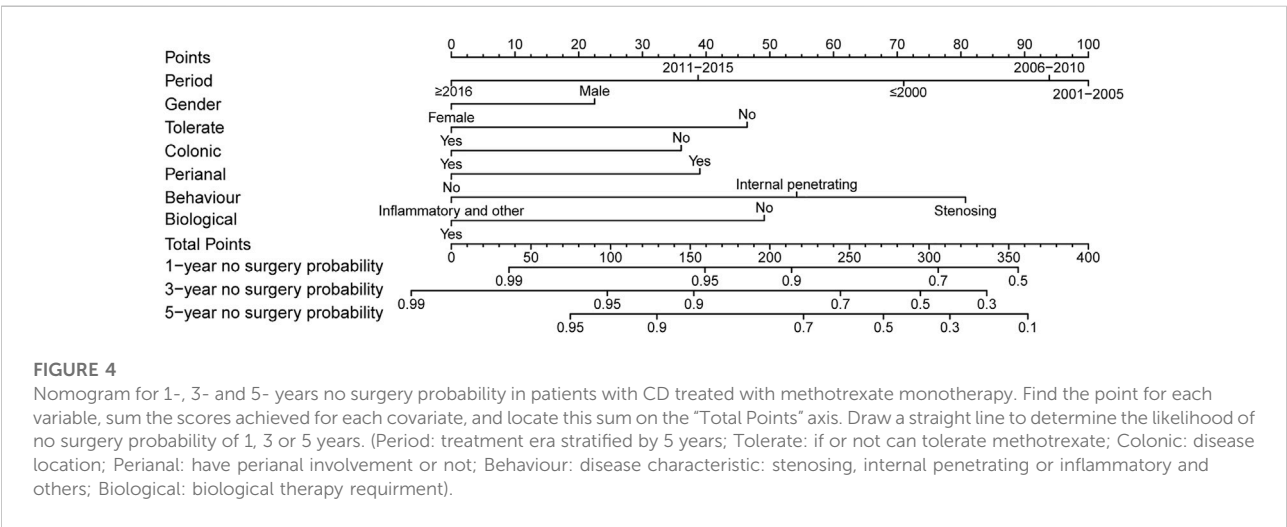
(Continued on following page)



TABLE 4 (Continued) Univariate and multivariable Cox regression for determining factors affecting surgery in patients with CD and UC treated with methotrexate monotherapy.

Factor	CD				UC			
	Univariable		Multivariable (backward stepwise)		Univariable		Multivariable (backward stepwise)	
	OR and 95% CI	<i>p</i> Value	OR and 95% CI	<i>p</i> Value	OR and 95% CI	<i>p</i> Value	OR and 95% CI	<i>p</i> Value
Yes	1.191 (0.750–1.892)				<0.001 (0- Infinity)			
No	Reference				Reference			

Significant *p* values shown in bold; CD, Crohn's disease; UC, ulcerative colitis; OR, odds ratio; CI, confidence interval; GI, gastrointestinal tract.



reaction, especially in the intolerance group; hepatotoxicity and fatigue were also observed without fatal adverse reactions. A retrospective study published in 2022 reported that methotrexate-induced nausea was noted in 34% of paediatric patients with IBD (Mehta et al., 2022). In our study, over 50% of methotrexate-effective patients were still on treatment at data lock in the two groups. Methotrexate treatment is relatively safe, with a low rate of adverse reactions and no fatal adverse reactions.

In this study, methotrexate appeared effective in both CD and UC, with no difference, consistent with a previous cohort study (Wahed et al., 2009). The ECCO Guidelines recommend methotrexate for the maintenance of remission in patients with steroid-dependent CD, however, for patients with UC, no clear application guidelines are available. In our study, the CMH test was more effective in UC than in CD; we also found evidence of increased methotrexate effectiveness in CD and a decreasing trend in UC (Supplementary Figure S1). Multivariable logistic regression analysis showed no statistical significance between CD and UC ( $p = 0.058$ ) in the adjusted models. By further

comparison, methotrexate had a better effect on patients with UC than on those with CD in avoiding escalation treatment (Figure 2D). Surgical risk factors include perianal involvement, internal penetration, and stenosis. After excluding these patients, the Kaplan-Meier curve showed that the protective effect of methotrexate on CD was significantly increased, and the gap between CD and UC was decreased (Supplementary Figure S2 vs. Figure 2D). We excluded patients with UC who had undergone colectomy, which resulted in a bias for milder disease among the participants. Those who had undergone CD-related surgery were analysed, showing a bias in disease severity. Our study is based in a single region of the United Kingdom with a limited number of cases, and endoscopy estimation was not available. In the future, prospective RCTs are needed to compare the efficacy of methotrexate in CD and UC.

A previous review considered that maintenance methotrexate treatment provides acceptable remission rates for treatment periods up to 3 years, after which relapse is frequent and occurs early (usually within 1 year) (Fraser et al.,

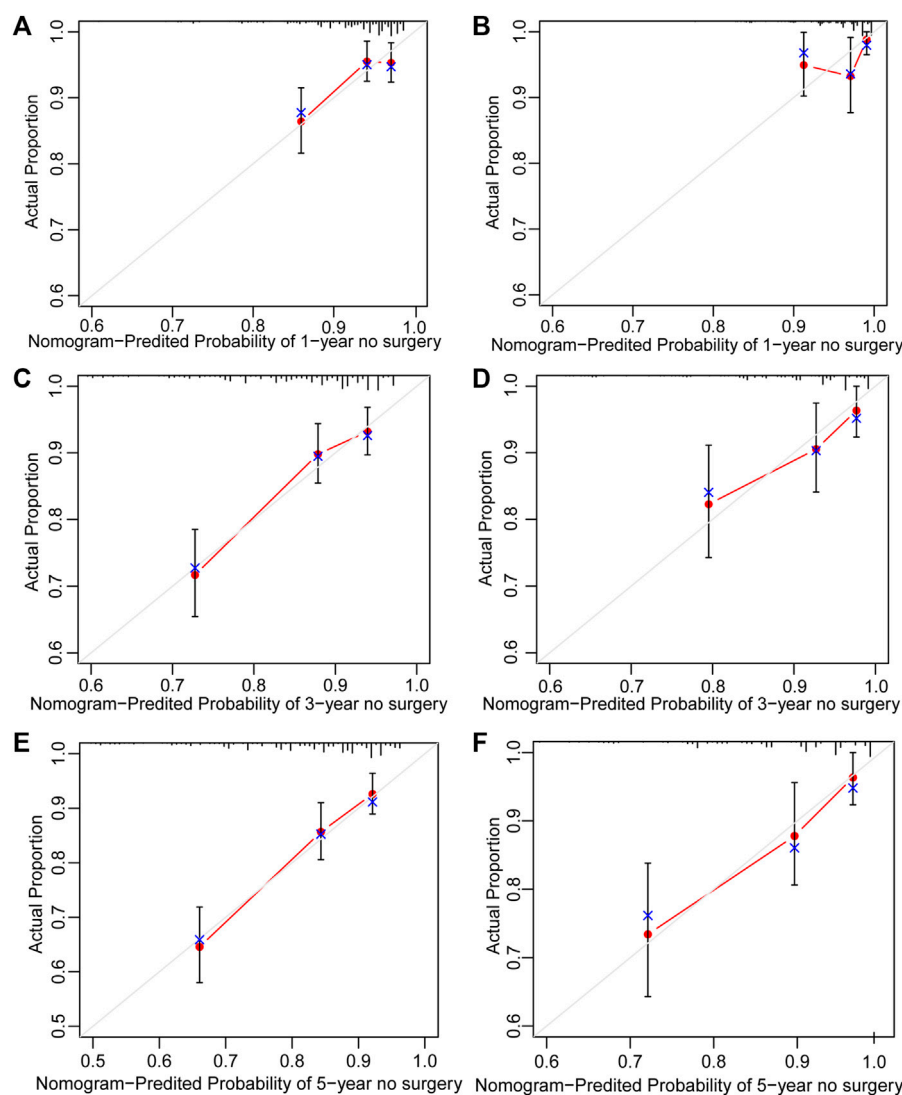


**FIGURE 5**

Calibration curve of nomogram for predicting no surgery occurrence at (A) 1-, (C) 3-, and (E) 5- years in the training cohort, and at (B) 1-, (D) 3-, and (F) 5- years in the validation cohort. The actual proportion is plotted on the Y-axis and the nomogram-predicted probability is plotted on the X-axis. (CD, Crohn's disease).

2002). In the current study, over 50% of the patients in whom treatment was deemed effective were still on methotrexate at the data lock, with a median treatment duration of 5 (CD) and 11 (UC) years. It seems that methotrexate is adhered to for prolonged periods (and effective), despite well-documented concerns about increased risk of hepatotoxicity and long-term blood cell reduction.

Our analysis identified specific patient subgroups that were most likely to respond to methotrexate. These included older patients treated in the recent period with exclusive upper GI disease for CD. Older patients with better outcomes may have a milder course (Charpentier et al., 2014). Although the  $p$  value of

upper GI disease was less than 0.05, the OR value contains 1, and previous studies have shown that upper GI disease ( $p = 0.042$ ) was significantly associated with an increased risk of surgical recurrence (Frolkis et al., 2013), larger trials are needed to confirm this. For UC, in multivariable analysis, the time interval from diagnosis to methotrexate initiation was an independent factor associated with effectiveness of treatment (OR: 1.056, 95% CI: 1.021–1.092 per year). After further analysis, we found that the methotrexate-tolerant group had a longer median time interval between diagnosis and methotrexate initiation than the methotrexate-intolerant group (5 years vs. 3 years).

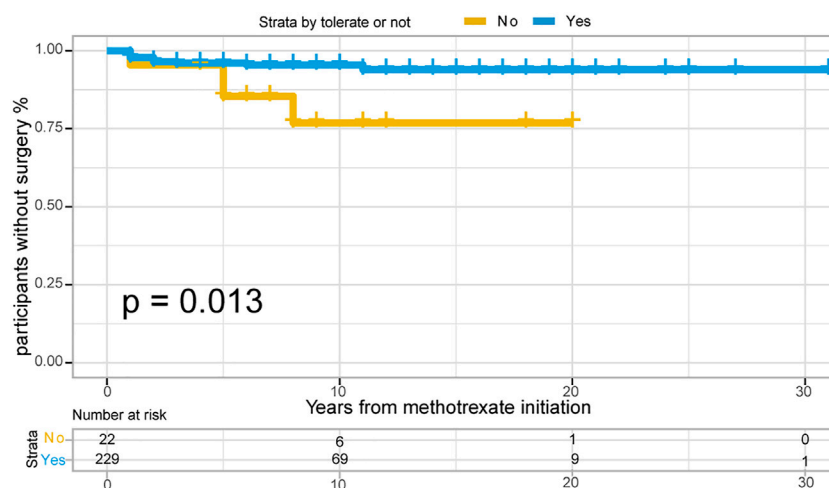


FIGURE 6

The Kaplan-Meier curve shows time interval from methotrexate initiation to surgery occurrence between "Able to tolerate" and "Unable to tolerate" groups of UC patients. ( $p = 0.013$  for log-rank test).

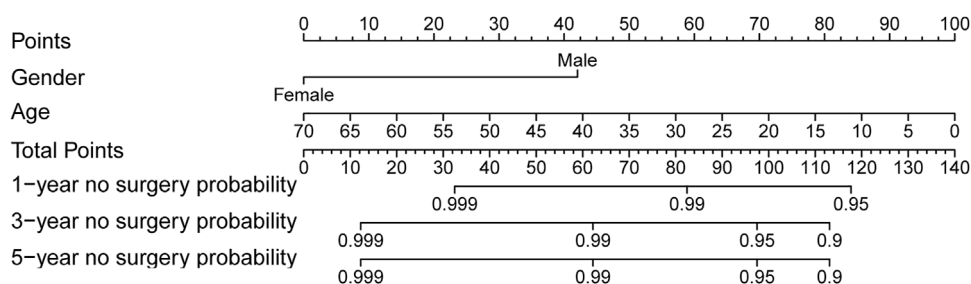


FIGURE 7

Nomogram for 1-, 3- and 5- years no surgery probability in UC patients treated with methotrexate monotherapy. Find the point for each variable, sum the scores achieved for each covariate, and locate this sum on the "Total Points" axis. Draw a straight line to determine the likelihood of no surgery probability of 1, 3 or 5 years. (Age: age at UC diagnosis).

We further analysed the patients' clinical characteristics and occurrence of surgery. Identification of patients at the highest risk of disease progression, who have the greatest chance of benefiting from early initiation of effective therapy, is an aspirational goal. For CD, 202/791 (25.5%) patients underwent at least two surgeries, and 198/791 (25.0%) underwent surgery after methotrexate initiation. We identified factors associated with surgery occurrence through univariate Cox regression as follows: age at diagnosis, gender, therapy era, disease location, perianal involvement, disease behaviour, tolerance, previous surgery history, biologics, and glucocorticoid treatment. For UC, 15/251 (6.0%) patients required colectomy after methotrexate treatment. Univariate Cox regression analysis revealed that the age at diagnosis, sex, and tolerance were significantly associated with early surgery. We then performed stepwise regression based on AIC to select factors into the final

prognostic model so that clinicians could identify patients at higher risk of surgery and implement more aggressive medical management as required.

Surgery is generally considered as a last-resort treatment for IBD. A review published in 2013 suggested that the 1- and 5- year surgery risk after diagnosis of UC was 4.9% and 11.6%, respectively, and that of CD was 16.3% and 33.3%, respectively (Samuel et al., 2013a). For patients diagnosed in the 21st century, the cumulative 5-year risk of surgery was 7.0% for UC and 17.8% for CD, substantially lower than the previous review (Tsai et al., 2021). In our study, for CD, the rates of 1- and 5- year surgery occurrence were 6.6% and 17.9%, respectively. For UC, the rates of 1- and 5- year surgery occurrence were 2.4% and 4.9%, respectively. In our study, the surgery rates were lower than those reported, reflecting the effectiveness of methotrexate. Although the number of surgeries

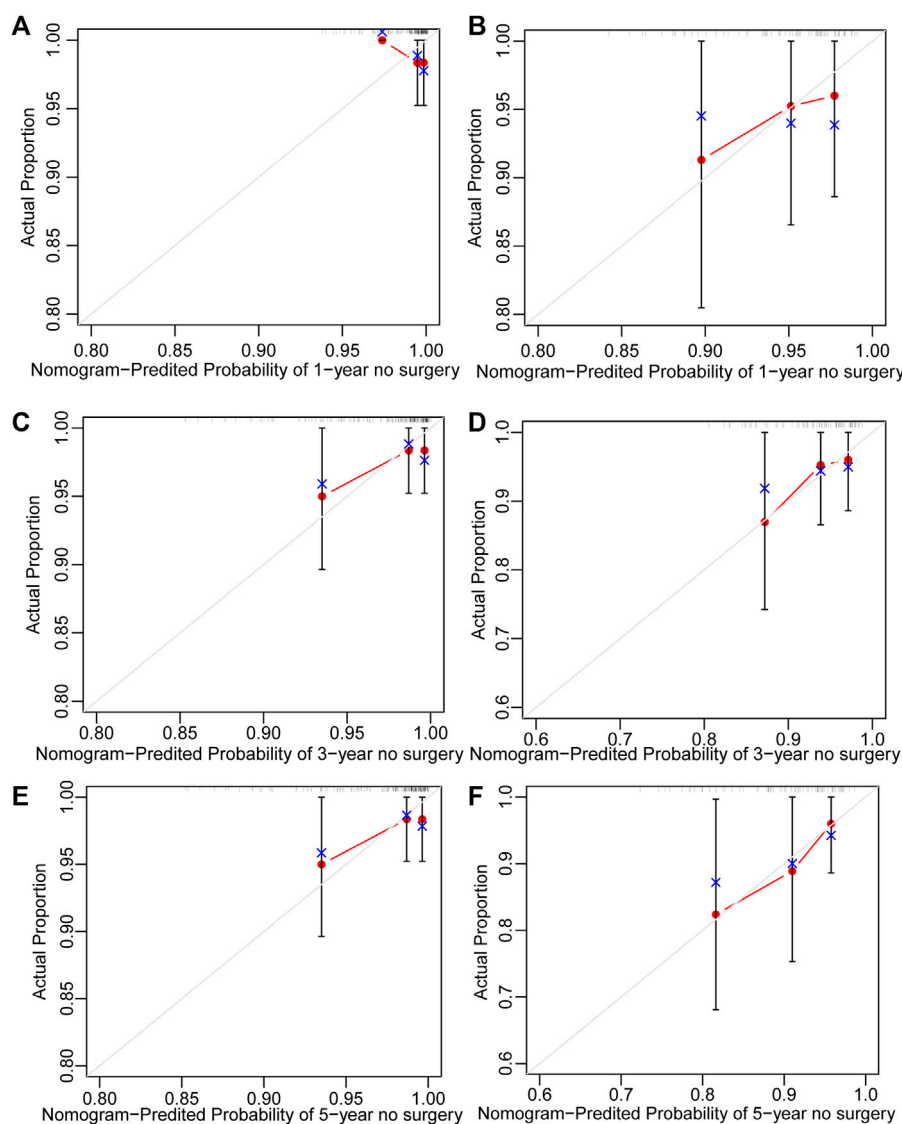


**FIGURE 8**

Calibration curve of nomogram for predicting no surgery occurrence at (A) 1-, (C) 3-, and (E) 5-years in the training cohort, and at (B) 1-, (D) 3-, and (F) 5- years in the validation cohort. The actual proportion is plotted on the Y-axis and the nomogram-predicted probability is plotted on the X-axis. (UC: ulcerative colitis).

has been decreasing, it still poses a huge burden to patients. One of the biggest challenges clinicians face today is predicting which patients are prone to surgery requirements. Those at the highest risk of surgery may benefit the most from early surgery.

As the nomograms show, female is a predictor of a lower risk of surgical treatment for both, patients with CD and UC. A consensus has been reached that male sex may be associated with a greater risk of growth impairment, and growth impairment diagnosis predicts an increased risk of bowel surgery (Ricciuto et al., 2021). A previous study of UC showed that male sex was significantly associated with colectomy risk (Samuel et al., 2013b; Macaluso et al., 2019). Jia-Yin et al. (Yao et al., 2020) developed a nomogram to predict 1-year

surgery risk in patients with CD without the sex variable. The people we enrolled were all from the United Kingdom, therefore, regional bias should be accounted for.

Smoking cessation is generally advised for patients with CD. However, in our study, smoking history was not a predictor of surgery occurrence in either UC or CD. Current smokers had a reduced risk of UC (odds ratio [OR]:0.61) and an increased risk of developing CD (OR: 1.74) (García Rodríguez et al., 2005). However, most studies showed that smoking status was not associated with surgical requirements (Hoie et al., 2007; Solberg et al., 2014). However, we could not confirm this association in the present study.

Regarding disease location, consistent with a previous study (Ricciuto et al., 2021), isolated colonic disease was associated with fewer surgeries. In our study, the colonic type had a lower surgery risk than the ileo-colonic type (OR: 0.537, 95% CI: 0.342–0.841), and was included in the nomogram as a predictor. For patients with UC, extensive disease is viewed as a risk factor for colectomy. Extensive colonic disease can be considered as a manifestation of severe disease (Hoie et al., 2007; Macaluso et al., 2019). In our study, the long-term efficacy of methotrexate for UC was independent of lesion location. Consistent with a previous study (Peyrin-Biroulet et al., 2010; Thia et al., 2010; Peyrin-Biroulet et al., 2012; Solberg et al., 2014; Yao et al., 2020), perianal involvement and behaviour were included in the nomogram as predictors of the occurrence of surgery. A review of 70 studies concluded that a younger age at diagnosis was associated with a higher risk of colectomy (Macaluso et al., 2019). Further analysis showed that colonic disease accounted for 28.5% (112/393) of patients below 30 years of age and 30.2% (120/398) of patients above 30 years of age. However, we believe that this is not enough to cause the difference and speculate that the risk of surgery is higher in young patients due to their own disease characteristics. Patients who received biologics after methotrexate initiation had a lower risk of surgery (OR: 0.605, 95% CI: 0.430–0.852). This suggests that for patients who cannot be controlled by traditional drugs or who do not respond to drugs, biologic agents should be sought in time to reduce the risk of surgery.

It is noteworthy that the value of surgery for IBD is changing (Buskens and Bemelman, 2019). We need to be aware that surgery should be considered as an alternative treatment rather than a salvage procedure after failed conservative treatment. We hope to use the nomograms to identify the high risk of surgery and administer more aggressive treatments to achieve better outcomes.

## Limitations

Our study had some limitations. In our study, the effectiveness of treatment was judged according to patients' subjective perception and whether there is treatment escalation. There is no standard disease activity score to evaluate the efficacy. Our study was based on IBD BioResource, a United Kingdom hospital-based program, and hence there may be regional limitations and disease severity bias, which may include individuals with more severe disease. Our results are based on a large sample, so we believe that this study is of certain significance.

## Conclusion

In conclusion, methotrexate was effective in both, patients with CD and UC, with no significant difference between two groups.

Methotrexate is well tolerated by most individuals. Male sex, methotrexate intolerance, and perianal involvement are predictors of early surgery. Treatment in the modern era, colonic and inflammatory diseases, and biological requirements are predictors of low surgery occurrence for CD. Male sex and younger age at diagnosis are predictors of early surgery in patients with UC. The nomograms can predict the 1-, 3- and 5- year risk of surgery for patients with CD and UC, who were initially treated with methotrexate monotherapy, with accuracy and discriminative ability.

## Data availability statement

Publicly available datasets were analyzed in this study. This data can be found here: We obtained the data from the United Kingdom IBD BioResource ([www.ibdbioresource.nihr.ac.uk](http://www.ibdbioresource.nihr.ac.uk)), which launched in 2016 as part of the United Kingdom National Institute for Health Research BioResource. To obtain these data, a data application was submitted to IBD BioResource (<https://www.ibdbioresource.nihr.ac.uk/index.php/resources/applying-for-access-to-the-ibd-bioresource-panel-2/>).

## Ethics statement

The studies involving human participants were reviewed and approved by Ethics Committee of Shengjing Hospital affiliated to China Medical University. Written informed consent to participate in this study was provided by the participants' legal guardian/next of kin.

## Author contributions

MW, LS, and BC contributed to the conception and design of the study, MW and LS contributed to the data collection, statistical analysis, MW, JZ, and HW contributed to manuscript drafting. CZ, LS, and BC contributed to study supervision and critically article revising. All authors contributed to the manuscript writing and approved to the submitted version.

## Funding

The authors have not declared a specific grant for this research from any funding agency in the public, commercial or not-for-profit sectors.

## Acknowledgments

We thank NIHR BioResource volunteers for their participation, and gratefully acknowledge NIHR BioResource



centres, NHS Trusts and staff for their contribution. We thank the National Institute for Health and Care Research, NHS Blood and Transplant, and Health Data Research United Kingdom as part of the Digital Innovation Hub Programme. The views expressed are those of the author(s) and not necessarily those of the NHS, the NIHR or the Department of Health and Social Care.

## Conflict of interest

The authors declare that the research was conducted in the absence of any commercial or financial relationships that could be construed as a potential conflict of interest.

## References

- Buskens, C. J., and Bemelman, W. A. (2019). The surgeon and inflammatory bowel disease. *Br. J. Surg.* 106 (9), 1118–1119. doi:10.1002/bjs.11282
- Carbonnel, F., Colombel, J. F., Filippi, J., Katsanos, K. H., Peyrin-Biroulet, L., Allez, M., et al. (2016). Methotrexate is not superior to placebo for inducing steroid-free remission, but induces steroid-free clinical remission in a larger proportion of patients with ulcerative colitis. *Gastroenterology* 150 (2), 380–388. e4. doi:10.1053/j.gastro.2015.10.050
- Cervoni, J. P., Alby-Lepresle, B., Weil, D., Zhong, P., Aubin, F., Wendling, D., et al. (2020). A pragmatic non-invasive assessment of liver fibrosis in patients with psoriasis, rheumatoid arthritis or Crohn's disease receiving methotrexate therapy. *Clin. Res. Hepatol. Gastroenterol.* 44S, 100003. doi:10.1016/j.clirex.2020.100003
- Charpentier, C., Salleron, J., Savoye, G., Fumery, M., Merle, V., Laberrenne, J. E., et al. (2014). Natural history of elderly-onset inflammatory bowel disease: A population-based cohort study. *Gut* 63 (3), 423–432. doi:10.1136/gutjnl-2012-303864
- Coward, S., Clement, F., Benchimol, E. I., Bernstein, C. N., Avina-Zubieta, J. A., Bitton, A., et al. (2019). Past and future burden of inflammatory bowel diseases based on modeling of population-based data. *Gastroenterology* 156 (5), 1345–1353. e4. doi:10.1053/j.gastro.2019.01.002
- Feagan, B. G., Rochon, J., Fedorak, R. N., Irvine, E. J., Wild, G., Sutherland, L., et al. (1995). Methotrexate for the treatment of Crohn's disease. The North American Crohn's study group investigators. *N. Engl. J. Med.* 332 (5), 292–297. doi:10.1056/NEJM199502033320503
- Fraser, A. G., Morton, D., McGovern, D., Travis, S., and Jewell, D. P. (2002). The efficacy of methotrexate for maintaining remission in inflammatory bowel disease. *Aliment. Pharmacol. Ther.* 16, 693–697. doi:10.1046/j.1365-2036.2002.01227.x
- Frolkis, A. D., Dykeman, J., Negrón, M. E., Debruyjn, J., Jette, N., Fiest, K. M., et al. (2013). Risk of surgery for inflammatory bowel diseases has decreased over time: A systematic review and meta-analysis of population-based studies. *Gastroenterology* 145 (5), 996–1006. doi:10.1053/j.gastro.2013.07.041
- Gabbani, T., Deiana, S., Lunardi, S., Manetti, N., and Annesse, V. (2016). Safety profile of methotrexate in inflammatory bowel disease. *Expert Opin. Drug Saf.* 15 (10), 1427–1437. doi:10.1080/14740338.2016.1218468
- García Rodríguez, L. A., González-Pérez, A., Johansson, S., and Gonzalez-Perez, A. (2005). Risk factors for inflammatory bowel disease in the general population. *Aliment. Pharmacol. Ther.* 22 (4), 309–315. doi:10.1111/j.1365-2036.2005.02564.x
- Herfarth, H. H., Kappelman, M. D., Long, M. D., and Isaacs, K. L. (2016). Use of methotrexate in the treatment of inflammatory bowel diseases. *Inflamm. Bowel Dis.* 22 (1), 224–233. doi:10.1097/MIB.0000000000000589
- Hoie, O., Wolters, F. L., Riis, L., Bernklev, T., Aamodt, G., Clofent, J., et al. (2007). Low colectomy rates in ulcerative colitis in an unselected European cohort followed for 10 years. *Gastroenterology* 132 (2), 507–515. doi:10.1053/j.gastro.2006.11.015
- Kaplan, G. G. (2015). The global burden of IBD: From 2015 to 2025. *Nat. Rev. Gastroenterol. Hepatol.* 12 (12), 720–727. doi:10.1038/nrgastro.2015.150
- Macaluso, F. S., Cavallaro, F., Felice, C., Mazza, M., Armuzzi, A., Gionchetti, P., et al. (2019). Risk factors and timing for colectomy in chronically active refractory ulcerative colitis: A systematic review. *Dig. Liver Dis.* 51 (5), 613–620. doi:10.1016/j.dld.2019.01.018
- Mehta, R. S., Taylor, Z. L., Martin, L. J., Rosen, M. J., and Ramsey, L. B. (2022). SLCO1B1 \*15 allele is associated with methotrexate-induced nausea in pediatric patients with inflammatory bowel disease. *Clin. Transl. Sci.* 15 (1), 63–69. doi:10.1111/cts.13130
- Ng, S. C., Shi, H. Y., Hamidi, N., Underwood, F. E., Tang, W., Benchimol, E. I., et al. (2017). Worldwide incidence and prevalence of inflammatory bowel disease in the 21st century: A systematic review of population-based studies. *Lancet* 390 (10114), 2769–2778. doi:10.1016/S0140-6736(17)32448-0
- Parkes, M. (2019). IBD BioResource: An open-access platform of 25 000 patients to accelerate research in Crohn's and colitis. *Gut* 68 (9), 1537–1540. doi:10.1136/gutjnl-2019-318835
- Peyrin-Biroulet, L., Harmsen, W. S., Tremaine, W. J., Zinsmeister, A. R., Sandborn, W. J., and Loftus, E. V. (2012). Surgery in a population-based cohort of Crohn's disease from Olmsted County, Minnesota (1970–2004). *Am. J. Gastroenterol.* 107, 1693–1701. doi:10.1038/ajg.2012.298
- Peyrin-Biroulet, L., Loftus, E. V., Jr., Colombel, J. F., and Sandborn, W. J. (2010). The natural history of adult Crohn's disease in population-based cohorts. *Am. J. Gastroenterol.* 105, 289–297. doi:10.1038/ajg.2009.579
- Raine, T., Bonovas, S., Burisch, J., Kucharzik, T., Adamina, M., Annesse, V., et al. (2022). ECCO guidelines on Therapeutics in ulcerative colitis: Medical treatment. *J. Crohns Colitis* 16 (1), 2–17. doi:10.1093/ecco-jcc/ijab178
- Rajitha, P., Biswas, R., Sabitha, M., and Jayakumar, R. (2017). Methotrexate in the treatment of psoriasis and rheumatoid arthritis: Mechanistic insights, current issues and novel delivery approaches. *Curr. Pharm. Des.* 23 (24), 3550–3566. doi:10.2174/1381612823666170601105439
- Ran, Z., Wu, K., Matsuoka, K., Jeon, Y. T., Wei, S. C., Ahuja, V., et al. (2021). Asian Organization for Crohn's and Colitis and Asia Pacific Association of Gastroenterology practice recommendations for medical management and monitoring of inflammatory bowel disease in Asia. *J. Gastroenterol. Hepatol.* 36 (3), 637–645. doi:10.1111/jgh.15185
- Ricciotti, A., Aardoom, M., Orlanski-Meyer, E., Navon, D., Carman, N., Aloï, M., et al. (2021). Predicting outcomes in pediatric Crohn's disease for management optimization: Systematic review and consensus statements from the pediatric inflammatory bowel disease-ahead program. *Gastroenterology* 160 (1), 403–436. e26. doi:10.1053/j.gastro.2020.07.065
- Rosen, M. J., Dhawan, A., and Saeed, S. A. (2015). Inflammatory bowel disease in children and adolescents. *JAMA Pediatr.* 169 (11), 1053–1060. doi:10.1001/jamapediatrics.2015.1982
- Sales-Campos, H., Basso, P. J., Alves, V. B., Fonseca, M. T. C., Bonfa, G., Nardini, V., et al. (2015). Classical and recent advances in the treatment of inflammatory bowel diseases. *Braz. J. Med. Biol. Res.* 48 (2), 96–107. doi:10.1590/1414-431X20143774
- Samuel, S., Ingle, S. B., Dhillon, S., Yadav, S., Harmsen, W. S., Zinsmeister, A. R., et al. (2013). Cumulative incidence and risk factors for hospitalization and surgery in a population-based cohort of ulcerative colitis. *Inflamm. Bowel Dis.* 19 (9), 1858–1866. doi:10.1097/MIB.0b013e31828c84c5
- Samuel, S., Ingle, S. B., Dhillon, S., Yadav, S., Harmsen, W. S., Zinsmeister, A. R., et al. (2013). Cumulative incidence and risk factors for hospitalization and surgery in a population-based cohort of ulcerative colitis. *Inflamm. Bowel Dis.* 19 (9), 1858–1866. doi:10.1097/MIB.0b013e31828c84c5

## Publisher's note

All claims expressed in this article are solely those of the authors and do not necessarily represent those of their affiliated organizations, or those of the publisher, the editors and the reviewers. Any product that may be evaluated in this article, or claim that may be made by its manufacturer, is not guaranteed or endorsed by the publisher.

## Supplementary material

The Supplementary Material for this article can be found online at: <https://www.frontiersin.org/articles/10.3389/fphar.2022.996065/full#supplementary-material>

- Seinen, M. L., Ponsioen, C. Y., de Boer, N. K., Oldenburg, B., Bouma, G., Mulder, C. J. J., et al. (2013). Sustained clinical benefit and tolerability of methotrexate monotherapy after thiopurine therapy in patients with Crohn's disease. *Clin. Gastroenterol. Hepatol.* 11 (6), 667–672. doi:10.1016/j.cgh.2012.12.026
- Solberg, I. C., Cvancarova, M., Vatn, M. H., and Moum, B. (2014). Risk matrix for prediction of advanced disease in a population-based study of patients with Crohn's Disease (the IBSEN Study). *Inflamm. Bowel Dis.* 20 (1), 60–68. doi:10.1097/01.MIB.0000436956.78220.67
- Thia, K. T., Sandborn, W. J., Harmsen, W. S., Zinsmeister, A. R., and Loftus, E. V. (2010). Risk factors associated with progression to intestinal complications of Crohn's disease in a population-based cohort. *Gastroenterology* 139, 1147–1155. doi:10.1053/j.gastro.2010.06.070
- Torres, J., Bonovas, S., Doherty, G., Kucharzik, T., Gisbert, J. P., Raine, T., et al. (2020). ECCO guidelines on Therapeutics in crohn's disease: Medical treatment. *J. Crohns Colitis* 14 (1), 4–22. doi:10.1093/ecco-jcc/jjz180
- Torres, J., Bonovas, S., Doherty, G., Kucharzik, T., Gisbert, J. P., Raine, T., et al. (2020). ECCO guidelines on Therapeutics in crohn's disease: Medical treatment. *J. Crohns Colitis* 14 (1), 4–22. doi:10.1093/ecco-jcc/jjz180
- Tsai, L., Ma, C., Dulai, P. S., Prokop, L. J., Eisenstein, S., Ramamoorthy, S. L., et al. (2021). Contemporary risk of surgery in patients with ulcerative colitis and crohn's disease: A meta-analysis of population-based cohorts. *Clin. Gastroenterol. Hepatol.* 19 (10), 2031–2045.e11. doi:10.1016/j.cgh.2020.10.039
- Tung, J. P., and Maibach, H. I. (1990). The practical use of methotrexate in psoriasis. *Drugs* 40 (5), 697–712. doi:10.2165/00003495-199040050-00005
- Vasudevan, A., Parthasarathy, N., Con, D., Nicolaides, S., Apostolov, R., Chauhan, A., et al. (2020). Thiopurines vs methotrexate: Comparing tolerability and discontinuation rates in the treatment of inflammatory bowel disease. *Aliment. Pharmacol. Ther.* 52 (7), 1174–1184. doi:10.1111/apt.16039
- Wahed, M., Louis-Auguste, J. R., Baxter, L. M., Limdi, J. K., McCartney, S. A., Lindsay, J. O., et al. (2009). Efficacy of methotrexate in Crohn's disease and ulcerative colitis patients unresponsive or intolerant to azathioprine/mercaptopurine. *Aliment. Pharmacol. Ther.* 30 (6), 614–620. doi:10.1111/j.1365-2036.2009.04073.x
- Yao, J. Y., Jiang, Y., Ke, J., Lu, Y., Hu, J., and Zhi, M. (2020). Development of a prognostic model for one-year surgery risk in crohn's disease patients: A retrospective study. *World J. Gastroenterol.* 26 (5), 524–534. doi:10.3748/wjg.v26.i5.524



## OPEN ACCESS

## EDITED BY

Adina Turcu-Stolica,  
University of Medicine and Pharmacy of  
Craiova, Romania

## REVIEWED BY

Renata Varut,  
University of Medicine and Pharmacy of  
Craiova, Romania  
Ali Hafez El-Far,  
Damanhour University, Egypt

## \*CORRESPONDENCE

Xiu-Juan Lei,  
xiujuanl@jlu.edu.cn  
Wei Li,  
liweili727@126.com

\*These authors have contributed equally  
to this work and share first authorship

## SPECIALTY SECTION

This article was submitted to  
Gastrointestinal and Hepatic  
Pharmacology,  
a section of the journal  
Frontiers in Pharmacology

RECEIVED 09 September 2022

ACCEPTED 27 September 2022

PUBLISHED 12 October 2022

## CITATION

Xia J, Hu J-N, Wang Z, Cai E-B, Ren S,  
Wang Y-P, Lei X-J and Li W (2022),  
Based on network pharmacology and  
molecular docking to explore the  
protective effect of Epimedii Folium  
extract on cisplatin-induced intestinal  
injury in mice.  
*Front. Pharmacol.* 13:1040504.  
doi: 10.3389/fphar.2022.1040504

## COPYRIGHT

© 2022 Xia, Hu, Wang, Cai, Ren, Wang,  
Lei and Li. This is an open-access article  
distributed under the terms of the  
[Creative Commons Attribution License](#)  
(CC BY). The use, distribution or  
reproduction in other forums is  
permitted, provided the original  
author(s) and the copyright owner(s) are  
credited and that the original  
publication in this journal is cited, in  
accordance with accepted academic  
practice. No use, distribution or  
reproduction is permitted which does  
not comply with these terms.

# Based on network pharmacology and molecular docking to explore the protective effect of Epimedii Folium extract on cisplatin-induced intestinal injury in mice

Juan Xia<sup>1,2,3,4†</sup>, Jun-Nan Hu<sup>3,4†</sup>, Zi Wang<sup>3</sup>, En-Bo Cai<sup>3</sup>,  
Shen Ren<sup>3</sup>, Ying-Ping Wang<sup>1,3,4</sup>, Xiu-Juan Lei<sup>3,4\*</sup> and  
Wei Li<sup>1,2,3,4\*</sup>

<sup>1</sup>Institute of Special Animal and Plant Sciences of Chinese Academy of Agricultural Sciences, Changchun, China, <sup>2</sup>College of Life Sciences, Jilin Agricultural University, Changchun, China, <sup>3</sup>College of Chinese Medicinal Materials, Jilin Agricultural University, Changchun, China, <sup>4</sup>National and Local Joint Engineering Research Center for Ginseng Breeding and Development, Changchun, China

**Background:** Epimedii Folium, as a natural botanical medicine, has been reported to have protective effects on intestinal diseases by modulating multiple signaling pathways. This study aimed to explore the potential targets and molecular mechanisms of Epimedii Folium extract (EFE) against cisplatin-induced intestinal injury through network pharmacology, molecular docking, and animal experiments.

**Methods:** Network pharmacology was used to predict potential candidate targets and related signaling pathways. Molecular docking was used to simulate the interactions between significant potential candidate targets and active components. For experimental validation, mice were intraperitoneally injected with cisplatin 20 mg/kg to establish an intestinal injury model. EFE (100, 200 mg/kg) was administered to mice by gavage for 10 days. The protective effect of EFE on intestinal injury was analyzed through biochemical index detection, histopathological staining, and western blotting.

**Results:** Network pharmacology analysis revealed that PI3K-Akt and apoptosis signaling pathways were thought to play critical roles in EFE treatment of the intestinal injury. Molecular docking results showed that the active constituents of Epimedii Folium, including Icariin, Epimedin A, Epimedin B, and Epimedin C, stably docked with the core AKT1, p53, TNF- $\alpha$ , and NF- $\kappa$ B. In verified experiments, EFE could protect the antioxidant defense system by increasing the levels of glutathione peroxidase (GSH-Px) and catalase (CAT) while reducing

**Abbreviations:** EFE, Epimedii Folium extract; cTnT, Plasma cardiac troponin T; TNF- $\alpha$ , Tumor necrosis factor- $\alpha$ ; GSH-Px, Glutathione peroxidase; MDA, Malondialdehyde; PI3K, Phosphatidylinositol 3-kinase; NF- $\kappa$ B, Nuclear factor-kappa B; CK-MB, Creatine kinase isoenzyme MB; LDH, Lactate dehydrogenase; IL-1 $\beta$ , Interleukin-1 $\beta$ ; CAT, Catalase; IL-6, Interleukin-6; Akt, Protein kinase B; Cyt-C, Cytochrome C

the content of malondialdehyde (MDA). EFE could also inhibit the expression of NF- $\kappa$ B and the secretion of inflammatory factors, including TNF- $\alpha$ , IL-1 $\beta$ , and IL-6, thereby relieving the inflammatory damage. Further mechanism studies confirmed that EFE had an excellent protective effect on cisplatin-induced intestinal injury by regulating PI3K-Akt, caspase, and NF- $\kappa$ B signaling pathways.

**Conclusion:** In summary, EFE could mitigate cisplatin-induced intestinal damage by modulating oxidative stress, inflammation, and apoptosis.

#### KEYWORDS

Epimedii Folium extract, cisplatin, intestinal injury, network pharmacology, PI3K/Akt signaling pathway

## Introduction

Cisplatin is a broad-spectrum and highly effective platinum-based antitumor drug, which is widely used in the treatment of various solid tumors such as lung cancer (Wang et al., 2021), gastric cancer, breast cancer (Vidra et al., 2022), ovarian cancer (Muhanmode et al., 2021), and bladder cancer. However, the dose-limiting toxicities of cisplatin, such as nephrotoxicity (Ma et al., 2021), ototoxicity (Tserga et al., 2020), neurotoxicity, hepatotoxicity (Abd Rashid et al., 2021), cardiotoxicity (Xu et al., 2021), and gastrointestinal toxicity (Lopez-Tofino et al., 2021), severely limit its application in clinical oncology. Among them, gastrointestinal toxicity is the most essential clinical dose-limiting side effect, which dramatically affects the antitumor efficacy of cisplatin, seriously affects the quality of life of patients, and even needs to stop chemotherapy (Blijlevens et al., 2000). Oxidative stress plays an essential role in the pathogenesis of cisplatin-induced cytotoxicity, which indicates that the application of antioxidants can effectively ameliorate cisplatin-induced toxicity (Mansour et al., 2006). For this purpose, past studies have demonstrated that various active extracts or active components obtained from herbal medicines have a significant activity in antagonizing the side effects caused by cisplatin (Awadalla et al., 2022; Gholampour et al., 2022; Pei et al., 2022). According to literature reports, flavonoids extracted from Epimedii Folium can effectively resist the toxicity caused by cisplatin (Ma et al., 2015).

Reactive oxygen species (ROS) react with biological macromolecules (including proteins, lipids, and nucleic acids), resulting in oxidative damage to cell membranes and lipid peroxidation, thus causing extensive tissue damage (Halliwell, 2006). Cisplatin treatment can increase the biochemical indicators of intestinal oxidative stress, thereby inducing epithelial apoptosis, and ultimately leading to small intestine injury (Rashid et al., 2017). In addition, the overproduction of ROS can cause inflammation by activating the transcription factor NF- $\kappa$ B, leading to the massive production of cell adhesion molecules, chemokines, and proinflammatory cytokines, thereby enhancing the cytotoxicity of cisplatin (Mukhopadhyay et al., 2011). Studies have shown that the inflammatory response activated by the NF- $\kappa$ B signaling pathway also plays a crucial role in cisplatin-induced intestinal injury (Lee et al., 2014).

Epimedii Folium, the dried aerial part of *Epimedium sagittatum* Maxim, *Epimedium koreanum* Naka, *Epimedium brevicornu* Maxim

or *Epimedium pubescens* Maxim (Chinese pharmacopoeia, 2020), is a well-known Chinese herb that has been used in functional foods and complementary medicines for more than 2000 years. Epimedii Folium has the effects of tonifying the kidney, strengthening the yang, dispelling wind, and removing dampness in the theory of traditional Chinese medicine (TCM). Hence, it is applied to prevent and treat sexual dysfunction, osteoporosis, rheumatism, neurasthenia, chronic nephritis, and cardiovascular diseases. Modern pharmacological studies have proved that Epimedii Folium has a variety of pharmacological activities, including antioxidant (Zhang et al., 2013), anti-inflammatory (Saba et al., 2020), anti-osteoporotic (Indran et al., 2016), antitumor (Song et al., 2014), anti-atherosclerosis (Xiao et al., 2017), neuroprotection (Wu et al., 2017), improving sexual function (Gu et al., 2018), and enhancing immune function (Lee et al., 2017). The intestinal tract is the most important immune organ and natural barrier, which can prevent pathogens, toxins, and other harmful substances from entering the circulation through the intestine and ensure a stable environment (Groschwitz and Hogan, 2009). Epimedii Folium combined with red ginseng synergistically relieved DSS-induced colitis in mice by modulating the NF- $\kappa$ B and MAPK pathways and the expression of NLRP3 (Saba et al., 2020).

Studies have shown that flavonoids extracted from Epimedii Folium have been proved to have various beneficial effects on intestinal lesions. Given this, this paper used the network pharmacology to explore the potential components, putative targets, and protective mechanisms of EFE in the treatment of cisplatin-induced intestinal injury, and conducted animal experiments for preliminary confirmation. Our findings provide a theoretical basis for the protective mechanism of EFE against cisplatin-induced intestinal damage.

## Materials and methods

### Screening active compounds of Epimedii Folium

The active ingredients of Epimedii Folium have collected through the Traditional Chinese Medicine Systems

Pharmacology (TCMSP, <http://tcmspw.com/tcmsp.php>) Database. Based on the Oral Bioavailability (OB)  $\geq 30\%$  and Drug-Like (DL)  $\geq 0.18$  as thresholds, the potential active compounds of Epimedii Folium were screened by ADME analysis.

## Candidate targets collection

All the possible targets against intestinal injury have retrieved from the OMIM (<https://www.omim.org/>), PharmGkb (<https://www.pharmgkb.org/>), and GeneCards (<https://www.genecards.org/>) database. Potential target genes of Epimedii Folium for the treatment of intestinal injury were obtained through the Veeny 2.1 (<https://bioinfo.gp.cnb.csic.es/tools/venny/>) intersection. Then we used Cytoscape (v.3.8.0) software to build the active compound-target-intestinal injury network.

## Construction of protein-protein interaction network

PPI network of acquired drug targets was created using the STRING database (<https://string-db.org/>). Then, the PPI network results were imported into Cytoscape v.3.8.0 ([www.cytoscape.org/](http://www.cytoscape.org/)) for network generation and further analysis. Moreover, the median of three topological parameters, “Betweenness Centrality,” “Closeness Centrality,” and “Degree,” were calculated to evaluate the topological importance of nodes in the PPI network.

## GO and KEGG pathway enrichment analysis

To explore the role of essential target genes through bioinformatics description and annotation, GO and KEGG pathway enrichment analysis on shared target genes was performed using R software with Bioconductor package under the conditions of  $p < 0.05$  and  $Q < 0.05$ , and the results were plotted in the form of a bubble chart. GO enrichment analysis includes three aspects: molecular function (MF), biological process (BP), and cellular components (CC). KEGG enrichment analysis was performed to screen out the potential signaling pathways of Epimedii Folium in the treatment of intestinal injury diseases.

## Molecular docking

To validate the association between compounds and targets, molecular docking simulations were performed using AutoDockTools-1.5.6 software. Crystal structures of crucial target

proteins were downloaded from the Protein Data Bank database (<http://www.rcsb.org/>) in PDB format. The chemical structures of Icariin, Epimedin A, Epimedin B, and Epimedin C were obtained from the PubChem database (<https://pubmed.ncbi.nlm.nih.gov/>). The 3D structures of active compounds were constructed and optimized by ChemBio3D Ultra 14.0.0.117 software, and their energy was minimized using the MM2 algorithm. PyMol software removed water molecules and organic compounds from receptor proteins. The target protein receptor molecules were hydrotreated and charged by AutoDockTools-1.5.6 software, and the compounds and target protein receptors were converted to PDBQT format. Finally, Auto Dock Vina software was used to verify the molecular docking of potential targets and components. Each group of molecular docking was run three times, and the ionization energy was recorded. The visualization of docking results with the best binding ability was presented using BIOVIA Discovery Studio (2019) Visualizer.

## Animal and experimental design

Forty male SPF ICR mice (6–8 weeks old, weighing 20–25 g) were provided by Beijing Hua-Fu-Kang Biotechnology Co., Ltd., license No. SCXK (Beijing) 2019-0008. Mice were allowed free access to food and water in a rearing chamber free of specific pathogens and a 12-h light/dark cycle. The temperature controlled at  $22.0^{\circ}\text{C} \pm 2.0^{\circ}\text{C}$ , and the humidity maintained at  $60.0\% \pm 10.0\%$ .

After 1 week of acclimatization, mice were randomly allocated into 4 groups ( $n = 10$ ): normal group, model group, cisplatin + EFE (100 mg/kg) group and cisplatin + EFE (200 mg/kg) group. Since there is currently no therapeutic agent for cisplatin-induced myocardial injury in the clinic, a group of positive drugs was not set up in the present work. EFE was dissolved in 0.05% carboxymethylcellulose sodium (CMC-Na) and administered to mice by gavage for ten consecutive days. On the 7th day of EFE administration, except the normal group, mice in the other groups were intraperitoneally injected with cisplatin 20 mg/kg to establish an acute intestinal injury model (Figure 3C).

## Ethical statement

All animal experiments were conducted according to the Guidelines for the Management and Use of Experimental Animals and were approved by the Experimental Animal Ethics Committee of Jilin Agricultural University (Animal Experiment Ethics No. 20190905002).

## Sampling

Epimedii Folium was obtained from Bozhou traditional Chinese medicine trading center (Anhui province, China), and



identified as *Epimedium brevicornu* Maxim by Professor Han Mei from the College of Chinese Medicinal Materials, Jilin Agricultural University. *Epimedium* Folium extract was prepared and quantified according to previous reports (Zhou et al., 2019). High-performance liquid chromatography (Waters HPLC, Milford, MA) was used to quantify EFE at 317 nm on a Hypersil ODS2 column (Figures 3A,B). The quantitative analysis of the main flavonoids in EFE was as follows: 0.61% of Epimedin A, 0.87% of Epimedin B, 2.82% of Epimedin C, and 1.84% of Icaritin.

## Reagents

The use of cisplatin in chemotherapy often leads to severe intestinal toxicity. Our research group has fully proved that cisplatin can cause intestinal toxicity in the body at a dose of 20 mg/kg in previous studies (Hu et al., 2021). Cisplatin (purity  $\geq$  99.0%) was provided by Shanghai Civic Chemical Technology Co., Ltd., (Shanghai, China); Glutathione peroxidase (GSH-Px), catalase (CAT) and malondialdehyde (MDA) detection kits and hematoxylin-eosin (H&E) staining kits were bought from Nanjing Jiancheng Bioengineering Institute (Nanjing, China); Tumor necrosis factor- $\alpha$  (TNF- $\alpha$ ), interleukin-1 $\beta$  (IL-1 $\beta$ ), interleukin-6 (IL-6) and diamine oxidase (DAO) enzyme-linked immunoassay (ELISA) kits were obtained from R&D Systems of the United States (Minneapolis, MN, United States); Hoechst 33258 staining kits and BCA protein concentration detection kits were acquired from Shanghai Beyotime Biotechnology Co., Ltd. (Shanghai, China); Cy3-SABC immunofluorescence staining kit was provided by BOSTER Biological Technology Co., Ltd. (Wuhan, China); Monoclonal antibodies: p-PI3K, PI3K, p-Akt, Akt, p-NF- $\kappa$ B, NF- $\kappa$ B, p-p53, p53, Bax, Bcl-2, cytochrome c, cleaved caspase-9, caspase-9, cleaved caspase-3, caspase-3,  $\beta$ -actin, and secondary antibodies were provided by Cell Signaling Technology (Danvers, MA, United States); Acetonitrile was chromatographic pure and obtained from Thermo Fisher Scientific Co., Ltd. (MERCK, Germany); Methanol, ethanol, and other chemical reagents were analytical pure and provided by Sinopharm Chemical Reagent Co., Ltd., (Shanghai, China).

## Determination of serum biochemical indicators

Blood samples were collected from mouse ocular venous plexus and centrifuged at 3,500 rpm for 10 min to separate serum samples. The levels of DAO, TNF- $\alpha$ , IL-1 $\beta$ , and IL-6 in serum samples were determined using ELISA kits according to the manufacturer's instructions. 10  $\mu$ l serum samples were added to 96 well plates coated with matrix and incubated at 37°C for 30 min, then chromogenic agent was added, and the absorbance of samples in each group at 450 nm was measured within 15 min. Finally, the content of biochemical indicators was calculated through the concentration-absorbance curve.

## Determination of biochemical indexes of tissue homogenate

Tissue samples were accurately weighed, 0.9% sterile saline was added according to weight (g): volume (ml) = 1:9, then homogenized with a tissue homogenizer, and finally centrifuged at 3,500 rpm for 10 min to collect the supernatant for subsequent biochemical parameter detection. The levels of MDA, GSH-Px, and CAT in tissue homogenate were determined using corresponding commercially available detection kits according to the instructions provided by Nanjing Jiancheng Bioengineering Institute.

## Histopathological examination

2~3 cm fresh mouse duodenum, jejunum, and ileum were immersed in 10% neutral buffered formalin for at least 48 h, routinely dehydrated and deparaffinized, embedded in paraffin, and then cut into 5  $\mu$ m thick sections. Paraffin sections were stained with H&E solution, and then pathological changes were observed with a light microscope, and images were collected. The degree of intestinal injury was assessed according to the histopathological scoring system.

## Hoechst 33258 staining analysis

5  $\mu$ m thick tissue sections were stained with Hoechst 33258 staining solution according to the kit instructions. After standing for 5 min, the sections were washed twice with phosphate buffer (0.01 M, pH 7.4) for 3 min each time and then sealed with anti-fluorescence quenching sealant. Finally, nuclear apoptosis was observed and photographed under a fluorescence microscope (Olympus BX-60, Tokyo, Japan). Hoechst 33258 staining results were quantified by Image-Pro Plus 6.0 software.

## Immunofluorometric analysis

Paraffin tissue sections were deparaffinized and hydrated with xylene and gradient ethanol solution and then repaired with citrate buffer (0.01 M, pH 6.0) under microwave conditions at medium-high temperature for 8 min. After returning to room temperature, 5% bovine serum albumin (BSA) was added dropwise to block the sections for 20 min, and then NF- $\kappa$ B P65 (1:100) primary antibody solution was added and incubated overnight at 4°C. Biotinylated goat anti-rabbit IgG solution was added and incubated at 37°C for 30 min. Diluted Cy3-SABC (1:400) solution was added dropwise to the sections and incubated at 37°C in the dark for 30 min. 4, 6-diamino-2-phenylindole (DAPI) solution was added for nuclear staining. Finally, the slices were sealed with anti-fluorescence quenching

sealant. The fluorescence expression intensity of the antibody was observed under a fluorescence microscope (Leica TCS SP8, Germany) and photographed. Immunofluorescence quantitative analysis was performed using Image-Pro Plus 6.0 software.

## Western blot analysis

Total protein samples were obtained by lysing mouse intestinal tissues with RIPA lysis buffer supplemented with protein phosphatase inhibitors. Total protein concentration in the tissues was determined using the BCA protein quantification kit according to the instructions provided by the manufacturer. The protein samples were separated on 15% SDS-PAGE gels and transferred to polyvinylidene fluoride (PVDF) membranes by electrophoresis. Then, the PVDF membranes were sealed with 5% skimmed milk at room temperature for at least 2 h and incubated with p-PI3K (1:1,000), PI3K (1:1,000), p-Akt (1:1,000), Akt (1:1,000), p-p53 (1:1,000), p53 (1:1,000), Bax (1:2000), Bcl-2 (1:2000), cleaved caspase-9 (1:1,000), caspase-9 (1:1,000), cleaved caspase-3 (1:1,000), caspase-3 (1:1,000), cytochrome c (1:1,000), and  $\beta$ -actin (1:2000) primary antibody solutions at 4°C overnight. The membranes were then incubated with the HRP-conjugated secondary antibody solution at room temperature for 1.5–2 h. Finally, the intensities of protein bands were quantified by Quantity One software (Bio-Rad Laboratories, Hercules, CA, United States).

## Statistical analysis

All experimental data were expressed as mean  $\pm$  standard deviation (Mean  $\pm$  S.D). Statistical significance was analyzed by SPSS version 19.0 software. The statistical histograms were made by GraphPad Prism 8.04 software (GraphPad Software, La Jolla, California, United States). In all cases,  $p < 0.05$  or  $p < 0.01$  was considered statistically significant.

## Results

### Active compounds in Epimedii Folium and candidate targets

Using the keyword “Epimedii Folium,” 23 active compounds were retrieved from TCMSP database. The potential active ingredients were collected under the screening conditions of OB  $\geq$  30% and DL  $\geq$  0.18. We searched through TCMSP, combined with Chinese and foreign literature supplements, deleted the active ingredients without targets, and finally obtained 25 active ingredients of Epimedii Folium, as shown in Table 1. In addition, 217 target genes were screened from the

TCMSP and Swiss target prediction databases for active components. Similarly, 8,226 target genes for intestinal injury were obtained from the GeneCards, OMIM, and PharmGkb databases (Figure 1A). To obtain the targets of Epimedii Folium against intestinal damage, the co-relative targets were identified using the online Draw Venn Diagram facility. Finally, 200 overlapping targets were obtained as candidate targets of Epimedii Folium in the treatment of intestinal injury (Figure 1B). Then, the candidate targets and corresponding active compounds were imported into Cytoscape 3.7.2 software to construct the “compound-target-intestinal injury” network diagram. As shown in Figure 1C, the network diagram contained 227 nodes (25 active compounds, 200 target genes, 1 drug, and 1 disease) and 686 edges, and purple circles represent the target genes, and light pink V shapes represent the active compounds, showing the direct relationship network of active compounds with intestinal injury and Epimedii Folium.

### Protein-protein interaction network analysis

The identifiable candidate targets of Epimedii Folium associated with intestinal injury were introduced into the STRING database to set up the PPI network diagram. Subsequently, the PPI network of candidate targets was inputted into Cytoscape-v3.8.0 software for visualization. We excluded disconnected nodes from the PPI network and finally obtained 197 nodes and 3,491 edges (Figure 1D). The network nodes delineate target proteins, and the edges represent protein-protein relationships. AKT1, TP53, TNF, RELA, CASP3, and CASP9 contained in the hub PPI network were considered as core targets (Figure 1E).

### GO and KEGG pathway enrichment analysis

To explore the biological functions and relevant pathways of Epimedii Folium associated with intestinal injury, GO and KEGG pathway enrichment analysis of the 200 candidate targets was carried out after calculation with R software. A total of 2768 GO terms ( $p < 0.05$ ) were obtained from GO enrichment analysis, including 2,437 biological process (BP) terms, 104 cellular components (CC) terms, and 227 molecular function (MF) terms. The top 10 markedly enriched biological processes of the 200 core targets were depicted in Figure 1F, including cellular response to chemical stress, response to oxidative stress, serine/threonine protein kinase complex, and DNA-binding transcription factor binding. Moreover, 170 signaling pathways were identified by the KEGG pathway enrichment analysis ( $p < 0.05$ ), and the finally sorted-out top 30 vital signaling pathways are shown in

TABLE 1 Candidate active components of Epimedii Folium.

Mol ID	Molecule name	OB (%)	DL
MOL001510	24-epicampestrol	37.58	0.71
MOL001645	Linoleyl acetate	42.1	0.2
MOL001771	poriferast-5-en-3beta-ol	36.91	0.75
MOL001792	DFV	32.76	0.18
MOL003044	Chryseriol	35.85	0.27
MOL003542	8-Isopentenyl-kaempferol	38.04	0.39
MOL000359	Sitosterol	36.91	0.75
MOL000422	Kaempferol	41.88	0.24
MOL004367	Olivil	62.23	0.41
MOL004373	Anhydroicaritin	45.41	0.44
MOL004380	C-Homoerythrinan,1,6-didehydro-3,15,16-trimethoxy-, (3.beta.)-	39.14	0.49
MOL004382	Yinyanghuo A	56.96	0.77
MOL004384	Yinyanghuo C	45.67	0.5
MOL004386	Yinyanghuo E	51.63	0.55
MOL004388	6-hydroxy-11,12-dimethoxy-2,2-dimethyl-1,8-dioxo-2,3,4,8-tetrahydro-1H-isochromeno [3,4-h] isoquinolin-2-ium	60.64	0.66
MOL004391	8-(3-methylbut-2-enyl)-2-phenyl-chromone	48.54	0.25
MOL004396	1,2-bis (4-hydroxy-3-methoxyphenyl) propan-1,3-diol	52.31	0.22
MOL004425	Icariin	41.58	0.61
MOL004427	Icariside A7	31.91	0.86
MOL000006	Luteolin	36.16	0.25
MOL000622	Magnograndiolide	63.71	0.19
MOL000098	Quercetin	46.43	0.28
MOL008865	Epimedin A	5.06	0.12
MOL004407	Epimedin B	8.65	0.13
MOL004409	Epimedin C	16.29	0.14

Figure 1G. The KEGG pathway enrichment analysis indicated that the mechanisms of Epimedii Folium against intestinal injury include the PI3K-Akt signaling pathway, apoptosis signaling pathway, p53 signaling pathway, and TNF- $\alpha$  signaling pathway. Additionally, the PI3K-Akt (hsa04151) and apoptosis (hsa04210) signaling pathways will be analyzed as critical pathways (Figures 1H,I).

## Molecular docking validation of core targets and active compounds

The PPI network screened out the core targets of Epimedii Folium against intestinal injury. To verify the reliability of candidate targets in the PPI network, four active compounds from Epimedii Folium were docked with AKT1, p53, TNF- $\alpha$ , NF- $\kappa$ B caspase 3, and caspase 9 using Auto Dock Vina software. The Vina score (kcal/mol) represented the binding affinity between the target protein and compounds. The lower the Vina score, the more stable the ligand binding to the receptor, and the greater the possibility of molecular interaction. As the score for molecular docking, the binding energy less than -5 kcal/mol indicates a

more vigorous binding activity. Interestingly, the results showed that Icariin, Epimedin A, Epimedin B, and Epimedin C readily bind to AKT1, p53, TNF- $\alpha$ , NF- $\kappa$ B, caspase3, and caspase9 due to their very low binding energies (Table 2). These results provide a basis for explaining the potential of AKT1, p53, TNF- $\alpha$ , NF- $\kappa$ B, caspase 3, and caspase 9 as the key therapeutic targets for intestinal injury. Finally, 3D maps of Icariin, Epimedin A, Epimedin B, and Epimedin C binding to AKT1, p53, TNF- $\alpha$ , NF- $\kappa$ B, caspase 3, and caspase 9 are shown in Figures 2A–F.

## Epimedii Folium extract improved cisplatin-induced intestinal injury

As can be seen from the line chart in Figure 3D that the weights of mice in the model group decreased significantly after intraperitoneal injection of cisplatin. EFE treatment (100 and 200 mg/kg) for 10 days effectively prevented weight loss in mice with no significant difference between the two-dose groups. As shown in Figure 3E, after intraperitoneal injection of cisplatin, the level of DAO was significantly increased, which was substantially different from that in the normal group ( $p <$

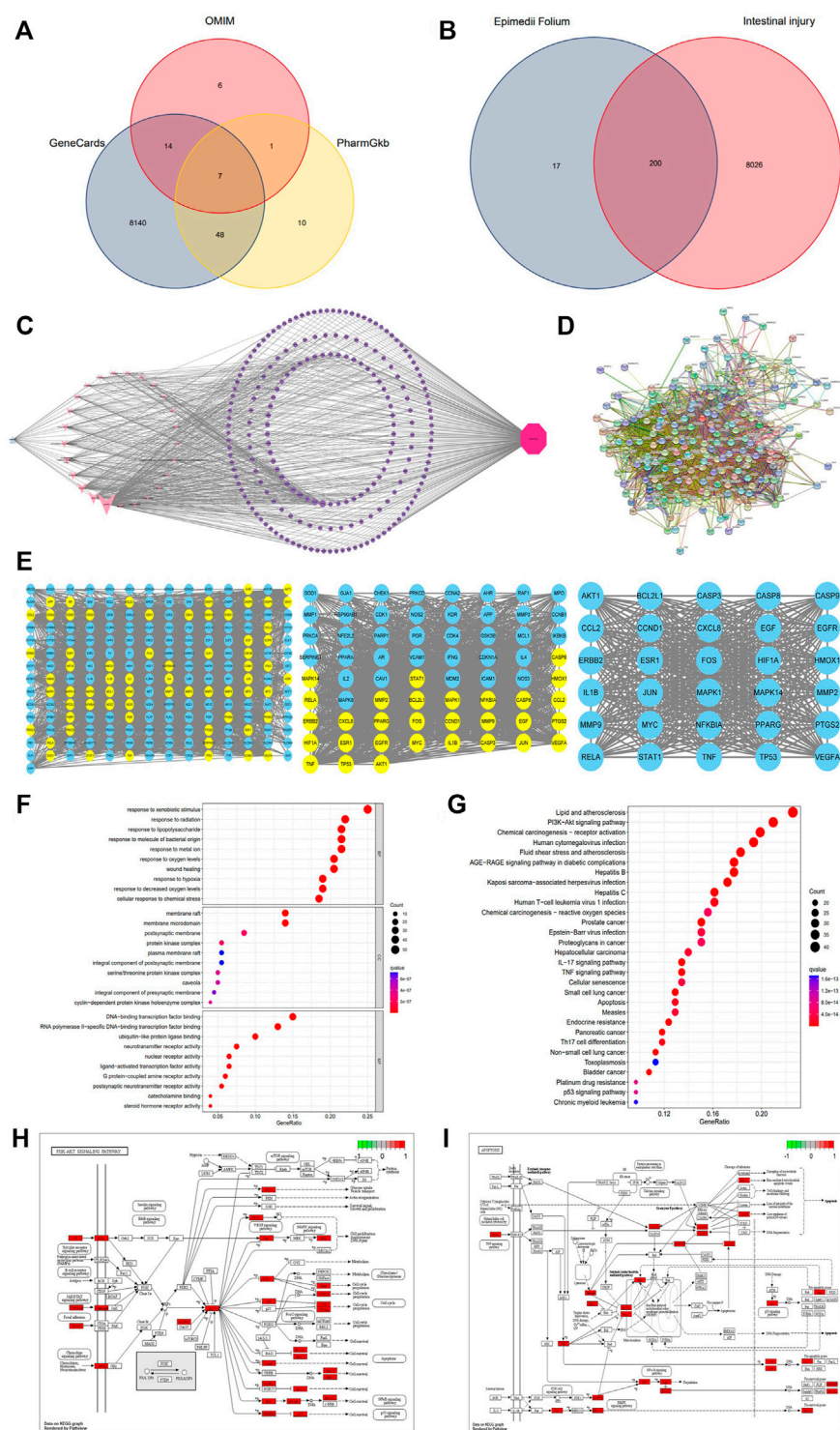


**FIGURE 1** Venn diagram of three databases of intestinal injury (A); Venny results of the potential target genes of Epimedii Folium in the treatment of intestinal injury (B); Compound-target-disease interaction network of Epimedii Folium and intestinal injury (C); The PPI network of disease-drug targets (D); Network diagram of the core targets of Epimedii Folium against intestinal injury (E); GO and KEGG enrichment analysis (F–G); The PI3K/Akt and apoptosis signaling pathways of potential target genes of EFE in intestinal injury (H,I).

TABLE 2 Molecular docking results of core targets and active ingredients.

Protein name	Molecule name	PDB	Vina scores (kcal/mol)	Mean	S	RMSD	Center		
							x	y	z
AKT1	Epimedin A	4GV1	-8.8						
			-8.9	-8.83	0.058	0	-26.571	2.775	16.251
			-8.8						
	Epimedin B		-8.7						
			-8.8	-8.7	0.1	0	-26.571	2.775	16.251
			-8.6						
Epimedin C	-9.1								
	-9.0		-9.13	0.15	0	-26.571	2.775	16.251	
	-9.3								
Icariin	-9.0								
	-9.1		-9.1	0.1	0	-26.571	2.775	16.251	
	-9.2								
P53	Epimedin A		-9.5						
			-9.4	-9.47	0.058	0	-40.261	27.583	-12.781
			-9.5						
	Epimedin B		-9.4						
			-9.5	-9.5	0.1	0	-40.261	27.583	-12.781
			-9.6						
Epimedin C	-9.4								
	-9.2	-9.4	0.2	0	-40.261	27.583	-12.781		
	-9.6								
TNF-α	Icariin	-9.3							
		-9.2	-9.3	0.1	0	-40.261	27.583	-12.781	
		-9.4							
	Epimedin A	-6.5							
		-6.5	-6.53	0.058	0	45.301	52.93	13.768	
		-6.6							
NF-κB	Epimedin B	-6.6							
		-6.7	-6.6	0.1	0	45.301	52.93	13.768	
		-6.5							
	Epimedin C	-6.6							
		-6.5	-6.63	0.15	0	45.301	52.93	13.768	
		-6.8							
NF-κB	Icariin	-6.6							
		-6.5	-6.57	0.058	0	45.301	52.93	13.768	
		-6.6							
	Epimedin A	-7.7							
		-7.6	-7.7	0.1	0	16.769	61.416	0.667	
		-7.8							
Epimedin B	-8.6								
	-8.7	-8.63	0.058	0	16.769	61.416	0.667		
	-8.6								
Epimedin C	-8.8								
	-8.7	-8.8	0.1	0	16.769	61.416	0.667		
	-8.9								

(Continued on following page)



TABLE 2 (Continued) Molecular docking results of core targets and active ingredients.

Protein name	Molecule name	PDB	Vina scores (kcal/mol)	Mean	S	RMSD	Center		
							x	y	z
Caspase3	Icariin	2J30	-8.4	-8.43	0.15	0	16.769	61.416	0.667
			-8.3						
			-8.6						
	Epimedin A		-6.1	-6.1	0.1	0	27.395	19.401	58.596
			-6.0						
			-6.2						
	Epimedin B		-6.6	-6.57	0.058	0	27.395	19.401	58.596
			-6.5						
			-6.6						
	Epimedin C		-6.8	-6.8	0.1	0	27.395	19.401	58.596
			-6.7						
			-6.9						
Caspase9	Icariin	3D9T	-6.0	-6.0	0.2	0	27.395	19.401	58.596
			-6.2						
			-8.2						
	Epimedin A		-8.0	-8.1	0.1	0	6.844	-11.718	-23.923
			-8.1						
			-7.8						
	Epimedin B		-7.7	-7.83	0.15	0	6.844	-11.718	-23.923
			-8.0						
			-7.6						
	Epimedin C		-7.5	-7.57	0.058	0	6.844	-11.718	-23.923
			-7.6						
			-7.6						
Icariin	-7.6	-7.63	0.058	0	6.844	-11.718	-23.923		
	-7.7								

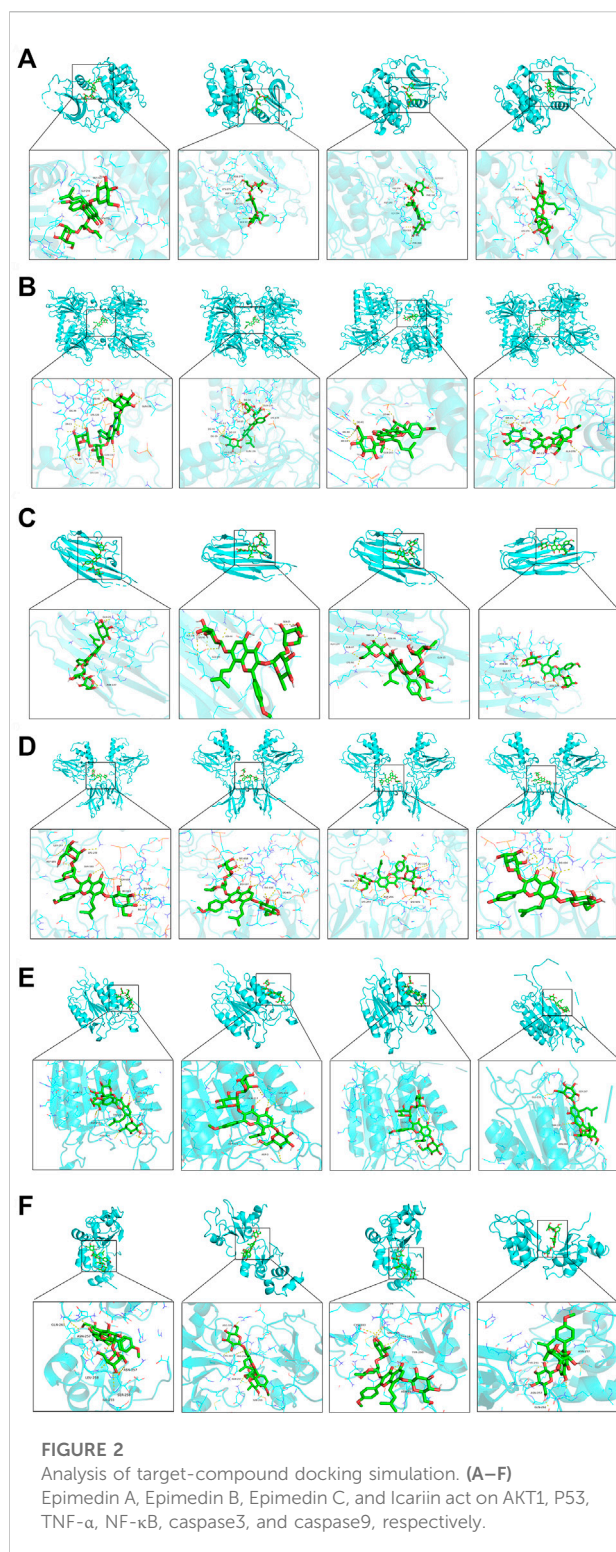
0.01). However, EFE administration could dramatically inhibit the increase of the biochemical index ( $p < 0.05$  or  $p < 0.01$ ), indicating that EFE could effectively alleviate the intestinal damage caused by cisplatin.

Gastrointestinal Morphology of mice in each experimental group was observed (Figure 4A). It was found that the stomach of cisplatin-treated mice became larger, the color of the intestine turned white, the intestinal wall became thinner, and multiple vacuoles appeared. EFE administration could significantly improve these pathological symptoms. Histopathological observation showed that the intestinal mucosa of mice in the cisplatin group was seriously damaged, villi degeneration and desquamation, mucosal glandular structure distortion, crypt ablation, and inflammatory cell infiltration. EFE could effectively alleviate cisplatin-induced intestinal injury and significantly restore the intestinal mucosal structure (Figure 4B). Furthermore, the histomorphology and pathological sections of the mouse intestines (duodenum,

jejunum, and ileum) showed that cisplatin had the most apparent damage to the duodenum. Therefore, the duodenum was selected as the research object of cisplatin-induced intestinal injury.

### Epimedii Folium extract alleviated cisplatin-induced inflammation and oxidative stress damage

To verify whether EFE could ameliorate cisplatin-induced intestinal injury through anti-inflammatory effects, the expression levels of NF- $\kappa$ B p65 in mouse intestinal tissues were detected by immunofluorescence staining. As shown in Figure 5A, NF- $\kappa$ B p65 had almost no fluorescence expression in the intestinal tissues of normal mice but was highly expressed in cisplatin-treated mice ( $p < 0.01$ ). Interestingly, the intensity of fluorescence expression was significantly attenuated after EFE



administration (Figure 5B) ( $p < 0.05$  or  $p < 0.01$ ). Moreover, as depicted in Figures 5C–E, the results showed that the serum levels of TNF- $\alpha$ , IL-1 $\beta$ , and IL-6 in the model group were significantly higher than those in the normal group ( $p < 0.01$ ).

However, the secretion levels of proinflammatory factors were suppressed considerably after EFE administration, especially in the high-dose EFE group ( $p < 0.05$  or  $p < 0.01$ ). These results suggested that EFE might effectively ameliorate cisplatin-induced intestinal injury through anti-inflammatory effects.

To evaluate whether EFE could protect intestinal tissues from oxidative stress damage caused by cisplatin, the levels of MDA, GSH-Px, and CAT in intestinal tissues were detected using corresponding kits (Figures 5F–H). The results showed that the levels of GSH-Px and CAT in the model group were significantly decreased, and the level of MDA was increased considerably, which was substantially different from those in the normal group ( $p < 0.01$ ). Interestingly, EFE could reverse the changes of these oxidative stress indices ( $p < 0.05$  or  $p < 0.01$ ).

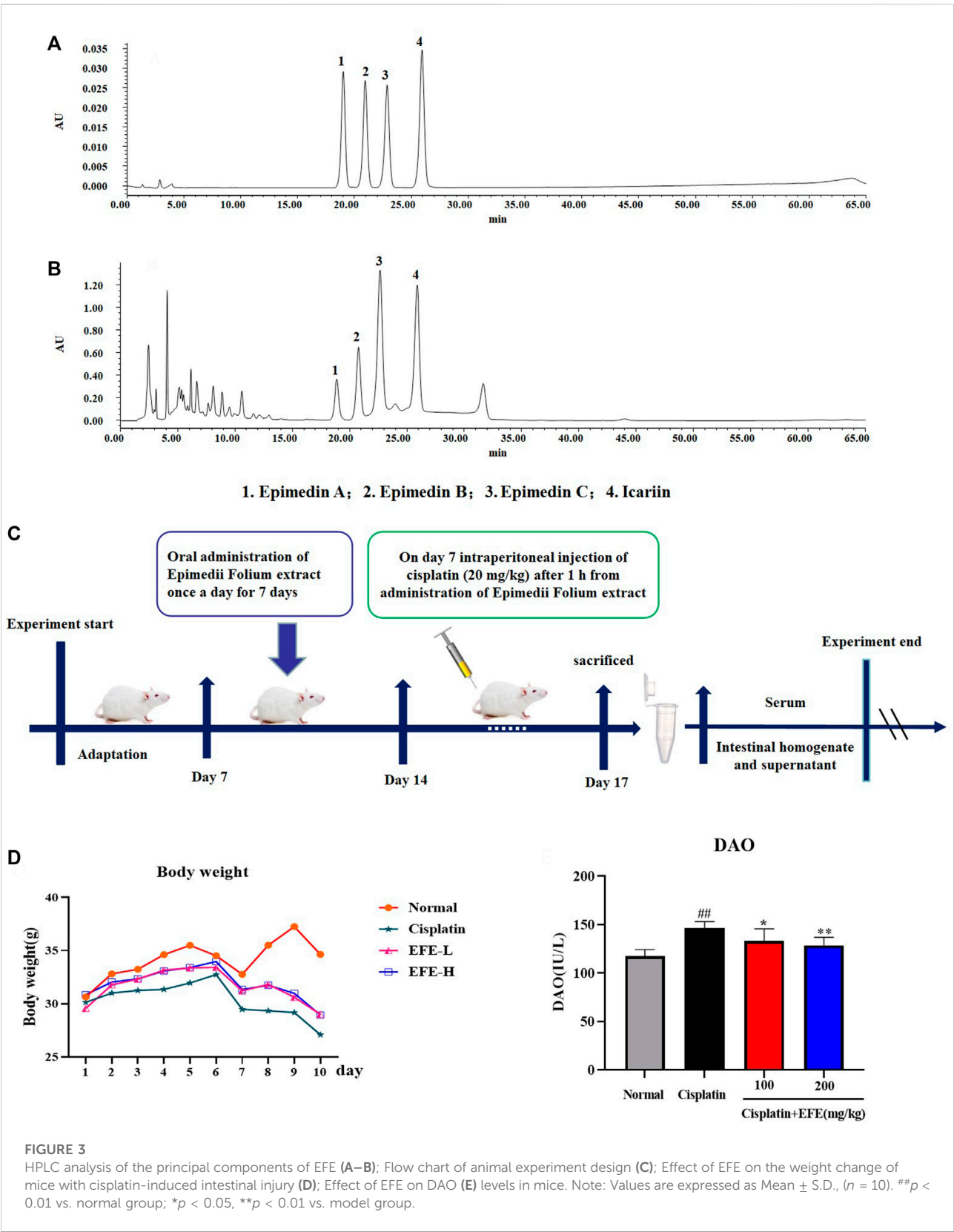
## Epimedium Folium extract inhibited cisplatin-induced intestinal apoptosis

As shown in Figure 6A, the intestinal histoarchitecture of normal mice was intact, neatly arranged with clear contours, and with no blue fluorescence of nuclei. Intestinal tissues of cisplatin-treated mice showed nuclear fragmentation and condensation and intense fluorescent signals, suggesting that cisplatin caused severe intestinal cell apoptosis. However, EFE could significantly reduce positive cells and improve cisplatin-induced intestinal apoptosis (Figure 6C) ( $p < 0.05$  or  $p < 0.01$ ).

To further explore the protective mechanism of EFE on cisplatin-induced intestinal apoptosis, western blotting was used to detect the expression levels of apoptosis-related proteins in mouse intestinal tissues (Figure 6B). The results showed that p-PI3K, p-Akt, and Bcl-2 proteins were significantly downregulated in the intestinal tissues of the model group, while p-p53, Bax, cleaved caspase-3, cleaved caspase-9, and cytochrome c proteins were upregulated considerably ( $p < 0.01$ ). However, the levels of these proteins were substantially reversed after EFE administration, and especially the high-dose EFE showed better effects (Figures 6D–J) ( $p < 0.05$  or  $p < 0.01$ ).

## Discussion

Epimedium Folium is a critical Chinese herbal medicine widely used to treat various malignant diseases. According to literature reports, flavonoids extracted from Epimedium Folium could ameliorate intestinal damage by regulating multiple signaling pathways. For example, icariin, the main flavonoid in Epimedium, effectively alleviated LPS-induced impairment of intestinal goblet cell function by modulating oxidative stress, inflammation, and apoptosis (Xiong et al., 2020b). Icariin pretreatment could improve the intestinal barrier dysfunction





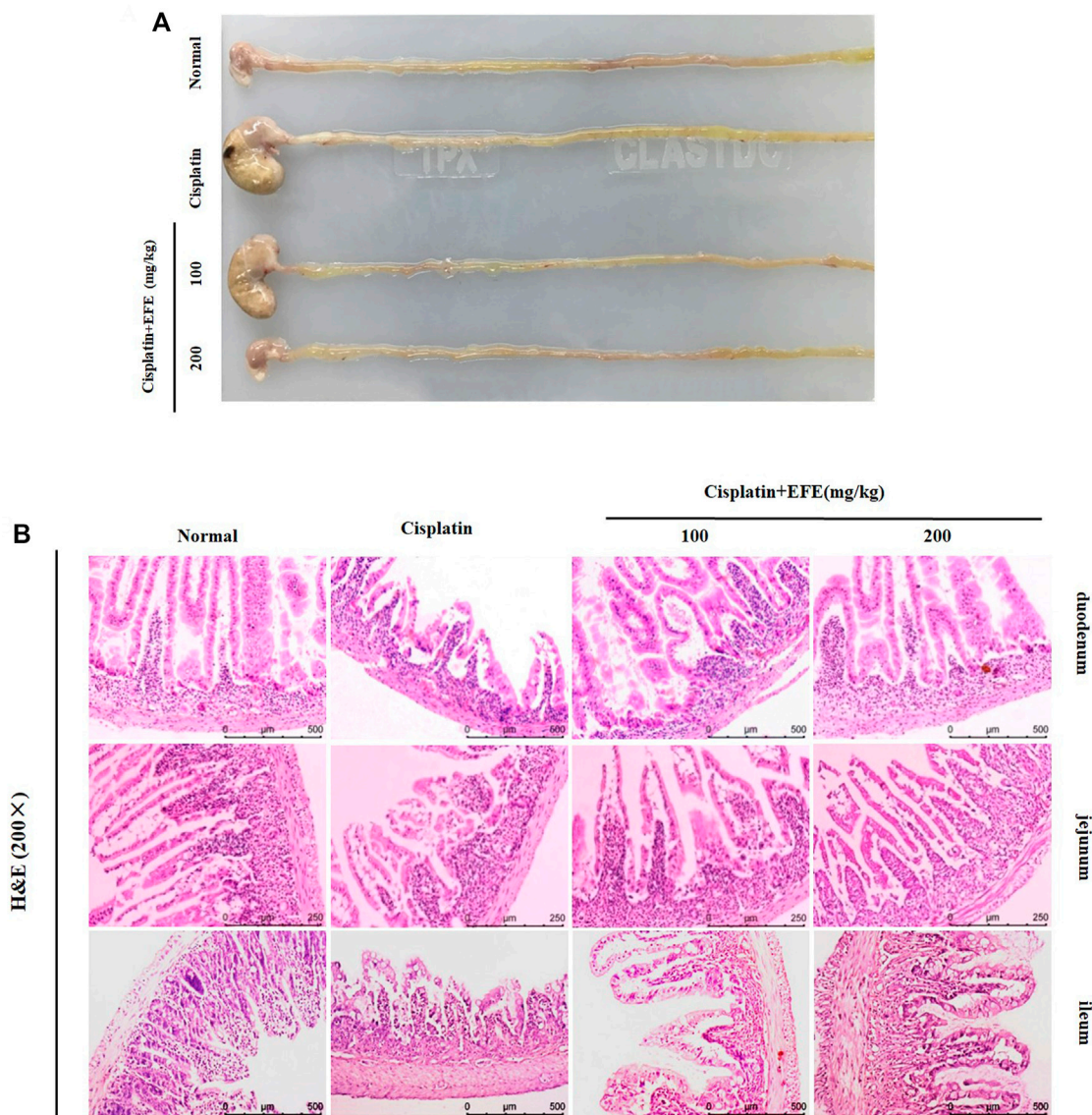
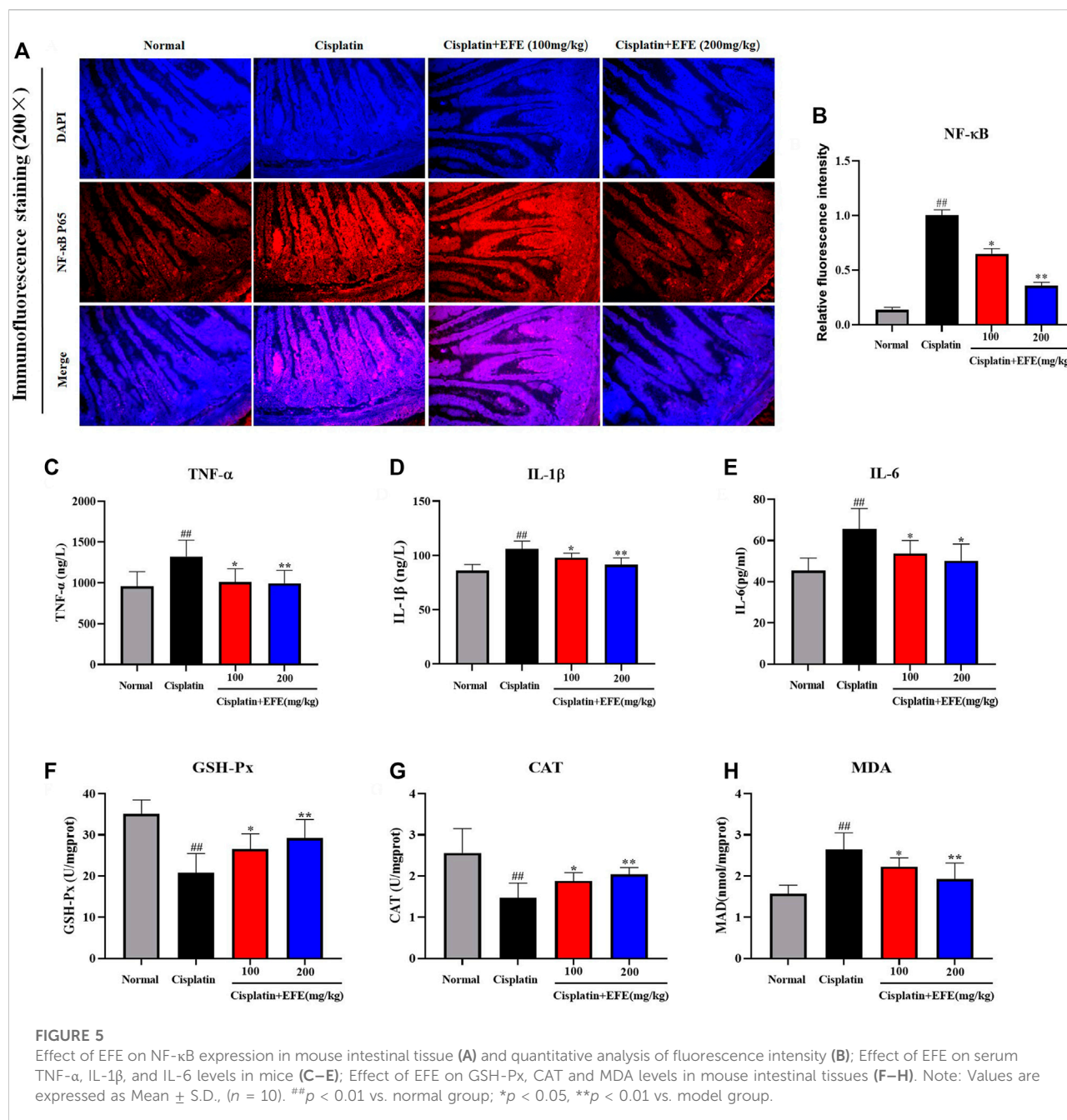


FIGURE 4

Effect of EFE on the gastrointestinal tissue morphology (A) of mice; Effect of EFE on intestinal histopathology in mice (B). Note: Values are expressed as Mean  $\pm$  S.D., ( $n = 10$ ).  $^{##}p < 0.01$  vs. normal group;  $^{*}p < 0.05$ ,  $^{**}p < 0.01$  vs. model group.

of piglets induced by *Escherichia coli* by regulating the p38 MAPKs signal pathway (Xiong et al., 2020a). Icarin could also protect intestinal cells from hypoxia-reoxygenation (H/R)-induced oxidative stress and apoptosis by activating the SIRT1/FOXO3 signaling pathway (Zhang F. et al., 2015). Cisplatin chemotherapy has serious side effects on intestinal tissues, which dramatically affects the prognosis and quality of life of patients, and severely limits its clinical application (Zou et al., 2021). While Epimedii Folium is rich in flavonoids, and these flavonoids have been reported to antagonize the toxicity of cisplatin (Ma et al., 2015; Zhou et al., 2019).

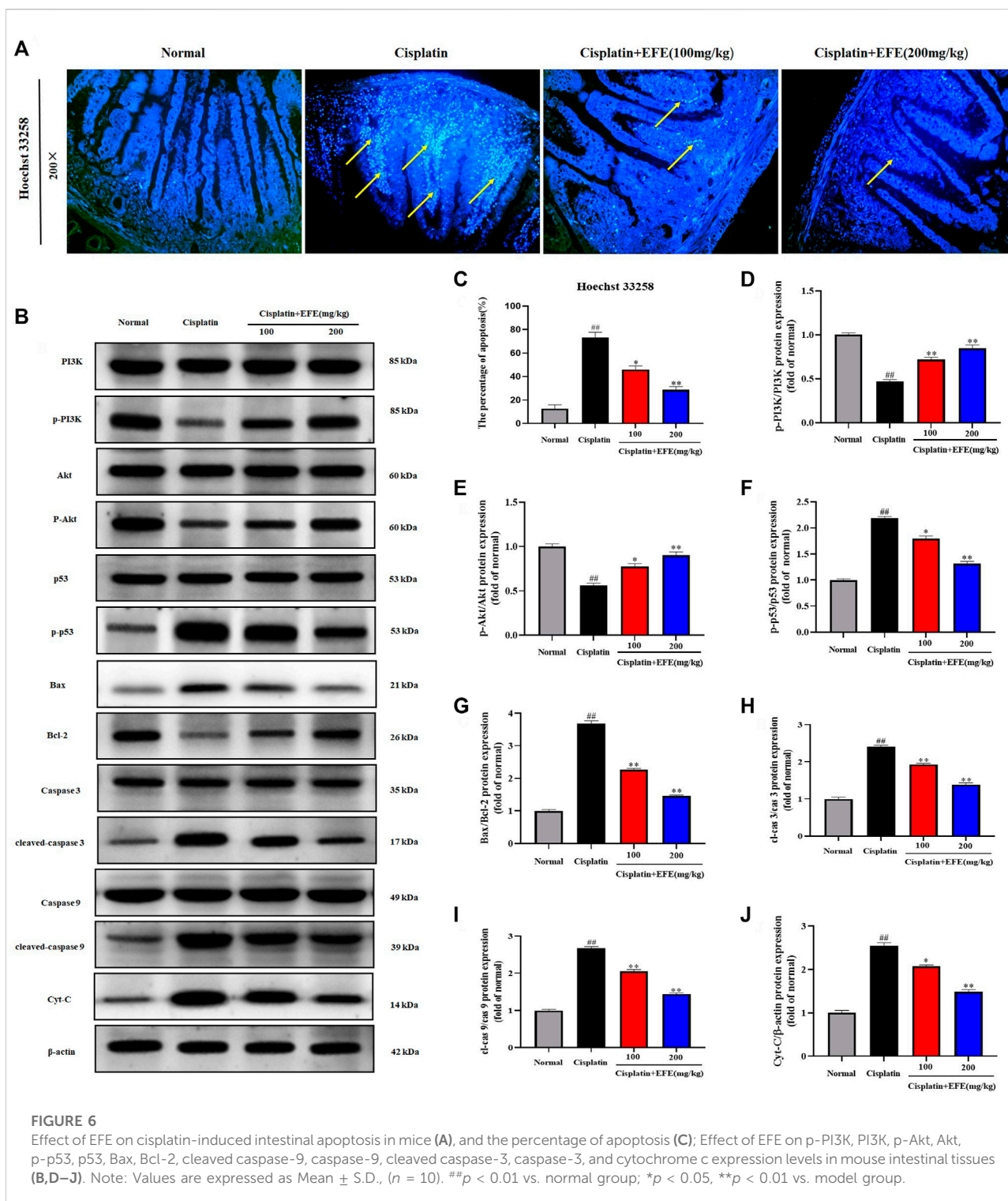
Chinese herbal medicines show good prospects in the treatment of complex diseases owing to their fewer side effects and multi-target effects. Due to the complexity of the ingredients of traditional Chinese medicine, it is difficult to comprehensively explore the potential pharmacological activities of the drugs through the research model of animal experiments. Network pharmacology is a novel method to reveal the active components and action mechanisms of Chinese herbal medicines (Zhang Y. et al., 2015). In light of this, we employed network pharmacology and animal experiments to explore the protective mechanism



of EFE on the cisplatin-induced intestinal injury. As a result, 200 drug-disease common targets were identified through database screening. Thirty key targets were selected in the hub PPI network. Molecular docking simulations indicated that the core target proteins AKT1, p53, TNF-α, NF-κB, caspase 3, and caspase 9 might play essential roles in Epimedii Folium's treatment of intestinal injury. GO and KEGG pathway enrichment analysis suggested that the treatment of intestinal damage by Epimedii Folium involves oxidative stress, inflammation, and apoptosis.

Oxidative stress is thought to play a crucial role in the mechanism of cisplatin-induced toxicity (Hazman et al., 2018). From this perspective, there is clear evidence that flavonoid compounds with antioxidant properties can reduce cisplatin-induced toxicity (Malik et al., 2015; Arab et al., 2016; Lu et al., 2022). Cisplatin exposure disrupts the endogenous antioxidant defense system, increases the production of ROS, reduces the activity of antioxidant enzymes and causes oxidative stress (Khan et al., 2012b). ROS-mediated oxidative stress plays a vital role in the





progression of cisplatin-induced intestinal dysfunction (Khan et al., 2012a). Lipid peroxidation is an important marker of oxidative stress. Cisplatin treatment significantly increased the level of MDA, a product of lipid peroxidation in tissues (Karadeniz et al., 2011). Studies have reported that the

activities of antioxidant enzymes GSH-Px and CAT in intestinal tissue of cisplatin-treated rats decreased, and the level of MDA increased (Shahid et al., 2017; Hu et al., 2021). Epimedium Folium, as a natural antioxidant, has been reported to protect the antioxidant defense system by increasing the

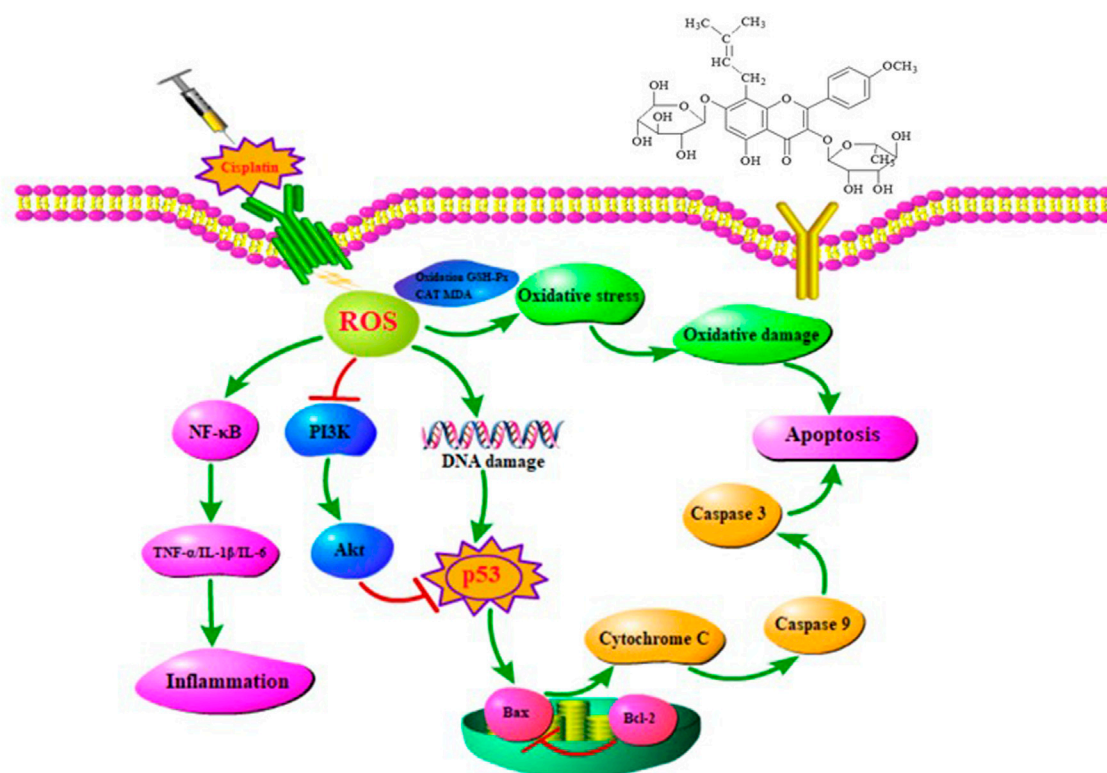


FIGURE 7

The mechanism of EFE attenuates cisplatin-induced intestinal injury in mice.

activity of antioxidant enzymes GSH-Px, CAT, and SOD while reducing the content of lipid peroxidation marker MDA (Yang et al., 2020; Zhao et al., 2022). Our results were consistent with literature reports, suggesting that EFE could exert an excellent protective role against cisplatin-induced intestinal injury by resisting oxidative stress.

Oxidative stress and inflammation are closely related in biological systems (Araujo et al., 2017). In addition to direct toxicity to the body, ROS can also induce the expression of the nuclear transcription factor NF-κB, thereby increasing the production of cell adhesion molecules, chemokines, and proinflammatory cytokines, and further enhancing the cytotoxicity of cisplatin (Li et al., 2017). Transcription of inflammatory markers such as iNOS, COX-2, TNF-α, and IL-1β can be triggered explicitly by activation of NF-κB (Liu et al., 2021). According to literature reports, Epimedii Folium can significantly reduce the expression of nuclear transcription factor NF-κB and the secretion of proinflammatory cytokines TNF-α and IL-1β (Huang et al., 2018; Yan et al., 2018). Our findings support this conclusion, showing that EFE can attenuate cisplatin-induced intestinal injury by inhibiting inflammation.

Previous studies have demonstrated that cisplatin-induced toxicity is closely related to oxidative stress-induced apoptosis (Shahid et al., 2018). When cisplatin induces ROS overproduction, it can cause mitochondrial dysfunction, change mitochondrial permeability, trigger the opening of the mitochondrial permeability transition pore (MPTP), release cytochrome c from mitochondria to the cytoplasm, and lead to the successive activation of caspase 9 and its downstream caspase 3, thereby inducing a mitochondrial-dependent pathway and ultimately leading to apoptosis (Kim et al., 2003). Cisplatin-induced intestinal toxicity mechanisms include oxidative stress, p53, and apoptosis through upregulation of caspase-3 and caspase-6 expression (Khan et al., 2012a). Bax and Bcl-2 are the most representative pro-apoptotic and anti-apoptotic factors. Cisplatin treatment significantly increased the expression of Bax and inhibited the expression of Bcl-2. Studies have shown that flavonoids extracted from Epimedii Folium can exert anti-apoptotic effects by increasing the ratio of Bcl-2/Bax and reducing the expression of caspase 3 (Liu et al., 2014; Hu and Ma, 2021). Our results also showed that EFE alleviated cisplatin-induced apoptosis by downregulating Bax

expression, upregulating Bcl-2 expression, reducing caspase-9 and caspase-3 expression, and cytochrome c release.

PI3K-Akt is a crucial intracellular signal transduction pathway that plays a crucial role in cell growth, proliferation, and migration (Zhang et al., 2020). It is also a survival signaling pathway that can resist various apoptotic injuries (Qin et al., 2021). Network pharmacology and molecular docking results suggested that the PI3K-Akt signaling pathway was the principal pathway of *Epimedii Folium* against intestinal damage. Furthermore, given the regulatory effects of *Epimedii Folium* on cell proliferation and the PI3K/Akt pathway (Song et al., 2014), this study validated the role of the PI3K-Akt pathway in the treatment of cisplatin-induced intestinal injury by EFE through western blotting. Excitingly, we demonstrated that EFE could significantly ameliorate cisplatin-induced intestinal injury by modulating the PI3K/Akt pathway.

Mitochondrial DNA is one of the main targets of cisplatin (Coskun et al., 2014). Cisplatin forms covalent adducts between platinum atoms and DNA bases, causing irreparable damage to DNA, inhibiting the synthesis of nucleic acids and proteins, and leading to apoptosis (Sancho-Martinez et al., 2012). Cisplatin-induced cell death is more intense in mitochondria-rich duodenal epithelial cells (Qian et al., 2005). p53, a tumor suppressor protein, is a crucial mediator of the DNA damage response and is considered to play a vital role in cisplatin-induced toxicity (Jiang and Dong, 2008). After cisplatin treatment, the p53 protein is activated and transferred to mitochondria, leading to the activation of the caspase pathway, which ultimately induces apoptosis (Khan et al., 2012b). EFE could inhibit cisplatin-induced apoptosis by reducing the expression of the p-p53 protein.

## Conclusion

In conclusion, combining with network pharmacology, molecular docking, and animal experiments, our study demonstrated for the first time that EFE could significantly attenuate cisplatin-induced intestinal damage by regulating oxidative stress, inflammation, and apoptosis. The molecular mechanism of action might be mainly related to PI3K/Akt, p53, and NF- $\kappa$ B signaling pathways (Figure 7). These findings could provide a theoretical basis for the clinical treatment of the toxic and side effects of cisplatin chemotherapy, guide the application of antitumor drugs, and provide new ideas for the application and development of *Epimedii Folium* in the future.

## References

Abd Rashid, N., Abd Halim, S. A. S., Teoh, S. L., Budin, S. B., Hussan, F., Ridzuan, N. R. A., et al. (2021). The role of natural antioxidants in cisplatin-induced hepatotoxicity. *Biomed. Pharmacother.* 144, 112328–112340. doi:10.1016/j.biopha.2021.112328

## Data availability statement

The original contributions presented in the study are included in the article/supplementary materials, further inquiries can be directed to the corresponding authors.

## Ethics statement

The animal study was reviewed and approved by the Experimental Animal Ethics Committee of Jilin Agricultural University.

## Author contributions

X-JL, WL, and Y-PW conceived and designed the experiments; ZW and SR and J-NH coordinated experimental arrangements; JX performed the experiments; J-NH and ZW analyzed the data; SR and E-BC contributed analysis tools; and JX wrote the paper. Y-PW revised this manuscript. All authors reviewed and approved the contents of the manuscript.

## Funding

This study was supported by the grants of the National key research and development project (No. 2021YFD1600901) and the Jilin Science and Technology Development Plan (No. 20200301037RQ).

## Conflict of interest

The authors declare that the research was conducted in the absence of any commercial or financial relationships that could be construed as a potential conflict of interest.

## Publisher's note

All claims expressed in this article are solely those of the authors and do not necessarily represent those of their affiliated organizations, or those of the publisher, the editors and the reviewers. Any product that may be evaluated in this article, or claim that may be made by its manufacturer, is not guaranteed or endorsed by the publisher.

Arab, H. H., Mohamed, W. R., Barakat, B. M., and Arafa el, S. A. (2016). Tangeretin attenuates cisplatin-induced renal injury in rats: Impact on the inflammatory cascade and oxidative perturbations. *Chem. Biol. Interact.* 258, 205–213. doi:10.1016/j.cbi.2016.09.008

- Araujo, R. S., Silveira, A. L. M., Souza, E. L. D. E., Freire, R. H., de Souza, C. M., Reis, D. C., et al. (2017). Intestinal toxicity evaluation of long-circulating and pH-sensitive liposomes loaded with cisplatin. *Eur. J. Pharm. Sci.* 106, 142–151. doi:10.1016/j.ejps.2017.05.046
- Awadalla, A., Mahdi, M. R., Zahran, M. H., Abdelbaset-Ismail, A., El-Dosoky, M., and Negm, A. (2022). Baicalein and alpha-tocopherol inhibit toll-like receptor pathways in cisplatin-induced nephrotoxicity. *Molecules* 27 (7), 2179–2195. doi:10.3390/molecules27072179
- Bljlevens, N. M., Donnelly, J. P., and De Pauw, B. E. (2000). Mucosal barrier injury: Biology, pathology, clinical counterparts and consequences of intensive treatment for hematological malignancy: An overview. *Bone Marrow Transpl.* 25 (12), 1269–1278. doi:10.1038/sj.bmt.1702447
- Coskun, R., Turan, M. I., Turan, I. S., and Gulapoglu, M. (2014). The protective effect of thiamine pyrophosphate, but not thiamine, against cardiotoxicity induced with cisplatin in rats. *Drug Chem. Toxicol.* 37 (3), 290–294. doi:10.3109/01480545.2013.851688
- Gholampour, F., Masoudi, R., Khaledi, M., Rooyeh, M. M., Farzad, S. H., Ataollahi, F., et al. (2022). Berberis integrifolia hydro-alcoholic root extract and its constituent berberine protect against cisplatin-induced nephro- and hepatotoxicity. *Am. J. Med. Sci.* 364, 76–87. doi:10.1016/j.amjms.2021.10.037
- Groschwitz, K. R., and Hogan, S. P. (2009). Intestinal barrier function: Molecular regulation and disease pathogenesis. *J. Allergy Clin. Immunol.* 124 (1), 3–20. doi:10.1016/j.jaci.2009.05.038
- Gu, S., Zhou, R., and Wang, X. Y. (2018). Comparison of enhanced male mice sexual function among three medicinal materials. *Andrologia* 50 (9), 13087–13094. doi:10.1111/and.13087
- Halliwell, B. (2006). Reactive species and antioxidants. Redox biology is a fundamental theme of aerobic life. *Plant Physiol.* 141 (2), 312–322. doi:10.1104/pp.106.077073
- Hazman, O., Bozkurt, M. F., Fidan, A. F., Uysal, F. E., and Celik, S. (2018). The effect of boric acid and borax on oxidative stress, inflammation, ER stress and apoptosis in cisplatin toxication and nephrotoxicity developing as a result of toxication. *Inflammation* 41 (3), 1032–1048. doi:10.1007/s10753-018-0756-0
- Hu, J. N., Yang, J. Y., Jiang, S., Zhang, J., Liu, Z., Hou, J. G., et al. (2021). Panax quinquefolium saponins protect against cisplatin evoked intestinal injury via ROS-mediated multiple mechanisms. *Phytomedicine* 82, 153446. doi:10.1016/j.phymed.2020.153446
- Hu, Y., and Ma, X. (2021). Icariin treatment protects against gentamicin-induced ototoxicity via activation of the AMPK-SIRT3 pathway. *Front. Pharmacol.* 12, 620741. doi:10.3389/fphar.2021.620741
- Huang, S., Meng, N., Chang, B., Quan, X., Yuan, R., and Li, B. (2018). Anti-inflammatory activity of Epimedium brevicornu Maxim ethanol extract. *J. Med. Food* 21 (7), 726–733. doi:10.1089/jmf.2017.4088
- Indran, I. R., Liang, R. L., Min, T. E., and Yong, E. L. (2016). Preclinical studies and clinical evaluation of compounds from the genus Epimedium for osteoporosis and bone health. *Pharmacol. Ther.* 162, 188–205. doi:10.1016/j.pharmthera.2016.01.015
- Jiang, M., and Dong, Z. (2008). Regulation and pathological role of p53 in cisplatin nephrotoxicity. *J. Pharmacol. Exp. Ther.* 327 (2), 300–307. doi:10.1124/jpet.108.139162
- Karadeniz, A., Simsek, N., Karakus, E., Yildirim, S., Kara, A., Can, I., et al. (2011). Can, IRoyal jelly modulates oxidative stress and apoptosis in liver and kidneys of rats treated with cisplatin. *Oxid. Med. Cell. Longev.* 2011, 981793. doi:10.1155/2011/981793
- Khan, R., Khan, A. Q., Qamar, W., Lateef, A., Ali, F., Rehman, M. U., et al. (2012a). Chrysin abrogates cisplatin-induced oxidative stress, p53 expression, goblet cell disintegration and apoptotic responses in the jejunum of Wistar rats. *Br. J. Nutr.* 108 (9), 1574–1585. doi:10.1017/S0007114511007239
- Khan, R., Khan, A. Q., Qamar, W., Lateef, A., Tahir, M., Rehman, M. U., et al. (2012b). Chrysin protects against cisplatin-induced colon, toxicity via amelioration of oxidative stress and apoptosis: Probable role of p38MAPK and p53. *Toxicol. Appl. Pharmacol.* 258 (3), 315–329. doi:10.1016/j.taap.2011.11.013
- Kim, J. S., He, L., and Lemasters, J. J. (2003). Mitochondrial permeability transition: A common pathway to necrosis and apoptosis. *Biochem. Biophys. Res. Commun.* 304 (3), 463–470. doi:10.1016/s0006-291x(03)00618-1
- Lee, C. S., Ryan, E. J., and Doherty, G. A. (2014). Gastro-intestinal toxicity of chemotherapeutics in colorectal cancer: The role of inflammation. *World J. Gastroenterol.* 20 (14), 3751–3761. doi:10.3748/wjg.v20.i14.3751
- Lee, W., Nam, J. H., Cho, H. J., Lee, J. Y., Cho, W. K., Kim, U., et al. (2017). Epimedium koreanum Nakai inhibits PMA-induced cancer cell migration and invasion by modulating NF- $\kappa$ B/MMP-9 signaling in monomorphic malignant human glioma cells. *Oncol. Rep.* 38 (6), 3619–3631. doi:10.3892/or.2017.6043
- Li, Y., Liu, M., Zuo, Z., Liu, J., Yu, X., Guan, Y., et al. (2017). TLR9 regulates the NF- $\kappa$ B-NLRP3-IL-1 $\beta$  pathway negatively in salmonella-induced nkg2d-mediated intestinal inflammation. *J. Immunol.* 199 (2), 761–773. doi:10.4049/jimmunol.1601416
- Liu, P., Jin, X., Lv, H., Li, J., Xu, W., Qian, H. H., et al. (2014). Icaritin ameliorates carbon tetrachloride-induced acute liver injury mainly because of the antioxidative function through estrogen-like effects. *Vitro Cell. Dev. Biol. Anim.* 50 (10), 899–908. doi:10.1007/s11626-014-9792-8
- Liu, X. Y., Su, J., Wang, G., Zheng, L. H., Wang, G. N., Sun, Y., et al. (2021). Discovery of phenolic Glycoside from Hyssopus cuspidatus attenuates LPS-induced inflammatory responses by inhibition of iNOS and COX-2 expression through suppression of NF- $\kappa$ B activation. *Int. J. Mol. Sci.* 22 (22), 12128–12144. doi:10.3390/ijms222212128
- Lopez-Tofino, Y., Vera, G., Lopez-Gomez, L., Giron, R., Nurgali, K., Uranga, J. A., et al. (2021). Effects of the food additive monosodium glutamate on cisplatin-induced gastrointestinal dysmotility and peripheral neuropathy in the rat. *Neurogastroenterol. Motil.* 33 (4), e14020. doi:10.1111/nmo.14020
- Lu, X., Deng, T., Dong, H., Han, J., Yu, Y., Xiang, D., et al. (2022). Novel application of eupatilin for effectively attenuating cisplatin-induced auditory hair cell death via mitochondrial apoptosis pathway. *Oxid. Med. Cell. Longev.* 2022, 1090034. doi:10.1155/2022/1090034
- Ma, P., Zhang, S., Su, X., Qiu, G., and Wu, Z. (2015). Protective effects of icariin on cisplatin-induced acute renal injury in mice. *Am. J. Transl. Res.* 7 (10), 2105–2114.
- Ma, S., Xu, H., Huang, W., Gao, Y., Zhou, H., Li, X., et al. (2021). Corrigendum: Chrysophanol Relieves cisplatin-induced nephrotoxicity via concomitant inhibition of oxidative stress, apoptosis, and inflammation. *Front. Physiol.* 12, 794302. doi:10.3389/fphys.2021.794302
- Malik, S., Bhatia, J., Suchal, K., Gamad, N., Dinda, A. K., Gupta, Y. K., et al. (2015). Nobiletin ameliorates cisplatin-induced acute kidney injury due to its anti-oxidant, anti-inflammatory and anti-apoptotic effects. *Exp. Toxicol. Pathol.* 67 (7–8), 427–433. doi:10.1016/j.etp.2015.04.008
- Mansour, H. H., Hafez, H. F., and Fahmy, N. M. (2006). Silymarin modulates cisplatin-induced oxidative stress and hepatotoxicity in rats. *J. Biochem. Mol. Biol.* 39 (6), 656–661. doi:10.5483/bmbrep.2006.39.6.656
- Muhanmode, Y., Mengke, W., Maitinuri, A., and Shen, G. Q. (2021). Curcumin and resveratrol inhibit chemoresistance in cisplatin-resistant epithelial ovarian cancer cells via targeting P13K pathway. *Hum. Exp. Toxicol.* 40 (12), S861–S868. doi:10.1177/09603271211052985
- Mukhopadhyay, P., Horvath, B., Kechrid, M., Tanchian, G., Rajesh, M., Naura, A. S., et al. (2011). Poly(ADP-ribose) polymerase-1 is a key mediator of cisplatin-induced kidney inflammation and injury. *Free Radic. Biol. Med.* 51 (9), 1774–1788. doi:10.1016/j.freeradbiomed.2011.08.006
- Pei, Z., Wu, M., Yu, H., Long, G., Gui, Z., Li, X., et al. (2022). Isoliquiritin ameliorates cisplatin-induced renal proximal tubular cell injury by antagonizing apoptosis, oxidative stress and inflammation. *Front. Med.* 9, 873739. doi:10.3389/fmed.2022.873739
- Qian, W., Nishikawa, M., Haque, A. M., Hirose, M., Mashimo, M., Sato, E., et al. (2005). Mitochondrial density determines the cellular sensitivity to cisplatin-induced cell death. *Am. J. Physiol. Cell Physiol.* 289 (6), C1466–C1475. doi:10.1152/ajpcell.00265.2005
- Qin, H., Zhang, H., Zhang, X., Zhang, S., Zhu, S., and Wang, H. (2021). Resveratrol attenuates radiation enteritis through the SIRT1/FOXO3a and PI3K/AKT signaling pathways. *Biochem. Biophys. Res. Commun.* 554, 199–205. doi:10.1016/j.bbrc.2021.03.122
- Rashid, S., Nafees, S., Siddiqi, A., Vafa, A., Afzal, S. M., Parveen, R., et al. (2017). Partial protection by 18 Glycrrhetic acid against Cisplatin induced oxidative intestinal damage in wistar rats: Possible role of NF $\kappa$ B and caspases. *Pharmacol. Rep.* 69 (5), 1007–1013. doi:10.1016/j.pharep.2017.02.013
- Saba, E., Lee, Y. Y., Kim, M., Hyun, S. H., Park, C. K., Son, E., et al. (2020). A novel herbal formulation consisting of red ginseng extract and Epimedium koreanum Nakai attenuated dextran sulfate sodium-induced colitis in mice. *J. Ginseng Res.* 44 (6), 833–842. doi:10.1016/j.jgr.2020.02.003
- Sancho-Martinez, S. M., Prieto-Garcia, L., Prieto, M., Lopez-Novoa, J. M., and Lopez-Hernandez, F. J. (2012). Subcellular targets of cisplatin cytotoxicity: An integrated view. *Pharmacol. Ther.* 136 (1), 35–55. doi:10.1016/j.pharmthera.2012.07.003
- Shahid, F., Farooqui, Z., and Khan, F. (2018). Cisplatin-induced gastrointestinal toxicity: An update on possible mechanisms and on available gastroprotective strategies. *Eur. J. Pharmacol.* 827, 49–57. doi:10.1016/j.ejphar.2018.03.009
- Shahid, F., Farooqui, Z., Rizwan, S., Abidi, S., Parwez, I., and Khan, F. (2017). Oral administration of Nigella sativa oil ameliorates the effect of cisplatin on brush



border membrane enzymes, carbohydrate metabolism and antioxidant system in rat intestine. *Exp. Toxicol. Pathol.* 69 (5), 299–306. doi:10.1016/j.etp.2017.02.001

Song, J., Zhong, R., Huang, H., Zhang, Z., Ding, D., Yan, H., et al. (2014). Combined treatment with Epimedium koreanum Nakai extract and gefitinib overcomes drug resistance caused by T790M mutation in non-small cell lung cancer cells. *Nutr. Cancer* 66 (4), 682–689. doi:10.1080/01635581.2014.895392

Tserga, E., Moreno-Pauble, R., Sarlus, H., Bjorn, E., Guimaraes, E., Goritz, C., et al. (2020). Circadian vulnerability of cisplatin-induced ototoxicity in the cochlea. *FASEB J.* 34 (10), 13978–13992. doi:10.1096/fj.202001236R

Vidra, R., Nemes, A., Vidrean, A., Pintea, S., Tintari, S., Deac, A., et al. (2022). Pathological complete response following cisplatin or carboplatin-based neoadjuvant chemotherapy for triple-negative breast cancer: A systematic review and meta-analysis. *Exp. Ther. Med.* 23 (1), 91. doi:10.3892/etm.2021.11014

Wang, Z., Mai, S., Lv, P., Xu, L., and Wang, Y. (2021). Etoposide plus cisplatin chemotherapy improves the efficacy and safety of small cell lung cancer. *Am. J. Transl. Res.* 13 (11), 12825–12833.

Wu, L., Du, Z. R., Xu, A. L., Yan, Z., Xiao, H. H., Wong, M. S., et al. (2017). Neuroprotective effects of total flavonoid fraction of the Epimedium koreanum nakai extract on dopaminergic neurons: *In vivo* and *in vitro*. *Biomed. Pharmacother.* 91, 656–663. doi:10.1016/j.biopha.2017.04.083

Xiao, H. B., Sui, G. G., and Lu, X. Y. (2017). Icaritin improves eNOS/NO pathway to prohibit the atherogenesis of apolipoprotein E-null mice. *Can. J. Physiol. Pharmacol.* 95 (6), 625–633. doi:10.1139/cjpp-2016-0367

Xiong, W., Huang, J., Li, X. Y., Zhang, Z., Jin, M. L., Wang, J., et al. (2020a). Icaritin and its phosphorylated derivatives alleviate intestinal epithelial barrier disruption caused by enterotoxigenic *Escherichia coli* through modulate p38 MAPK *in vivo* and *in vitro*. *FASEB J.* 34 (1), 1783–1801. doi:10.1096/fj.201902265R

Xiong, W., Ma, H., Zhang, Z., Jin, M., Wang, J., Xu, Y., et al. (2020b). The protective effect of icaritin and phosphorylated icaritin against LPS-induced intestinal goblet cell dysfunction. *Innate Immun.* 26 (2), 97–106. doi:10.1177/1753425919867746

Xu, J., Zhang, B., Chu, Z., Jiang, F., and Han, J. (2021). Wogonin alleviates cisplatin-induced cardiotoxicity in mice via inhibiting Gasdermin D-mediated Pyroptosis. *J. Cardiovasc. Pharmacol.* 78 (4), 597–603. doi:10.1097/FJC.0000000000001085

Yan, N., Wen, D. S., Zhao, Y. R., and Xu, S. J. (2018). Epimedium sagittatum inhibits TLR4/MD-2 mediated NF- $\kappa$ B signaling pathway with anti-inflammatory activity. *BMC Complement. Altern. Med.* 18 (1), 303. doi:10.1186/s12906-018-2363-x

Yang, X. H., Li, L., Xue, Y. B., Zhou, X. X., and Tang, J. H. (2020). Flavonoids from Epimedium pubescens: Extraction and mechanism, antioxidant capacity and effects on CAT and GSH-px of *Drosophila melanogaster*. *PeerJ* 8, 8361–8382. doi:10.7717/peerj.8361

Zhang, E., Yang, H., Li, M., and Ding, M. (2020). A possible underlying mechanism behind the cardioprotective efficacy of tangeretin on isoproterenol triggered cardiotoxicity via modulating PI3K/Akt signaling pathway in a rat model. *J. Food Biochem.* 44 (9), e13368. doi:10.1111/jfbc.13368

Zhang, F., Hu, Y., Xu, X. M., Zhai, X. H., Wang, G. Z., Ning, S. L., et al. (2015). Icaritin protects against intestinal ischemia-reperfusion injury. *J. Surg. Res.* 194 (1), 127–138. doi:10.1016/j.jss.2014.10.004

Zhang, W., Chen, H., Wang, Z., Lan, G., and Zhang, L. (2013). Comparative studies on antioxidant activities of extracts and fractions from the leaves and stem of Epimedium koreanum Nakai. *J. Food Sci. Technol.* 50 (6), 1122–1129. doi:10.1007/s13197-011-0447-4

Zhang, Y., Bai, M., Zhang, B., Liu, C., Guo, Q., Sun, Y., et al. (2015). Uncovering pharmacological mechanisms of Wu-tou decoction acting on rheumatoid arthritis through systems approaches: Drug-target prediction, network analysis and experimental validation. *Sci. Rep.* 5, 9463. doi:10.1038/srep09463

Zhao, H. Y., Zhao, T. T., Yang, J. H., Huang, Q. Q., Wu, H., Pan, Y. Y., et al. (2022). Epimedium protects against dyszoospermia in mice with Pex3 knockout by exerting antioxidant effects and regulating the expression level of P16. *Cell Death Dis.* 13 (1), 69–80. doi:10.1038/s41419-021-04435-8

Zhou, Y. D., Hou, J. G., Yang, G., Jiang, S., Chen, C., Wang, Z., et al. (2019). Icaritin ameliorates cisplatin-induced cytotoxicity in human embryonic kidney 293 cells by suppressing ROS-mediated PI3K/Akt pathway. *Biomed. Pharmacother.* 109, 2309–2317. doi:10.1016/j.biopha.2018.11.108

Zou, Y. T., Zhou, J., Wu, C. Y., Zhang, W., Shen, H., Xu, J. D., et al. (2021). Protective effects of Poria cocos and its components against cisplatin-induced intestinal injury. *J. Ethnopharmacol.* 269, 113722–113732. doi:10.1016/j.jep.2020.113722





## OPEN ACCESS

EDITED BY  
Maria Dimitrova,  
Medical University Sofia, Bulgaria

REVIEWED BY  
Rita Leporati,  
Fondazione IRCCS Istituto Nazionale  
dei Tumori, Italy  
Caren Lee Hughes,  
Mayo Clinic Florida, United States

\*CORRESPONDENCE  
Cristina Lungulescu,  
cristina.lungulescu@yahoo.com

SPECIALTY SECTION  
This article was submitted to  
Gastrointestinal and Hepatic  
Pharmacology,  
a section of the journal  
Frontiers in Pharmacology

RECEIVED 11 September 2022  
ACCEPTED 30 September 2022  
PUBLISHED 13 October 2022

CITATION  
Sur D, Lungulescu C, Spînu Ș, Gorzo A,  
Dumitrescu E-A, Gheonea DI and  
Lungulescu C-V (2022), Trifluridine/  
tipiracil as a therapeutic option in real  
life setting of metastatic colorectal  
cancer: An efficacy and safety analysis.  
*Front. Pharmacol.* 13:1041927.  
doi: 10.3389/fphar.2022.1041927

COPYRIGHT  
© 2022 Sur, Lungulescu, Spînu, Gorzo,  
Dumitrescu, Gheonea and Lungulescu.  
This is an open-access article  
distributed under the terms of the  
[Creative Commons Attribution License](https://creativecommons.org/licenses/by/4.0/)  
(CC BY). The use, distribution or  
reproduction in other forums is  
permitted, provided the original  
author(s) and the copyright owner(s) are  
credited and that the original  
publication in this journal is cited, in  
accordance with accepted academic  
practice. No use, distribution or  
reproduction is permitted which does  
not comply with these terms.

# Trifluridine/tipiracil as a therapeutic option in real life setting of metastatic colorectal cancer: An efficacy and safety analysis

Daniel Sur<sup>1,2</sup>, Cristina Lungulescu<sup>3\*</sup>, Ștefan Spînu<sup>1</sup>,  
Alecsandra Gorzo<sup>1</sup>, Elena-Adriana Dumitrescu<sup>4</sup>,  
Dan Ionut Gheonea<sup>5</sup> and Cristian-Virgil Lungulescu<sup>6</sup>

<sup>1</sup>Department of Medical Oncology, The Oncology Institute, Cluj-Napoca, Romania, <sup>2</sup>Department of Medical Oncology, University of Medicine and Pharmacy, Cluj-Napoca, Romania, <sup>3</sup>Doctoral School, University of Medicine and Pharmacy of Craiova, Craiova, Romania, <sup>4</sup>Institute of Oncology, Bucharest, Romania, <sup>5</sup>Gastroenterology Department, University of Medicine and Pharmacy of Craiova, Craiova, Romania, <sup>6</sup>Oncology Department, University of Medicine and Pharmacy of Craiova, Craiova, Romania

**Background:** In the phase III RECURSE trial, the orally administered combination trifluridine/tipiracil (FTD/TPI) demonstrated a survival benefit and an acceptable safety profile, earning approval as a third-line therapy in metastatic colorectal cancer (mCRC). This study aimed to assess the efficacy and safety of FTD/TPI in daily clinical practice in Romanian population.

**Methods:** A single-center, retrospective, and observational study analyzed patients with mCRC that received chemotherapy with trifluridine/tipiracil between May 2019 and May 2022 at the Oncology Institute Prof. Dr. Ion Chiricuță in Cluj-Napoca, Romania. Study endpoints included safety, and median progression-free survival (PFS).

**Results:** In this Romanian cohort ( $n = 50$ ) the most common treatment-emergent adverse event was haematological toxicity (76%): anemia (50%), leucopenia (38%), neutropenia (34%), and thrombocytopenia (30%), followed by fatigue (60%), and abdominal pain (18%). Overall, the median progression-free survival was 3.85 months (95% CI: 3.1–4.6 months). PFS was significantly correlated with the number of FTD/TPI administrations and prior surgery.

**Conclusion:** Our study corroborated the previously described safety profile for FTD/TPI in the third-line setting, and demonstrated relatively superior mPFS.

## KEYWORDS

metastatic colorectal cancer, trifluridine/tipiracil, Romanian population, toxicity analysis, real-world data

## Introduction

Colorectal cancer (CRC) is one of the most frequent malignancies and leading causes of cancer-related mortality worldwide (Ferlay et al., 2015; Favoriti et al., 2016). Although overall survival (OS) has improved, there are few regimens available for patients who progress beyond first- and second-line treatment (Vogel et al., 2017; Arnold et al., 2018).

Fluoropyrimidines have been generally regarded an essential component of colorectal cancer treatment (Meyerhardt & Mayer, 2005). These agents predominantly inhibit thymidylate synthase, an enzyme involved in pyrimidine nucleotide synthesis. The ability of fluorouracil (5-FU) to bind to thymidylate synthase has been improved by combining it with folinic acid (Sobrero et al., 2000). The current standard of care for mCRC includes the addition of oxaliplatin (FOLFOX) or irinotecan (FOLFIRI) to fluorouracil and folinic acid, along with a vascular endothelial growth factor (VEGF) inhibitor (e.g., bevacizumab) or an epidermal growth factor receptor (EGFR) inhibitor for RAS wild-type tumors (e.g., cetuximab or panitumumab) (Yoshino et al., 2018). Trifluridine (FTD) was developed nearly 50 years ago, close to the introduction of fluorouracil, and demonstrated antitumoral activity (Heidelberger & Anderson, 1964; Heidelberger et al., 1965; Dexter et al., 1972). However, subsequent drug development was terminated because the required dosing schedule for trifluridine exhibited a toxicity profile that was unacceptable for long-term use (Dexter et al., 1972). It was not until approximately 15 years ago that tipiracil (TPI) hydrochloride, which inhibits the fast degradation of trifluridine and enables the preservation of acceptable plasma concentrations of the active medication, was developed (Fukushima et al., 2000).

The subsequent combination of trifluridine and tipiracil (FTD/TPI) to develop TAS-102 prompted the preclinical and clinical trials that led to its approval for refractory mCRC in Japan in March 2014 (Yoshino et al., 2016). Firstly, a Japanese phase II study (JapicCTI-090880) established the safety and efficacy of TAS-102 monotherapy in patients with refractory mCRC (Yoshino et al., 2012). Following that, the RECOURSE trial (Mayer et al., 2015) was successful in gaining authorization in both the United States and Europe in September 2015, and April 2016, respectively (Mulet et al., 2018). According to the phase III study (NCT01607957), FTD/TPI increased both median progression-free survival (mPFS) and median overall survival (mOS) when compared to placebo, from 1.7 to 2.0 months and 5.3–7.1 months, respectively (Mayer et al., 2015).

These findings were corroborated by a second phase III trial (TERRA) conducted in an all-Asian demographic (Xu et al., 2018). In light of the promising outcomes of the clinical studies, an international phase IIIb research, PRECONNECT (NCT03306394), was launched to further analyze FTD/TPI in a sizable cohort of patients engaged in normal clinical practice (Bachet et al., 2020).

Post hoc analyses of the PRECONNECT research are being conducted on a country-specific basis due to disparities in disease treatment between states, with publications so far available for Italy (Zaniboni et al., 2021), and Turkey (Ozet et al., 2022).

In February 2017, the National Oncology Program of Romania covered trifluridine/tipiracil for patients with mCRC who had previously had two or more lines of treatment or who were ineligible for intense chemotherapy.

To the best of our knowledge, this is the first study to document real-world experience of using FTD/TPI in mCRC in Romania.

## Materials and methods

### Study design

The present investigation is non-interventional, retrospective, single-center study that analyzed patients with metastatic colorectal cancer that received chemotherapy with trifluridine/tipiracil between May 2019 and May 2022 at the Oncology Institute Prof. Dr. Ion Chiricuță in Cluj-Napoca, Romania. The study was conducted in compliance with the principles of the Declaration of Helsinki, and all participants provided written, informed consent.

### Patients

Patients included in the study had to be at least 18 years old, have a biopsy-confirmed adenocarcinoma of the colon or rectum with metastatic lesions, and have an Eastern Cooperative Oncology Group performance status (ECOG PS) of 0–2. Patients were required to have undergone a minimum of two prior regimens of standard chemotherapy consisting of fluoropyrimidine, oxaliplatin, and irinotecan (which included adjuvant setting if recurrence happened within 6 months), and bevacizumab, or anti-epidermal growth factor receptor (EGFR) monoclonal antibody for RAS-wild-type tumors.

Baseline information such as demographic data, ECOG PS, disease characteristics, RAS-mutation status, treatment description (prior systemic regimens and surgeries), number of trifluridine/tipiracil cycles, toxicities, disease response, and date of progression were collected from patients' medical records.

### Treatment

Trifluridine/tipiracil was given orally twice daily at a dosage of 35 mg/m<sup>2</sup>, in a 28-day cycle that included five treatment days and 2 rest days for 2 weeks, followed by a 14-day rest period. This completed one treatment cycle, which was repeated every

TABLE 1 Baseline patients' characteristics.

Characteristics	Patients given FTD/TPI ( <i>n</i> = 50)
Age (mean ± SD)	62.9 ± 12.9
≤45	8 (16%)
46–69	23 (46%)
≥70	19 (38%)
Gender	26 (52%)
Male	24 (48%)
Female	
Comorbidities	
Yes	30 (60%)
No	8 (16%)
N/A	12 (24%)
Type of comorbidities	
Hypertension	9 (18%)
Heart disease	15 (30%)
Smoking/alcohol	0
Diabetes	2 (4%)
Others	25 (50%)
Primary tumor site	
Left	37 (74%)
Right	8 (16%)
Rectum	18 (36%)
RAS status	
Wild-type	19 (38%)
Mutated	19 (38%)
N/A	12 (24%)
Lymph node involvement	
Yes	45 (90%)
No	0
Missing data	5 (10%)
Lymph node involvement	
N0	8 (16%)
N1	17 (34%)
N2	20 (40%)
No	0
Missing data	5 (10%)
Location of metastases	
Peritoneal	18 (36%)
Liver	39 (78%)
Lung	28 (56%)
Lymph nodes	11 (22%)
Bone	8 (16%)
Brain	2 (4%)
Others	3 (6%)
Number of metastatic organ locations	
1	10 (20%)
2	18 (36%)
≥3	22 (44%)

(Continued on following page)

TABLE 1 (Continued) Baseline patients' characteristics.

Characteristics	Patients given FTD/TPI ( <i>n</i> = 50)
Surgery	
No surgery delivered	23 (26%)
Yes	37 (74%)
First-line chemotherapy regimens	
Oxaliplatin-based chemotherapy + Bevacizumab/cetuximab	33 (66%)
Irinotecan-based chemotherapy + Bevacizumab/cetuximab	7 (14%)
Second-line chemotherapy regimens	
Oxaliplatin-based chemotherapy + Bevacizumab/cetuximab	1 (2%)
Irinotecan-based chemotherapy + Bevacizumab/cetuximab	24 (48%)
Number of FTD/TPI administrations in 3rd line	
Mean ± SD	4.58 ± 3.91
≤5	25 (80%)
6–9	3 (10%)
≥10	3 (10%)
Missing data	—
Number of FTD/TPI administrations in 4th line	
Mean ± SD	4.0 ± 2.1
≤5	10 (83%)
6–9	2 (17%)
≥10	0
Missing data	—
Post-FTD/TPI adverse events	
Yes	40 (80%)
No	3 (6%)
N/A	7 (14%)
ECOG Status	
0	5 (10%)
1	20 (40%)
2	18 (36%)
3	7 (14%)

Data are presents as frequency (percentage) or mean (±SD).

4 weeks. Treatment continued until disease progression, unacceptable toxicity, or withdrawal of consent.

## Outcomes

Study endpoints included safety, and median progression-free survival (PFS). PFS was defined as the time elapsed between the beginning of trifluridine/tipiracil treatment and the first recorded disease progression or death from any cause. Treating physicians determined the intervals at which tumor response was measured using RECIST 1.1. The National Cancer Institute Common Terminology Criteria for Adverse Events (NCI CTCAE), version 4.0, was used to grade all toxicities.

## Statistical analysis

All the data was collected in an Excel worksheet and analyzed using GraphPad 9.4.1 (GraphPad Software, San Diego, CA, United States). Continuous variables were presented as mean ± standard deviation, and categorical variables as number (percentages). The Kaplan-Meier method was used to estimate the curve corresponding to the progression-free survival (PFS). The patients alive at the time of last follow-up were censored. Cox regression was performed for PFS with the main known prognostic factors: age, gender, tumor sidedness, RAS mutation, lymph node involvement, surgery, number of metastatic locations, number of FTD/TPI administrations. The threshold for statistical significance was 5%.

TABLE 2 Reported toxicities (CTCAE).

Reported toxicities	Patients given FTD/TPI (n = 50)
Any Grade AE	
Low blood count	38 (76%)
Leucopenia	19 (38%)
Anemia	25 (50%)
Thrombocytopenia	15 (30%)
Neutropenia	17 (34%)
Tiredness (fatigue/weakness)	30 (60%)
Nausea	4 (8%)
Vomiting	2 (4%)
Decreased appetite	6 (12%)
Diarrhea	2 (4%)
Abdominal pain	9 (18%)
Fever	1 (2%)
Grade 3 AEs	
Leucopenia	9 (18%)
Anemia	2 (4%)
Neutropenia	12 (24%)
Tiredness (fatigue/weakness)	1 (2%)

Data are presents as frequency (percentage).

## Results

A total of 50 patients with metastatic colorectal cancer were included in the study. Baseline characteristics of enrolled patients and reported toxicities are summarized in Table 1. There were 26 male and 24 female patients with a median age of 65.5 (range, 31–86) years. Young ( $\leq 45$  years) and elderly ( $\geq 70$  years) patients represented 16% and 38% of our sample, respectively. The bulk of study participants had an ECOG performance level of 1–40%, followed by ECOG 2 (36%), ECOG 3 (14%), and ECOG 0 (10%). Studying the comorbidities (60% patients had comorbidities), most of them had heart disease (30%) and hypertension (18%). Left-sided tumors were the most common (74%) presenting with cancers in the rectum (36%). Of 50 patients, 19 (38%) had wild type RAS status and 19 (38%) were mutated. Lymph node involvement was observed in 90% of patients, among which 8 (16%) were N0, 17 (34%) were N1 and 20 (40%) were N2. The liver was the principal common metastatic site (78%), followed by lung (56%), peritoneal (36%), lymph nodes (22%), bone (16%) or brain (4%). Most of the patients had more than 3 metastatic organ locations (44%). Surgery was performed for most of the patients (74%) (Table 1).

Regarding first-line, oxaliplatin-based chemotherapy combined with bevacizumab or cetuximab was the dominant choice (66%), whereas irinotecan-based chemotherapy combined with bevacizumab or cetuximab was chosen for 14% cases.

Recorded post-FTD/TPI toxicities were registered in 80% of the study population (Table 2). The most common adverse event

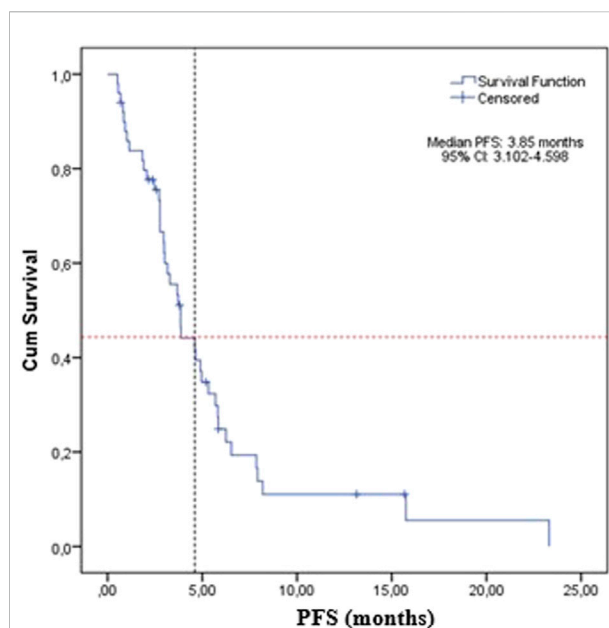


FIGURE 1  
Progression-free survival of the sample treated with FTD/TPI.

was low blood count (76%), followed by fatigue (60%), anemia (50%), leucopenia (38%), neutropenia (34%), thrombocytopenia (30%) and abdominal pain (18%). Interestingly, when grade 3 AEs are considered—respecting CTCAE v5.0 grading, the majority of patients (24%) encountered grade 3 neutropenia, followed by grade 3 leucopenia (18%), grade 3 anemia (4%) and only one patient experienced Grade 3 fatigue (2%).

The median PFS was 3.85 months (95% CI: 3.1–4.6) for the whole study group (Figure 1).

For male patients with metastatic colorectal cancer, the median PFS was 3.16 months (95% CI: 1.94–4.38) and for female patients, the median PFS increased to 4.9 months (95% CI: 2.5–7.3), but the differences were not significant ( $p$ -value = 0.446) (Figure 2A).

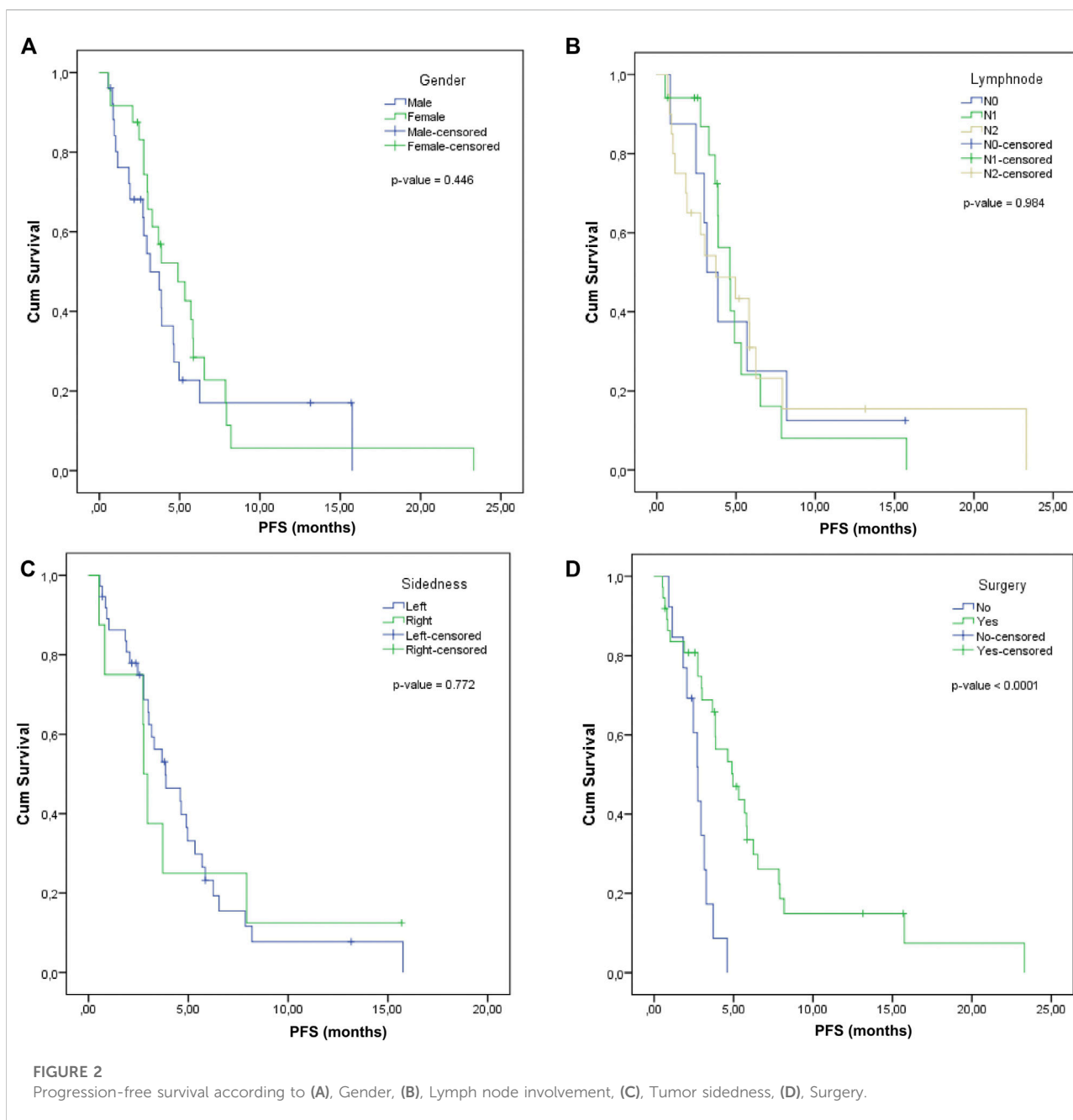
The median PFS was calculated according to the lymph nodal status: for N0, it was 3.16 months (95% CI: 0.97–4.35), for N1, it was 4.6 months (95% CI: 3.32–5.88), and for N2, it was 3.88 months (95% CI: 2.79–4.97). The comparative difference between them was not statistically significant ( $p$ -value = 0.984) (Figure 2B).

Log Rank comparison on sidedness showed no statistically significant differences between the left and right: 3.85 months (2.14–5.56) vs. 2.76 months (2.44–3.08),  $p$ -value = 0.772 (Figure 2C).

A significantly superior median PFS was observed in the case of patients that previously received surgery (4.96, 95% CI: 3.03–6.89) compared to those without surgery (2.76, 95% CI: 2.29–3.23), with log rank  $p$ -value < 0.0001 (Figure 2D).

The potential predictors of PFS were investigated based on Kaplan-Meier, univariate and multivariate Cox regression and





only number of FTD/TPI administrations and surgery were significantly associated with PFS (Table 3). We confirmed the prognostic value of number of FTD/TPI administrations ( $p$ -value < 0.0001) and surgery ( $p$ -value < 0.0001) on PFS. On univariate Cox regression analysis, patients with less than five doses had significantly inferior median PFS (3.16 months vs. 7.92 months), HR = 0.18 (95% CI: 0.07–0.51),  $p$ -value < 0.0001. Moreover, previous surgery was also associated with PFS (log rank  $p$ -value < 0.0001): the impact of previous surgery was associated with a superior PFS compared to patients who did not benefit from any surgery. Notably, these

observations were confirmed on multivariate analysis after adjustment for covariates.

## Discussion

FTD/TPI is an anti-tumor medication administered orally that consists of trifluridine (a nucleoside analogue), and tipiracil (a thymidine phosphorylase inhibitor), and is registered for mCRC refractory to standard regimens in over 93 countries (Bachet et al., 2020). Specifically, thymidine kinase

TABLE 3 Association of baseline characteristics with PFS.

Characteristics	Kaplan-meier survival analysis with log-rank test		Univariate cox regression analysis		Multivariate cox regression analysis	
	PFS (95%CI)	p-value	HR (95%CI)	p-value	HR (95%CI)	p-value
Gender (female vs. male)	3.85 (3.1–4.6)	0.446	1.27 (0.68–2.38)	0.449	—	—
Age (<50 years vs. ≥ 50 years)	3.85 (3.1–4.6)	0.949	0.97 (0.43–2.21)	0.950	—	—
Comorbid conditions (yes vs. no)	3.68 (2.5–4.9)	0.844	1.09 (0.46–2.58)	0.845	—	—
Tumor sidedness (left-sided vs. right-sided)	3.68 (2.7–4.7)	0.772	1.13 (0.49–2.61)	0.775	—	—
Lymph node involvement (N2 vs. N0/N1)	3.88 (2.8–4.97)	0.858	0.94 (0.48–1.85)	0.858	—	—
Number of metastatic organ locations (<3 vs. ≥3)	3.85 (3.1–4.6)	0.759	1.1 (0.6–2.1)	0.760	—	—
Number of FTD/TPI administrations (≤5 vs. >5)	3.85 (3.1–4.6)	<0.0001	0.18 (0.07–0.51)	0.001	0.21 (0.07–0.59)	0.003
Surgery (no vs. yes)	3.85 (3.1–4.6)	<0.0001	0.26 (0.12–0.58)	0.001	0.34 (0.15–0.76)	0.008

phosphorylates FTD, which is then incorporated into DNA, leading to DNA malfunction and cytotoxicity. This mechanism of action differs from that of 5-FU and other fluoropyrimidines, which inhibit thymidylate synthase (Sunakawa et al., 2017).

The results of this real-world investigation corroborate the findings of phase III studies and worldwide recommendations, which demonstrate that FTD/TPI is a safe and effective therapy in this setting (Mulet et al., 2018; Andersen et al., 2019). Real-world, country-specific studies are significant because of the disparities in disease management that exist between regions and because of their potential to highlight treatment gaps (Ozet et al., 2022).

A systematic analysis was conducted which synthesizes published and unpublished data using FTD/TPI in clinical practice settings, comparing the outcomes of pooled analyses of observational studies, the Japanese phase II study, and the RECURSE and TERRA phase III trials (Andersen et al., 2019). A total of 1,008 patients from 64 hospitals in Japan and Europe were compiled throughout 7 published papers between 2016 and 2018, and 2 unpublished investigations (Japanese and Danish).

Furthermore, PRECONNECT was a multicenter, open-label, phase IIb trial, that aimed to facilitate access for eligible mCRC patients to FTD/TPI, and to further evaluate its safety and efficacy in ordinary clinical practice. 793 patients received oral FTD/TPI until disease progression, unacceptable toxicity, significant protocol deviation, physician or patient's decision, or when the medication became commercially available (Bachet et al., 2020). PRECONNECT applied the same inclusion criteria as the RECURSE study: adult patients with histologically proven metastatic colorectal cancer, an Eastern Cooperative Oncology Group (ECOG) performance status (PS) of 0 or 1 and at least two prior regimens of conventional chemotherapy (Mayer et al., 2015; Van Cutsem et al., 2018). Unlike RECURSE and PRECONNECT, neither Yoshino et al.

nor TERRA required patients to have had bevacizumab (or an anti-EGFR antibody for KRAS wild-type tumors) before enrollment (Yoshino et al., 2012; Xu et al., 2018; Andersen et al., 2019).

In general, the three RCTs—the Japanese phase II trial (Yoshino et al., 2012), the RECURSE phase III trial (Mayer et al., 2015), and the TERRA phase III trial (Xu et al., 2018), the pooled analysis of observational studies (Andersen et al., 2019), the PRECONNECT trial (Bachet et al., 2020), and the present study had cohorts with baseline similar characteristics. The patients in the Romanian population were slightly older (median age of 65.5 years; patients ≥70 years represented 38% of our sample) compared to the pooled real life studies (median age of 63.5 years), Yoshino et al. (2012) and RECURSE (median age of 63 years for both cohorts), PRECONNECT study (median age of 62 years), and TERRA trial (median age of 58 years) (Mayer et al., 2015; Xu et al., 2018; Andersen et al., 2019; Bachet et al., 2020).

Although they still accounted for more than half of the sample, male patients in the current study (52%) were relatively less prevalent than in previous investigations: Japanese phase II trial (57%), PRECONNECT population (59%), RECURSE and the pooled observational studies (61%), and TERRA study (63%) (Yoshino et al., 2012; Mayer et al., 2015; Xu et al., 2018; Bachet et al., 2020).

Nineteen (38%) of 50 patients included in this study were RAS wild-type, whereas 19 (38%) were RAS mutant. In RECURSE and TERRA (Mayer et al., 2015; Xu et al., 2018), mOS and mPFS were not influenced by KRAS status, whereas in the Japanese phase II study (Yoshino et al., 2012) TAS-102 was more effective in individuals with KRAS mutations. However, TAS-102 was proven effective regardless of KRAS mutational status (Yoshino et al., 2012; Andersen et al., 2019).

Overall, the median PFS for the current study was 3.85 months (95% CI: 3.1–4.6 months), higher than previously

reported. A meta-analysis assessing real life experience with FTD/TPI from more than 1,000 patients reported a mPFS of 2.2 months (95% CI: 2.1–2.3 months). The randomized controlled trials had comparable median PFS: 2.0 months (95% CI: 1.9–2.8 months) for the phases II trial and TERRA study, and 2.0 months for RECURSE (95% CI: 1.9–2.1 months). Final results from PRECONNECT study show a median PFS of 2.8 months (CI 95%: 2.7–3.0 months) (Andersen et al., 2019).

PFS is a popular endpoint that is utilized in clinical studies for third line treatment of mCRC, with radiologic testing often used as the primary basis for assessing the course of an illness. Because the true date of progression is somewhere between two radiological evaluations, using the date of scanning as the date of progression overestimates the PFS (Panageas et al., 2007). As a result, varied scanning intervals may render comparisons of median PFS across trials less relevant, as surveillance intervals may influence PFS (Andersen et al., 2019). Given the retrospective nature of this study, follow-up imaging was not subjected to the same strict requirements as a randomized clinical trial, and may account for the variations in PFS findings.

PRECONNECT study showed that the median PFS increased with duration of treatment as follows: 0–3 cycles: 2.2 (CI 95%: 2.0–2.3 months); 4–7 cycles: 5.3 (CI 95%: 4.6–5.6 months);  $\geq 8$  cycles: 9.4 (CI 95%: 8.7–10.5 months) (Bachet et al., 2020). Similarly, on the basis of univariate Cox regression analysis, our data revealed that patients who received less than five cycles of treatment had significantly inferior median PFS (3.16 months versus 7.92 months), HR = 0.18 (95% CI: 0.07–0.51),  $p$  0.0001.

A significantly superior median PFS was observed in the case of patients benefitting from surgery (4.96, 95% CI: 3.03–6.89) compared to those who did not (2.76, 95% CI: 2.29–3.23), with log rank  $p$ -value < 0.0001. Surgical procedures performed in this study were either excision of the primary tumor, liver metastasectomy, palliative surgery (diverting colostomy), or debulking. No evidence connecting surgical procedures to FTD/TPI efficacy was mentioned in the literature.

Toxicities were recorded in 80% of the study population. Haematological toxicity (76%)—specifically anemia (50%), leucopenia (38%), neutropenia (34%), and thrombocytopenia (30%)—was the most prevalent adverse event, followed by fatigue (60%), and abdominal pain (18%). These results are consistent with the safety profiles of the RTCs (Yoshino et al., 2012; Mayer et al., 2015; Xu et al., 2018) and PRECONNECT study (Bachet et al., 2020).

Our study yielded results that were in line with the safety profile that had already been established for FTD/TPI, and it also showed relatively superior mPFS. This is extremely noteworthy given that both FTD/TPI and regorafenib are approved for third-line treatment in mCRC patients (Van Cutsem et al., 2018), and regorafenib is not presently covered by Romanian National Oncology Program, despite being available in several other European countries (Bullement et al., 2018). Although FTD/TPI and regorafenib have not been directly compared in a clinical

study, but rather in observational series, both efficacy (Abrahao et al., 2018) and effectiveness appear comparable for mCRC patients as third line option (Masuishi et al., 2017; Moriwaki et al., 2018). A research undertaken in the United Kingdom sought to quantify the cost-effectiveness of FTD/TPI compared to other existing treatment choices for patients in this setting (best supportive care and regorafenib) from the standpoint of the National Health Service (NHS). The findings demonstrate that FTD/TPI outperforms regorafenib in terms of cost-effectiveness, with clinical outcomes much above those of patients receiving best supportive care (BSC) alone (Bullement et al., 2018).

Our study has a number of limitations. First, the research was limited by the fact that it was a retrospective, non-randomized study done at a single institution, and it only included 50 patients from a single region in Romania. Secondly, since the purpose of the study was to determine the efficacy and safety of FTD/TPI in routine clinical settings, there was no control group. Third, the lack of follow-up data required for overall survival prevented the evaluation of this endpoint. Finally, the data collection was not conducted with the same level of rigor as a randomized clinical study, and there are gaps in the information that have been provided. Real world data, despite these limitations, is crucial for consolidating clinical trial outcomes and establishing the utility of treatments among clinicians and patient subgroups.

## Conclusion

In clinical settings, new medications are often administered to a more diverse patient group in a less structured way (Andersen et al., 2019). Our study's findings supported the safety profile for FTD/TPI that had previously been published, and demonstrated relatively superior mPFS. The results of this Romanian study support the routine use of FTD/TPI in the treatment of patients with mCRC and reflect the findings of RCTs as well as post hoc analyses conducted in other countries.

## Data availability statement

The original contributions presented in the study are included in the article/Supplementary Material, further inquiries can be directed to the corresponding author.

## Ethics statement

The studies involving human participants were reviewed and approved by Ethics Committees of the Oncology Institute Prof. Dr. Ion Chiricuta and the University of Medicine and Pharmacy Iuliu Hatieganu, Cluj-Napoca, Romania. The patients/participants provided their written informed consent to participate in this study.

## Author contributions

Conceptualization, DS and CL; Methodology, DS, SS, CL, and AG; Software, E-AD; Validation, DS, CL, and SS; Formal Analysis, DS and E-AD; Resources, SS and AG; Writing–Original Draft Preparation, DS, CL, SS, E-AD, and C-VL; Writing–Review and Editing, DS, CL, SS, AG, E-AD, DG, and C-VL; Visualization, DS, CL, and SS; Supervision, DG and DS.

## Acknowledgments

The authors want to acknowledge the support of the Romanian Society of Medical Oncology (SNOMR) for the payment of the APC.

## References

- Abrahao, A. B. K., Ko, Y. J., Berry, S., and Chan, K. K. W. (2018). A comparison of regorafenib and TAS-102 for metastatic colorectal cancer: A systematic review and network meta-analysis. *Clin. Colorectal Cancer* 17 (2), 113–120. doi:10.1016/j.clcc.2017.10.016
- Andersen, S. E., Andersen, I. B., Jensen, B. V., Pfeiffer, P., Ota, T., and Larsen, J. S. (2019). A systematic review of observational studies of trifluridine/tipiracil (TAS-102) for metastatic colorectal cancer. *Acta Oncol.* 58 (8), 1149–1157. doi:10.1080/0284186X.2019.1605192
- Arnold, D., Prager, G. W., Quintela, A., Stein, A., Moreno Vera, S., Mounedji, N., et al. (2018). Beyond second-line therapy in patients with metastatic colorectal cancer: A systematic review. *Ann. Oncol.* 29 (4), 835–856. doi:10.1093/annonc/mdy038
- Bachet, J. B., Wyrwicz, L., Price, T., Cremolini, C., Phelip, J. M., Portales, F., et al. (2020). Safety, efficacy and patient-reported outcomes with trifluridine/tipiracil in pretreated metastatic colorectal cancer: Results of the PRECONNECT study. *ESMO Open* 5 (3), e000698. doi:10.1136/esmoopen-2020-000698
- Bullement, A., Underhill, S., Fougerey, R., and Hatswell, A. J. (2018). Cost-effectiveness of trifluridine/tipiracil for previously treated metastatic colorectal cancer in england and wales. *Clin. Colorectal Cancer* 17 (1), e143–e151. doi:10.1016/j.clcc.2017.09.001
- Dexter, D. L., Wolberg, W. H., Ansfield, F. J., Helson, L., and Heidelberger, C. (1972). The clinical pharmacology of 5-trifluoromethyl-2'-deoxyuridine. *Cancer Res.* 32 (2), 247–253. PMID: 4333494.
- Favoriti, P., Carbone, G., Greco, M., Pirozzi, F., Pirozzi, R. E., and Corcione, F. (2016). Worldwide burden of colorectal cancer: A review. *Updat. Surg.* 68 (1), 7–11. doi:10.1007/s13304-016-0359-y
- Ferlay, J., Soerjomataram, I., Dikshit, R., Eser, S., Mathers, C., Rebelo, M., et al. (2015). Cancer incidence and mortality worldwide: Sources, methods and major patterns in GLOBOCAN 2012. *Int. J. Cancer* 136 (5), E359–E386. doi:10.1002/ijc.29210
- Fukushima, M., Suzuki, N., Emura, T., Yano, S., Kazuno, H., Tada, Y., et al. (2000). Structure and activity of specific inhibitors of thymidine phosphorylase to potentiate the function of antitumor 2'-deoxyribonucleosides. *Biochem. Pharmacol.* 59 (10), 1227–1236. doi:10.1016/s0006-2952(00)00253-7
- Heidelberger, C., and Anderson, S. W. (1964). Fluorinated pyrimidines. Xxi. The tumor-inhibitory activity of 5-trifluoromethyl-2'-deoxyuridine. *Cancer Res.* 24, 1979–1985. PMID: 14247510.
- Heidelberger, C., Boohar, J., and Kampschroer, B. (1965). Fluorinated pyrimidines. Xxiv. *in vivo* metabolism of 5-trifluoromethyluracil-2-C-14 and 5-trifluoromethyl-2'-deoxyuridine-2-C-14. *Cancer Res.* 25, 377–381. PMID: 14281103.
- Masuishi, T., Taniguchi, H., Hamauchi, S., Komori, A., Kito, Y., Narita, Y., et al. (2017). Regorafenib versus trifluridine/tipiracil for refractory metastatic colorectal

## Conflict of interest

The authors declare that the research was conducted in the absence of any commercial or financial relationships that could be construed as a potential conflict of interest.

## Publisher's note

All claims expressed in this article are solely those of the authors and do not necessarily represent those of their affiliated organizations, or those of the publisher, the editors and the reviewers. Any product that may be evaluated in this article, or claim that may be made by its manufacturer, is not guaranteed or endorsed by the publisher.

- cancer: A retrospective comparison. *Clin. Colorectal Cancer* 16 (2), e15–e22. doi:10.1016/j.clcc.2016.07.019
- Mayer, R. J., Van Cutsem, E., Falcone, A., Yoshino, T., Garcia-Carbonero, R., Mizunuma, N., et al. (2015). Randomized trial of TAS-102 for refractory metastatic colorectal cancer. *N. Engl. J. Med.* 372 (20), 1909–1919. doi:10.1056/NEJMoa1414325
- Meyerhardt, J. A., and Mayer, R. J. (2005). Systemic therapy for colorectal cancer. *N. Engl. J. Med.* 352 (5), 476–487. doi:10.1056/NEJMra040958
- Moriwaki, T., Fukuoka, S., Taniguchi, H., Takashima, A., Kumekawa, Y., Kajiura, T., et al. (2018). Propensity score analysis of regorafenib versus trifluridine/tipiracil in patients with metastatic colorectal cancer refractory to standard chemotherapy (regotas): A Japanese society for cancer of the colon and rectum multicenter observational study. *Oncologist* 23 (1), 7–15. doi:10.1634/theoncologist.2017-0275
- Mulet, N., Matos, I., Noguerido, A., Martini, G., Elez, M. E., Argiles, G., et al. (2018). Evaluating trifluridine + tipiracil hydrochloride in a fixed combination (TAS-102) for the treatment of colorectal cancer. *Expert Opin. Pharmacother.* 19 (6), 623–629. doi:10.1080/14656566.2018.1453497
- Ozet, A., Dane, F., Aykan, N. F., Yalcin, S., Evrensel, T., Ozkan, M., et al. (2022). Safety and efficacy of trifluridine/tipiracil in previously treated metastatic colorectal cancer: PRECONNECT Turkey. *Future Oncol.* ahead of printdoi:10.2217/fon-2022-0455
- Panageas, K. S., Ben-Porat, L., Dickler, M. N., Chapman, P. B., and Schrag, D. (2007). When you look matters: The effect of assessment schedule on progression-free survival. *J. Natl. Cancer Inst.* 99 (6), 428–432. doi:10.1093/jnci/djk091
- Sobrero, A., Guglielmi, A., Grossi, F., Puglisi, F., and Aschele, C. (2000). Mechanism of action of fluoropyrimidines: Relevance to the new developments in colorectal cancer chemotherapy. *Semin. Oncol.* 27 (5), 72–77. PMID: 11049035.
- Sunakawa, Y., Izawa, N., Mizukami, T., Horie, Y., Hirakawa, M., Arai, H., et al. (2017). Profile of trifluridine/tipiracil hydrochloride in the treatment of metastatic colorectal cancer: Efficacy, safety, and place in therapy. *Onco. Targets. Ther.* 10, 4599–4605. doi:10.2147/OTT.S106101
- Van Cutsem, E., Mayer, R. J., Laurent, S., Winkler, R., Gravalos, C., Benavides, M., et al. (2018). The subgroups of the phase III RECOUSE trial of trifluridine/tipiracil (TAS-102) versus placebo with best supportive care in patients with metastatic colorectal cancer. *Eur. J. Cancer* 90, 63–72. doi:10.1016/j.ejca.2017.10.009
- Vogel, A., Hofheinz, R. D., Kubicka, S., and Arnold, D. (2017). Treatment decisions in metastatic colorectal cancer - beyond first and second line combination therapies. *Cancer Treat. Rev.* 59, 54–60. doi:10.1016/j.ctrv.2017.04.007
- Xu, J., Kim, T. W., Shen, L., Sriuranpong, V., Pan, H., Xu, R., et al. (2018). Results of a randomized, double-blind, placebo-controlled, phase III trial of trifluridine/tipiracil (TAS-102) monotherapy in asian patients with previously treated

metastatic colorectal cancer: The TERRA study. *J. Clin. Oncol.* 36 (4), 350–358. doi:10.1200/JCO.2017.74.3245

Yoshino, T., Arnold, D., Taniguchi, H., Pentheroudakis, G., Yamazaki, K., Xu, R. H., et al. (2018). Pan-asian adapted ESMO consensus guidelines for the management of patients with metastatic colorectal cancer: A JSMO-ESMO initiative endorsed by CSCO, KACO, MOS, SSO and TOS. *Ann. Oncol.* 29 (1), 44–70. doi:10.1093/annonc/mdx738

Yoshino, T., Mizunuma, N., Yamazaki, K., Nishina, T., Komatsu, Y., Baba, H., et al. (2012). TAS-102 monotherapy for pretreated metastatic colorectal cancer: A double-blind, randomised, placebo-controlled phase

2 trial. *Lancet. Oncol.* 13 (10), 993–1001. doi:10.1016/S1470-2045(12)70345-5

Yoshino, T., Uetake, H., Fujita, N., Furuta, T., Katori, J., Hara, N., et al. (2016). TAS-102 safety in metastatic colorectal cancer: Results from the first postmarketing surveillance study. *Clin. Colorectal Cancer* 15 (4), e205–e211. doi:10.1016/j.clcc.2016.04.004

Zaniboni, A., Barone, C. A., Banzi, M. C., Bergamo, F., Blasi, L., Bordonaro, R., et al. (2021). Italian results of the PRECONNECT study: Safety and efficacy of trifluridine/tipiracil in metastatic colorectal cancer. *Future Oncol.* 17 (18), 2315–2324. doi:10.2217/fon-2020-1278





## OPEN ACCESS

## EDITED BY

Adina Turcu-Stolica,  
University of Medicine and Pharmacy of  
Craiova, Romania

## REVIEWED BY

Bogdan Procopet,  
Iuliu Hațieganu University of Medicine  
and Pharmacy, Romania  
Larisa Sandulescu,  
University of Medicine and Pharmacy of  
Craiova, Romania

## \*CORRESPONDENCE

Simona Dima,  
dima.simona@gmail.com

<sup>†</sup>These authors have contributed equally  
to this work and share first authorship

## SPECIALTY SECTION

This article was submitted to  
Gastrointestinal and Hepatic  
Pharmacology,  
a section of the journal  
Frontiers in Pharmacology

RECEIVED 12 September 2022

ACCEPTED 27 September 2022

PUBLISHED 18 October 2022

## CITATION

Iacob S, Iacob R, Manea I, Uta M,  
Chiosa A, Dumbrava M, Becheanu G,  
Stoica L, Popa C, Brasoveanu V,  
Hrehoret D, Gheorghe C, Gheorghe L,  
Dima S and Popescu I (2022), Host and  
immunosuppression-related factors  
influencing fibrosis occurrence post  
liver transplantation.  
*Front. Pharmacol.* 13:1042664.  
doi: 10.3389/fphar.2022.1042664

## COPYRIGHT

© 2022 Iacob, Iacob, Manea, Uta,  
Chiosa, Dumbrava, Becheanu, Stoica,  
Popa, Brasoveanu, Hrehoret, Gheorghe,  
Gheorghe, Dima and Popescu. This is an  
open-access article distributed under  
the terms of the [Creative Commons  
Attribution License \(CC BY\)](https://creativecommons.org/licenses/by/4.0/). The use,  
distribution or reproduction in other  
forums is permitted, provided the  
original author(s) and the copyright  
owner(s) are credited and that the  
original publication in this journal is  
cited, in accordance with accepted  
academic practice. No use, distribution  
or reproduction is permitted which does  
not comply with these terms.

# Host and immunosuppression-related factors influencing fibrosis occurrence post liver transplantation

Speranta Iacob<sup>1,2,3†</sup>, Razvan Iacob<sup>1,2,3†</sup>, Ioana Manea<sup>1,2</sup>,  
Mihaela Uta<sup>2,3</sup>, Andrei Chiosa<sup>2,3</sup>, Mona Dumbrava<sup>2,3</sup>,  
Gabriel Becheanu<sup>1,2,3</sup>, Luminita Stoica<sup>2,3</sup>, Codruta Popa<sup>1,2,3</sup>,  
Vlad Brasoveanu<sup>2,3</sup>, Doina Hrehoret<sup>2,3</sup>, Cristian Gheorghe<sup>1,2,3</sup>,  
Liana Gheorghe<sup>1,2,3</sup>, Simona Dima<sup>2,3\*</sup> and Irinel Popescu<sup>2,3</sup>

<sup>1</sup>Gastroenterology Department, University of Medicine and Pharmacy “Carol Davila”, Bucharest, Romania, <sup>2</sup>Center for Excellence in Translational Medicine, Bucharest, Romania, <sup>3</sup>Fundeni Clinical Institute, Bucharest, Romania

Post liver transplantation (LT) fibrosis has a negative impact on graft function. Cytokine production in the host immune response after LT may contribute to the variable CYP3A-dependent immunosuppressive drug disposition, with subsequent impact on liver fibrogenesis, together with host-related factors. We aimed to investigate whether the cytochrome P4503A5\*3 (CYP3A5\*3) or TBX21 genotypes impact post-LT liver fibrogenesis. Furthermore, the impact of immunosuppressants on cellular apoptosis has been evaluated using human hepatocytes harvested from cirrhotic explanted livers. We have enrolled 98 LT recipients that were followed for occurrence of liver fibrosis for at least 12 months. There was a statistically significant higher trough level of TAC in patients with homozygous CC-TBX21 genotype ( $7.83 \pm 2.84$  ng/ml) vs.  $5.66 \pm 2.16$  ng/ml in patients without this genotype ( $p = 0.009$ ). The following variables were identified as risk factors for fibrosis  $\geq 2$ : donor age ( $p = 0.02$ ), neutrophil to lymphocyte ratio ( $p = 0.04$ ) and TBX21 genotype CC ( $p = 0.009$ ). In the cell culture model cytometry analysis has indicated the lowest apoptotic cells percentage in human cirrhotic hepatocytes cultures treated with mycophenolate mofetil (MMF) (5%) and TAC + MMF (2%) whereas the highest apoptosis percentage was registered for the TAC alone (11%). The gene expression results are concordant to cytometry study results, indicating the lowest apoptotic effect for MMF and MMF + TAC immunosuppressive regimens. The allele 1993C of the SNP rs4794067 may predispose to the development of late significant fibrosis of the liver graft. MMF-based regimens have a favourable anti-apoptotic profile *in vitro*, supporting its use in case of LT recipients at high risk for liver graft fibrosis.

## KEYWORDS

graft fibrosis, tacrolimus, mycophenolate mofetil, CYP3A5 genotype, apoptosis, hepatocytes culture, liver transplant, TBX21

# 1 Introduction

The availability of the calcineurin inhibitors (CNIs) cyclosporine (CsA) (Calne et al., 1978) and tacrolimus (TAC) (Starzl et al., 1989) has completely changed the prognosis of transplanted patients. Currently, more than 90% of all patients receiving a graft are treated post-transplant with CNIs. The combination of a CNI and mycophenolate mofetil (MMF) or sirolimus (SRL) are commonly used for maintenance immunosuppression following liver transplantation (LT) (Iacob et al., 2009). However, there are post-LT complications immunosuppression-related that negatively impact survival and quality of life. *In vitro* and *in vivo* studies have demonstrated profibrogenic properties of CNIs with increased hepatic and renal collagen deposition triggered by a high expression of transforming growth factor beta 1 and extracellular matrix genes (Frizzell et al., 1994). Newer studies suggest a role of these agents in promoting and enhancing cell-death in non-liver cell types like pancreatic cells, renal and prostate cells, thereby driving an inflammatory response that promotes fibrosis (Khanna et al., 1997; Giordano et al., 2006; Choi et al., 2008; Bouvier et al., 2009). On the other hand, CNIs at therapeutic concentrations did not affect murine hepatocyte apoptosis, but combination with MMF significantly enhanced cell death. By contrast, SRL/MMF combination did not significantly reduce hepatocyte viability or promote apoptosis (Nguyen et al., 2009). However, hepatic stellate cells (HSCs) play the critical role in liver fibrosis; reversal of liver fibrosis can be achieved through the apoptosis of activated HSCs. Immunosuppressive agents may also affect the life cycle of HSCs. One study (Kabat-Koperska et al., 2016) showed that the treatment with MMF induced human HSC apoptosis and reduced collagen alpha 1 expression compared to CsA or SRL treatment. Thus, some immunosuppressive agents may have antifibrotic properties and not profibrotic.

As previously mentioned, the immunosuppressive regimen with TAC is essential for patients after LT. The cytochrome P450 3A (CYP3A) subfamily and P-glycoprotein in human liver and intestine can contribute to inter and intra-individual differences in the pharmacokinetics of TAC (Thervet et al., 2003; Rojas et al., 2015). A single nucleotide polymorphism (SNP) in the CYP3A5 gene involving an A to G transition at position 6986 within intron 3 was found strongly associated with CYP3A5 protein expression. At least one CYP3A5\*1 allele were found to express large amounts of CYP3A5 protein, whereas homozygous for the CYP3A5\*3 allele did not express significant quantities of CYP3A5 protein, which results in a truncated protein and a severe decrease of functional CYP3A5 (Hesselink et al., 2014). The CYP3A5\*1 SNP is currently the most promising biomarker for tailoring TAC treatment.

There is accumulating evidence that regulatory T cells (Tregs) have a crucial role in immune tolerance and long-term graft survival.

T-box21 gene (transcription factor T-bet – T-box expressed in T cells – TBX21), as well as GATA 3 (GATA binding protein 3) and FOXP3 (forkhead box P3) genes constitute the principle regulators for the differentiation of Th1, Th2 and Tregs (Szabo et al., 2000; Evans and Jenner, 2013). These T cells are implicated in different post-transplant complications and are influenced by the immunosuppressive drugs. TBX21 is a key transcriptional activator of Th1 cell differentiation. T-bet plays an essential role in Th1/Th2 balance, where it is the master regulator of Th1 cell fate through promotion of Th1 cytokines and inhibition of Th2 cytokines (Szabo et al., 2000; Usui et al., 2006).

The SNP rs4794067 represents a T to C substitution at position -1993 in the promoter region of the TBX21 gene. The -1993C allele of the SNP rs4794067 is associated with a reduced promoter activity, when compared with the -1993T allele. The expression level of TBX21 is lower in individuals with the -1993C allele than in individuals with the -1993T allele (Suttner et al., 2009; Li et al., 2011) and hence there is a decreased proinflammatory cytokines generated by Th2 or Th17 cells.

The main objective of the present paper was to investigate whether the cytochrome P450 3A5\*3 (CYP3A5\*3) or TBX21 genotypes affect TAC pharmacokinetics and to evaluate their potential impact on liver fibrogenesis post-LT, after controlling for the host-related factors. Furthermore, the impact of immunosuppressants on cellular apoptosis has been evaluated using human hepatocytes harvested from cirrhotic explanted livers.

# 2 Materials and methods

## 2.1 Clinical study

Between October 2018 and March 2020, we have enrolled 98 LT recipients that were followed for occurrence of liver fibrosis for at least 12 months. Non-invasive evaluation of the liver was performed at the moment of inclusion into the study (Fibroscan® with CAP and FIB4) for detection of fibrosis stage  $\geq 2$  and/or steatosis grade 3 occurrence. All clinical data were collected in a database. Buffy coat from patients were obtained for genotyping of CYP3A5\*3 (rs776746) and TBX21 (rs4794067) polymorphisms by Taqman SNP Genotyping Assays (Thermo Scientific). All patients signed an informed consent; the study was approved by the Ethics Committee of Fundeni Clinical Institute (126769/29.09.2018) and conducted in accordance with guidelines for human studies.

## 2.2 Statistical analysis

Quantitative variables were expressed as mean  $\pm$  standard deviation or median and interquartile range. Categorical variables were expressed as frequencies and percentages. Quantitative variables were compared by T-Student test or Mann Whitney U test. Pearson correlation coefficient was

used to correlate quantitative variables. Qualitative variables were compared by Chi-squared or Fisher exact test. Cox regression analysis was performed to identify predictors of the outcome and log-rank test was used for comparison of Kaplan Meyer curves. Results with  $p \leq 0.05$  were considered statistically significant.

## 2.3 Cell culture models

In this study human hepatocytes were isolated from cirrhotic explanted livers. All livers were processed within a few hours after harvesting. They were transferred to the hepatocyte isolation lab on ice, in University of Wisconsin solution under sterile conditions. Human hepatocyte isolation was performed using collagenase perfusion with the technique described by Seglen et al. (Seglen, 1976; Mitry et al., 2002).

Cirrhotic hepatocytes have been cultured in low glucose DMEM culture medium and have been treated for 24 h with different concentrations and of immunosupresants ranging from 10 nM to 100  $\mu$ M: TAC, SRL, MMF, or combinations (TAC + SRL, MMF + TAC). At 24 h apoptosis and necrosis was assessed using Tali™ Apoptosis Kit - Annexin V Alexa Fluor™ 488 & Propidium Iodide (Thermo Scientific). Gene expression has been assessed by qRT-PCR using a microarray of 19 genes significant for apoptosis. Relative expression of selected genes was evaluated by the Real-Time PCR System using SYBR Green Master Mix (Thermo Fisher Scientific Waltham, MA, United States), with beta-actin as a reference gene. Cirrhotic liver hepatocytes cultures, untreated with immunosupresants were used as a reference for gene expression quantification. The studied genes and the primers used for specific amplification of the mRNA are depicted in Supplementary Table S1.

Cirrhotic human hepatocytes differ from hepatocytes isolated from normal liver by a rapid *in vitro* conversion to a mesenchymal proliferative phenotype that offers advantages as a study *in vitro* model due to the cellular expansion capacity permitting experimental repeatability.

During our study there were used 3 different cellular cultures isolated from explanted liver during LT procedures. During the same procedure were isolated hepatocytes and also non-parenchymal hepatic cells by centrifugation technique on Percoll gradient of the supernatant obtained at the first wash of the cellular suspension resulting from the enzymatic digestion of the hepatic parenchyma by collagenase solution.

## 3 Results

### 3.1 Study of the impact of the CYP3A5 and TBX21 genotypes following LT

#### 3.1.1 General characteristics of the LT patients

There were included 98 patients: 56.1% men and 43.9% women, median age at inclusion 59 years and median time

**TABLE 1 Biochemical characteristics and noninvasive liver fibrosis assessment of the analysed cohort.**

Variable	Median value (range)
ALT (U/L)	27.5 (9.5–183)
AST (U/L)	24 (12.2–101)
GGT (U/L)	23 (6–887)
Alkaline phosphatase (U/L)	92 (25.2–417)
Total bilirubin (mg/dl)	0.69 (0.2–4.84)
Creatinine (mg/dl)	1.08 (0.56–2.36)
Uric acid (mg/dl)	5.4 (2.7–12.4)
Serum albumine (mg/dl)	4.56 (2.9–5.62)
Glycemia (mg/dl)	108.6 (72.1–209)
Total Cholesterol (mg/dl)	189 (40–331)
LDL cholesterol (mg/dl)	115.6 (51.4–261)
HDL cholesterol (mg/dl)	50.1 (27–91)
Triglycerides (mg/dl)	106 (40–306)
NLR (neutrophil to lymphocyte ratio)	2.42 (0.78–12.16)
PLR (platelet to lymphocyte ratio)	119.5 (42.3–304.7)
FIB-4	1.51 (0.57–11.58)
Liver stiffness measurement by Fibroscan (kPa)	5.5 (2.8–48)
CAP (dB/m)	274.5 (100–400)

since LT was 62.6 months; the median age of the donors (91 cadaveric and 7 living) was 42 years; gender of the donors were: 42.3% women and 57.7% men. The median time of warm ischemia was 39 min and the median cold ischemia time was 4.75 h.

Etiology of liver cirrhosis was: hepatitis C (HCV) in 59.2%, hepatitis B and delta coinfection in 19.4%, alcohol related cirrhosis in 7.1%, autoimmune liver disease in 8.1% and others in 6.2% of cases. Hepatocellular carcinoma (HCC) was present in 30.6% of patients. All patients transplanted for HCV had cured hepatitis C after LT with the new direct antivirals. Diabetes mellitus was encountered in 20.4% of patients after LT. 73.5% of patients received TAC, 7.1% CsA and 19.4% SRL. MMF was associated in 28.6% of patients. A significantly higher proportion of patients with HCC received SRL (33.3% vs. 8.8%,  $p = 0.002$ ). Table 1 shows the biochemical parameters studied in our cohort. In Table 2 are shown the differences between LT recipients with and without HCV-related cirrhosis.

There was a moderate correlation between FIB-4 values and liver stiffness measured by Fibroscan® ( $r = 0.51$ ,  $p < 0.0001$ ).

#### 3.1.2 Analysis of studied variables according to the CYP3A5 or TBX21 genes

In the studied cohort the frequency of CYP3A5-CC genotype was 88% and of CT genotype 12%; whereas the distribution of the TBX21 genotypes was as follows: CC genotype 17.5%; CT genotype 36.1% and TT genotype 46.4%.

Aminotransferases and gamma glutamyl transpeptidase did not differ at 7 and 14 days following LT according to the CYP3A5 or

TABLE 2 Analysis of the variables in patients with cured recurrent C hepatitis after LT vs. patients transplanted for other causes of cirrhosis.

Variable	HCV (+) group (n = 58)	HCV (-) group (n = 40)	p value
Age (years)	59.8 ± 7.8	52.6 ± 11.8	<b>0.0005</b>
FIB-4	2.41 ± 0.3	1.65 ± 0.2	<b>0.04</b>
Liver stiffness (kPa)	8.08 ± 0.8	7.31 ± 1.3	0.56
CAP (dB/m)	273.2 ± 65.0	252.1 ± 62.5	0.11
NLR (neutrophil to lymphocyte ratio)	2.79 ± 0.2	2.72 ± 0.2	0.83
PLR (platelet to lymphocyte ratio)	122.8 ± 46.2	127.3 ± 51.2	0.65
ALT (UI/L)	35.1 ± 3.8	34.6 ± 4.8	0.92
AST (UI/L)	30.4 ± 2.5	26.5 ± 2.2	0.28
GGT (UI/L)	54.2 ± 16.2	69.8 ± 23.1	0.57
Diabetes mellitus type II	25.9%	12.5%	0.10
TBX21_CC genotype	8.6%	27.5%	<b>0.01</b>
TBX21_CT genotype	43.1%	27.5%	0.11
TBX21_TT genotype	47.4%	45%	0.81
CYP3A5_CT genotype	13.8%	22.5%	0.26
CYP3A5_CC genotype	91.5%	82.1%	0.23

TBX21 genotypes. However, total bilirubin value was significantly higher at Day 7 and 14 post-LT in patients with CYP3A5-CC vs. CT genotype; creatinine values at 1 year after LT were significantly higher in patients with CYP3A5 CT vs. CC genotypes ( $1.22 \pm 0.34$  mg/dl vs.  $1.05 \pm 0.24$  mg/dl,  $p = 0.01$ ) where as glomerular filtration rates (GFR) were significantly lower in CT vs. CC genotypes ( $p = 0.04$ ). TBX21 genotype did not influence the total bilirubin value early after LT or the creatinine/GFR values 1 year after LT.

There was no statistically significant difference between dose used or trough levels of TAC/SRL or CsA in patients with CC vs. CT CYP3A5 genotypes. On the other hand, TBX21 CC genotype was associated with a higher trough levels of TAC compared to other genotypes ( $p = 0.009$ ), but not with a higher dose of TAC taken by the patient.

There was also no statistical difference between patients with CYP3A5 - CC genotype vs. CT with regard to FIB-4 values ( $p = 0.26$ ), liver stiffness ( $p = 0.51$ ) or CAP ( $p = 0.15$ ) obtained by Fibroscan®. Patients with genotype TT of TBX21 gene had a statistically significantly higher steatosis grade evaluated by CAP compared to other genotypes ( $p = 0.009$ ), but fibrosis stage evaluated by FIB-4 or liver stiffness did not vary according to genotype.

Inflammatory markers such as PLR or NLR did not differ according to CYP3A5 or TBX21 genotypes.

### 3.1.3 Results of the cox regression analysis

The following variables were included in the univariate Cox regression analysis having as outcome occurrence of significant fibrosis stage ( $\geq 2$ ) after LT (fibrosis evaluated by both concordant Fibroscan  $>8.1$  kPa and FIB-4  $>1.45$ ): genotype CC of CYP3A5 gene; genotypes TT and CC of TBX21 gene; age of recipient and of the donor; presence of post-LT diabetes mellitus;

HCV etiology of liver cirrhosis at LT; use of TAC, SRL and MMF; NLR and PLR values as well as steatosis grade evaluated by CAP.

Risk factors for fibrosis stage  $\geq 2$  were: TBX21 CC genotype (HR = 2.53,  $p = 0.009$ ), NLR value (HR = 1.2,  $p = 0.04$ ) and older donor age (HR = 1.1,  $p = 0.02$ ). Independent risk factors for significant fibrosis stage after LT were only TBX21 CC genotype ( $p = 0.0001$ ) and increased donor age ( $p = 0.0008$ ).

Patients with TBX21 gene CC allele had a significantly lower graft survival rate compared to patients with CT/TT genotypes of TBX21 gene (median survival 51.4 vs. 102.6 months,  $p = 0.007$ ). Patients receiving a combination of low dose TAC (aiming a trough level of 2–4 ng/ml) and MMF had a significantly lower percentage of significant graft fibrosis compared to patients with TAC monotherapy (27.4% vs. 47.1%,  $p = 0.03$ ).

## 3.2 Study of the apoptosis process in liver cell culture models

### 3.2.1 Apoptosis induced by the immunosuppression medication in the hepatocytes cultures

Apoptosis process induced by IS was studied in hepatocytes isolated from cirrhotic livers after treatment with TAC, SRL, MMF and combinations (TAC + SRL; TAC + MMF) according to the current standards of therapy of the LT recipients. There were studied the following increasing IS concentrations in order to identify an apoptotic effect different from the toxic-necrotic effect (10nM, 100nM, 1  $\mu$ M, 10  $\mu$ M, 100  $\mu$ M).

For the concentration of 10 nM of the IS the maximum percentage of apoptotic and necrotic cells for the combination of



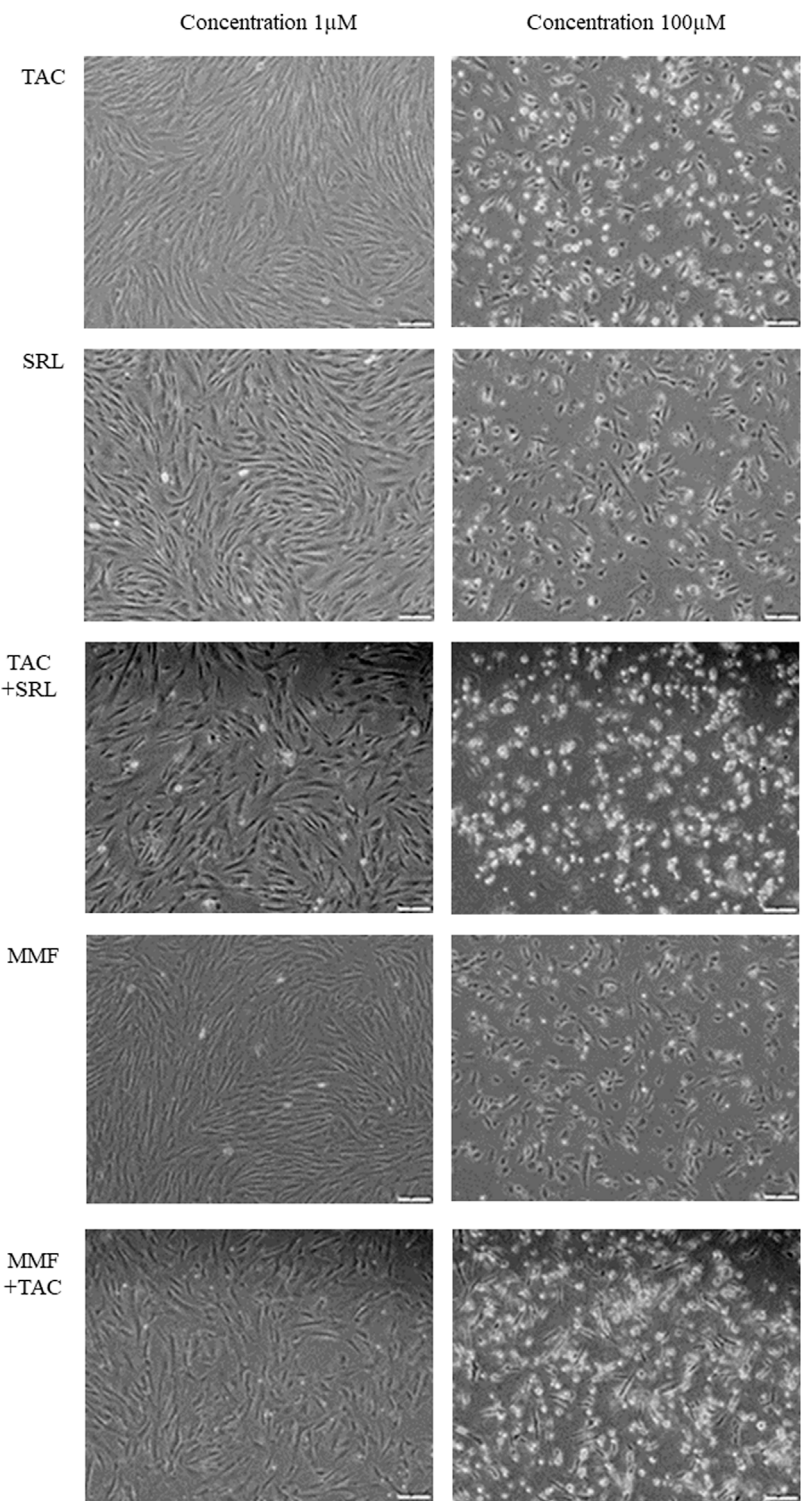


**FIGURE 1**  
Examination of the hepatocyte cultures isolated from human cirrhotic liver after treatment with immunosuppression medication at a concentration of 1 μM and respectively 100 μM (Inverted microscope, phase contrast, 40X).



TAC + SRL was 19% and a low level of apoptosis of only 2% was noted for MMF or TAC + MMF. At a concentration of 1  $\mu$ M the cumulated maximum apoptotic and necrotic cell percentage was 17% for TAC + SRL and only 3–5% of apoptotic cells for MMF or TAC + MMF. At a high concentration of 100  $\mu$ M of IS, the level of apoptosis for TAC and MMF was still reduced, but for SRL and the combination of TAC and MMF there were registered high levels of cellular toxicity manifested by both apoptosis and cellular necrosis. Association of TAC + SRL at this concentration led to apoptosis and massive cellular necrosis with marked alteration of the cellular viability. According to the data obtained in the study of the cellular apoptosis induced by the IS on the adherent cultures of hepatocytes isolated from the human cirrhotic liver, we established as a study model for other cellular types the concentration of 1  $\mu$ M where the apoptotic effect is evident, but without any significant toxic effect, manifested by the rate of cellular proliferation and cell death (Figure 1).

### 3.2.2 Culture of non-parenchymal hepatic cells

For liver non-parenchymal cells, the level of apoptosis induced by the IS at a concentration of 1  $\mu$ M is similar to that registered for the hepatocytes isolated from the cirrhotic liver, of approximate 5–7% of the cellular population without significant variations according to the type of IS. The most pronounced toxic effect is registered for the association of TAC + SRL and is significantly higher compared to the hepatocytes and is attributed to the cell necrosis.

### 3.2.3 3D Co-culture of hepatocytes and non-parenchymal liver cells

In the co-culture systems the level of cellular apoptosis is low between 4 and 6%, even at high doses of immunosuppression.

## 3.3 Quantification of the gene expression for the significant genes for the cellular apoptosis

### 3.3.1 In human hepatocyte cell cultures isolated from cirrhotic liver

The following genes were analysed according to their function: cellular receptors mediating a cellular apoptosis (TNFRSF1A-TNFR1, TNFRSF10A-TRAILR1, TNFRSF10B-TRAILR2, CD40 and FAS), genes specific to mitochondrial apoptosis (BAK1, BAX, RIPK1, ASK1-MAP3K5, SMAC-DIABLO, AIFM1, HTRA2) and effector proteins of apoptosis (CASP3, CASP8, CASP9, CASP10, DFFB-CAD), as well as the transcription factor significant for the cellular apoptosis NFkB1. In Figure 2 are presented the results of the relative quantification of the gene expression for the significant genes implicated in the cellular apoptosis in the hepatocyte cultures isolated from the cirrhotic liver following treatment with immunosuppressive drugs. Gene expression analysis indicated that MMF induces

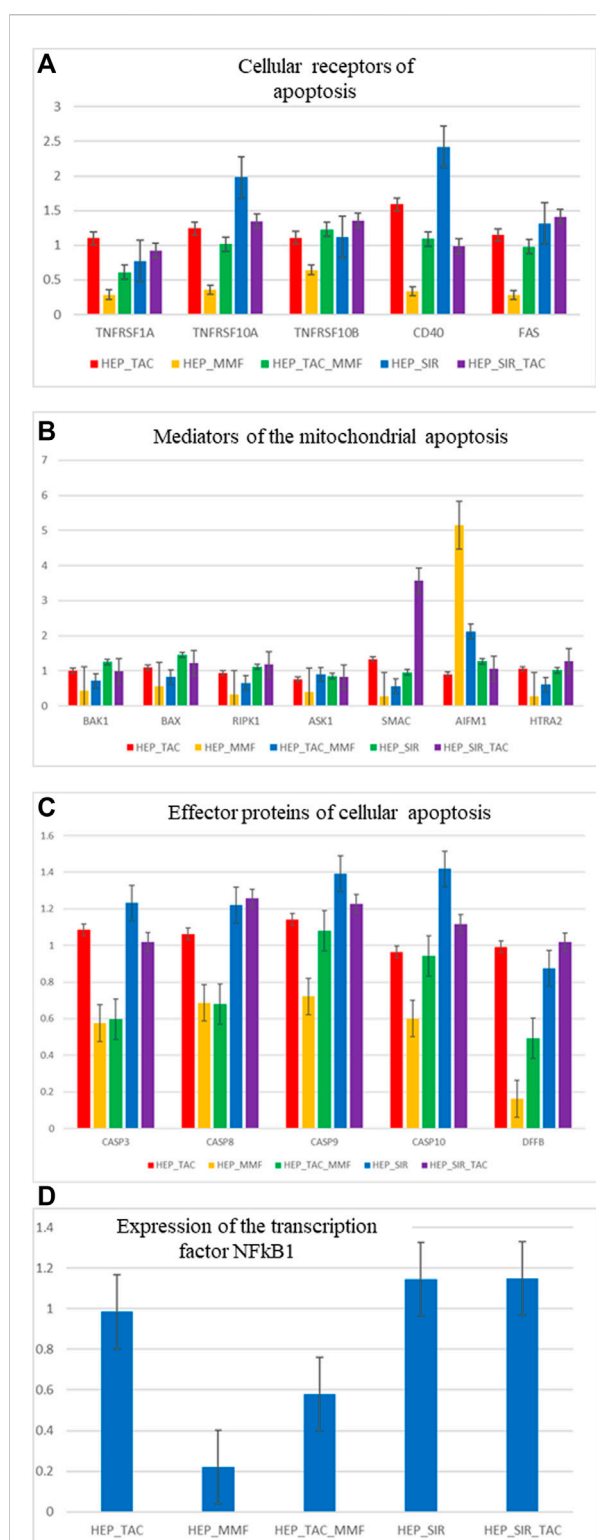


**FIGURE 2**

(A,B,C,D) Relative gene expression quantification (fold change) for significant genes involved in the process of cellular apoptosis, in hepatocyte cultures isolated from the cirrhotic liver after treatment with immunosuppressive drugs (1  $\mu$ M).

an antiapoptotic effect mediated by the decrease of the membrane receptors expression of the apoptosis, decrease of the gene expression that mediates cellular apoptosis, decrease of the genes that mediates mitochondrial apoptosis (excepting AIFM1), decrease of the effector proteins receptors of the apoptosis especially DFFB-CAD and a significant decrease of the transcription factor NFkB1. These results are concordant with the effects demonstrated in the cytometry studies of the cell cultures that indicated the lowest level of cellular apoptosis after treatment of the hepatocytes with MMF and MMF + TAC.

In the non-parenchymal hepatic cell cultures there is an unchanged expression for the studied genes with the exception of the overexpression of the SMAC gene in cell cultures treated with TAC. Results are also concordant to the cytometry studies.

Quantification of the apoptosis gene expression in the 3D co-culture of hepatocytes and non-parenchymal liver cells revealed a favourable profile of the markers of cellular apoptosis in case of the MMF and TAC combination. For this association there is a significant underexpression of the TRAILR1, BAK, BAX and SMAC-DIABLO genes, specific markers of mitochondrial apoptosis and underexpression of the caspases 8, 9 and 10. There is also an overexpression of RIPK1, specific marker for necroptosis in the 3D cultures treated with TAC. There is also an overexpression of AIFM1 concordant with the results registered for the 2D hepatocyte cultures.

## 4 Discussions

LT is an established therapy associated with an excellent improvement in patients' life expectancy over 70% at 10 years (Jadlowiec and Taner, 2016). However, an accelerated course of hepatic fibrosis may occur in LT patients despite normal or slightly abnormal liver blood tests (Gelson et al., 2010; Feng et al., 2018.), with concomitant allograft dysfunction. This late graft dysfunction is usually multifactorial (Kok et al., 2019; Iacob et al., 2021). Tailoring the immunosuppressive regimen has been proposed as a strategy to regulate fibrogenesis in the post-transplant period. Numerous intrinsic and extrinsic parameters influence TAC pharmacokinetic parameters, and variations in the expression and/or activity of drug metabolizing enzymes and transporters, in general supported by single nucleotide polymorphisms (SNPs), received much attention in the last years (Sakaeda, 2004). Of particular importance is the impact of variants in the genes encoding P450 cytochromes 3A (CYP3A4 and 3A5), which control TAC hepatic metabolism and intestinal absorption (Uesugi et al., 2014). However, in our paper this SNP had no influence on TAC trough levels and fibrosis occurrence after LT.

On the other hand, profile and Th1/Th2 ratio plays a strong role in fibrosis occurrence and can be affected by the activation of the hepatic stellate cells (Xu et al., 2012). Co-culture of the hepatic stellate cells with T CD4<sup>+</sup> lymphocytes lead to inhibition of the Th1 cells response and increase of the Th2 response. In the presence of the SNP rs4794067, representing a T to C substitution at position -1993 in the promoter region of the TBX21 gene, associated with a reduced promoter activity and a lower TBX21 (Suttner et al., 2009; Li et al., 2011), as well as a shift of the Th1/Th2 ratio towards Th2, activation of these cells leading to a more pronounced fibrosis in this subgroup of patients. In addition, there is activation of the Th17 cells with liberation of proinflammatory cytokines. Induction of Th17 cells, defined as CD4<sup>+</sup> or CD8<sup>+</sup> IL17 producing cells, is highly dependent of the signals of cytokines produced by other T cells populations or dendritic cells (Tesmer et al., 2008). Th17 cell response is propagated by the IL23 and IL21 cytokines and IL17 production is antagonized by T-bet transcription factor and by the IFN gamma, IL4 and IL2 cytokines (Bettelli et al., 2008). Thus, in the case of TBX21 -1993C allele of the SNP rs4794067 there is association with the predominance of the Th17 cell activity. TBX21 SNP rs4794067 was already associated with reumathoid arthritis, asthma or type 1 diabetes mellitus (Sasaki et al., 2004; Chae et al., 2009), but no association was found with acute cellular LT rejection (Thude et al., 2019).

The role of TBX21 as a determinant signal for maturation of NK cells in late stages and their effector function is largely accepted nowadays. Recent studies have shown that non-parenchymal liver cells have important function in the tolerance induction following LT (Knechtle and Kwun., 2009). Kupffer cells proved to have a dual performance in the pathological changes that occur after LT, Th1 cells correlated with rejection and Th2 predominance favoured graft acceptance and immunological tolerance (Li et al., 2022).

Programmed cellular death occurs through different pathways including autophagy, necroptosis and apoptosis. There are lots of data that establish hepatocyte apoptosis as a leading force for fibrogenesis in various causes of hepatocyte injury (Guicciardi and Gores, 2010). Apoptotic hepatocytes are eliminated by Kupffer and hepatic stellate cells. Elimination of the apoptotic bodies by hepatic stellate cells results in their activation and TGF-beta secretion, a key factor in stimulation of liver fibrosis. Kupffer cells with phagocytated apoptotic hepatocytes secrete TGF-beta leading to a pro-apoptotic response through stellate cells activation. There was demonstrated that patients with LT had significantly higher apoptotic markers compared to subjects with normal liver (Shojaie et al., 2020). This fact is linked to the immunosuppressor agents used following transplantation that have cytotoxic and pro-apoptotic effects. Studies of the

CNIs on cellular death are conflictual. Cyclosporine proved to increase hepatocyte expression of Bak1, a pro-apoptotic protein, in a model of liver injury; however, it had also an effect of preventing human gingival fibroblast apoptosis (Jung et al., 2008; Rao et al., 2018). Tacrolimus had also both pro and antiapoptotic effects in variate non-liver cellular lines (Johnson et al., 2009). In the study by Lim et al. (Lim et al., 2015), at therapeutic concentrations, none of the CNIs promoted hepatocyte cell death.

Despite the presence of multiple publications investigating functional and molecular cellular effects of MMF, cytotoxic action of MMF remains weakly defined. In a study published in 2008 (Chaigne-Delalande et al., 2008), mycophenolic acid induced a caspase dependant apoptosis in a minor cellular population. Recently, MMF therapy was associated with decreased incidence of tumors compared to untreated patients (Leckel et al., 2003). MMF treatment increased apoptosis of epithelial cells in the gastrointestinal tract, as well as apoptosis of the insular pancreatic cells, but reduced apoptosis of the renal tubular epithelium, in the glomerular and interstitial cells (Pardo-Mindan et al., 1999; Johnson et al., 2009). In contrast with other drugs, MMF therapy improved cellular viability and reduced apoptosis in primary hepatocytes, suggesting a hepatoprotector effect compared to other immunosuppressor drugs (Smiley et al., 2000). This effect was proved in our study in LT recipients with reduced fibrosis if they received MMF (Iacob et al., 2015). On the other hand, in other studies it was shown that the hepatoprotective effect of MMF is lost if this is used together with CNIs due to increased hepatocyte apoptosis. Also, based on the literature data, immunosuppression medication with serum concentrations over the therapeutic levels (>10–100 times) induces hepatocyte apoptosis. *In vitro* studies done by our team demonstrated the apoptotic and necrotic effect of the immunosuppressive medication on both cell populations hepatocytes and non-parenchymal liver cells. Studies have investigated the level of apoptosis and necrosis induced *in vitro* by different concentrations of immunosuppression medication certifying an evident relation of the toxic-necrotic and apoptotic effect with the dose of the drugs. Gene expression studies have indicated an antiapoptotic effect of MMF at doses close to the therapeutic levels through action of several apoptotic pathways (decrease of the cellular apoptosis receptors, of the genes specific to the mitochondrial apoptosis, of the effectors of apoptosis such as caspases or DFFB-CAD). In the co-culture systems, MMF + TAC association has induced antiapoptotic effects, decreasing the expression of the following genes: TRAILR1, BAK1, BAX, SMAC and of the effector proteins of apoptosis CASP8, CASP9 and CASP10.

Our results support the idea of using a low dose TAC and MMF association in case a genetic profile with a high risk of posttransplant fibrogenesis, such as the CC genotype of the

TBX21 gene promoter SNP. Literature data demonstrated that SRL at therapeutic levels did not lead to the death of hepatocytes. Also, SRL proved to be less toxic compared to cyclosporine/TAC + MMF; in addition SRL + MMF led to a reduced apoptosis of hepatocytes. Other studies (Iacob et al., 2007; Manzia et al., 2011) have established also a reduced progression of posttransplant fibrosis, of the inflammation and aminotransferases levels in patients with chronic hepatitis C treated with low dose CNI and MMF.

The goal of optimum immunosuppression is to increase drug effectiveness while lowering the adverse effects, as well as a long-term graft and recipient survival with a good quality of life. Every transplant recipient needs an immunosuppression regimen tailored to their: age, comorbid conditions, transplantation indications, behavior of the allograft, complications related to immunosuppression and post-LT physiologic conditions.

This study supports the role of MMF in liver fibrosis modulation and apoptosis after LT in a clinical setting and suggests that tailoring immunosuppression could avoid fibrosis progression in the allograft.

## Data availability statement

The raw data supporting the conclusions of this article can be made available by the authors upon reasonable request.

## Ethics statement

The studies involving human participants were reviewed and approved by Ethics Committee of Fundeni Clinical Institute. The patients/participants provided their written informed consent to participate in this study.

## Author contributions

SI and RI designed the study, performed experiments, collected data, interpreted data, wrote the manuscript, had equal contribution and share first authorship; IM, MU, AC, MD, GB, and CP—performed the experiments, contributed to analysis of data; LS, VB, and DH—collected data, contributed to analysis of data; CG, LG, SD, and IP—wrote, review and edited manuscript; all authors read and approved the final version of the manuscript.

## Funding

This work was supported by UEFISCDI Project TE120/2018 (APOHEPI).

## Conflict of interest

The authors declare that the research was conducted in the absence of any commercial or financial relationships that could be construed as a potential conflict of interest.

## Publisher's note

All claims expressed in this article are solely those of the authors and do not necessarily represent those of their affiliated organizations, or those of the publisher, the

editors and the reviewers. Any product that may be evaluated in this article, or claim that may be made by its manufacturer, is not guaranteed or endorsed by the publisher.

## Supplementary material

The Supplementary Material for this article can be found online at: <https://www.frontiersin.org/articles/10.3389/fphar.2022.1042664/full#supplementary-material>

## References

- Bettelli, E., Korn, T., Oukka, M., and Kuchroo, V. (2008). Induction and effector functions of T<sub>H</sub>17 cells. *Nature* 453, 1051–1057. doi:10.1038/nature07036
- Bouvier, N., Flinois, J. P., Gilleron, J., Sauvage, F. L., Legendre, C., Beaune, P., et al. (2009). Cyclosporine triggers endoplasmic reticulum stress in endothelial cells: A role for endothelial phenotypic changes and death. *Am. J. Physiol. Ren. Physiol.* 296, F160–F169. doi:10.1152/ajprenal.90567.2008
- Calne, R. Y., White, D. J., Thiru, S., Evans, D. B., McMaster, P., Dunn, D. C., et al. (1978). Cyclosporin A in patients receiving renal allografts from cadaver donors. *Lancet* 2, 1323–1327. doi:10.1016/s0140-6736(78)91970-0
- Chae, S. C., Shim, S. C., and Chung, H. T. (2009). Association of TBX21 polymorphisms in a Korean population with rheumatoid arthritis. *Exp. Mol. Med.* 41, 33–41. doi:10.3858/emmm.2009.41.1.005
- Chaigne-Delalande, B., Guidicelli, G., Couzi, L., Merville, P., Mahfouf, W., Bouchet, S., et al. (2008). The immunosuppressor mycophenolic acid kills activated lymphocytes by inducing a nonclassical actin-dependent necrotic signal. *J. Immunol.* 181, 7630–7638. doi:10.4049/jimmunol.181.11.7630
- Choi, S. J., You, H. S., and Chung, S. Y. (2008). Tacrolimus-induced apoptotic signal transduction pathway. *Transpl. Proc.* 40, 2734–2736. doi:10.1016/j.transproceed.2008.08.028
- Evans, C., and Jenner, R. (2013). Transcription factor interplay in T helper cell differentiation. *Brief. Funct. Genomics* 12, 499–511. doi:10.1093/bfgp/elt025
- Feng, S., Bucuvalas, J. C., Demetris, A. J., Burrell, B. E., Spain, K. M., Kanaparthi, S., et al. (2018). Evidence of chronic allograft injury in liver biopsies from long-term pediatric recipients of liver transplants. *Gastroenterology* 155, 1838–1851. doi:10.1053/j.gastro.2018.08.023
- Frizell, E., Abraham, A., Doolittle, M., Bashey, R., Kresina, T., Van, T. D., et al. (1994). FK506 enhances fibrogenesis in *in vitro* and *in vivo* models of liver fibrosis in rats. *Gastroenterology* 107, 492–498. doi:10.1016/0016-5085(94)90176-7
- Gelson, W., Hoare, M., Unitt, E., Palmer, C., Gibbs, P., Coleman, N., et al. (2010). Heterogeneous inflammatory changes in liver graft recipients with normal biochemistry. *Transplantation* 89, 739–748. doi:10.1097/TP.0b013e3181c96b32
- Giordano, A., Avellino, R., Ferraro, P., Romano, S., Corcione, N., and Romano, M. F. (2006). Rapamycin antagonizes NF-kappaB nuclear translocation activated by TNF-alpha in primary vascular smooth muscle cells and enhances apoptosis. *Am. J. Physiol. Heart Circ. Physiol.* 290, H2459–H2465. doi:10.1152/ajpheart.00750.2005
- Guicciardi, M. E., and Gores, G. J. (2010). Apoptosis as a mechanism for liver disease progression. *Semin. Liver Dis.* 30, 402–410. doi:10.1055/s-0030-1267540
- Hesselink, D. A., Bouamar, R., Elens, L., van Schaik, R. H. N., and van Gelder, T. (2014). The role of pharmacogenetics in the disposition of and response to tacrolimus in solid organ transplantation. *Clin. Pharmacokinet.* 53, 123–139. doi:10.1007/s40262-013-0120-3
- Iacob, S., Cicinnati, V., Kabar, I., Hüsing-Kabar, A., Radtke, A., Iacob, R., et al. (2021). Prediction of late allograft dysfunction following liver transplantation by immunological blood biomarkers. *Transpl. Immunol.* 69, 101448. doi:10.1016/j.trim.2021.101448
- Iacob, S., Cicinnati, V. R., and Beckebaum, S. (2009). Current immunosuppressive approaches in liver transplantation. *Panminerva Med.* 51, 215–225.
- Iacob, S., Cicinnati, V. R., Hilgard, P., Iacob, R. A., Gheorghe, L. S., Popescu, I., et al. (2007). Predictors of graft and patient survival in hepatitis C virus (HCV) recipients: Model to predict HCV cirrhosis after liver transplantation. *Transplantation* 84, 56–63. doi:10.1097/01.tp.0000267916.36343.ca
- Iacob, S., Cicinnati, V. R., Lindemann, M., Heinemann, F. M., Radtke, A., Kaiser, G. M., et al. (2015). Donor-specific anti-HLA antibodies and endothelial C4d deposition-association with chronic liver allograft failure. *Transplantation* 99, 1869–1875. doi:10.1097/TP.0000000000000613
- Jadlowiec, C. C., and Taner, T. (2016). Liver transplantation: Current status and challenges. *World J. Gastroenterol.* 22, 4438–4445. doi:10.3748/wjg.v22.i18.4438
- Johnson, J. D., Ao, Z., Ao, P., Li, H., Dai, L. J., He, Z., et al. (2009). Different effects of FK506, rapamycin, and mycophenolate mofetil on glucose-stimulated insulin release and apoptosis in human islets. *Cell Transpl.* 18, 833–845. doi:10.3727/096368909X471198
- Jung, J. Y., Jeong, Y. J., Jeong, T. S., Chung, H. J., and Kim, W. J. (2008). Inhibition of apoptotic signals in overgrowth of human gingival fibroblasts by cyclosporin A treatment. *Arch. Oral Biol.* 53, 1042–1049. doi:10.1016/j.archoralbio.2008.03.008
- Kabat-Koperska, J., Kolasa-Wolosiuk, A., Baranowska-Bosiacka, I., Safranow, K., Kosik-Bogacka, D., Gutowska, I., et al. (2016). The influence of exposure to immunosuppressive treatment during pregnancy on renal function and rate of apoptosis in native kidneys of female Wistar rats. *Apoptosis* 21, 1240–1248. doi:10.1007/s10495-016-1281-y
- Khanna, A., Kapur, S., Sharma, V., Li, B., and Suthanthiran, M. (1997). *In vivo* hyperexpression of transforming growth factor-beta1 in mice: Stimulation by cyclosporine. *Transplantation* 63, 1037–1039. doi:10.1097/00007890-199704150-00026
- Knechtle, S. J., and Kwun, J. (2009). Unique aspects of rejection and tolerance in liver transplantation. *Semin. Liver Dis.* 29, 91–101. doi:10.1055/s-0029-1192058
- Kok, B., Dong, V., and Karvellas, C. J. (2019). Graft dysfunction and management in liver transplantation. *Crit. Care Clin.* 35, 117–133. doi:10.1016/j.ccc.2018.08.002
- Leckel, K., Beecken, W. D., Jonas, D., Oppermann, E., Coman, M. C., Beck, K. F., et al. (2003). The immunosuppressive drug mycophenolate mofetil impairs the adhesion capacity of gastrointestinal tumour cells. *Clin. Exp. Immunol.* 134, 238–245. doi:10.1046/j.1365-2249.2003.02290.x
- Li, J. R., Li, J. G., Deng, G. H., Zhao, W. L., Dan, Y. J., Wang, Y. M., et al. (2011). A common promoter variant of TBX21 is associated with allele specific binding to Yin-Yang 1 and reduced gene expression. *Scand. J. Immunol.* 73, 449–458. doi:10.1111/j.1365-3083.2011.02520.x
- Li, W., Chang, N., and Li, L. (2022). Heterogeneity and function of kupffer cells in liver injury. *Front. Immunol.* 13, 940867. doi:10.3389/fimmu.2022.940867
- Lim, E. J., Chin, R., Nachbur, U., Silke, J., Jia, Z., Angus, P. W., et al. (2015). Effect of immunosuppressive agents on hepatocyte apoptosis post-liver transplantation. *PLoS ONE* 10, e0138522. doi:10.1371/journal.pone.0138522
- Manzia, T. M., Angelico, R., Toti, L., Bellini, M. I., Sforza, D., Palmieri, G., et al. (2011). Long-term, maintenance MMF monotherapy improves the fibrosis progression in liver transplant recipients with recurrent hepatitis C. *Transpl. Int.* 24, 461–468. doi:10.1111/j.1432-2277.2011.01228.x
- Mitry, R. R., Hughes, R. D., and Dhawan, A. (2002). Progress in human hepatocytes: Isolation, culture & cryopreservation. *Semin. Cell Dev. Biol.* 13, 463–467. doi:10.1016/s1084952102001350

- Nguyen, T., Park, J. Y., Scudiere, J. R., and Montgomery, E. (2009). Mycophenolic acid (cellcept and myofortic) induced injury of the upper GI tract. *Am. J. Surg. Pathol.* 33, 1355–1363. doi:10.1097/PAS.0b013e3181a755bd
- Pardo-Mindan, F. J., Errasti, P., Panizo, A., Sola, I., de Alava, E., and Lozano, M. D. (1999). Decrease of apoptosis rate in patients with renal transplantation treated with mycophenolate mofetil. *Nephron* 82, 232–237. doi:10.1159/000045407
- Rao, S. R., Ajitkumar, S., Subbarayan, R., and Girija, D. M. (2018). Cyclosporine-A induces endoplasmic reticulum stress in human gingival fibroblasts – an *in vitro* study. *J. Oral Biol. Craniofac. Res.* 8, 165–167. doi:10.1016/j.jobcr.2016.11.002
- Rojas, L., Neumann, I., Herrero, M. J., Boso, V., Reig, J., Poveda, J. L., et al. (2015). Effect of CYP3A5\*3 on kidney transplant recipients treated with tacrolimus: A systematic review and meta-analysis of observational studies. *Pharmacogenomics J.* 15, 38–48. doi:10.1038/tpj.2014.38
- Sakaeda, T., Nakamura, T., and Okumura, K. (2004). Pharmacogenetics of drug transporters and its impact on the pharmacotherapy. *Curr. Top. Med. Chem.* 4, 1385–1398. doi:10.2174/1568026043387692
- Sasaki, Y., Ihara, K., Matsuura, N., Kohno, H., Nagafuchi, S., Kuromaru, R., et al. (2004). Identification of a novel type 1 diabetes susceptibility gene, T-bet. *Hum. Genet.* 115, 177–184. doi:10.1007/s00439-004-1146-2
- Seglen, P. O. (1976). Preparation of isolated rat liver cells. *Methods Cell Biol.* 13, 29–83. doi:10.1016/s0091-679x(08)61797-5
- Shojaie, L., Iorga, A., and Dara, L. (2020). Cell death in liver diseases: A review. *Int. J. Mol. Sci.* 21, 9682. doi:10.3390/ijms21249682
- Smiley, S. T., Csizmadia, V., Gao, W., Turka, L. A., and Hancock, W. W. (2000). Differential effects of cyclosporine A, methylprednisolone, mycophenolate, and rapamycin on CD154 induction and requirement for NFkappaB: Implications for tolerance induction. *Transplantation* 70, 415–419. doi:10.1097/00007890-200008150-00005
- Starzl, T. E., Todo, S., Fung, J., Demetris, A. J., Venkataramman, R., and Jain, A. (1989). FK 506 for liver, kidney, and pancreas transplantation. *Lancet* 2, 1000–1004. doi:10.1016/s0140-6736(89)91014-3
- Suttner, K., Rosenstiel, P., Depner, M., Schedel, M., Pinto, L. A., Ruether, A., et al. (2009). TBX21 gene variants increase childhood asthma risk in combination with HLX1 variants. *J. Allergy Clin. Immunol.* 123, 1062–1068. doi:10.1016/j.jaci.2009.02.025
- Szabo, S., Kim, S., Costa, G., Zhang, X., Fathman, C., and Glimcher, L. (2000). A novel transcription factor, T-bet, directs Th1 lineage commitment. *Cell* 100, 655–669. doi:10.1016/s0092-8674(00)80702-3
- Tesmer, L. A., Lundy, S. K., Sarkar, S., and Fox, D. A. (2008). Th17 cells in human disease. *Immunol. Rev.* 223, 87–113. doi:10.1111/j.1600-065X.2008.00628.x
- Thervet, E., Anglicheau, D., King, B., Schlageter, M. H., Cassinat, B., Beaune, P., et al. (2003). Impact of cytochrome p450 3A5 genetic polymorphism on tacrolimus doses and concentration-to-dose ratio in renal transplant recipients. *Transplantation* 76, 1233–1235. doi:10.1097/01.TP.0000090753.99170.89
- Thude, H., Tiede, P., Sterneck, M., Nashan, B., and Koch, M. (2019). Impact of TBX21, GATA3, and FOXP3 gene polymorphisms on acute cellular rejection after liver transplantation. *HLA* 93, 97–101. doi:10.1111/tan.13458
- Uesugi, M., Kikuchi, M., Shinke, H., Omura, T., Yonezawa, A., Matsubara, K., et al. (2014). Impact of cytochrome P450 3A5 polymorphism in graft livers on the frequency of acute cellular rejection in living-donor liver transplantation. *Pharmacogenet. Genomics* 24, 356–366. doi:10.1097/FPC.0000000000000060
- Usui, T., Preiss, J. C., Kanno, Y., Yao, Z. J., Bream, J. H., O'Shea, J. J., et al. (2006). T-bet regulates Th1 responses through essential effects on GATA-3 function rather than on IFNG gene acetylation and transcription. *J. Exp. Med.* 203, 755–766. doi:10.1084/jem.20052165
- Xu, R., Zhang, Z., and Wang, F. S. (2012). Liver fibrosis: Mechanisms of immune-mediated liver injury. *Cell. Mol. Immunol.* 9, 296–301. doi:10.1038/cmi.2011.53





## OPEN ACCESS

## EDITED BY

Mariana Jinga,  
Carol Davila University of Medicine and  
Pharmacy, Romania

## REVIEWED BY

Jun Ren,  
Fudan University, China  
Prasanna K. Santhekadur,  
JSS Academy of Higher Education and  
Research, India

## \*CORRESPONDENCE

Shizhen Zhao,  
zhaoshizhen1987@163.com  
Yunfu Li,  
ligeng528@126.com  
Wenling Ye,  
hexi81@163.com

<sup>†</sup>These authors have contributed equally  
to this work.

## SPECIALTY SECTION

This article was submitted to  
Gastrointestinal and Hepatic  
Pharmacology,  
a section of the journal  
Frontiers in Pharmacology

RECEIVED 20 June 2022

ACCEPTED 18 October 2022

PUBLISHED 02 November 2022

## CITATION

Fu Y, Zhou Y, Shen L, Li X, Zhang H, Cui Y,  
Zhang K, Li W, Chen W-d, Zhao S, Li Y  
and Ye W (2022), Diagnostic and  
therapeutic strategies for non-alcoholic  
fatty liver disease.  
*Front. Pharmacol.* 13:973366.  
doi: 10.3389/fphar.2022.973366

## COPYRIGHT

© 2022 Fu, Zhou, Shen, Li, Zhang, Cui,  
Zhang, Li, Chen, Zhao, Li and Ye. This is  
an open-access article distributed  
under the terms of the [Creative  
Commons Attribution License \(CC BY\)](#).  
The use, distribution or reproduction in  
other forums is permitted, provided the  
original author(s) and the copyright  
owner(s) are credited and that the  
original publication in this journal is  
cited, in accordance with accepted  
academic practice. No use, distribution  
or reproduction is permitted which does  
not comply with these terms.

# Diagnostic and therapeutic strategies for non-alcoholic fatty liver disease

Yajie Fu<sup>1†</sup>, Yanzhi Zhou<sup>1†</sup>, Linhu Shen<sup>1</sup>, Xuewen Li<sup>1</sup>,  
Haorui Zhang<sup>1</sup>, Yeqi Cui<sup>1</sup>, Ke Zhang<sup>1</sup>, Weiguo Li<sup>1</sup>,  
Wei-dong Chen<sup>1,2</sup>, Shizhen Zhao<sup>1\*</sup>, Yunfu Li<sup>1\*</sup> and Wenling Ye<sup>1\*</sup>

<sup>1</sup>Key Laboratory of Receptors-Mediated Gene Regulation, Hebi Key Laboratory of Liver Disease, School of Basic Medical Sciences, The People's Hospital of Hebi, Henan University, Kaifeng, China, <sup>2</sup>Key Laboratory of Receptors-Mediated Gene Regulation and Drug Discovery, School of Basic Medical Science, Inner Mongolia Medical University, Hohhot, China

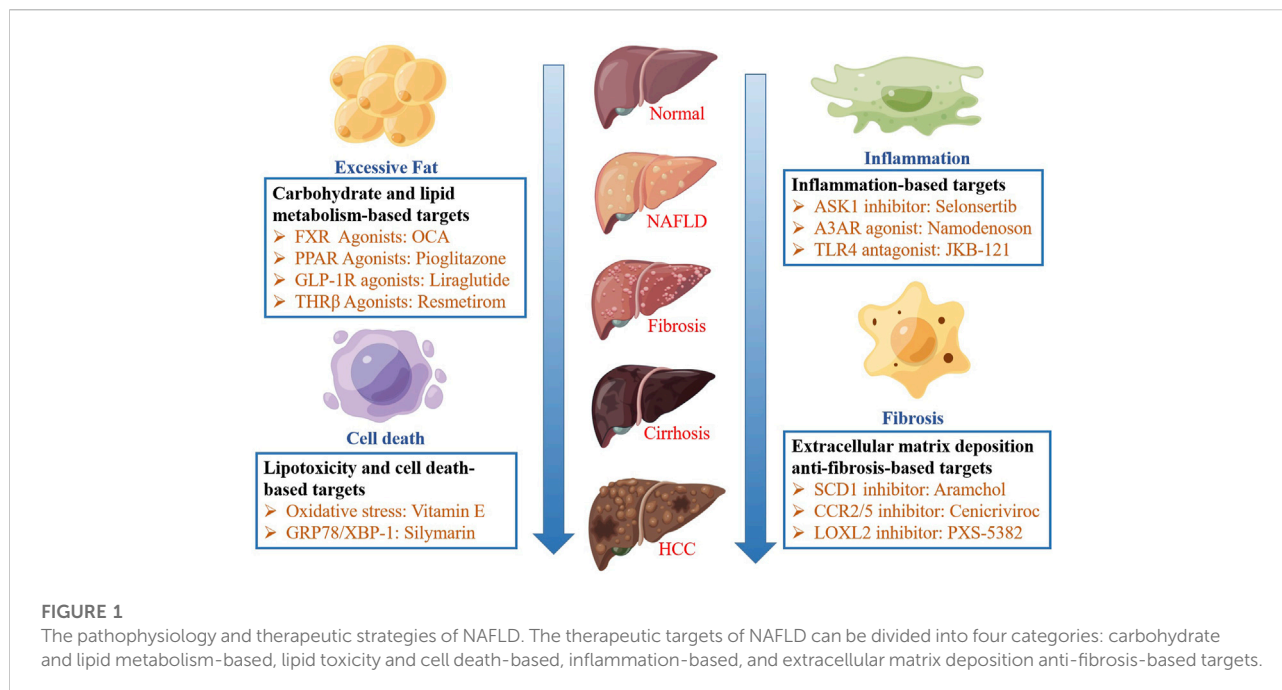
The global incidence rate of non-alcoholic fatty liver disease (NAFLD) is approximately 25%. With the global increase in obesity and its associated metabolic syndromes, NAFLD has become an important cause of chronic liver disease in many countries. Despite recent advances in pathogenesis, diagnosis, and therapeutics, there are still challenges in its treatment. In this review, we briefly describe diagnostic methods, therapeutic targets, and drugs related to NAFLD. In particular, we focus on evaluating carbohydrate and lipid metabolism, lipotoxicity, cell death, inflammation, and fibrosis as potential therapeutic targets for NAFLD. We also summarized the clinical research progress in terms of drug development and combination therapy, thereby providing references for NAFLD drug development.

## KEYWORDS

NAFLD, NASH, diagnostic, therapeutic strategies, drug development

## 1 Introduction

Non-alcoholic fatty liver disease (NAFLD) is a liver disease, which encompasses diffuse non-alcoholic liver steatosis, non-alcoholic steatohepatitis (NASH), and other features of liver damage, such as liver cirrhosis and hepatocellular carcinoma (Friedman et al., 2018a). NAFLD is defined by the presence of steatosis in more than 5% of liver cells and in the absence of excessive alcohol consumption (men  $\geq$  30 g per day and women  $\geq$  20 g per day) or other chronic liver diseases (Cobbina and Akhlaghi, 2017). In addition, NASH can occur if steatosis is accompanied by inflammation and hepatocyte ballooning (Yeh and Brunt, 2014). NAFLD has become increasingly common in recent years, and it is now the leading cause of chronic liver disease in many countries. The pathogenesis of NAFLD has not yet been fully elucidated; however, obesity, type 2 diabetes mellitus (T2DM), and other metabolic disorders (Akhtar et al., 2019) play key roles in increasing the incidence and prevalence of NAFLD. The global prevalence of NAFLD is approximately 25.2%, and the overall prevalence of NASH is approximately 1.5%–6.5%. People with obesity are more likely to develop NAFLD. Approximately 50%



and 80% of patients with NAFLD and NASH, respectively, are overweight. Patients with T2DM also have a high prevalence of NAFLD (56%–59%), and the prevalence of NASH in patients with T2DM is 37% (Younossi et al., 2019a). The prevalence of NAFLD and NASH in patients with dyslipidemia has also increased significantly (Wu et al., 2016). NAFLD is a multisystem disease; however, the only clinical symptom is liver disease. It also affects the cardiovascular, excretory, and endocrine systems and carries the risk of extrahepatic malignant tumors. The most common cause of death in NAFLD is cardiovascular disease, followed by malignant tumors and liver-related complications (Li and Ahmed, 2020).

The pathogenesis of NAFLD is unclear, and the “two-hit” theory is widely accepted in the early stage. This theory suggests that lipid metabolism disorder triggers the “first blow” and causes fatty degeneration of liver parenchymal cells. On this basis, a “second blow” can occur, wherein oxidative stress and mitochondrial dysfunction take place in the liver with over-deposition of lipids, forming lipid peroxide products and eventually damaging liver cells (Day and James, 1998). Further research found, that the two-hit theory cannot fully explain the pathogenesis of NAFLD, and therefore, the “multiple-hit” theory has gradually attracted attention. At the same time, available evidence suggests that genetic factors are also important in the pathogenesis of NAFLD. Family studies show that the risk of NAFLD is significantly higher in patients who have first-degree relatives affected by this disease compared with the normal population. (Del Campo et al., 2018). Over 100 loci have been examined in genome-wide association studies and candidate gene studies, and five genes (PNPLA3, TM6SF2,

GCKR, MBOAT7, and HSD17B13) have been identified as reliably and robustly predisposing individuals to MAFLD. (Valenti and Baselli, 2018; Sookoian and Pirola, 2019). All five genes are involved in glucose and fat homeostasis regulatory pathways. Although the current study of these mechanisms is incomplete, these findings may provide some scientific information for targeted therapy of NAFLD (Carlsson et al., 2020). Due to its complex pathogenesis and absence of specific drugs, NAFLD treatment mainly involves lifestyle intervention. However, the efficacy of this treatment is limited. This article summarizes the diagnostic methods and therapeutic drugs in development for NAFLD, including the targets that regulate each pathway. This review also outlines the current state of NAFLD drug development and combination therapy.

## 2 Diagnostic progress

The current diagnostic methods for NAFLD include ultrasound diagnosis, computed tomography (CT), magnetic resonance imaging (MRI), liver biopsy, and laboratory testing. When NAFLD is suspected, the patient should first be evaluated using non-invasive imaging. Although ultrasound has a high detection rate for moderate and severe liver steatosis, its sensitivity and specificity are low for mild liver steatosis. Hence, ultrasound cannot be used to diagnose steatohepatitis or fibrosis (Bril et al., 2015). CT can also be used to diagnose NAFLD with the same level of sensitivity and specificity as ultrasound. Hyodo et al. (Hyodo et al., 2017) found that the multi-substance analysis algorithm of dual-energy CT allows for

TABLE 1 Mechanism and Research Progress of drugs targeting carbohydrate and lipid metabolism.

Drug name	Drug targets	NCT number	Current research progress	Status	Reference
Dapagliflozin	SGLT2 Inhibitors. Improve steatosis and fibrosis	NCT05459701	Phase IV	Recruiting	<a href="https://clinicaltrials.gov">https://clinicaltrials.gov</a>
Liraglutide	GLP-1 Receptor Agonist. Increase fatty acid oxidation and reduce <i>de novo</i> lipogenesis	NCT02654665	Phase III	Completed	Khoo et al. (2019)
Oltipraz	LXR Agonist. Inhibit fatty acid synthesis through AMPK-S6K1 pathway and LXR-SREBP-1c pathway in liver	NCT02068339	Phase III	Completed	<a href="https://clinicaltrials.gov">https://clinicaltrials.gov</a>
Resmetirom (MGL-3196)	Selective Thyroid Hormone Receptor $\beta$ Agonist. Reduce liver fat and lipoprotein	NCT04951219, NCT03900429	Phase III	Recruiting	<a href="https://clinicaltrials.gov">https://clinicaltrials.gov</a>
Elafibranor	PPAR- $\alpha/\delta$ Agonist. Improve insulin sensitivity, glucose homeostasis, and lipid metabolism and reduce inflammation	NCT02704403	Phase III	Terminated	<a href="https://clinicaltrials.gov">https://clinicaltrials.gov</a>
6-ethylchenodeoxycholic acid (OCA)	FXR Agonist. Induce the expression of intestinal sex hormones, especially fibroblast growth factor 19. Improve liver blood index and reduce liver fibrosis	NCT02548351	Phase III	Not yet recruiting	<a href="https://clinicaltrials.gov">https://clinicaltrials.gov</a>
Semaglutide	GLP-1 Receptor Agonist. Increase fatty acid oxidation and reduce <i>de novo</i> lipogenesis	NCT02970942, NCT05067621	Phase II/III	Completed/Not yet recruiting	Newsome et al. (2021)
Omega-3 polyunsaturated fatty acids	Inhibit hepatic <i>de novo</i> lipogenesis and increase fat oxidation	NCT00681408	Phase II/III	Completed	Argo et al. (2015)
Synbiotic	Improve insulin resistance by changing gut microbiota	NCT01791959	Phase II/III	Completed	Eslamparast et al. (2014)
Licogliflozin	SGLT2 Inhibitors. Improve steatosis and fibrosis	NCT03205150	Phase II	Completed	<a href="https://clinicaltrials.gov">https://clinicaltrials.gov</a>
Vitamin D	Regulate oxidation, improve inflammation, lipotoxicity, and fibrosis	NCT01571063, NCT01792115	Phase II	Completed	<a href="https://clinicaltrials.gov">https://clinicaltrials.gov</a>
Px-104	FXR Agonist. Improve insulin sensitivity and liver enzymes	NCT01999101	Phase II	Completed	Traussnigg et al. (2021)
Cilofexor	FXR Agonist. Reduce hepatic steatosis and serum bile acid	NCT02854605	Phase II	Completed	Patel et al. (2020)
EDP-305	FXR Agonist. Reduce inflammation and liver fat content	NCT03421431	Phase II	Completed	Ratziu et al. (2022)
Ervogastat (PF-06865571)	DGAT Inhibitors. Reduced liver fat fraction	NCT03776175	Phase II	Completed	<a href="https://clinicaltrials.gov">https://clinicaltrials.gov</a>
Saroglitazar	PPAR- $\alpha/\gamma$ Agonist. Improve insulin resistance and increase lipid oxidation	NCT03061721, NCT03863574	Phase II	Completed	<a href="https://clinicaltrials.gov">https://clinicaltrials.gov</a>
VK-2809 (MB07811)	Selective Thyroid Hormone Receptor $\beta$ Agonist. Reduce liver fat and lipoprotein	NCT04173065	Phase II	Recruiting	<a href="https://clinicaltrials.gov">https://clinicaltrials.gov</a>
TERN-501	Selective Thyroid Hormone Receptor $\beta$ Agonist. Reduce liver fat and lipoprotein	NCT05415722	Phase II	Recruiting	<a href="https://clinicaltrials.gov">https://clinicaltrials.gov</a>
ION224 (IONIS-DGAT2 <sub>Rx</sub> )	DGAT Inhibitors. Reduced liver fat fraction	NCT04932512	Phase II	Recruiting	<a href="https://clinicaltrials.gov">https://clinicaltrials.gov</a>
ASC40(TVB-2640)	FASN Inhibitor. Reduce excessive fat in the liver and inhibit inflammation and fibrosis	NCT04906421	Phase II	Recruiting	<a href="https://clinicaltrials.gov">https://clinicaltrials.gov</a>
Tropifexor (LJN452)	FXR Agonist. Reduced steatohepatitis, fibrosis, and profibrogenic gene expression	NCT02855164	Phase II	Terminated	<a href="https://clinicaltrials.gov">https://clinicaltrials.gov</a>
Nidufexor (LMB763)	FXR Agonist. Reduce steatosis, inflammation and fibrosis	NCT02913105	Phase II	Terminated	<a href="https://clinicaltrials.gov">https://clinicaltrials.gov</a>
Seladelpar	PPAR- $\delta$ Agonist. Improve glucose homeostasis, lipid metabolism and reduce inflammation	NCT03551522	Phase II	Terminated	<a href="https://clinicaltrials.gov">https://clinicaltrials.gov</a>
MET-409	FXR Agonist. Reduce hepatic steatosis, inflammation and fibrosis	NCT04702490	Phase II	Not yet recruiting	<a href="https://clinicaltrials.gov">https://clinicaltrials.gov</a>
PXL065	PPAR- $\gamma$ Agonist. Increase the levels of plasma adiponectin, thus playing anti-inflammatory and anti-fibrosis roles	NCT04321343	Phase II	Not yet recruiting	<a href="https://clinicaltrials.gov">https://clinicaltrials.gov</a>

(Continued on following page)

TABLE 1 (Continued) Mechanism and Research Progress of drugs targeting carbohydrate and lipid metabolism.

Drug name	Drug targets	NCT number	Current research progress	Status	Reference
ASC41	Selective Thyroid Hormone Receptor $\beta$ Agonist. Reduce liver fat and lipoprotein	NCT05462353, NCT05118360	Phase II	Not yet recruiting	<a href="https://clinicaltrials.gov">https://clinicaltrials.gov</a>
BAR502	Steroidal dual ligand for FXR and GPBAR1. Promote adipose tissue browning, prevent liver injury caused by HFD.	NCT05203367	Phase I	Not yet recruiting	<a href="https://clinicaltrials.gov">https://clinicaltrials.gov</a>
Dulaglutide	GLP-1 Receptor Agonist. Increase fatty acid oxidation and reduce <i>de novo</i> lipogenesis	NCT03590626	Clinical phase	Completed	Kuchay et al. (2020)
InT-767	FXR Agonist. Restore lipid and glucose metabolism, reduce insulin resistance and inhibit TNF- $\alpha$ And NF- $\kappa$ B to attenuate the pro-inflammatory response	-	Preclinical study	Completed	Hu et al. (2018b)
Altenusin	FXR Agonist. Reduce body weight and fat mass, reduce blood glucose, and reverse HFD induced liver lipid droplet accumulation and bullous steatosis	-	Preclinical study	Completed	Zheng et al. (2017)
Yangonin	FXR Agonist. Activate FXR signal to inhibit hepatic lipogenesis and gluconeogenesis, promote lipid metabolism and glycogen synthesis, and improve insulin sensitivity	-	Preclinical study	Completed	Dong et al. (2019)
Isoschimgine	Improved steatosis and inflammation and fibrosis	-	Preclinical study	Completed	Li et al. (2021)

PPAR, peroxisome proliferator-activated receptor; GLP-1RA, glucagon-like peptide receptor agonist; SGLT, sodium-glucose cotransporter; FXR, farnesoid X receptor; TNF- $\alpha$ ,  $\alpha$ -tumor necrosis factor; NF- $\kappa$ B, Nuclear factor kappa-B; HFD, High-fat diet; HSC, hepatic stellate cell; TG, triglyceride; MCD, methionine and choline deficient.

quantitative evaluation of liver steatosis. However, this is expensive and involves exposure to radiation, which limits its clinical application. MRI is the most sensitive detection method and can detect approximately 5% of hepatocyte steatosis. However, its accuracy may be affected by fibrosis and severe steatosis (Lee and Kim, 2019). Liver biopsy is the “gold standard” for NAFLD diagnosis, and can be used to accurately assess liver cell inflammation, liver fibrosis, and liver steatosis (Nalbantoglu and Brunt, 2014). When non-invasive imaging is not sufficient to accurately diagnose NAFLD, liver biopsy can assist in the diagnosis. Meanwhile, laboratory testing can predict NAFLD early and assess the risk and prognosis of cardiovascular and other dangerous events in patients with NAFLD; therefore, it is also worthy of attention.

The most important histological feature of advanced NAFLD is fibrosis (Chalasani and Younossi, 2018). Therefore, the evaluation of liver fibrosis is essential. The imageological examinations mentioned above do not reliably reflect the progression of liver fibrosis in patients with NAFLD. Consequently, there has been significant interest in developing noninvasive biomarkers and clinical prediction rules. Simple biochemical markers of fibrosis such as low albumin, prolonged prothrombin time and thrombocytopenia are markers of advanced cirrhosis. These biochemical markers are non-invasive and inexpensive, but they are less reliable (Jennison et al., 2019). Currently, several methods have been developed to assess hepatic fibrosis, such as the NAFLD Fibrosis Score (NFS),

Fibrosis-4 (FIB-4) Score and Enhanced Liver Fibrosis (ELF) test (Shah et al., 2009). The NFS is based on six variables: age, BMI, hyperglycemia, platelet count, albumin, and AST/ALT ratio. FIB-4 index is an algorithm based on platelet count, age, AST, and ALT (Kaswala et al., 2016). A previous study showed that NFS and FIB-4 were better than other indices such as AST to Platelet Ratio Index (APRI) and AST/ALT ratio in predicting advanced fibrosis (Imajo et al., 2016). The Enhanced Liver Fibrosis (ELF) panel consisting of plasma levels of three matrix turnover proteins (tissue inhibitor of metalloproteinase 1, hyaluronic acid and N-terminal procollagen III-peptide) have an AUROC of 0.90 with 90% specificity and 80% sensitivity for detecting advanced fibrosis (Angulo et al., 2007). In addition, ELF is approved for commercial use in Europe.

### 3 Therapeutic targets and related drugs for NAFLD

Studies show that the therapeutic targets of NAFLD can be divided into four categories: carbohydrate and lipid metabolism-based, lipid toxicity and cell death-based, inflammation-based, and extracellular matrix deposition anti-fibrosis-based targets. Various drugs can improve NASH by acting on different targets. These therapeutic targets and their related drugs are schematically depicted in Figure 1.

### 3.1 Carbohydrate and lipid metabolism-based targets

Excessive fatty acids in the liver lead to excess energy and the production of lipotoxic metabolites by hepatocytes, thereby damaging hepatocytes (Neuschwander-Tetri, 2010). Therefore, reducing intrahepatic free fatty acids is a potential strategy for NAFLD treatment, which can be achieved by increasing insulin sensitivity, fatty acid oxidation, or fatty acid export and storage by peripheral tissues and reducing *de novo* lipogenesis (DNL). The research progress on drugs targeting carbohydrate and lipid metabolism is summarized in Table 1.

#### 3.1.1 Farnesoid X receptor agonists

The farnesoid X receptor (FXR) is a bile acid receptor that regulates bile acid absorption, metabolism, and secretion and is closely associated with the development of cholestasis, fatty liver disease, cholesterol stones, enteritis and tumors (Koutsounas et al., 2015). FXR shares a common architecture with classical nuclear receptors, which are composed of an N-terminal ligand-independent activation domain, conserved DNA-binding domain (DBD), and C-terminal ligand-binding domain (LBD) (Weikum and Liu, 2018). FXR agonists can improve insulin sensitivity, inhibit DNL and reduce bile acid synthesis (Neuschwander-Tetri et al., 2015; Harrison et al., 2018b). In addition, FXR activation can inhibit sterol regulatory element-binding protein 1c (SREBP-1c), a key transcription factor for lipid regeneration that regulates triglyceride metabolism and lipid regeneration (Watanabe et al., 2004). Therefore, FXR is considered the most promising target for NAFLD treatment.

##### 3.1.1.1 Obeticholic acid

Obeticholic acid (OCA) is a steroidal FXR agonist that has completed phase III clinical trials for NASH treatment. As its safety and effectiveness are still not guaranteed, the FDA rejected a new application for NASH treatment submitted by Intercept Pharmaceuticals Inc. in 2019 (Younossi et al., 2021). Pruritus, a common symptom of cholestatic diseases, and is a common side effect of FXR agonists (Srivastava, 2014; Hirschfield et al., 2015; Kowdley et al., 2018). Generally, mild pruritus occurs at the beginning of OCA treatment and does not deteriorate over time (Younossi et al., 2019b).

Recent studies show that low doses of OCA are a safe and effective treatment for NASH and cholestatic liver disease. A double-blind study showed that OCA can improve NASH fibrosis [OR: 1.95 (1.47–2.59;  $p < 0.001$ )]. The probability of improvement was 1.61 (1.03–2.51;  $p = 0.03$ ) in the 10 mg OCA dose group and 2.23 (1.55–3.18;  $p < 0.001$ ) in the 25 mg OCA dose group. However, in patients with NASH, 25 mg OCA resulted in significant adverse events and drug discontinuation reactions compared with 10 mg OCA [0.95 (0.6–1.5);  $p = 0.84$ ] [2.8 (1.42–3.02);  $p < 0.001$ ]. OCA (5 mg) was associated with the lowest risk of itching (Kulkarni et al., 2021). Another study

showed that compared with the placebo, OCA increased the liver transport of bound bile acid tracer 11C CSAR, thereby increasing the transport of endogenous bound bile acids from hepatocytes to bile ducts. Therefore, OCA shortens the exposure time of hepatocytes to potentially cytotoxic bile acids and reduces hepatocellular injury (Kjærgaard et al., 2021). In conclusion, as a representative steroid FXR agonist, OCA should be considered in terms of safety and selectivity.

##### 3.1.1.2 Tropifexor

Tropifexor, also known as LJN-452, is a highly potent non-steroidal FXR agonist. It can activate FXR and regulate FXR target genes at very low doses and upon systemic exposure. Studies show that the efficacy of tropifexor at a dose of  $<1$  mg/kg is superior to that 25 mg/kg OCA in the liver of insulin-resistant NASH obesity models (islet amyloid liver NASH model and chemical and dietary models of NASH stelic animal model) (Hernandez et al., 2019). Some steroidal FXR agonists are agonists of GPBAR1 (also known as TGR5), another bile acid receptor that is the main cause of side effects, including pruritus (Kowdley et al., 2018). Unlike steroidal drugs, non-steroidal drugs do not usually interact with non-target proteins, such as GPBAR1; that is, they have higher selectivity. A previous study showed that the  $EC_{50}$  of OCA on GPBAR1 was  $0.918 \mu\text{M}$ , whereas tropifexor had no detectable activity on GPBAR1 ( $EC_{50} > 10 \mu\text{M}$ ) (Tully et al., 2017). Moreover, in clinical trials, itching was not observed in healthy volunteers within 2 weeks of daily administration (Badman et al., 2020). Phase II clinical trials for the evaluation of the safety and efficacy of tropifexor in treating primary biliary cirrhosis and NASH are currently ongoing (Kowdley et al., 2020). The crystal structure of the FXR-tropifexor complex has been resolved, and the molecular mechanism of the combination of tropifexor and FXR-LBD has been proposed (Jiang et al., 2021). In addition, the highly selective structures of tropifexor to FXR and GPBAR1 were analyzed, which provided a better understanding of the development of new compounds targeting FXR (Jiang et al., 2021). As a representative non-steroidal drug, tropifexor is preferable to steroidal drugs in terms of selectivity and is expected to become the first-line drug for NASH treatment.

#### 3.1.2 Peroxisome proliferator-activated receptor agonists

Peroxisome proliferator-activated receptors (PPARs) are ligand-activated receptors in the nuclear hormone receptor family and include three subtypes: PPAR $\alpha$ , PPAR $\beta/\delta$  and PPAR $\gamma$ . PPAR $\alpha$  is highly expressed in the liver, skeletal muscle, kidney, heart and vascular wall, but at relatively low levels in fatty tissues and cartilage. It regulates fatty acid metabolism, including absorption, transport and  $\alpha$ -oxidation. PPAR $\beta$  is widely expressed throughout the body and regulates the  $\beta$ -oxidation of free fatty acids, improving glucose



homeostasis and exerting anti-inflammatory effects. PPAR $\gamma$  is expressed in adipose, vascular smooth muscle and myocardial tissues in mammals. It can regulate adipogenesis and fatty acid storage, and improve insulin sensitivity. Therefore, PPARs agonists may be efficacious in NAFLD treatment. Among them, PPAR- $\alpha$  agonists are expected to reduce the metabolic overload of NASH. However, clinical trials of fibrates are not satisfactory (Laurin et al., 1996; Basaranoglu et al., 1999; Fernández-Miranda et al., 2008). Therefore, people begin to study selective PPAR agonists, such as pioglitazone (PPAR- $\gamma$  agonist), saroglitazar (PPAR- $\alpha/\gamma$  agonist) (Kumar et al., 2020), elafibranor (PPAR- $\alpha/\delta$  agonist) (Ratziu et al., 2016).

### 3.1.2.1 Pioglitazone

Pioglitazone is a PPAR $\gamma$  agonist that can increase levels of plasma adiponectin, through anti-inflammatory and anti-fibrosis action (Bajaj et al., 2004). To investigate the efficacy and safety of long-term pioglitazone treatment for patients with NASH and T2DM, 101 patients with prediabetes or T2DM were randomly divided into 45 mg/d pioglitazone treatment and placebo groups for 18 months in a randomized, double-blind, placebo-controlled trial (NCT00994682). The results showed that 58% patients treated with pioglitazone had a reduction of at least two points on the NAFLD activity score without worsening fibrosis, and 51% reached a resolution of NASH compared with the placebo group. In addition, the group treated with pioglitazone showed improvement in their fibrosis score, hepatic triglyceride content, and insulin sensitivity (Cusi et al., 2016). However, pioglitazone has some side effects, such as the increased risk of body weight gain, fluid retention, bladder cancer, bone fracture, and increased incidence of hospitalization for heart failure. These side effects may be mitigated by altering the pioglitazone dose (Giles et al., 2008; Satirapoj et al., 2018; Tang et al., 2018; Portillo-Sanchez and Bril, 2019). In summary, on the premise of biopsy-proven NASH, pioglitazone can be used to treat NASH patients with or without T2DM according to guidelines (Chalasani and Younossi, 2018).

### 3.1.2.2 PXL065

PXL065 is a newly patented deuterium-stabilized R-stereoisomer of pioglitazone. It has anti-inflammatory and anti-NASH properties related to pioglitazone and causes little or no weight gain or fluid retention, thus, it may have a better therapeutic effect on NASH than pioglitazone. To evaluate the efficacy and safety of PXL065 in patients with NASH confirmed by non-cirrhotic biopsies, a 36-week, randomized, double-blind, placebo-controlled phase II clinical trial is in progress (NCT04321343). In this trial, 123 participants were randomly divided into three PXL065 treatment groups (7.5, 15, and 22.5 mg) and a placebo group. The primary endpoint of the trial was the relative change in the percentage of liver fat content measured using MRI-PDFF at 36 weeks. The phase II clinical trial of the PXL065 were completed in August 2022,

but no results have been posted on [ClinicalTrials.gov](https://clinicaltrials.gov) at present.

## 3.1.3 Glucagon-like peptide receptor agonists

Glucagon-like peptide-1 (GLP-1) is an incretin mainly produced by intestinal L cells. Glucagon-like peptide-1 receptor (GLP-1R) agonists can enhance insulin secretion, inhibit glucagon secretion in a glucose concentration-dependent manner, and delay gastric emptying. It can also reduce food intake through central appetite inhibition by activating the GLP-1 receptor, thereby reducing blood glucose levels (Gupta et al., 2010). GLP-1R agonists are anti-diabetic drugs that potentially affect on NAFLD. However, owing to a lack of sufficient evidence, it is premature to consider them for the specific treatment of liver disease in patients with NAFLD or NASH, according to the guidelines of the American Association for the Study of Liver Diseases in 2018 (Chalasani and Younossi, 2018).

### 3.1.3.1 Liraglutide

Liraglutide, the most widely used GLP-1R agonist, was approved T2DM treatment in 2010 (Drucker et al., 2010). It has been shown to have a potential benefit in preventing cardiovascular events (Marso et al., 2016b). Several clinical trials have reported the potential efficacy of liraglutide in patients with NAFLD. A phase II trial (NCT01237119) evaluated the safety and efficacy of liraglutide in the treatment of NASH. 52 patients with NASH were randomly assigned to the liraglutide treatment group (1.8 mg daily) and the placebo group. At week 48, there were fewer patients with fibrosis progression and a higher proportion of patients with improved steatosis and hepatocyte ballooning in the treatment group than in the placebo group. Liraglutide was generally well tolerated by subjects, and the most common side effects were mild, transient gastrointestinal adverse events, such as constipation, diarrhea, and loss of appetite (Armstrong et al., 2016). A phase III trial (NCT02654665) comparing the effects of liraglutide and lifestyle changes on weight loss in patients with NAFLD showed that once-daily liraglutide was as effective as diet and exercise for over 26 weeks in adult patients with NAFLD and obesity. Liraglutide could reduce weight and improve liver steatosis, insulin resistance, and hepatocyte injury; however, these improvements were not sustained after treatment withdrawal (Khoo et al., 2019). Few trials have evaluated the efficacy of liraglutide in patients with NAFLD, and larger trials are needed to evaluate the potential of liraglutide in NAFLD treatment.

### 3.1.3.2 Semaglutide

Semaglutide, a novel GLP-1R agonist, reduces cardiovascular risk (Marso et al., 2016a) and levels of alanine aminotransferase (ALT) and inflammatory markers (Newsome et al., 2019); it is a potential treatment for NAFLD. A 72-week, double-blind, phase

II trial (NCT02970942) was conducted to evaluate the efficacy and safety of semaglutide in patients with NASH. The 320 patients were randomly divided into three treatment groups and three placebo groups. The patients in the treatment groups were subcutaneously injected with 0.1, 0.2, or 0.4 mg semaglutide once daily. The results showed that the proportion of patients with NASH remission treated with semaglutide was significantly higher than those treated with the placebo (Newsome et al., 2021). This study lays a good foundation for larger trials to evaluate the efficacy of Semaglutide on NAFLD in the future.

### 3.1.4 Omega-3 polyunsaturated fatty acids

The n-3 polyunsaturated fatty acid (n-3 PUFA) family contains several long-chain fatty acids including docosahexaenoic acid (DHA), eicosapentaenoic acid (EPA), stearic acid (SDA), docosahexaenoic acid (DPA), and  $\alpha$ -linolenic acid (ALA). Humans and other mammals can synthesize EPA and DHA from ALA through a series of desaturases and carbon chain-lengthening enzymes. However, the conversion efficiency is low, and ALA cannot be synthesized in the body and must be absorbed from food. Marine fish are known sources of EPA and DHA (Siriwardhana et al., 2012).

N-3 PUFAs are a potential treatment for NAFLD as they can inhibit hepatic DNL and increase fat oxidation. However, n-3 PUFAs supplementation also leads to a significant increase in fasting and postprandial blood glucose concentration (Green et al., 2020). Several trials have been conducted to study its safety and efficacy in NAFLD treatment (Li et al., 2015; Eriksson et al., 2018; Oscarsson et al., 2018; Manousopoulou et al., 2019; Parker et al., 2019; Cansanção et al., 2020; Climax et al., 2020). In a randomized, double-blind, placebo-controlled trial, 78 patients with NASH were randomly divided into a control group and a PUFA therapy group (50 ml PUFA with a 1:1 ratio of dietary DHA and EPA daily). The results showed that steatosis grade, fibrosis stage, ballooning score, and necrotizing inflammatory grade were significantly improved in the treatment group after 6 months of treatment compared to that in the control group (Li et al., 2015). Moreover, in another randomized, double-blind, placebo-controlled clinical trial, alkaline phosphatase (ALP) and liver fibrosis decreased significantly after 6 months of supplementation with fish oil containing DHA and EPA in patients with NAFLD (Cansanção et al., 2020). Thus, n-3 PUFAs supplementation may improve NAFLD in several ways.

However, in a double-blind randomized controlled trial in 2019, 50 apparently healthy overweight men (BMI 25.0–29.9 kg/m<sup>2</sup>; waist circumference >94 cm) between 18 and 60 years old were randomly divided into a control group receiving olive oil capsules and a PUFA therapy group receiving 1728 mg fish oil per day (containing 588 mg EPA and 412 mg DHA) for 12 weeks. The results showed that compared to the control, PUFA treatment had no significant effect on liver fat or enzymes (Parker et al., 2019). This suggests that n-3 PUFAs do not

effectively reduce liver fat in overweight men. Moreover, 1,000 mg of EPA and DHA per day may not be sufficient to reduce liver or visceral fat in apparently healthy men who are overweight and have an increased risk of NAFLD.

Hence, the efficacy of n-3 PUFAs in NAFLD treatment may be heterogeneous in terms of sex and age. Overall, the effects of different treatment dosages, durations, age, sex, and race of the subjects on the efficacy of n-3 PUFAs in the treatment of NAFLD need to be further studied.

### 3.1.5 Synbiotics

Gut microbiota disorder is a pathogenic factor of NAFLD because it is linked to NAFLD through microbial metabolites and the gut-liver axis. NAFLD progression is regulated by the effect of gut microbiota on intestinal epithelial barrier function, the Toll-like receptor (TLR) signaling pathway, and choline metabolism (Dong and Jacobs, 2019). Therefore, gut microbiota can be a therapeutic target for NAFLD (Zhou and Fan, 2019). At present, gut microbiota therapy is in development; large-scale and well-organized RCT trials are needed to confirm the clinical efficacy of gut microbiota therapy for NAFLD (Ma et al., 2017). Some drugs, including antibiotics, probiotics, prebiotics, and synbiotics, can potentially regulate gut microbiota and thus have a therapeutic effect on NAFLD.

Synbiotics are biological agents that consist of probiotics and prebiotics. Synbiotics may improve insulin resistance by altering the gut microbiota, and trials investigating the efficacy of synbiotics in NAFLD treatment have been conducted (Eslamparast et al., 2014; Mofidi et al., 2017; Bakhshimoghaddam et al., 2018; Scorletti et al., 2020). In a 24-week open-label, randomized controlled clinical trial (IRCT2017020932417N2), 102 overweight [BMI 31.2  $\pm$  4.9 kg/m<sup>2</sup> (mean  $\pm$  SD)] patients, including 50 males and 52 females, with an average age of 40, were randomly divided into a control group (no supplementation) and two intervention groups. The patients were administered 300 g synbiotic yogurt containing 10<sup>8</sup> colony-forming units of *Bifidobacterium* per mL and 1.5 g inulin or conventional yogurt daily. The results show that compared with the conventional and control groups, patients with NAFLD in the synbiotic group had significantly improved liver steatosis and liver enzyme concentration (Bakhshimoghaddam et al., 2018). Moreover, in another randomized, double-blind, placebo-controlled clinical trial (NCT02530138), 50 lean patients with NAFLD (BMI  $\leq$  25) were randomly divided into a synbiotic group, which was administered synbiotic capsules containing 200 million bacteria of seven strains and fructo-oligosaccharide, and a placebo group which was administered maltodextrin capsules for 28 weeks. The results showed that hepatic steatosis and fibrosis were significantly alleviated in the synbiotic group compared to the placebo group (Mofidi et al., 2017). The two trials suggest that synbiotic supplementation can improve NAFLD symptoms in patients with high, normal, or low BMI.

TABLE 2 Mechanism and Research Progress of drugs targeting lipotoxicity and cell death.

Drug name	Drug targets	NCT number	Current research progress	Status	Reference
Ornithine Aspartic Acid	Targeted oxidative stress. Ammonia-lowering action	NCT05042245	Phase IV	Recruiting	<a href="https://clinicaltrials.gov">https://clinicaltrials.gov</a>
Resveratrol	Targeted oxidative stress. Regulate Sirtuin-1 autophagy pathway. Reduce ER stress	NCT02030977	Phase II/III	Completed	Faghihzadeh et al. (2014)
Vitamin E	Targeted oxidative stress. Improve inflammation and fibrosis	NCT01792115	Phase II	Completed	Podszun et al. (2020)
Silymarin	Targeted endoplasmic reticulum stress. Improve inflammation and fibrosis	NCT02006498	Phase II	Completed	Wah Kheong et al. (2017)
Niacin	Targeted oxidative stress. Improve hepatic steatosis, inflammation and lipid accumulation	NCT04330326	Phase II	Unknown	<a href="https://clinicaltrials.gov">https://clinicaltrials.gov</a>
Anthocyanins	Targeted oxidative stress. Decrease sembp1c. Induced PPAR $\alpha$ Activity	NCT01940263	Phase I	Completed	Zhang et al. (2015)
Bicyclol	Inhibition of MAPK and NF- $\kappa$ B signal path	-	Preclinical study	Completed	Zhao et al. (2021)
Piceatannol	Targeted oxidative stress. Reduce fat accumulation	-	Preclinical study	Completed	Yang et al. (2020)
Polydatin	Targeted oxidative stress. Improve inflammation and fibrosis	-	Preclinical study	Completed	Li et al. (2018)

PPAR  $\alpha$ , peroxisome proliferator-activated receptor  $\alpha$ ; MAPK, mitogen-activated protein kinase; NF- $\kappa$ B, nuclear factor- $\kappa$ B.

However, another randomized, double-blind, placebo-controlled phase II trial conducted in 2020 (NCT01680640), in which participants were given synbiotic agents containing fructo-oligosaccharides and *Bifidobacterium* spp. for 10–14 months, showed that synbiotic supplementation had no effect on liver fat or fibrosis (Scorletti et al., 2020). This may be because only one combination of probiotics and prebiotics was tested in this trial, which did not have a significant effect on NAFLD.

In conclusion, more trials are needed to study the efficacy of different combinations of synbiotics on NAFLD, as well as the effects of race, sex, age, body type, and other factors on the efficacy of synbiotics.

### 3.1.6 Thyroid hormone receptor $\beta$ (THR $\beta$ ) agonists

Thyroid hormone receptors (THRs), belong to the nuclear receptor superfamily, are ligand-dependent transcription factors regulated by endogenous thyroid hormones. THRs consists of two subtypes, THR $\alpha$ , which is a major subtype in the heart and bone, and THR $\beta$ , which is a major subtype in the liver (Sinha et al., 2019). Selective THR- $\beta$  agonists mainly provide metabolic benefits of thyroid hormones to the liver while avoiding unwanted systemic effects caused by excessive thyroid hormones in the heart and bones (Harrison et al., 2019). Selective THR  $\beta$  agonists are currently being developed including resmetirom (MGL-3196), VK2809 (MB 07811), TERN501, ASC41 for the treatment of NAFLD. It has been proved that normal hypothyroidism and subclinical hypothyroidism are independent risk factors for NASH and advanced fibrosis, which is one of the reasons why THR  $\beta$  agonists are still being studied (Kim et al., 2018).

#### 3.1.6.1 Resmetirom (MGL-3196)

In a 36-week randomized, double-blind, placebo-controlled, phase 2 study (NCT02912260), 125 patients with NASH and  $\geq 10\%$  hepatic steatosis confirmed by biopsy were randomly assigned to Resmetirom (80 mg) and placebo group. The results showed that compared with placebo, resmetirom had statistically significant effects in reducing liver enzymes, liver fat, lipoprotein (a), atherogenic lipids, inflammation and fibrosis markers, and improving NASH of liver biopsy. Generally, Resmetirom is well tolerated, the most common adverse events are nausea and diarrhea. This study provides a theoretical basis for three ongoing phase 3 trials (NCT04197479, NCT04951219, NCT03900429) to further evaluate the efficacy and safety of resmetirom in the treatment of NAFLD (Harrison et al., 2019). The results of the clinical trials will guide the pharmacological treatment of NAFLD.

## 3.2 Lipotoxicity and cell death-based targets

Lipotoxic mediators may include free (unesterified) cholesterol, saturated free fatty acids, diacylglycerol, lysophosphatidylcholine, sphingolipids, and ceramide (Farrell et al., 2018). Lipotoxicity can induce endoplasmic reticulum (ER) stress in hepatocytes, which restores ER homeostasis by activating the unfolded protein response (UPR) (Lebeau et al., 2018). If ER homeostasis cannot be restored, prolonged activation of the unfolded protein response may initiate apoptotic cell death by upregulating C/EBP homologous protein (CHOP) (Hu H. et al., 2018). Mitochondrial dysfunction and ER stress caused by lipotoxicity lead to an

TABLE 3 Mechanism and Research Progress of drugs targeting inflammation.

Drug name	Drug targets	NCT number	Current research progress	Status	Reference
Berberine	Inhibit nod-like receptor family Pyrin domain containing 3 inflammasome activation and pyroptosis in nonalcoholic steatohepatitis <i>via</i> the ROS/TXNIP Axis	NCT03198572	Phase IV	Recruiting	<a href="https://clinicaltrials.gov">https://clinicaltrials.gov</a>
Selonsertib	ASK1 inhibitor. Improve inflammation and fibrosis	NCT03053063	Phase III	Terminated	Harrison et al. (2020)
Namodenoson	ADORA3 Agonist. Induce a robust anti-inflammatory effect in the liver through de-regulation of the Wnt/ $\beta$ -catenin pathway	NCT02927314	Phase II	Completed	Safadi et al. (2021)
Amlexanox	IKK $\epsilon$ and TBK1 inhibitor. Inhibit the activation of KCs and induce polarization of KCs toward the M2 phenotype	NCT01975935	Phase II	Completed	<a href="https://clinicaltrials.gov">https://clinicaltrials.gov</a>
JKB-121	TLR4 antagonist. Decrease fibrosis and inhibit hepatic stellate cell activation and collagen expression <i>in vitro</i>	NCT02442687	Phase II	Completed	<a href="https://clinicaltrials.gov">https://clinicaltrials.gov</a>

ASK1, apoptosis signal-regulating kinase 1; A3AR, A3 adenosine receptor; IKK $\epsilon$ , I $\kappa$ B kinase epsilon; TBK1, activator-binding kinase 1; TLR4, toll-like receptor 4.

imbalance between oxidants and antioxidants, resulting in oxidative stress (Arroyave-Ospina et al., 2021). ER stress and oxidative stress can lead to the activation of c-Jun N-terminal kinase (JNK) and other pathways, thus resulting in apoptosis. The synergistic effect of ER stress and oxidative stress leads to the occurrence and development of NAFLD (Fujii et al., 2018). The research progress on drugs targeting lipotoxicity and cell death is summarized in Table 2.

### 3.2.1 Vitamin E

Oxidative stress is a promising therapeutic target in NAFLD. Vitamin E is an effective antioxidant that reduces liver inflammation (Nagashimada and Ota, 2019). A meta-analysis of the effect of vitamin E supplementation on adult patients with NAFLD showed that the value of liver enzymes was reduced by vitamin E administration compared to the placebo (−5.71 IU/L, 95% CI: −9.49 to −1.93 for AST and −7.37 IU/L, 95% CI: −10.11 to −4.64 for ALT) (Vadarlis and Antza, 2021). In an experiment on the accumulation pathway of intrahepatic triglyceride (IHTG) in the liver (NCT01792115), 20 patients with NAFLD were randomly sorted into groups to receive 200, 400, or 800 IU/D vitamin E for 24 weeks; 50% of patients had a  $\geq 25\%$  relative decrease in IHTG (Podszun et al., 2020). The antioxidant, anti-inflammatory, and antiapoptotic properties and ease of use of vitamin E make it a practical treatment choice for patients with NAFLD (Perumpail et al., 2018). Vitamin E is a highly effective antioxidant obtained through diet; it can inhibit the development of oxidative stress and inflammation and thus, has a positive impact on NAFLD. However, long-term use of vitamin E may lead to an increase in all-cause mortality, so more accurate methods are still needed to prove its safety (Perumpail et al., 2018).

### 3.2.2 Silymarin

Silymarin, a bioactive component of milk thistle, has anti-inflammatory, anti-fibrosis, and antioxidant effects (Federico

et al., 2017). Silymarin can reduce ER stress proteins GRP78 and XBP-1, thereby relieving the NAFLD symptoms; it can be used to treat diseases caused by ER stress (Sahin and Bagci, 2020). A meta-analysis of silymarin in patients with NAFLD showed that silymarin treatment resulted in a statistically significant reduction in transaminase levels compared to a placebo (Kalopitas et al., 2021). According to the clinical manifestations of NAFLD, a low-calorie diet and physical activity supplemented with silymarin are the correct methods for NAFLD treatment (Colica et al., 2017).

A randomized, double-blind, placebo-controlled trial (NCT02006498) was conducted in adults with biopsy-confirmed NASH and NAFLD activity scores (NAS)  $\geq 4$ . Patients were randomly divided into two groups and administered silymarin (700 mg; n = 49) or a placebo (n = 50) thrice daily for 48 weeks. The results showed that silymarin could improve liver fibrosis compared to the placebo, but the NAS score decreased by no more than 30% in patients with NASH (Wah Kheong et al., 2017). A phase II trial (NCT00680407) was conducted at five medical centers in the United States to test a patented standardized silymarin preparation (Legalon<sup>®</sup>, Rottapharm Madaus, Mylan) on patients with NAS  $\geq 4$ . Patients were randomly divided into groups that were administered 420 mg (n = 26) or 700 mg (n = 27) of silymarin or placebo (n = 25) three times a day for 48 weeks. The primary endpoint in NAS was a histological improvement of more than two points. The results showed that after 48–50 weeks, 5/26 (19%) of participants in the 420 mg group, 4/27 (15%) in the 700 mg group, and 3/25 (12%) of placebo participants reached the primary endpoint ( $p = 0.79$ ), indicating that silymarin (Legalon<sup>®</sup>) had no significant benefit in terms of histological improvement (Navarro et al., 2019). Silymarin alone did not significantly improve NAS; however, it can resist the development of fibrosis and reduce the level of aminotransferase. Therefore,

TABLE 4 Mechanism and Research Progress of drugs targeting extracellular matrix deposition antifibrosis.

Drug name	Drug targets	NCT number	Current research progress	Statue	Reference
Belapectin	gal-3 inhibitor. Reduce liver fibrosis and portal hypertension	NCT04365868	Phase III	Recruiting	<a href="https://clinicaltrials.gov">https://clinicaltrials.gov</a>
Aramchol	SCD1 inhibitor. Directly inhibit HSCs and induce the protective gene PPARc	NCT04104321	Phase III	Recruiting	<a href="https://clinicaltrials.gov">https://clinicaltrials.gov</a>
Cenicriviroc	CCR2/CCR5 dual inhibitor. Inhibit macrophage accumulation in the liver and ameliorates fibrosis	NCT03028740/ NCT02217475	Phase II/III	Terminated/ Completed	Anstee et al. (2020); Ratziu et al. (2020)
Pegbelfermin	PEGylated analogue of FGF21. Improve insulin sensitivity, lipid and adiponectin concentrations, and biomarkers of fibrosis	NCT02413372	Phase II	Completed	Sanyal et al. (2019)
NGM282	Non-tumorigenic analogue of FGF19. Retain the ability to suppress CYP7A1 without activating STAT3 signalling	NCT02443116	Phase II	Completed	Harrison et al. (2018b)
PXS-5382	LOXL2 inhibitor. Decrease cell numbers, proliferation, colony formations and cell growth, induce cell cycle arrest and increase apoptosis	NCT04183517	Phase I	Completed	<a href="https://clinicaltrials.gov">https://clinicaltrials.gov</a>
Oxy210	hedgehog and TGF- $\beta$ signalling inhibitor. Attenuated expression of TGF- $\beta$ -induced pro-fibrotic genes <i>in vitro</i>	-	Preclinical study	Completed	Hui et al. (2021)
HMGB1 peptide	Induce anti-inflammatory macrophages and inactivate T cells	-	Preclinical study	Completed	Nojiri et al. (2021)
JT 003	AdipoR1/AdipoR2 dual agonist. improve insulin resistance in high fat diet induced NASH mice and suppress hepatic stellate cells activation in CCl	-	Preclinical study	Completed	Xu et al. (2020)
TM5275	plasminogen activator inhibitor-1 inhibitor. Ameliorat the development of hepatic fibrosis and suppressed the proliferation of activated hepatic stellate cells	-	Preclinical study	Completed	Noguchi et al. (2020)
DZNep	EZH2 Inhibitor. inhibit multiple histone methylation modifications	-	Biological Testing	Completed	Zeybel et al. (2017)

CCR2/CCR5, C-C chemokine receptors type 2 and 5; gal-3, galectin-3; TGF- $\beta$ , transforming growth factor-beta; AdipoR1/AdipoR2, adiponectin receptors 1/2; PAI-1, plasminogen activator inhibitor-1; HSCs, hepatic stellate cells; LOXL2, Lysyl oxidase-like 2.

the combination of silymarin is a more feasible method for NAFLD treatment. Therapeutic doses of silymarin have been shown to be safe for humans, but more clinical trials for pregnant women are needed. And it must be cautious when combined with drugs with narrow therapeutic windows (Soleimani et al., 2019). Further clinical trials are needed to better use silymarin.

### 3.3 Inflammation-based targets

Liver inflammation is caused by innate immune cells, mainly macrophages. Monocytes are mainly recruited through CCR2-CCL2 interaction (Baeck et al., 2012). Other chemokine pathways, such as CXCR3-CXCL10, CCR1-CCL5, and CCR8-CCL1, may also contribute to monocyte recruitment (Tacke, 2017). Ly-6C + monocyte infiltration is a key factor in NAFLD, which promotes hepatitis and subsequent fibrosis progression. Liver macrophages of patients with NASH have an obvious inflammatory phenotype, which may be the result of excess lipids and free fatty acids (Jindal et al., 2015). Accumulation of liver macrophages and inflammation are considered hallmarks of the progression of liver disease in patients with NASH. Experimental evidence shows that inflammatory macrophages

promote NASH progression through a variety of mechanisms, including liver cell steatosis (Navarro et al., 2015), inflammatory lymphocytes (Wehr et al., 2013), angiogenesis (Ehling et al., 2014), and liver fibrosis (Ju and Tacke, 2016). The research progress on drugs targeting inflammation is summarized in Table 3.

#### 3.3.1 Selonsertib

Selonsertib (formerly GS-4997) is a selective inhibitor of apoptotic signal-regulated kinase 1 (ASK1) activated by oxidative stress. Selonsertib acts on the effector kinases p38 and c-Jun N-terminal kinase *via* the mitogen-activated protein kinase pathway, which regulates liver pro-inflammatory and pro-fibrotic changes (Harrison et al., 2020). In a randomized, open-label, phase II trial, 72 patients were randomly assigned to receive 24 weeks of treatment with six or 18 mg selonsertib alone, six or 18 mg selonsertib with 125 mg simtuzumab, or 125 mg simtuzumab alone. Simtuzumab, a humanized monoclonal antibody directed against lysyl oxidase-like molecule 2, has been proved to be ineffective at reducing hepatic fibrosis (Harrison et al., 2018a). Evaluation of the treatment effectiveness involved liver biopsy, magnetic resonance imaging (MRI), and non-invasive liver injury



TABLE 5 Mechanism and research progress of combination therapy for NAFLD.

Drug name	Mechanism	NCT number	Current research progress	Status	Reference
Vitamin E and Pioglitazone	Improve inflammation and steatosis	NCT01002547	Phase IV	Completed	Bril et al. (2019)
Vitamin E and Hydroxytyrosol	Improve oxidative stress, insulin resistance, and steatosis	NCT02842567	Phase III	Completed	Mosca et al. (2021)
Pentoxiphylline and Vitamin E	Reduce hepatic inflammation and fibrosis	NCT01384578	Phase III	Withdrawn	Kedarisetty et al. (2021)
Tropifexor and Cenicriviroc	Improve fibrosis and steatohepatitis	NCT03517540	phase IIb	Completed	Pedrosa et al. (2020)
Obeticholic acid and atorvastatin	Ameliorate the OCA-induced side effects on plasma lipoprotein spectrum	NCT02633956	Phase II	Completed	Pockros et al. (2019)
Cilofexor and Firsocostat	Improve fibrosis	NCT03449446	Phase II	Completed	Loomba et al. (2021)
Omega-3 fatty acids and probiotic	Reduce liver fat, improve metabolism and inflammation	NCT03528707	Clinical phase	Completed	Kobyliak et al. (2018)
N-3 fatty acids and phytosterol esters	Improve the efficacy on hepatic steatosis and decrease the levels of inflammation	ChiCTR1800014419	Clinical phase	Completed	Song et al. (2020)
Synbiotic and sitagliptin	Improve the efficacy on steatosis and inflammation of liver	-	Clinical phase	Completed	Sayari et al. (2018)
Vitamin E and Vitamin D and Silybin	Reduce hepatic inflammation and fibrosis	NCT04640324	Clinical phase	Completed	Federico and Dallio, (2019)
Vitamin E, artichoke leaf extract and metformin	Improve inflammation and fat accumulation	IRCT2017040429278N1	Clinical phase	Completed	Majnooni et al. (2021)
Obeticholic acid and elafbranor	Improve the interaction with lipid treatment and insulin signal transduction, inhibit immune response and reduce the formation of extracellular matrix	-	Preclinical study	Completed	Roth et al. (2019)
SUMOylation inhibitors and FXR agonists	SUMOylation inhibitors rescue FXR signaling and thereby increasing the efficacy of OCA against HSC activation and fibrosis	-	Preclinical study	Completed	Zhou and Cui, (2020)
Metformin and genistein	Reduce blood glucose and the level of TG in the liver and affect the pathway of gluconeogenesis	-	Preclinical study	Completed	Zamani-Garmsiri et al. (2021)
Luteolin and lycopene	Improve the cell viability and lipid accumulation of HepG2 cells and primary hepatocytes induced by PA, and improve weight gain and hepatocyte steatosis	-	Preclinical study	Completed	Zhu et al. (2020)
Glucagon-like peptide-1 receptor agonist and obeticholic acid	Reduce liver steatosis, inflammation and fibrosis	-	Preclinical study	Completed	Jouihaan et al. (2017)

Sirt1, Sirtuins1; AMPK, AMP-activated protein kinase; TG, triglyceride.

markers. After 24-week of treatment, selonsertib-treated patients had higher rates of fibrosis improvement and lower rates of fibrosis progression than that in patients treated with simtuzumab alone. The proportion of patients with at least a one-stage reduction in fibrosis after 24 weeks of treatment in the 18 mg selonsertib group was 13 of 30 (43%; 95% CI, 26–63); compared to eight of 27 in the 6 mg selonsertib group (30%; 95% CI, 14–50); and two of 10 in the simtuzumab-alone group (20%; 95% CI, 3–56) (Loomba et al., 2018). Selonsertib improved liver fibrosis in a considerable number of patients with NASH and stage 2 or three fibrosis, indicating its potential as a future treatment for NAFLD. However, in two large, randomized, phase III trials in patients with bridging fibrosis or compensated cirrhosis due to NASH, treatment for 48 weeks with the ASK1 inhibitor selonsertib was ineffective (Harrison et al., 2020). Selonsertib monotherapy had no effect in these

trials, but when used in combination with other drugs, there can be a significant effect. Research is still underway into selonsertib combination treatment.

### 3.3.2 Namodenoson

Namodenoson is a selective A3 adenosine receptor (A3AR) agonist. It is highly selective for A3AR in pathological liver cells and can produce powerful anti-inflammatory effects (Cohen et al., 2011). The A3AR belongs to the family of the Gi-protein associated cell membrane receptors. And the anti-inflammatory mechanism of the A3AR agonist involves deregulation of the NF- $\kappa$ B signaling pathway and induction of apoptosis of inflammatory cells (Ochaion et al., 2008). Namodenoson can also inhibit ischemia-reperfusion injury and act as a protective agent in the liver (Ohana et al., 2016). Namodenoson exhibits a triple mechanism of action in the liver.

It exerts anti-inflammatory and anti-fibrosis effects by activating A3AR and relaxing the regulation of the NF- $\kappa$ B and Wnt/ $\beta$ -catenin pathways (Fishman et al., 2019). A phase II double-blind trial randomized 60 patients with NAFLD (ALT  $\geq$  60 IU/L) (1:1:1) and divided them into oral namodenoson groups administered 12.5 mg b.d. (n = 21), 25 mg b.d. (n = 19), or placebo (n = 20) groups for 12 weeks (total follow-up: 16 weeks). The primary efficacy endpoint was the normalization of serum ALT levels. After 12 weeks of treatment, serum ALT levels decreased in a dose-dependent manner with namodenoson over time. At week 12, 31.6% of the namodenoson 25 mg b.d. group and 20.0% of the placebo group achieved ALT normalization ( $p = 0.405$ ). At week 16, 36.8% and 10.0% ( $p = 0.038$ ) patients achieved ALT normalization in the namodenoson 25 mg b.d. and placebo groups, respectively. In addition, approximately one-quarter (23.8%) of the 12.5 mg b.d. group achieved normalization of serum ALT levels at week 16 (Safadi et al., 2021). During the entire phase II clinical trial period, namodenoson significantly reduced liver fat and inflammation and was well tolerated without serious adverse reactions. Various liver parameters, such as ALT and AST levels, improved significantly. Namodenoson also has cardioprotective and neuroprotective characteristics that may compensate NAFLD patients with comorbid cardiovascular and diabetic diseases (Cross et al., 2002). In conclusion, namodenoson can be a potential treatment option for NAFLD.

### 3.4 Extracellular matrix deposition anti-fibrosis-based targets

Hepatic fibrosis is characterized by the overexpression and accumulation of extracellular matrix (ECM) proteins in the liver as a result of the parenchymal cell damage caused by different hepatotoxic agents and mechanisms. The main stroma-producing cell types in liver fibrosis are hepatic stellate cells (HSCs), which are used for lipid storage, and which transform into myofibroblasts (Tacke and Weiskirchen, 2021). However, prolonged liver injury activates them from a resting state to a pro-inflammatory/pro-fibrotic fibroblast-like phenotype, which can contribute to ECM remodeling (Gabbia et al., 2021). The pathways that activate HSCs are diverse, including transforming growth factor (TGF)- $\beta$ , the hormone fibroblast growth factor 21 (FGF21) (Le et al., 2018) and newly discovered pathways such as hedgehog, autophagy, free cholesterol, YAP1, hepcidin, and nuclear/G-protein-coupled receptor-mediated signals (Tsuchida, 2019).

In response to these mechanisms, drug targets can be divided into two categories: inhibition of fibril formation and enhancement of fibrinolysis. Cenicriviroc is an antagonist of C-C motif chemokine receptor-2/5 (CCR2/5) and is anti-fibrotic as it inhibits collagen activation, HSCs activation, and proliferation (Puengel et al., 2017). However, studies on drugs

that increase fibrinolysis are lacking. A recent study shows that the HMGB one peptide can induce fibrinolysis (Nojiri et al., 2021). Drugs targeting extracellular matrix deposition anti-fibrosis and their research progress are summarized in Table 4.

#### 3.4.1 Cenicriviroc

C chemokine receptor types 2 (CCR2) and 5 (CCR5) mediate fibrosis by recruiting inflammatory monocytes and macrophages and activating lymphocytes and hepatic stellate cells (Lefebvre et al., 2016; Tacke, 2018). Cenicriviroc (CVC), a dual antagonist of CCR2/CCR5, has anti-inflammatory and anti-fibrosis effects in animal models (Pedrosa et al., 2020). A randomized, double-blind, multinational CENTAUR study randomly assigned 298 participants with NASH to take 150 mg CVC or a placebo daily for 2 years (NCT02217475). Of these 298 participants, 242 entered the second year of the trial, 24% switched to CVC, and 17% remained on the placebo. Twice as many CVC patients whose fibrosis improved in year one maintained the benefit in year two compared with patients receiving the placebo. However, over 2 years, the same proportion of patients taking CVC or placebo met the primary endpoint of hepatic histology improvement in NAS by more than two points with no fibrous deterioration. Interestingly, patients with stage F2 or F3 fibrosis were more likely to benefit from treatment. Moreover, the safety and tolerability of CVC are similar to those of the placebo (Friedman et al., 2018b; Ratziu et al., 2020). Based on these results, the efficacy and safety of CVC will be comprehensively evaluated in a global, multicenter, randomized, double-blind, placebo-controlled study (AURORA, NCT03028740) in patients with stage F2 or F3 NASH (Anstee et al., 2020). However, the highly anticipated Phase III clinical trial of AURORA was terminated in early 2021. This is due to the lack of validity of some of its findings. At present, the combination therapy of CVC and Tropifexor has entered the phase II clinical study and achieved good results (Pedrosa et al., 2020). We do not know whether CVC monotherapy is feasible and need to wait for follow-up studies.

#### 3.4.2 Belapectin

Galectins belong to the non-integrin  $\beta$ -galactoside-binding lectin family. Increased galectin-3 levels are strongly associated with fibrosis, cancer, and inflammation. However, the exact mechanisms of its action are currently unknown (Harrison and Dennis, 2018; Al Attar et al., 2021). Belapectin (GR-MD-02) is a galectin-3 inhibitor derived from plants. It had good anti-fibrotic effects in mouse models and was well-tolerated and safe in phase I clinical trials (Harrison et al., 2016).

The hepatic venous pressure gradient (HVPG) can be used to assess improvements in portal pressure. Portal hypertension is associated with mortality in patients with NASH. In a randomized, double-blind, placebo-controlled phase II trial (NCT02462967), patients with NASH, cirrhosis, or portal

hypertension were randomly assigned to two groups. The treatment groups were administered two or 8 mg/kg belapectin ( $n = 54$  each) biweekly and compared to the placebo group ( $n = 54$ ) for 52 weeks. These results did not meet the primary or secondary endpoints for either dose. This indicates that belapectin was not significantly correlated with HVPg, the incidence of cirrhotic complications, or liver histology. However, a subgroup analysis showed that 2 mg/kg belapectin reduced HVPg and prevented the development of new varices in another group of patients without esophageal varices (Chalasani et al., 2020). The results of phase I and IIb trials indicate that treatment should target patients with NASH cirrhosis without esophageal varices. Moreover, a phase IIb/III study will further investigate the benefits of belapectin in the prevention of other liver-related complications.

### 3.4.3 3 $\beta$ -arachidinoyl amide cholic acid

3 $\beta$ -arachidinoyl amide cholic acid (Aramchol) is fatty acid-bile acid conjugate that partially inhibits hepatic stearyl-CoA desaturase (SCD1) protein expression (Bhattacharya et al., 2021). In animal experiments, Aramchol reduced hepatic steatosis and improved steatohepatitis and fibrosis (Iruarizaga-Lejarreta et al., 2017; Aljohani and Khan, 2019). Aramchol was shown to be safe and well tolerated in an early clinical trial and significantly reduced liver fat in NAFLD patients (NCT01094158) (Safadi et al., 2014).

In a 52-week, double-blind, placebo-controlled, phase 2b clinical trial, 247 NASH patients were randomized to 400 or 600 mg/day Aramchol or placebo (NCT 02279524). There was a significant reduction in liver fat in the 400 mg group ( $p = 0.045$ ) and a reduction in liver triglycerides in the 600 mg group compared with placebo ( $p = 0.066$ ). However, aramchol 600 mg decreased liver triglycerides without meeting the prespecified primary end point for statistical significance. Happily, aramchol ameliorated liver histology in patients with T2D or prediabetes with histologically confirmed steatohepatitis and with high disease activity and precirrhotic stages of fibrosis. (Ratziu et al., 2021). A Phase 3 trial is currently underway, allowing patients to receive a different regimen (Aramchol 300 mg bid) to achieve higher exposures in an attempt to detect the magnitude difference observed in this study (NCT04104321). We will continue to pay attention to the follow-up experimental results of this drug and have certain expectations for it.

## 4 Combination therapy

Owing to the limited efficacy and side effects of monotherapy, other methods are being investigated to treat NAFLD. Moreover, there are various therapeutic targets for NAFLD. An increasing number of studies have shown the limitations of monotherapy and suggested instead developing combination therapies. The advantages of combination therapy include improving the response rate and reducing the side effects

of drugs. For example, the response rate of drugs used in NASH monotherapy is <32% compared with a placebo. Combination therapy may increase the response rate by converting non-responders or partial responders into responders. Additionally, combination therapy may treat the side effects of a given drug through the effects of additional drugs or by reducing its dose-dependent side effects without compromising its efficacy, i.e. adding another drug can allow for a reduction in the dose of the original drug (Dufour et al., 2020). Many trials have investigated combination therapies for NAFLD. The drug combinations for NAFLD are listed in Table 5.

### 4.1 Combination of OCA and atorvastatin

Several studies have demonstrated the effectiveness of OCA in NAFLD treatment (Kowdley et al., 2018; Younossi et al., 2019b; Kjærgaard et al., 2021; Kulkarni et al., 2021). However, OCA can increase the concentration of serum total cholesterol and low-density lipoprotein cholesterol (LDLc) and decrease the concentration of high-density lipoprotein cholesterol (HDLc), which limits its clinical application (Neuschwander-Tetri et al., 2015). Statins can reduce LDL and triglyceride (TG) levels and slightly increase HDL (McTaggart and Jones, 2008). Thus, a combination of OCA and statins may alleviate the side effects of OCA on the plasma lipoprotein spectrum.

A randomized, double-blind, placebo-controlled phase II study (NCT02633956) was conducted to investigate the efficacy and safety of OCA combined with atorvastatin in NAFLD treatment. In this study, 84 patients with NASH were randomly divided into three treatment groups (5, 10, or 25 mg OCA once daily) and one placebo group for 16 weeks. Each group was additionally administered atorvastatin (10 mg/day) once a day beginning at week 4. In the fourth week, the mean LDLc and mean LDL particle concentration (LDLpc) in all OCA groups were higher than the baseline, and in the eighth week, 10 mg atorvastatin treatment resulted in LDLc and LDLpc levels lower than the baseline in all OCA groups. Additionally, atorvastatin improved the increase in serum total cholesterol and the reduction in HDL caused by OCA (Pockros et al., 2019). Thus, atorvastatin can ameliorate OCA-induced side effects in the plasma lipoprotein spectrum. The combination of OCA and atorvastatin seems to be a good choice for the treatment of NAFLD, trials with larger sample sizes and longer study periods are required to further evaluate the efficacy of combination therapy with OCA and atorvastatin.

### 4.2 Combination of FXR agonists and SUMOylation inhibitors

Hepatic stellate cells (HSCs) play key roles in the pathological development of liver fibrosis (Kowdley et al., 2020). HSCs

activation is a marker of liver fibrosis. Loss of lipid droplets (LDS) is a key step in promoting HSC activation (Pawella et al., 2014; Kory et al., 2016; Koyama and Brenner, 2017; Jiang et al., 2021). Plin1 was identified as an FXR target gene responsible for stabilizing LDS in HSCs. Furthermore, FXR agonists can stabilize LDS in HSCs by activating the FXR target gene plin1, but SUMOylation gradually increases during the activation of HSCs, thus inhibiting the FXR signaling pathway. Hence, SUMOylation inhibitors can reduce FXR signaling, which amplifies the effect of FXR agonists, thereby improving the therapeutic efficacy of FXR agonists for activated HSCs and liver fibrosis.

Compared to individual administration, a combination of OCA and spectinomycin (SP, a SUMOylation inhibitor) increased lipid storage and reduced all pre-fibrosis biomarkers. Combined treatment with OCA and SP significantly decreased levels of serum ALT and AST, but there was no significant decrease upon treatment with OCA or SP alone (Čopić et al., 2018). Combined treatment significantly reduced serum aminotransferase levels and improved the histological characteristics of the liver, including steatosis, inflammatory infiltration, ballooning, and a series of liver fibrosis diseases. In addition, the SUMOylation inhibitor ginkgolic acid had a significant effect on activated HSC when combined with OCA. Overall, a combination of a SUMOylation inhibitor and FXR agonist is a promising treatment for liver fibrosis, including NASH, indicating another potential treatment option for utilizing FXR against various types of liver fibrosis.

### 4.3 Combination of vitamin E and silymarin

Vitamin E exhibits antioxidant, anti-inflammatory, and anti-apoptotic activities, along with a favorable clinical profile, making it an appropriate therapeutic choice for NAFLD. However, vitamin E does not affect liver fibrosis. Therefore, vitamin E combined with other anti-fibrotic agents (silymarin) may provide improved treatment for patients with NAFLD.

In a randomized clinical trial of silymarin with vitamin E for NAFLD treatment, 36 patients were randomly divided into two groups. The first group was administered 540.3 mg *Silybum marianum* Gaerth in tablet form and 36 mg vitamin E once daily (Eurosil 85<sup>®</sup>, MEDAS SL) and underwent lifestyle changes, including eating a low-calorie diet. The second group only underwent lifestyle changes. The results show that gamma glutamine transpeptidase levels, fatty liver index, and liver fibrosis scores decreased in both groups. However, the patients in the first group who did not lose 5% of their bodyweight still showed improvement in these parameters, whereas the patients in the second group did not. Therefore, both this drug treatment and lifestyle improvements can improve disease status (Aller et al., 2015), i.e., a combination of silymarin and vitamin E can improve liver function in patients with

NAFLD. However, there are few clinical research results, and further clinical trials are needed to determine the efficacy of combination therapy.

## 5 Discussion

NAFLD has no obvious symptoms until it reaches an advanced stage, at which point many patients are diagnosed. Liver biopsy has long been the “gold standard” for diagnosing NAFLD; however, it has well-known limitations, such as sampling bias and serious complications. Therefore, in clinical practice, it is best to adopt an accurate non-invasive method to diagnose different disease stages. Non-invasive tests can also be used as screening tools in the general population to identify high-risk groups. In recent years, non-invasive methods for diagnosing NAFLD have been widely developed, for example, serum biomarkers and imaging techniques. In the current study, US and H-MRI could be used to accurately diagnose NAFLD. US is widely used in clinical practice owing to its low cost and practicality. VCTE was the first FDA-approved elastography model used to assess the severity of fibrosis. It has short processing times and good reproducibility and can be combined with biomarkers to further improve diagnostic performance. More effective non-invasive biomarkers and imaging techniques are needed in the future to diagnose NAFLD and track disease progression.

Overall, studies show that it is not only the selection of a drug that must be considered to maximize the effects of a treatment scheme, other influencing factors determining the final outcome should also be considered. Individualized therapy is the selection of the best drug regimen based on individual patients' factors. In the case of NAFLD, the main considerations are the patient's disease state, physiological characteristics, and genetic characteristics at the molecular level.

First, the pathophysiological state was considered, i.e., the screening of appropriate target populations based on disease status. For example, belapectin is more effective in patients with NASH but without esophageal varices, so patients with NASH without esophageal varices can be treated with belapectin. Another example is vitamin E, which is indicated in patients with NASH but without T2DM. In addition to the different disease states, the stage of the disease of the target population must be considered. For example, studies have confirmed that CVC is more beneficial for patients with NASH at stages F2–F3. Moreover, there is heterogeneity in drug therapy for patients with NAFLD of different races, ages, sexes, and body types, and the impact of these factors should be considered when selecting participants.

It is also important to weigh efficacy against adverse effects. For example, some adverse effects of pioglitazone are a major cause of discontinuation, including fluid retention, fractures, and, more seriously, an increased risk of hospitalization for heart

failure. Pioglitazone should be administered with caution, particularly in patients with heart disease. Therefore, when individualizing medication, especially in special populations, a thorough assessment of its efficacy and side effects should be considered, including timing, dose, frequency, duration, combination, and the need to change medication. This should be evaluated regularly during treatment, and the continuation or change of the treatment regimen should be decided based on the results.

In addition, the determination of gene polymorphisms can provide relevant information on treatment response. In recent years, multiple genome-wide associations and large candidate gene studies have enriched our knowledge of the genetics of NAFLD. Notably, the I148M PNPLA3 variant has been identified as a major co-genetic determinant of NAFLD (Wang et al., 2011; Valenti and Dongiovanni, 2017). Precision medicine can modulate the activity of a specific gene (PNPLA3) in specific organs in specific patient populations. And other NASH-related genes may provide targets for future intervention strategies. In addition, a genome-wide analysis study identified several loci associated with response to OCA in NASH patients. These variant-associated genetic variants may improve the effectiveness and accuracy of selecting NASH patients for OCA therapy, as these variants can increase NASH resolution (Gawrieh et al., 2019). NASH patients with these genetic variants may then be directed to individualized treatment. However, more research and evidence are needed before speculating whether genotyping can be used to guide treatment decisions in patients at risk for NASH.

Finally, considering the complexity of the pathophysiology of the disease and the heterogeneity of the individual, the detection of specific biological markers should be considered when administering drugs to identify genetic polymorphisms, develop more precise dosing regimens and achieve better therapeutic results (Dufour et al., 2020).

The pathogenesis of NAFLD is complex and involves many factors. Due to the complexity of NAFLD pathophysiology, many targets have potential therapeutic effects, including carbohydrate and lipid metabolism, fibrosis, and inflammation. At present, there have been many studies on NAFLD drugs, most of which are monotherapies, and their efficacy is generally unsatisfactory. Recently, an increasing number of studies have been conducted on NAFLD combination therapy, and some drug combinations have entered clinical phases II or III, indicating their feasibility. Although combination therapy can be more effective than monotherapy and could potentially reduce side effects, its clinical application still has limitations.

The first limitation is the choice of drug. Many drugs are potentially effective against NAFLD, and it is difficult to select a suitable combination from a large number of possibilities. Moreover, the selection of drugs should not be limited to those that are effective against NAFLD; drugs that have no individual efficacy but have synergistic effects with others should not be excluded. Therefore, many studies are needed

to screen and combine various drugs, which will be a lengthy process. Second, although combination therapy can be more efficacious, it may also produce further side effects. Therefore, attention should be paid to both side effects and efficacy. In addition, the increase in the types of drugs used in combination therapy also brings some difficulties to the design of the trials, including the allocation of trial groups and the selection of participants. Despite these challenges, combined drug therapy remains a promising treatment option for NAFLD.

It is worth mentioning that dual-target drugs are another current research hotspot. These drugs can act on two or more targets simultaneously and exhibit significant efficacy. Some patients who are difficult to treat with single-target drugs can respond well to these drugs. Therefore, the design and application of dual-target drugs for NAFLD may be beneficial.

## 6 Conclusion

NAFLD pathogenesis is a complicated process that has not yet been fully elucidated. In this review, we briefly introduced diagnostic methods, therapeutic targets, and drugs related to NAFLD. In particular, we focused on the role of carbohydrate and lipid metabolism, lipotoxicity, cell death, inflammation, and fibrosis as potential therapeutic targets for NAFLD. We also summarized the clinical research progress in terms of drug development and combination therapy. Numerous drugs have progressed into clinical studies and have achieved excellent results in clinical NAFLD treatment. However, owing to the complexity of NAFLD and drug side effects, no effective drugs are available on the market. Additionally, combination therapy may have curative effects on NAFLD and NASH by affecting multiple pathways. In the near future, renewed and sustained efforts must be made to provide patients with NAFLD and NASH with safe and effective drugs.

## Author contributions

YF, YZ, LS, XL, YC, KZ, and HZ wrote the article. WL, W-dC, SZ, YL, and WY reviewed and revised the article. All authors contributed to the article and approved the submitted version.

## Funding

This work were supported by the National Natural Science Foundation of China (Grant Nos. 81970726 and 81903444), Innovation Talent of Henan Province, Key Program for Science and Technology of Henan Province (Grant No. 202102310808), College Students' Innovative Entrepreneurial Training Plan Program (No. 20210475084, 202010475032, and 202210475053), Major Scientific and Technological Innovation



Project of Hebi, First Class Discipline Cultivation Project of Henan University (Grant No. 2019YLZDYJ19).

## Conflict of interest

The authors declare that the research was conducted in the absence of any commercial or financial relationships that could be construed as a potential conflict of interest.

## References

- Akhtar, D. H., Iqbal, U., Vazquez-Montesino, L. M., Dennis, B. B., and Ahmed, A. (2019). Pathogenesis of insulin resistance and atherogenic dyslipidemia in nonalcoholic fatty liver disease. *J. Clin. Transl. Hepatol.* 7 (4), 362–370. doi:10.14218/jcth.2019.00028
- Al Attar, A., Antaramian, A., and Nouredin, M. (2021). Review of galectin-3 inhibitors in the treatment of nonalcoholic steatohepatitis. *Expert Rev. Clin. Pharmacol.* 14 (4), 457–464. doi:10.1080/17512433.2021.1894127
- Aljohani, A., Khan, M. I., Bonneville, A., Guo, C., Jeffery, J., O'Neill, L., et al. (2019). Hepatic stearoyl CoA desaturase 1 deficiency increases glucose uptake in adipose tissue partially through the PGC-1 $\alpha$ -FGF21 axis in mice. *J. Biol. Chem.* 294 (51), 19475–19485. doi:10.1074/jbc.RA119.009868
- Aller, R., Izaola, O., Gómez, S., Tafur, C., González, G., Berroa, E., et al. (2015). Effect of silymarin plus vitamin E in patients with non-alcoholic fatty liver disease. A randomized clinical pilot study. *Eur. Rev. Med. Pharmacol. Sci.* 19 (16), 3118–3124.
- Angulo, P., Hui, J. M., Marchesini, G., Bugianesi, E., George, J., Farrell, G. C., et al. (2007). The NAFLD fibrosis score: A noninvasive system that identifies liver fibrosis in patients with NAFLD. *Hepatology* 45 (4), 846–854. doi:10.1002/hep.21496
- Anstee, Q. M., Neuschwander-Tetri, B. A., Wong, V. W., Abdelmalek, M. F., Younossi, Z. M., Yuan, J., et al. (2020). Cenicriviroc for the treatment of liver fibrosis in adults with nonalcoholic steatohepatitis: AURORA phase 3 study design. *Contemp. Clin. Trials* 89, 105922. doi:10.1016/j.cct.2019.105922
- Argo, C. K., Patrie, J. T., Lackner, C., Henry, T. D., de Lange, E. E., Weltman, A. L., et al. (2015). Effects of n-3 fish oil on metabolic and histological parameters in NASH: A double-blind, randomized, placebo-controlled trial. *J. Hepatol.* 62 (1), 190–197. doi:10.1016/j.jhep.2014.08.036
- Armstrong, M. J., Gaunt, P., Aithal, G. P., Barton, D., Hull, D., Parker, R., et al. (2016). Liraglutide safety and efficacy in patients with non-alcoholic steatohepatitis (LEAN): A multicentre, double-blind, randomised, placebo-controlled phase 2 study. *Lancet* 387 (10019), 679–690. doi:10.1016/s0140-6736(15)00803-x
- Arroyave-Ospina, J. C., Wu, Z., Geng, Y., and Moshage, H. (2021). Role of oxidative stress in the pathogenesis of non-alcoholic fatty liver disease: Implications for prevention and therapy. *Antioxidants* 10 (2), 174. doi:10.3390/antiox10020174
- Badman, M. K., Chen, J., Desai, S., Vaidya, S., Neelakantham, S., Zhang, J., et al. (2020). Safety, tolerability, pharmacokinetics, and pharmacodynamics of the novel non-bile acid FXR agonist tropifexor (LJN452) in healthy volunteers. *Clin. Pharmacol. Drug Dev.* 9 (3), 395–410. doi:10.1002/cpdd.762
- Baeck, C., Wehr, A., Karlmark, K. R., Heymann, F., Vucur, M., Gassler, N., et al. (2012). Pharmacological inhibition of the chemokine CCL2 (MCP-1) diminishes liver macrophage infiltration and steatohepatitis in chronic hepatic injury. *Gut* 61 (3), 416–426. doi:10.1136/gutjnl-2011-300304
- Bajaj, M., Suramornkul, S., Piper, P., Hardies, L. J., Glass, L., Cersosimo, E., et al. (2004). Decreased plasma adiponectin concentrations are closely related to hepatic fat content and hepatic insulin resistance in pioglitazone-treated type 2 diabetic patients. *J. Clin. Endocrinol. Metab.* 89 (1), 200–206. doi:10.1210/jc.2003-031315
- Bakhshimoghaddam, F., Shateri, K., Sina, M., Hashemian, M., and Alizadeh, M. (2018). Daily consumption of synbiotic yogurt decreases liver steatosis in patients with nonalcoholic fatty liver disease: A randomized controlled clinical trial. *J. Nutr.* 148 (8), 1276–1284. doi:10.1093/jn/nxy088
- Basaranoglu, M., Achay, O., and Somsuz, A. (1999). A controlled trial of gemfibrozil in the treatment of patients with nonalcoholic steatohepatitis. *J. Hepatol.* 31 (2), 384. doi:10.1016/s0168-8278(99)80243-8
- Bhattacharya, D., Basta, B., Mato, J. M., Craig, A., Fernández-Ramos, D., Lopitz-Otsoa, F., et al. (2021). Aramchol downregulates stearoyl CoA-desaturase 1 in hepatic stellate cells to attenuate cellular fibrogenesis. *JHEP Rep.* 3 (3), 100237. doi:10.1016/j.jhepr.2021.100237
- Bril, F., Ortiz-Lopez, C., Lomonaco, R., Orsak, B., Freckleton, M., Chintapalli, K., et al. (2015). Clinical value of liver ultrasound for the diagnosis of nonalcoholic fatty liver disease in overweight and obese patients. *Liver Int.* 35 (9), 2139–2146. doi:10.1111/liv.12840
- Bril, F., Biernacki, D. M., Kalavalapalli, S., Lomonaco, R., Subbarayan, S. K., Lai, J., et al. (2019). Role of vitamin E for nonalcoholic steatohepatitis in patients with type 2 diabetes: A randomized controlled trial. *Diabetes Care* 42 (8), 1481–1488. doi:10.2337/dc19-0167
- Cansanção, K., Citelli, M., Carvalho Leite, N., López de Las Hazas, M. C., Davalos, A., Tavares do Carmo, M. d. G., et al. (2020). Impact of long-term supplementation with fish oil in individuals with non-alcoholic fatty liver disease: A double blind randomized placebo controlled clinical trial. *Nutrients* 12 (11), E3372. doi:10.3390/nut12113372
- Carlsson, B., Lindén, D., Brolén, G., Liljeblad, M., Bjursell, M., Romeo, S., et al. (2020). Review article: The emerging role of genetics in precision medicine for patients with non-alcoholic steatohepatitis. *Aliment. Pharmacol. Ther.* 51 (12), 1305–1320. doi:10.1111/apt.15738
- Chalasani, N., Younossi, Z., Lavine, J. E., Charlton, M., Cusi, K., Rinella, M., et al. (2018). The diagnosis and management of nonalcoholic fatty liver disease: Practice guidance from the American Association for the Study of Liver Diseases. *Hepatology* 67 (1), 328–357. doi:10.1002/hep.29367
- Chalasani, N., Abdelmalek, M. F., Garcia-Tsao, G., Vuppalanchi, R., Alkhouri, N., Rinella, M., et al. (2020). Effects of belapactin, an inhibitor of galectin-3, in patients with nonalcoholic steatohepatitis with cirrhosis and portal hypertension. *Gastroenterology* 158 (5), 1334–1345. e1335. doi:10.1053/j.gastro.2019.11.296
- Climax, J., Newsome, P. N., Hamza, M., Weissbach, M., Coughlan, D., Sattar, N., et al. (2020). Effects of epeleuton, a novel synthetic second-generation n-3 fatty acid, on non-alcoholic fatty liver disease, triglycerides, glycemic control, and cardiometabolic and inflammatory markers. *J. Am. Heart Assoc.* 9 (16), e016334. doi:10.1161/jaha.119.016334
- Cobbina, E., and Akhlaghi, F. (2017). Non-alcoholic fatty liver disease (NAFLD) - pathogenesis, classification, and effect on drug metabolizing enzymes and transporters. *Drug Metab. Rev.* 49 (2), 197–211. doi:10.1080/03602532.2017.1293683
- Cohen, S., Stemmer, S. M., Zozulya, G., Ochaion, A., Patoka, R., Barer, F., et al. (2011). CF102 an A3 adenosine receptor agonist mediates anti-tumor and anti-inflammatory effects in the liver. *J. Cell. Physiol.* 226 (9), 2438–2447. doi:10.1002/jcp.22593
- Colica, C., Boccuto, L., and Abenavoli, L. (2017). Silymarin: An option to treat non-alcoholic fatty liver disease. *World J. Gastroenterol.* 23 (47), 8437–8438. doi:10.3748/wjg.v23.i47.8437
- Čopić, A., Antoine-Bally, S., Giménez-Andrés, M., La Torre Garay, C., Antonny, B., Manni, M. M., et al. (2018). A giant amphipathic helix from a perilipin that is adapted for coating lipid droplets. *Nat. Commun.* 9 (1), 1332. doi:10.1038/s41467-018-03717-8
- Cross, H. R., Murphy, E., Black, R. G., Auchampach, J., and Steenbergen, C. (2002). Overexpression of A(3) adenosine receptors decreases heart rate, preserves energetics, and protects ischemic hearts. *Am. J. Physiol. Heart Circ. Physiol.* 283 (4), H1562–H1568. doi:10.1152/ajpheart.00335.2002
- Cusi, K., Orsak, B., Bril, F., Lomonaco, R., Hecht, J., Ortiz-Lopez, C., et al. (2016). Long-term pioglitazone treatment for patients with nonalcoholic steatohepatitis and prediabetes or type 2 diabetes mellitus: A randomized trial. *Ann. Intern. Med.* 165 (5), 305–315. doi:10.7326/m15-1774
- Day, C. P., and James, O. F. (1998). Steatohepatitis: A tale of two "hits". *Gastroenterology* 114 (4), 842–845. doi:10.1016/s0016-5085(98)70599-2

## Publisher's note

All claims expressed in this article are solely those of the authors and do not necessarily represent those of their affiliated organizations, or those of the publisher, the editors and the reviewers. Any product that may be evaluated in this article, or claim that may be made by its manufacturer, is not guaranteed or endorsed by the publisher.

- Del Campo, J. A., Gallego-Durán, R., Gallego, P., and Grande, L. (2018). Genetic and epigenetic regulation in nonalcoholic fatty liver disease (NAFLD). *Int. J. Mol. Sci.* 19 (3), E911. doi:10.3390/ijms19030911
- Dong, T. S., and Jacobs, J. P. (2019). Nonalcoholic fatty liver disease and the gut microbiome. *Exp. Biol. Med.* 244 (6), 408–418. doi:10.1177/1535370219836739
- Dong, R., Yang, X., Wang, C., Liu, K., Liu, Z., Ma, X., et al. (2019). Yanganin protects against non-alcoholic fatty liver disease through farnesoid X receptor. *Phytomedicine* 53, 134–142. doi:10.1016/j.phymed.2018.09.006
- Drucker, D. J., Dritselis, A., and Kirkpatrick, P. (2010). Liraglutide. *Nat. Rev. Drug Discov.* 9 (4), 267–268. doi:10.1038/nrd3148
- Dufour, J. F., Caussy, C., and Loomba, R. (2020). Combination therapy for non-alcoholic steatohepatitis: Rationale, opportunities and challenges. *Gut* 69 (10), 1877–1884. doi:10.1136/gutjnl-2019-319104
- Ehling, J., Bartneck, M., Wei, X., Gremse, F., Fech, V., Möckel, D., et al. (2014). CCL2-dependent infiltrating macrophages promote angiogenesis in progressive liver fibrosis. *Gut* 63 (12), 1960–1971. doi:10.1136/gutjnl-2013-306294
- Eriksson, J. W., Lundkvist, P., Jansson, P. A., Johansson, L., Kvarnström, M., Moris, L., et al. (2018). Effects of dapagliflozin and n-3 carboxylic acids on non-alcoholic fatty liver disease in people with type 2 diabetes: A double-blind randomised placebo-controlled study. *Diabetologia* 61 (9), 1923–1934. doi:10.1007/s00125-018-4675-2
- Eslamparast, T., Poustchi, H., Zamani, F., Sharafkhan, M., Malekzadeh, R., and Hekmatdoost, A. (2014). Synbiotic supplementation in nonalcoholic fatty liver disease: A randomized, double-blind, placebo-controlled pilot study. *Am. J. Clin. Nutr.* 99 (3), 535–542. doi:10.3945/ajcn.113.068890
- Faghihzadeh, F., Adibi, P., Rafiei, R., and Hekmatdoost, A. (2014). Resveratrol supplementation improves inflammatory biomarkers in patients with nonalcoholic fatty liver disease. *Nutr. Res.* 34 (10), 837–843. doi:10.1016/j.nutres.2014.09.005
- Farrell, G. C., Haczeyni, F., and Chitturi, S. (2018). Pathogenesis of NASH: How metabolic complications of overnutrition favour lipotoxicity and pro-inflammatory fatty liver disease. *Adv. Exp. Med. Biol.* 1061, 19–44. doi:10.1007/978-981-10-8684-7\_3
- Federico, A., and Dallio, M. (2019). Evaluation of the Effect Derived from Silybin with Vitamin D and Vitamin E Administration on Clinical, Metabolic, Endothelial Dysfunction, Oxidative Stress Parameters, and Serological Worsening Markers in Nonalcoholic Fatty Liver Disease Patients. *Oxid Med Cell Longev* 2019, 8742075. doi:10.1155/2019/8742075
- Federico, A., Dallio, M., and Loguercio, C. (2017). Silymarin/silybin and chronic liver disease: A marriage of many years. *Molecules* 22 (2), E191. doi:10.3390/molecules22020191
- Fernández-Miranda, C., Pérez-Carreras, M., Colina, F., López-Alonso, G., Vargas, C., and Solís-Herruzo, J. A. (2008). A pilot trial of fenofibrate for the treatment of non-alcoholic fatty liver disease. *Dig. Liver Dis.* 40 (3), 200–205. doi:10.1016/j.dld.2007.10.002
- Fishman, P., Cohen, S., Itzhak, I., Amer, J., Salhab, A., Barer, F., et al. (2019). The A3 adenosine receptor agonist, namodenoson, ameliorates non-alcoholic steatohepatitis in mice. *Int. J. Mol. Med.* 44 (6), 2256–2264. doi:10.3892/ijmm.2019.4364
- Friedman, S. L., Neuschwander-Tetri, B. A., Rinella, M., and Sanyal, A. J. (2018a). Mechanisms of NAFLD development and therapeutic strategies. *Nat. Med.* 24 (7), 908–922. doi:10.1038/s41591-018-0104-9
- Friedman, S. L., Ratziu, V., Harrison, S. A., Abdelmalek, M. F., Aithal, G. P., Caballeria, J., et al. (2018b). A randomized, placebo-controlled trial of cenicriviroc for treatment of nonalcoholic steatohepatitis with fibrosis. *Hepatology* 67 (5), 1754–1767. doi:10.1002/hep.29477
- Fujii, J., Homma, T., Kobayashi, S., and Seo, H. G. (2018). Mutual interaction between oxidative stress and endoplasmic reticulum stress in the pathogenesis of diseases specifically focusing on non-alcoholic fatty liver disease. *World J. Biol. Chem.* 9 (1), 1–15. doi:10.4331/wjbc.v9.i1.1
- Gabbia, D., Carpi, S., Sarcognato, S., Cannella, L., Colognesi, M., Scaffidi, M., et al. (2021). The extra virgin olive oil polyphenol oleocanthal exerts antifibrotic effects in the liver. *Front. Nutr.* 8, 715183. doi:10.3389/fnut.2021.715183
- Gawrieh, S., Guo, X., Tan, J., Lauzon, M., Taylor, K. D., Loomba, R., et al. (2019). A pilot genome-wide analysis study identifies loci associated with response to obeticholic acid in patients with NASH. *Hepatol. Commun.* 3 (12), 1571–1584. doi:10.1002/hep4.1439
- Giles, T. D., Miller, A. B., Elkayam, U., Bhattacharya, M., and Perez, A. (2008). Pioglitazone and heart failure: Results from a controlled study in patients with type 2 diabetes mellitus and systolic dysfunction. *J. Card. Fail.* 14 (6), 445–452. doi:10.1016/j.cardfail.2008.02.007
- Green, C. J., Pramfalk, C., Charlton, C. A., Gunn, P. J., Cornfield, T., Pavlides, M., et al. (2020). Hepatic de novo lipogenesis is suppressed and fat oxidation is increased by omega-3 fatty acids at the expense of glucose metabolism. *BMJ Open Diabetes Res. Care* 8 (1), e000871. doi:10.1136/bmjdr-2019-000871
- Gupta, N. A., Mells, J., Dunham, R. M., Grakoui, A., Handy, J., Saxena, N. K., et al. (2010). Glucagon-like peptide-1 receptor is present on human hepatocytes and has a direct role in decreasing hepatic steatosis *in vitro* by modulating elements of the insulin signaling pathway. *Hepatology* 51 (5), 1584–1592. doi:10.1002/hep.23569
- Harrison, S. A., Dennis, A., Fiore, M. M., Kelly, M. D., Kelly, C. J., Paredes, A. H., et al. (2018). Utility and variability of three non-invasive liver fibrosis imaging modalities to evaluate efficacy of GR-MD-02 in subjects with NASH and bridging fibrosis during a phase-2 randomized clinical trial. *PLoS One* 13 (9), e0203054. doi:10.1371/journal.pone.0203054
- Harrison, S. A., Marri, S. R., Chalasani, N., Kohli, R., Aronstein, W., Thompson, G. A., et al. (2016). Randomised clinical study: GR-MD-02, a galectin-3 inhibitor, vs. placebo in patients having non-alcoholic steatohepatitis with advanced fibrosis. *Aliment. Pharmacol. Ther.* 44 (11–12), 1183–1198. doi:10.1111/apt.13816
- Harrison, S. A., Abdelmalek, M. F., Caldwell, S., Shiffman, M. L., Diehl, A. M., Ghalib, R., et al. (2018a). Simtuzumab is ineffective for treatment of non-bridging fibrosis or compensated cirrhosis caused by nonalcoholic steatohepatitis. *Gastroenterology* 155 (4), 1140–1153. doi:10.1053/j.gastro.2018.07.006
- Harrison, S. A., Rinella, M. E., Abdelmalek, M. F., Trotter, J. F., Paredes, A. H., Arnold, H. L., et al. (2018b). NGM282 for treatment of non-alcoholic steatohepatitis: A multicentre, randomised, double-blind, placebo-controlled, phase 2 trial. *Lancet* 391 (10126), 1174–1185. doi:10.1016/s0140-6736(18)30474-4
- Harrison, S. A., Bashir, M. R., Guy, C. D., Zhou, R., Moylan, C. A., Frias, J. P., et al. (2019). Resmetirom (MGL-3196) for the treatment of non-alcoholic steatohepatitis: A multicentre, randomised, double-blind, placebo-controlled, phase 2 trial. *Lancet* 394 (10213), 2012–2024. doi:10.1016/s0140-6736(19)32517-6
- Harrison, S. A., Wong, V. W., Okanoue, T., Bzowej, N., Vuppalanchi, R., Younes, Z., et al. (2020). Selonsertib for patients with bridging fibrosis or compensated cirrhosis due to NASH: Results from randomized phase III STELLAR trials. *J. Hepatol.* 73 (1), 26–39. doi:10.1016/j.jhep.2020.02.027
- Hernandez, E. D., Zheng, L., Kim, Y., Fang, B., Liu, B., Valdez, R. A., et al. (2019). Tropifexor-mediated abrogation of steatohepatitis and fibrosis is associated with the antioxidative gene expression profile in rodents. *Hepatol. Commun.* 3 (8), 1085–1097. doi:10.1002/hep4.1368
- Hirschfield, G. M., Mason, A., Luketic, V., Lindor, K., Gordon, S. C., Mayo, M., et al. (2015). Efficacy of obeticholic acid in patients with primary biliary cirrhosis and inadequate response to ursodeoxycholic acid. *Gastroenterology* 148 (4), 751–761. e758. doi:10.1053/j.gastro.2014.12.005
- Hu, H., Tian, M., Ding, C., and Yu, S. (2018a). The C/EBP homologous protein (CHOP) transcription factor functions in endoplasmic reticulum stress-induced apoptosis and microbial infection. *Front. Immunol.* 9, 3083. doi:10.3389/fimmu.2018.03083
- Hu, Y. B., Liu, X. Y., and Zhan, W. (2018b). Farnesoid X receptor agonist INT-767 attenuates liver steatosis and inflammation in rat model of nonalcoholic steatohepatitis. *Drug Des. devel. Ther.* 12, 2213–2221. doi:10.2147/dddt.s170518
- Hui, S. T., Wang, F., Stappenbeck, F., French, S. W., Magyar, C. E., Parhami, F., et al. (2021). Oxy210, a novel inhibitor of hedgehog and TGF- $\beta$  signalling, ameliorates hepatic fibrosis and hypercholesterolemia in mice. *Endocrinol. Diabetes Metab.* 4 (4), e00296. doi:10.1002/edm.2.296
- Hyodo, T., Yada, N., Hori, M., Maenishi, O., Lamb, P., Sasaki, K., et al. (2017). Multimaterial decomposition algorithm for the quantification of liver fat content by using fast-kilovolt-peak switching dual-energy CT: Clinical evaluation. *Radiology* 283 (1), 108–118. doi:10.1148/radiol.2017160130
- Imajo, K., Kessoku, T., Honda, Y., Tomeno, W., Ogawa, Y., Mawatari, H., et al. (2016). Magnetic resonance imaging more accurately classifies steatosis and fibrosis in patients with nonalcoholic fatty liver disease than transient elastography. *Gastroenterology* 150 (3), 626–637. e627. doi:10.1053/j.gastro.2015.11.048
- Iruarizaga-Lejarreta, M., Varela-Rey, M., Fernández-Ramos, D., Martínez-Arranz, I., Delgado, T. C., Simon, J., et al. (2017). Role of Aramchol in steatohepatitis and fibrosis in mice. *Hepatol. Commun.* 1 (9), 911–927. doi:10.1002/hep4.1107
- Jennison, E., Patel, J., Scorletti, E., and Byrne, C. D. (2019). Diagnosis and management of non-alcoholic fatty liver disease. *Postgrad. Med. J.* 95 (1124), 314–322. doi:10.1136/postgradmedj-2018-136316
- Jiang, L., Xiao, D., Li, Y., Dai, S., Qu, L., Chen, X., et al. (2021). Structural basis of tropifexor as a potent and selective agonist of farnesoid X receptor. *Biochem. Biophys. Res. Commun.* 534, 1047–1052. doi:10.1016/j.bbrc.2020.10.039
- Jindal, A., Bruzzi, S., Sutti, S., Locatelli, I., Bozzola, C., Paternostro, C., et al. (2015). Fat-laden macrophages modulate lobular inflammation in nonalcoholic steatohepatitis (NASH). *Exp. Mol. Pathol.* 99 (1), 155–162. doi:10.1016/j.yexmp.2015.06.015

- Jouihan, H., Will, S., Guionaud, S., Bolland, M. L., Oldham, S., Ravn, P., et al. (2017). Superior reductions in hepatic steatosis and fibrosis with co-administration of a glucagon-like peptide-1 receptor agonist and obeticholic acid in mice. *Mol. Metab.* 6 (11), 1360–1370. doi:10.1016/j.molmet.2017.09.001
- Ju, C., and Tacke, F. (2016). Hepatic macrophages in homeostasis and liver diseases: From pathogenesis to novel therapeutic strategies. *Cell. Mol. Immunol.* 13 (3), 316–327. doi:10.1038/cmi.2015.104
- Kalopitas, G., Antza, C., Doundoulakis, I., Siargkas, A., Kouroumalis, E., Germanidis, G., et al. (2021). Impact of silymarin in individuals with nonalcoholic fatty liver disease: A systematic review and meta-analysis. *Nutrition* 83, 111092. doi:10.1016/j.nut.2020.111092
- Kaswala, D. H., Lai, M., and Afdhal, N. H. (2016). Fibrosis assessment in nonalcoholic fatty liver disease (NAFLD) in 2016. *Dig. Dis. Sci.* 61 (5), 1356–1364. doi:10.1007/s10620-016-4079-4
- Kedarisetty, C. K., Bhardwaj, A., Kumar, G., Rastogi, A., Bihari, C., Kumar, M., et al. (2021). Efficacy of combining pentoxifylline and vitamin E versus vitamin E alone in non-alcoholic steatohepatitis—A randomized pilot study. *Indian J. Gastroenterol.* 40 (1), 41–49. doi:10.1007/s12664-020-01131-x
- Khoo, J., Hsiang, J. C., Taneja, R., Koo, S. H., Soon, G. H., Kam, C. J., et al. (2019). Randomized trial comparing effects of weight loss by liraglutide with lifestyle modification in non-alcoholic fatty liver disease. *Liver Int.* 39 (5), 941–949. doi:10.1111/liv.14065
- Kim, D., Kim, W., Joo, S. K., Bae, J. M., Kim, J. H., and Ahmed, A. (2018). Subclinical hypothyroidism and low-normal thyroid function are associated with nonalcoholic steatohepatitis and fibrosis. *Clin. Gastroenterol. Hepatol.* 16 (1), 123–131. e121. doi:10.1016/j.cgh.2017.08.014
- Kjærsgaard, K., Frisch, K., Sorensen, M., Munk, O. L., Hofmann, A. F., Horsager, J., et al. (2021). Obeticholic acid improves hepatic bile acid excretion in patients with primary biliary cholangitis. *J. Hepatol.* 74 (1), 58–65. doi:10.1016/j.jhep.2020.07.028
- Kobyliak, N., Abenavoli, L., Falalyeyeva, T., Mykhalchysyn, G., Boccuto, L., Kononenko, L., et al. (2018). Beneficial effects of probiotic combination with omega-3 fatty acids in NAFLD: A randomized clinical study. *Minerva Med.* 109 (6), 418–428. doi:10.23736/s0026-4806.18.05845-7
- Kory, N., Farese, R. V., Jr., and Walther, T. C. (2016). Targeting fat: Mechanisms of protein localization to lipid droplets. *Trends Cell Biol.* 26 (7), 535–546. doi:10.1016/j.tcb.2016.02.007
- Koutsounas, I., Theocharis, S., Delladetsima, I., Patsouris, E., and Giaginis, C. (2015). Farnesoid x receptor in human metabolism and disease: The interplay between gene polymorphisms, clinical phenotypes and disease susceptibility. *Expert Opin. Drug Metab. Toxicol.* 11 (4), 523–532. doi:10.1517/17425255.2014.999664
- Kowdley, K. V., Luketic, V., Chapman, R., Hirschfield, G. M., Poupon, R., Schramm, C., et al. (2018). A randomized trial of obeticholic acid monotherapy in patients with primary biliary cholangitis. *Hepatology* 67 (5), 1890–1902. doi:10.1002/hep.29569
- Kowdley, K. V., Vuppalanchi, R., Levy, C., Floreani, A., Andreone, P., LaRusso, N. F., et al. (2020). A randomized, placebo-controlled, phase II study of obeticholic acid for primary sclerosing cholangitis. *J. Hepatol.* 73 (1), 94–101. doi:10.1016/j.jhep.2020.02.033
- Koyama, Y., and Brenner, D. A. (2017). Liver inflammation and fibrosis. *J. Clin. Invest.* 127 (1), 55–64. doi:10.1172/jci88881
- Kuchay, M. S., Krishan, S., Mishra, S. K., Choudhary, N. S., Singh, M. K., Wasir, J. S., et al. (2020). Effect of dulaglutide on liver fat in patients with type 2 diabetes and NAFLD: Randomised controlled trial (D-LIFT trial). *Diabetologia* 63 (11), 2434–2445. doi:10.1007/s00125-020-05265-7
- Kulkarni, A. V., Tevethia, H. V., Arab, J. P., Candia, R., Premkumar, M., Kumar, P., et al. (2021). Efficacy and safety of obeticholic acid in liver disease—A systematic review and meta-analysis. *Clin. Res. Hepatol. Gastroenterol.* 45 (3), 101675. doi:10.1016/j.clinre.2021.101675
- Kumar, D. P., Caffrey, R., Marioneaux, J., Santhekadur, P. K., Bhat, M., Alonso, C., et al. (2020). The PPAR  $\alpha/\gamma$  agonist saroglitazar improves insulin resistance and steatohepatitis in a diet induced animal model of nonalcoholic fatty liver disease. *Sci. Rep.* 10 (1), 9330. doi:10.1038/s41598-020-66458-z
- Laurin, J., Lindor, K. D., Crippin, J. S., Gossard, A., Gores, G. J., Ludwig, J., et al. (1996). Ursodeoxycholic acid or clofibrate in the treatment of non-alcohol-induced steatohepatitis: A pilot study. *Hepatology* 23 (6), 1464–1467. doi:10.1002/hep.510230624
- Le, C. T., Nguyen, G., Park, S. Y., Choi, D. H., and Cho, E. H. (2018). LY2405319, an analog of fibroblast growth factor 21 ameliorates  $\alpha$ -smooth muscle actin production through inhibition of the succinate-G-protein couple receptor 91 (GPR91) pathway in mice. *PLoS One* 13 (2), e0192146. doi:10.1371/journal.pone.0192146
- Lebeaupin, C., Vallée, C., Hazari, Y., Hetz, C., Chevet, E., and Bailly-Maitre, B. (2018). Endoplasmic reticulum stress signalling and the pathogenesis of non-alcoholic fatty liver disease. *J. Hepatol.* 69 (4), 927–947. doi:10.1016/j.jhep.2018.06.008
- Lee, S. J., and Kim, S. U. (2019). Noninvasive monitoring of hepatic steatosis: Controlled attenuation parameter and magnetic resonance imaging-proton density fat fraction in patients with nonalcoholic fatty liver disease. *Expert Rev. Gastroenterol. Hepatol.* 13 (6), 523–530. doi:10.1080/17474124.2019.1608820
- Lefebvre, E., Moyle, G., Reshef, R., Richman, L. P., Thompson, M., Hong, F., et al. (2016). Antifibrotic effects of the dual CCR2/CCR5 antagonist cenicriviroc in animal models of liver and kidney fibrosis. *PLoS One* 11 (6), e0158156. doi:10.1371/journal.pone.0158156
- Li, A. A., Ahmed, A., and Kim, D. (2020). Extrahepatic manifestations of nonalcoholic fatty liver disease. *Gut Liver* 14 (2), 168–178. doi:10.5009/gnl19069
- Li, Y. H., Yang, L. H., Sha, K. H., Liu, T. G., Zhang, L. G., and Liu, X. X. (2015). Efficacy of poly-unsaturated fatty acid therapy on patients with nonalcoholic steatohepatitis. *World J. Gastroenterol.* 21 (22), 7008–7013. doi:10.3748/wjg.v21.i22.7008
- Li, R., Li, J., Huang, Y., Li, H., Yan, S., Lin, J., et al. (2018). Polydatin attenuates diet-induced nonalcoholic steatohepatitis and fibrosis in mice. *Int. J. Biol. Sci.* 14 (11), 1411–1425. doi:10.7150/ijbs.26086
- Li, J., Liu, C., Zhou, Z., Dou, B., Huang, J., Huang, L., et al. (2021). Isotachismine alleviates nonalcoholic steatohepatitis and fibrosis via FXR agonism in mice. *Phytother. Res.* 35 (6), 3351–3364. doi:10.1002/ptr.7055
- Loomba, R., Lawitz, E., Mantry, P. S., Jayakumar, S., Caldwell, S. H., Arnold, H., et al. (2018). The ASK1 inhibitor selonsertib in patients with nonalcoholic steatohepatitis: A randomized, phase 2 trial. *Hepatology* 67 (2), 549–559. doi:10.1002/hep.29514
- Loomba, R., Noureddin, M., Kowdley, K. V., Kohli, A., Sheikh, A., Neff, G., et al. (2021). Combination therapies including clobefoxor and firsocostat for bridging fibrosis and cirrhosis attributable to NASH. *Hepatology* 73 (2), 625–643. doi:10.1002/hep.31622
- Ma, J., Zhou, Q., and Li, H. (2017). Gut microbiota and nonalcoholic fatty liver disease: Insights on mechanisms and therapy. *Nutrients* 9 (10), E1124. doi:10.3390/nu9101124
- Majnooni, M. B., Ataee, M., Bahrami, G., Heydarpour, F., Aneva, I. Y., Farzaei, M. H., et al. (2021). The effects of co-administration of artichoke leaf extract supplementation with metformin and vitamin E in patients with nonalcoholic fatty liver disease: A randomized clinical trial. *Phytother. Res.* 35 (11), 6324–6334. doi:10.1002/ptr.7279
- Manousopoulou, A., Scorletti, E., Smith, D. E., Teng, J., Fotopoulos, M., Roumeliotis, T. I., et al. (2019). Marine omega-3 fatty acid supplementation in non-alcoholic fatty liver disease: Plasma proteomics in the randomized WELCOME\* trial. *Clin. Nutr.* 38 (4), 1952–1955. doi:10.1016/j.clnu.2018.07.037
- Marso, S. P., Bain, S. C., Consoli, A., Eliaschewitz, F. G., Jódar, E., Leiter, L. A., et al. (2016a). Semaglutide and cardiovascular outcomes in patients with type 2 diabetes. *N. Engl. J. Med.* 375 (19), 1834–1844. doi:10.1056/NEJMoa1607141
- Marso, S. P., Daniels, G. H., Brown-Frandsen, K., Kristensen, P., Mann, J. F., Nauck, M. A., et al. (2016b). Liraglutide and cardiovascular outcomes in type 2 diabetes. *N. Engl. J. Med.* 375 (4), 311–322. doi:10.1056/NEJMoa1603827
- McTaggart, F., and Jones, P. (2008). Effects of statins on high-density lipoproteins: A potential contribution to cardiovascular benefit. *Cardiovasc. Drugs Ther.* 22 (4), 321–338. doi:10.1007/s10557-008-6113-z
- Mofidi, F., Poustchi, H., Yari, Z., Nourinayyer, B., Merat, S., Sharafkhan, M., et al. (2017). Synbiotic supplementation in lean patients with non-alcoholic fatty liver disease: A pilot, randomised, double-blind, placebo-controlled, clinical trial. *Br. J. Nutr.* 117 (5), 662–668. doi:10.1017/s0007114517000204
- Mosca, A., Crudele, A., Smeriglio, A., Braghini, M. R., Panera, N., Comparcola, D., et al. (2021). Antioxidant activity of Hydroxytyrosol and Vitamin E reduces systemic inflammation in children with paediatric NAFLD. *Dig. Liver Dis.* 53 (9), 1154–1158. doi:10.1016/j.dld.2020.09.021
- Nagashimada, M., and Ota, T. (2019). Role of vitamin E in nonalcoholic fatty liver disease. *IUBMB Life* 71 (4), 516–522. doi:10.1002/iub.1991
- Nalbantoglu, I. L., and Brunt, E. M. (2014). Role of liver biopsy in nonalcoholic fatty liver disease. *World J. Gastroenterol.* 20 (27), 9026–9037. doi:10.3748/wjg.v20.i27.9026
- Navarro, L. A., Wree, A., Povero, D., Berk, M. P., Eguchi, A., Ghosh, S., et al. (2015). Arginase 2 deficiency results in spontaneous steatohepatitis: A novel link between innate immune activation and hepatic de novo lipogenesis. *J. Hepatol.* 62 (2), 412–420. doi:10.1016/j.jhep.2014.09.015



- Navarro, V. J., Belle, S. H., D'Amato, M., Adfhal, N., Brunt, E. M., Fried, M. W., et al. (2019). Silymarin in non-cirrhotics with non-alcoholic steatohepatitis: A randomized, double-blind, placebo controlled trial. *PLoS One* 14 (9), e0221683. doi:10.1371/journal.pone.0221683
- Neuschwander-Tetri, B. A., Loomba, R., Sanyal, A. J., Lavine, J. E., Van Natta, M. L., Abdelmalek, M. F., et al. (2015). Farnesoid X nuclear receptor ligand obeticholic acid for non-cirrhotic, non-alcoholic steatohepatitis (FLINT): A multicentre, randomised, placebo-controlled trial. *Lancet* 385 (9972), 956–965. doi:10.1016/s0140-6736(14)61933-4
- Neuschwander-Tetri, B. A. (2010). Hepatic lipotoxicity and the pathogenesis of nonalcoholic steatohepatitis: The central role of nontriglyceride fatty acid metabolites. *Hepatology* 52 (2), 774–788. doi:10.1002/hep.23719
- Newsome, P., Francque, S., Harrison, S., Ratziu, V., Van Gaal, L., Calanna, S., et al. (2019). Effect of semaglutide on liver enzymes and markers of inflammation in subjects with type 2 diabetes and/or obesity. *Aliment. Pharmacol. Ther.* 50 (2), 193–203. doi:10.1111/apt.15316
- Newsome, P. N., Buchholtz, K., Cusi, K., Linder, M., Okanou, T., Ratziu, V., et al. (2021). A placebo-controlled trial of subcutaneous semaglutide in nonalcoholic steatohepatitis. *N. Engl. J. Med.* 384 (12), 1113–1124. doi:10.1056/NEJMoa2028395
- Noguchi, R., Kaji, K., Namisaki, T., Moriya, K., Kawaratani, H., Kitade, M., et al. (2020). Novel oral plasminogen activator inhibitor-1 inhibitor TM5275 attenuates hepatic fibrosis under metabolic syndrome via suppression of activated hepatic stellate cells in rats. *Mol. Med. Rep.* 22 (4), 2948–2956. doi:10.3892/mmr.2020.11360
- Nojiri, S., Tsuchiya, A., Natsui, K., Takeuchi, S., Watanabe, T., Kojima, Y., et al. (2021). Synthesized HMGB1 peptide attenuates liver inflammation and suppresses fibrosis in mice. *Inflamm. Regen.* 41 (1), 28. doi:10.1186/s41232-021-00177-4
- Ochaion, A., Bar-Yehuda, S., Cohen, S., Amital, H., Jacobson, K. A., Joshi, B. V., et al. (2008). The A3 adenosine receptor agonist CF502 inhibits the PI3K, PKB/Akt and NF-kappaB signaling pathway in synoviocytes from rheumatoid arthritis patients and in adjuvant-induced arthritis rats. *Biochem. Pharmacol.* 76 (4), 482–494. doi:10.1016/j.bcp.2008.05.032
- Ohana, G., Cohen, S., Rath-Wolfson, L., and Fishman, P. (2016). A3 adenosine receptor agonist, CF102, protects against hepatic ischemia/reperfusion injury following partial hepatectomy. *Mol. Med. Rep.* 14 (5), 4335–4341. doi:10.3892/mmr.2016.5746
- Oscarsson, J., Önnérhag, K., Risérus, U., Sundén, M., Johansson, L., Jansson, P. A., et al. (2018). Effects of free omega-3 carboxylic acids and fenofibrate on liver fat content in patients with hypertriglyceridemia and non-alcoholic fatty liver disease: A double-blind, randomized, placebo-controlled study. *J. Clin. Lipidol.* 12 (6), 1390–1403. e1394. doi:10.1016/j.jacl.2018.08.003
- Parker, H. M., Cohn, J. S., O'Connor, H. T., and Garg, M. L. (2019). Effect of fish oil supplementation on hepatic and visceral fat in overweight men. *A Randomized Control. Trial* 11 (2), 475. doi:10.3390/nu11020475
- Patel, K., Harrison, S. A., Elkhatab, M., Trotter, J. F., Herring, R., Rojter, S. E., et al. (2020). Cilofexor, a nonsteroidal FXR agonist, in patients with noncirrhotic NASH: A phase 2 randomized controlled trial. *Hepatology* 72 (1), 58–71. doi:10.1002/hep.31205
- Pawella, L. M., Hashani, M., Eiteneuer, E., Renner, M., Bartenschlager, R., Schirmacher, P., et al. (2014). Perilipin discloses chronic from acute hepatocellular steatosis. *J. Hepatol.* 60 (3), 633–642. doi:10.1016/j.jhep.2013.11.007
- Pedrosa, M., Seyedkazemi, S., Francque, S., Sanyal, A., Rinella, M., Charlton, M., et al. (2020). A randomized, double-blind, multicenter, phase 2b study to evaluate the safety and efficacy of a combination of tropifexor and cenicriviroc in patients with nonalcoholic steatohepatitis and liver fibrosis: Study design of the TANDEM trial. *Contemp. Clin. Trials* 88, 105889. doi:10.1016/j.cct.2019.105889
- Perumpail, B. J., Li, A. A., John, N., Sallam, S., Shah, N. D., Kwong, W., et al. (2018). The role of vitamin E in the treatment of NAFLD. *Diseases* 6 (4), E86. doi:10.3390/diseases6040086
- Pockros, P. J., Fuchs, M., Freilich, B., Schiff, E., Kohli, A., Lawitz, E. J., et al. (2019). Control: A randomized phase 2 study of obeticholic acid and atorvastatin on lipoproteins in nonalcoholic steatohepatitis patients. *Liver Int.* 39 (11), 2082–2093. doi:10.1111/liv.14209
- Podszus, M. C., Alawad, A. S., Lingala, S., Morris, N., Huang, W. A., Yang, S., et al. (2020). Vitamin E treatment in NAFLD patients demonstrates that oxidative stress drives steatosis through upregulation of de-novo lipogenesis. *Redox Biol.* 37, 101710. doi:10.1016/j.redox.2020.101710
- Portillo-Sanchez, P., Bril, F., Lomonaco, R., Barb, D., Orsak, B., Bruder, J. M., et al. (2019). Effect of pioglitazone on bone mineral density in patients with nonalcoholic steatohepatitis: A 36-month clinical trial. *J. Diabetes* 11 (3), 223–231. doi:10.1111/1753-0407.12833
- Puengel, T., Krenkel, O., Kohlhepp, M., Lefebvre, E., Luedde, T., Trautwein, C., et al. (2017). Differential impact of the dual CCR2/CCR5 inhibitor cenicriviroc on migration of monocyte and lymphocyte subsets in acute liver injury. *PLoS One* 12 (9), e0184694. doi:10.1371/journal.pone.0184694
- Ratziu, V., Harrison, S. A., Francque, S., Bedossa, P., Leher, P., Serfaty, L., et al. (2016). Elafibranor, an agonist of the peroxisome proliferator-activated receptor- $\alpha$  and - $\delta$ , induces resolution of nonalcoholic steatohepatitis without fibrosis worsening. *Gastroenterology* 150 (5), 1147–1159. e1145. doi:10.1053/j.gastro.2016.01.038
- Ratziu, V., Sanyal, A., Harrison, S. A., Wong, V. W., Francque, S., Goodman, Z., et al. (2020). Cenicriviroc treatment for adults with nonalcoholic steatohepatitis and fibrosis: Final analysis of the phase 2b CENTAUR study. *Hepatology* 72 (3), 892–905. doi:10.1002/hep.31108
- Ratziu, V., de Guevara, L., Safadi, R., Poordad, F., Fuster, F., Flores-Figueroa, J., et al. (2021). Aramchol in patients with nonalcoholic steatohepatitis: A randomized, double-blind, placebo-controlled phase 2b trial. *Nat. Med.* 27 (10), 1825–1835. doi:10.1038/s41591-021-01495-3
- Ratziu, V., Rinella, M. E., Neuschwander-Tetri, B. A., Lawitz, E., Denham, D., Kayali, Z., et al. (2022). EDP-305 in patients with NASH: A phase II double-blind placebo-controlled dose-ranging study. *J. Hepatol.* 76 (3), 506–517. doi:10.1016/j.jhep.2021.10.018
- Roth, J. D., Veidal, S. S., Fensholdt, L. K. D., Rigbolt, K. T. G., Papazyan, R., Nielsen, J. C., et al. (2019). Combined obeticholic acid and elafibranor treatment promotes additive liver histological improvements in a diet-induced ob/ob mouse model of biopsy-confirmed NASH. *Sci. Rep.* 9 (1), 9046. doi:10.1038/s41598-019-45178-z
- Safadi, R., Konikoff, F. M., Mahamid, M., Zelber-Sagi, S., Halpern, M., Gilat, T., et al. (2014). The fatty acid-bile acid conjugate Aramchol reduces liver fat content in patients with nonalcoholic fatty liver disease. *Clin. Gastroenterol. Hepatol.* 12 (12), 2085–2091. e2081. doi:10.1016/j.cgh.2014.04.038
- Safadi, R., Braun, M., Francis, A., Milgrom, Y., Massarwa, M., Hakimian, D., et al. (2021). Randomised clinical trial: A phase 2 double-blind study of namodenoson in non-alcoholic fatty liver disease and steatohepatitis. *Aliment. Pharmacol. Ther.* 54 (11–12), 1405–1415. doi:10.1111/apt.16664
- Sahin, E., Bagci, R., Bektur Aykanat, N. E., Kacar, S., and Sahinturk, V. (2020). Silymarin attenuated nonalcoholic fatty liver disease through the regulation of endoplasmic reticulum stress proteins GRP78 and XBP-1 in mice. *J. Food Biochem.* 44 (6), e13194. doi:10.1111/jfbc.13194
- Sanyal, A., Charles, E. D., Neuschwander-Tetri, B. A., Loomba, R., Harrison, S. A., Abdelmalek, M. F., et al. (2019). Pegbelfermin (BMS-986036), a PEGylated fibroblast growth factor 21 analogue, in patients with non-alcoholic steatohepatitis: A randomised, double-blind, placebo-controlled, phase 2a trial. *Lancet* 392 (10165), 2705–2717. doi:10.1016/s0140-6736(18)31785-9
- Satirapoj, B., Watanakijthavonkul, K., and Supasindh, O. (2018). Safety and efficacy of low dose pioglitazone compared with standard dose pioglitazone in type 2 diabetes with chronic kidney disease: A randomized controlled trial. *PLoS One* 13 (10), e0206722. doi:10.1371/journal.pone.0206722
- Sayari, S., Neishaboori, H., and Jameshorani, M. (2018). Combined effects of synbiotic and sitagliptin versus sitagliptin alone in patients with nonalcoholic fatty liver disease. *Clin. Mol. Hepatol.* 24 (3), 331–338. doi:10.3350/cmh.2018.0006
- Scorletti, E., Afolabi, P. R., Miles, E. A., Smith, D. E., Almeshmadi, A., Alshathry, A., et al. (2020). Synbiotics alter fecal microbiomes, but not liver fat or fibrosis, in a randomized trial of patients with nonalcoholic fatty liver disease. *Gastroenterology* 158 (6), 1597–1610. e1597. doi:10.1053/j.gastro.2020.01.031
- Shah, A. G., Lydecker, A., Murray, K., Tetri, B. N., Contos, M. J., Sanyal, A. J., et al. (2009). Comparison of noninvasive markers of fibrosis in patients with nonalcoholic fatty liver disease. *Clin. Gastroenterol. Hepatol.* 7 (10), 1104–1112. doi:10.1016/j.cgh.2009.05.033
- Sinha, R. A., Bruinstroop, E., Singh, B. K., and Yen, P. M. (2019). Nonalcoholic fatty liver disease and hypercholesterolemia: Roles of thyroid hormones, metabolites, and agonists. *Thyroid* 29 (9), 1173–1191. doi:10.1089/thy.2018.0664
- Siriwardhana, N., Kalupahana, N. S., and Moustaid-Moussa, N. (2012). Health benefits of n-3 polyunsaturated fatty acids: Eicosapentaenoic acid and docosahexaenoic acid. *Adv. Food Nutr. Res.* 65, 211–222. doi:10.1016/b978-0-12-416003-3.00013-5
- Soleimani, V., Delghandi, P. S., Moallem, S. A., and Karimi, G. (2019). Safety and toxicity of silymarin, the major constituent of milk thistle extract: An updated review. *Phytother. Res.* 33 (6), 1627–1638. doi:10.1002/ptr.6361
- Song, L., Zhao, X. G., Ouyang, P. L., Guan, Q., Yang, L., Peng, F., et al. (2020). Combined effect of n-3 fatty acids and phytosterol esters on alleviating hepatic steatosis in non-alcoholic fatty liver disease subjects: A double-blind placebo-

- controlled clinical trial. *Br. J. Nutr.* 123 (10), 1148–1158. doi:10.1017/s0007114520000495
- Sookoian, S., and Pirola, C. J. (2019). Genetics of nonalcoholic fatty liver disease: From pathogenesis to therapeutics. *Semin. Liver Dis.* 39 (2), 124–140. doi:10.1055/s-0039-1679920
- Srivastava, A. (2014). Progressive familial intrahepatic cholestasis. *J. Clin. Exp. Hepatol.* 4 (1), 25–36. doi:10.1016/j.jceh.2013.10.005
- Tacke, F., and Weiskirchen, R. (2021). Non-alcoholic fatty liver disease (NAFLD)/non-alcoholic steatohepatitis (NASH)-related liver fibrosis: Mechanisms, treatment and prevention. *Ann. Transl. Med.* 9 (8), 729. doi:10.21037/atm-20-4354
- Tacke, F. (2017). Targeting hepatic macrophages to treat liver diseases. *J. Hepatol.* 66 (6), 1300–1312. doi:10.1016/j.jhep.2017.02.026
- Tacke, F. (2018). Cenicriviroc for the treatment of non-alcoholic steatohepatitis and liver fibrosis. *Expert Opin. Investig. Drugs* 27 (3), 301–311. doi:10.1080/13543784.2018.1442436
- Tang, H., Shi, W., Fu, S., Wang, T., Zhai, S., Song, Y., et al. (2018). Pioglitazone and bladder cancer risk: A systematic review and meta-analysis. *Cancer Med.* 7 (4), 1070–1080. doi:10.1002/cam4.1354
- Traussnigg, S., Halilbasic, E., Hofer, H., Munda, P., Stojakovic, T., Fauler, G., et al. (2021). Open-label phase II study evaluating safety and efficacy of the non-steroidal farnesoid X receptor agonist PX-104 in non-alcoholic fatty liver disease. *Wien. Klin. Wochenschr.* 133 (9–10), 441–451. doi:10.1007/s00508-020-01735-5
- Tsuchida, T. (2019). Mechanisms of hepatic stellate cell activation as a therapeutic target for the treatment of non-alcoholic steatohepatitis. *Nihon Yakurigaku Zasshi.* 154 (4), 203–209. doi:10.1254/fpj.154.203
- Tully, D. C., Rucker, P. V., Chianelli, D., Williams, J., Vidal, A., Alper, P. B., et al. (2017). Discovery of tropifexor (LJN452), a highly potent non-bile acid FXR agonist for the treatment of cholestatic liver diseases and nonalcoholic steatohepatitis (NASH). *J. Med. Chem.* 60 (24), 9960–9973. doi:10.1021/acs.jmedchem.7b00907
- Vadarlis, A., Antza, C., Bakaloudi, D. R., Doundoulakis, I., Kalopitas, G., Samara, M., et al. (2021). Systematic review with meta-analysis: The effect of vitamin E supplementation in adult patients with non-alcoholic fatty liver disease. *J. Gastroenterol. Hepatol.* 36 (2), 311–319. doi:10.1111/jgh.15221
- Valenti, L. V. C., and Baselli, G. A. (2018). Genetics of nonalcoholic fatty liver disease: A 2018 update. *Curr. Pharm. Des.* 24 (38), 4566–4573. doi:10.2174/1381612825666190119113836
- Valenti, L., and Dongiovanni, P. (2017). Mutant PNPLA3 I148M protein as pharmacological target for liver disease. *Hepatology* 66 (4), 1026–1028. doi:10.1002/hep.29298
- Wah Kheong, C., Nik Mustapha, N. R., and Mahadeva, S. (2017). A randomized trial of silymarin for the treatment of nonalcoholic steatohepatitis. *Clin. Gastroenterol. Hepatol.* 15 (12), 1940–1949. e1948. doi:10.1016/j.cgh.2017.04.016
- Wang, C. W., Lin, H. Y., Shin, S. J., Yu, M. L., Lin, Z. Y., Dai, C. Y., et al. (2011). The PNPLA3 I148M polymorphism is associated with insulin resistance and nonalcoholic fatty liver disease in a normoglycaemic population. *Liver Int.* 31 (9), 1326–1331. doi:10.1111/j.1478-3231.2011.02526.x
- Watanabe, M., Houten, S. M., Wang, L., Moschetta, A., Mangelsdorf, D. J., Heyman, R. A., et al. (2004). Bile acids lower triglyceride levels via a pathway involving FXR, SHP, and SREBP-1c. *J. Clin. Invest.* 113 (10), 1408–1418. doi:10.1172/jci21025
- Wehr, A., Baeck, C., Heymann, F., Niemietz, P. M., Hammerich, L., Martin, C., et al. (2013). Chemokine receptor CXCR6-dependent hepatic NK T Cell accumulation promotes inflammation and liver fibrosis. *J. Immunol.* 190 (10), 5226–5236. doi:10.4049/jimmunol.1202909
- Weikum, E. R., Liu, X., and Ortlund, E. A. (2018). The nuclear receptor superfamily: A structural perspective. *Protein Sci.* 27 (11), 1876–1892. doi:10.1002/pro.3496
- Wu, K. T., Kuo, P. L., Su, S. B., Chen, Y. Y., Yeh, M. L., Huang, C. L., et al. (2016). Nonalcoholic fatty liver disease severity is associated with the ratios of total cholesterol and triglycerides to high-density lipoprotein cholesterol. *J. Clin. Lipidol.* 10 (2), 420–425. e421. doi:10.1016/j.jacl.2015.12.026
- Xu, H., Zhao, Q., Song, N., Yan, Z., Lin, R., Wu, S., et al. (2020). AdipoR1/AdipoR2 dual agonist recovers nonalcoholic steatohepatitis and related fibrosis via endoplasmic reticulum-mitochondria axis. *Nat. Commun.* 11 (1), 5807. doi:10.1038/s41467-020-19668-y
- Yang, J. S., Tongson, J., Kim, K. H., and Park, Y. (2020). Piceatannol attenuates fat accumulation and oxidative stress in steatosis-induced HepG2 cells. *Curr. Res. Food Sci.* 3, 92–99. doi:10.1016/j.crrfs.2020.03.008
- Yeh, M. M., and Brunt, E. M. (2014). Pathological features of fatty liver disease. *Gastroenterology* 147 (4), 754–764. doi:10.1053/j.gastro.2014.07.056
- Younossi, Z. M., Golabi, P., de Avila, L., Paik, J. M., Srishord, M., Fukui, N., et al. (2019a). The global epidemiology of NAFLD and NASH in patients with type 2 diabetes: A systematic review and meta-analysis. *J. Hepatol.* 71 (4), 793–801. doi:10.1016/j.jhep.2019.06.021
- Younossi, Z. M., Ratziu, V., Loomba, R., Rinella, M., Anstee, Q. M., Goodman, Z., et al. (2019b). Obeticholic acid for the treatment of non-alcoholic steatohepatitis: Interim analysis from a multicentre, randomised, placebo-controlled phase 3 trial. *Lancet* 394 (10215), 2184–2196. doi:10.1016/s0140-6736(19)33041-7
- Younossi, Z. M., Stepanova, M., Nader, F., Loomba, R., Anstee, Q. M., Ratziu, V., et al. (2021). Obeticholic acid impact on quality of life in patients with nonalcoholic steatohepatitis: REGENERATE 18-month interim analysis. *Clin. Gastroenterol. Hepatol.* 20, 2050–2058.e12. doi:10.1016/j.cgh.2021.07.020
- Zamani-Garmsiri, F., Hashemnia, S. M. R., Shabani, M., Bagherieh, M., Emamgholipour, S., and Meshkani, R. (2021). Combination of metformin and genistein alleviates non-alcoholic fatty liver disease in high-fat diet-fed mice. *J. Nutr. Biochem.* 87, 108505. doi:10.1016/j.jnutbio.2020.108505
- Zeybel, M., Luli, S., Sabater, L., Hardy, T., Oakley, F., Leslie, J., et al. (2017). A proof-of-concept for epigenetic therapy of tissue fibrosis: Inhibition of liver fibrosis progression by 3-deazaneplanocin A. *Mol. Ther.* 25 (1), 218–231. doi:10.1016/j.ymthe.2016.10.004
- Zhang, P. W., Chen, F. X., Li, D., Ling, W. H., and Guo, H. H. (2015). A CONSORT-compliant, randomized, double-blind, placebo-controlled pilot trial of purified anthocyanin in patients with nonalcoholic fatty liver disease. *Med. Baltim.* 94 (20), e758. doi:10.1097/md.0000000000000758
- Zhao, W., Yan, Y., Xiao, Z., Wang, M., Xu, M., Wang, Z., et al. (2021). Bicyclol ameliorates nonalcoholic fatty liver disease in mice via inhibiting MAPKs and NF- $\kappa$ B signaling pathways. *Biomed. Pharmacother.* 141, 111874. doi:10.1016/j.biopha.2021.111874
- Zheng, Z., Zhao, Z., Li, S., Lu, X., Jiang, M., Lin, J., et al. (2017). Altenusin, a nonsteroidal microbial metabolite, attenuates nonalcoholic fatty liver disease by activating the farnesoid X receptor. *Mol. Pharmacol.* 92 (4), 425–436. doi:10.1124/mol.117.108829
- Zhou, J., Cui, S., He, Q., Guo, Y., Pan, X., Zhang, P., et al. (2020). SUMOylation inhibitors synergize with FXR agonists in combating liver fibrosis. *Nat. Commun.* 11 (1), 240. doi:10.1038/s41467-019-14138-6
- Zhou, D., and Fan, J. G. (2019). Microbial metabolites in non-alcoholic fatty liver disease. *World J. Gastroenterol.* 25 (17), 2019–2028. doi:10.3748/wjg.v25.i17.2019
- Zhu, Y., Liu, R., Shen, Z., and Cai, G. (2020). Combination of luteolin and lycopene effectively protect against the “two-hit” in NAFLD through Sirt1/AMPK signal pathway. *Life Sci.* 256, 117990. doi:10.1016/j.lfs.2020.117990





## OPEN ACCESS

## EDITED BY

Mariana Jinga,  
Carol Davila University of Medicine and  
Pharmacy, Romania

## REVIEWED BY

Sumei Liu,  
University of Wisconsin–La Crosse,  
United States  
Huang Wu,  
Shanghai University of Traditional  
Chinese Medicine, China  
Vijay Shankar,  
Clemson University, United States

## \*CORRESPONDENCE

Bo Tan,  
tannyhy@gzucm.edu.cn

<sup>†</sup>These authors have contributed equally  
to this work

## SPECIALTY SECTION

This article was submitted to  
Gastrointestinal and Hepatic  
Pharmacology,  
a section of the journal  
Frontiers in Pharmacology

RECEIVED 13 May 2022

ACCEPTED 31 October 2022

PUBLISHED 14 November 2022

## CITATION

Chen W, Liao L, Huang Z, Lu Y, Lin Y,  
Pei Y, Yi S, Huang C, Cao H and Tan B  
(2022), Patchouli alcohol improved  
diarrhea-predominant irritable bowel  
syndrome by regulating excitatory  
neurotransmission in the myenteric  
plexus of rats.  
*Front. Pharmacol.* 13:943119.  
doi: 10.3389/fphar.2022.943119

## COPYRIGHT

© 2022 Chen, Liao, Huang, Lu, Lin, Pei,  
Yi, Huang, Cao and Tan. This is an open-  
access article distributed under the  
terms of the [Creative Commons  
Attribution License \(CC BY\)](#). The use,  
distribution or reproduction in other  
forums is permitted, provided the  
original author(s) and the copyright  
owner(s) are credited and that the  
original publication in this journal is  
cited, in accordance with accepted  
academic practice. No use, distribution  
or reproduction is permitted which does  
not comply with these terms.

# Patchouli alcohol improved diarrhea-predominant irritable bowel syndrome by regulating excitatory neurotransmission in the myenteric plexus of rats

Wanyu Chen <sup>1†</sup>, Lu Liao <sup>2†</sup>, Zitong Huang <sup>1</sup>, Yulin Lu <sup>1</sup>,  
Yukang Lin <sup>3</sup>, Ying Pei <sup>1</sup>, Shulin Yi <sup>1</sup>, Chen Huang <sup>1</sup>, Hongying Cao <sup>4</sup>  
and Bo Tan <sup>1\*</sup>

<sup>1</sup>Research Centre of Basic Integrative Medicine, School of Basic Medical Sciences, Guangzhou University of Chinese Medicine, Guangzhou, China, <sup>2</sup>Shenzhen Hospital of Shanghai University of Traditional Chinese Medicine, Guangzhou, China, <sup>3</sup>College of Integrated Chinese and Western Medicines, Hunan University of Chinese Medicine, Changsha, Hunan, China, <sup>4</sup>School of Chinese Materia Medica, Guangzhou University of Chinese Medicine, Guangzhou, China

**Background and Purpose:** Irritable bowel syndrome (IBS) is usually associated with chronic gastrointestinal disorders. Its most common subtype is accompanied with diarrhea (IBS-D). The enteric nervous system (ENS) modulates major gastrointestinal motility and functions whose aberration may induce IBS-D. The enteric neurons are susceptible to long-term neurotransmitter level alterations. The patchouli alcohol (PA), extracted from *Pogostemonis Herba*, has been reported to regulate neurotransmitter release in the ENS, while its effectiveness against IBS-D and the underlying mechanism remain unknown.

**Experimental Approach:** In this study, we established an IBS-D model in rats through chronic restraint stress. We administered the rats with 5, 10, and 20 mg/kg of PA for intestinal and visceral examinations. The longitudinal muscle myenteric plexus (LMMP) neurons were further immunohistochemically stained for quantitative, morphological, and neurotransmitters analyses.

**Key Results:** We found that PA decreased visceral sensitivity, diarrhea symptoms and intestinal transit in the IBS-D rats. Meanwhile, 10 and 20 mg/kg of PA significantly reduced the proportion of excitatory LMMP neurons in the distal colon, decreased the number of acetylcholine (ACh)- and substance P (SP)-positive neurons in the distal colon and restored the levels of ACh and SP in the IBS-D rats.

**Conclusion and Implications:** These findings indicated that PA modulated LMMP excitatory neuron activities, improved intestinal motility and alleviated IBS-induced diarrheal symptoms, suggesting the potential therapeutic efficacy of PA against IBS-D.

## KEYWORDS

patchouli alcohol, irritable bowel syndrome with diarrhea, colonic longitudinal muscle myenteric plexus, excitatory neurons, intestinal motility

## 1 Introduction

The irritable bowel syndrome (IBS) is a common gastrointestinal disorder affecting physical symptoms and social functioning. Although IBS is not associated with serious complications or mortality, abdominal pain and bloating are often of chronic nature. The pathophysiological mechanisms of IBS remain unknown (Niesler et al., 2021). Several factors have been implicated, including the microbiota, the gut-brain axis (De Palma et al., 2014; Thumann et al., 2019) and psychosocial and environmental factors (Dunn and Adams, 2014; Zhu et al., 2019; van Thiel et al., 2020). The microenvironment of peripheral neurons in the gut wall is presumably involved (Buhner et al., 2014), suggesting the importance local transmitters in the mediation of abdominal pain,

discomfort and motility (Knowles et al., 2013). The diagnostic criteria of IBS changed to the Rome IV, which indicated that IBS with diarrhea (IBS-D) is the most common subtype (Ford et al., 2020; Bb et al., 2021).

The digestive system is innervated through its connections with the central nervous system (CNS) and by the enteric nervous system (ENS) within the wall of the gastrointestinal tract (Neunlist & Schemann, 2014). The ENS mainly modulates gastrointestinal motility and functions like secretion, absorption, permeability of epithelial cells and immune activities (Furness & Stebbing, 2018). In the wall of the gut, enteric neurons are susceptible to long-term changes in neurotransmitter levels that ultimately impact the gastrointestinal function (Altaf & Sood, 2008; Neunlist & Schemann, 2014). Acetylcholine (ACh) and substance P (SP) are the principal excitatory neurotransmitters (Clemens et al.,

TABLE 1 Antibodies used for immunohistochemistry.

Antigen	Host	Code	Dilution	Source
HuC/HuD	Rabbit	ab184267	1:500	Abcam
ChAT	Goat	AB144P	1:100	Chemicon
Substance P	Rat	MAB356	1:200	Chemicon
Mouse IgG	Goat Alexa Fluor 488	1010–30	1:100	SouthernBiotech
Rabbit IgG	Goat Alexa Fluor 555	4010–32	1:200	SouthernBiotech
Goat IgG	Donkey Cy3	705–165–147	1:100	Jackson
Rabbit IgG	DyLight 405	711–475–152	1:100	Jackson
Rat IgG	Donkey Alexa Fluor 488	712–545–153	1:100	Jackson

Note: ChAT, choline acetyltransferase; IgG, immunoglobulin G; Cy3, indocarbocyanine.

TABLE 2 Primer sequences.

Gene	Forward primer (5'–3')	Reverse primer (5'–3')
SP	TTAATGGGCAAACGGGATGC	GCGCTTCTTCATAAGCCACAG
ChAT	TTGTGCAAGCCATGACTGAC	ATGGTTGTCAATGGCCATGC
GAPDH	TGAGCATCTCCCTCACAATTCC	TTTTTGAGGGTGCAGCGAAC

TABLE 3 Antibodies used for western blot.

Antigen	Host	Code	Dilution	Source
ChAT	Goat	AB144P	1:1000	Chemicon
Substance P	Rat	MAB356	1:1000	Chemicon
Rabbit anti-Goat IgG (h + l)	HRP	FDR007	1:5000	Fudebio
Goat anti-Rat IgG (h + l)	HRP	FDM007	1:5000	Fudebio

Note: ChAT, choline acetyltransferase; IgG, immunoglobulin G; Cy3, indocarbocyanine.

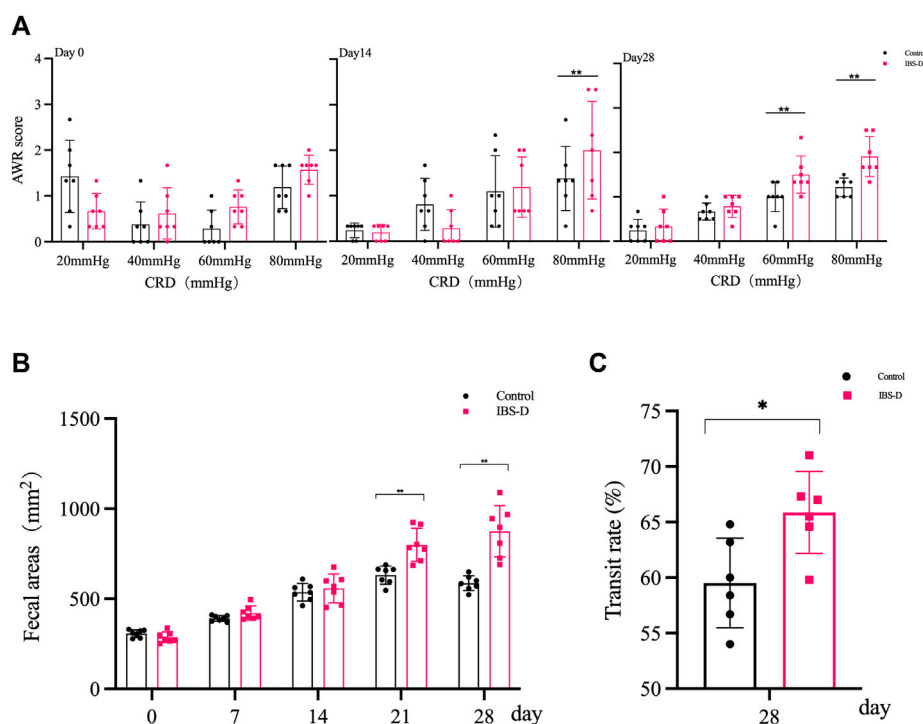


FIGURE 1

Evaluation of the IBS-D model. (A) Abdominal withdrawal reflex assessment in IBS-D rats. The AWR scores were used to assess visceral sensitivity in IBS-D rats at baseline, day 14 and day 28. (B) The defecation area evaluated diarrhea symptoms at baseline, day 7, day 14, day 21, and day 28 in different groups. (C) The intestinal transit rate revealed the changes in colon motility among model groups. Data are presented as mean  $\pm$  SD ( $n = 6$ ). \*\* $p < 0.01$  vs. controls, \* $p < 0.05$  vs. controls.

2003). In the gastrointestinal tract, Ach transmits excitatory signals through the receptors expressed by smooth muscle cells. SP can cause contractions of the smooth muscles, promoting intestinal peristalsis and provoking diarrhea (Smith et al., 2007).

The patchouli alcohol (PA) is a tricyclic sesquiterpene extracted from *Pogostemonis Herba* (Cho et al., 2015). PA has been associated with different pharmacological effects, including anti-inflammatory, antibacterial and anticancer properties (Hu et al., 2017). In addition, PA regulates colonic smooth muscle activity through cholinergic and non-cholinergic nerves. Zhou et al. (2018) reported that PA might potentially treat IBS-D by influencing the neurotransmitter release in the ENS. Although PA may affect the release of gastrointestinal transmitters through multiple pathways and targets, whether it would be of benefit for IBS-D is unknown.

## 2 Methods

### 2.1 Animals and treatments

Fifty-four male Sprague-Dawley rats were randomly divided into six model groups and three control groups

( $n = 6$  per group). Initially, rats in model groups were stressed between 4:00 and 6:00 p.m. for 14 days. The upper limbs, shoulders and chest were bound with a medical elastic mesh bandage, the rats were restricted from scratching the head and face, but other activities were not restricted. After modeling, the rats were divided into three model groups and three PA groups with low (5 mg/kg), medium (10 mg/kg), and high (20 mg/kg) doses. PA groups received gavage administration for 2 weeks, while control and model groups received an equal volume of Tween 80.

### 2.2 Visceral sensitivity assessment

Behavioral responses to colorectal distention (40 and 60 mmHg) were assessed by measuring the abdominal withdrawal reflex (AWR) on day 14, day 21, and day 28 after modeling, as previously described (Williams et al., 1988). Briefly, rats were anesthetized with diethyl ether after fasting for 12 h. Then, a catheter was inserted through the anus and the outer end of the distention balloon was secured by taping the attached

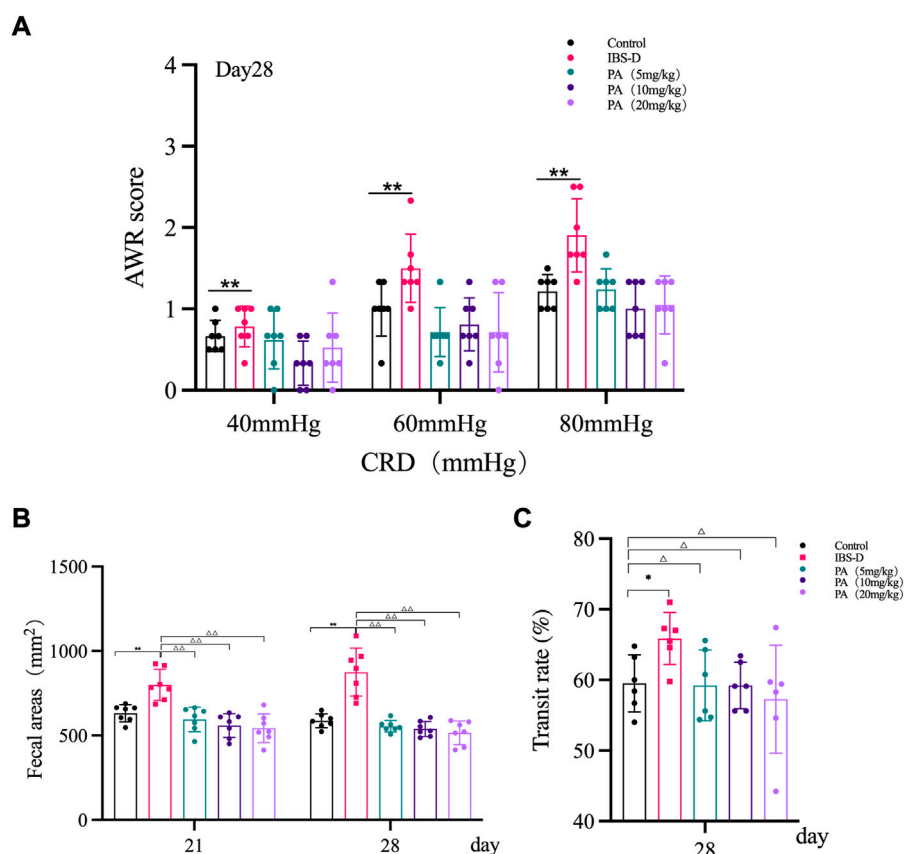


FIGURE 2

Effects of patchouli alcohol (PA) in IBS-D rats. (A) Abdominal withdrawal reflex assessment in different groups after PA. The AWR scores were used to assess visceral sensitivity at day 21 and day 28 after PA. (B) The defecation area evaluated diarrhea symptoms at day 7 and day 14 after PA. (C) The intestinal transit rate revealed the changes in colon motility among PA groups. Data are presented as mean  $\pm$  SD ( $n = 6$ ). \* $p < 0.05$ , \*\* $p < 0.01$ , vs. controls;  $\Delta p < 0.05$ ,  $\Delta\Delta p < 0.01$ , vs. models.

tubing to the rat's tail. After adaption for 1 h, animal responses to colorectal distention were blindly examined by two investigators.

## 2.3 Evaluation of defecation

On day 14, day 21, and day 28 after modeling, rats were placed individually in clean cages with food and water *ad libitum*. The defecation area was monitored within 4 h and evaluated with the ImageJ Software.

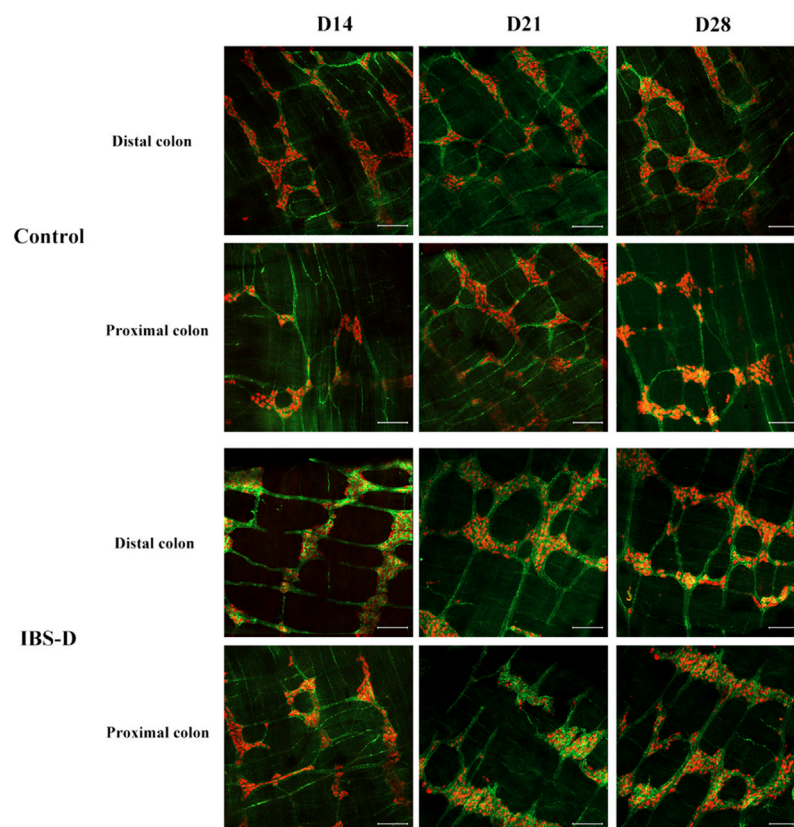
## 2.4 Intestinal transit

After modeling, rats fasted for 24 h with free access to water on day 14, day 21, and day 28. Then, they received 1 ml of powdered carbon (Activated Carbon Powder) *via* gastric

gavage. Thirty minutes later, rats were euthanized and the bowel was removed. The length of the intestinal tract from the gastroduodenal junction to the anus and the length of the tract containing the carbon were measured. The intestinal transit rate was calculated through the following equation: length of the intestinal tract containing the carbon/length of the intestinal tract  $\times 100\%$ .

## 2.5 Tissues preparation

The colon was dissected and placed in ice-cold Krebs solution. The Krebs solution was pretreated with 95% oxygen and 5% CO<sub>2</sub> for at least 30 min. Then, the colon was cut into several segments and flushed with ice-cold Krebs solution to clean the fecal matter. The longitudinal muscle myenteric plexus (LMMP) was separated and placed on polylysine glass slides. Cold paraformaldehyde (PFA) was

**FIGURE 3**

Substance P (SP) was altered in IBS-D rats. SP proteins photographed by laser confocal microscopy. Immunofluorescence results of SP positive neurons in the proximal and distal colon of IBS-D rats at day 14, day 21, and day 28. HuC/D (Red), SP(Green). Scale Bar = 100  $\mu$ m.

added in 0.1 M of sodium phosphate buffer saline (PBS) and LMMP was bathed for 4–6 h at 4°C. After fixture, the samples were washed with PBS and cryoprotected overnight with 30% sucrose dissolved in PBS at 4°C. The longitudinal muscle strips were separated with the same procedure and placed at liquid nitrogen for RNA extraction.

## 2.6 Immunohistochemistry

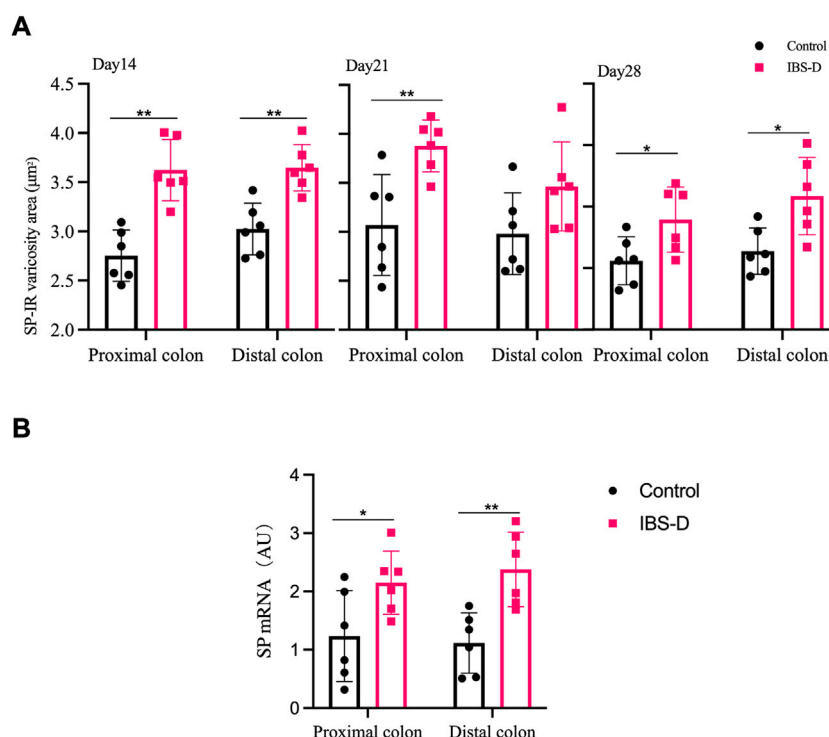
After cryoprotection, LMMP was rinsed with PBS and cut into 10 \* 10 mm pieces. Tissue wholemounts were placed in 5% bovine serum albumin and 0.3% Triton X-100 in PBS for 2 h at room temperature. Later, LMMP samples were exposed to primary antibodies diluted in PBS at 4°C for 21–24 h. The wholemounts were washed with PBS supplemented with 0.05% tween-20 (TPBS) for 5 min and rinsed three times with PBS (5 min each time). Then, the samples were incubated with secondary antibodies for 2 h at room temperature. After incubation, tissue wholemounts were rinsed with TPBS for 15 min, washed with PBS (5 min

each time) and coverslipped with fluorescence decay-resistant medium. Concerning choline acetyltransferase (ChAT) and SP immunohistochemistry, tissue wholemounts were heated by water-bath for antigen retrieval. Briefly, samples were placed in 0.01 M citrate buffer (pH 6.0) and heated for 10 min at 100°C. After being washed three times with PBS, the samples were cut into pieces and blocked in 10% donkey serum albumin and 0.3% Triton X-100 in PBS. Primary and secondary antibodies used in this study are provided in [Table 1](#).

## 2.7 Quantitative analysis

The quantitative analysis for immunoreactive neurons was performed according to the neuronal density (neurons/mm<sup>2</sup>). Images were obtained using a 10X microscope objective. The ImageJ software was used to calculate the proportion of ChAT-positive and SP-positive neurons.



**FIGURE 4**

(A) SP-immunoreactive varicosities in the distal and proximal colon. (B) SP mRNA expression in model groups. RNA was isolated with TRIzol reagent and qRT-PCR was utilized to analyze the gene expression of SP. The GAPDH gene was defined as internal reference. Data were presented as mean  $\pm$  SD ( $n = 6$ ). \* $p < 0.05$ , \*\* $p < 0.01$ , vs. controls.

## 2.8 Morphological analysis

The morphometric analysis of HuC/D-immunoreactive neurons was performed in an area ( $\mu\text{m}^2$ ) with 100 neuronal cell bodies. Regarding the SP-immunoreactive neurons, an average area of 400 nerve varicosities from each animal (2,400/group) was used for morphometric analysis.

## 2.9 The mRNA quantification

The total RNA was extracted from LMMP preparations through the TRIzol Reagent method (GIBCO, US). The concentration of mRNAs was evaluated by quantitative polymerase chain reaction (qPCR) analysis. The qPCR was performed using CFX 96 Real-Time Detection System (Bio-Rad, Germany). The concentration was normalized for RNA loading using GAPDH primers. Sequences of the PCR primers are listed in Table 2.

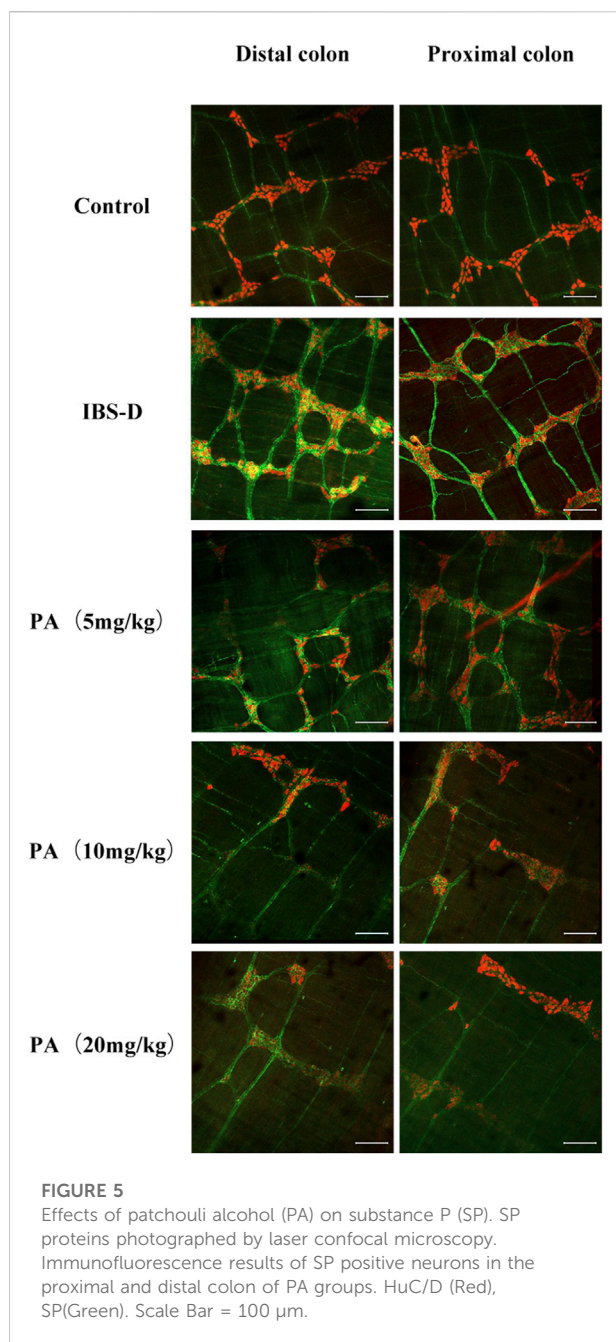
## 2.10 Western blot

The LMMP layers were frozen in liquid nitrogen and stored at  $-80^\circ\text{C}$  until processed. Then, cell lysis was

performed with ice-cold RIPA lysis buffer and protease inhibitor cocktail. The total protein concentrations in the extracts were measured with a BCA protein assay kit (Pierce). The membranes were blocked for 1 h at room temperature with nonfat dry milk in Tris-buffered saline (TBS) supplemented with 0.1% tween-20 and incubated overnight with primary antibodies at  $4^\circ\text{C}$ . After repeated washing, the membranes were incubated with a horseradish peroxidase-conjugated anti-rabbit secondary antibody at room temperature for 2 h and visualized with a chemiluminescence substrate. Primary and secondary antibodies used in this study are provided in Table 3.

## 2.11 Statistical analysis

Data are presented as mean  $\pm$  standard deviation (SD). Group comparisons were performed using the one-way ANOVA test. Values of  $p < 0.05$  were considered statistically significant. Tukey's post hoc test was then used to compare significant differences between groups. Statistical analysis was performed using GraphPad Prism software.



## 2.12 Patchouli alcohol

Patchouli alcohol (purity >99%) was kindly provided by the Mathematical Engineering Academy of Chinese Medicine, and the quality of PA was confirmed by melting point, infrared spectroscopy,  $^1\text{H}$  and  $^{13}\text{C}$  NMR, and mass spectrometry. DMSO was used to dissolve PA. DMSO <0.5% in all experiments.

## 3 Results

### 3.1 Patchouli alcohol improved intestinal symptoms in Irritable bowel syndrome with diarrhea rats

#### 3.1.1 Visceral sensitivity

As shown in Figure 1A, the AWR scores of the model group were significantly increased at day 14 and day 28 compared to the control group ( $p < 0.01$ ), indicating the occurrence of visceral hypersensitivity. As shown in Figure 2A, at day 28 the AWR scores of each PA group were significantly reduced compared to the model group ( $p < 0.05$  and  $p < 0.01$ ).

#### 3.1.2 Diarrhea symptoms

As shown in Figure 1B, the defecation area in the model group was significantly increased at day 21 and day 28 compared to the control group ( $p < 0.01$ ), indicating that the defecation frequency increased in the model group. As shown in Figure 2B, the defecation area in each PA group significantly decreased compared to the model group ( $p < 0.01$ ).

#### 3.1.3 Intestinal transit

As shown in Figure 1C, the intestinal transit rate was faster in the model group than the control group. The rate in the model group was  $65.9 \pm 0.87\%$ , while the rate in the control group was  $59.5 \pm 4.0\%$  ( $n = 6$ ,  $p = 0.032$ ). As shown in Figure 2C, the intestinal transit rate significantly decreased after treatment with PA.

### 3.2 Patchouli alcohol improved intestinal motility by modulating excitatory neurotransmitters

#### 3.2.1 Substance P

As shown in Figures 3, 4A, immunofluorescence results showed that SP-immunoreactive neurons were significantly increased in the model group compared to the control group ( $p < 0.05$ ). As shown in Figure 4B, the qRT-PCR analysis revealed significantly increased SP expression in the distal and proximal colon of the IBS-D group compared with the control group ( $p < 0.05$ ). As shown in Figure 5, Figure 6A, after treatment with PA for 14 days, the area of SP-immunoreactive varicosities in the distal and proximal colon was significantly decreased in the PA group compared with the IBS-D group ( $p < 0.01$ ). As shown in Figure 6B, the expression of SP mRNA in

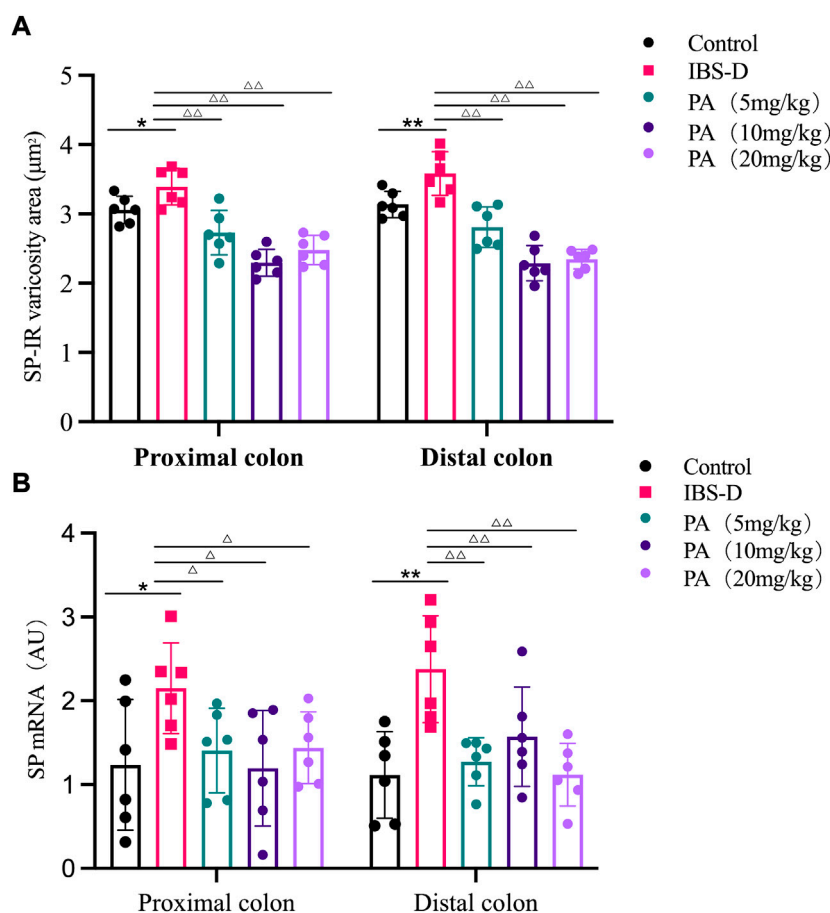


FIGURE 6

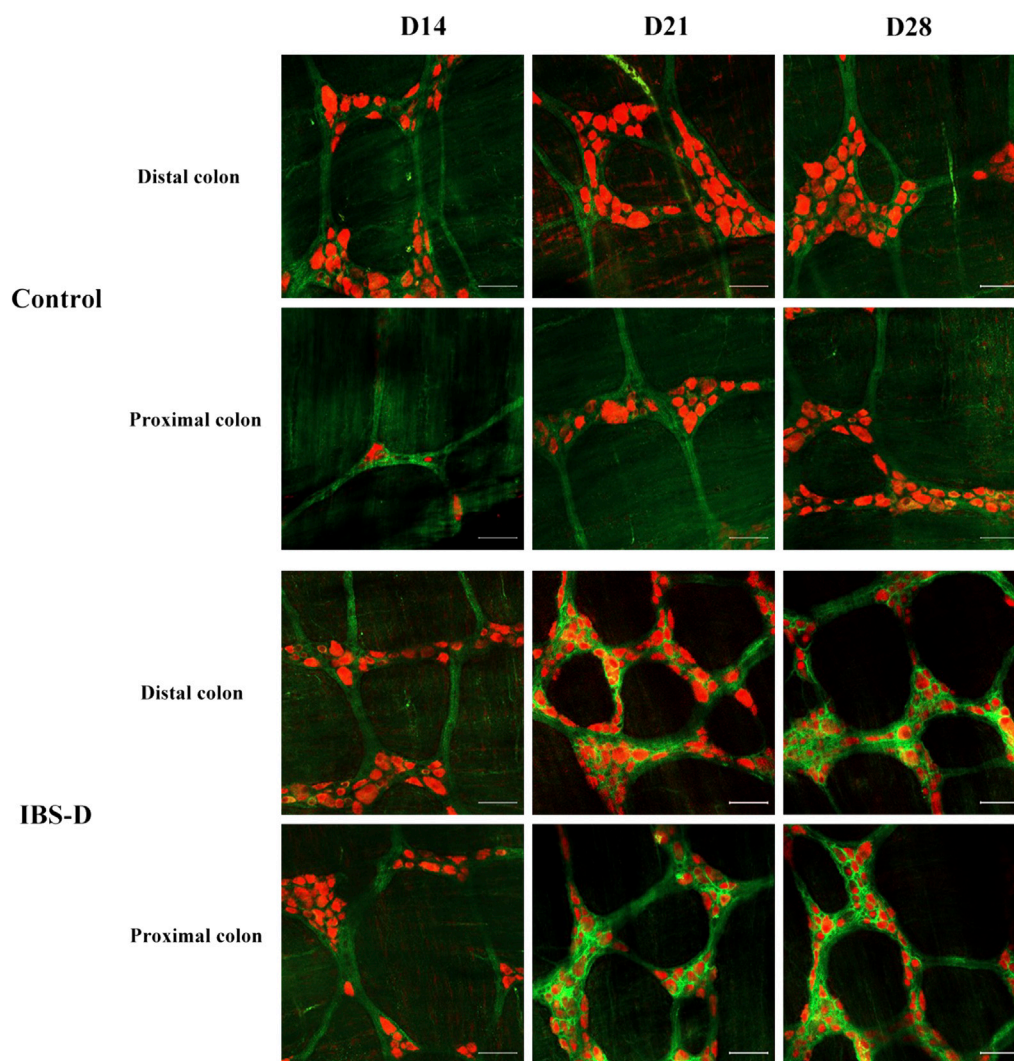
(A) SP-immunoreactive varicosities in the distal and proximal colon of PA groups. (B) SP mRNA expression in PA groups. RNA was isolated with TRIzol reagent and qRT-PCR was utilized to analyze the gene expression of SP. The GAPDH gene was used as internal reference. Data are presented as mean  $\pm$  SD ( $n = 6$ ). \* $p < 0.05$ , \*\* $p < 0.01$ , vs. controls. ^ $p < 0.05$ , vs. models, ^^ $p < 0.01$ , vs. models.

the distal and proximal colon was significantly decreased in the PA group compared with the IBS-D group ( $p < 0.05$ ).

As shown in Figures 11, 12A, western blot revealed a specific band at approximately 40 kDa in LMMP preparations, representing a post-translational modification of SP. The expression of SP in the proximal colon of the model group was significantly increased compared with the control group ( $p < 0.05$ ). The expression of SP in the distal colon was not significantly elevated. After administration of PA for 14 days, SP levels were downregulated in the distal and proximal colon.

### 3.2.2 Choline acetyltransferase

As shown in Figures 7, 8A, the proportion of ChAT positive neurons in the distal colon of IBS-D rats was significantly increased ( $p < 0.01$ ). At the same time, there was no significant difference in the proximal colon between the two groups. As shown in Figure 8B, the qRT-PCR analysis revealed significantly increased ChAT expression in the distal colon of IBS-D rats ( $p < 0.05$ ). As shown in Figure 9 and Figure 10A, the proportion of ChAT positive neurons in the distal colon was significantly decreased after treatment with PA ( $p < 0.01$ ), and as shown in Figure 10B, ChAT mRNA expression levels was significantly decreased in the PA group.

**FIGURE 7**

Choline acetyltransferase (ChAT) is altered in IBS-D rats. ChAT proteins photographed by laser confocal microscopy. Immunofluorescence results of ChAT positive neurons in the proximal and distal colon of IBS-D rats at day 14, day 21, and day 28. HuC/D (Red), ChAT (Green). Scale Bar = 50  $\mu$ m.

compared with the IBS-D group ( $p < 0.05$ ). On the contrary, the expression of ChAT in the distal colon of IBS-D rats increased ( $p < 0.05$ ). The expression of ChAT in the proximal colon was not significantly elevated. After administration of PA for 14 days (D28), the expression of ChAT in the proximal colon decreased.

As shown in Figures 11, 12B, western blot found a significant difference regarding the expression of ChAT between the high dose group and the model group after PA administration ( $p = 0.003$ ). A significant difference was also found between the model group and the control group ( $p = 0.003$ ). At D28, the expression of ChAT in the distal colon of high, medium and low dosing groups was significantly downregulated ( $p = 0.001$ ,  $p < 0.01$  and

$p < 0.01$ , respectively). High dose of PA treatment significantly decreased ChAT protein expression in the proximal colon comparing to the model group.

## 4 Discussion

Different physiological activities of the intestine depend on neurons. The ENS is a critical controller of the innervation of the large intestine (Bayliss & Starling, 1901), but its relevance in gastrointestinal diseases has largely been overlooked (Furness, 2012; Knowles et al., 2013; Spencer & Hu, 2020). Previous studies identified

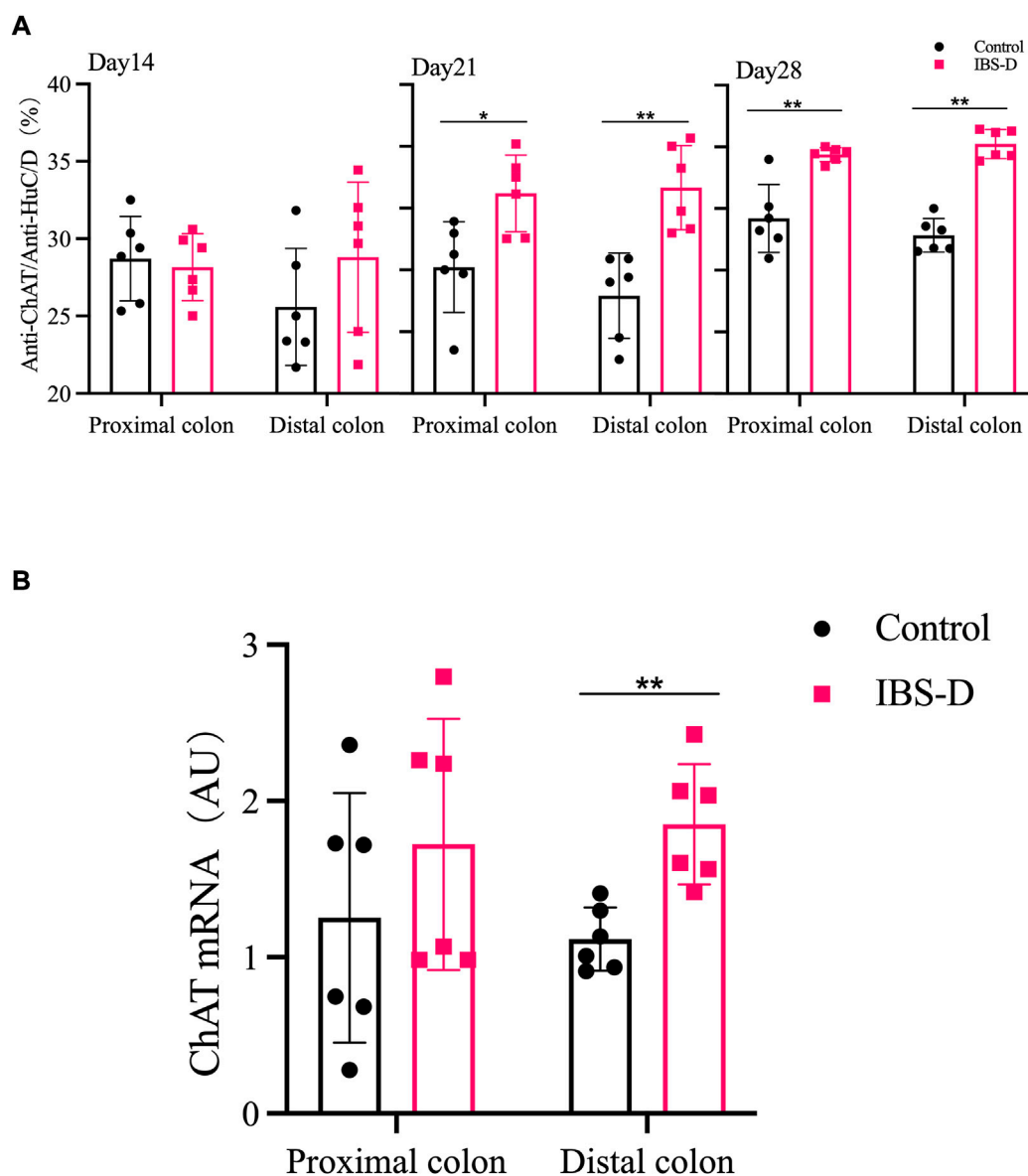


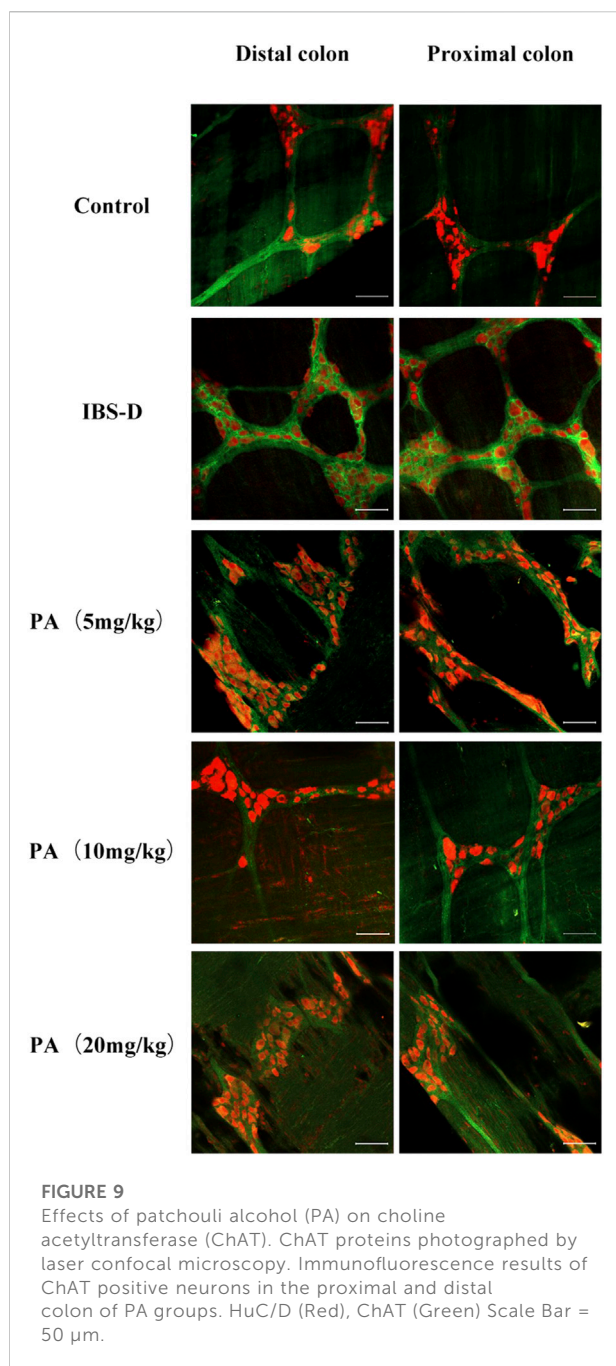
FIGURE 8

(A) The proportion of ChAT positive neurons in the distal and proximal colon. (B) ChAT mRNA expression in model groups. RNA was isolated with TRIzol reagent and qRT-PCR was used to analyze the gene expression of ChAT. The GAPDH gene was used as internal reference. Data are presented as mean  $\pm$  SD ( $n = 6$ ). \* $p < 0.05$ , \*\* $p < 0.01$ , vs. controls.

the relationship between intestinal activity and neurons in different regions of the colon (Costa et al., 2013). Li et al. (2019) designed a  $Ca^{2+}$  imaging approach revealing that different regions of the gut exhibited specific motility patterns regulated by myenteric neurons. Hibberd et al. (2018) found that optogenetic control of enteric neurons can increase gut motility and fecal output. However, local effects of myenteric neurons on intestinal function have

been insufficiently investigated in drug development. In this study, we focused on the neuronal activities of the myenteric plexus, which innervates the longitudinal and circular muscles in the intestine. We used a previously implemented technique isolating LMMP preparations to observe the morphological changes of the entire colon (Huang et al., 2021). Immunoreactivity for ChAT and SP identified the corresponding neurons in the myenteric





plexus (Sang & Young, 1996; Sang et al., 1997). The aim of the present study was to investigate the ENS remodeling in rats with IBS-D and the potential mechanisms of PA for IBS-D treatment. In the wrap-restraint stressed IBS-D rats, the total number of neurons increased in the myenteric plexus

of the distal colon, as indicated by an increased number of varicosities and an augmented expression of ChAT and SP. Previous studies found that stress increased colonic motility in animals and human volunteers (Williams et al., 1988). In animal models, diarrhea associated with stress may be related to a local imbalance of neurotransmitters. We further investigated the effects of PA, demonstrating that PA significantly decreased the number of neurons, reduced varicosities and restored the expression of SP and ChAT to normal levels. These findings suggested that PA might restore the local imbalance of neurotransmitters in the colonic myenteric plexus.

Our rat model of IBS-D was optimized through wrap-restraint stress as a single inducing factor. After 2 weeks, the IBS-D rats were characterized by an increased defecation area and augmented AWR responses to rectal distention, mimicking some clinical traits of IBS-D. This model can be reproducible and could therefore be utilized to investigate IBS-D and the mechanism of action of potential drugs. Interestingly, our study indicated that PA was beneficial in IBS-D rats by ameliorating intestinal transit and visceral hypersensitivity.

PA is an active ingredient of *Pogostemonis Herba*, an herb used for vomiting, diarrhea and other gastrointestinal diseases. Studies have shown that patchouli alcohol extracted from patchouli can produce antifungal and anti-inflammatory pharmacological effects, enhance the body's resistance; PA also has a bidirectional effect on the stomach and intestines, promote gastric acid secretion, enhance gastrointestinal activity, regulate digestive function, while calming the smooth muscle of the gastrointestinal tract, and alleviate the spasmodic contraction of the gastrointestinal tract caused by irritating substances; Reduce the activity of enzymes that reflect gastrointestinal inflammation, prevent ulcerative gastroenteritis, protect the gastrointestinal mucosal barrier. (Chen et al., 1998; Hu et al., 2017; Liu et al., 2017). Previously, we showed that PA exerted an inhibitory effect on the spontaneous contraction of the colonic longitudinal smooth muscle in IBS-D rats (Sah et al., 2011). In this study, we showed that PA can downregulate the expression of ChAT by influencing proximal and distal colonic myenteric neurons.

At present, many animal models of IBS-D have been studied. Different animal models may reflect several pathological aspects of the disease, resulting in heterogeneous and inconsistent results. For example, the proportion of ChAT-immunoreactive neurons was significantly increased in the model of water avoidance

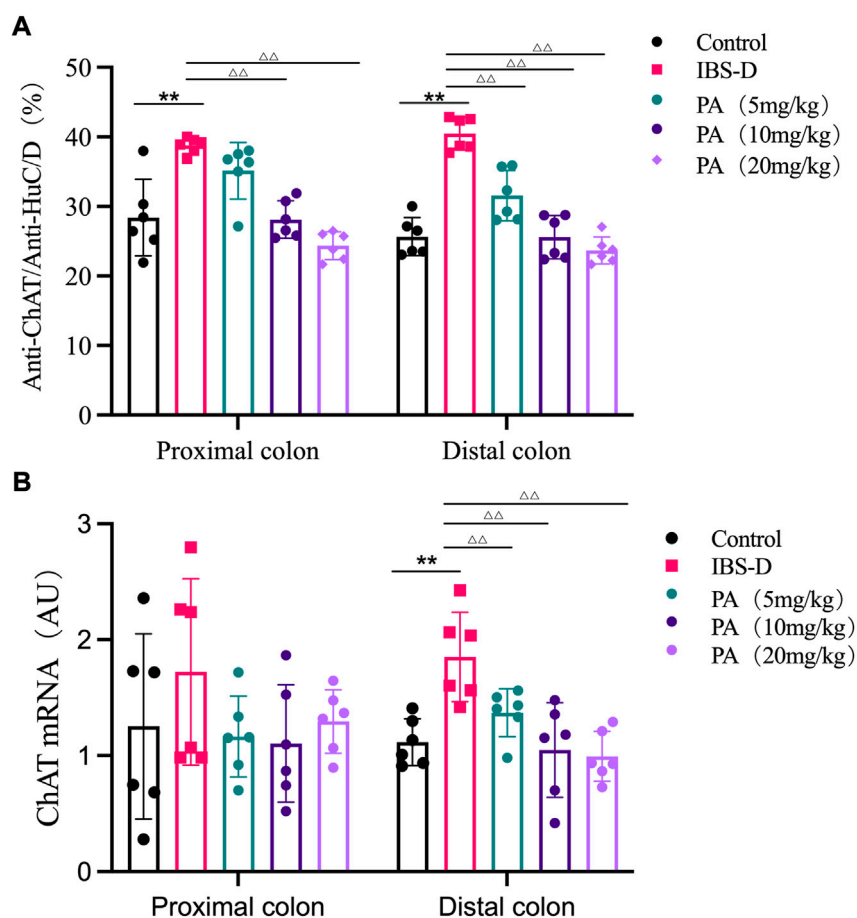


FIGURE 10

(A) The proportion of ChAT positive neurons in the distal and proximal colon of PA groups. (B) ChAT mRNA expression in PA groups. RNA was isolated with Trizol reagent and qRT-PCR was utilized to analyze the gene expression of ChAT. The GAPDH gene was used as internal reference. Data are presented as mean  $\pm$  SD ( $n = 6$ ). \* $p < 0.05$ , \*\* $p < 0.01$ , vs. controls.  $\Delta p < 0.05$ , vs. models,  $\Delta\Delta p < 0.01$ , vs. models.

stress (MAS), compared with controls. At the same time, no difference was found regarding the total number of neurons (Aubert et al., 2019).

The IBS-D disorder is closely related to an abnormal activation and proliferation of gastrointestinal neurons. Recent studies have demonstrated that the proliferation of gastrointestinal neurons is finely balanced. On the one hand, apoptotic neurons are efficiently removed by macrophages. On the other hand, the homeostasis of gastrointestinal neurons mainly depends on enteric glial cells with neuronal stem/progenitor properties (ENPCs). The enteric glial cells interact with neurons and participate in the regulation of gastrointestinal motility (Rao et al., 2017). In the gastrointestinal tract of

mice, ENPCs can replace about 90% of neurons in around 2 weeks. Selective knockdown of PTEN gene in glial cells contributed to the regeneration of neurons (Kulkarni et al., 2017). If nestin and glial cells were selectively knocked out, the neurons proliferated (Kulkarni et al., 2017). In a rat model of constipation irritable bowel syndrome (IBS-C), the total number of neurons and the subtypes of excitatory and inhibitory neurons changed significantly. The total number of neurons per high-power field increased, while the proportion of cholinergic acetyltransferase immunoreactive neurons and activated vasoactive intestinal peptide positive neurons decreased. The proportion of NOS positive neurons increased, suggesting

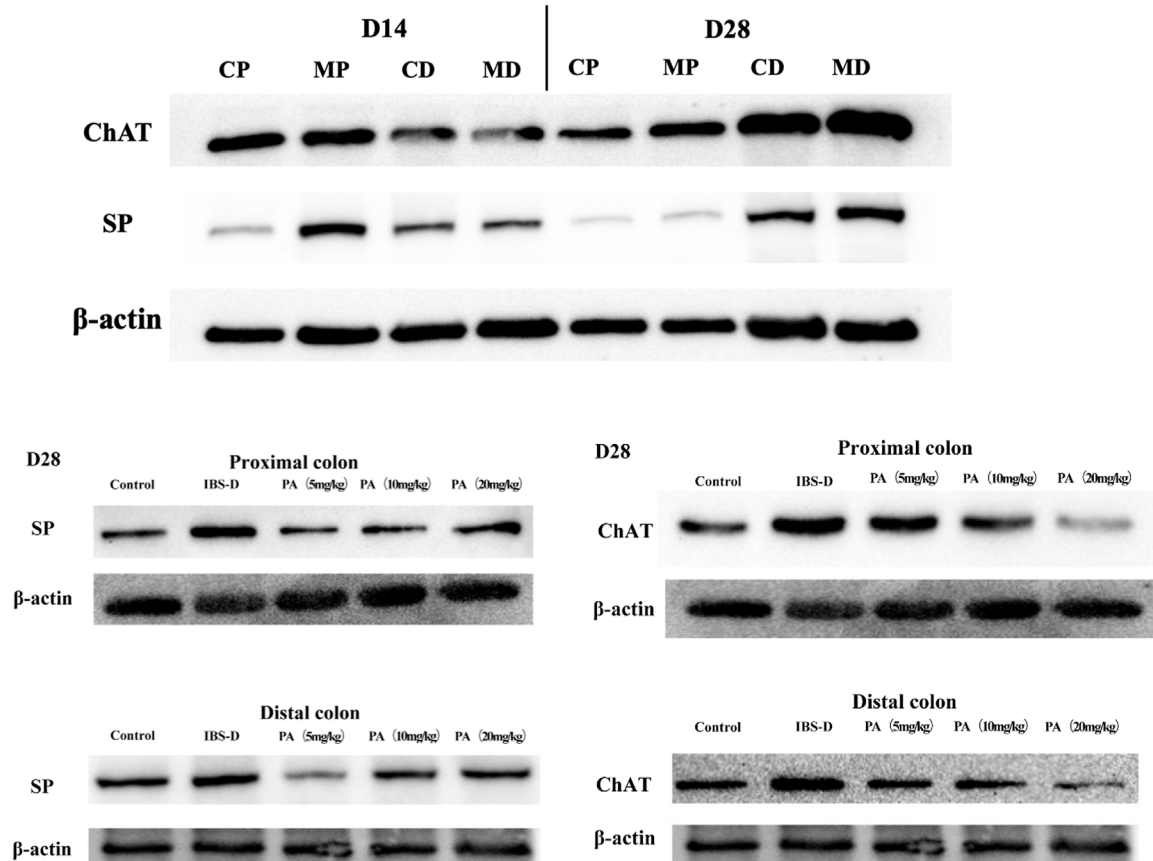


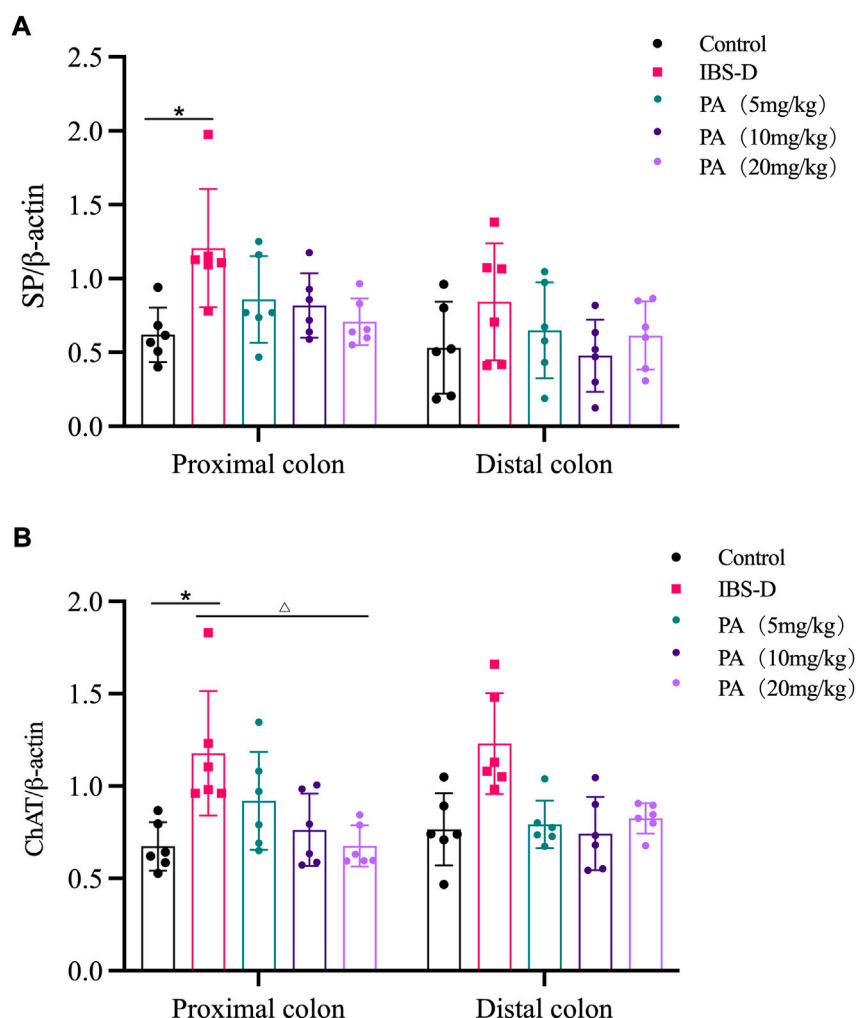
FIGURE 11

Effects of patchouli alcohol (PA) on substance P (SP) and choline acetyltransferase (ChAT) protein expression (SP and ChAT bands). SP and ChAT proteins were quantified by western blot. CP = proximal colon in control groups, CD = distal colon in control groups, MP = proximal colon in model groups, MD = distal colon in model groups.

that these changes might be relevant in the pathogenesis of IBS-C (Fei et al., 2018).

The intestinal neurons, along with the microbiota, immune and glial cells have a key role in IBS-D (Collins et al., 2014; Neunlist et al., 2014; Sharkey, 2015; Veiga-Fernandes & Pachnis, 2017; Yoo & Mazmanian, 2017; Chandrasekharan et al., 2019). In a series of recent studies, the mouse and human gut advanced our understanding of the ENS (Amit et al., 2018; Drokhyansky et al., 2020; Elmentaite et al., 2021; May-Zhang et al., 2021). A single-cell transcriptome analysis revealed different myenteric neuron classes in the small intestine of the mouse (Morarach et al., 2021). A comprehensive atlas of the cellular landscape across the

human intestine was suggested by different studies (Elmentaite et al., 2021; Holloway et al., 2021). Another research provided new compelling evidence revealing the role of the ENS on immune cells. IL-6 secreted by enteric neurons was able to influence the number and phenotypes of regulatory T cells, which in turn modulated the structure and activity of ENS (Yan et al., 2021). In the future, the role of ENS in IBS-D will be further clarified. The use of more advanced technology such as transcriptomics and neuroimmunology will shed more light on enteric neural circuits and their relevance in gut motility, helping us to explore novel strategies to prevent or treat gastrointestinal diseases.

**FIGURE 12**

Effects of patchouli alcohol (PA) on substance P (SP) and choline acetyltransferase (ChAT) protein expression. SP and ChAT proteins were quantified by western blot.  $\beta$ -actin was used as internal reference. **(A)** SP protein in the distal and proximal colon of PA groups. **(B)** ChAT protein in the distal and proximal colon of PA groups. Data are presented as mean  $\pm$  SD ( $n = 6$ ). \* $p < 0.05$ , vs. controls.  $\Delta p < 0.05$ , vs. models.

## Data availability statement

The original contributions presented in the study are included in the article/supplementary material, further inquiries can be directed to the corresponding author.

## Ethics statement

This study and included experimental procedures were approved by the Institutional Animal Care and Use Committee of Guangzhou University of Chinese Medicine (approval No. 20210316003). All animal housing and

experiments were conducted in strict accordance with the institutional Guidelines for Care and Use of Laboratory Animals.

## Author contributions

WC: Designed The Research Studies, Writing, Investigation. LL: Conducted Experiments, Data Analysis, Investigation. ZH: Conducted Experiments. YL: Conducted Experiments. YL: Assisted Experiments. YP: Assisted Experiments. SY: Investigation. CH: Investigation. HC: Supervision, Project administration. BT: Supervision, Obtained Funding, Project administration.

## Funding

This work was funded by National Natural Science Foundation of China (grant number 8197141628); Key Project of Department of Education of Guangdong Province (grant number 2022ZDZX2019); “Double First-class” and High-level University Discipline collaborative innovation team project of Guangzhou University of Chinese Medicine (grant number 2021xk37).

## Conflict of interest

The authors declare that the research was conducted in the absence of any commercial or financial relationships that could be construed as a potential conflict of interest.

## References

- Altaf, M. A., and Sood, M. R. (2008). The nervous system and gastrointestinal function. *Dev. Disabil. Res. Rev.* 14 (2), 87–95. doi:10.1002/ddrr.15
- Amit, Z., Hannah, H., Peter, L., Anna, J., Fatima, M., Job, V., et al. (2018). Molecular architecture of the mouse nervous system. *Cell* 174 (4), 999e1022–1014. doi:10.1016/j.cell.2018.06.021
- Aubert, P., Oleynikova, E., Rizvi, H., Ndjim, M., Le Berre-Scoull, C., Grohard, P., et al. (2019). Maternal protein restriction induces gastrointestinal dysfunction and enteric nervous system remodeling in rat offspring. *FASEB J. official Publ. Fed. Am. Soc. Exp. Biol.* 33 (1), 770–781. doi:10.1096/fj.201800079R
- Bayliss, W. M., and Starling, E. H. (1901). The movements and the innervation of the large intestine. *J. Physiol.* 26 (1–2), 107–118. doi:10.1113/jphysiol.1900.sp000825
- Bb, A., Cjm, B., Pevs, A., and Pacfc, D. (2021). Global prevalence of functional constipation according to the Rome criteria: A systematic review and meta-analysis. *Lancet Gastroenterology Hepatology* 6, 638–648. doi:10.1016/s2468-1253(21)00111-4
- Buhner, S., Braak, B., Li, Q., Kugler, E., Klooker, T., Wouters, M., et al. (2014). Neuronal activation by mucosal biopsy supernatants from irritable bowel syndrome patients is linked to visceral sensitivity. *Exp. Physiol.* 99 (10), 1299–1311. doi:10.1113/expphysiol.2014.080036
- Chandrasekharan, B., Saeedi, B., Alam, A., Houser, M., Srinivasan, S., Tansey, M., et al. (2019). Interactions between commensal bacteria and enteric neurons, via FPR1 induction of ROS, increase gastrointestinal motility in mice. *Gastroenterology* 157 (1), 179–192. e172. doi:10.1053/j.gastro.2019.03.045
- Chen, X., He, B., Li, X., and Luo, J. (1998). Effects of herba Pogostemonis on gastrointestinal tract. *Zhong yao cai = Zhongyaocai = J. Chin. Med. Mater.* 21 (9), 462–466.
- Cho, S. I., Lim, C. Y., Kim, B. Y., and Lim, S. H. (2015). Effects of Pogostemon cablin Blanco extract on hypoxia induced rabbit cardiomyocyte injury. *Pharmacogn. Mag.* 11 (42), 311–319. doi:10.4103/0973-1296.153084
- Clemens, C., Samsom, M., Henegouwen, G., and Smout, A. (2003). Abnormalities of left colonic motility in ambulant nonconstipated patients with irritable bowel syndrome. *Dig. Dis. Sci.* 48 (1), 74–82. doi:10.1023/a:1021734414976
- Collins, J., Borojcic, R., Verdu, E., Huizinga, J., and Ratcliffe, E. (2014). Intestinal microbiota influence the early postnatal development of the enteric nervous system. *Neurogastroenterol. Motil.* 26 (1), 98–107. doi:10.1111/nmo.12236
- Costa, M., Dodds, K., Wiklundt, L., Spencer, N., Brookes, S., and Dinning, P. (2013). Neurogenic and myogenic motor activity in the colon of the Guinea pig, mouse, rabbit, and rat. *Am. J. Physiol. Gastrointest. Liver Physiol.* 305 (10), G749–G759. doi:10.1152/ajpgi.00227.2013
- De Palma, G., Collins, S., and Bercik, P. (2014). The microbiota-gut-brain axis in functional gastrointestinal disorders. *Gut microbes* 5 (3), 419–429. doi:10.4161/gmic.29417
- Drokhlyansky, E., Smillie, C., Van Wittenberghe, N., Ericsson, M., Griffin, G., Eraslan, G., et al. (2020). The human and mouse enteric nervous system at

## Publisher's note

All claims expressed in this article are solely those of the authors and do not necessarily represent those of their affiliated organizations, or those of the publisher, the editors and the reviewers. Any product that may be evaluated in this article, or claim that may be made by its manufacturer, is not guaranteed or endorsed by the publisher.

## Supplementary material

The Supplementary Material for this article can be found online at: <https://www.frontiersin.org/articles/10.3389/fphar.2022.973612/full#supplementary-material>

single-cell resolution. *Cell* 182 (6), 1606–1622. e1623. doi:10.1016/j.cell.2020.08.003

Dunn, T. N., and Adams, S. H. (2014). Relations between metabolic homeostasis, diet, and peripheral afferent neuron biology. *Adv. Nutr.* 5, 386–393. doi:10.3945/an.113.005439

Elmentaite, R., Kumasaka, N., Roberts, K., Fleming, A., Dann, E., King, H., et al. (2021). Cells of the human intestinal tract mapped across space and time. *Nature* 597 (7875), 250–255. doi:10.1038/s41586-021-03852-1

Fei, G., Fu-Jing, H. U., Fan, W. J., Liang, L. X., Fang, X. C., and Gastroenterology, D. O. (2018). Changes in submucosal plexus neurons of colon in a rat model of irritable bowel syndrome with constipation. *Basic & Clin. Med.*

Ford, A., Sperber, A., Corsetti, M., and Camilleri, M. (2020). Irritable bowel syndrome. *Lancet (London, Engl.)* 396 (10263), 1675–1688. doi:10.1016/s0140-6736(20)31548-8

Furness, J. B. (2012). The enteric nervous system and neurogastroenterology. *Nat. Rev. Gastroenterol. Hepatol.* 9 (5), 286–294. doi:10.1038/nrgastro.2012.32

Furness, J., and Stebbing, M. (2018). The first brain: Species comparisons and evolutionary implications for the enteric and central nervous systems. *Neurogastroenterol. Motil.* 30 (2), e13234. doi:10.1111/nmo.13234

Hibberd, T., Feng, J., Luo, J., Yang, P., Samineni, V., Gereau, R., et al. (2018). Optogenetic induction of colonic motility in mice. *Gastroenterology* 155 (2), 514–528. e516. doi:10.1053/j.gastro.2018.05.029

Holloway, E., Czerwinski, M., Tsai, Y., Wu, J., Wu, A., Childs, C., et al. (2021). Mapping development of the human intestinal niche at single-cell resolution. *Cell stem Cell* 28 (3), 568–580.e4. e564. doi:10.1016/j.stem.2020.11.008

Hu, G., Peng, C., Xie, X., Zhang, S., and Cao, X. (2017). Availability, pharmacokinetics, security, pharmacokinetics, and pharmacological activities of patchouli alcohol. *eCAM. Evidence-based complementary and alternative medicine*, 4850612. doi:10.1155/2017/4850612

Huang, Z., Liao, L., Wang, Z., Lu, Y., Yan, W., Cao, H., et al. (2021). An efficient approach for wholemount preparation of the myenteric plexus of rat colon. *J. Neurosci. Methods* 348, 109012. doi:10.1016/j.jneumeth.2020.109012

Knowles, C., Lindberg, G., Panza, E., and De Giorgio, R. (2013). New perspectives in the diagnosis and management of enteric neuropathies. *Nat. Rev. Gastroenterol. Hepatol.* 10 (4), 206–218. doi:10.1038/nrgastro.2013.18

Kulkarni, S., Micci, M., Leser, J., Shin, C., Tang, S., Fu, Y., et al. (2017). Adult enteric nervous system in health is maintained by a dynamic balance between neuronal apoptosis and neurogenesis. *Proc. Natl. Acad. Sci. U. S. A.* 114 (18), E3709–E3718. doi:10.1073/pnas.1619406114

Li, Z., Hao, M., Van den Haute, C., Baekelandt, V., Boesmans, W., and Vanden Berghe, P. (2019). Regional complexity in enteric neuron wiring reflects diversity of motility patterns in the mouse large intestine. *eLife* 8, e42914. doi:10.7554/eLife.42914

Liu, Y., Liang, J., Wu, J., Chen, H., Zhang, Z., Yang, H., et al. (2017). Transformation of patchouli alcohol to  $\beta$ -patchoulene by gastric juice:  $\beta$ -Patchoulene is more effective in preventing ethanol-induced gastric injury. *Sci. Rep.* 7 (1), 5591. doi:10.1038/s41598-017-05996-5



- May-Zhang, A., Tycksen, E., Southard-Smith, A., Deal, K., Benthall, J., Buehler, D., et al. (2021). Combinatorial transcriptional profiling of mouse and human enteric neurons identifies shared and disparate subtypes *in situ*. *Gastroenterology* 160 (3), 755–770.e26. e726. doi:10.1053/j.gastro.2020.09.032
- Morarach, K., Mikhailova, A., Knoflach, V., Memic, F., Kumar, R., Li, W., et al. (2021). Diversification of molecularly defined myenteric neuron classes revealed by single-cell RNA sequencing. *Nat. Neurosci.* 24 (1), 34–46. doi:10.1038/s41593-020-00736-x
- Neunlist, M., Rolli-Derkinderen, M., Latorre, R., Van Landeghem, L., Coron, E., Derkinderen, P., et al. (2014). Enteric glial cells: Recent developments and future directions. *Gastroenterology* 147 (6), 1230–1237. doi:10.1053/j.gastro.2014.09.040
- Neunlist, M., and Schemann, M. (2014). Nutrient-induced changes in the phenotype and function of the enteric nervous system. *J. Physiol.* 592 (14), 2959–2965. doi:10.1113/jphysiol.2014.272948
- Niesler, B., Kuerten, S., Demir, I., and Schäfer, K. (2021). Disorders of the enteric nervous system - a holistic view. *Nat. Rev. Gastroenterol. Hepatol.* 18 (6), 393–410. doi:10.1038/s41575-020-00385-2
- Rao, M., Rastelli, D., Dong, L., Chiu, S., Corfas, G., Gershon, M. D., et al. (2017). Enteric glia regulate gastrointestinal motility but are not required for maintenance of the epithelium in mice. *Gastroenterology* 153 (4), 1068–1081. doi:10.1053/j.gastro.2017.07.002
- Sah, S., Mathela, C., and Chopra, K. (2011). Antidepressant effect of Valeriana wallichii patchouli alcohol chemotype in mice: Behavioural and biochemical evidence. *J. Ethnopharmacol.* 135 (1), 197–200. doi:10.1016/j.jep.2011.02.018
- Sang, Q., Williamson, S., and Young, H. (1997). Projections of chemically identified myenteric neurons of the small and large intestine of the mouse. *J. Anat.* 190 ( Pt 2), 209–222. doi:10.1046/j.1469-7580.1997.19020209.x
- Sang, Q., and Young, H. (1996). Chemical coding of neurons in the myenteric plexus and external muscle of the small and large intestine of the mouse. *Cell Tissue Res.* 284 (1), 39–53. doi:10.1007/s004410050565
- Sharkey, K. (2015). Emerging roles for enteric glia in gastrointestinal disorders. *J. Clin. Invest.* 125 (3), 918–925. doi:10.1172/jci76303
- Smith, T., Spencer, N., Hennig, G., and Dickson, E. (2007). Recent advances in enteric neurobiology: Mechanosensitive interneurons. *Neurogastroenterol. Motil.* 19 (11), 869–878. doi:10.1111/j.1365-2982.2007.01019.x
- Spencer, N., and Hu, H. (2020). Enteric nervous system: Sensory transduction, neural circuits and gastrointestinal motility. *Nat. Rev. Gastroenterol. Hepatol.* 17 (6), 338–351. doi:10.1038/s41575-020-0271-2
- Thumann, T., Pferschy-Wenzig, E., Moissl-Eichinger, C., and Bauer, R. (2019). The role of gut microbiota for the activity of medicinal plants traditionally used in the European Union for gastrointestinal disorders. *J. Ethnopharmacol.* 245, 112153. doi:10.1016/j.jep.2019.112153
- van Thiel, L., de Jonge, W., Chiu, I., and van den Wijngaard, R. (2020). Microbiota-neuroimmune cross talk in stress-induced visceral hypersensitivity of the bowel. *Am. J. Physiol. Gastrointest. Liver Physiol.* 318 (6), G1034–G1041. doi:10.1152/ajpgi.00196.2019
- Veiga-Fernandes, H., and Pachnis, V. (2017). Neuroimmune regulation during intestinal development and homeostasis. *Nat. Immunol.* 18 (2), 116–122. doi:10.1038/ni.3634
- Williams, C. L., Villar, R. G., Peterson, J. M., and Burks, T. F. (1988). Stress-induced changes in intestinal transit in the rat: A model for irritable bowel syndrome. *Gastroenterology* 94 (3), 611–621. doi:10.1016/0016-5085(88)90231-4
- Yan, Y., Ramanan, D., Rozenberg, M., McGovern, K., Rastelli, D., Vijaykumar, B., et al. (2021). Interleukin-6 produced by enteric neurons regulates the number and phenotype of microbe-responsive regulatory T cells in the gut. *Immunity* 54 (3), 499–513.e5. e495. doi:10.1016/j.immuni.2021.02.002
- Yoo, B., and Mazmanian, S. (2017). The enteric network: Interactions between the immune and nervous systems of the gut. *Immunity* 46 (6), 910–926. doi:10.1016/j.immuni.2017.05.011
- Zhou, T., Huang, J., Huang, Z., Cao, H., and Tan, B. (2018). Inhibitory effects of patchouli alcohol on stress-induced diarrhea-predominant irritable bowel syndrome. *World J. Gastroenterol.* 24 (6), 693–705. doi:10.3748/wjg.v24.i6.693
- Zhu, S., Liu, S., Li, H., Zhang, Z., Zhang, Q., Chen, L., et al. (2019). Identification of gut microbiota and metabolites signature in patients with irritable bowel syndrome. *Front. Cell. Infect. Microbiol.* 9, 346. doi:10.3389/fcimb.2019.00346



## OPEN ACCESS

## EDITED BY

Maria Dimitrova,  
Medical University Sofia, Bulgaria

## REVIEWED BY

Alice Bonomi,  
Monzino Cardiology Center (IRCCS),  
Italy  
Jinhang Gao,  
Sichuan University, China

## \*CORRESPONDENCE

Xiaoyu Wen,  
xywen@jlu.edu.cn

## SPECIALTY SECTION

This article was submitted to Drugs  
Outcomes Research and Policies,  
a section of the journal  
Frontiers in Pharmacology

RECEIVED 12 July 2022

ACCEPTED 26 October 2022

PUBLISHED 16 November 2022

## CITATION

Zhang R, Li T, Shao Y, Bai W and Wen X  
(2022), Efficacy evaluation of pulmonary  
hypertension therapy in patients with  
portal pulmonary hypertension: A  
systematic review and meta-analysis.  
*Front. Pharmacol.* 13:991568.  
doi: 10.3389/fphar.2022.991568

## COPYRIGHT

© 2022 Zhang, Li, Shao, Bai and Wen.  
This is an open-access article  
distributed under the terms of the  
[Creative Commons Attribution License](#)  
(CC BY). The use, distribution or  
reproduction in other forums is  
permitted, provided the original  
author(s) and the copyright owner(s) are  
credited and that the original  
publication in this journal is cited, in  
accordance with accepted academic  
practice. No use, distribution or  
reproduction is permitted which does  
not comply with these terms.

# Efficacy evaluation of pulmonary hypertension therapy in patients with portal pulmonary hypertension: A systematic review and meta-analysis

Ruihua Zhang<sup>1,2</sup>, Tengfei Li<sup>1</sup>, Yueming Shao<sup>3</sup>, Wei Bai<sup>4</sup> and  
Xiaoyu Wen<sup>1,2\*</sup>

<sup>1</sup>Department of Hepatology, The First Hospital of Jilin University, Changchun, Jilin, China, <sup>2</sup>Center of Infectious Diseases and Pathogen Biology, The First Hospital of Jilin University, Changchun, Jilin, China, <sup>3</sup>Department of Infectious Diseases and Immunology, Shanghai Public Health Clinical Center, Fudan University, Shanghai, China, <sup>4</sup>Unit of Psychiatry, Department of Public Health and Medicinal Administration, and Institute of Translational Medicine, Faculty of Health Sciences, University of Macau, Macao, Macao SAR, China

**Objective:** To determine the therapeutic effect of pulmonary arterial hypertension (PAH) agents for portal pulmonary hypertension (POPH).

**Design:** Systematic review and meta-analysis.

**Background:** POPH is a serious complication of end-stage liver disease with a low survival rate. Liver transplantation (LT) is an effective treatment. Due to the presence of POPH, some patients cannot undergo LT. After PAH treatment, patients with POPH can obtain good hemodynamics and cardiac function for LT, but there are no standard guidelines.

**Methods:** Two independent researchers searched PubMed, EMBASE, Cochrane Library, and Web of Science for studies published from inception to 27 September 2022, focusing on the changes in hemodynamics and cardiac function in all patients with POPH to understand the effect of PAH treatment on the entire population of POPH patients. Among these, we specifically analyzed the changes in hemodynamics and cardiac function in moderate and severe POPH patients. After collecting the relevant data, a meta-analysis was carried out using the R program meta-package.

**Results:** A total of 2,775 literatures were retrieved, and 24 literatures were included. The results showed that in all POPH patients ( $n = 1,046$ ), the following indicators were significantly improved with PAH agents: mPAP:

**Abbreviations:** 6MWD, 6-minutes walking distance; 95%CI, 95%confidence interval; CO, cardiac output; ERA, endothelin receptor antagonist; LT, liver transplantation; MELD, model for end-stage liver disease; mPAP, mean pulmonary artery pressure; NYHA, New York heart association; PAH, pulmonary arterial hypertension; PAWP, pulmonary arterial wedge pressure; PDE-5, phosphodiesterase type 5; POPH, portal pulmonary hypertension; PVR, pulmonary vascular resistance; RAP, right atrial pressure; RCT, randomized controlled trial; RHC, right heart catheterization; RV, right ventricle; SvO<sub>2</sub>, mixed venous oxygen saturation; TPG, transpulmonary gradient; WHO FC, WHO functional classification.

(MD =  $-9.11$  mmHg,  $p < 0.0001$ ); PVR: (MD =  $-239.33$  dyn·s·cm $^{-5}$ ,  $p < 0.0001$ ); CO: (MD =  $1.71$  L/min,  $p < 0.0001$ ); cardiac index: (MD =  $0.87$  L/(min·m $^2$ ),  $p < 0.0001$ ); 6MWD: (MD =  $43.41$  m,  $p < 0.0001$ ). In patients with moderate to severe POPH ( $n = 235$ ), the following indicators improved significantly with PAH agents: mPAP (MD =  $-9.63$  mmHg,  $p < 0.0001$ ); PVR (MD =  $-259.78$  dyn·s·cm $^{-5}$ ,  $p < 0.0001$ ); CO (MD =  $1.76$  L/min,  $p < 0.0001$ ); Cardiac index: (MD =  $1.01$  L/(min·m $^2$ ),  $p = 0.0027$ ); 6MWD: (MD =  $61.30$  m,  $p < 0.0001$ ).

**Conclusion:** The application of PAH agents can improve cardiopulmonary hemodynamics and cardiac function in patients with POPH, especially in patients with moderate to severe POPH, and the above changes are more positive.

**Systematic Review Registration:** <https://inplasy.com>, identifier INPLASY202250034.

#### KEYWORDS

portal pulmonary hypertension, pulmonary arterial hypertension, portal hypertension, curative effect, meta-analysis

## 1 Introduction

Pulmonary arterial hypertension (PAH) is a clinical and pathophysiological syndrome of altered pulmonary vascular structure or function caused by a variety of etiologies and pathogenesis, leading to increased PVR (pulmonary vascular resistance) and pulmonary arterial pressure, which progresses to right heart failure or even death. The pathology is characterized by the proliferation of endothelial cells, smooth muscle cells, and fibroblasts in the vascular wall, leading to pulmonary artery stenosis and occlusion (Tuder et al., 2013). The increase in pulmonary vascular resistance may lead to severe PAH. Portal pulmonary hypertension (POPH) is a clinical symptom with elevated pulmonary artery pressure based on portal hypertension (with or without chronic liver disease). In 1951, Mantz and Craige (Mantz and Craige, 1951) identified the first case of POPH. The Sixth World Conference on pulmonary hypertension (Xu and Jing, 2018) in 2018 classified POPH as Group 1 PAH. According to the 2016 practice guideline of the International Society for LT (Liu and Li, 2016), POPH is graded according to mPAP (mean pulmonary artery pressure) measured by RHC (right heart catheterization), which can be classified as mild ( $25$  mmHg  $\leq$  mPAP  $< 35$  mmHg), moderate ( $35$  mmHg  $\leq$  mPAP  $< 45$  mmHg) and severe (mPAP  $\geq 45$  mmHg).

The incidence of POPH varies in different studies, accounting for 5%–10% (Badesch et al., 2010) in PAH, 1%–2% (Mancuso et al., 2013) in patients with portal hypertension, and 2%–6% (Savale et al., 2017) in patients with LT. Unfortunately, the survival rate is low. The median survival time of untreated POPH has been reported to be as low as 6 months (Robalino and Moodie, 1991), with a 5-year survival rate of 14%–28% and a 5-year survival rate of 35%–45% after treatment with pulmonary vasodilators alone (Krowka et al., 2000; Bremer et al., 2007; Galiè et al., 2009; Johnson et al., 2012).

Currently, LT is considered to be an attractive treatment as it can cure potential liver diseases (Safdar et al., 2012), and it has been proven that pulmonary vascular diseases may be reversible in some POPH patients who survive transplantation (Scott et al., 1993; Csete, 1997; Schott et al., 1999; Krowka et al., 2000). However, the presence of PAH was found to increase mortality and prolong the time of hospitalization for LT (Krowka et al., 2016). Patients with mild POPH have mostly survivable conditions after transplantation, while patients with moderate and severe POPH have a mortality rate as high as 50%–100% after transplantation. Due to the high perioperative mortality, moderate and severe diseases are contraindications to LT, but if patients can obtain good right heart function and hemodynamics (mPAP  $< 35$  mmHg and PVR  $< 400$  dyn·s·cm $^{-5}$ ) after pulmonary vasodilator therapy, some can successfully undergo LT. Therefore, PAH treatment is essential in patients with POPH, especially in patients with moderate and severe POPH.

At present, there are no formal guidelines on the clinical management of POPH. Because POPH is pathologically similar to other forms of PAH, the current clinical treatment of POPH is related to the treatment of PAH. The meta-analysis we conducted aimed to complement the existing clinical studies of POPH to evaluate the effectiveness and safety of specific treatment for pulmonary hypertension in patients with portal pulmonary hypertension to provide a basis for rational clinical drug use.

## 2 Materials and methods

### 2.1 Search strategy and study selection

This meta-analysis was conducted following the recommendations of the Preferred Reporting Items for

Systematic Reviews and Meta-Analyses (PRISMA) and was registered in INPLASY (registration number: INPLASY202250034; <https://inplasy.com>). Two researchers (RHZ and TFL) searched PubMed, EMBASE, Web of Science and the Cochrane library for clinical studies related to the application of PAH treatment in patients with POPH. The search was conducted from the time the database was created to 27 September 2022. The following terms were applied to search the title and abstracts: “portalpulmonary hypertension” or “portal pulmonary hypertension” or “POPH” or “PPHTN.”

The titles and abstracts of retrieved studies were screened independently by two researchers, who then read the full text of the potentially included studies to select those for inclusion in the meta-analysis. All selected studies needed to meet the following criteria according to the PICOS acronym: Participants (P): POPH patients identified by RHC and identified as POPH patients in each study; Intervention (I): Specific treatment of PAH (including prostacyclin and its analogs, endothelin receptor antagonists, phosphodiesterase 5 inhibitors, soluble guanylate cyclase stimulants, *etc.*), regardless of whether LT was performed after drug treatment; Control (C): Baseline hemodynamic (mPAP, PVR, PAWP (pulmonary arterial wedge pressure), TPG (transpulmonary gradient), SvO<sub>2</sub> (mixed venous oxygen saturation), CO (cardiac output), Cardiac index, RAP (right atrial pressure) or cardiac function [6MWD (6-min walking distance), NYHA (New York Heart Association) grade, WHO FC (WHO functional classification), *etc.*] were available in the study; Outcome (O): There are corresponding follow-up values in the study: hemodynamics (mPAP, PVR, PAWP, TPG, SvO<sub>2</sub>, CO, cardiac index, RAP), cardiac function (6MWD, NYHA grade, WHO FC, *etc.*) and other relevant data. Study (S): RCTs, prospective studies and retrospective studies were included. Exclusion criteria included the following: 1) Studies with <5 patients with POPH; 2) On-English articles; 3) Review, comments, conference paper, guidelines, editorial, letter, note, poster, erratum, replies, short surveys, clinical trials registration, meta; 4) Pediatric research; and 5) Incomplete data. Any discrepancies in the selection process of the included studies in the meta-analysis were resolved by consensus through discussion with a third researcher (XYW).

## 2.2 Data extraction and quality assessment

The following information was independently extracted by two researchers (YMS and WB): author name, year, country, study duration, study design, sample size, mean age, severity of underlying liver disease, etiology, treatment regimen, hemodynamic indices (mPAP, PVR, PAWP, TPG, SvO<sub>2</sub>, CO, cardiac index, RAP), 6MWD, NYHA grade, WHO FC, survival rate, adverse events, *etc.*). Study quality was assessed using the NIH Quality Assessment Tool for Case Series Studies or

Controlled Intervention Studies (<https://www.nhlbi.nih.gov/health-topics/study-quality-assessment-tools>). Quality assessment consisted of 9 parts for case series studies and 14 parts for controlled intervention studies. The results were marked as Yes, NO, Other (cannot determine, CD; not applicable, NA; not reported, NR) (Supplementary Table S1). Any discrepancies in these processes were resolved by consensus through discussion with a third researcher (XYW).

## 2.3 Statistical analyses

Meta-analysis was conducted using a meta-package (version 5.1–0) in the R program (version 4.1.1). Mean and standard deviation (SD) were used to calculate the pooled results using a random-effects model, and for studies with median and interquartile ranges, they were transformed to mean and SD to combine data. The heterogeneity of the studies was evaluated using  $I^2$ , and a value of  $I^2$  above 50% indicated high heterogeneity. Subgroup and meta-regression analyses were performed to explore potential sources of heterogeneity. For changes in indicators with significant heterogeneity and more than 3 studies, the sources of heterogeneity were discussed according to the following categorical variables: age  $\geq 55$  and  $< 55$ ; sample size  $\geq 20$  and  $< 20$ ; proportion of women  $\geq 50\%$  and  $< 50\%$ ; prostacyclin and its analogs and nonprostacyclin and its analogs (e.g., endothelin receptor antagonists and phosphodiesterase 5 inhibitors). Meta-regression analysis was performed by the following continuous variables: the effects of baseline mPAP and PVR on the changes in mPAP and PVR in all patients with POPH and patients with moderate and severe POPH. Publication bias was evaluated by funnel plots and Egger's test. A statistically significant level was set as  $p < 0.05$  (two-tailed) for all tests.

## 3 Results

### 3.1 Basic characteristics

Figure 1 shows the selection process of studies included in the meta-analysis. A total of 2,775 literatures were introduced into the search strategy. Of these, 24 literatures and 27 studies met the inclusion criteria (Krowka et al., 1999; Hoeper et al., 2005; Reichenberger et al., 2006; Sussman et al., 2006; Ashfaq et al., 2007; Fix et al., 2007; Hoeper et al., 2007; Gough and White, 2009; Hemnes and Robbins, 2009; Melgosa et al., 2010; Cartin-Ceba et al., 2011; Halank et al., 2011; Hollatz et al., 2012; Awdish and Cajigas, 2013; Savale et al., 2013; Khaderi et al., 2014; Fisher et al., 2015; Legros et al., 2017; Sitbon et al., 2019; DuBrock et al., 2020; Preston et al., 2020; Savale et al., 2020; Rossi et al., 2021; Sadd et al., 2021). Of these studies, 9 were in Europe [4 in Germany,

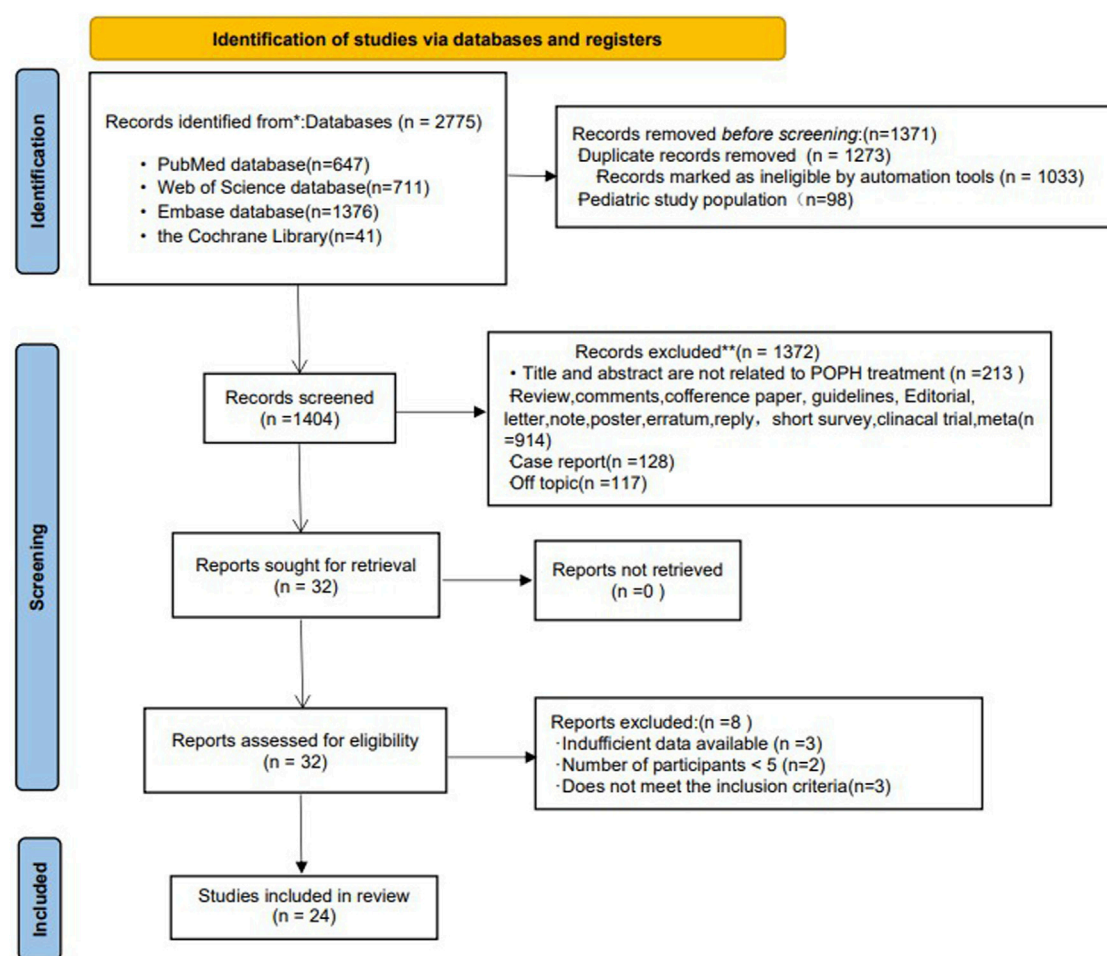


FIGURE 1  
Flow chart of the selection of studies for inclusion in the meta-analysis.

3 in France, 1 in Italy and 1 in Spain), 12 in the United States, 1 in Canada, and 1 in Europe/the United States/Brazil (the only RCT (randomized controlled trial) (Sitbon et al., 2019)] (Detail informations were shown in Table 1). Among the included studies, 3 were prospective studies (Gough and White, 2009; Cartin-Ceba et al., 2011; Awdish and Cajigas, 2013), 1 was an RCT (Sitbon et al., 2019), 1 was an open-label study (Preston et al., 2020), and the others were retrospective studies.

The basic characteristics of the studies are shown in Table 1. A total of 1,046 POPH patients with a mean age of 54.49 years were included in these studies. Among them, women accounted for 44.16%. The most common cause of portal hypertension was alcoholic liver disease (49.15%) (Table 2). Patients in the study received various PAH-specific treatments (Table 1), including prostacyclin and its analogs (epoprostenol, treprostinil, remodulin, inhaled iloprost), endothelin receptor antagonists (ambrisentan, macitentan, bosentan), and phosphodiesterase 5 inhibitors (sildenafil, tadalafil). There were 15 literature on

the treatment of patients with moderate and severe POPH ( $n = 235$ ), including 18 studies (Table 1).

### 3.2 Effect of PAH-specific treatment on pulmonary hemodynamics in all patients with POPH

In all POPH patients, the following indices were significantly improved after PAH treatment: mPAP (MD =  $-9.11$  mmHg,  $p < 0.0001$ ); PVR (MD =  $-239.33$  dyn·s·cm $^{-5}$ ,  $p < 0.0001$ ); PAWP (MD =  $1.36$  mmHg,  $p = 0.0303$ ); TPG (MD =  $-13.81$  mmHg,  $p < 0.0001$ ); and SvO $_2$  (MD =  $5.16\%$ ,  $p < 0.0001$ ). After 6 months of PAH treatment, mPAP (MD =  $-7.5$  mmHg,  $p < 0.0001$ ) and PVR (MD =  $-176.66$  dyn·s·cm $^{-5}$ ,  $p < 0.0001$ ) were significantly improved, and the change in PAWP (MD =  $0$  mmHg,  $p = 0.9938$ ) was not obvious. After 1 year of PAH treatment, PVR (MD =  $-236.54$  dyn·s·cm $^{-5}$ ,  $p = 0.0433$ ) improved significantly,



TABLE 1 Characteristics of the 27 included studies.

Author name	year	Country	Patients,n	Male (%)	Mean age (Years)	Mean MELD	Child-pugh A/B/C/- or mean points	PAH Therapy, n	PAH therapy
Rossi.R	2021	Italy	64	65.63	60	10	7.5	64	Sildenafil:38; Macitentan + Sildenafil:26
Sadd.C J**	2021	United States	24	37.5	52.8	13	NA	24	Sildenafil monotherapy:4; Sildenafil + epoprostenol:6; Sildenafil + treprostinil:3; Treprostinil:3; Sildenafil + ambrisentan:3; Sildenafil + bosentan:1; Sildenafil + inhaled iloprost:1; Ambrisentan monotherapy:1
Sadd.C J**	2021	United States	25	72	56.2	12.5	NA	25	Sildenafil:14; Sildenafil + epoprostenol:4; Sildenafil + treprostinil:5; Sildenafil + ambrisentan:1:Sildenafil + macitentan:1
DuBrock.H M**	2020	United States	16	31.25	49.5	19.5	NA	16	Sildenafil:5; Sildenafil + epoprostenol: 3; epoprostenol:2; Ambrisentan + Tadalafil:1; NO:1; Ambrisentan:1; Ambrisentan + epoprostenol:1; Remodulin + sildenafil:1; Remodulin:1
Savale.L	2020	France	637	58.4	55	11.5	328/192/57/-	574	sildenafil:239; tadalafil:97; bosentan: 90; ambrisentan: 36; maci-tentan: 2; bosentan + sildenafil:31; bosentan + tadalafil:15; ambrisentan + sildenafil: 17; ambrisentan + tadalafil:24; macitentan + tadalafil:2
Preston.I R	2020	NA	31	41.94	62.6	11.1	13/18/-/-	23	Ambrisentan:23
Sitbon.O	2019	Europe/the United States/ Brazil	43	51.16	58	8.5	20/3/-/20	43	macitentan:43
Legros.L	2017	France	20	65	52.25	11.75	8/10/2/-	20	sildenafil:10; bosentan:5; bosentan + sildenafil:3; bosentan + tadalafil:1; ambrisentan:1; associated IV epoprostenol:2
Fisher.J H	2015	Canada	20	60	54.5	15.25	3/7/3/7	20	sildenafil:19; tadalafil:1
Khaderi.S**	2014	United States	7	42.86	45	NA	NA	7	IV EPO:6; sildenafil:1
Savale.L	2013	France	34	47.06	50	NA	19/9/-/-	34	bosentan:34
Awdish.R L A	2013	United States	21	52.38	55	12.5	5/11/5/-	21	Prostacyclin IV:14; Prostacyclin inhaled:1; PDE5; ETRA:1
Hollatz.T J**	2012	United States	11	45.45	51.4	15.4	NA	11	Sildenafil:2; treprostinil:4; Sildenafil + epoprostenol:3; Sildenafil + inhaled iloprost:1; bosentan + Sildenafil + epoprostenol:1
Halank.M**	2011	Germany	14	35.71	55.75	10.5	12/-/-/2	14	ambrisentan + sildenafil:1; ambrisentan + tadalafil:1; ambrisentan:12
Cartin-Ceba.R**	2011	United States	13	53.85	56.5	10.88	8/-/-/5	13	ambrisentan:13
Melgosa.M T	2010	Spain	12	66.67	51	11.1	NA	12	inhaled iloprost:9; bosentan + inhaled iloprost:3; add sildenafil:1
Hemnes.A R**	2009	United States	10	50	51	14.3*	NA	10	Sildenafil:10
Gough.M S**	2009	United States	11	36.36	50.36	13.73	0/7/4/-	11	sildenafil:11

(Continued on following page)

TABLE 1 (Continued) Characteristics of the 27 included studies.

Author name	year	Country	Patients,n	Male (%)	Mean age (Years)	Mean MELD	Child-pugh A/B/C/- or mean points	PAH Therapy, n	PAH therapy
Ashfaq.M**	2007	United States	8	75	52.4	11.9	7.3	6	Epoprostenol:5; Bosentan + epoprostenol:1
Ashfaq.M**	2007	United States	12	41.67	51.8	15.2	8.9	10	Epoprostenol:8; Bosentan + diltiazem + epoprostenol:1; Diltiazem:1
Hoeper.M M**	2007	Germany	13	38.46	44	12	10/3/-/-	13	inhaled iloprost:9; bosentan + inhaled iloprost:4
Hoeper.M M**	2007	Germany	18	50	48	10	18/-/-/-	18	bosentan:16; Sildenafil + bosentan:2
Fix.O K**	2007	United States	19	63.16	49.9	15.25	6/8/5/-	19	Epoprostenol:10; Epoprostenol + Sildenafil:7; Sildenafil:2
Reichenberger**	2006	Germany	12	33.33	55	NA	7/5/-/-	12	sildenafil:7; sildenafil + inhaled iloprost:5
Sussman.N**	2006	United States	8	62.5	45.75	17.38	NA	8	Epoprostenol:8
Hoeper.M M**	2005	Germany	11	45.45	51.55	NA	11/-/-/-	11	bosentan:11
Krowka.M J**	1999	United States	7	71.43	45.43	NA	3/3/1/-	7	Epoprostenol:7

Note: PAH, Pulmonary hypertension; \*:Mean MELD, in 7 patients; NA:Not available. \*\*: 18 studies on the treatment of patients with moderate and severe POPH.

while mPAP (MD = -3.46 mmHg,  $p = 0.2176$ ) did not improve significantly (Detail informations were shown in Table 3, Supplementary Figure S1).

### 3.3 Effects of PAH-specific treatment on cardiac hemodynamics and cardiac function of all patients with POPH

In all POPH patients, the following indices were significantly improved after PAH treatment: CO: (MD = 1.71 L/min,  $p < 0.0001$ ); cardiac index: (MD = 0.87 L/(min·m<sup>2</sup>),  $p < 0.0001$ ); RAP (MD = -1.22 mmHg,  $p = 0.0479$ ); 6MWD (MD = 43.41 m,  $p < 0.0001$ ). Three studies (Hollatz et al., 2012; Preston et al., 2020; Rossi et al., 2021) reported changes in right ventricular function or size. Hollatz et al. (2012) followed up eight patients and found no change in right ventricular size in two patients. The expansion degree of five patients was reduced, and that of one patient was increased. In right ventricular function, six patients improved, and two remained unchanged. Preston et al. (2020) followed patients and found reduced right ventricular enlargement in six patients and enlargement in three patients. In terms of right ventricular function, eight patients improved, and two worsened. Rossi et al. (2021) found that after 6 months of sildenafil application, overall RV performance improved significantly in patients with POPH, with significant increases in RV volume (+33%), RV ejection fraction (+31%), and RV work index

(+17.5%). After PAH treatment, except for the unclear change in 6MWD at 3 months (MD = 33.56 m,  $p = 0.0657$ ), 6MWD at 6 months (MD = 22.97 m,  $p = 0.0004$ ) and 6MWD at 1 year (MD = 66.84 m,  $p < 0.0001$ ) were significantly improved. Four studies (Hoeper et al., 2005; Hoeper et al., 2007; Swanson et al., 2008; Savale et al., 2013) showed that the proportion of patients with NYHA grade III/IV decreased after PAH treatment. Three studies (Gough and White, 2009; Fisher et al., 2015; Preston et al., 2020) reported a decrease in the proportion of WHO FC III/IV patients (Detail informations were shown in Table 3, Supplementary Figure S1).

### 3.4 Effects of PAH-specific treatment on cardiopulmonary hemodynamics and 6MWD of patients with moderate and severe POPH

In patients with moderate to severe POPH, except for the insignificant improvement in SvO<sub>2</sub> (MD = 3.36%,  $p = 0.1714$ ) and RAP (MD = -0.53 mmHg,  $p = 0.6473$ ), the following indices were significantly improved after PAH treatment: mPAP (MD = -9.63 mmHg,  $p < 0.0001$ ); PVR (MD = -259.78 dyn·s·cm<sup>-5</sup>,  $p < 0.0001$ ); PAWP (MD = 2.45 mmHg,  $p = 0.0217$ ); TPG (MD = -14.86 mmHg,  $p < 0.0001$ ); CO (MD = 1.76 L/min,  $p < 0.0001$ ); Cardiac index (MD = 1.01 L/(min·m<sup>2</sup>),  $p = 0.0027$ ); 6MWD (MD = 61.30 m,

TABLE 2 Characteristics of the 27 Included Studies: etiology of liver Disease.

First author	year	patients, n	ALD	Viral (HCV/ HBV)	ALD + viral	Autoimmune (AIH/ PBC/PSC)	Cryptogenic	Cholestatic	Metabolic	Other
Rossi.R	2021	64	11	32 (–/–)	7	0	0	0	8	6
Sadd.C J	2021	24	11	3 (3-/)	4	0	1	1	3	1
Sadd.C J	2021	25	10	4 (4-/)	6	0	2	0	2	1
DuBrock.H M	2020	16	7	7 (7-/)	0	2 (1-/1)	2	0	1	2
Savale.L	2020	637	370	83 (–/–)	100	21 (–/–/–)	15	0	22	26
Preston.I R	2020	31	10	11	0	6 (–/4-/)	0	0	5	1
Sitbon.O	2019	43	24	9 (9-/)	3	4 (–/1-/)	0	0	2	1
Legros.L	2017	20	13	2 (2-/)	1	1 (–/–/–)	0	0	0	3
Fisher.J H	2015	20	11	2 (–/–)	0	1 (–/–/–)	0	0	2	4
Khaderi.S	2014	7	2	3 (3-/)	0	0	2	0	0	0
Savale.L	2013	28	20	4 (4-/)	3	1 (–/–/–)	0	0	0	0
Awdish.R L A	2013	21	NA	NA	NA	NA	NA	NA	NA	NA
Hollatz.T J	2012	11	5	1 (1-/)	3	0	0	1	0	1
Halank.M	2011	14	8	1 (–/1)	0	1 (–/1-/)	3	0	0	1
Cartin-Ceba.R	2011	13	6	3 (3-/)	0	1 (–/–/–)	0	0	1	2
Melgosa.M T	2010	12	2	5 (4/1)	0	2 (–/2-/)	0	0	0	4
Hemnes.A R	2009	10	0	7 (7-/)	1	1 (–/1-/)	0	0	0	1
Gough.M S	2009	11	4	2 (2-/)	4	0	0	0	0	1
Ashfaq.M	2007	8	0	3 (3-/)	0	0	1	3	0	1
Ashfaq.M	2007	12	0	4 (4-/)	0	0	3	1	0	4
Hoeper.M M	2007	13	6	2 (–/–)	0	4 (–/–/–)	0	1	0	0
Hoeper.M M	2007	18	11	3 (–/–)	0	2 (–/–/–)	0	2	0	0
Fix.O K	2007	36*	7	9 (9-/)	10	3 (–/2-/)	3	1	0	3
Reichenberger	2006	12	7	2 (–/–)	0	3 (–/–/–)	0	0	0	0
Sussman.N	2006	8	4	1 (1-/)	1	0	2	0	0	0
Hoeper.M M	2005	11	7	1 (1-/)	0	0	2	1	0	0
Krowka.M J	1999	7	0	1 (1-/)	2	3 (1/–/2)	1	0	0	0

Note: AIH, autoimmune hepatitis; ALD, alcoholic liver disease; HBV, hepatitis B virus; HCV, hepatitis C virus; PBC, primary biliary cholangitis; PSC, primary sclerosing cholangitis; \*: Epoprostenol group:19 + Nonepoprostenol:17.

$p < 0.0001$ ). The 6MWD (MD = 66.67 m,  $p < 0.0001$ ) also showed significant improvement after 1 year of PAH treatment (Detail informations were shown in Table 4, Supplementary Figure S2).

### 3.5 Effect of PAH treatment on the survival rate of patients with POPH

The survival rates of POPH from the date of diagnosis of POPH were as follows (Sadd et al., 2021): after PAH treatment, the 1-year survival rate was 74.5%, the 3-year survival rate was 59.3%, and the 5-year survival rate was 35.9%; after PAH combined with LT, the 1-year survival rate was 95.8%, the 3-year survival rate was 90.9%, and the 5-year survival rate was 90.9%.

From the date of PAH treatment, the survival rates for POPH were as follows: the 6-month survival rate after PAH treatment alone (Melgosa et al., 2010) was 91%, and three studies (Hoeper et al., 2007; Melgosa et al., 2010) showed that the 1-year survival rates were 77%, 83% and 94%, respectively. Two studies (Hoeper et al., 2007) showed that the 2-year survival rates were 62% and 89%, respectively, and two studies (Hoeper et al., 2007) showed that the 3-year survival rates were 46% and 89%, respectively.

Starting from the date of LT, three studies (Ashfaq et al., 2007; DuBrock et al., 2020; Sadd et al., 2021) reported 1-year survival rates of 69%, 86.9% and 90.9%, respectively, one study (Ashfaq et al., 2007) showed a 2-year survival rate of 80.8%, two studies (DuBrock et al., 2020; Sadd et al., 2021) showed 3-year survival rates of 53.8% and 86.9%, and three

TABLE 3 Changes of hemodynamics and 6 MWD in all patients with POPH.

	Number of studies	Merge results	95%CI	I <sup>2</sup> (%)	p-Value
Overall mPAP change	25	-9.11	(-10.97,-7.26)	54	<0.0001
Changes in mPAP at 6 months	3	-7.5	(-10.40,-4.59)	0	<0.0001
Changes in mPAP at 1 year	3	-3.46	(-8.97,2.04)	0	0.2176
Overall PVR change	25	-239.33	(-272.28,-206.37)	77	<0.0001
Changes in PVR at 6 months	3	-176.66	(-247.89,-105.43)	11	<0.0001
Changes in PVR at 1 year	3	-236.54	(-465.96,-7.13)	0	0.0433
Overall PAWP change	14	1.36	(0.13,2.59)	74	0.0303
Changes in PAWP at 6 months	3	0	(-1.12,1.13)	0	0.9938
Overall TPG change	5	-13.81	(-15.95,-11.67)	29	<0.0001
Overall SVO <sub>2</sub> change	8	5.16%	(3.19%,7.14%)	38	<0.0001
Overall CO change	19	1.71	(1.28,2.14)	54	<0.0001
Overall Cardiac index change	11	0.87	(0.61,1.12)	93	<0.0001
Overall RAP change	12	-1.22	(-2.44,-0.01)	62	0.0479
Overall 6MWD change	16	43.41	(29.48,57.34)	39	<0.0001
Changes in 6MWD at 3 months	3	33.56	(-2.18,69.30)	16	0.0657
Changes in 6MWD at 6 months	4	22.97	(10.37,35.56)	0	0.0004
Changes in 6MWD at 1 year	7	66.84	(47.48,86.20)	0	<0.0001

Note: 6MWD, 6-minutes walking distance; 95%CI, 95%confidence interval; CO, cardiac output; mPAP, mean pulmonary artery pressure; PAWP, pulmonary wedge pressure; PVR, pulmonary vascular resistance; RAP, right atrial pressure; SvO<sub>2</sub>, mixed venous oxygen saturation; TPG, transpulmonary gradient.

TABLE 4 Changes of hemodynamics and 6MWD in patients with moderate and severe POPH.

	Number of studies	Merge results	95%CI	I <sup>2</sup> (%)	p-Value
Overall mPAP change	17	-9.63	(-12.49,-6.78)	62	<0.0001
Overall PVR change	17	-259.78	(-301.56,-218.01)	23	<0.0001
Overall PAWPchange	7	2.45	(0.36,4.54)	76	0.0217
Overall TPG change	4	-14.86	(-16.23,-13.50)	0	<0.0001
Overall SVO <sub>2</sub> change	4	3.36%	(-1.46%,8.19%)	30	0.1714
Overall CO change	15	1.76	(1.16,2.36)	58	<0.0001
Overall Cardiac index change	4	1.01	(0.35,1.67)	83	0.0027
Overall RAP change	6	-0.53	(-2.83,1.76)	57	0.6473
Overall 6MWD change	8	61.3	(41.38,81.21)	0	<0.0001
Changes in 6MWD at 1 year	7	66.67	(38.58,94.76)	0	<0.0001

Note: 6MWD, 6-minutes walking distance; 95%CI, 95%confidence interval; CO, cardiac output; mPAP, mean pulmonary artery pressure; PAWP, pulmonary wedge pressure; PVR, pulmonary vascular resistance; RAP, right atrial pressure; SvO<sub>2</sub>, mixed venous oxygen saturation; TPG, transpulmonary gradient.

studies (Ashfaq et al., 2007; DuBrock et al., 2020; Sadd et al., 2021) showed 5-year survival rates of 53.8%, 67.63% and 86.9%, respectively.

### 3.6 Stop PAH treatment

After PAH combined with LT, twelve studies reported that the proportion of successful cessation of PAH treatment after LT ( $n = 77$ ) was 53.25% ( $n = 41$ ), and one study (Khaderi et al., 2014) had a recurrence of POPH after LT.

### 3.7 Adverse reactions after PAH treatment

A total of 12 studies reported adverse reactions after medication, and four studies (Krowka et al., 1999; Sussman et al., 2006; Ashfaq et al., 2007; Hoeper et al., 2007) noted adverse reactions after prostacyclin application. Six studies (Hoeper et al., 2007; Cartin-Ceba et al., 2011; Halank et al., 2011; Legros et al., 2017; Sitbon et al., 2019; Preston et al., 2020) reported adverse reactions after the application of endothelin receptor antagonists. One study (Fisher et al., 2015) reported adverse reactions after the application of PDE-5 inhibitors.

### 3.8 Subgroup analysis

The results showed that PAH treatment could improve cardiopulmonary hemodynamics and cardiac function, but there was significant heterogeneity ( $I^2 > 50\%$ ) in the changes in overall mPAP, PVR, PAWP, CO, cardiac index, and RAP in enrolled patients with POPH and the changes in overall mPAP, PAWP, CO, cardiac index and RAP in patients with moderate and severe POPH. For the index changes with obvious heterogeneity and  $\geq 3$  studies (overall changes in mPAP, PVR, PAWP and CO, cardiac index and RAP in all patients with POPH, and overall changes in mPAP and CO in patients with moderate and severe POPH), the sources of heterogeneity were discussed according to the following categorical variables: age, sample size, proportion of women and drug type, and no obvious sources of heterogeneity (Supplementary Tables S2, S3 for detailed data). A meta-regression analysis of the change in overall mPAP and PVR in all POPH patients and in patients with moderate and severe POPH using the continuous variables baseline mPAP and PVR was performed to explore the sources of heterogeneity. The results showed that in all POPH patients, baseline mPAP was negatively correlated with the change in PVR ( $\beta = -10.91558$ ,  $z = -2.00480$ ,  $p = 0.04498$ ; Supplementary Table S4); in the meta-regression analysis of patients with moderate and severe POPH, the baseline PVR was positively correlated with the change in PVR ( $\beta = 0.00331$ ,  $z = 3.29822$ ,  $p = 0.00097$ ; Supplementary Table S5), and no statistical significance was found in other regression analyses.

### 3.9 Publication bias detection

Funnel plots were made for the outcome indicators (overall changes in mPAP, PVR, PAWP, CO, cardiac index, RAP and 6MWD in all patients with POPH and overall changes in mPAP, PVR and CO in patients with moderate and severe POPH) with  $\geq 10$  studies to test publication bias. The results showed that there was no publication bias in the remaining index studies, except for an asymmetric scatter distribution corresponding to the change in overall PVR in all POPH patients, which was publication biased ( $t = -2.45$ ;  $p = 0.0222$ ; Supplementary Figure S3).

## 4 Discussion

At present, there are no clear guidelines for the specific treatment of POPH. Clinical practice is guided by PAH guidelines and expert opinions to carry out multidisciplinary treatment for patients with POPH. Due to the poor prognosis of POPH patients, few RCTs have been performed for POPH. In this meta-analysis, only one study was a randomized trial of macitentan. This meta-analysis mainly comes from retrospective studies and prospective observational studies.

### 4.1 PAH-specific treatment can significantly improve pulmonary hemodynamics in patients with POPH

Ideally, the optimal regimen of PAH-targeted drugs for POPH should reduce pulmonary artery pressure and PVR without obvious damage to liver function and improve right heart function and symptoms. In this meta-analysis, we first counted the effects of PAH treatment on mPAP, PVR, PAWP and TPG in all patients with POPH: mPAP decreased by 9.11 mmHg, PVR decreased by 239.33 dyn·s·cm<sup>-5</sup>, TPG decreased by 13.81 mmHg and PAWP increased by 1.36 mmHg, which were statistically significant. In current clinical practice, mPAP is used to stratify the severity of patients with POPH. If mPAP  $\geq 35$  mmHg, PAH therapy should be started for POPH. mPAP and PVR were used to assess the hemodynamics of POPH and the risk of mortality after LT. It has been reported that the posttransplant mortality in patients with moderate and severe POPH was 50%–100% (Krowka et al., 2000). In terms of treatment, the 2016 international guidelines for LT practice (Krowka et al., 2016) stated that if PAH targeted therapy leads to mPAP  $< 35$  mmHg and PVR  $< 400$  dyn·s·cm<sup>-5</sup>, MELD exception can be considered; if treated POPH fails to bring mPAP down to  $< 35$  mmHg, but with normal PVR ( $< 240$  dyn·s·cm<sup>-5</sup>) and RV function, the MELD exception can also be considered. Regarding PAWP, Swanson et al. (2008) found in their analysis that PAWP  $< 10$  mmHg was associated with death after transplantation; therefore, lowering PAWP by PAH treatment is beneficial for patients. TPG is calculated as the mean pulmonary artery pressure minus the left atrial pressure; if the TPG is high enough, it will lead to right ventricular pressure overload. Under normal circumstances, the right ventricle is a thin-walled chamber responsible for volume transmission. In the acute phase, the right ventricle is poorly adapted to the increased pressure load, which is more likely to cause right ventricular dysfunction. Overall, the above indicators improved in a “statistically significant” way ( $p < 0.05$ ), indicating that PAH-specific treatment can significantly improve pulmonary hemodynamics in patients with POPH.

### 4.2 PAH-specific treatment significantly improved cardiac blood flow and cardiac function in patients with POPH

The meta-analysis found a 1.71 L/min increase in CO, a 0.87 L/(min·m<sup>2</sup>) increase in cardiac index, a 1.22 mmHg decrease in RAP, a 5.16% increase in SvO<sub>2</sub>, and a 43.41 m increase in 6MWD. The amount of blood delivered to the heart during liver graft reperfusion increased significantly, which may cause right heart failure in the already stiff and poorly compliant right ventricle (De Wolf et al., 1993; Ramsay et al., 1997; Martínez-



Palli et al., 2005). The increase in CO and cardiac index after PAH treatment before LT is relatively beneficial to patients. RAP is also an indicator of right ventricular function. Recent registry data from trials evaluating early and long-term PAH disease management have shown that mean RAP is a predictor of survival (Krowka et al., 2012). Usually, patients with POPH often suffer from fatigue and insufficient exercise tolerance, which are thought to be related to insufficient cardiac output and tissue perfusion. After PAH-specific treatment, hemodynamics such as CO, cardiac index, RAP and SvO<sub>2</sub> improved, the 6MWD increased, and the proportion of patients with NYHA and WHO FC III/IV decreased, indicating that PAH-specific treatment can significantly improve the hemodynamics and cardiac function of patients with POPH.

In the meta-analysis, we also compared the phased changes in mPAP, PVR and 6MWD. Interestingly, mPAP improved significantly after 6 months of PAH treatment, but its improvement at 1 year was not statistically significant. The reasons are as follows: 1) Hemnes and Robbins (2009) only followed 5 patients at 1 year, which was a small sample size; only 2 of these 5 patients received sildenafil 50 mg tid po, and the remaining patients received 20–25 mg, which is a low dose. Of note, although there was no statistically significant difference in hemodynamics at the first year, the mPAP decreased or remained unchanged in 4 of 5 patients, and the PVR decreased in 3 of 5 patients. 2) Reichenberger et al. (2006) followed 12 patients with RHC after 1 year of sildenafil treatment, five of whom had received prostacyclin drugs for several months before sildenafil application. 3) Hoeper et al. (2005) found that although the change in mPAP was not statistically significant after 1 year of bosentan treatment, the follow-up value decreased by 10% compared with the baseline. Therefore, although there was no “statistically” improvement in mPAP after 1 year of PAH treatment, the overall trend was improved. Next, although the 6MWD improved after 3 months of PAH treatment, the difference was not statistically significant. There was a statistical improvement after 6 months and 1 year of application. The lack of improvement in the 6MWD is related to the fact that the 6MWD may not accurately reflect the cardiopulmonary limitations of patients with severe comorbidities. In addition, the short treatment time, ascites, indication, sarcopenia, anemia and encephalopathy and other factors (Fisher et al., 2015) also make it difficult to confirm the improvement of 6MWD in some patients with POPH.

### 4.3 PAH drugs have more positive effects on cardiopulmonary hemodynamics and cardiac function in patients with moderate and severe POPH

In this meta-analysis, there were 18 studies on the treatment of moderate and severe POPH, comparing them with the changes

in all POPH, and more positive changes in hemodynamic and functional status were found in patients with moderate and severe POPH treated with PAH-specific therapy. According to this result, early and appropriate PAH treatment was recommended for patients with moderate and severe POPH, considering its severity and poor prognosis. PAH treatment can reduce mPAP to <35 mmHg, allowing such patients to qualify for the MELD exception score earlier; thus, registering the waiting list for LT will be beneficial for obtaining good survival rates after LT.

### 4.4 Drug discontinuation after PAH treatment

In this meta-analysis, more than half of the patients were able to stop PAH therapy after PAH therapy combined with LT. Although some patients still needed to continue treatment, they were able to maintain a good quality of life and functional status. This suggests that PAH treatment is very meaningful for patients with POPH. Khaderi et al. (2014) identified a patient with recurrence of POPH after LT, who was also the only patient with recurrent cirrhosis and portal hypertension after LT. This patient had pulmonary arterial hypertension that resolved after transplantation but recurred at the time of relapse of portal hypertension, suggesting an unexplained susceptibility to POPH.

### 4.5 Some adverse drug reactions may occur after PAH treatment

Krowka et al. (1999) found that patients treated with epoprostenol might experience different levels of facial flushing, jaw pain, dyspareunia and calf discomfort. One patient had a lower platelet count after medication. Sussman et al. (2006) reported facial flushing, nausea, anorexia and diarrhea during the application of epoprostenol and postoperative bleeding in 2 patients. This may be related to the anticoagulant effect of epoprostenol. In the study of Ashfaq et al. (2007), one patient discontinued epoprostenol due to intolerance. Hoeper et al. (2007) found that all patients tolerated inhaled iloprost well without side effects except for mild flushing, headache and cough. Several studies have reported that patients treated with ERA are prone to liver enzyme elevation, which usually recovers after dose reduction or discontinuation. Preston et al. (2020) found an asymptomatic elevation of AST (275 IU/L, more than five times the ULN) in one patient, which led to the discontinuation of ambrisentan, and the liver enzyme improved without sequelae. Hoeper et al. (2007) reported that liver aminotransferase increased to more than three times the upper limit in one patient after administration of bosentan and returned to normal after halving the dose. Sitbon et al. (2019) also reported that liver aminotransferase increased to three times or more in one

patient after the application of macitentan. Therefore, in patients with POPH, ERA drugs should be used with caution if liver enzymes are elevated. Even if a patient has normal liver function, liver function needs to be monitored regularly after the application of ERA. Three studies (Cartin-Ceba et al., 2011; Halank et al., 2011; Preston et al., 2020) reported that patients developed edema after the application of Ambrisentan, which disappeared after discontinuation of the drug. Legros et al. (2017) reported a patient with moderate cytotoxicity after bosentan application. Fisher et al. (2015) reported that some patients experienced dyspepsia, loose stool, back pain and myalgia after PDE5 inhibitors, but the incidence was less than 10% and was generally well tolerated.

## 4.6 Heterogeneity analysis of statistical results

This meta-analysis shows that PAH treatment can improve cardiopulmonary hemodynamics and cardiac function, but there is significant heterogeneity in some statistical results ( $I^2 > 50\%$ ). We conducted a subgroup analysis but did not find a source of significant heterogeneity. This may be related to the following factors: the included studies were mainly retrospective; different studies were conducted in various periods, and the treatment regimens and follow-up times were inconsistent. Subsequently, we performed a meta-regression analysis to explore the source of heterogeneity. The results showed that in all POPH patients, the baseline mPAP was negatively correlated with the change in PVR. However, in patients with moderate and severe POPH, the baseline PVR was positively correlated with the change in PVR, while no statistical significance was found in the other regression analyses, suggesting that PVR may be an indicator affected by multiple factors, and the factors affecting changes in cardiopulmonary outcome indicators may be different for patients with different degrees of POPH, which needs to be further explored in our future studies.

## 4.7 Limitations of the meta-analysis

There were some limitations in this meta-analysis: 1) Only one of the 24 included studies was an RCT. Patients with POPH are usually excluded from prospective studies of pulmonary hypertension because of their frequent concomitant liver disease. Thus, compared with randomized controlled trials, the quality of the included studies is poor, since they mainly include observational cohort studies and retrospective case studies. 2) Most studies had relatively small samples. 3) Different studies were conducted at different periods, with different treatment schemes and inconsistent follow-up times; for this, we performed statistical analysis on some studies that had the same follow-up time. 4) Due to the lack of data regarding

the severity of liver diseases (e.g., MELD score, Child–Pugh grade, etc.), in some studies, it was impossible to determine whether the efficacy of drugs used by patients was affected by their liver diseases. 5) We made a funnel chart for the publication bias test, and the results showed that the distribution of scattered points corresponding to the study of PVR changes was asymmetric in all POPH patients. Therefore, the results of this meta-analysis should be interpreted with caution.

## 5 Conclusion

In conclusion, PAH-specific treatment in POPH can significantly improve cardiopulmonary hemodynamics and cardiac function. As multiple drug regimens were used in clinical studies and the duration of treatment varied between studies, it is difficult to propose a specific PAH drug or drug combinations, as well as dosing regimen or duration of treatment. Considering the poor prognosis of untreated POPH patients, it is unlikely that placebo control will be used in future studies. More prospective studies or larger multicenter studies in the POPH population should be performed to confirm the current findings and adequately control for important confounding factors to expand our understanding of the effectiveness, safety, cost and optimal timing of PAH treatment in POPH patients and assist in formulating guidelines in the future. In addition, better drug regimens and treatment timing should be selected according to the clinical characteristics of patients.

## Data availability statement

The original contributions presented in the study are included in the article/Supplementary Material, further inquiries can be directed to the corresponding author.

## Author contributions

RZ was responsible for data analysis and drafting the original manuscript; TL was responsible for consulting the literature; YS was responsible for revising the paper; WB was responsible for collecting data; XW was responsible for formulating writing ideas, guiding the writing of articles and finalizing them.

## Funding

The study was sponsored by the Foundation of Science and Technology Commission of Jilin Province (20190201065JC), and the Foundation of Science and Technology Commission of Jilin Province (20220203126SF). The funders had no role in the study design, data collection and analysis, preparation of the manuscript, or decision to publish.

## Conflict of interest

The authors declare that the research was conducted in the absence of any commercial or financial relationships that could be construed as a potential conflict of interest.

## Publisher's note

All claims expressed in this article are solely those of the authors and do not necessarily represent those of their affiliated organizations, or those of the publisher, the

editors and the reviewers. Any product that may be evaluated in this article, or claim that may be made by its manufacturer, is not guaranteed or endorsed by the publisher.

## Supplementary material

The Supplementary Material for this article can be found online at: <https://www.frontiersin.org/articles/10.3389/fphar.2022.991568/full#supplementary-material>

## References

- Ashfaq, M., Chinnakotla, S., Rogers, L., Ausloos, K., Saadeh, S., Klintmalm, G. B., et al. (2007). The impact of treatment of portopulmonary hypertension on survival following liver transplantation. *Am. J. Transpl.* 7 (5), 1258–1264. doi:10.1111/j.1600-6143.2006.01701.x
- Awdish, R. L., and Cajigas, H. R. (2013). Early initiation of prostacyclin in portopulmonary hypertension: 10 years of a transplant center's experience. *Lung* 191 (6), 593–600. doi:10.1007/s00408-013-9501-5
- Badesch, D. B., Raskob, G. E., Elliott, C. G., Krichman, A. M., Farber, H. W., Frost, A. E., et al. (2010). Pulmonary arterial hypertension: Baseline characteristics from the REVEAL registry. *Chest* 137 (2), 376–387. doi:10.1378/chest.09-1140
- Bremer, H. C., Kreisel, W., Roecker, K., Dreher, M., Koenig, D., Kurz-Schmieg, A. K., et al. (2007). Phosphodiesterase 5 inhibitors lower both portal and pulmonary pressure in portopulmonary hypertension: A case report. *J. Med. Case Rep.* 1, 46. doi:10.1186/1752-1947-1-46
- Cartin-Ceba, R., Swanson, K., Iyer, V., Wiesner, R. H., and Krowka, M. J. (2011). Safety and efficacy of ambrisentan for the treatment of portopulmonary hypertension. *Chest* 139 (1), 109–114. doi:10.1378/chest.10-0574
- Csete, M. (1997). Intraoperative management of liver transplant patients with pulmonary hypertension. *Liver Transpl. Surg.* 3 (4), 454–455. doi:10.1002/lt.500030422
- De Wolf, A. M., Scott, V. L., Gasior, T., and Kang, Y. (1993). Pulmonary hypertension and liver transplantation. *Anesthesiology* 78 (1), 213–214. doi:10.1097/00000542-199301000-00037
- DuBrock, H. M., Runo, J. R., Sadd, C. J., Burger, C. D., Cartin-Ceba, R., Rosen, C. B., et al. (2020). Outcomes of liver transplantation in treated portopulmonary hypertension patients with a mean pulmonary arterial pressure  $\geq 35$  mm Hg. *Transpl. Direct* 6 (12), e630. doi:10.1097/txd.0000000000001085
- Fisher, J. H., Johnson, S. R., Chau, C., Kron, A. T., and Granton, J. T. (2015). Effectiveness of phosphodiesterase-5 inhibitor therapy for portopulmonary hypertension. *Can. Respir. J.* 22 (1), 42–46. doi:10.1155/2015/810376
- Fix, O. K., Bass, N. M., De Marco, T., and Merriman, R. B. (2007). Long-term follow-up of portopulmonary hypertension: Effect of treatment with epoprostenol. *Liver Transpl.* 13 (6), 875–885. doi:10.1002/lt.21174
- Galiè, N., Hoeper, M. M., Humbert, M., Torbicki, A., Vachiery, J. L., Barbera, J. A., et al. (2009). Guidelines for the diagnosis and treatment of pulmonary hypertension: The task force for the diagnosis and treatment of pulmonary hypertension of the European society of Cardiology (ESC) and the European respiratory society (ERS), endorsed by the international society of heart and lung transplantation (ISHLT). *Eur. Heart J.* 30 (20), 2493–2537. doi:10.1093/eurheartj/ehp297
- Gough, M. S., and White, R. J. (2009). Sildenafil therapy is associated with improved hemodynamics in liver transplantation candidates with pulmonary arterial hypertension. *Liver Transpl.* 15 (1), 30–36. doi:10.1002/lt.21533
- Halank, M., Knudsen, L., Seyfarth, H. J., Ewert, R., Wiedemann, B., Kolditz, M., et al. (2011). Ambrisentan improves exercise capacity and symptoms in patients with portopulmonary hypertension. *Z. Gastroenterol.* 49 (9), 1258–1262. doi:10.1055/s-0031-1273393
- Hemnes, A. R., and Robbins, I. M. (2009). Sildenafil monotherapy in portopulmonary hypertension can facilitate liver transplantation. *Liver Transpl.* 15 (1), 15–19. doi:10.1002/lt.21479
- Hoeper, M. M., Halank, M., Marx, C., Hoeffken, G., Seyfarth, H. J., Schauer, J., et al. (2005). Bosentan therapy for portopulmonary hypertension. *Eur. Respir. J.* 25 (3), 502–508. doi:10.1183/09031936.05.00080804
- Hoeper, M. M., Seyfarth, H. J., Hoeffken, G., Wirtz, H., Speikerkoetter, E., Pletz, M. W., et al. (2007). Experience with inhaled iloprost and bosentan in portopulmonary hypertension. *Eur. Respir. J.* 30 (6), 1096–1102. doi:10.1183/09031936.00032407
- Hollatz, T. J., Musat, A., Westphal, S., Decker, C., D'Alessandro, A. M., Keevil, J., et al. (2012). Treatment with sildenafil and treprostinil allows successful liver transplantation of patients with moderate to severe portopulmonary hypertension. *Liver Transpl.* 18 (6), 686–695. doi:10.1002/lt.23407
- Johnson, S. R., Granton, J. T., Tomlinson, G. A., Grosbein, H. A., Le, T., Lee, P., et al. (2012). Warfarin in systemic sclerosis-associated and idiopathic pulmonary arterial hypertension. A Bayesian approach to evaluating treatment for uncommon disease. *J. Rheumatol.* 39 (2), 276–285. doi:10.3899/jrheum.110765
- Khaderi, S., Khan, R., Safdar, Z., Stribling, R., Vierling, J. M., Goss, J. A., et al. (2014). Long-term follow-up of portopulmonary hypertension patients after liver transplantation. *Liver Transpl.* 20 (6), 724–727. doi:10.1002/lt.23870
- Krowka, M. J., Fallon, M. B., Kawut, S. M., Fuhrmann, V., Heimbach, J. K., Ramsay, M. A., et al. (2016). International liver transplant society practice guidelines: Diagnosis and management of hepatopulmonary syndrome and portopulmonary hypertension. *Transplantation* 100 (7), 1440–1452. doi:10.1097/tp.0000000000001229
- Krowka, M. J., Frantz, R. P., McGoon, M. D., Severson, C., Plevak, D. J., and Wiesner, R. H. (1999). Improvement in pulmonary hemodynamics during intravenous epoprostenol (prostacyclin): A study of 15 patients with moderate to severe portopulmonary hypertension. *Hepatology* 30 (3), 641–648. doi:10.1002/hep.510300307
- Krowka, M. J., Miller, D. P., Barst, R. J., Taichman, D., Dweik, R. A., Badesch, D. B., et al. (2012). Portopulmonary hypertension: A report from the US-based REVEAL registry. *Chest* 141 (4), 906–915. doi:10.1378/chest.11-0160
- Krowka, M. J., Plevak, D. J., Findlay, J. Y., Rosen, C. B., Wiesner, R. H., and Krom, R. A. (2000). Pulmonary hemodynamics and perioperative cardiopulmonary-related mortality in patients with portopulmonary hypertension undergoing liver transplantation. *Liver Transpl.* 6 (4), 443–450. doi:10.1053/jlts.2000.6356
- Legros, L., Chabanne, C., Camus, C., Fournet, M., Houssel-Debry, P., Latournerie, M., et al. (2017). Oral pulmonary vasoactive drugs achieve hemodynamic eligibility for liver transplantation in portopulmonary hypertension. *Dig. Liver Dis.* 49 (3), 301–307. doi:10.1016/j.jltd.2016.10.010
- Liu, Y. J., and Li, T. (2016). An excerpt of international liver transplant society Practice guidelines: Diagnosis and management of hepatopulmonary hypertension. *J. Clin. Hepatol.* 32 (10), 1838–1842. doi:10.3969/j.issn.1001-5256.2020.01.051
- Mancuso, L., Scordato, F., Pieri, M., Valerio, E., and Mancuso, A. (2013). Management of portopulmonary hypertension: New perspectives. *World J. Gastroenterol.* 19 (45), 8252–8257. doi:10.3748/wjg.v19.i45.8252
- Mantz, F. A., Jr., and Craige, E. (1951). Portal axis thrombosis with spontaneous portacaval shunt and resultant cor pulmonale. *AMA. Arch. Pathol.* 52 (1), 91–97.
- Martínez-Palli, G., Taurà, P., Balust, J., Beltrán, J., Zavala, E., and García-Valdecasas, J. C. (2005). Liver transplantation in high-risk patients: Hepatopulmonary syndrome and portopulmonary hypertension. *Transpl. Proc.* 37 (9), 3861–3864. doi:10.1016/j.transproceed.2005.09.119

- Melgosa, M. T., Ricci, G. L., García-Pagan, J. C., Blanco, I., Escribano, P., Abalde, J. G., et al. (2010). Acute and long-term effects of inhaled iloprost in portopulmonary hypertension. *Liver Transpl.* 16 (3), 348–356. doi:10.1002/lt.21997
- Preston, I. R., Burger, C. D., Bartolome, S., Safdar, Z., Krowka, M., Sood, N., et al. (2020). Ambrisentan in portopulmonary hypertension: A multicenter, open-label trial. *J. Heart Lung Transpl.* 39 (5), 464–472. doi:10.1016/j.healun.2019.12.008
- Ramsay, M. A., Simpson, B. R., Nguyen, A. T., Ramsay, K. J., East, C., and Klintmalm, G. B. (1997). Severe pulmonary hypertension in liver transplant candidates. *Liver Transpl. Surg.* 3 (5), 494–500. doi:10.1002/lt.500030503
- Reichenberger, F., Voswinckel, R., Steveling, E., Enke, B., Kreckel, A., Olschewski, H., et al. (2006). Sildenafil treatment for portopulmonary hypertension. *Eur. Respir. J.* 28 (3), 563–567. doi:10.1183/09031936.06.00030206
- Robalino, B. D., and Moodie, D. S. (1991). Association between primary pulmonary hypertension and portal hypertension: Analysis of its pathophysiology and clinical, laboratory and hemodynamic manifestations. *J. Am. Coll. Cardiol.* 17 (2), 492–498. doi:10.1016/s0735-1097(10)80121-4
- Rossi, R., Talarico, M., Schepis, F., Coppi, F., Sgura, F. A., Monopoli, D. E., et al. (2021). Acute hemodynamic effects of intravenous adenosine in patients with associated pulmonary arterial hypertension: Comparison with intravenous epoprostenol. *Pulm. Pharmacol. Ther.* 70, 147–151. doi:10.1016/j.pupt.2017.06.005
- Sadd, C. J., Osman, F., Li, Z., Chybowski, A., Decker, C., Henderson, B., et al. (2021). Long-term outcomes and survival in moderate-severe portopulmonary hypertension after liver transplant. *Transplantation* 105 (2), 346–353. doi:10.1097/tp.0000000000003248
- Safdar, Z., Bartolome, S., and Sussman, N. (2012). Portopulmonary hypertension: An update. *Liver Transpl.* 18 (8), 881–891. doi:10.1002/lt.23485
- Savale, L., Guimas, M., Ebstein, N., Fertin, M., Jevnikar, M., Renard, S., et al. (2020). Portopulmonary hypertension in the current era of pulmonary hypertension management. *J. Hepatol.* 73 (1), 130–139. doi:10.1016/j.jhep.2020.02.021
- Savale, L., Magnier, R., Le Pavec, J., Jaïs, X., Montani, D., O'Callaghan, D. S., et al. (2013). Efficacy, safety and pharmacokinetics of bosentan in portopulmonary hypertension. *Eur. Respir. J.* 41 (1), 96–103. doi:10.1183/09031936.00117511
- Savale, L., Sattler, C., Coilly, A., Conti, F., Renard, S., Francoz, C., et al. (2017). Long-term outcome in liver transplantation candidates with portopulmonary hypertension. *Hepatology* 65 (5), 1683–1692. doi:10.1002/hep.28990
- Schott, R., Chaouat, A., Launoy, A., Pottecher, T., and Weitzenblum, E. (1999). Improvement of pulmonary hypertension after liver transplantation. *Chest* 115 (6), 1748–1749. doi:10.1378/chest.115.6.1748
- Scott, V., De Wolf, A., Kang, Y., Martin, M., Selby, R., Fung, J., et al. (1993). Reversibility of pulmonary hypertension after liver transplantation: A case report. *Transpl. Proc.* 25 (2), 1789–1790.
- Sitbon, O., Bosch, J., Cottrel, E., Csonka, D., de Groote, P., Hoeper, M. M., et al. (2019). Macitentan for the treatment of portopulmonary hypertension (PORTICO): A multicentre, randomised, double-blind, placebo-controlled, phase 4 trial. *Lancet. Respir. Med.* 7 (7), 594–604. doi:10.1016/s2213-2600(19)30091-8
- Sussman, N., Kaza, V., Barshes, N., Stribling, R., Goss, J., O'Mahony, C., et al. (2006). Successful liver transplantation following medical management of portopulmonary hypertension: A single-center series. *Am. J. Transpl.* 6 (9), 2177–2182. doi:10.1111/j.1600-6143.2006.01432.x
- Swanson, K. L., Wiesner, R. H., Nyberg, S. L., Rosen, C. B., and Krowka, M. J. (2008). Survival in portopulmonary hypertension: Mayo Clinic experience categorized by treatment subgroups. *Am. J. Transpl.* 8 (11), 2445–2453. doi:10.1111/j.1600-6143.2008.02384.x
- Tuder, R. M., Archer, S. L., Dorfmueller, P., Erzurum, S. C., Guignabert, C., Michelakis, E., et al. (2013). Relevant issues in the pathology and pathobiology of pulmonary hypertension. *J. Am. Coll. Cardiol.* 62 (25), D4–D12. doi:10.1016/j.jacc.2013.10.025
- Xu, X. Q., and Jing, Z. C. (2018). The 6th World symposium on pulmonary hypertension: Focus on updates on definition and clinical classification of pulmonary hypertension. *Med. J. Peking Union Med. Coll. Hosp.* 9 (3), 197–201. doi:10.3969/j.issn.1674-9081.2018.03.002



## OPEN ACCESS

EDITED BY  
Maria Dimitrova,  
Medical University Sofia, Bulgaria

REVIEWED BY  
Magda Rotaru,  
Medicover Hospital, Romania  
Klejda Harasani,  
University of Medicine, Tirana, Albania  
Daniela Grekova-Kafalova,  
Medical University of Plovdiv, Bulgaria

\*CORRESPONDENCE  
Andrei Lucian Groza,  
✉ dr.andreigroza@gmail.com

SPECIALTY SECTION  
This article was submitted to  
Gastrointestinal and  
Hepatic Pharmacology,  
a section of the journal  
Frontiers in Pharmacology

RECEIVED 11 September 2022  
ACCEPTED 08 December 2022  
PUBLISHED 19 December 2022

CITATION  
Groza AL, Ungureanu BS, Tefas C,  
Miutescu B and Tanțau M (2022),  
Correlation between adenoma  
detection rate and other quality  
indicators, and its variability depending  
on factors such as sedation or indication  
for colonoscopy.  
*Front. Pharmacol.* 13:1041915.  
doi: 10.3389/fphar.2022.1041915

COPYRIGHT  
© 2022 Groza, Ungureanu, Tefas,  
Miutescu and Tanțau. This is an open-  
access article distributed under the  
terms of the [Creative Commons  
Attribution License \(CC BY\)](https://creativecommons.org/licenses/by/4.0/). The use,  
distribution or reproduction in other  
forums is permitted, provided the  
original author(s) and the copyright  
owner(s) are credited and that the  
original publication in this journal is  
cited, in accordance with accepted  
academic practice. No use, distribution  
or reproduction is permitted which does  
not comply with these terms.

# Correlation between adenoma detection rate and other quality indicators, and its variability depending on factors such as sedation or indication for colonoscopy

Andrei Lucian Groza<sup>1\*</sup>, Bogdan Silviu Ungureanu<sup>2,3</sup>,  
Cristian Tefas<sup>1,4</sup>, Bogdan Miutescu<sup>5</sup> and Marcel Tanțau<sup>1,4</sup>

<sup>1</sup>Iuliu Hațieganu University of Medicine and Pharmacy, 3rd Department of Internal Medicine, Cluj-Napoca, Romania, <sup>2</sup>Research Center of Gastroenterology and Hepatology, University of Medicine and Pharmacy of Craiova, Craiova, Romania, <sup>3</sup>Department of Gastroenterology, University of Medicine and Pharmacy of Craiova, Craiova, Romania, <sup>4</sup>Regional Institute of Gastroenterology and Hepatology "Prof. dr. Octavian Fodor", Cluj-Napoca, Romania, <sup>5</sup>Department of Gastroenterology and Hepatology, "Victor Babeș" University of Medicine and Pharmacy, Timisoara, Romania

Colorectal cancer (CRC) is an important worldwide public health burden and colonoscopy is the main diagnostic and most importantly, preventive method. For this reason, many countries have implemented national or regional CRC screening programs. High-quality colonoscopy is a prerequisite to effectively detect premalignant lesions, like adenomas. The quality of colonoscopy is assessed using several quality indicators, the main one being adenoma detection rate (ADR). In Romania, despite CRC having the highest incidence of all cancers, there is no national screening program and quality in colonoscopy is not routinely assessed. We therefore wanted to evaluate the actual level of quality in colonoscopy in a region of Romania. Our study was conducted in two private endoscopy clinics over a period of 7 months. 1,440 consecutive colonoscopies performed by five physicians were included in the study. We found that the quality level is above the minimum one recommended by international societies and that the ADR calculation method does not significantly influence its value. Furthermore, ADR correlated well with other quality indicators such as polyp detection rate (PDR) and adenoma per colonoscopy (APC). An interesting finding was that ADR was higher among colonoscopies performed without sedation. Thus, our data encourage endoscopists to adopt a sedation-free colonoscopy in their practice without an impact on the quality of the procedure.

## KEYWORDS

adenoma detection rate, screening colonoscopy, quality indicators, adenoma per colonoscopy, colorectal cancer, sedation



## Introduction

Colorectal cancer (CRC) is one of the worldwide leading causes of cancer death and colonoscopy is the most important method of screening and diagnosis. To provide accurate results, endoscopists must be sure that they have performed a high-quality colonoscopy. The quality of colonoscopy is routinely assessed in countries where there are national CRC screening programs, using several quality indicators. The main one is adenoma detection rate (ADR), representing the proportion of screening colonoscopies in which at least one adenoma has been detected. However, there is uncertainty in the literature regarding the inclusion or exclusion criteria of patients whose ADR is reported. The American Society of Gastrointestinal Endoscopy (ASGE) defines ADR as the proportion of screening colonoscopies in average-risk individuals aged 50 years or older in which at least one adenoma has been detected (Rizk et al., 2015). The minimum standard proposed by ASGE is 30% for male and 20% for female patients. The European Society of Gastrointestinal Endoscopy (ESGE) reports the ADR to the total number of screening and diagnostic colonoscopies in individuals aged 50 years or older, mentioning some exclusion criteria like workup of previously detected lesion or follow-up in inflammatory bowel disease (Kaminski et al., 2017). The minimum standard proposed by ESGE is 25% regardless of gender.

In Romania, despite CRC having the highest incidence of all cancers, there is no national screening program, thus screening is conducted opportunistically. In addition, quality in colonoscopy is not routinely assessed and there are no national guidelines for quality assessment.

In this study we wanted to determine the proportion of screening colonoscopies and the current level of quality in endoscopy in a region in Romania, based on the quality indicators recommended by ESGE. We also wanted to establish if there are any statistical differences in calculating ADR depending on the indication for colonoscopy, and to compare it with other newly proposed quality indicators like adenoma per colonoscopy (APC) and adenoma per positive participant (APP).

## Materials and methods

We conducted a prospective observational study in two private endoscopy clinics from two cities in northwestern Romania (Cluj-Napoca and Zalau), between July 1 and 31 December 2021.

We recorded all colonoscopies performed by five endoscopists with at least 5 years of experience and a minimum of 300 colonoscopies per year. The exclusion criteria were emergency colonoscopies, patients without a

clear indication for colonoscopy, patients with indication for sigmoidoscopy or patients with a specific therapeutic indication. All endoscopies were performed using HD equipment with virtual chromoendoscopy and magnification. In both clinics the data were recorded electronically in a different system than the main patient record system, due to the lack of a standardized endoscopy reporting system.

The recorded data were related to patients' demographics and quality of the procedures. The quality indicators we followed were time slot for colonoscopy, reason for admission, quality of bowel preparation (defined as adequate or inadequate, based on the Boston Bowel Preparation Score), cecal intubation rate, use of sedation, number of detected polyps and their histology. Based on these parameters we calculated the polyp detection rate (PDR), ADR, APC, APP.

Endoscopists were not aware of the recorded parameters, but they agreed to participate in this study to find out their level of performance.

## Definition of quality indicators

We used both definitions from ESGE and ASGE guidelines in calculating PDR, ADR, APC and APP to see if there are differences determined by certain indications for colonoscopy, keeping in mind that ASGE reports ADR only for screening colonoscopies, while ESGE reports it for all colonoscopies with a screening or diagnostic indication (Table 1).

Summarizing these guidelines, we also defined high-quality colonoscopy as an examination complete to cecum in a patient with adequate bowel preparation (Boston Bowel Preparation Score  $\geq 6$ ), performed by a physician with an appropriate ADR, who carefully inspected the colonic mucosa (withdrawal time of at least 6 min) and applied the correct therapeutic procedures.

## Statistical analysis

Statistical analysis was performed using Graph Pad (GraphPad Software, San Diego, CA, United States). Descriptive statistics were reported as mean  $\pm$  standard deviation (SD), median (interquartile range) and range for continuous variables and as frequency and percentages for discrete variables. The two-tailed Mann-Whitney *U* test was used to compare two continuous variables and the Kruskal-Wallis *H* test for more than two variables. Violin plots were created to also evaluate the visual differences between two patient groups. Correlations were realized using heatmap (colors range from bright blue for strong positive

TABLE 1 ESGE and ASGE definitions of quality indicators.

	ESGE definition <a href="#">Kaminski et al. (2017)</a>	ASGE definition <a href="#">Rizk et al. (2015)</a>
PDR	Number of screening or diagnostic colonoscopies in patients aged 50 years or older in which one or more polyps were detected, divided by the total number of diagnostic colonoscopies	Number of screening colonoscopies in patients aged 50 years or older in which one or more polyps were detected, divided by the total number of screening colonoscopies
ADR	Number of screening or diagnostic colonoscopies in patients aged 50 years or older in which one or more adenomas were detected, divided by the total number of diagnostic colonoscopies	Number of screening colonoscopies in patients aged 50 years or older in which one or more adenomas were detected, divided by the total number of screening colonoscopies
APC	Number of detected adenomas in screening or diagnostic colonoscopies in patients aged 50 years or older divided by the total number of diagnostic colonoscopies	Number of detected adenomas in screening colonoscopies in patients aged 50 years or older divided by the total number of screening colonoscopies
APP	Number of detected adenomas in screening or diagnostic colonoscopies in patients aged 50 years or older divided by the number of diagnostic colonoscopies in which one or more adenomas were detected	Number of detected adenomas in screening colonoscopies in patients aged 50 years or older divided by the number of screening colonoscopies in which one or more adenomas were detected
Exclusion criteria	Colonoscopies with a therapeutic indication or follow-up of inflammatory bowel disease	Patients with family history of CRC or advanced adenoma, or patients with other conditions that classified them as high-risk patients for CRC.

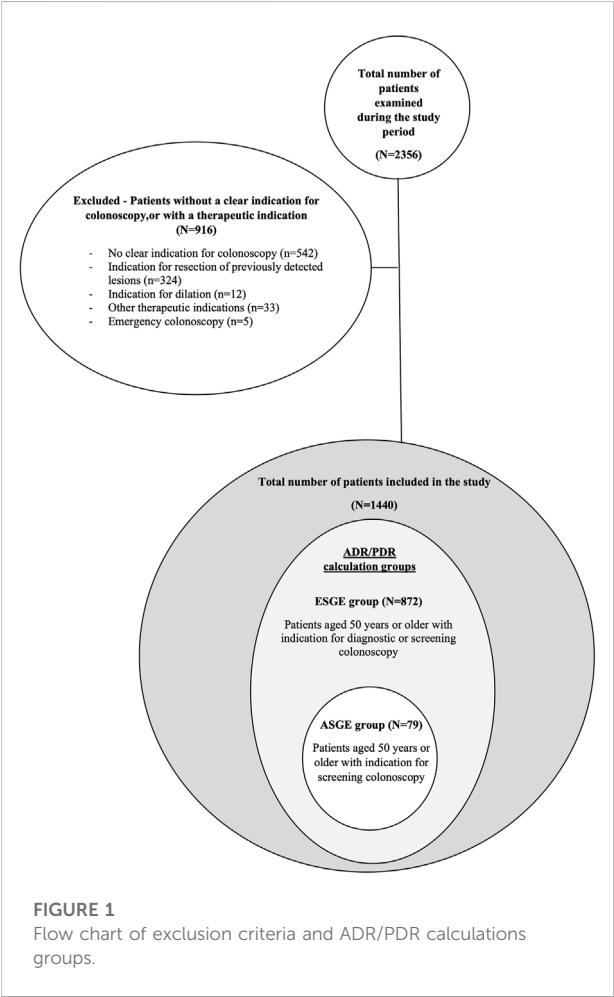


FIGURE 1  
Flow chart of exclusion criteria and ADR/PDR calculations groups.

correlations to bright olive, for strong negative correlations) and Spearman's correlation coefficient ( $\rho$ ). A  $p$ -value of less than 0.05 was statistically significant.

TABLE 2 List of recorded indications for colonoscopy.

	Patients	Percentage (%)
Lower gastrointestinal bleeding	281	19.51
Abdominal pain	240	16.67
Post polypectomy follow-up	148	10.28
Diarrhea	121	8.40
Post CRC follow-up	106	7.36
Constipation	97	6.74
Screening (positive family history)	95	6.60
Screening (average risk population)	91	6.32
Other reasons	89	6.18
Proctalgia	53	3.68
Abnormality on imaging study	41	2.85
IBD follow-up	36	2.50
Screening (positive FOBT)	21	1.46
Anemia	21	1.46

Results

During the study period a total of 2,356 colonoscopies were performed in the two clinics, 1,440 of which were included in the study. The most frequent exclusion criterion was the lack of an indication for colonoscopy. A flow chart of exclusion criteria and study groups is represented in Figure 1.

A list of the recorded indications for colonoscopy is shown in Table 2. The percentage of screening colonoscopies (all ages) was 14.38%, 6.32% of which were patients with a family history of CRC or advanced adenoma, and 1.46% were patients with previously positive FOBT.

**TABLE 3 Physician characteristics.**

	Physician 1	Physician 2	Physician 3	Physician 4	Physician 5
Age, years	47	42	37	57	36
Experience, years	18	14	10	30	9
Number of colonoscopies performed during the study period	243	813	252	381	667
Cecal intubation rate	92.15%	98.20%	96%	98.73%	93.25%
ADR <sub>ESGE</sub>	36.67%	49.46%	37.39%	40.48%	50.47%
PDR <sub>ESGE</sub>	40.00%	52.72%	43.48%	40.48%	62.46%
APC <sub>ESGE</sub>	0.80	1.01	0.59	0.86	1.05
APP <sub>ESGE</sub>	2.18	2.03	1.58	2.12	2.08
ADR <sub>ASGE</sub>	—	70.59%	42.86%	—	49.09%
ADR <sub>ASGE-male</sub>	—	91.67%	25.00%	—	38.46%
ADR <sub>ASGE-female</sub>	—	20.00%	66.67%	—	58.62%
PDR <sub>ASGE</sub>	—	76.47%	42.86%	—	58.18%
APC <sub>ASGE</sub>	—	2.12	0.71	—	0.84
APP <sub>ASGE</sub>	—	3.00	1.67	—	1.70

**TABLE 4 Characteristics of the patients in ESGE group.**

	Physician 1	Physician 2	Physician 3	Physician 4	Physician 5	<i>p</i> -value
	<i>N</i> = 30	<i>N</i> = 368	<i>N</i> = 115	<i>N</i> = 42	<i>N</i> = 317	
Age	62.50 ± 7.83	62.76 ± 7.86	61.58 ± 7.07	66.10 ± 10.65	62.67 ± 8.15	0.183
	61 (55–69.25)	62 (57–68)	61 (56–66)	65 (59–71.50)	62 (56–68)	
	51–77	50–100	50–83	52–110	50–88	
Gender, male	11 (36.7%)	153 (41.6%)	44 (38.3%)	20 (47.6%)	148 (46.7%)	0.411
Sedation						<0.0001
Midazolam	21 (70%)	340 (92.4%)	111 (96.5%)	34 (81%)	—	
Propofol	6 (20%)	11 (3%)	—	6 (14.3%)	—	
No	3 (10%)	17 (4.6%)	4 (3.5%)	2 (4.8%)	317 (100%)	
Sedation, yes	27 (90%)	351 (95.4%)	111 (96.5%)	40 (95.2%)	0 (0%)	
Rate of adequate bowel preparation	94.11%	86.11%	80.50%	97.46%	87.61%	0.002

Time slot for colonoscopy was 1 h for all examinations, regardless of the indication.

The overall rate of adequate bowel preparation (Boston Bowel Preparation Score  $\geq 6$ ) was 90.34%, with lower scores among patients who used a single dose administration of purgative.

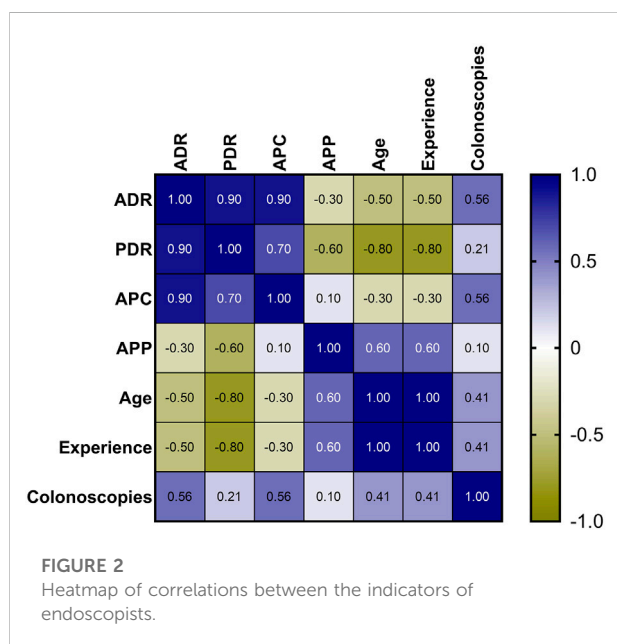
Withdrawal time was recorded in less than half of the diagnostic procedures, so we did not include it in the study.

Characteristics of the endoscopists are shown in Table 3. Only three of them had performed more than 300 examinations during the study period.

For the calculation of PDR, ADR, APC and APP 872 patients according to ESGE definition and 79 patients according to ASGE definition were included. Further on we will refer to these patients as the ESGE and ASGE groups.

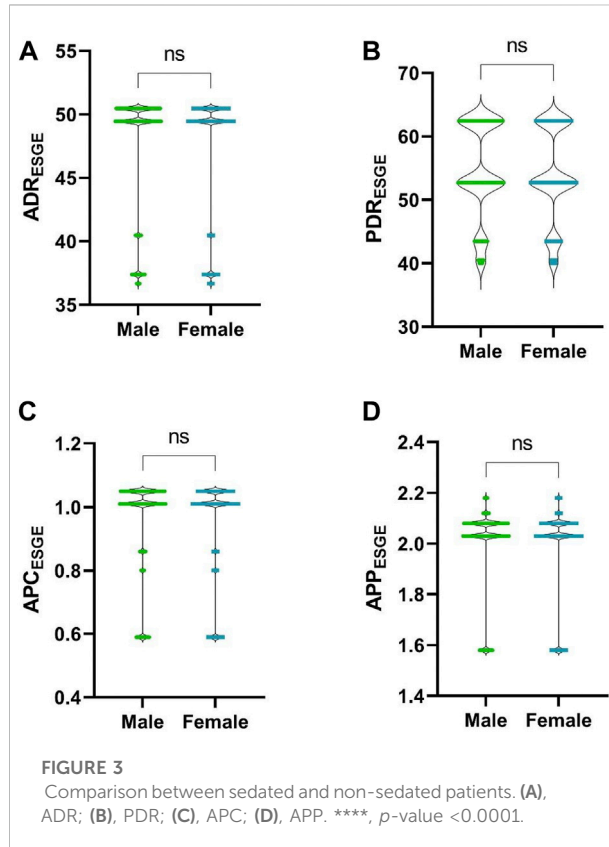
TABLE 5 Characteristics of the patients in ASGE group.

	Physician 2	Physician 3	Physician 5	<i>p</i> -value
	<i>N</i> = 17	<i>N</i> = 7	<i>N</i> = 55	
Age	61.18 ± 4.92	57.86 ± 4.53	60.51 ± 6.25	0.366
	61 (56.5–65)	58 (53–60)	61 (56–66)	
	54–70	53–66	50–79	
Gender, male	12 (70.6%)	4 (57.1%)	26 (47.3%)	0.241
Sedation				<0.0001
Midazolam	2 (11.8%)	7 (100.00%)	-	
No	15 (88.2%)	-	317 (100%)	
Sedation, yes	15 (88.2%)	7 (100.00%)	0 (0%)	<0.0001
Rate of adequate bowel preparation	86.59%	85.66%	87.18%	0.002



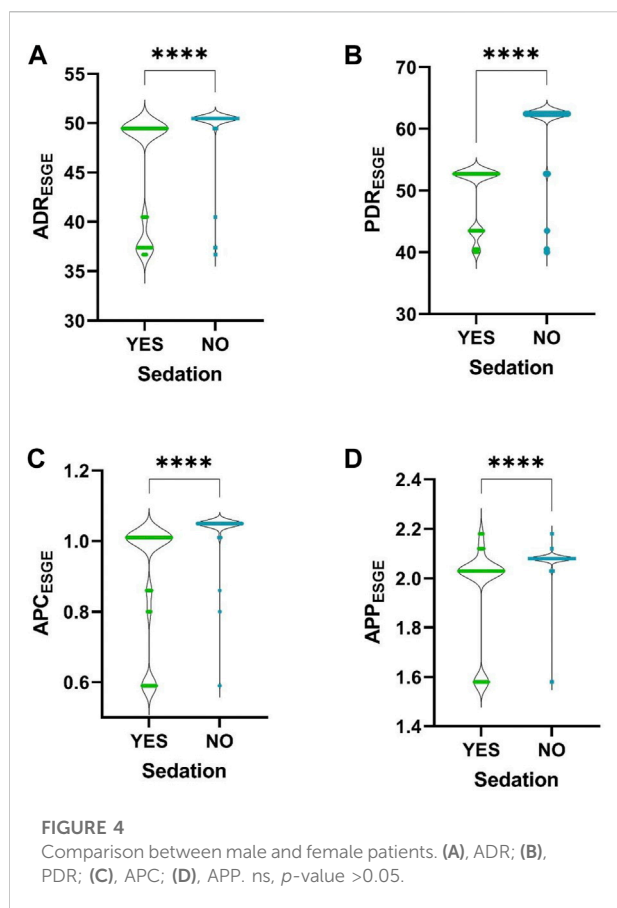
The ESGE group of patients had a mean age ( $\pm$ SD) of 62.72 ( $\pm$ 8.05) years. In this group the overall PDR was 54.02% and ADR was 47.36%. After applying the Kruskal–Wallis H test, no significant differences were noted between physician subgroups regarding age and gender of the patients, only regarding sedation and rate of adequate bowel preparation. One endoscopist did not use sedation, while the others used sedation in over 90% of the procedures, as seen in Table 4.

The ASGE group of patients had a mean age ( $\pm$ SD) of 60.42 ( $\pm$ 5.86) years. Regarding age and gender, no differences



were observed between patients. Use of sedation was different depending on the evaluated endoscopist, as seen in Table 5.

In the ESGE group there was a strong positive correlation between ADR and PDR ( $\rho = 0.90$ ) and between ADR and APC ( $\rho = 0.90$ ), but without a significant *p*-value due to the small



number of endoscopists included in our study ( $0.083 > 0.05$ ). (Figure 2).

In the same group we observed significant differences between sedated and non-sedated patients: better ADR (median of sedated vs. non-sedated, 49.46 vs. 50.47), PDR (52.72 vs. 62.46), APC (1.01 vs. 1.05) and APP (2.03 vs. 2.08) were obtained for non-sedated patients (Figure 3). Cecal intubation rate (CIR) was higher when colonoscopies were performed with sedation: OR = 20.62 (95% CI, 6.64–64.18),  $p$ -value  $<0.0001$ .

Among the patients in the ESGE group, taking gender into account (376, 43%, male vs. 493, 57%, female), no differences were observed for PDR ( $p$ -value = 0.1233), ADR ( $p$ -value = 0.0945), APC ( $p$ -value = 0.0977) or APP ( $p$ -value = 0.1364), (Figure 4).

In the ASGE group we noted significant differences between sedated and non-sedated patients: a higher ADR (median of sedated vs. non-sedated, 49.09 vs. 70.59), ADR for male patients (38.46 vs. 91.67), PDR (58.18 vs. 76.47), APC (0.84 vs. 2.12) and APP (1.7 vs. 3.0) in the case of non-sedated patients. A higher ADR was noted for female (58.62 vs. 20.00) sedated patients (Figure 5).

In the ESGE group we also wanted to see which of the indications for colonoscopy significantly influence quality

indicators. The one with the highest impact on PDR and ADR calculations are diarrhea, screening (especially in case of positive FOBT), and proctalgia. (Table 6).

We also conducted crude and adjusted linear regression analysis to fully examine the association between ADR and different indications for colonoscopy. As such, ADR was negatively associated with diarrhea and positively associated with the indication for screening in the adjusted analysis. Their coefficients barely changed and, most importantly, kept the direction of the association as in unadjusted analysis (Table 7).

## Discussions

The demographic data of the patients included in the study were very similar between all five endoscopists, both in terms of average age and gender, with a higher percentage of women examined.

The characteristics of the physicians were different both in terms of age and years of experience, but also in terms of the average number of colonoscopic examinations per year. We did not identify a correlation between the ADR value and any physician characteristics, although in previous similar studies they represented an important variable in the calculation of ADR (Lee et al., 2014; Jover et al., 2016; James et al., 2018). A slightly higher ADR was observed in younger doctors, with a higher average number of colonoscopies per year.

The most common indications for colonoscopy were lower digestive bleeding and abdominal pain. The percentage of screening examinations was low compared with other similar studies (Gupta et al., 2010; Boroff et al., 2017), the number of screening colonoscopies for patients with average risk of CRC representing only 6.32% of the total examinations included in the study. In the mentioned studies, the percentage of screening colonoscopies varied between 8.4% and 49.2%. For this reason, the calculation of ADR according to ASGE definition generated results with few statistically significant data. To be able to correctly calculate the ADR according to the ASGE definition, a follow-up for at least 1 year of each endoscopist under the given conditions would be necessary, or it would be necessary to introduce automatic digital calculation of the ADR. The only statistically significant conclusion from the ASGE patient group was that the ADR is higher among examinations performed without sedation than those performed with sedation. The same could be observed in the ESGE group. In the literature, there are conflicting data regarding the influence of sedation on ADR. In some studies ADR was significantly higher when colonoscopies were performed with sedation (Khan et al., 2020; Zhang et al., 2020), and in others ADR was not influenced by sedation (Bannert et al., 2012; Lee et al., 2014; Zhao et al., 2020) but the frequency of major complications increased among sedated patients (Zhao et al., 2020). We have not found studies in which



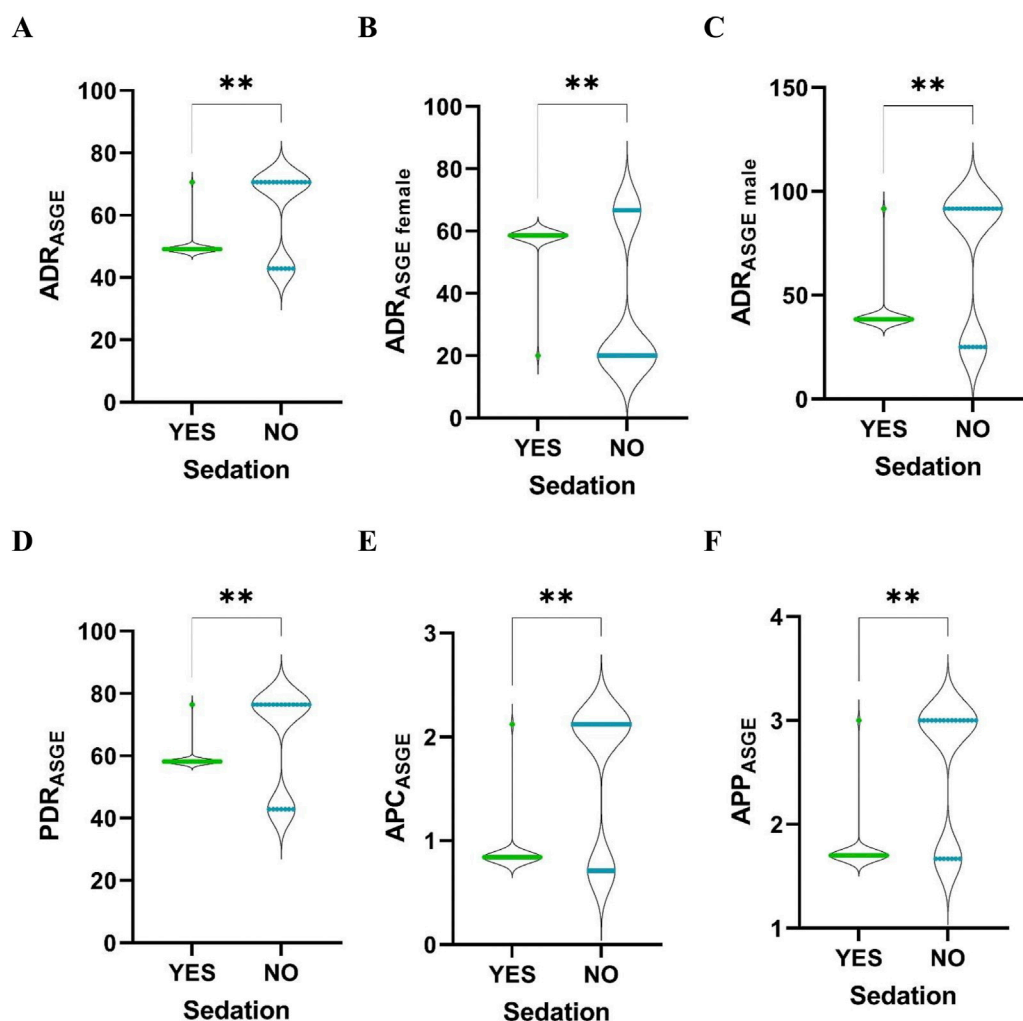


FIGURE 5

Comparison between sedated and non-sedated patients. (A), ADR; (B), ADR for female; (C), ADR for male; (D), PDR; (E), APC; (F), APP. \*\*,  $p$ -value  $< 0.01$ .

sedation negatively influences ADR, and the data we obtained may represent a particularity that deserves to be studied further or may be a false positive finding determined by the limitations of the study. Cecal intubation rate was higher when colonoscopies were performed with sedation which is in accordance with the data from the literature. There is a new measure of quality in colonoscopy that is being studied, called Performance Indicator of Colonic Intubation (PICI), which is defined as the rate of cecal intubation without significant discomfort and use of minimal sedation (Nass et al., 2021). The study of this indicator shows that there is an interest in reducing the amount of sedation during colonoscopy, or in performing as many examinations as possible without sedation, while maintaining the comfort of the patient and the quality of the examination. Our data may be of interest for the further study of PICI.

The ESGE group of patients was the reference group in this study. In this group overall PDR was 54.02% and ADR was 47.36%, significantly higher than the minimum values recommended by ESGE (Kaminski et al., 2017). The rate of adequate bowel preparation was lower than the minimum recommended standard by ESGE in three out of five examiners and we would have expected it to generate lower PDR and ADR values, but we did not find a positive correlation between these indicators. We tried to find an explanation for the increased ADR and PDR values and thus performed an analysis of the indicators related to the indication for colonoscopy. We found that ADR was negatively associated with diarrhea and positively associated with screening. None of the other indications for colonoscopy had a significant influence on its calculation. This means that the calculation method proposed by

**TABLE 6 Correlation between the indication for colonoscopy and PDR, ADR, APC, and APP calculation.**

Examination reason	N total = 872 number (percentage)	<i>p</i> -value			
		PDR	ADR	APC	APP
Anemia	15 (1.72%)	0.147	0.182	0.151	0.434
Constipation	61 (7.00%)	0.610	0.590	0.627	0.979
Diarrhea	62 (7.11%)	0.004	0.003	0.002	0.013
Abdominal pain	139 (15.94%)	0.303	0.286	0.371	0.664
Lower gastrointestinal bleeding	128 (14.68%)	0.932	0.827	0.894	0.565
Abnormality on imaging study	35 (4.01%)	0.056	0.050	0.050	0.049
Proctalgia	28 (3.21%)	0.056	0.046	0.054	0.167
Screening (positive FOBT)	19 (2.18%)	<0.001	<0.001	<0.001	<0.001
Screening (average risk population)	80 (9.17%)	<0.001	<0.001	<0.001	0.001
Screening (positive family history)	40 (4.59%)	0.023	0.034	0.052	0.532
Post CCR follow-up	92 (10.55%)	0.718	0.737	0.858	0.733
Post polypectomy follow-up	123 (14.11%)	0.291	0.312	0.217	0.216
Other reasons	50 (5.73%)	0.203	0.234	0.354	0.374

**TABLE 7 Crude and adjusted linear regression models for ADR calculation.**

Examination reason	N total = 872 number (percentage)	Crude coefficients		Adjusted coefficients	
		$\beta$ (95% CI)	<i>p</i> -value	$\beta$ (95% CI)	<i>p</i> -value
Anemia	15 (1.72%)	−1.34 (−3.88,1.21)	0.303	—	-
Constipation	61 (7.00%)	0.48 (−0.82,1.77)	0.472	—	-
Diarrhea	62 (7.11%)	−1.73 (−3.0,−0.44)	0.008	−1.47 (−2.74,−0.19)	0.025
Abdominal pain	139 (15.94%)	−0.05 (−0.95,0.86)	0.920	—	-
Lower gastrointestinal bleeding	128 (14.68%)	0.15 (−0.79,1.08)	0.757	—	-
Abnormality on imaging study	35 (4.01%)	0.43 (−1.25,2.12)	0.613	—	-
Proctalgia	28 (3.21%)	−1.15 (−3.02,0.73)	0.229	—	-
Screening (positive FOBT)	19 (2.18%)	3.12 (0.87,5.38)	0.007	3.19 (0.95, 5.43)	0.005
Screening (average risk population)	80 (9.17%)	1.92 (0.78,3.06)	0.001	1.88 (0.74, 3.02)	0.001
Screening (positive family history)	40 (4.59%)	−0.3 (−1.88,1.28)	0.707	—	-
Post CCR follow-up	92 (10.55%)	−0.12 (−1.19,0.96)	0.834	—	-
Post polypectomy follow-up	123 (14.11%)	−0.54 (−1.49,0.4)	0.261	—	-
Other reasons	50 (5.73%)	−0.66 (−2.08,0.76)	0.361	—	-

CI, confidence intervals.

ESGE does not increase the ADR or PDR values, compared to the method proposed by ASGE. On the contrary, in our patient group, these indicators were higher when reporting was done

only at screening colonoscopies. The negative influence of diarrhea on ADR may be due to the overuse of colonoscopy in cases of infectious or functional diarrhea.

Time slot for colonoscopy was higher than the minimum standard recommended by ESGE (30 min for clinical and primary screening colonoscopy; 45 min for colonoscopy following positive FOBD) (Kaminski et al., 2017), and perhaps this led to a more thorough examination of the colonic mucosa, with more frequent detection of polyps and a higher ADR.

There were no differences in the calculation of ADR, PDR, APC and APP regarding patient gender, so we consider that it is not necessary to establish a minimum target of these indicators according to gender, contrary to ASGE recommendations (Rizk et al., 2015).

## Limitations of the study

Considering that this was an observational study, it was not possible to impose the parameters that had to be followed and thus indicators such as withdrawal time or indication for colonoscopy were poorly recorded. This led to the exclusion of many patients from the study.

The total number of examinations as well as the number of endoscopists was low and some of the results had no statistical significance. Nevertheless, the power test was done and assuming an alpha level of 0.05, the correlations between the endoscopists indicators yielded the power between 84% and 95% for the different analysis.

The study followed the activity of endoscopists over a period and not several of consecutive examinations. Thus, significant differences appeared between physicians in terms of the number of examinations performed, which led to results without statistical significance in some instances. We believe that for a correct ADR calculation it is necessary to include at least 300 consecutive diagnostic colonoscopies for each physician, and in our study only three endoscopists met this condition.

## Conclusion

Even if in Romania the quality in colonoscopy is not routinely monitored, according to our data, endoscopists seem to exceed the minimum standards recommended by international societies. The lower rate of screening

colonoscopies does not influence the ADR calculation and any of the definitions proposed by international societies can be used for its assessment.

Also, ADR correlated well with PDR, APC and APP and we think that it could be used as the only quality indicator in countries where there is no quality monitoring in endoscopy until other indicators can be evaluated and calculated automatically.

## Data availability statement

The original contributions presented in the study are included in the article/Supplementary Material, further inquiries can be directed to the corresponding author.

## Author contributions

AG and MT planned and conducted the study, interpreted the data, and drafted the manuscript. BU interpreted the data and drafted the manuscript. CT and BM interpreted the data and reviewed the manuscript.

## Conflicts of interest

The authors declare that the research was conducted in the absence of any commercial or financial relationships that could be construed as a potential conflict of interest.

The reviewer MR declared a shared affiliation with the authors AG, CT, and MT to the handling editor at the time of review.

## Publisher's note

All claims expressed in this article are solely those of the authors and do not necessarily represent those of their affiliated organizations, or those of the publisher, the editors and the reviewers. Any product that may be evaluated in this article, or claim that may be made by its manufacturer, is not guaranteed or endorsed by the publisher.

## References

- Bannert, C., Reinhart, K., Dunkler, D., Trauner, M., Renner, F., Knoflach, P., et al. (2012). Sedation in screening colonoscopy: impact on quality indicators and complications. *Am. J. Gastroenterol.* 107 (12), 1837–1848. doi:10.1038/ajg.2012.347
- Boroff, E. S., Disbrow, M., Crowell, M. D., and Ramirez, F. C. (2017). Adenoma and polyp detection rates in colonoscopy according to indication. *Gastroenterol. Res. Pract.* 2017, 7207595. doi:10.1155/2017/7207595
- Gupta, M., Holub, J. L., and Eisen, G. (2010). Do indication and demographics for colonoscopy affect completion? A large national database evaluation. *Eur. J. Gastroenterol. Hepatol.* 22 (5), 620–627. doi:10.1097/MEG.0b013e3283352cd6
- James, P., Hegagi, M., Hegagi, M., Antonova, L., Rostom, A., Dube, C., et al. (2018). Variable endoscopist performance in proximal and distal adenoma detection during colonoscopy: a retrospective cohort study. *BMC Gastroenterol.* 18 (1), 73. doi:10.1186/s12876-018-0800-4

- Jover, R., Zapater, P., Bujanda, L., Hernández, V., Cubiella, J., Pellisé, M., et al. (2016). Endoscopist characteristics that influence the quality of colonoscopy. *Endoscopy* 48 (3), 241–247. doi:10.1055/s-0042-100185
- Kaminski, M. F., Thomas-Gibson, S., Bugajski, M., Bretthauer, M., Rees, C. J., Dekker, E., et al. (2017). Performance measures for lower gastrointestinal endoscopy: a European society of gastrointestinal endoscopy (ESGE) quality improvement initiative. *Endoscopy* 49 (4), 378–397. doi:10.1055/s-0043-103411
- Khan, F., Hur, C., Lebwohl, B., and Krigel, A. (2020). Unsedated colonoscopy: Impact on quality indicators. *Dig. Dis. Sci.* 65 (11), 3116–3122. doi:10.1007/s10620-020-06491-0
- Lee, T. J., Rees, C. J., Blanks, R. G., Moss, S. M., Nickerson, C., Wright, K. C., et al. (2014). Colonoscopic factors associated with adenoma detection in a national colorectal cancer screening program. *Endoscopy* 46 (3), 203–211. doi:10.1055/s-0033-1358831
- Nass, K. J., van Doorn, S. C., van der Vlugt, M., Fockens, P., and Dekker, E. (2021). Impact of sedation on the performance indicator of colonic intubation. *Endoscopy* 53 (6), 619–626. doi:10.1055/a-1254-5182
- Rizk, M. K., Sawhney, M. S., Cohen, J., Pike, I. M., Adler, D. G., Dominitz, J. A., et al. (2015). Quality indicators common to all GI endoscopic procedures. *Gastrointest. Endosc.* 81 (1), 3–16. doi:10.1016/j.gie.2014.07.055
- Zhang, Q., Dong, Z., Jiang, Y., Zhan, T., Wang, J., and Xu, S. (2020). The impact of sedation on adenoma detection rate and cecal intubation rate in colonoscopy. *Gastroenterol. Res. Pract.* 2020, 3089094. doi:10.1155/2020/3089094
- Zhao, S., Deng, X. L., Wang, L., Ye, J. W., Liu, Z. Y., Huang, B., et al. (2020). The impact of sedation on quality metrics of colonoscopy: a single-center experience of 48, 838 procedures. *Int. J. Colorectal Dis.* 35 (6), 1155–1161. doi:10.1007/s00384-020-03586-y



## OPEN ACCESS

## EDITED BY

Mariana Jinga,  
Carol Davila University of Medicine and  
Pharmacy, Romania

## REVIEWED BY

Luiz Jardelino De Lacerda Neto,  
Federal University of Campina Grande,  
Brazil  
Adina Turcu-Stiolica,  
University of Medicine and Pharmacy of  
Craiova, Romania

## \*CORRESPONDENCE

Ahuo Ma,  
✉ [maahuo@sohu.com](mailto:maahuo@sohu.com)

## SPECIALTY SECTION

This article was submitted to  
Gastrointestinal and Hepatic  
Pharmacology,  
a section of the journal  
Frontiers in Pharmacology

RECEIVED 09 June 2022

ACCEPTED 30 December 2022

PUBLISHED 24 January 2023

## CITATION

Ding L, Duan J, Yang T, Jin C, Luo J and  
Ma A (2023), Advanced intestinal  
regulation improves bowel preparation  
quality in patients with constipation: A  
systematic review and network meta-  
analysis.  
*Front. Pharmacol.* 13:964915.  
doi: 10.3389/fphar.2022.964915

## COPYRIGHT

© 2023 Ding, Duan, Yang, Jin, Luo and Ma.  
This is an open-access article distributed  
under the terms of the [Creative Commons  
Attribution License \(CC BY\)](https://creativecommons.org/licenses/by/4.0/). The use,  
distribution or reproduction in other  
forums is permitted, provided the original  
author(s) and the copyright owner(s) are  
credited and that the original publication in  
this journal is cited, in accordance with  
accepted academic practice. No use,  
distribution or reproduction is permitted  
which does not comply with these terms.

# Advanced intestinal regulation improves bowel preparation quality in patients with constipation: A systematic review and network meta-analysis

Liang Ding<sup>1</sup>, JinNan Duan<sup>2</sup>, Tao Yang<sup>1</sup>, ChaoQiong Jin<sup>1</sup>, Jun Luo<sup>1</sup>  
and Ahuo Ma<sup>1\*</sup>

<sup>1</sup>Department of Gastroenterology, Shaoxing People's Hospital, Shaoxing, Zhejiang, China, <sup>2</sup>Department of Infectious Diseases, Shaoxing People's Hospital, Shaoxing, Zhejiang, China

**Background:** Inadequate bowel preparation (IBP) has a critical influence on the colonoscopy procedure and is associated with significantly lower rates of detection of colorectal lesions. Constipation is an important risk factor of IBP, and some studies have attempted to address the bowel cleansing for constipated patients. However, there is still lack of consensus to guide the clinical work of bowel preparation (BP) for patients with constipation. Therefore, we aimed to perform a network meta-analysis to compare the overall efficacy of various regimens for BP in constipated patients.

**Methods:** We performed a comprehensive search of PubMed, MEDLINE, EMBASE, Cochrane, and Web of science to identify randomized controlled trials (RCTs) of bowel preparation regimens in constipated patients, update to January 2021. Two investigators independently evaluated articles and extracted data. The odds ratio (OR) with a 95% confidence interval (CI) was used to combine dichotomous data of the primary outcome which was defined as adequate bowel preparation (ABP). Rank probability was used to exhibit the outcome of the network meta-analysis.

**Results:** Eleven studies that included 1891 constipated patients were identified as suitable for inclusion. The proportion of ABP was associated with the administration of intensive regimen (OR 2.19, 95% CI 1.16–4.17,  $p = .02$ ,  $I^2 = 84\%$ ). Moreover, an intensive regimen had a significant efficacy and light heterogeneity when the same basic laxative program was used (OR 4.06, 95% CI 3.04–5.43,  $p < .0001$ ,  $I^2 = 0\%$ ). In the network meta-analysis, the protocol of a normal regimen + A (normal regimen plus advanced intestinal regulation) had a significant effect for bowel preparation compared with a normal regimen + IR (normal regimen plus irritating laxative regimen) (OR 5.21, 95% CI 1.18–24.55), H PEG (4L- polyethylene glycol) (OR 8.70, 95% CI 1.75–52.56), and normal regimen (NR) (OR 7.37, 95% CI 2.33–26.39). In the remaining protocols, no significant difference was observed in any comparison. No significant severe adverse events (AEs) associated with bowel preparation were reported in included studies.

**Conclusion:** Intensive regimens could improve bowel cleansing quality for patients with constipation, and advanced intestinal regulation regimens may be superior to others.

## KEYWORDS

bowel preparation, colonoscopy, constipation, network meta-analysis, regimens



# 1 Introduction

Colonoscopy is considered the most valuable screening tool for gastrointestinal disease especially for colorectal cancer and precancerous lesions as successful colonoscopy can improve the mortality rate of colorectal cancer through detection and resection of tumors at an early and treatable stage; about every 1% increase in the adenoma detection rate will decrease 3% incidence and 5% mortality in colorectal cancer (Corley et al., 2014). The success of colonoscopy to find colorectal lesions is associated with the quality of the bowel visibility, and IBP significantly decreases the rate of detection of colorectal lesions with about .53 odds ratio in early adenomas and .74 odds ratio in advanced adenomas comparing inadequate with adequate bowel preparation (Sulz et al., 2016).

With a global prevalence of 15%, constipation is a manifestation gastrointestinal dysmotility in clinic, and its prevalence would steadily rise after the age of 50 years, which is the recommended age to perform colonoscopy for colorectal lesion screening (Bharucha and Lacy, 2020). However, constipation is an important risk factor for inadequate bowel preparation (IBP) and difficulty in colonoscopy which may lead to lesion missing, patient suffering, and time cost (Takahashi et al., 2005). A meta-analysis which included 67 studies and 75,818 patients finds that constipation adds the risk of IBP nearly up to twofold (Gandhi et al., 2018). There is little resolution when patients have IBP on the colonoscopy procedure, thus optimizing that the bowel preparation (BP) regimen is the critical measure to ensure the examination quality. In clinical practice, we empirically reinforce the BP program such as increasing laxative amount or adding adjuvants to address the BP of constipation, but the efficacy is under debate. Some RCT studies have been designed to verify the effect of “empirical” intensive regimens, and they provide some optional choices for clinical work (Hassan et al., 2019). However, these options have extremely diverse, and there is still lack of arbitrary and objective evidence to recommend a special regimen; even some RCTs have attempted to address the obstacle by comparing a series of BP regimens (Saltzman et al., 2015; Hassan et al., 2019).

Therefore, we aimed to perform a network meta-analysis as it allows us evaluating the indirectly comparative efficacy of multiple treatments in individual RCTs to determine the ideal bowel preparation regimen for constipated patients.

# 2 Methods

We performed a systematic review and network meta-analysis according to the Cochrane Handbook (<https://training.cochrane.org/handbook>) and reported according to Preferred Reporting Items (Liberati et al., 2009). The registration number is CRD42021238380 in PROSPERO. We claim that there is no ethical approval or patient consent was required.

## Search methods

The databases of PubMed, MEDLINE, EMBASE, Cochrane, and Web of science were searched, update to January 2021. The search strategy identified in [All Fields] with the term: (prepar\* OR clean\*) AND (bowel\* OR colon\* OR intestin\*) AND (colonoscopy) AND (constipat\* OR fecal impaction), and the article type was restricted in “trial.”

# 2.1 Inclusion and exclusion criteria

Inclusion criteria: 1) studies were randomized controlled trials and report ABP, 2) subjects should be constipated adult patients (as diagnosed by a clinician, or using any recognized diagnostic criteria) that prepare to colonoscopy, 3) study purpose should be related with bowel preparation quality, 4) study interventions were pharmacological therapies, and 5) outcome should include dichotomous data about ABP.

Exclusion criteria: 1) studies not adhering to the inclusion criteria, 2) studies with only an abstract or commentary, and 3) studies that include other interventions like diet, education, and exercise.

# 2.2 Outcome assessment

The primary outcome is ABP, which is defined as follows: 1) total score more than 6 of the Boston Bowel Preparation Scale (BBPS), 2) total score less than 6 of the Ottawa Bowel Preparation Quality Scale (OBPS), 3) grade between 1 and 2 of the Aronchick Scale, and 4) grade 1 or 2 of the bowel preparation quality grading score.

The secondary outcome is the adverse events and tolerability of different bowel preparation regimens.

# 2.3 Data extraction

Two investigators independently extracted the intent-to-treat data from eligible studies. Disagreements were resolved by discussion with an additional reviewer. The data included the first author, country, publication years, recruitment criteria, intervention, assessment, sample size, age, sex, adequate preparation number, and adverse events.

# 2.4 Assessment of quality

Two independent investigators assess the methodological quality of the included studies, and disagreements will be resolved by consensus and discussion with a senior investigator. The Cochrane risk of bias tool will be used to assess the risk of bias at the individual study. Using this tool, studies will be classified to be at high, low, or unclear risk of bias based on seven items (<https://training.cochrane.org/handbook>): 1. random sequence generation, 2. allocation concealment, 3. blinding of participants, 4. blinding of outcome data, 5. incomplete data, 6. selective reporting, and 7. other biases.

# 2.5 Statistical analysis

The estimated effects of OR with 95% CI were used to evaluate dichotomous data by Review Manager version 5.3 (The Cochrane Collaboration, Oxford, UK). Heterogeneity was calculated with I<sup>2</sup> statistics. A fixed-effects model was used only in I<sup>2</sup> < 50%. Single study deletion was used to assess the sensitivity of estimated effects.

Bayesian network meta-analysis with convergence estimate was used to compare all possible comparisons by Stata SE 15 (StataCorp. College Station, Texas, USA) and Gemtc (GitHub). The parameters of the network meta-analysis were set as follows: 4 of

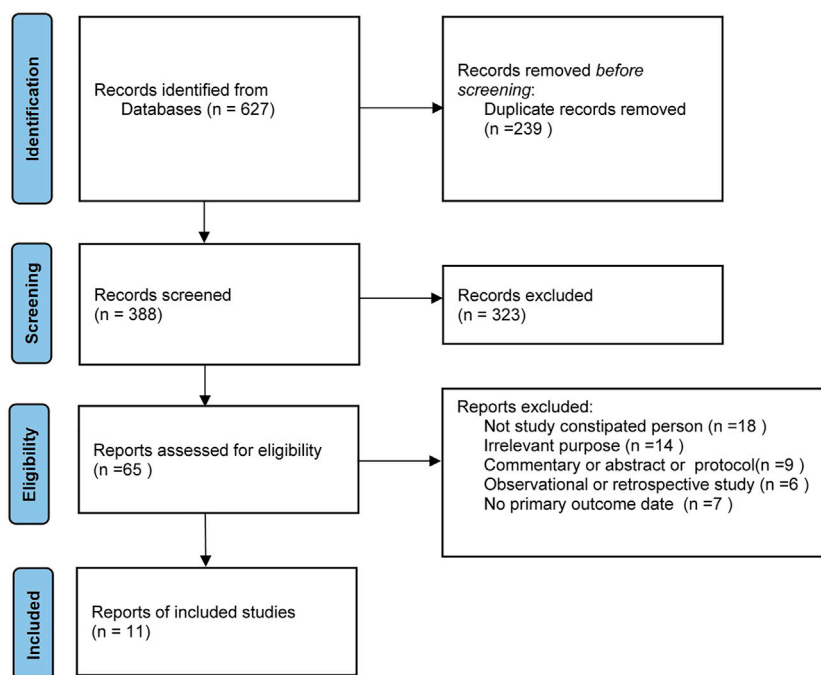


**FIGURE 1**  
Prisma flowchart.

chains, 20,000 of the tuning iterations, 50,000 of simulation iterations, 10 of thinning interval, 10,000 of inference samples, and 2.5 of variance scaling factor.  $p < .05$  was judged as statistically significant. If the study has two or more intervention arms, we divide the “shared” group into two or more equal groups (reasonably independent comparisons) according to the Cochrane handbook (<https://training.cochrane.org/handbook>).

## 3 Result

### 3.1 Search result

The search strategy identified a total of 627 citations; after removing 239 duplicates and 323 obviously irrelevant articles, we retrieved 65 articles for full-text appraisal (Figure 1). Finally, 11 articles were included in qualitative synthesis; 54 studies did not meet the inclusion criteria because of the reasons listed in Figure 1, most often because the participant was not a constipated person. It is worth mentioning that seven studies that included 868 patients were excluded because there was no primary outcome, and these study characteristics are shown in Supplementary Table S1.

### 3.2 Study characteristics

Fourteen regimens were studied for intestinal cleansing in 1,891 patients from 11 studies (Arezzo, 2000; De Salvo et al., 2006; Lee et al., 2010; Tajika et al., 2012; Tian et al., 2012; Pereyra et al., 2013; Parente et al., 2015; Li et al., 2017; Yu et al., 2018; Zhong et al., 2018;

Chancharoen et al., 2019). The test groups usually choose the regimen of conventional laxatives plus additional stimulant laxatives, prokinetic drugs, or advanced intestinal regulation such as using probiotics and dietary fiber, and the control group usually chooses low-dose laxative such as 2 L polyethylene glycol (PEG) or sodium phosphate (NaP). More information about study characteristics is summarized in Table 1.

### 3.3 Risk of bias in included studies

A majority of bias items showed low risk and unclear risk, but most studies showed a high risk in the item of performance bias since the fact that experimenters or medical workers must give the details of a BP plan to ensure the compliance of participants. More details are shown in Figure 2 and Supplementary Table S2.

### 3.4 Direct meta-analysis

We first divided the BP regimens into “intensive regimen” (combination of extra preparation program with conventional single laxative) and “standard regimen” (conventional single laxative like PEG and NaP). In total, 789 (77.5%) participants in the intensive group achieved ABP and 554 (63.5%) in the standard group. The estimated effect for the primary outcome was significantly higher in the intensive regimen (OR 2.19, 95% CI 1.16–4.17,  $p = .02$ ,  $I^2 = 84\%$ ) (Figure 3A).

We observed that the studies of Arezzo (2000), De Salvo et al. (2006), and Parente et al. (2015) conducted a completely different program in comparison which is not consistent in the use of laxative,

TABLE 1 Main characteristics of included studies.

Author	Year	Country	Constipation criterion	BP quality assessment	BP regimen	NP (f)	Age (M± SD)
Arezzo, A	2000	Germany	Asked if he or she experienced constipation	Non-validate score	Senna + MgSO <sub>4</sub>	40 (NA)	NA
					4L PEG	43 (NA)	NA
					NaP	48 (NA)	NA
De Salvo, L	2006	Italy	Rome II	Non-validate score	Senna + MgSO <sub>4</sub>	36 (NA)	61.4 ± 12.0
					2L PEG + bisacodyl	40 (NA)	60.5 ± 10.9
					NaP	25 (NA)	61.9 ± 12.6
Lee, H	2010	Korea	Rome III	BP quality grading	Probiotic 14 days + NaP	51 5)	40.5 ± 11.4
					NaP	53 5)	42.2 ± 11.7
Tajika, M	2012	Japan	<2 bowel movements per week more than a year	Aronchick's criteria	Mosapride+2L PEG	16 (11)	67.3 ± 8.6
					2L PEG	5 4)	67.8 ± 10.1
Tian, Xia	2012	China	Asked if he or she experienced constipation	BP quality grading	Probiotic 3 days + mosapride 3 days +2L PEG	86 (40)	NA
					Mosapride 3 days +2L PEG	82 (44)	NA
					2L PEG	80 (42)	NA
Pereyra, Lisandro	2013	Argentina	Rome II	BP quality grading	NaP	22 (NA)	59 ± 13.2
					NaP + bisacodyl	20 (NA)	57 ± 11.1
					4L PEG	15 (NA)	60 ± 13.8
					2L PEG + bisacodyl	20 (NA)	59 ± 10.9
Parente, Fabrizio	2015	Italy	Rome III	OBPS	2L PEG + simethicone + citrates + bisacodyl	193 (105)	60 ± 13
					4L PEG	189 (113)	59 ± 14
Li, Y	2017	China	1 or 2 on the Bristol Stool Form Scale	BBPS	2L PEG + bisacodyl	234 (160)	52.1 ± 9.8
					2L PEG	233 (156)	52.2 ± 9.7
Yu, Z. B	2018	China	Rome III	BBPS	Lactulose 2 days+2L PEG	36 (NA)	NA
					2L PEG + senna	36 (NA)	NA
					2L PEG	36 (NA)	NA
Zhong, Shishun	2018	China	Chinese chronic constipation guide	BBPS	Testa triticum tricum 7 days +3L PEG	93 (61)	52.9 ± 12.3
					3L PEG	97 (60)	53.3 ± 12.6
Chancharoen, A	2019	Thailand	Rome III or a score of 1 or 2 on the Bristol Stool Form Scale	OBPS	4L PEG + pre-2L PEG	37 (23)	57.6 ± 9.4
					4L PEG	39 (25)	59.2 ± 7.2

BP, bowel preparation; BBPS, Boston Bowel Preparation Scale; OBPS, Ottawa Bowel Preparation Scale; NaP, sodium phosphate; PEG, polyethylene glycol; NA, not available; NP, number of patients; f, female; M±SD, mean ± standard deviation.

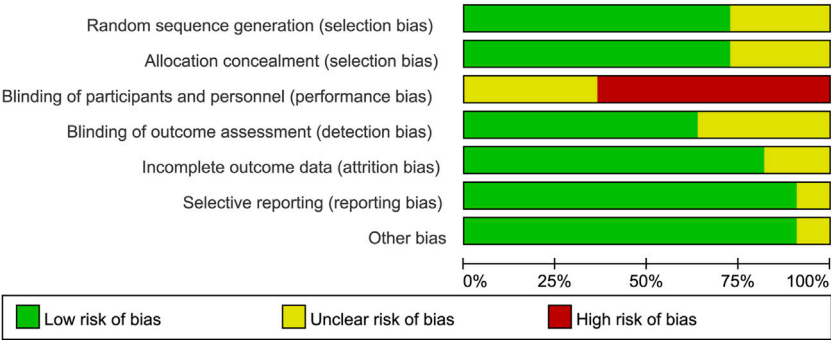


**FIGURE 2**  
Risk of bias graph: review authors' judgements about each risk of bias item presented as percentages across all included studies.

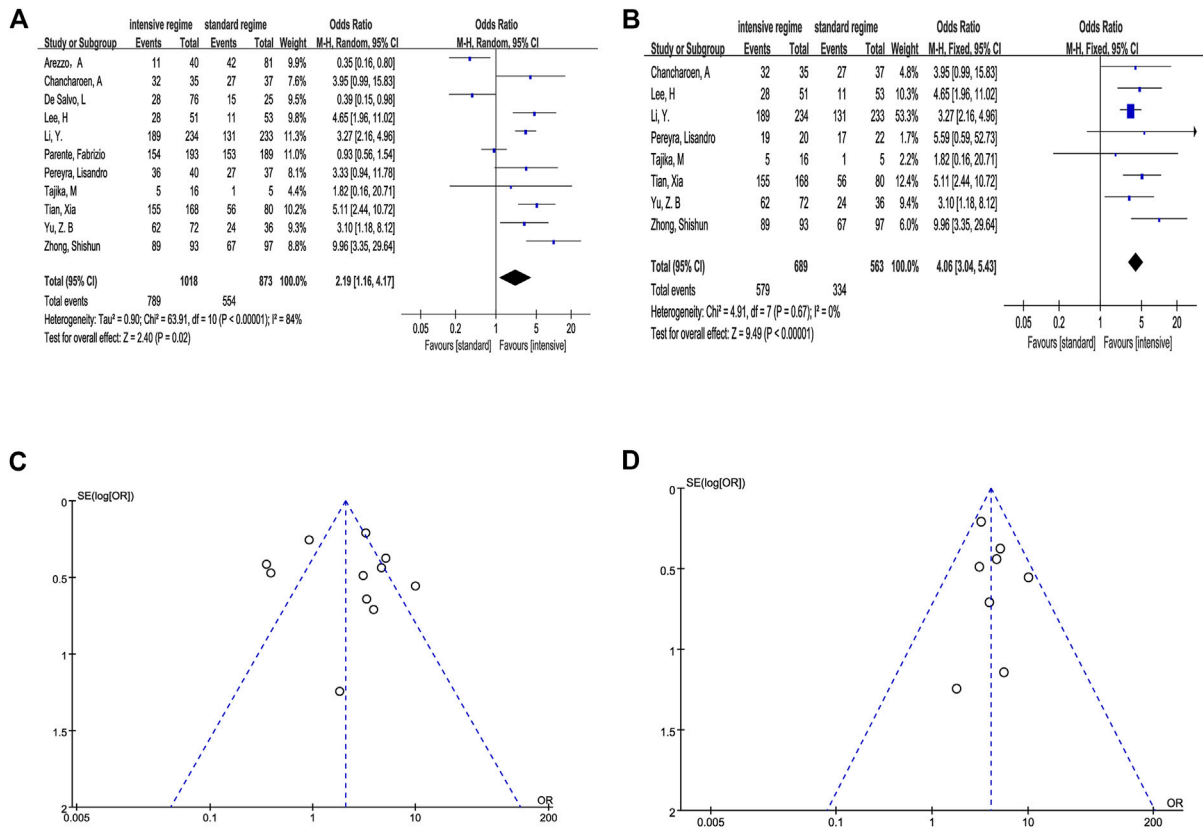
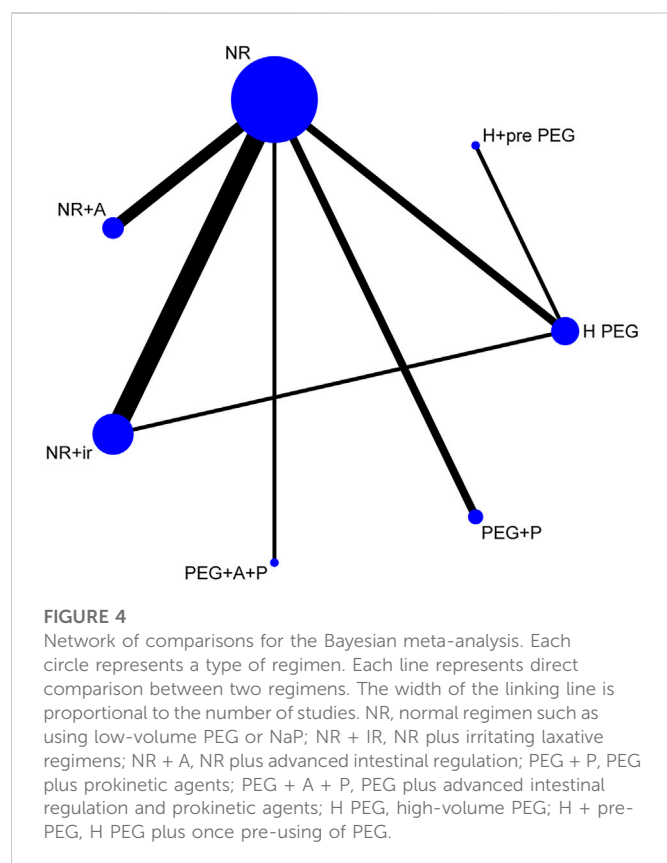


**FIGURE 3**  
Outcome of direct meta-analysis. (A, C) Forest graph and funnel graph of intensive regimen vs. standard regimen. (B, D) Forest graph and funnel graph of intensive regimen vs. standard regimen based on the same laxative.

and Pereyra et al. (2013) also had the same question in a certain way. Hence, we performed the analysis based on the same basic laxative program (4L PEG, 2L PEG or NaP) after removing inconsistent data. The result still indicated that the intensive regimen has a significant efficacy compared with the standard regimen when the same basic laxative program was used (OR 4.06, 95% CI 3.04–5.43,  $p < .0001$ ,  $I^2 = 0\%$ ) (Figure 3B).

Sensitivity analysis proved that all estimate effect maintained stability in the process of single study deletion (Supplementary Table S3).

We seemingly observed potential asymmetry in the funnel plots (Figures 3C,D). In order to further evaluate the publication bias, we conducted Begg's and Egger's tests, and the results suggested no evidence proving publication bias ( $p > .1$ ) (Supplementary Table S4).



## 3.5 Network meta-analysis

### 3.5.1 Regimens and sample size

In order to further explore the efficacy of different schemes, we classified them into seven types according to the mechanisms and eliminated the program of Senna + MgSO<sub>4</sub> because its effectiveness was as low as 27.6%. The seven types include normal regimen such as using low-volume PEG or NaP (NR), NR plus irritating laxative regimens (NR + IR), NR plus advanced intestinal regulation (NR + A), PEG plus prokinetic agents (PEG + P), PEG plus advanced intestinal regulation and prokinetic agents (PEG + A + P), high-volume PEG (H PEG), and H PEG plus once pre-using of PEG (H+pre-PEG).

The sample size and comparisons of each regimen showed the network map that was made by Stata software (Figure 4). The circle represented different regimens, and the size of the circle was proportional to the regimen sample. The lines indicated direct comparisons between regimens, and the thickness of the line was proportional to the weight of each regimen comparing others.

### 3.5.2 Quality assessment

The result of inconsistency factors was .53 with 95% CI .84–2.40, and the Random Effects Standard Deviation of Consistency model and the Inconsistency model kept a good consistency (.70 with 95% CI 0.31–1.51, .65 with 95% CI 0.22–1.47, respectively). Hence, we selected a consistency model for the network meta-analysis. In addition, a favorable convergence efficiency was provided by all PSRF values which were limited to 1.

## 3.6 Efficacy and rank probability analysis

Except for NR + A, any comparison of remaining six regimens showed no significant difference in the ABP rate. However, we found that the NR + A regimen showed significant superior efficacy than NR + IR (OR 5.21, 95% CI 1.18–24.55), H PEG (OR 8.70, 95% CI 1.75–52.56), and NR (OR 7.37, 95% CI 2.33–26.39) (Table 2).

In the ranking table, NR + A (33% with Rank 1 and 39% with Rank 2) and PEG + A + P (38% with Rank 1 and 27% with Rank 2) had priority of ranking top; other probability data are shown in Table 3.

## 3.7 Adverse events and tolerability with bowel preparation

In general, each regimen has a low rate of AEs and good tolerability although the definition was not according to a homogeneous standardized role. Only one serious adverse event (intestinal occlusion) was reported in the 4L PEG group, but it was not considered as the cause of colonic lavage solution (Parente et al., 2015). Other AEs mainly include gastrointestinal symptoms and are often mild and transient. Statistically significant difference was not obvious for secondary outcomes, except vomiting (OR 0.60, 95% CI 0.38–.97) (Table 4). However, we found that the AEs of vomiting were rare, and sensitivity analysis indicated two studies (Tajika et al., 2012; Zhong et al., 2018) which contributed to the major advantage of vomiting, meaning the difference was unstable.

## 4 Discussion

Constipation is a frequent risk factor of poor BP quality, and empirically strengthening bowel cleansing is a common clinical coping strategy (Hassan et al., 2019). In the article, we systematically investigated the efficacy and safety of the additional BP program for constipated patients to find the best solution. To our knowledge, this study is the first conducted network meta-analysis to address this clinical problem.

Two reviewers independently undertook a contemporaneous and exhaustive literature search which included searching the “grey” literature and [clinicaltrials.gov](http://clinicaltrials.gov), and recruited 11 studies which provide binary information about ABP or IBP but excluded seven articles that only provide the bowel score. The main reason for our choice is that IBP is more clinically meaningful premonition in the omission of intestinal lesions than the difference of bowel score (Clark et al., 2014). In addition, there was substantial variation in the definition of the bowel cleansing score which will cause great heterogeneity in the statistical process.

In total, 1,891 patients were studied for intestinal cleansing from 11 studies. To our knowledge, this is the largest meta-analysis of bowel preparation in patients with constipation. In the traditional meta-analysis, our results found that intensive regimens could acquire a high rate of ABP (OR 2.19, 95% CI 1.16–4.17) although there is major heterogeneity ( $I^2 = 84\%$ ). Moreover, pairwise results also exhibited significant superiority (OR 4.06, 95% CI 3.04–5.43) in intensive regimens but only with light heterogeneity ( $I^2 = 0\%$ ) when we eliminate the studies that compare double intervention factors: intensive measure and inconsistent laxative, meaning that large heterogeneity comes



**TABLE 2 Network meta-analysis of adequate bowel preparation.**

NR + A	PEG + A + P	H + pre-PEG	PEG + P	NR + IR	H PEG	NR
1.01 (.10, 11.29)						
1.97 (.12, 32.99)	1.94 (.07, 48.21)					
2.16 (.28, 17.20)	2.09 (.17, 28.98)	1.10 (.05, 21.70)				
5.21 (1.18, 24.55)	5.14 (.56, 48.51)	2.66 (.21, 48.70)	2.43 (.38, 16.92)			
8.70 (1.75, 52.56)	8.66 (.87, 96.40)	4.42 (.49, 45.30)	4.09 (.55, 33.15)	1.67 (.49, 6.02)		
7.37 (2.33, 26.39)	7.43 (.96, 55.09)	3.80 (.32, 48.70)	3.47 (.68, 19.02)	1.43 (.59, 3.41)	.85 (.24, 2.71)	

NR, normal regimen such as using low-volume PEG or NaP; NR + IR, NR plus irritating laxative regimens; NR + A, NR plus advanced intestinal regulation; PEG + P, PEG plus prokinetic agents; PEG + A + P, PEG plus advanced intestinal regulation and prokinetic agents; H PEG, high-volume PEG; H + pre-PEG, H PEG plus once pre-using of PEG.

Effect estimates presented as odds ratio (OR) with 95% confidence interval (CI).

*p*value < .05 are in bold.

**TABLE 3 Rank probability of bowel preparation regimens.**

Regimen	Rank 1	Rank 2	Rank 3	Rank 4	Rank 5	Rank 6	Rank 7
NR + A	.33	.39	.2	.07	.01	0	0
PEG + A + P	.38	.27	.2	.1	.02	.01	.02
H + pre-PEG	.2	.16	.23	.21	.07	.07	.06
PEG + P	.09	.17	0.3	.29	.08	.04	.03
NR + IR	0	.01	.05	.23	.46	.18	.06
H PEG	0	0	.01	.05	.15	.28	.5
NR	0	0	.01	.05	.21	.41	.32

NR, normal regimen such as using low-volume PEG or NaP; NR + IR, NR plus irritating laxative regimens; NR + A, NR plus advanced intestinal regulation; PEG + P, PEG plus prokinetic agents; PEG + A + P, PEG plus advanced intestinal regulation and prokinetic agents; H PEG, high-volume PEG; H + pre-PEG, H PEG plus once pre-using of PEG.

**TABLE 4 Secondary outcomes of intensive regimen vs. standard regimen.**

Outcome	N1 (E/S)	N2 (E/S)	OR	95% CI	I2 (%)
Nausea	115/902	135/767	.75	.57–1.00	19
Vomiting	32/709	45/578	.60	.38–.97	11
Bloating	96/902	101/767	.72	.40–1.30	61
Abdominal pain	70/902	50/767	1.21	.83–1.79	32
Tolerability	786/874	600/723	1.19	.56–2.54	68

N1, number of intensive regimens; N2, number of standard regimens; E/S, event/sample size; OR, odds ratio; CI, confidence interval; I2 >50% indicates high heterogeneity.

from the difference of basic purgative. As a control group, the “standard regimen” includes the two most common laxatives in clinical practice (Parra-Blanco et al., 2014; Hassan et al., 2019): PEG scheme and NaP scheme that indicate that constipated patients could usually benefit from extra bowel preparation in practice. Meanwhile, all intensive regimens show the same safety as the standard regimen despite the fact that adverse events were not reported according to a homogeneous standardized role. Those outcomes are inspiring and therefore likely to be important in medical field, in order to help inform treatment decisions.

However, it remains confusing until we explain the effectiveness of the specific regimen. Thus, in the subsequent Bayesian network meta-analysis, which integrates the superiority of direct and indirect

evidence, we tried to explore the effects of different regimens for prokinetics, intestinal regulation, combined stimulant laxatives, and high-dose laxative regimens. The first enlightening result is that NR + A, PEG + A + P, and H+ pre-PEG had the three top ranks which indicated that advanced intestinal regulation or pre-bowel preparation could maximize the benefits of cleansing quality for constipation. Five RCTs provide five different pre-bowel preparations including PEG (Chancharoen et al., 2019), lactulose (Yu et al., 2018), testa triticum (Zhong et al., 2018), and two probiotic products (*Bacillus subtilis* and *Streptococcus faecium* in the study of Lee et al. (2010) and *Clostridium butyricum* in the study of Tian et al. (2012)). Both lactulose and PEG which could increase the water amount of stool are commonly used osmotic laxatives in the treatment of chronic constipation (Lee-

Robichaud et al., 2010). By taking additional laxatives on the basis of the standard bowel preparation program, RCTs of both PEG (Chancharoen et al., 2019) and lactulose (Yu et al., 2018) exhibit improvement in the bowel quality in constipation. In addition, a multicenter retrospective study from Japan found that the improved rate by using short-duration PEG was 72.6% for chronic constipation whose previous bowel preparation had been fair or poor (Yoshida et al., 2020). Despite differences in results, at least on some options, dietary fiber and probiotics were commonly considered as functional supplements/food that could improve defecation in constipated patients (Ford et al., 2014). Correspondingly, the three RCTs (Lee et al., 2010; Tian et al., 2012; Zhong et al., 2018) in our study demonstrate that taking probiotics or dietary fiber in advance can improve the quality of bowel preparation. However, in view of the huge and complex of human flora, the role of probiotics, prebiotics, and synbiotics in intestinal function is still being further explored. For example, insoluble fibers can increase a regulatory stool frequency but wheat dextrin and finely ground wheat bran would decrease stool water content and bowel sensation, potentially aggravating constipation symptoms (Gill et al., 2021). Therefore, raising knowledge of functional supplements/food with different characteristics may help us choose the ideal product for prebowel preparation.

Another issue worth exploring is the duration of constipation management since preparation time ranges from 1 day to 2 weeks. It seems to be mechanism oriented, because high-dose laxatives can empty the intestines in a short time, while low-dose laxatives or functional supplements need more time to adjust intestinal function. Considering patient tolerance, symptom-oriented management may be able to guide the preparation time because if patients feel that difficult defecation is relieved, they are more likely to achieve qualified bowel preparation (Safder et al., 2008). Unfortunately, there is a lack of enough explanation of specific relationship between the disease severity and bowel preparation. The RCTs in our study also provide insufficient information about baseline characteristics and improvement degree of constipation. A few studies prove that bowel symptoms such as type 1 or 2 of the Bristol stool form scale (BSFS), starting-to-defecation interval  $\geq 4$  h, and infrequent bowel movement ( $<3$ /week) could predict IBP (Lee et al., 2017; Guo et al., 2020). Some studies found that the colon transit time test represents a useful mean for predicting IBP before colonoscopy (Park et al., 2015; Zhai et al., 2019). These evidences may be valuable for formulating individualized BP strategies in constipated patients until verified by a large cohort study. Regardless of the gap, our network meta-analysis intends to that reasonable symptom management before colonoscopy could maximize bowel cleansing to reach the standard of “adequate” for patients with constipation.

Abundant evidence indicates that high-volume PEG could provide the highest quality preparation (Johnson et al., 2014). However, volume-related discomfort and unpleasant taste may hinder the acceptability. Considering the limitations, several studies have suggested that low-volume PEG plus adjuvants such as ascorbate, citrate, and sports drinks may have the potentiality of addressing the issues under certain conditions (Saltzman et al., 2015; Hassan et al., 2019). Parente et al. (2015) discussed the role of previous two measures in patients with constipation, and they found that 2L PEG plus adjuvants perform equivalent in terms of bowel cleansing but better in

patient tolerability and compliance. In our study, we observed that increasing the amount of PEG may be ineffective in constipation according to the data in [table2](#). We speculate that high-dose laxatives may not be able to fully empty the constipated intestines in a short time because of colonic sensorimotor disturbances and pelvic floor dysfunction. However, since there is no direct comparison, it remains unclear if this is because of insufficient data, mix factor, or equivalent outcomes. In summary, we need head-to-head experiments and related mechanism examine to confirm the hypothesis.

One of the strengths in our study is that we help address clinical needs in practical settings by traditional and network meta-analysis. Another strength is the strict quality control of statistics which include mild heterogeneity, insignificant publication bias, and good index of sensitivity, consistency, and convergence, meaning that all results have a good credibility. There also are several limitations in the present study. First, there are differences in the preparation process, severity of symptom, and the endpoint used to define ABP. These are inevitable weakness in any meta-analysis because of the difference in individual trials which means we need to cautiously interpret outcomes even in mild heterogeneity (Nakagawa et al., 2017). Second, some studies may be underpowered owing to the relatively small sample. Third, inadequate participants blinding may elicit bias and impact the accuracy of the estimate. Fortunately, single-blind trials are more likely to influence the outcome of subjectively reported. In the definition of bowel cleanliness, it is more important to keep the endoscopists blind before observation. Our network meta-analysis may be criticized due to the absence of direct comparisons between most arms that may lead to confounding due to underlying differences, but the universality of various preparations raises the results of consistency and convergence that increase the credibility of outcome (Cipriani et al., 2013). In addition, our results tend to provide principled guidance for clinical decision-making, but the specific selection still needs to rely on the individualized characteristics of the patient.

In summary, we found that the intensive regimen and advanced intestinal regulation could increase the ABP rate, but increasing the amount of PEG may be ineffective in patients with constipation. Further checking the relationship between constipation severity/improvement and bowel preparation quality will help policy-makers refine clinical guidelines so that health-care providers can more efficiently and effectively develop a bowel cleaning strategy for constipated patients.

## Data availability statement

The original contributions presented in the study are included in the article/[Supplementary Material](#), further inquiries can be directed to the corresponding author.

## Author contributions

AM contributed to the conception and design of the review. LD wrote the manuscript. AM revised the manuscript. JD and TY contributed toward the statistical analysis of this work. LD and CJ interpreted the data. All authors contributed to manuscript revision, and read and approved the submitted version.

## Conflict of interest

The authors declare that the research was conducted in the absence of any commercial or financial relationships that could be construed as a potential conflict of interest.

## Publisher's note

All claims expressed in this article are solely those of the authors and do not necessarily represent those of their affiliated

organizations, or those of the publisher, the editors, and the reviewers. Any product that may be evaluated in this article, or claim that may be made by its manufacturer, is not guaranteed or endorsed by the publisher.

## Supplementary material

The Supplementary Material for this article can be found online at: <https://www.frontiersin.org/articles/10.3389/fphar.2022.964915/full#supplementary-material>

## References

- Arezzo, A. (2000). Prospective randomized trial comparing bowel cleaning preparations for colonoscopy. *Surg. Laparosc. Endosc. Percutan Tech.* 10, 215–217. doi:10.1097/00129689-200008000-00006
- Bharucha, A. E., and Lacy, B. E. (2020). Mechanisms, evaluation, and management of chronic constipation. *Gastroenterology* 158, 1232–1249. e3. doi:10.1053/j.gastro.2019.12.034
- Chancharoen, A., Mairiang, P., Sawadpanich, K., Suttichaimongkol, T., Kunyakhom, W., Limpapanasit, U., et al. (2019). Triple-dose vs. Split-dose PEG-ELS bowel preparation before colonoscopy in constipated patients: A prospective, endoscopist-blinded, randomized controlled trial[J]. *J. Med. Assoc. Thai.* 102 (10), 113–119.
- Cipriani, A., Higgins, J. P., Geddes, J. R., and Salanti, G. (2013). Conceptual and technical challenges in network meta-analysis. *Ann. Intern. Med.* 159, 130–137. doi:10.7326/0003-4819-159-2-201307160-00008
- Clark, B. T., Rustagi, T., and Laine, L. (2014). What level of bowel prep quality requires early repeat colonoscopy: Systematic review and meta-analysis of the impact of preparation quality on adenoma detection rate. *Am. J. Gastroenterol.* 109, 1714–1723. quiz 1724. doi:10.1038/ajg.2014.232
- Corley, D. A., Jensen, C. D., Marks, A. R., Zhao, W. K., Lee, J. K., Doubeni, C. A., et al. (2014). Adenoma detection rate and risk of colorectal cancer and death. *N. Engl. J. Med.* 370, 1298–1306. doi:10.1056/NEJMoa1309086
- De Salvo, L., Borgonovo, G., Ansaldo, G. L., Varaldo, E., Floris, F., Assalino, M., et al. (2006). The bowel cleansing for colonoscopy. A randomized trial comparing three methods. *Ann. Ital. Chir.* 77, 143–146. discussion 147.
- Ford, A. C., Quigley, E. M., Lacy, B. E., Lembo, A. J., Saito, Y. A., Schiller, L. R., et al. (2014). Efficacy of prebiotics, probiotics, and synbiotics in irritable bowel syndrome and chronic idiopathic constipation: Systematic review and meta-analysis. *Am. J. Gastroenterol.* 109, 15471562–15481561. quiz 1546. doi:10.1038/ajg.2014.202
- Gandhi, K., Tofani, C., Sokach, C., Patel, D., Kastenber, D., and Daskalakis, C. (2018). Patient characteristics associated with quality of colonoscopy preparation: A systematic review and meta-analysis. *Clin. Gastroenterol. Hepatol.* 16, 357–369. e10. doi:10.1016/j.cgh.2017.08.016
- Gill, S. K., Rossi, M., Bajka, B., and Whelan, K. (2021). Dietary fibre in gastrointestinal health and disease. *Nat. Rev. Gastroenterol. Hepatol.* 18, 101–116. doi:10.1038/s41575-020-00375-4
- Guo, X., Shi, X., Kang, X., Luo, H., Wang, X., Jia, H., et al. (2020). Risk factors associated with inadequate bowel preparation in patients with functional constipation. *Dig. Dis. Sci.* 65, 1082–1091. doi:10.1007/s10620-019-05847-5
- Hassan, C., East, J., Radaelli, F., Spada, C., Benamouzig, R., Bisschops, R., et al. (2019). Bowel preparation for colonoscopy: European society of gastrointestinal endoscopy (ESGE) guideline - update 2019. *Endoscopy* 51, 775–794. doi:10.1055/a-0959-0505
- Johnson, D. A., Barkun, A. N., Cohen, L. B., Dominitz, J. A., Kaltenbach, T., Martel, M., et al. (2014). Optimizing adequacy of bowel cleansing for colonoscopy: Recommendations from the US multi-society task force on colorectal cancer. *Gastroenterology* 147, 903–924. doi:10.1053/j.gastro.2014.07.002
- Lee, D. W., Koo, J. S., Kang, S., Kim, S. Y., Hyun, J. J., Jung, S. W., et al. (2017). Association between bowel habits and quality of bowel preparation for colonoscopy. *Med. (Abingdon)* 96, e7319. doi:10.1097/MD.00000000000007319
- Lee, H., Kim, Y. H., Kim, J. H., Chang, D. K., Kim, J. Y., Son, H. J., et al. (2010). A feasibility study of probiotics pretreatment as a bowel preparation for colonoscopy in constipated patients. *Dig. Dis. Sci.* 55, 2344–2351. doi:10.1007/s10620-009-1011-1
- Lee-Robichaud, H., Thomas, K., Morgan, J., and Nelson, R. L. (2010). Lactulose versus polyethylene glycol for chronic constipation. *Cochrane Database Syst. Rev.*, CD007570. doi:10.1002/14651858.CD007570.pub2
- Li, Y., Jia, X., Liu, B., Qi, Y., Zhang, X., Ji, R., et al. (2017). Randomized controlled trial: Standard versus supplemental bowel preparation in patients with Bristol stool form 1 and 2. *PLoS ONE* 12, e0171563. doi:10.1371/journal.pone.0171563
- Liberati, A., Altman, D. G., Tetzlaff, J., Mulrow, C., Gotzsche, P. C., Ioannidis, J. P., et al. (2009). The PRISMA statement for reporting systematic reviews and meta-analyses of studies that evaluate healthcare interventions: Explanation and elaboration. *BMJ Clin. Res. ed.* 339, b2700. doi:10.1136/bmj.b2700
- Nakagawa, S., Noble, D. W., Senior, A. M., and Lagisz, M. (2017). Meta-evaluation of meta-analysis: Ten appraisal questions for biologists. *BMC Biol.* 15, 18. doi:10.1186/s12915-017-0357-7
- Parente, F., Vailati, C., Bargiggia, S., Manes, G., Fontana, P., Masci, E., et al. (2015). 2-Litre polyethylene glycol-citrate-simethicone plus bisacodyl versus 4-litre polyethylene glycol as preparation for colonoscopy in chronic constipation. *Dig. Liver Dis.* 47, 857–863. doi:10.1016/j.dld.2015.06.008
- Park, H. J., Chae, M. H., Kim, H. S., Kim, J. W., Kim, M. Y., Baik, S. K., et al. (2015). Colon transit time may predict inadequate bowel preparation in patients with chronic constipation. *Intest. Res.* 13, 339–345. doi:10.5217/ir.2015.13.4.339
- Parra-Blanco, A., Ruiz, A., Alvarez-Lobos, M., Amorós, A., Gana, J. C., Ibáñez, P., et al. (2014). Achieving the best bowel preparation for colonoscopy. *World J. Gastroenterol.* 20, 17709–17726. doi:10.3748/wjg.v20.i47.17709
- Pereyra, L., Cimmino, D., González Malla, C., Laporte, M., Rotholtz, N., Peczan, C., et al. (2013). Colonic preparation before colonoscopy in constipated and non-constipated patients: A randomized study. *World J. Gastroenterol.* 19, 5103–5110. doi:10.3748/wjg.v19.i31.5103
- Safder, S., Demintieva, Y., Rewalt, M., and Elitsur, Y. (2008). Stool consistency and stool frequency are excellent clinical markers for adequate colon preparation after polyethylene glycol 3350 cleansing protocol: A prospective clinical study in children. *Gastrointest. Endosc.* 68, 1131–1135. doi:10.1016/j.gie.2008.04.026
- Saltzman, J. R., Cash, B. D., Pasha, S. F., Early, D. S., Muthusamy, V. R., Khashab, M. A., et al. (2015). Bowel preparation before colonoscopy. *Gastrointest. Endosc.* 81, 781–794. doi:10.1016/j.gie.2014.09.048
- Sulz, M. C., Kröger, A., Prakash, M., Manser, C. N., Heinrich, H., and Misselwitz, B. (2016). Meta-analysis of the effect of bowel preparation on adenoma detection: Early adenomas affected stronger than advanced adenomas. *PLoS ONE* 11, e0154149. doi:10.1371/journal.pone.0154149
- Tajika, M., Niwa, Y., Bhatia, V., Kawai, H., Kondo, S., Sawaki, A., et al. (2012). Efficacy of mosapride citrate with polyethylene glycol solution for colonoscopy preparation. *World J. Gastroenterol.* 18, 2517–2525. doi:10.3748/wjg.v18.i20.2517
- Takahashi, Y., Tanaka, H., Kinjo, M., and Sakumoto, K. (2005). Prospective evaluation of factors predicting difficulty and pain during sedation-free colonoscopy. *Dis. Colon Rectum* 48, 1295–1300. doi:10.1007/s10350-004-0940-1
- Tian, X., Zheng, H., Wang, C., Chen, W., and Zhu, Q. X. (2012). Analysis of the effects of prokinetic drug combined with probiotics of bowel preparation before colonoscopy in patients with constipation. *Chin. J. Hosp. Pharm.* 32, 1634–1636. doi:10.13286/j.cnki.chinhosppharmacj.2012.20.017
- Yoshida, N., Inagaki, Y., Fukumoto, K., Yoriki, H., Inada, Y., Murakami, T., et al. (2020). The efficacy of short-duration polyethylene glycol plus electrolytes for improving bowel preparation of colonoscopy in patients with chronic constipation. *Gastroenterol. Res. Pract.* 2020, 8886073. doi:10.1155/2020/8886073
- Yu, Z. B., Jiang, J. P., and Qu, Z. Y. (2018). Effects of polyethylene glycol electrolyte powder combined with different agents in bowel preparation for colonoscopy in elderly patients with constipation. *World Chin. J. Dig.* 26, 1268–1272. doi:10.11569/wcj.v26.i20.1268
- Zhai, C., Huang, Q., Chai, N., Zhang, W., and Linghu, E. (2019). Prediction of inadequate bowel preparation using total and segmental colon transit time in patients with chronic constipation: Some different outcomes. *Gastroenterol. Res. Pract.* 2019, 2328054. doi:10.1155/2019/2328054
- Zhong, S. S., Liang, W., Chen, Y. Y., Chen, X. Q., Zheng, X. L., Chen, L., et al. (2018). Application of testa tritum tricum purif to colonoscopy bowel preparation in constipation patients. *Chin. J. Dig. Endosc.* 35 (1), 55–57. doi:10.3760/cma.j.issn.1007-5232.20

# Frontiers in Pharmacology

Explores the interactions between chemicals and living beings

The most cited journal in its field, which advances access to pharmacological discoveries to prevent and treat human disease.

## Discover the latest Research Topics

[See more →](#)

### Frontiers

Avenue du Tribunal-Fédéral 34  
1005 Lausanne, Switzerland  
[frontiersin.org](https://frontiersin.org)

### Contact us

+41 (0)21 510 17 00  
[frontiersin.org/about/contact](https://frontiersin.org/about/contact)



### Frontiers in Pharmacology

